สารออกฤทธิ์ทางชีวภาพจากจิงจาบและจันทิมาดอย

นางสาวกนกภรณ์ สวัสดี

วิทยานิพนธ์นี้เป็นส่วนหนึ่งของการศึกษาตามหลักสูตรปริญญาวิทยาศาสตรดุษฎีบัณฑิต
สาขาวิชาเภสัชเวท ภาควิชาเภสัชเวทและเภสัชพฤกษศาสตร์
คณะเภสัชศาสตร์ จุฬาลงกรณ์มหาวิทยาลัย
ปีการศึกษา 2554
ลิขสิทธิ์ของจุฬาลงกรณ์มหาวิทยาลัย

BIOACTIVE CONSTITUENTS OF *MILIUSA MOLLIS* AND *MILIUSA* CF. *FUSCA*

Miss Kanokporn Sawasdee

A Dissertation Submitted in Partial Fulfillment of the Requirements

for the Degree of Doctor of Philosophy Program in Pharmacognosy

Department of Pharmacognosy and Pharmaceutical Botany

Faculty of Pharmaceutical Sciences

Chulalongkorn University

Academic year 2011

Thesis Title	BIOACTIVE CONSTITUENTS OF *MILIUSA MOLLIS* AND *MILIUSA* CF. *FUSCA*
By	Miss Kanokporn Sawasdee
Field of Study	Pharmacognosy
Thesis Advisor	Professor Kittisak Likhitwitayawuid, Ph.D.

Accepted by the Faculty of Pharmaceutical Sciences, Chulalongkorn University in Partial Fulfillment of the Requirements for the Doctoral Degree

……Dean of the Faculty of Pharmaceutical Sciences

(Associate Professor Pintip Pongpech, Ph.D.)

THESIS COMMITTEE

……Chairman

(Associate Professor Nijsiri Ruangrungsi, Ph.D.)

……...Thesis Advisor

(Professor Kittisak Likhitwitayawuid, Ph.D.)

……Examiner

(Associate Professor Vimolmas Lipipun, Ph.D.)

……Examiner

(Associate Professor Boonchoo Sritularak, Ph.D.)

……External Examiner

(Associate Professor Sumphan Wongseripipatana, Ph.D.)

……External Examiner

(Assistant Professor Lalita Wirasathien, Ph.D.)

……External Examiner

(Anong Teeravanichpong, Ph.D.)

กนกภรณ์ สวัสดี : สารออกฤทธิ์ทางชีวภาพจากจิงจาบและจันทิมาดอย (BIOACTIVE CONSTITUENTS OF *MILIUSA MOLLIS* AND *MILIUSA* CF. *FUSCA*) อ. ที่ปรึกษาวิทยานิพนธ์หลัก : ศ. ดร. กิตติศักดิ์ ลิขิตวิทยาวุฒิ, 336 หน้า.

การศึกษาองค์ประกอบทางเคมีของกิ่งและใบของจิงจาบและจากใบและต้นของจันทิมาดอย สามารถแยกสารชนิดใหม่ในกลุ่ม neolignan ได้ 15 ชนิด คือ (2*S*,3*S*)-2,3-dihydro-2-(4-methoxyphenyl)-3-methyl-5-(*E*)-propenylbenzofuran, (7*S*,8*S*)-*threo*-$\Delta^{8'}$-4-methoxy-8.O.4′-neolignan, (2*S*,3*S*)-5-allyl-2-(4-methoxyphenyl)-3-methyl-2,3-dihydrobenzofuran, (7*R*,8*R*)-*threo*-$\Delta^{8'}$-7-acethoxy-4-methoxy-8.O.4′-neolignan, (2*R*,3*R*)-5-allyl-2-(4-hydroxy-3-methoxyphenyl)-3-methyl-2,3-dihydrobenzofuran, (2*R*,3*R*)-5-allyl-2-(4-hydroxyphenyl)-3-methyl-2,3-dihydrobenzofuran, (2*R*,3*R*)-5-allyl-2-(4-hydroxyphenyl)-7-methoxy-3-methyl-2,3-dihydrobenzofuran, (2*R*,3*R*)-2-(4-hydroxyphenyl)-3-methyl-5-(2-oxopropyl)-2,3-dihydrobenzofuran, (7*S*,8*R*)-$\Delta^{8'}$-5-hydroxy-3,4,5′-trimethoxy-7.O.3′,8.O.4′-neolignan, (7*S*,8*R*)-$\Delta^{8'}$-4-hydroxy-3,5,5′-trimethoxy-7.O.3′,8.O.4′-neolignan, (7*R*,8*R*)-$\Delta^{8'}$-4-hydroxy-3,5′-dimethoxy-7.O.3′,8.O.4′-neolignan, (7*R*,8*R*)-$\Delta^{8'}$-3,4,5′-trimethoxy-7.O.3′,8.O.4′-neolignan, 3,4,5,4′,5′-pentamethoxy-3′,β-epoxy-γ,2′-neolign-8′-ene, (7*R*,8*R*)-$\Delta^{8'}$-3,4,5,5′-tetramethoxy-7.O.3′,8.O.4′-neolignan, $\Delta^{7'}$-9′-hydroxy-4,5,3′,5′-tetramethoxy-8.O.4′-neolignan, กลุ่ม phenolic glycoside 1 ชนิด คือ tyrosol-1-*O*-β-xylopyranosyl-(1$\rightarrow$6)-*O*-β-glucopyranoside และกลุ่ม lignan 1 ชนิด คือ *rel*-(7*S*,8*S*,7′*R*,8′*S*)-5-hydroxy-3,4,3′,4′-tetramethoxy-7,7′-epoxylignan รวมทั้งสารที่เคยมีการรายงานมาแล้ว 17 ชนิด ได้แก่ (2*R*,3*R*)-2,3-dihydro-2-(4-hydroxy-3-methoxyphenyl)-3-methyl-5-(*E*)-propenylbenzofuran, conocarpan, (−)-epicatechin, liriodenine, asimilobine, (−)-norushinsunine, icariside D_2, decurrenal, 2-methoxy-4-[2-[2-methoxy-4-(2-propen-1-yl)phenoxy]propyl]phenol, licarin A, eusiderin D, (7*S*,8*R*)-*erythro*-7-hydroxy-3,4,3′-trimethoxy-$\Delta^{1,3,5,1',3',5',8'}$-8.O.4′-neolignan, 2-(4-allyl-2,6-dimethoxyphenoxy)-1-(3,4-dimethoxyphenyl)propane, virolongin B, eusiderin C, (+)-veraguensin และ (7*S*,8*S*,7′*R*,8′*S*)-3,4,5,3′,4′-pentamethoxy-7,7′-epoxylignan การพิสูจน์โครงสร้างทางเคมีของสารที่แยกได้นี้ โดยวิเคราะห์สเปคตรัมของ UV, IR, MS และ NMR ร่วมกับการเปรียบเทียบข้อมูลของสารที่ทราบโครงสร้างแล้ว ได้ทำการทดสอบฤทธิ์จับอนุมูลอิสระ, ฤทธิ์ความเป็นพิษต่อเซลล์และฤทธิ์ต้านไวรัสเริม พบว่าสาร 3 ชนิด ได้แก่ (2*R*,3*R*)-2,3-dihydro-2-(4-hydroxy-3-methoxyphenyl)-3-methyl-5-(*E*)-propenylbenzofuran, (−)-epicatechin และ asimilobine มีฤทธิ์อ่อนในการจับอนุมูลอิสระ ในส่วนของใบจากจิงจาบและจันทิมาดอยพบสารบางชนิดมีฤทธิ์ปานกลางถึงอ่อนที่เป็นพิษต่อเซลล์มะเร็ง สารที่น่าสนใจในกลุ่มนี้และมีฤทธิ์ดีที่สุดต่อเซลล์มะเร็งชนิด KB, MCF7 และ NCI-H187 โดยไม่เป็นพิษต่อเซลล์ปกติชนิด ATCC CCL-81 คือ (7*S*,8*R*)-*erythro*-7-hydroxy-3,4,3′-trimethoxy-$\Delta^{1,3,5,1',3',5',8'}$-8.O.4′-neolignan นอกจากนี้พบสาร (2*R*,3*R*)-2-(4-hydroxyphenyl)-3-methyl-5-(2-oxopropyl)-2,3-dihydrobenzofuran, (7*S*,8*R*)-$\Delta^{8'}$-4-hydroxy-3,5,5′-trimethoxy-7.O.3′,8.O.4′-neolignan และ licarin A มีฤทธิ์อ่อนในการต้านเชื้อไวรัสเริมชนิด 1 และ 2

ภาควิชา เภสัชเวทและเภสัชพฤกษศาสตร์ ลายมือชื่อนิสิต .....

สาขาวิชา เภสัชเวท ลายมือชื่ออ.ที่ปรึกษาวิทยานิพนธ์หลัก .....

ปีการศึกษา 2554 .....

5076951833 : MAJOR PHARMACOGNOSY
KEYWORDS : NEOLIGNANS / PHENOLIC GLYCOSIDE / LIGNAN/ FREE RADICAL SCAVENGING ACTIVITY / CYTOTOXIC ACTIVITY / ANTI-HERPES SIMPLEX VIRUS ACTIVITY / *MILIUSA MOLLIS* / *MILIUSA* CF. *FUSCA*

KANOKPORN SAWASDEE: BIOACTIVE CONSTITUENTS OF *MILIUSA MOLLIS* AND *MILIUSA* CF. *FUSCA*. THESIS ADVISOR: PROF. KITTISAK LIKHITWITAYAWUID, Ph.D., 336 pp.

Chemical investigations of the twigs and leaves of *Miliusa mollis*, and from the leaves and the stems of *Miliusa* cf. *fusca* led to the isolation of fifteen new neolignans, namely, (2*S*,3*S*)-2,3-dihydro-2-(4-methoxyphenyl)-3-methyl-5-(*E*)-propenylbenzofuran, (7*S*,8*S*)-*threo*-$\Delta^{8'}$-4-methoxy-8.O.4′-neolignan, (2*S*,3*S*)-5-allyl-2-(4-methoxyphenyl)-3-methyl-2,3-dihydrobenzofuran, (7*S*,8*S*)-*threo*-$\Delta^{8'}$-7-acethoxy-4-methoxy-8.O.4′-neolignan, (2*R*,3*R*)-5-allyl-2-(4-hydroxy-3-methoxyphenyl)-3-methyl-2,3-dihydrobenzofuran, (2*R*,3*R*)-5-allyl-2-(4-hydroxyphenyl)-3-methyl-2,3-dihydrobenzo furan, (2*R*,3*R*)-5-allyl-2-(4-hydroxyphenyl)-7-methoxy-3-methyl-2,3-dihydrobenzofuran, (2*R*,3*R*)-2-(4-hydroxyphenyl)-3-methyl-5-(2-oxopropyl)-2,3-dihydrobenzofuran, (7*S*,8*R*)-$\Delta^{8'}$-5-hydroxy-3,4,5′-trimethoxy-7.O.3′,8.O.4′-neolignan, (7*S*,8*R*)-$\Delta^{8'}$-4-hydroxy-3,5,5′-trimethoxy-7.O.3′,8.O.4′-neolignan, (7*R*,8*R*)-$\Delta^{8'}$-4-hydroxy-3,5′-dimethoxy-7.O.3′,8.O.4′-neolignan, (7*R*,8*R*)-Δ8′-3,4,5′-trimethoxy-7.O.3′,8.O.4′-neolignan, 3,4,5,4′,5′-pentamethoxy-3′,β-epoxy-γ,2′-neolign-8′-ene, (7*R*,8*R*)-$\Delta^{8'}$-3,4,5,5′-tetramethoxy-7.O.3′,8.O.4′-neolignan, $\Delta^{7'}$-9′-hydroxy-4,5,3′,5′-tetramethoxy-8.O.4′-neolignan, a new phenolic glycosides, namely, tyrosol-1-*O*-*β*-xylopyranosyl-(1→6)-*O*-*β*-glucopyranoside, and a new lignan, namely, *rel*-(7*S*,8*S*,7′*R*,8′*S*)-5-hydroxy-3,4,3′,4′-tetramethoxy-7,7′-epoxylignan. In addition, seventeen known compounds were identified including (2*R*,3*R*)-2,3-dihydro-2-(4-hydroxy-3-methoxyphenyl)-3-methyl-5-(*E*)-propenylbenzofuran, conocarpan, (−)-epicatechin, liriodenine, asimilobine, (−)-norushinsunine, icariside D_2, decurrenal, 2-methoxy-4-[2-[2-methoxy-4-(2-propen-1-yl)phenoxy]propyl]phenol, licarin A, eusiderin D, (7*S*,8*R*)-*erythro*-7-hydroxy-3,4,3′-trimethoxy-$\Delta^{1,3,5,1',3',5',8'}$-8.O.4′-neolignan, 2-(4-allyl-2,6-dimethoxyphenoxy)-1-(3,4-dimethoxyphenyl)propane, virolongin B, eusiderin C, (+)-veraguensin and (7*S*,8*S*,7′*R*,8′*S*)-3,4,5,3′,4′-pentamethoxy-7,7′-epoxylignan. The structures of these compounds were determined by means of spectroscopic analysis, as well as comparison of their UV, IR, MS and NMR properties with previously reported data. These isolated compounds were evaluated for free radical scavenging, cytotoxic and anti-herpes simplex virus activities. Three compounds including (2*R*,3*R*)-2,3-dihydro-2-(4-hydroxy-3-methoxyphenyl)-3-methyl-5-(*E*)-propenylbenzofuran, (−)-epicatechin and asimilobine showed weak free radical scavenging activity. Some compounds from the leaves of *M. mollis* and *M.* cf. *fusca* showed moderate to weak cytotoxicity. Interestingly, (7*S*,8*R*)-*erythro*-7-hydroxy-3,4,3′-trimethoxy-$\Delta^{1,3,5,1',3',5',8'}$-8.O.4′-neolignan showed potent cytotoxicity against KB, MCF7 and NCI-H187 cell lines without toxicity against ATCC CCL-81 (Vero cells). In addition, (2*R*,3*R*)-2-(4-hydroxyphenyl)-3-methyl-5-(2-oxopropyl)-2,3-dihydrobenzofuran, (7*S*,8*R*)-$\Delta^{8'}$-4-hydroxy-3,5,5′-trimethoxy-7.O.3′,8.O.4′-neolignan and licarin A showed weak activity against herpes simplex type 1 and type 2.

Department : Pharmacognosy and Pharmaceutical Botany Student's Signature .....

Field of Study : Pharmacognosy Advisor's Signature .....

Academic Year : 2011

Acknowledgements

The author would like to express her deepest gratitude to her thesis advisor, Professor Dr. Kittisak Likhitwitayawuid of the Department of Pharmacognosy and Pharmaceutical botany, Faculty of Pharmaceutical Sciences, Chulalongkorn University, for his invaluable advice, useful guidance, endless support, concern, patience and encouragement throughout the course of this study.

The author wishes to express her sincere thanks to Professor Dr. Sylvie Michel and Associate Professor Dr. Thi-Hanh Dufat of Département de Physico-chimie du medicament, Faculté des sciences pharmaceutiques et biologiques, Université Paris Descartes for providing research opportunities and invaluable suggestions during her stay in France.

The author would like to thank Associate Professor Dr. Vimolmas Lipipun of the Department of Biochemistry and Microbiology for her kind assistance in the determination of the anti-herpes simplex virus activity and Associate Professor Dr. Boonchoo Sritularak of the Department of Pharmacognosy and Pharmaceutical botany, Faculty of Pharmaceutical Sciences, Chulalongkorn University for his beneficial guidance and encouragements.

The author would like to acknowledge the thesis committee for their constructive suggestions and critical review of her thesis.

The author would like to thank the Thailand Research Fund for a 2006 Royal Golden Jubilee Scholarship, the French Embassy in Thailand and Chulalongkorn University Graduate Scholarship in Commemoration of HM King Bhumibol Adulyadej's 72nd Anniversary for financial supports.

The author would also like to thank all lecturers and staff members of the Department of Pharmacognosy and Pharmaceutical Botany, and the people at the Pharmaceutical Research Instrument Center, Faculty of Pharmaceutical Sciences, Chulalongkorn University for their support and facilities.

The author is grateful to all students of the Department of Pharmacognosy and Pharmaceutical Botany, Faculty of Pharmaceutical Sciences, Chulalongkorn University, for their unforgettable friendship and warmth.

Finally, the author wishes to express her infinite gratitude to her family for their love, understanding, assistance and encouragement.

CONTENTS

CHAPTER Page

CHAPTER Page

CHAPTER Page

CHAPTER Page

CHAPTER Page

LIST OF TABLES

TABLE Page

TABLE Page

LIST OF FIGURES

FIGURE Page

FIGURE Page

FIGURE Page

FIGURE Page

FIGURE Page

FIGURE Page

FIGURE Page

FIGURE Page

FIGURE Page

FIGURE Page

FIGURE Page

LIST OF SCHEMES

ABBREVIATIONS

$[\alpha]_D^{20}$	=	Specific rotation at 20° and sodium D line (589 nm)
α	=	Alpha
ACC CCL-81	=	African green monkey kidney cell (vero cell)
Acetone-d_6	=	Deuterated acetone
β	=	Beta
br	=	Broad (for NMR spectra)
C	=	Concentration
ºC	=	Degree Celsius
calcd	=	Calculated
CD	=	Circular Dichroism
$CDCl_3$	=	Deuterated chloroform
CH_2Cl_2	=	Dichloromethane
cm	=	Centimeter
^{13}C NMR	=	Carbon-13 Nuclear Magnetic Resonance
Col-2	=	Colon cancer cell line
1-D	=	One dimensional (for NMR spectra)
2-D	=	Two dimensional (for NMR spectra)
d	=	Doublet (for NMR spectra)
dd	=	Doublet of doublets (for NMR spectra)
δ	=	Chemical shift
DEPT	=	Distortionless Enhancement by Polarization Transfer
DMSO-d_6	=	Deuterated dimethylsulfoxide
DNA	=	Deoxyribonucleic acid
DPPH	=	1,1-Diphenyl-2-picrylhydrazyl
EIMS	=	Electron Impact Mass Spectrometry
ESIMS	=	Electrospray Ionization Mass Spectrometry
EtOAc	=	Ethyl acetate
FCC	=	Flash Column Chromatography
g	=	Gram

GF	=	Gel Filtration Chromatography
Hep-G2	=	Human hepatocellular liver carcinoma cell line
Hr	=	Hour
HIV	=	Human immunodeficiency virus
^{1}H-NMR	=	Proton Nuclear Magnetic Resonance
HMBC	=	^{1}H-detected Heteronuclear Multiple Bond Correlation
HMQC	=	^{1}H-detected Heteronuclear Multiple Quantum Coherence
H_2O	=	Water
HRESIMS	=	High Resolution Electrospray Ionization Mass Spectrrmetry
HSV-1	=	Herpes Simplex Virus type 1
HSV-2	=	Herpes Simplex Virus type 2
Hz	=	Hertz
HUVEC	=	Human umbilical vein endothelial cell line
IC_{50}	=	Concentration showing 50% inhibition
IR	=	Infrared
J	=	Coupling constant
KB	=	oral cavity carcer cell line
Kg	=	Kilogram
L	=	Liter
µL	=	Microliter
λmax	=	Wavelength at maximal absorption
LNCaP	=	Human prostate cancer cell line
Lu-1	=	Lung cancer cell line
ε	=	Molar absorptivity
M^+	=	Molecular ion
m	=	Multiplet (for NMR spectra)
MCF-7	=	Breast cancer cell line
MeOH	=	Methanol
MeOH-d_4	=	Deuterated methanol
mg	=	Milligram
µg	=	Microgram
µL	=	Microliter

µM	=	Micromolar
MHz	=	Mega Hertz
MIC	=	Minimum inhibitory concentration
Min	=	Minute
mL	=	Milliliter
mm	=	Millimeter
MLPC	=	Medium Pressure Liquid Chromatography
MS	=	Mass spectrum
MTT	=	3-[4,5-Dimethylthiazol-2-yl]-2,5-diphenyltetrazolium bromide
MW	=	Molecular weight
m/z	=	Mass to charge ratio
N-04	=	Human neuroma cell line
NCI-H187	=	Small cell lung cancer cell line
nm	=	Nanometer
NMR	=	Nuclear Magnetic Resonance
NOESY	=	Nuclear Overhauser Effect Spectroscopy
ppm	=	Part per million
prep TLC	=	Preparative Thin Layer Chromatography
q	=	Quartet (for NMR spectra)
quint	=	Quintet (for NMR spectra)
RD	=	Rhabdomyosarcoma cell line
s	=	Singlet (for NMR spectra)
sext	=	Sextet (for NMR spectra)
t	=	Triplet (for NMR spectra)
TLC	=	Thin Layer Chromatography
UV-VIS	=	Ultraviolet and Visible spectrophotometry
VLC	=	Vacuum Liquid Column Chromatography

CHAPTER I

INTRODUCTION

Free radicals are defined as molecules having an unpaired electron in the outer orbit. They are generally unstable and very reactive. Examples of oxygen free radicals, known as reactive oxygen species (ROS), include superoxide ($O_2^{\bullet -}$), hydroxyl ($OH^{\bullet}$), peroxyl ($RO_2^{\bullet}$), alkoxyl ($RO^{\bullet}$), hydroperoxyl ($H_2O_2^{\bullet}$), and nitric oxide ($NO^{\bullet}$) radicals (Fang, Yang, and Wu, 2002; Pietta, 2000). It is accepted that ROS play different roles in vivo. Some are positive and are related to their involvement in energy production, phagocytosis, regulation of cell growth and intercellular signaling, and synthesis of biologically important compounds. However, ROS may be very damaging, since they can attack lipids in cell membranes, proteins in tissues or enzymes, carbohydrates, and DNA, to induce oxidations, which cause membrane damage, protein modification (including enzymes), and DNA damage. This oxidative damage is considered to play a causative role in aging and several degenerative diseases associated with it, such as heart diseases, cataracts, cognitive dysfunction, and cancer (Pietta, 2000).

Defense mechanisms against free radical-induced oxidative stress involve: (i) preventative mechanisms, (ii) repair mechanisms, (iii) physical defenses, and (iv) antioxidant defenses. Enzymatic antioxidant defenses include superoxide dismutase (SOD), glutathione peroxidase (GPx), and catalase (CAT). Non-enzymatic antioxidants are represented by ascorbic acid (Vitamin C), α-tocopherol (Vitamin E), glutathione (GSH), carotenoids, and plant polyphenols such as phenol, phenolic acids, flavonoids, tannins, and lignans (Valko *et al*., 2007; Pietta, 2000).

Based on the GLOBOCAN 2008 report, about 12.7 million cancer cases and 7.6 million cancer deaths are estimated to have occurred in 2008; of these, 56% of the cases and 64% of the deaths occurred in the economically developing world (Jemal *et al*., 2011). Plants have played an important role as a source of effective anticancer agents, and it is significant that over 60% of currently used anti-cancer agents are

derived in one way or another from natural sources, including plants, marine organisms and micro-organisms (Cragg and Newman, 2005).

The search for anti-cancer agents from plant sources started in earnest in the 1950s with the discovery and development of the vinca alkaloids, vinblastine and vincristine, and the isolation of the cytotoxic podophyllotoxins. As a result, the United States National Cancer Institute (NCI) initiated an extensive plant collection program in 1960, focused mainly in temperate regions. This led to the discovery of many novel chemotypes showing a range of cytotoxic activities, including the taxanes and camptothecins, but their development into clinically active agents spanned a period of some 30 years, from the early 1960s to the 1990s. This plant collection program was terminated in 1982, but the development of new screening technologies led to the revival of collections of plants and other organisms in 1986, with a focus on the tropical and sub-tropical regions of the world.

Herpes simplex virus (HSV) causes a contagious infection that affects approximately 60% to 95% of adults worldwide. HSV-1 and HSV-2 primarily infect human populations. HSV-1 is primarily associated with oral, pharyngeal, facial, ocular, and central nervous system infections and largely transmitted by oral secretions and nongenital contact. Sixty-seven percent of those with herpes simplex labialis (HSL) are reported to have HSV-1 on their hands, indicating the likelihood of horizontal spread. HSV-1 can remain viable on the skin, clothing, or plastic for brief periods, facilitating transmission through close nonsexual contact, such as kissing on the cheeks or sharing common utensils. HSV-2 is frequently involved with anal and genital infections and is mainly transmitted sexually by genital secretions. The risk of HSV-2 transmission through oral shedding and intimate nonsexual contact is minimal (Fatahzadeh and Schwartz, 2007). The clinical manifestation of the disease exhibits different severity in normal and immuno-competent hosts; in addition, several patients always encounter recurrent attacks. It should be pointed out that in immuno-compromised patients and neonates, HSV infections can cause serious systemic illnesses. Drug-resistant strains of HSV frequently develop following therapeutic treatment. Resistance to acyclovir and related nucleoside analogues can occur following mutation in either HSV thymidine kinase (TK) or DNA polymerase. Virus strains associated with clinical resistance are almost always defective in TK

production. Therefore, new antiviral agents exhibiting different mechanisms of action are urgently needed (Khan *et al*., 2005).

The genus *Miliusa* Lesch. ex. A. DC. (Annonaceae) comprises 30-40 species, which can be found from India and Bhutan to Australia and New Guinea. Most species occur in mainland Asia (Mols and Keßler, 2003). It has formerly been grouped in the tribe Miliuseae (Chaowasku and Keßler, 2006).

Plants in genus *Miliusa* are trees or erect shrubs. The flowers are in axils of leaves, or fallen leaves. They are solitary or in fascicles or cymes. The flowers have 3 sepals, small, valvate. The outer petals are small, cylyx-like. The inner petals are much larger than the outer petals, erect, cohering at the edges at first, readily free. The torus is cylindrical. The stamens are numerus, connective narrow, not concealing the cells. The ovaries are numerous, 1-2 ovuled. The stigmas are oblong or conical. The ripe carpels are numerus, stalk, globose or ellipsoid. They have 1-2 seeds (Backer and Bakhuizen van der Brink 1963).

According to Chalermglin (2005), nine species of *Miliusa* plants have been identified in Thailand:

Miliusa amplexicaulis Ridl.	ใบเบี้ยว bi buai
M. campanulata Pierre	ระฆังภู ra kang bhuu
M. cuneata Craib	ระฆังเขียว ra kang khuai
M. lineate (Craib) Aston	อีแรด ee rad, ปอขี้แฮด por khee had (chiang Mai), สะโงง sa ngong (Udonthani) Synonym *Saccopetalum lineatum* Craib
M. longipes King	ระฆังสายยาว ra kang sai yao
M. mollis Pierre var. *mollis*	จิงจาบ jing jaab, ตีนก้อง teen kong, คู่ขน ku khon, เหลืองดง leung dong
M. smithiae Craib	ระฆังใต้ ra kang tai
M. thorelii Finet & Gagnep.	หมาดำ ma dam

M. velutina (Dunal) Hook. F. & Thomson ขางหัวหมู khang hua muu, โกงกาง kong kang, จอแจ jor jae (Nakhon ratchasima, Prachinburi), โจรเจ็ดนาย joan jed nai, หัวใจไมยราบ hua jai mai ya rab (Prachuab khiri khan), เต็งใบใหญ่ teng bai yai, บังรอก bang rork, หางค่าง hang kang, หำรอก ham rork (Ratchaburi, Prachuab khiri khan), ยางโดน yang don, หางรอก hang rork (Pichit), สะแมะ sa mae (Suay- Surin)

M. mollis Pierre is a small shrub, 2-4 m height. The stem bark is dark brown and glabrous. The young twig has densely brown pilose. The branch is parallel with the ground. The leaves are ovate to oblong, 2-2.5 x 5.5-6 cm, base obtuse to oblique, apex acute, margin entire, thin lamina. The lower surface of midrib has densely villous, secondary vein 10-12 pairs per leaf, leaf stalk 1-2 mm long. The flowers are yellowish solitary, axillary, densely pilose pedicels 1-1.5 cm long. The sepals and the outer petals are nearly size, 1 mm. The inner petals are thick yellowish broadly ovate, 3-4 x 2-3 cm, 4 mm in diameter. The fruits are aggregate fruits (5-8 fruits), orbicular, 0.7-1 cm in diameter. Ripening fruits are black, peel is soft, 1 seed per fruit (Chalermklin, 2005).

M. cf. *fusca* Pierre is a shrub, 4-15 m height. The branch is small and slender. The young twig has red or reddish villous. The stem bark is blackish glabrous The leaves are ovate to oblong, 3 x 8 cm, base obtuse to oblique, apex acute, margin entire, thin lamina, secondary vein 8-10 pairs per leaf, leaf stalk 1-2 mm long. The leaf stock has villous. The flower is a small solitary, axillary, 4-5 mm diameter, 2-3 bracts. The sepals are ovate to triangular. The outer sepals have a little villous, but the inner sepals are glabrous. The petals are triangular to obtuse. The outer petals are longer and bigger than the sepals. The stamens are elliptical in 2-3 rows, appendix to connect almost indistinct. The carpels are glabrous and ovate. The stigma is glabrous,

1 ovule, insert to the middle of the ventral suture. Flowers are seen in April to May (Gagnepain, 1907).

To date, no studies on the phytochemical and the biological properties in *M. mollis* and *M.* cf. *fusca* have been reported. The MeOH extracts of two plants were screened for free radical scavenging activity, the cytotoxic activity and the antiviral, and the results are summarized in Table 1.

Table 1 Percentages of DPPH reduction, cytotoxic activity and anti-herpes simplex virus activity of the MeOH extracts prepared from *M. mollis* and *M.* cf. *fusca*

MeOH extract	% DPPH reduction (100 μg/mL)	% inhibition (50 μg/mL)			% inhibition (μg/mL)			
		KB	MCF7	NCI-H187	post-treatment		inactivation-treatment	
					HSV-1	HSV-2	HSV-1	HSV-2
M. mollis twigs	95.3	31	-4	28	inactive[a]	inactive[a]	inactive[a]	inactive[a]
M. mollis leaves	50.0	92	76	92	60[b]	60[b]	60[b]	inactive[b]
M. cf. *fusca* leaves	94.5	94	59	93	70[a]	60[a]	70[a]	60[a]
M. cf. *fusca* stems	95.1	-8	-6	42	80[a]	80[a]	85[a]	85[a]

[a] at concentration of 100 μg/mL; [b]at concentration of 50 μg/mL

It can be seen that the MeOH extracts prepared from the twigs of *M. mollis* and the leaves and stems of *M.* cf. *fusca* showed positive DPPH reduction. For cytotoxic activity, the MeOH extracts prepared from the leaves of *M. mollis* and *M.* cf. *fusca* exhibited positive results against KB, MCF7 and NCI-H187 cell lines. In

addition, the MeOH extracts prepared from the leaves of *M. mollis*, and the leaves and the stems of *M.* cf. *fusca* showed positive anti-herpes simplex virus activity against HSV-1 and HSV-2.

The main objectives in this investigation are as follows.

1. To isolate and purify the constituents from *M. mollis* and *M.* cf. *fusca*.
2. To determine the chemical structures of each isolated compound.
3. To evaluate the isolates for free radical scavenging activity, cytotoxic activity and antiherpetic potential.

Figure 1a Flower of *Miliusa mollis* Pierre (by Thanawat Chaowasku)

Figure 1b Leaves of *Miliusa mollis* Pierre

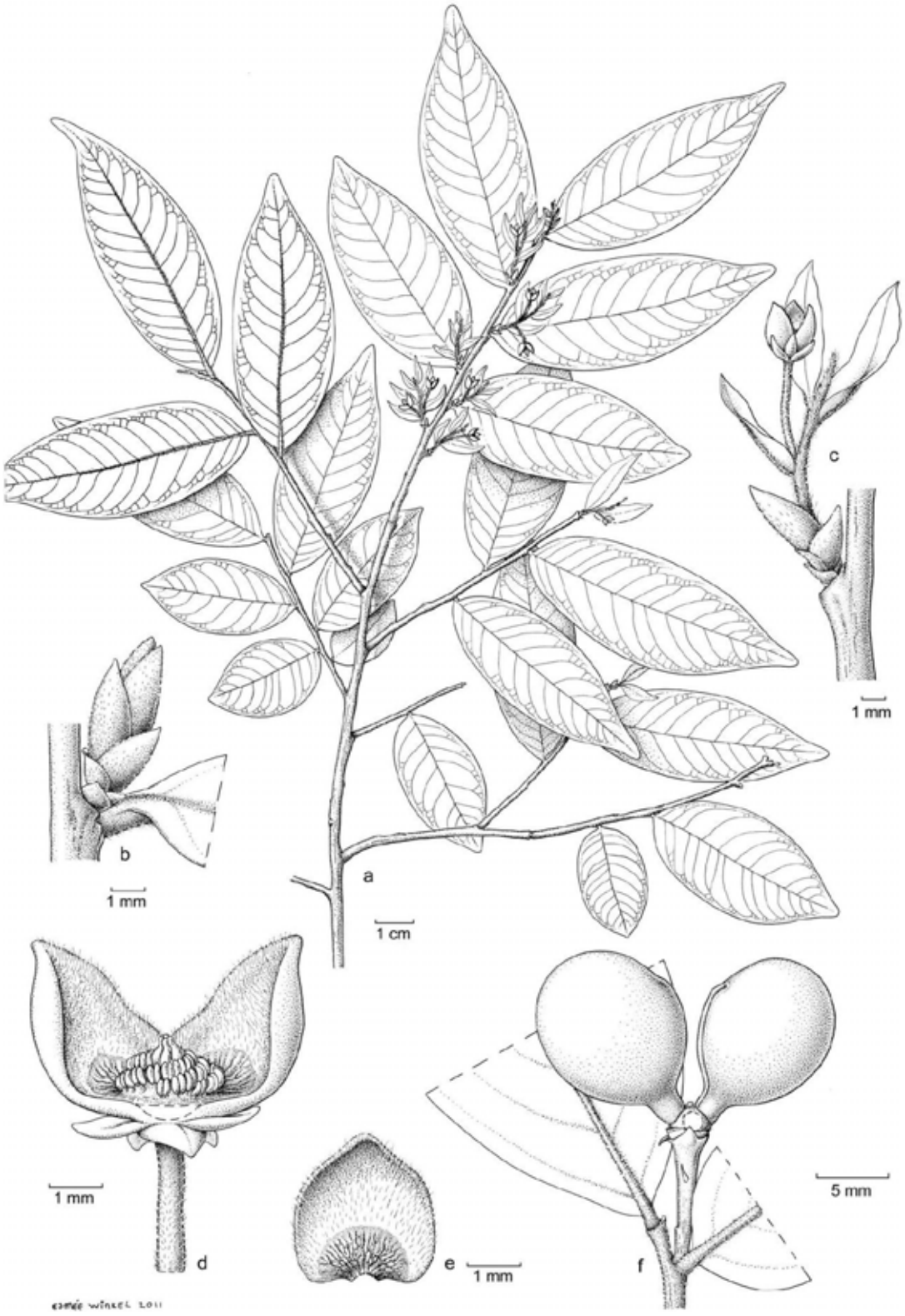

Figure 2 *Miliusa* cf. *fusca* Pierre (by Tanawat Chaowasku)

CHAPTER II

HISTORICAL

1. Chemical Constituents of *Miliusa*

Several types of compounds have been isolated from the genus *Miliusa*. They can be classified as terpenoids, homogentisic acids derivatives, alkaloids, flavonoids and miscellaneous compounds as shown in Tables 2-6.

Table 2 Distribution of terpenoids in the genus *Miliusa*

Plant and compound	Category	Plant part	Reference
Miliusa brahei			
(*Z*)-*β*-Ocimene [**1**]	Monoterpene	leaves	Brophy, Goldsack and Forster, 2004
α-Terpinenol [**2**]	Monoterpene	leaves	Brophy, Goldsack and Forster, 2004
Linalool [**3**]	Monoterpene	leaves	Brophy, Goldsack and Forster, 2004
Geraniol [**4**]	Monoterpene	leaves	Brophy, Goldsack and Forster, 2004
Geranyl acetate [**5**]	Monoterpene	leaves	Brophy, Goldsack and Forster, 2004
β-Caryophyllene [**6**]	Sesquiterpene	leaves	Brophy, Goldsack and Forster, 2004
α-Humulene [**7**]	Sesquiterpene	leaves	Brophy, Goldsack and Forster, 2004
Bicyclogermacrene [**8**]	Sesquiterpene	leaves	Brophy, Goldsack and Forster, 2004
Miliusa horsfieldii			
β-Caryophyllene [**6**]	Sesquiterpene	leaves	Brophy, Goldsack and Forster, 2004

Table 2 (continued)

Miliusa horsfieldii			
Caryophyllene oxide [**9**]	Sesquiterpene	leaves	Brophy, Goldsack and Forster, 2004
Miliusa sinensis			
24-Methylenecycloartane-3β-21-diol [**10**]	Triterpene	leaves and branches	Thanh Thuy *et al*., 2011
Miliusa traceyi			
α-Pinene [**11**]	Monoterpene	leaves	Brophy, Goldsack and Forster, 2004
β-Pinene [**12**]	Monoterpene	leaves	Brophy, Goldsack and Forster, 2004
β-Caryophyllene [**6**]	Sesquiterpene	leaves	Brophy, Goldsack and Forster, 2004
Miliusa velutina			
Spathulenol [**13**]	Sesquiterpene	stem bark	Jumana, Hasan and Rashid, 2000

Table 3 Distribution of homogentisic acid derivatives in the genus *Miliusa*

Plant and compound	Plant part	Reference
Miliusa balansae		
Miliusate [**14**]	not specified	Wu *et al*., 2001
Miliusol [**15**]	leaves and branches	Kamperdick *et al*., 2002
Miliusolide [**16**]	leaves and branches	Huong *et al*., 2004
Miliusa sinensis		
Miliusate [**14**]	leaves, twigs and flowers	Zhang *et al*., 2006
Miliusol [**15**]	leaves, twigs and flowers	Zhang *et al*., 2006

Table 3 (continued)

Plant and compound	Plant part	Reference
Miliusa sinensis		
(+)-Miliusane I [**17**]	leaves, twigs and flowers	Zhang *et al*., 2006
(+)-Miliusane II [**18**	leaves, twigs and flowers	Zhang *et al*., 2006
(+)-Miliusane III [**19**]	leaves, twigs and flowers	Zhang *et al*., 2006
(+)-Miliusane IV [**20**]	leaves, twigs and flowers	Zhang *et al*., 2006
(+)-Miliusane V [**21**]	leaves, twigs and flowers	Zhang *et al*., 2006
(+)-Miliusane VI [**22**]	leaves, twigs and flowers	Zhang *et al*., 2006
(+)-Miliusane VII [**23**]	leaves, twigs and flowers	Zhang *et al*., 2006
(+)-Miliusane VIII [**24**]	leaves, twigs and flowers	Zhang *et al*., 2006
(+)-Miliusane IX [**25**]	leaves, twigs and flowers	Zhang *et al*., 2006
(+)-Miliusane X [**26**]	leaves, twigs and flowers	Zhang *et al*., 2006
(+)-Miliusane XI [**27**]	leaves, twigs and flowers	Zhang *et al*., 2006
(+)-Miliusane XII [**28**]	leaves, twigs and flowers	Zhang *et al*., 2006
(+)-Miliusane XIII [**29**]	leaves, twigs and flowers	Zhang *et al*., 2006
(+)-Miliusane XIV [**30**]	leaves, twigs and flowers	Zhang *et al*., 2006

Table 3 (continued)

Plant and compound	Plant part	Reference
Miliusa sinensis		
(+)-Miliusane XV [**31**]	leaves, twigs and flowers	Zhang *et al*., 2006
(–)-Miliusane XVI [**32**]	leaves, twigs and flowers	Zhang *et al*., 2006
(+)-Miliusane XVII [**33**]	leaves, twigs and flowers	Zhang *et al*., 2006

Table 4 Distribution of alkaloids in the genus *Miliusa*

Plant and compound	Category	Plant part	Reference
Miliusa balansae			
Liriodenine [**34**]	Aporphine	not specified	Chen *et al*., 2002
(–)-caseamine [**35**]	Protoberberine	not specified	Chen *et al*., 2002
5,6,7,8-Tetramethoxyonychine [**36**]	Azafluorene	not specified	Chen *et al*., 2002
Oncodine [**37**]	Azafluorene	not specified	Chen *et al*., 2002
Polyfothine [**38**]	Azafluorene	not specified	Chen *et al*., 2002
6,7-Dimethoxy-5-hydroxyony-chine [**39**]	Azafluorene	not specified	Chen *et al*., 2002
Miliusa cf. banacea			
Lauterine [**40**]	Aporphine	not specified	Harrigan *et al*., 1994
10-Hydroxyliriodenine [**41**]	Aporphine	not specified	Harrigan *et al*., 1994

Table 4 (continued)

Plant and compound	Category	Plant part	Reference
Miliusa cuneata			
Liriodenine [**34**]	Aporphine	leaves and stem	Kamperdick, 2002
1,9-Dihydroxy-2,11-dimethoxy-4,5-dihydro-7-oxoaporphine [**42**]	Aporphine	leaves and stem	Kamperdick, 2002
Lanuginosine [**43**]	Aporphine	leaves and stem	Kamperdick, 2002
Dehydroxylopine [**44**]	Aporphine	leaves and stem	Kamperdick, 2002
(+)-Liriotulipiferine [**45**]	Aporphine	leaves and stem	Kamperdick, 2002
Norisocorytuberine [**46**]	Aporphine	leaves and stem	Kamperdick, 2002
N,O-Dimethylharnovine [**47**]	Aporphine	leaves and stem	Kamperdick, 2002
(–)-Nordicentrine [**48**]	Aporphine	leaves and stem	Kamperdick, 2002
Wilsonirine [**49**]	Aporphine	leaves and stem	Kamperdick, 2002
N-methyllindcarpine [**50**]	Aporphine	leaves and stem	Kamperdick, 2002
2,10-Dimethoxy-3,11-dihydroxy-5,6-dihydroprotoberberine [**51**]	Protoberberine	leaves and stem	Kamperdick, 2002
Pseudocolumbamine [**52**]	Protoberberine	leaves and stem	Kamperdick, 2002
Salutarine [**53**]	Morphine	leaves and stem	Kamperdick, 2002
N-methylcorydaldine [**54**]	Isoquuinoline	leaves and stem	Kamperdick, 2002

Table 4 (continued)

Plant and compound	Category	Plant part	Reference
Miliusa cuneata			
Kinabaline [**55**]	Azofluorene	leaves and stem	Kamperdick, 2002
Miliusa sinensis			
Liriodenine [**34**]	Aporphine	leaves and branches	Thanh Thuy *et al*., 2011
Miliusa velutina			
Liriodenine [**34**]	Aporphine	stem bark	Jumana, Hasan and Rashid, 2000
Norcorydine [**56**]	Aporphine	stem bark	Jumana, Hasan and Rashid, 2000
Isocorydine [**57**]	Aporphine	stem bark	Jumana, Hasan and Rashid, 2000
Reticuline [**58**]	Benzylisoqui-noline	stem bark	Jumana, Hasan and Rashid, 2000

Table 5 Distribution of flavonoids in the genus *Miliusa*

Plant and compound	Category	Plant part	Reference
Miliusa balansae			
5-Hydroxy-7-methoxyflavanone [**59**]	Flavanone	leaves and branches	Kamperdick *et al*., 2002
5-Hydroxy-7,4′-dimethoxyflava-none [**60**]	Flavanone	leaves and branches	Kamperdick *et al*., 2002
5-Hydroxy-7,8-dimethoxyflava-none [**61**]	Flavanone	leaves and branches	Kamperdick *et al*., 2002

Table 5 (continued)

Plant and compound	Category	Plant part	Reference
Miliusa balansae			
5-Hydroxy-6,7-dimethoxyflavanone [**62**]	Flavanone	leaves and branches	Kamperdick *et al*., 2002
Miliufavol [**63**]	Flavanone	leaves and branches	Huong *et al*., 2005
Ombuine [**64**]	Flavanone	leaves and branches	Huong *et al*., 2005
Pachypodol [**65**]	Flavanone	leaves and branches	Huong *et al*., 2005
Chrysoplenol B [**66**]	Flavanone	leaves and branches	Huong *et al*., 2005
Chrysoplenol C [**67**]	Flavanone	leaves and branches	Kamperdick *et al*., 2002
2′,6′-Dihydroxy-3′,4′-dimethoxydihydrochalcone [**68**]	Dihydrochalcone	leaves and branches	Huong *et al*., 2004
2′,6′-Dihydroxy-4′-methoxydihydrochalcone [**69**]	Dihydrochalcone	leaves and branches	Kamperdick *et al*., 2002
Miliusa sinensis			
5-Hydroxy-7-methoxyflavanone [**59**]	Flavanone	leaves and branches	Thanh Thuy *et al*., 2011

Table 5 (continued)

Miliusa sinensis			
5-Hydroxy-7,4′-dimethoxyflavanone [**60**]	Flavanone	leaves and branches	Thanh Thuy *et al*., 2011
5-Hydroxy-7,8-dimethoxyflavanone [**61**]	Flavanone	leaves and branches	Thanh Thuy *et al*., 2011
5-Hydroxy-6,7-dimethoxyflavanone [**62**]	Flavanone	leaves and branches	Thanh Thuy *et al*., 2011
7,3′,4′-Trimethoxyflavone [**70**]	Flavone	leaves and branches	Thanh Thuy *et al*., 2011
2′,6′-Dihydroxy-3′,4′-dimethoxydihydrochalcone [**68**]	Dihydrochalcone	leaves and branches	Thanh Thuy *et al*., 2011
4′,6′-Dihydroxy-2′,3′,4-trimethoxydihydrochalcone [**71**]	Dihydrochalcone	leaves and branches	Thanh Thuy *et al*., 2011
Pashanone [**72**]	Chalcone	leaves and branches	Thanh Thuy *et al*., 2011

Table 6 Distribution of miscellaneous compounds in the genus *Miliusa*

Plant and compound	Category	Plant part	Reference
Miliusa balansae			
3,4-Dimethoxy-6-styrylpyran-2-one [**73**]	Styrylpyrone	leaves and branches	Kamperdick *et al*., 2002

Table 6 (continued)

Plant and compound	Category	Plant part	Reference
Miliusa balansae			
(2*E*,5*E*)-2-methoxy-4-oxo-6-phenylhexa-2,5-dienoic acid methyl ester [**74**]	Styrylpyrone	leaves and branches	Kamperdick *et al*., 2002
Miliubisstyryl A [**75**]	Bis-styryl	leaves and branches	Huong *et al*., 2008
Miliubisstyryl B [**76**]	Bis-styryl	leaves and branches	Huong *et al*., 2008
Miliusoside A [**77**]	Phenolic glycoside	stem	Lei *et al*., 2008
Miliusoside B [**78**]	Phenolic glycoside	stem	Lei *et al*., 2008
Osmanthuside H [**79**]	Phenolic glycoside	stem	Lei *et al*., 2008
Cuchiloside [**80**]	Phenolic glycoside	stem	Lei *et al*., 2008
Bis(2-hydroxyphenyl)-methyl ether [**81**]	Phenolic compound	leaves and branches	Huong *et al*., 2004
1-(α-L-rhamnosyl-(1$\rightarrow$6)-β-D-glucopyranosyloxy)-3,4,5-trimethoxy benzene [**82**]	Phenolic compound	stem	Lei *et al*., 2008
3,4,5-Trimethoxyphenol-β-D-glucopyranoside [**83**]	Phenolic compound	stem	Lei *et al*., 2008
Alanginoside B [**84**]	Megastigmane glycoside	stem	Lei *et al*., 2008

Table 6 (continued)

Plant and compound	Category	Plant part	Reference
Miliusa balansae Megastigm-7-ene-3,6,9-triol-9-*O*-α-D-apifuranosyl-(1$\rightarrow$6)-*O*-β-D-glucopyranoside [**85**]	Megastigmane glycoside	stem	Lei *et al*., 2008
Miliusa velutina Goniothalamusin [**86**]	Acetogenin	stem bark	Jumana, Hasan and Rashid, 2000a

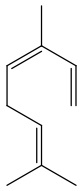

(*Z*)-*β*-Ocimene [**1**]

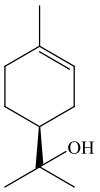

α-Terpinenol [**2**]

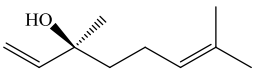

Linalool [**3**]

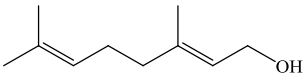

Geraniol [**4**]

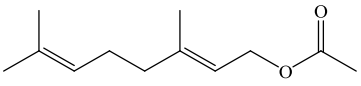

Geranyl acetate [**5**]

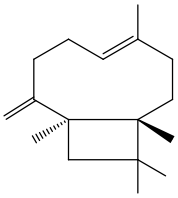

β-Caryophyllene [**6**]

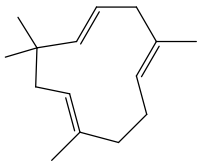

α-Humulene [**7**]

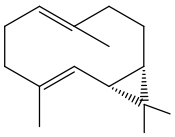

Bicyclogermacrene [**8**]

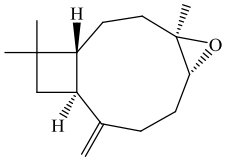

Caryophyllene oxide [**9**]

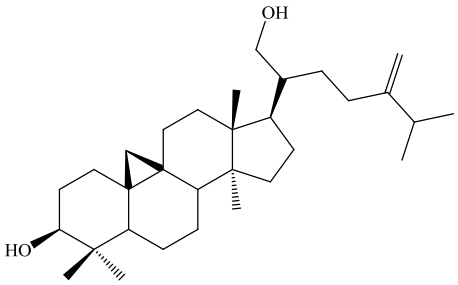

24-Methylenecycloartane-3*β*-21-diol [**10**]

***α*-Pinene [11]**

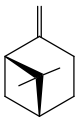

***β*-Pinene [12]**

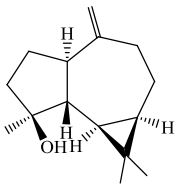

Spathulenol [**13**]

Figure 3 Structures of terpenoids previously isolated from the genus *Miliusa*

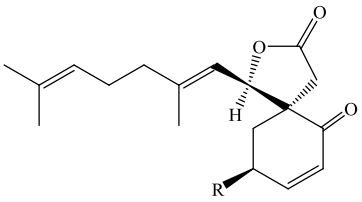

	R
Miliusate [**14**]	OAc
Miliusol [**15**]	OH

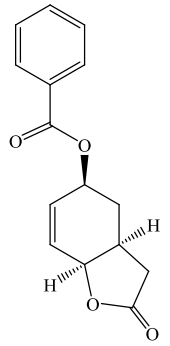

Miliusolide [**16**]

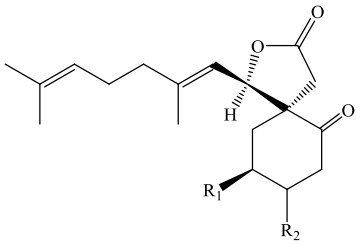

	R_1	R_2
(+)-Miliusane I [**17**]	OH	β-OCH_3
(+)-Miliusane II [**18**]	OH	α-OCH_3
(+)-Miliusane III [**19**]	OH	β-OH
(+)-Miliusane IV [**20**]	OH	α-OH
(+)-Miliusane V [**21**]	OH	β-NHAc
(+)-Miliusane VI [**22**]	OAc	β-OCH_3
(+)-Miliusane VII[**23**]	OAc	α-OCH_3

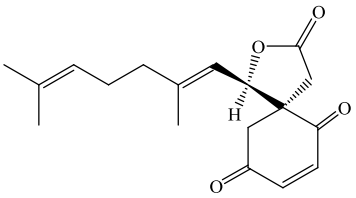

(+)-Miliusane VIII [**24**]

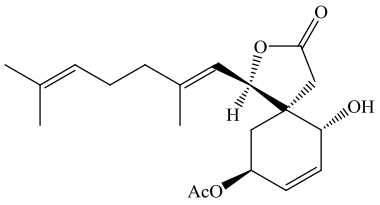

(+)-Miliusane IX [**25**]

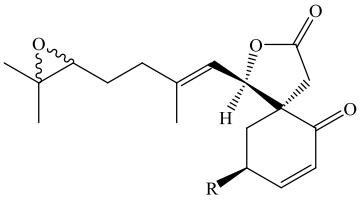

	R
(+)-Miliusane X [**26**]	OH
(+)-Miliusane XI [**27**]	OAc

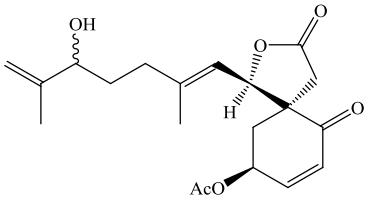

(+)-Miliusane XII [**28**]

Figure 4 Structures of homogentisic acid derivatives previously isolated from the genus *Miliusa*

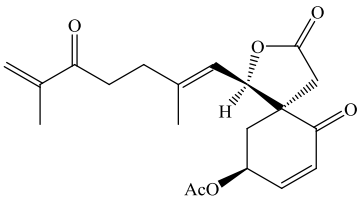

(+)-Miliusane XIII [**29**]

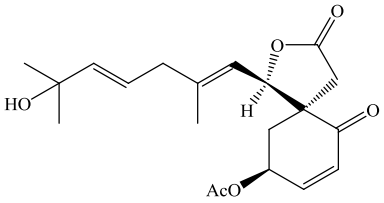

(+)-Miliusane XIV [**30**]

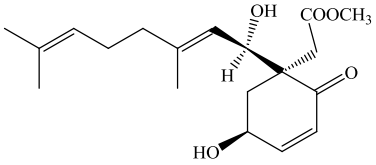

(+)-Miliusane XV [**31**]

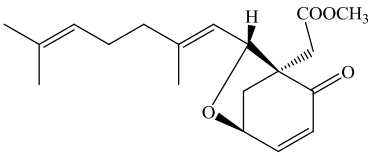

(–)-Miliusane XVI [**32**]

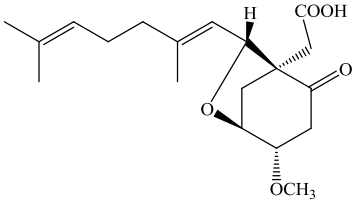

(+)-Miliusane XVII [**33**]

Figure 4 Structures of homogentisic acid derivatives previously isolated from the genus *Miliusa* (continued)

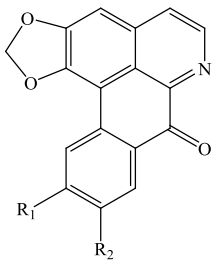

	R_1	R_2
Liriodenine **[34]**	H	H
Lauterine [**40**]	OCH_3	H
10-Hydroxyliriodenine [**41**]	OH	H
Lanuginosine [**43**]	H	OCH_3

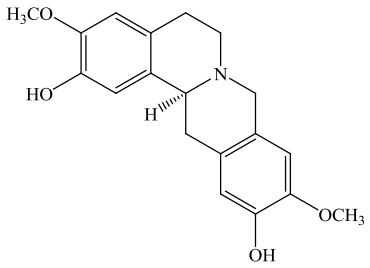

(–)-caseamine [**35**]

Figure 5 Structures of alkaloids previously isolated from the genus *Miliusa*

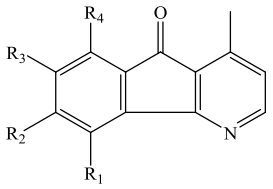

	R_1	**R_2**	**R_3**	**R_4**
5,6,7,8-Tetramethoxyonychine [**36**]	OCH_3	OCH_3	OCH_3	OCH_3
Oncodine [**37**]	H	OH	OCH_3	H
Polyfothine [**38**]	H	OCH_3	OCH_3	H
6,7-Dimethoxy-5-hydroxyonychine [**39**]	OH	OCH_3	OCH_3	H
Kinabaline [**55**]	OCH_3	OH	H	OCH_3

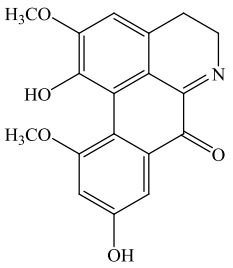

1,9-Dihydroxy-2,11-dimethoxy-4,5-dihydro-7-oxoaporphine [**42**]

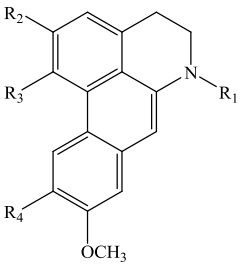

	R_1	**R_2**	**R_3**	**R_4**
Dehydroxylopine [**44**]	H	$–OCH_2O–$		H
(+)-Liriotulipiferine [**45**]	CH_3	OH	OCH_3	OH

Figure 5 Structures of alkaloids previously isolated from the genus *Miliusa* (continued)

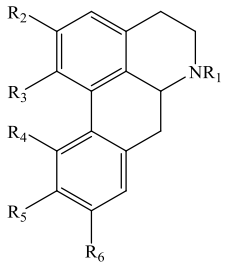

	R_1	R_2	R_3	R_4	R_5	R_6
Norisocorytuberine [**46**]	H	OCH_3	OH	OCH_3	OH	H
N,O-Dimethylharnovine [**47**]	CH_3	OH	OCH_3	OCH_3	OCH_3	H
(–)-Nordicentrine [**48**]	H	–OCH_2O–		H	OCH_3	OCH_3
Wilsonirine [**49**]	H	OCH_3	OH	H	OCH_3	OCH_3
N-methyllindcarpine [**50**]	CH_3	OH	OCH_3	OH	OCH_3	H
Norcorydine [**56**]	H	OCH_3	OH	OCH_3	OCH_3	H
Isocorydine [**57**]	CH_3	OCH_3	OCH_3	OH	OCH_3	H

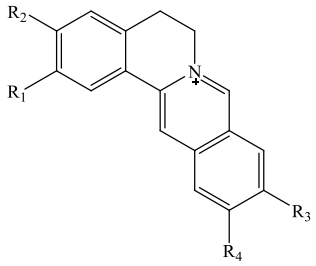

	R_1	R_2	R_3	R_4
2,10-Dimethoxy-3,11-dihydroxy-5,6-dihydroprotoberberine [**51**]	OCH_3	OH	OCH_3	OH
Pseudocolumbamine [**52**]	OH	OCH_3	OCH_3	OCH_3

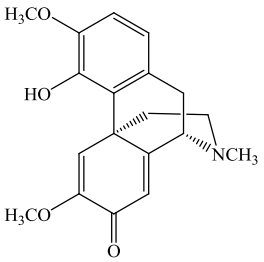

Salutarine [**53**]

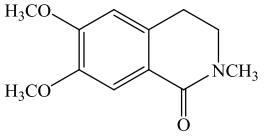

N-methylcorydaldine [**54**]

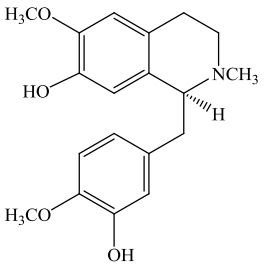

Reticuline [**58**]

Figure 5 Structures of alkaloids previously isolated from the genus *Miliusa* (continued)

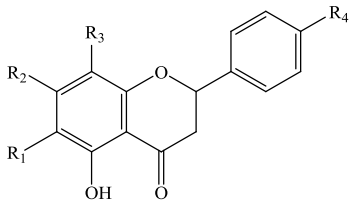

	R_1	R_2	R_3	R_4
5-Hydroxy-7-methoxyflavanone [**59**]	H	OCH_3	H	H
5-Hydroxy-7,4'-dimethoxyflavanone [**60**]	H	OCH_3	H	OCH_3
5-Hydroxy-7,8-dimethoxyflavanone [**61**]	H	OCH_3	OCH_3	H
5-Hydroxy-6,7-dimethoxyflavanone [**62**]	OCH_3	OCH_3	H	H

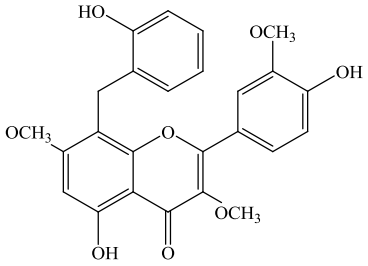

Miliufavol [**63**]

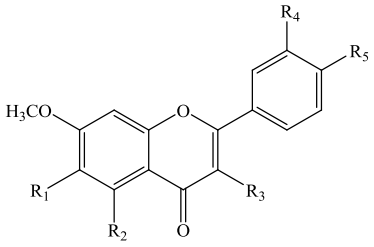

	R_1	R_2	R_3	R_4	R_5
Ombuine [**64**]	H	OH	OH	OH	OCH_3
Pachypodol [**65**]	H	OH	OCH_3	OCH_3	OH
Chrysoplenol B [**66**]	OCH_3	H	OCH_3	OCH_3	OH
Chrysoplenol C [**67**]	OH	OH	OCH_3	OCH_3	OH
7,3',4'-Trimethoxyflavone [**70**]	H	OH	OH	OCH_3	OCH_3

Figure 6 Structures of flavonoids previously isolated from the genus *Miliusa*

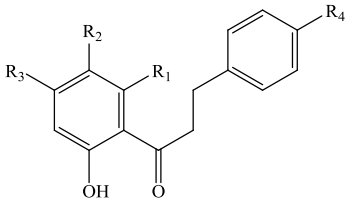

	R_1	R_2	R_3	R_4
2',6'-Dihydroxy-3',4'-dimethoxydihydrochalcone [**68**]	OH	OCH_3	OCH_3	H
2',6'-Dihydroxy-4'-methoxydihydrochalcone [**69**]	OH	H	OCH_3	H
4',6'-Dihydroxy-2',3',4-trimethoxydihydrochalcone [**71**]	OCH_3	OCH_3	OH	OCH_3

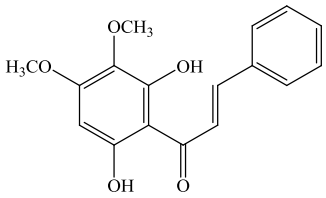

Pashanone [**72**]

Figure 6 Structures of flavonoids previously isolated from the genus *Miliusa* (continued)

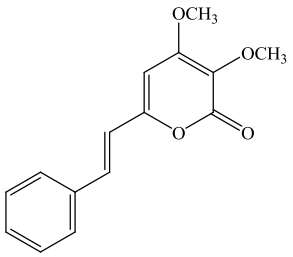

3,4-Dimethoxy-6-styrylpyran-2-one [**73**]

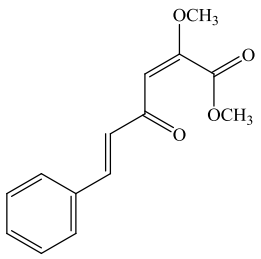

(2*E*,5*E*)-2-methoxy-4-oxo-6-phenylhexa-2,5-dienoic acid methyl ester [**74**]

Figure 7 Structures of miscellaneous compounds previously isolated from the genus *Miliusa*

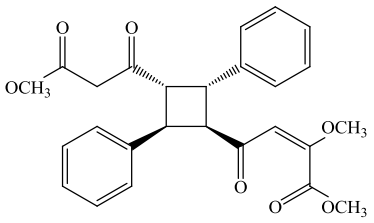

Miliubisstyryl A [**75**]

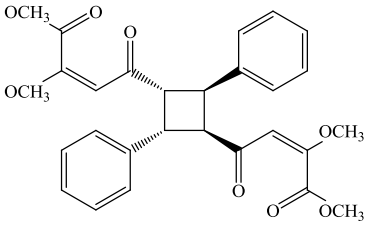

Miliubisstyryl B [**76**]

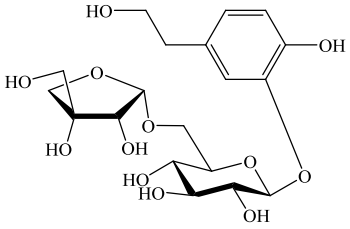

Miliusoside A [**77**]

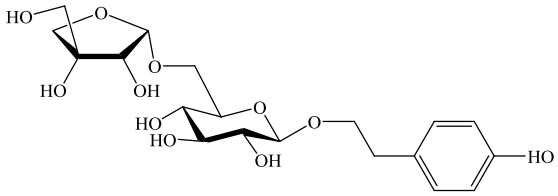

Miliusoside B [**78**]

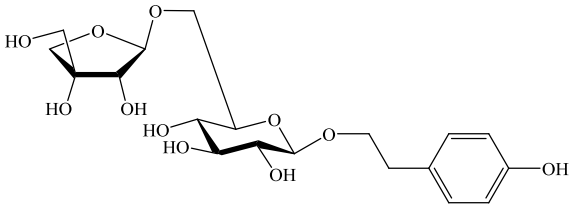

Osmanthuside H [**79**]

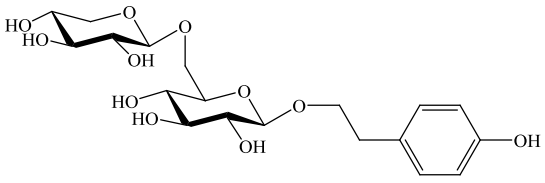

Cuchiloside [**80**]

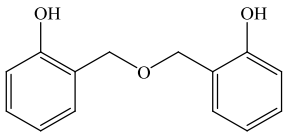

Bis(2-hydroxyphenyl)-methyl ether [**81**]

Figure 7 Structures of miscellaneous compounds previously isolated from the genus *Miliusa* (continued)

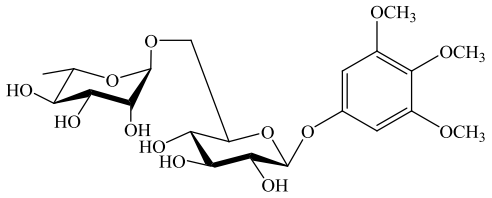

1-(α-L-rhamnosyl-(1→6)-β-D-glucopyranosyloxy)-3,4,5-trimethoxy benzene [**82**]

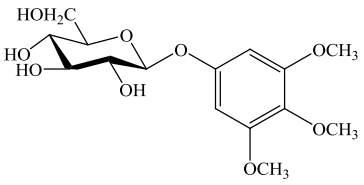

3,4,5-Trimethoxyphenol-β-D-glucopyranoside [**83**]

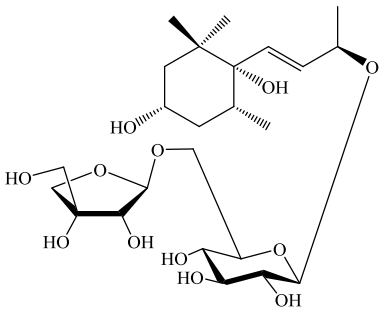

Alanginoside B [**84**]

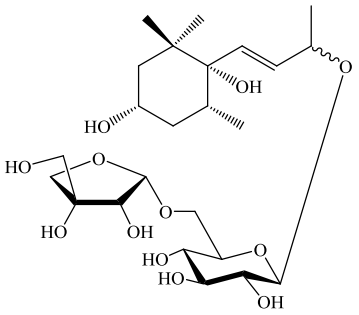

Megastigm-7-ene-3,6,9-triol-9-*O*-α-D-apifuranosyl-(1→6)-*O*-β-D-glucopyranoside [**85**]

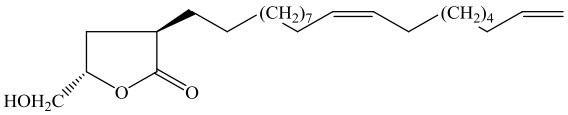

Goniothalamusin [**86**]

Figure 7 Structures of miscellaneous compounds previously isolated from the genus *Miliusa* (continued)

2. Traditional uses and biological activity of *Miliusa*

Several plants of the genus *Miliusa* have been used in traditional medicine. *Miliusa balansae* Finet et Gagnep is used to treat different symptoms, for example, gastropathy and glomerulonephropathy (Wu *et al*., 2001). In Thailand, the boiling water containing the stem wood of *Miliusa velutina*, the stem wood or the root of *Lasianthus cyanocarpus* and the stem of *Betula alnoides* is used for tonic and aphrodisiac properties (มูลนิธิมหาวิทยาลัยมหิดล 2548).

The flavonoids from *Miliusa balansae,* such as ombuine [**64**], pachypodol [**65**], chrysoplenol B [**66**] and chrysoplenol C [**67**], have been reported for cytotoxic activity against KB, Hep-G2 and RD cells with IC_{50} less than 5 μg/ml. In particular, pachypodol [**65**] has strong activity against KB and Hep-G2 cell lines with IC_{50} 0.7 and 0.55 μg/ml, respectively (Huong *et al*., 2005). The butanone extract of the roots of *Miliusa* cf. *banacea* showed activity against the *rad 52. Top 1* mutant of yeast *Saccharomyces cerevisiae*. Lauterine [**40**] and 10-hydroxyliriodenine [**41**] from this plant showed toxicity towards the *rad 52. Top 1* mutant and showed inhibitory activity against purified mammalian DNA topoisomerase II. 10-Hydroxyliriodenine [**41**] (IC_{50} 12.5 μg/ml) was about twice as active as lauterine [**40**] (IC_{50} 25.0 μg/ml) (Harrigan *et al*., 1994). *Miliusa cuneata* Graib has been reported for cytotoxic activity. The ethanolic extracts of the stem and leaves of this plant exhibited weak cytotoxicity *in vitro* against human Lu-02, N-04 and Bre-04 (breast cancer cell) carcinoma cell lines (Chen *et al*., 2003). The dichloromethane extract of the leaves, twigs and flowers of *Miliusa sinensis* Finet and Gagnep. exhibited cytotoxicity against KB cells with an IC_{50} value of 2.0 μg/ml. The homogentisic acid derivatives of this plant extract, such as miliusate [**14**], miliusol [**15**], (+)-miliusane I [**17**], (+)-miliusane III [**19**], (+)-miliusane VI [**22**], (+)-miliusane VII [**23**], (+)-miliusane XIII [**29**], (+)-miliusane XV [**31**] and (–)-miliusane XVI [**32**], demonstrated significant cytotoxic activity in KB, Col-2, LNCaP, Lu-1, MCF-7 and HUVEC cancer cell lines (Zhang *et al*., 2006). The volatile oil isolated from the leaves of *Miliusa tomentosa* (Roxb.) J Sinclair showed strong and moderate activity against the bacteria and fungi (Menon and Kar, 1970). In addition, a petroleum ether extract of the stem bark of *Miliusa velutina* exhibited significant antibacterial and cytotoxic activities (Jumana,

Hasan, Rashid, 2000a). Goniothalamusin [**86**] from this extract exhibited moderate antibacterial activity and showed significant cytotoxic activity in the brine shrimp lethality bioassay (Jumara, Hasan and Rashid, 2000a).

CHAPTER III

EXPERIMENTAL

1. Source of plant materials

The twigs and leaves of *Miliusa mollis* Pierre were collected in Bangkok, Thailand by Tanawat Chaowasku and identified by R. W. J. M. van der Ham, as previously described (Chaowasku, Mols, and Van Der Ham, 2008).

The leaves and stems of *Miliusa* cf. *fusca* Pierre were collected in Chiang Mai, Thailand by Tanawat Chaowasku and identified by Tanawat Chaowasku and colleagues (Chaowasku *et al*., submitted).

2. General techniques

2.1 Analytical thin-layer chromatography (TLC)

Technique	:	One dimension, ascending
Adsorbent	:	Silica gel 60 F254 (E. Merck) precoated plate
Layer thickness	:	0.2 mm
Distance	:	6 cm
Temperature	:	Laboratory temperature (30-35ºC)
Detection	:	1. Ultraviolet light at wavelengths of 254 and 365 nm. 2. Anisaldehyde/hydrochloric acid and heating at 105°C for 10 min. 3. Vanillin/sulfuric acid and heating at 105°C for 5 min.

2.2 Preparative thin-layer chromatography (TLC)

Technique	:	One dimension, ascending
Adsorbent	:	Silica gel 60 F254 (E. Merck) precoated plate
Layer thickness	:	0.2 mm
Distance	:	16 cm
Temperature	:	Laboratory temperature (30-35ºC)
Detection	:	Ultraviolet light at wavelengths of 254 and 365 nm.

2.3 Column chromatography

2.3.1 Vacuum liquid column chromatography

Adsorbent	:	Silica gel 60 (No.7734) particle size 0.063-0.200 mm (70-230 mesh ASTM) (E. Merck)
Packing method	:	Dry packing
Sample loading	:	The sample was dissolved in a small amount of organic solvent, mixed with a small quantity of adsorbent, triturated, dried and then placed gently on top of the column.
Detection	:	Fractions were examined by TLC under UV light at the wavelengths of 254 and 365 nm.

2.3.2 Flash column chromatography

Adsorbent	:	Silica gel 60 (No.9385) particle size 0.040-0.063 mm (70-230 mesh ASTM) (E. Merck) or silica gel 60 particle size (0.035-0.070 mm and 0.020-0.045 mm) (Carlo Erba Reactifs-SDS)
Packing method	:	Wet packing
Sample loading	:	The sample was dissolved in a small amount of eluent and then applied gently on top of the column, Alternatively, the sample was dissolved in a small amount of organic solvent, mixed with a small quantity of adsorbent, triturated, dried and then placed gently on top of the column.
Detection	:	Fractions were examined in the same way as described in section 2.3.1

2.3.3 Medium pressure liquid chromatography

Adsorbent	:	Silica gel 60 (No.9385) particle size 0.040-0.063 mm (70-230 mesh ASTM) (E. Merck)
Packing method	:	Dry packing
Sample loading	:	The sample was dissolved in a small amount of organic solvent, mixed with a small quantity of adsorbent,

triturated, dried and then placed gently on top of the column.

Detection : Fractions were examined in the same way as described in section 2.3.1

2.2.4 Gel filtration chromatography

Adsorbent : Sephadex LH 20 (Pharmacia)

Packing method : Gel filter was suspended in the eluent and left standing to swell for 24 hours prior to use. It was then poured into the column and allowed to set tightly.

Sample loading : The sample was dissolved in a small amount eluent and then applied gently on top of the column.

2.4 Spectroscopy

2.4.1 Ultraviolet (UV) absorption spectra

UV (in methanol) spectra were obtained on a Shimadzu UV-160A UV/vis spectrophotometer (Pharmaceutical Research Instrument Center, Faculty of Pharmaceutical Sciences, Chulalongkorn University).

2.4.2 Mass spectra

Mass spectra were recorded on a Micromass LCT spectrtometer or a Thermo-Finnigan Polaris Q mass spectrometer (Department of Chemistry, Faculty of Science, Mahidol University), or a Bruker microTOF mass spectrometer (National Center for Genetic Engineering and Biotechnology), or a Thermo Finnergan LCQ Advantage (ESI-ion trap) or a LCT Premier Waters® (ESI-TOF) (Faculté des sciences pharmaceutiques et biologiques, Université Paris Descartes, Paris, France).

2.4.3 Proton and carbon-13 nuclear magnetic resonance (^{1}H and ^{13}C-NMR) spectra

^{1}H NMR (300 MHz) and ^{13}C NMR (75 MHz) spectra were obtained with a Bruker Avance DPX-300 FT-NMR spectrometer (Faculty of Pharmaceutical Sciences, Chulalongkorn University) or a Bruker AC300 NMR spectrometer (Faculté des sciences pharmaceutiques et biologiques, Université Paris Descartes, Paris, France).

^{1}H NMR (400 MHz) and ^{13}C NMR (100 MHz) spectra were obtained with a Bruker Avance 400 NMR spectrometer (Faculté des sciences pharmaceutiques et biologiques, Université Paris Descartes, Paris, France).

^{1}H NMR (500 MHz) and ^{13}C NMR (125 MHz) spectra were obtained with a JEOL JMN-A 500 NMR spectrometer (Scientific and Technological Research Equipment Center, Chulalongkorn University).

Solvents for NMR spectra were deuterated chloroform (chloroform-*d*) and deuterated acetone (acetone-d_6), deuterated methanol (MeOH-d_4) and deuterated dimethyl sulfoxide (DMSO-d_6). Chemical shifts were reported in ppm scale using the chemical shift of the solvent as the reference signal.

2.5 Physical property

2.5.1 Optical rotation

Optical rotations were measured on a Perkin Elmer Polarimeter 341 (Pharmaceutical Research Instrument Center, Faculty of Pharmaceutical Sciences, Chulalongkorn University or Laboratoire de Pharmocognosie, Faculté des sciences pharmaceutiques et biologiques, Université Paris Descartes, Paris, France). Optical rotation was calculated by the following equation:

$$[\alpha]_{\lambda}^{t} = \frac{\alpha_{D}^{20} \text{ x } 100}{\text{l x c}}$$

α	=	specific rotation
t	=	temperature (°C)
λ	=	wavelength (nm)
l	=	path-length of cell (dm)
c	=	concentration (g/100 mL)

2.5.2 Circular dichroism (CD) spectra

CD spectra were recorded on a JASCO J-715 spectropolarimeter (Pharmaceutical Research Instrument Center, Faculty of Pharmaceutical Sciences, Chulalongkorn University). Molar ellipticity was calculated by the following equation:

$$[\theta] = \frac{\theta}{10 \times c \times l}$$

θ = ellipticity (mdeg)

c = concentration (M)

l = path-length of cell (cm)

2.6 Solvents

All organic solvents employed throughout this work were of commercial grade and were redistilled prior to use.

3. Extraction and isolation

3.1 Extraction and isolation of compounds from twigs of *Miliusa mollis*

3.1.1 Extraction

The dried and powdered twigs of *Miliusa mollis* (380.0 g) were macerated with methanol (3 x 3L) to give, after removal of the solvent, a methanol extract (24.3 g, 6.41% based on dried weight of twigs).

3.1.2 Isolation

3.1.2.1 Isolation of compound TMM1

The methanol extract (12.1 g) was fractionated by vacuum liquid column chromatography using a sintered glass filter column of silica gel (No.7734, 260 g). Elution was performed using solvent mixtures of increasing polarity (hexane-CH_2Cl_2 (1:0 to 0:1), CH_2Cl_2-EtOAc (1:0 to 0:1) to MeOH). The eluates (200 ml per fraction) were collected and examined by TLC (silica gel, CH_2Cl_2) to yield 105 fractions. Another portion of methanol extract (12.3 g) was separated in the same manner to give 68 fractions. Fractions (173 fractions) with similar chromatographic patterns were combined to yield 8 fractions: A (32 mg), B (6 mg), C (49 mg), D (98 mg), E (321 mg), F (1.9 g), G (1.6 g) and H (16.5 g).

Fraction D (98 mg) was further separated by flash column chromatography (silica gel 60 No. 9385; hexane-CH_2Cl_2, 1:0 to 0:1). Fractions (69 fractions) showing similar chromatographic patterns (TLC, silica gel, hexane-CH_2Cl_2, 7:3) were combined to yield 7 fractions: D1 (3 mg), D2 (25 mg), D3 (12 mg), D4 (33 mg), D5 (4 mg), D6 (2 mg) and D7 (14 mg).

Fraction D4 (33 mg) was purified on Sephadex LH-20 (CH_2Cl_2-MeOH, 1:1) to give compound TMM1 as a colorless oil (22 mg). This compound was characterized as a new dihydrobenzofuran neolignan named (2*S*,3*S*)-2,3-dihydro-2-(4-methoxy-phenyl)-3-methyl-5-(*E*)-propenylbenzofuran [**87**].

3.1.2.2 Isolation of compound TMM2

Fraction E (321 mg) was separated on silica gel 60 (No. 9385) with hexane-CH_2Cl_2 gradient elution. Eighty-seven fractions with similar chromatographic patterns (TLC, silica gel, hexane-CH_2Cl_2 1:1) were combined to give 10 fractions: E1 (4 mg), E2 (2 mg), E3 (1 mg), E4 (3 mg), E5 (54 mg), E6 (184 mg), E7 (22 mg), E8 (9 mg), E9 (3 mg) and E10 (23 mg).

Fraction E6 (184 mg) was purified on Sephadex LH-20 (CH_2Cl_2-MeOH, 1:1) to give compound TMM2 as white amorphous solid (100 mg). This compound was identified as (2*R*,3*R*)-2,3-dihydro-2-(4-hydroxy-3-methoxyphenyl)-3-methyl-5-(*E*)-propenylbenzofuran [**88**].

3.1.2.3 Isolation of compound TMM3

Fraction F (1.9 g) was separated by medium pressure liquid chromatography (MPLC) (silica gel, No. 9385; gradient mixture of hexane-CH_2Cl_2, 1:0 to 0:1). The eluates were collected 200 ml per fraction to give 73 fractions. Seventy-three fractions with similar chromatographic patterns (TLC, silica gel, CH_2Cl_2) were combined to give 11 fractions: F1 (14 mg), F2 (5 mg), F3 (6 mg), F4 (9 mg), F5 (167 mg), F6 (2878 mg), F7 (172 mg), F8 (378 mg), F9 (51 mg), F10 (629 mg) and F11 (14 mg).

Fraction F7 (172 mg) was further separated on Sephadex LH-20 (CH_2Cl_2-MeOH, 1:1) to give 5 fractions: F7-1 (3 mg), F7-2 (24 mg), F7-3 (22 mg), F7-4 (7 mg), and F7-5 (100 mg).

Fraction F7-4 (7 mg) was purified by preparative TLC (silica gel, hexane-EtOAc-acetone 90:8:2, 7-time development) to give compound TMM3 as a colorless oil (2 mg). This compound was determined as a new 8.*O*.4′-neolignan namely (7*S*,8*S*)- *threo*-$\Delta^{8'}$-4-methoxy-8.O.4′-neolignan [**89**].

3.1.2.4 Isolation of compound TMM4

Fraction F8 (378 mg) was purified on a Sephadex LH-20 column (CH_2Cl_2-MeOH, 1:1) to give compound TMM4 as a white amorphous solid (339 mg). This compound was characterized as conocarpan [**90**].

3.1.2.5 Isolation of compound TMM5

Fraction G (1.6 g) was separated by MPLC (silica gel, No. 9385; gradient mixture of hexane-EtOAc, 1:0 to 0:1). The eluates (200 ml per fraction) were collected to yield 120 fractions. Fractions showing similar chromatographic patterns (TLC, silica gel, hexane-EtOAc, 1:9) were combined to give 12 fractions: G1 (34 mg), G2 (8 mg), G3 (56 mg), G4 (145 mg), G5 (29 mg), G6 (124 mg), G7 (27 mg), G8 (70 mg), G9 (433 mg), G10 (104 mg), G11 (270 mg) and G12 (398 mg).

Fraction G9 (433 mg) was separated on Sephadex LH-20 (acetone) to give compound TMM5 as a white amorphous powder (163 mg). This compound was identified as (−)-epicatechin [**91**].

3.1.2.6 Isolation of compound TMM6

Fraction H (16.5 g) was divided into 4 portions. Each portion was fractionated on Diaion HP20SS, then eluted with H_2O-MeOH (100:0 to 0:100) to give 7 fractions: H1 (7.1 g), H2 (2.2 g), H3 (0.3 g), H4 (0.3 g), H5 (5. 4 g), H6 (0.6 g) and H7 (0.4 g).

Fraction H7 (406 mg) was separated on silica gel (No. 9385) with EtOAc-MeOH-H_2O gradient elution (100:0:0 to 0:90:10). Sixty-two fractions showing similar chromatographic patterns (TLC, silica gel, EtOAc:MeOH:H_2O, 75:15:10) were combined to give 14 fractions: H7-1 (76 mg), H7-2 (25 mg), H7-3 (44 mg), H7-4 (20 mg), H7-5 (25 mg), H7-6 (52 mg), H7-7 (38 mg), H7-8 (4 mg), H7-9 (58 mg), H7-10 (10 mg), H7-11 (8 mg), H7-12 (11 mg), H7-13 (14 mg) and H7-14 (4 mg).

Fraction H7-2 (25 mg) was further purified on Sephadex-LH-20 (CH_2Cl_2-MeOH, 1:1) to give compound TMM6 as a yellow powder (2 mg). This compound was determined as liriodenine [**34**].

3.1.2.7 Isolation of compound TMM7

Fraction H7-6 (52 mg) was separated on Sephadex LH-20 and eluted with CH_2Cl_2-MeOH (1:1). All twenty-four fractions with similar chromatographic patterns (TLC, silica gel, CH_2Cl_2-MeOH, 9:1) were combined to give 4 fractions: H7-6-1 (28 mg), H7-6-2 (4 mg), H7-6-3 (6 mg) and H7-6-4 (10 mg).

Fraction H7-6-4 (10 mg) was further purified by flash column chromatography (silica gel, No. 9385; CH_2Cl_2-acetone, 1:4) to give compound TMM7 as a light brownish viscous residue (2 mg). This compound was identified as asimilobine [**92**].

3.1.2.8 Isolation of compounds TMM7 and TMM8

Fraction H7-7 (38 mg) was separated on Sephadex LH-20 (CH_2Cl_2-MeOH, 1:1). Fractions (14 fractions) with similar chromatographic patterns (TLC, silica gel, CH_2Cl_2-MeOH, 9:1) were combined to give 4 fractions: H7-7-1 (10 mg), H7-7-2 (6 mg), H7-7-3 (4 mg) and H7-7-4 (15 mg).

Fraction H7-7-4 (15 mg) was further purified by flash column chromatography on silica gel (No. 9385) and eluted with CH_2Cl_2-acetone (1:4) to give 2 compounds: TMM**7** (1 mg) and TMM8 (4 mg), which were subsequently identified as asimilobine [**92**] and (–)-norushinsunine [**93**], respectively.

3.1.2.9 Isolation of compound TMM9

Fraction H4 (282 mg) was separated on a silica gel (No. 9385) column with EtOAC-MeOH-H_2O gradient elution (100:0:0 to 0:100:10). Sixty-six fractions with similar chromatographic patterns (TLC, silica gel, EtOAc-MeOH-H_2O, 90:6:4 and 75:15:10) were combined to give 12 fractions: H4-1 (3 mg), H4-2 (7 mg), H4-3 (16 mg), H4-4 (24 mg), H4-5 (21 mg), H4-6 (39 mg), H4-7 (10 mg), H4-8 (41 mg), H4-9 (35 mg), H4-10 (14 mg), H4-11 (6 mg) and H4-12 (28 mg).

Fraction H4-3 (16 mg) was further separated on Sephaddex LH-20 (MeOH) to give 8 fractions showing similar chromatographic pattern (TLC, silica gel, EtOAc-MeOH-H_2O, 90:6:4), which were combined to give 3 fractions: H4-3-1 (14 mg), H4-3-2 (1 mg) and H4-3-3(1 mg).

Fraction H4-3-1 (14 mg) was further purified by preparative TLC (silica gel) with EtOAc-MeOH-H_2O (92:6:2) to give compound TMM9 as a white amorphous powder (10 mg). This compound was identified as icariside D_2 [**94**].

3.1.2.10 Isolation of compound TMM10

Fraction H4-6 (39 mg) was separated on Sephadex LH-20 (MeOH) and gave 25 fractions with similar chromatographic patterns (TLC, silica gel, EtOAc-MeOH-H_2O, 75:15:10), which were combined to give 6 fractions: H4-6-1 (1 mg), H4-6-2 (4 mg), H4-6-3 (3 mg), H4-6-4 (26 mg), H4-6-5 (3 mg) and H4-6-6 (3 mg).

Fraction H4-6-4 (26 mg) was further purified by flash column chromatography (silica gel, No. 9385; EtOAc-MeOH-H_2O, 80:12:8) to give compound TMM10 as a colorless amorphous powder (3 mg). This was characterized as a new phenolic

glycoside compound, namely tyrosol-1-*O*-*β*-xylopyranosyl-(1→6)-*O*-*β*-gluco-pyranoside [**95**].

3.2 Extraction and isolation of compounds from leaves of *Miliusa mollis*

3.2.1 Extraction

The dried and powdered leaves of *Miliusa mollis* (198 g) were macerated with methanol (3 x 3L) to give, after removal of the solvent, a methanol extract (36 g, 18.16% based on dried weight of leaves).

3.2.2 Isolation

3.2.2.1 Isolation of compound LMM1

The methanol extract (36 g) was fractionated by vacuum liquid column chromatography using a sintered glass filter column of silica gel (No.7734, 556 g). Elution was performed using solvent mixtures of increasing polarity (hexane-CH_2Cl_2 (1:0 to 0:1), CH_2Cl_2-EtOAc (1:0 to 0:1) to MeOH). The eluates (500 ml per fraction) were collected and examined by TLC (silica gel, CH_2Cl_2) to yield 54 fractions. Fractions with similar chromatographic patterns were combined to yield 8 fractions: A (22 mg), B (22 mg), C (141 mg), D (314 mg), E (2.2 g), F (5.2 g), G (3.9 g) and H (23.1 g).

Fraction D (314 mg) was fractionated on a silica gel (No. 9385) column. Elution was performed in a polarity gradient manner with mixtures of hexane and CH_2Cl_2 (10:0 to 0:10). Fractions (72 fractions) showing similar chromatographic patterns (TLC, silica gel, hexane-CH_2Cl_2, 85:15) were combined to yield 9 fractions: D1 (13 mg), D2 (3 mg), D3 (6 mg), D4 (11 mg), D5 (90 mg), D6 (97 mg), D7 (35 mg), D8 (20 mg) and D9 (30 mg).

Fraction D5 (90 mg) was further fractionated by column chromatography (silica gel, No. 9385, hexane-EtOAc, 98:2). Twenty-nine fractions with similar chromatographic patterns (TLC, silica gel, hexane-EtOAc, 98:2) were combined to give 3 fractions: D5-1 (7 mg.), D5-2 (32 mg) and D5-3 (1 mg).

Fraction D5-2 (32 mg) was repeatedly separated on silica gel (No. 9385) and eluted with hexane-CH_2Cl_2 (4:1) to give compound LMM1 as a colorless oil (13 mg). This compound was a new dihydrobenzofuran neolignan. It was characterized as (2*S*,3*S*)-5-allyl-2-(4-methoxyphenyl)-3-methyl-2,3-dihydrobenzofuran [**96**].

3.2.2.2 Isolation of compound LMM2

Fraction E (2.2 g) was separated on a flash column (silica gel, No. 9385, gradient mixtures of hexane-CH_2Cl_2 10:0 to 0:10). Twenty-two fractions were combined on the basis of their TLC composition (silica gel, hexane-CH_2Cl_2, 3:7) to yield 7 fractions: E1 (10 mg), E2 (17 mg), E3 (194 mg), E4 (790 mg), E5 (29 mg), E6 (21 mg), and E7 (668 mg).

Fraction E4 (790 mg) was repeatedly fractionated on Sephadex LH-20 (CH_2Cl_2-MeOH, 1:1). Eleven fractions with similar chromatographic patterns (TLC, silica gel, hexane-EtOAc, 95:5) were combined to yield 5 fractions: E4-1 (50 mg), E4-2 (84 mg), E4-3 (110 mg), E4-4 (531 mg) and E4-5 (12 mg).

Fraction E4-2 (84 mg) was purified by flash column chromatography (silica gel, No. 9385, hexane-EtOAc, 96:4) to give compound LMM2 as a colorless oil (11 mg). This compound was a new 8.O.4′ neolignan, and its structure was determined as (7*R*,8*R*)-threo-$\Delta^{8'}$-7-acetoxy-4-methoxy-8.O.4′-neolignan [**97**].

3.2.2.3 Isolation of compound LMM3

Fraction E4-4 (531 mg) was fractionated by repeated column chromatography (silica gel, No. 9385, hexane-EtOAc, 94:6) to afford compound LMM3 as a colorless oil (161 mg). This compound was a new dihydrobenzofuran neolignan named (2*R*,3*R*)-5-allyl-2-(4-hydroxy-phenyl)-3-methyl-2,3-dihydro-benzofuran [**98**].

3.2.2.4 Isolation of compounds LMM4 and LMM5

Fraction F (5.2 g) was fractionated by vacuum liquid column chromatography using a sintered glass filter column of silica gel (No.7734, 154 g). Elution was performed in a polarity gradient manner with mixtures of hexane and EtOAc (10:0 to 0:10). The eluates (100 ml per fraction) were collected and examined by TLC (silica gel, hexane-EtOAc, 7:3) to yield 32 fractions. Fractions with similar chromatographic patterns were combined to yield 7 fractions: F1 (102 mg), F2 (259 mg), F3 (2.4 g), F4 (674 mg), F5 (991 mg), F6 (370 mg) and F7 (410 mg).

Fraction F4 (674 mg) was further fractionated on Sephadex LH-20 (CH_2Cl_2-MeOH, 1:1). Twenty fractions with similar chromatographic patterns (TLC, silica gel, hexane-EtOAc, 7:3) were combined to give 7 fractions: F4-1 (156 mg), F4-2 (49 mg), F4-3 (60 mg), F4-4 (71 mg), F4-5 (121 mg), F4-6 (167 mg) and F4-7 (1 mg).

Fraction F4-5 (121 mg) was purified by flash column chromatography (silica gel, No. 9385, gradient mixture of hexane-EtOAc) to give compound LMM4 as a colorless oil (8 mg) and LMM5 as a colorless oil (6 mg). They were new dihydrobenzofurans characterized as (2*R*,3*R*)-5-allyl-2-(4-hydroxyphenyl)-3-methyl-2,3-dihydrobenzofuran [**99**] and (2*R*,3*R*)-5-allyl-2-(4-hydroxyphenyl)-7-methoxy-3-methyl-2,3-dihydrobenzofuran [**100**], repectively.

3.2.2.5 Isolation of compounds LMM6 and LMM7

Fraction F5 (991 mg) was separated on a Sephadex LH-20 column (CH_2Cl_2-MeOH, 1:1). Fractions (20 fractions) were combined according to their TLC patterns (silica gel, hexane:EtOAc, 6:4) to give 5 fractions: F5-1 (140 mg), F5-2 (428 mg), F5-3 (347 mg), F5-4 (174 mg) and F5-5 (101 mg).

Purification of fraction F5-4 (174 mg) by flash column chromatography (silica gel, No. 9385, gradient mixture of hexane-EtOAc) gave 2 compounds: LMM6 as a colorless oil (63.7 mg) and LMM7 as a white amorphous powder (26.9 mg). They were characterized to be decurrenal [**101**] and a new dihydrobenzofuran neolignan, namely (2*R*,3*R*)-2-(4-hydroxyphenyl)-3-methyl-5-(2-oxopropyl)-2,3-dihydrobenzofuran [**102**], respectively.

3.3 Extraction and isolation of compounds from leaves of *Miliusa* cf. *fusca*

3.3.1 Extraction

The dried and powdered leaves of *Miliusa* cf. *fusca* (199 g) were macerated with methanol (9 x 1L) to give, after removal of the solvent, a methanol extract (40.1 g, 20.17% based on dried weight of leaves).

3.3.2 Isolation

3.3.2.1 Isolation of compounds LMF1 and LMF2

The methanol extract (40.1 g) was fractionated by vacuum liquid column chromatography using a sintered glass filter column of silica gel (No.7734, 569 g). Elution was performed using solvent mixtures of increasing polarity (hexane-CH_2Cl_2 (1:0 to 0:1), CH_2Cl_2-EtOAc (1:0 to 0:1) to EtOAc-MeOH (1:0 to 0:1)). The eluates (500 ml per fraction) were collected and examined by TLC (silica gel, CH_2Cl_2) to yield 55 fractions. Fractions with similar chromatographic patterns were combined to

yield 8 fractions: A (12 mg), B (42 mg), C (119 mg), D (352 mg), E (8.3 g), F (1.8 g), G (973 g) and H (16.1 g).

Fraction E (8.3 g) was further divided into 8 fractions. Each portion was fractionated on Sephadex LH-20 (CH_2Cl_2-MeOH, 1:1). The eluates (75 ml per fractions) were examined by TLC (TLC, silica gel, CH_2Cl_2) and combined according to their TLC patterns to afford 4 fractions: E1 (3.2 g), E2 (2.9 g), E3 (2.8 g) and E4 (13 mg).

Fraction E3 (2.8 g) was further separated by flash column chromatography (silica gel, size 0.035-0.037 mm; gradient mixture solvent of cyclohexane-EtOAc). Fractions (142 fractions) were collected and combined based on chromatographic patterns (TLC, silica gel, cyclohexane-EtOAc, 7:3) to give 14 fractions: E3-1 (121 mg), E3-2 (52 mg), E3-3 (61 mg), E3-4 (126 mg), E3-5 (967 mg), E3-6 (407 mg), E3-7 (112 mg), E3-8 (23 mg), E3-9 (69 mg), E3-10 (71 mg), E3-11 (524 mg), E3-12 (69 mg) and E3-13 (132 mg). Two new 7.O.3′,8.O.4′ neolignans were isolated from fractions E3-7 (LMF1) and E3-11 (LMF2). They were colorless oils and characterized as (7*S*,8*R*)-$\Delta^{8'}$-5-hydroxy-3,4,5′-trihydroxy-7.O.3′,8.O.4′-neolignan [**103**] and (7*S*,8*R*)-$\Delta^{8'}$-4-hydroxy-3,5,5′-trihydroxy-7.O.3′,8.O.4′-neolignan [**104**], respectively.

3.3.2.2 Isolation of compound LMF3

Fraction E3-2 (52 mg) was purified on Sephadex LH-20 (CH_2Cl_2-MeOH, 1:1). Eight fractions with similar chromatographic pattern were combined (TLC, silica gel, cyclohexane-EtOAc, 9:1) to give compound LMF3 as a colorless oil (12 mg). It was determined as 2-methoxy-4-[2-[2-methoxy-4-(2-propen-1-yl)phenoxy]propyl] phenol [**105**].

3.3.2.3 Isolation of compound LMF4

Fraction E3-4 (126 mg) was further separated on a flash column (silica gel, size 0.020-0.045 mm, cyclohexane-CH_2Cl_2, 1:9). Thirty-two fractions were combined on the basis of their TLC composition (silica gel, cyclohexane-CH_2Cl_2, 1:9) to yield 4 fractions: E3-4-1 (2 mg), E3-4-2 (38 mg), E3-4-3 (74 mg) and E3-4-4 (19 mg).

Fraction E3-4-3 (74 mg) was purified on Sephadex LH-20 column (CH_2Cl_2-MeOH, 1:1) to furnish compound LMF4 as white solid (16.8 mg), which is Licarin A [**106**].

3.3.2.4 Isolation of compound LMF5

Fraction E3-5 (967 mg) was purified by flash column chromatography (silica gel, size 0.020-0.045 mm, cyclohexane-CH_2Cl_2, 1:9) to give 2 compounds: LMF5 (366 mg) as a white solid and LMF6 (126 mg) as a colorless oil. They were characterized as a new 7.O.3′,8.O.4′ neolignan, which are (7*R*,8*R*)-$\Delta^{8'}$-4-hydroxy-3,5′-dihydroxy-7.O.3′,8.O.4′-neolignan [**107**] and eusiderin D [**108**], respectively.

3.3.2.5 Isolation of compound LMF7

Fraction F (1.8 g) was fractionated on a flash column (silica gel, size 0.020-0.045 mm, gradient mixtures of cyclohexane-acetone, 10:0 to 0:10). Forty-eight fractions were collected and combined based on chromatographic patterns (TLC, silica gel, cyclohexane-acetone, 8:2) to yield 8 fractions: F1 (428 mg), F2 (96 mg), F3 (328 mg), F4 (378 mg), F5 (71 mg), F6 (312 mg), F7 (226 mg) and F8 (146 mg).

Fraction F3 (328 mg) was re-chromatographed on a Sephadex LH-20 column (CH_2Cl_2-MeOH, 1:1). Eleven fractions with similar chromatographic patterns (TLC, silica gel, cyclohexane-acetone, 75:25) were combined to yield 3 fractions: F3-1 (59 mg), F3-2 (145 mg) and F3-3 (82 mg).

Fraction F3-3 (82 mg) was purified by flash column chromatography (silica gel, size 0.020-0.045 mm, CH_2Cl_2-EtOAc, 95:5) to give compound LMF7 as a colorless oil (28 mg). This compound was identified as (7*S*,8*R*)-*erythro*-7-hydroxy-3,4,3′-trimethoxy-$\Delta^{1,3,5,1',3',5',8'}$-8.O.4′-neolignan [**109**].

3.3.2.6 Isolation of compound LMF8

Fraction G (973 mg) was separated on a flash column (silica gel, size 0.020-0.045 mm, gradient mixture solvent of CH_2Cl_2-MeOH). Fractions (63 fractions) with similar chromatographic patterns (TLC, silica gel, CH_2Cl_2-MeOH, 9:1) were combined to give 7 fractions: G1 (369 mg), G2 (26 mg), G3 (29 mg), G4 (190 mg), G5 (97 mg), G6 (23 mg) and G7 (73 mg).

Fraction G4 (190 mg) was further purified on a Sephadex LH-20 column and eluted with MeOH to give compound LMF8 as a white amorphous powder (140 mg). It was identified as (–)-epicatechin **[91]**.

3.4 Extraction and isolation of compounds from stem of *Miliusa* cf. *fusca*

3.4.1 Extraction

The dried and powdered stems of *Miliusa* cf. *fusca* (1.2 kg) were macerated with methanol (3 x 4L) to give, after removal of the solvent, a methanol extract (99.3 g, 8.27% based on dried weight of stem).

3.4.2 Isolation

3.4.2.1 Isolation of compound SMF1

The methanol extract (99.3 g) was fractionated by vacuum liquid column chromatography using a sintered glass filter column of silica gel (No.7734, 570 g). Elution was performed using solvent mixtures of increasing polarity (hexane-EtOAc (1:0 to 0:1) to EtOAc-MeOH (1:0 to 0:1)). The eluates (500 ml per fraction) were collected and examined by TLC (silica gel, hexane-EtOAc, 1:1) to yield 41 fractions. Fractions with similar chromatographic patterns were combined to yield 7 fractions: A (61.2 mg), B (1.2 g), C (2.6 g), D (6.6 g), E (1.9 g), F (4.8 g) and G (68.1 g).

Fraction D (6.6 g) was repeatedly separated on a flash column (silica gel, sixe 0.020-0.045 mm, gradient mixtures of cyclohexane-EtOAc). Fractions (227 fractions) were combined on the basis of their TLC composition (silica gel, cyclohexane-EtOAc, 8:2) to yield 15 fractions: D1 (174 mg), D2 (72 mg), D3 (474 mg), D4 (896 mg), D5 (1.2 g), D6 (702 mg), D7 (320 mg), D8 (660 mg), D9 (510 mg), D10 (144 mg), D11 (140 mg), D12 (454 mg), D13 (279 mg), D14 (103 mg) and D15 (147 mg).

Fraction D2 (72 mg) was further purified on a Sephadex LH-20 column (CH_2Cl_2-MeOH, 1:1) to furnish compound SMF1 as a colorless oil (38.4 mg), which is characterized as 2-(4-allyl-2,6-dimethoxyphenoxy)-1-(3,4-dimethoxyphenyl) propane [**110**].

3.4.2.2 Isolation of compounds SMF2 and SMF3

Fraction D4 (896 mg) was purified by flash column chromatography (silica gel, size 0.020-0.045 mm, cyclohexane-EtOAc, 98:2) to give 2 colorless oily compounds: SMF2 (87 mg) and SMF3 (291 mg). They were identified as (7*R*,8*R*)-$\Delta^{8'}$-3,4,5′-trimethoxy-7-O-3′,8-O-4′-neolignan [**111**] and 3,4,5,4′,5′-pentamethoxy-3′,β-epoxy-γ,2′-neolign-8′-ene [**112**], respectively.

3.4.2.3 Isolation of compounds SMF4, SMF5, SMF6 and SMF7

Fraction D5 (1.2 g) was purified on a silica gel (size 0.020-0.045 mm) column, eluted with gradient mixture of cyclohexane-EtOAc to give 4 colorless oily compounds: SMF4 (32 mg), SMF5 (310 mg), SMF6 (58 mg) and SMF7 (46 mg). They were identified as (7*R*,8*R*)-$\Delta^{8'}$-4-hydroxy-3,5′-dimethoxy-7.O.3′,8.O.4′-neolignan [**107**], eusiderin D [**108**], (7*S*,8*S*)-$\Delta^{8'}$-3,4,5,5′-tetramethoxy-7.O.3′,8.O.4′-neolignan [**113**] and virolongin B [**114**], respectively.

3.4.2.4 Isolation of compound SMF8

Fraction D6 (702 mg) was re-chromatographed on silica gel (size 0.020-0.045 mm, gradient mixture of CH_2Cl_2-EtOAc) to afford compound SMF8 as a colorless oil (347 mg). This compound was determined as eusiderin C [**115**].

3.4.2.5 Isolation of compounds SMF9 and SMF10

Fraction D8 (660 mg) was fractionated on Sephadex LH-20 with CH_2Cl_2-MeOH (1:1). Eleven fractions with similar chromatographic patterns were combined (TLC, silica gel, cyclohexane-EtOAc, 7:3) to give 4 fractions: D8-1 (7 mg), D8-2 (532 mg), D8-3 (4 mg) and D8-4 (3 mg).

Fraction D8-2 (532 mg) was further separated on a flash column (silica gel, sixe 0.020-0.045 mm, cyclohexane-EtOAc, 96:4) to give SMF9 (205 mg) and SMF10 (50 mg), which were identified as (+)-veraguensin [**116**] and (7*S*,8*S*, 7′*R*, 8′*S*)-3,4,5,3′,4′-Pentamethoxy-7,7′-epoxylignan [**117**], respectively.

3.4.2.6 Isolation of compound SMF11

Fraction D12 (454 mg) was separated on a flash column (silica gel, size 0.020-0.0045 mm) using mixture solvent of CH_2Cl_2-EtOAc (95:5) as the eluent. Twenty-nine fractions were combined on the basis of their TLC patterns (silica gel, CH_2Cl_2-EtOAc, 95:5) to yield 6 fractions: D12-1 (118 mg), D12-2 (10 mg), D12-3 (86 mg), D12-4 (92 mg), D12-5 (100 mg) and D12-6 (20 mg). Fraction D12-1 (SMF11), a solid after solvent evaporation, was identified as (7*S*,8*R*)-$\Delta^{8'}$-4-hydroxy-3,5,5′-trimethoxy-7.O.3′,8.O.4′-neolignan [**104**].

3.4.2.7 Isolation of compound SMF12

Fraction D12-5 (100 mg) was purified on a flash column (silica gel, size 0.020-0.045 mm, gradient mixture of CH_2Cl_2-EtOAc) to give SMF12 as a colorless

oil (58 mg). It was determined as a new tetrahydrofuran lignan, which characterized as *rel*-(7*S*,8*S*,7′*R*,8′*S*)-5-hydroxy-3,4,3′,4′-tetramethoxy-7,7′-epoxylignan [**118**].

3.4.2.8 Isolation of compound SMF13

Fraction E (1.9 g) was fractionated on Sephadex LH20 (MeOH). The eluates (60 ml per fractions) were examined by TLC (TLC, silica gel, CH_2Cl_2-MeOH, 9:1) and combined according to their TLC patterns to afford 6 fractions: E1 (193 mg), E2 (609 mg), E3 (398.2 mg), E4 (17 mg), E5 (79 mg) and E6 (579 mg).

Fraction E2 (609 mg) was separated on a flash column (silica gel, size 0.020-0.045 mm, gradient mixtures of CH_2Cl_2-EtOAc) to furnish compound SMF13 as a colorless oil (7 mg). This was a new 8.O.4′-neolignan, which was determined as $\Delta^{7'}$-9′-Hydroxy-4,5,3′,5′-tetramethoxy-8.O.4′-neolignan [**119**].

3.4.2.9 Isolation of compound SMF14

Fraction E6 (579 mg) was repeatedly fractionated by flash column chromatography (silica gel, size 0.020-0.045 mm; gradient mixture solvent of CH_2Cl_2-MeOH). Thirty fractions were collected and combined based on chromatographic patterns (TLC, silica gel, CH_2Cl_2-MeOH, 8:2) to give 4 fractions: E6-1 (82 mg), E6-2 (80 mg), E6-3 (37 mg) and E3-4 (265 mg).

Fraction E6-2 (80.0 mg) was purified on a Sephadex LH-20 column (MeOH) to afford compound SMF14 (47.1 mg), which was identified as (–)-epicatechin [**91**].

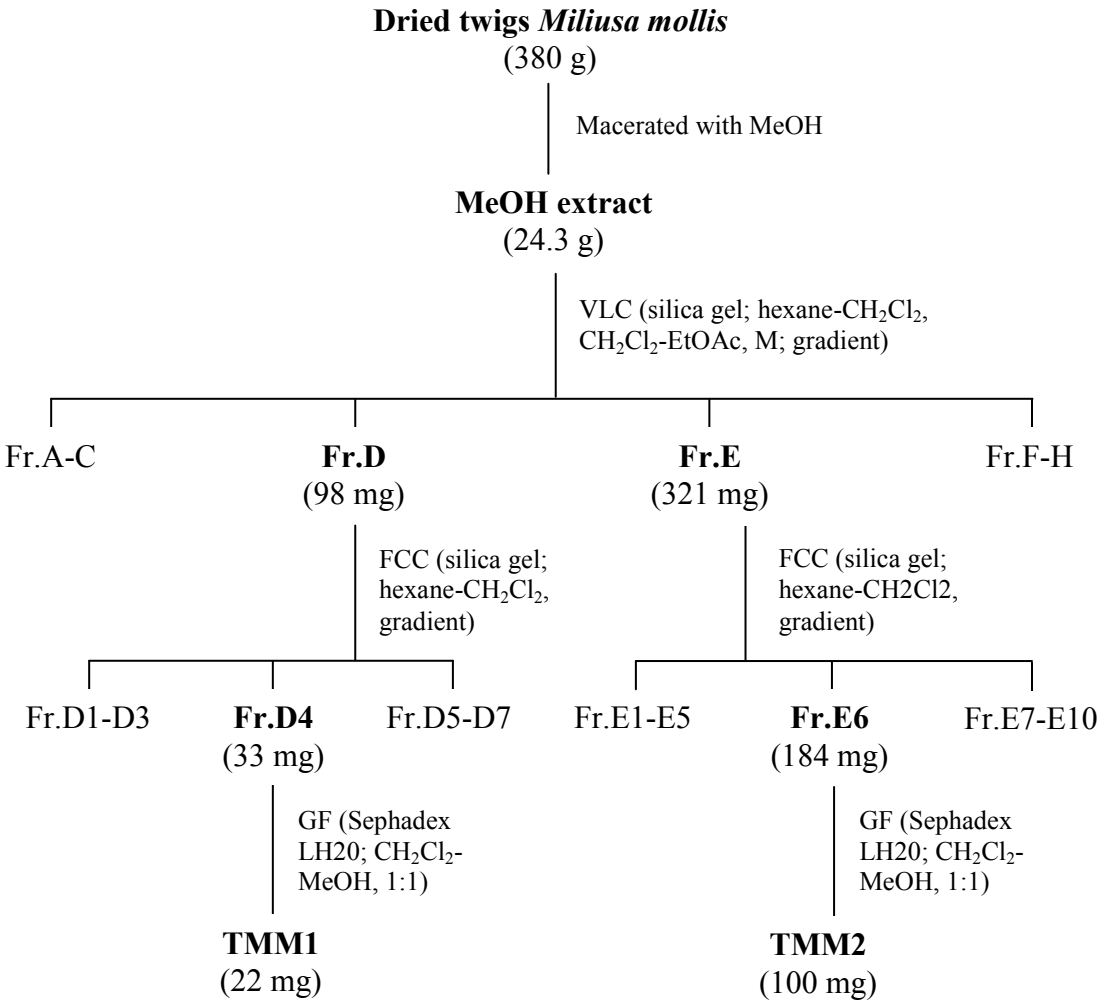

Scheme 1 Extraction and chromatographic separation of *M. mollis* twigs

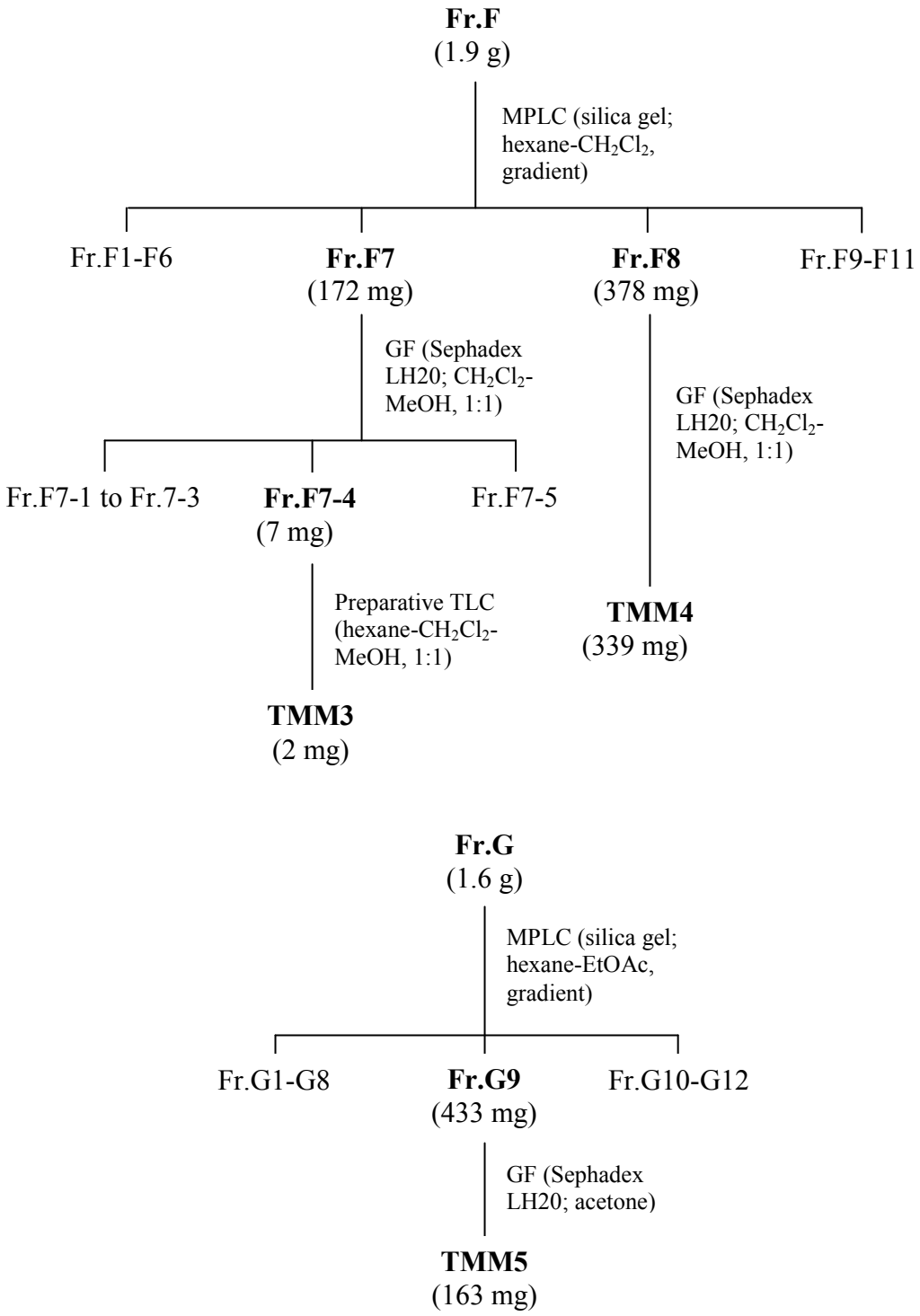

Scheme 1 Extraction and chromatographic separation of *M. mollis* twigs (continued)

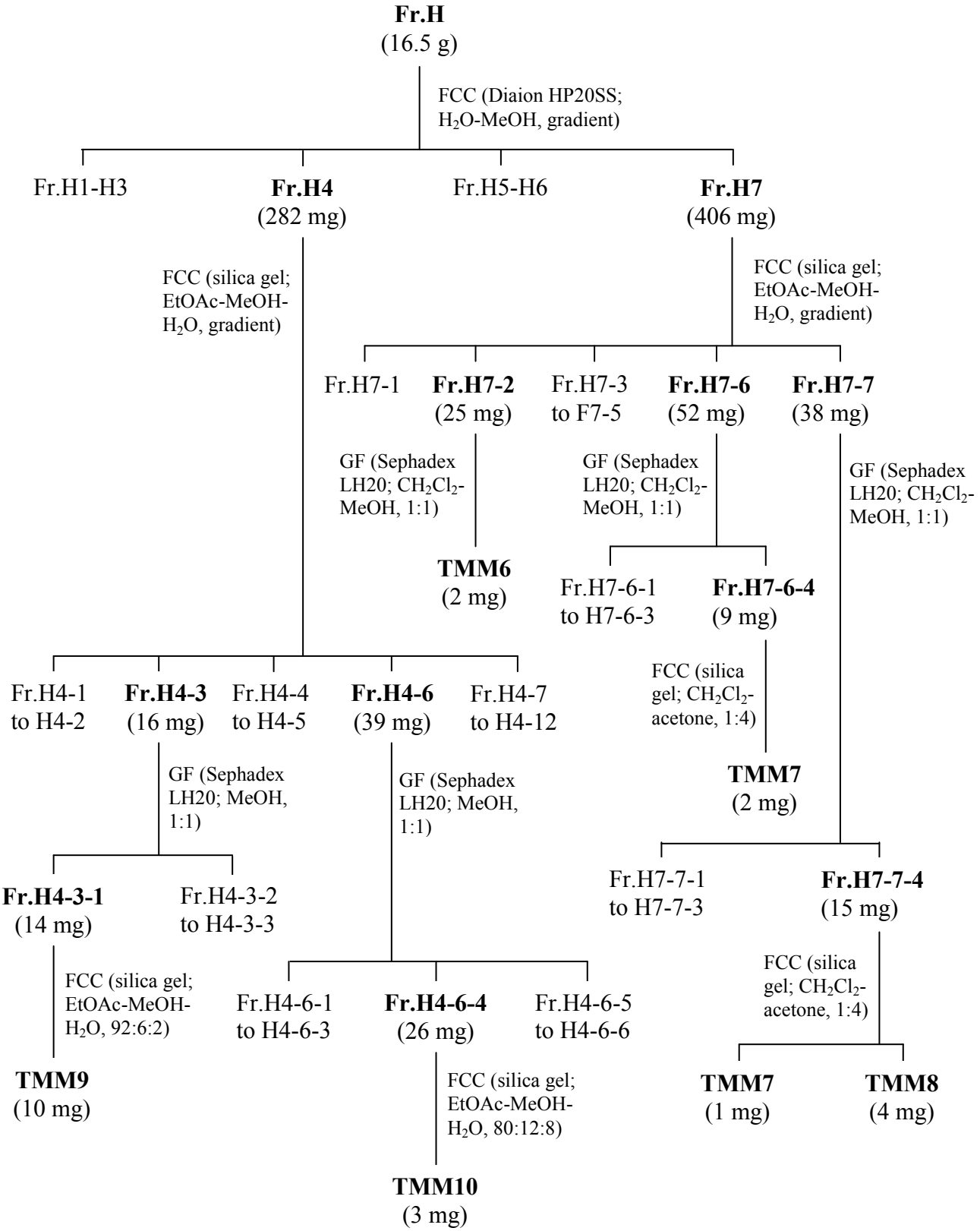

Scheme 1 Extraction and chromatographic separation of *M. mollis* twigs (continued)

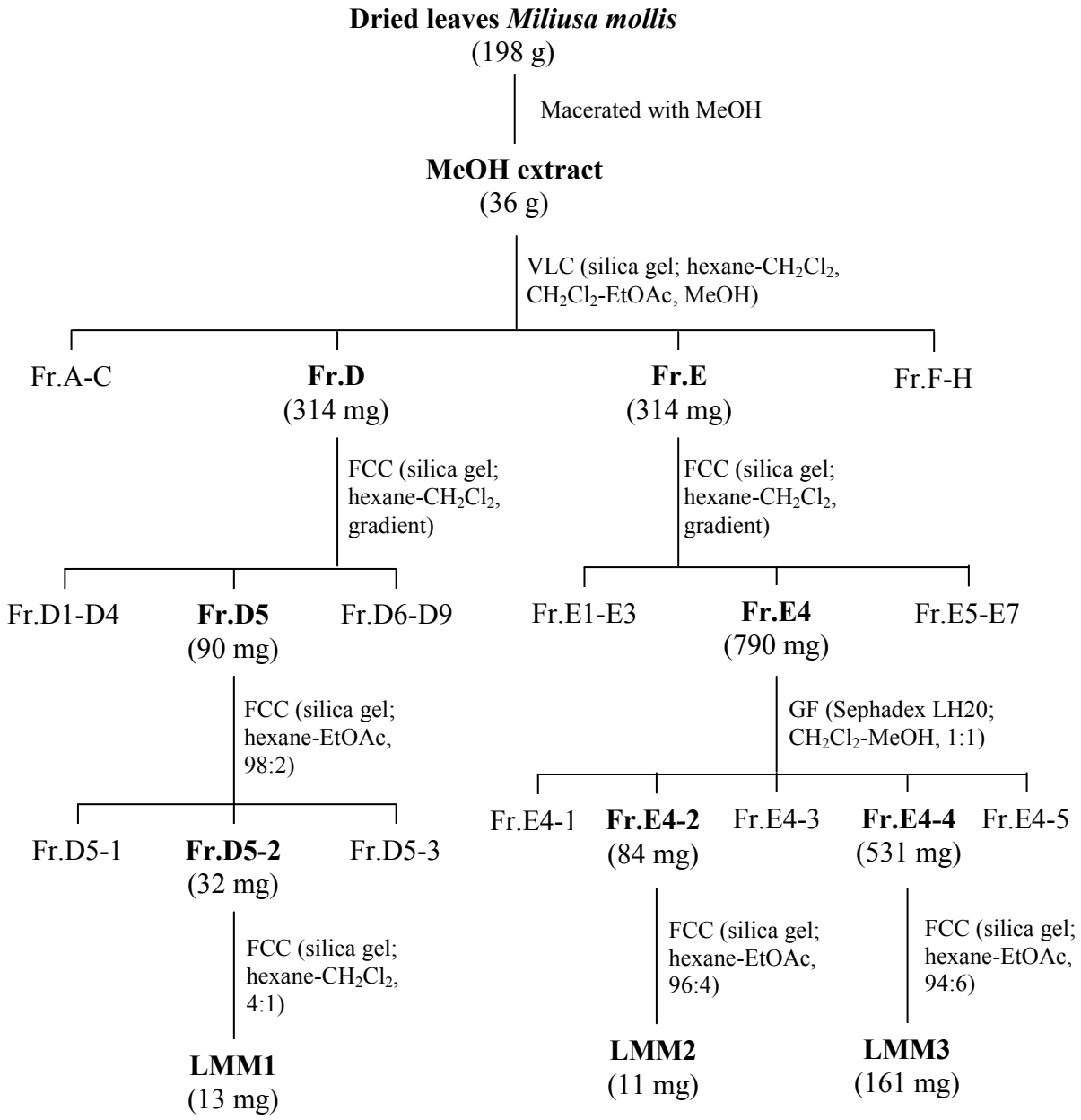

Scheme 2 Extraction and chromatographic separation of *M. mollis* leaves

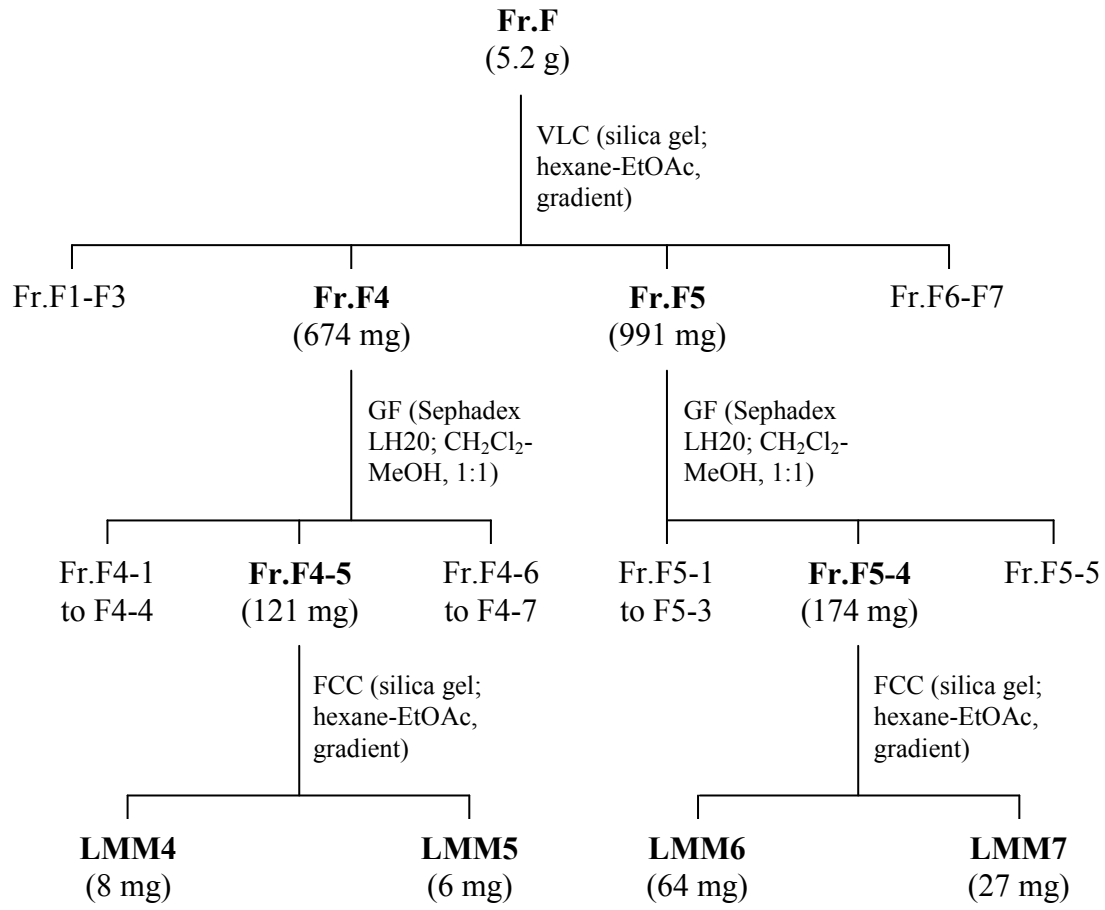

Scheme 2 Extraction and chromatographic separation of *M. mollis* leaves (continued)

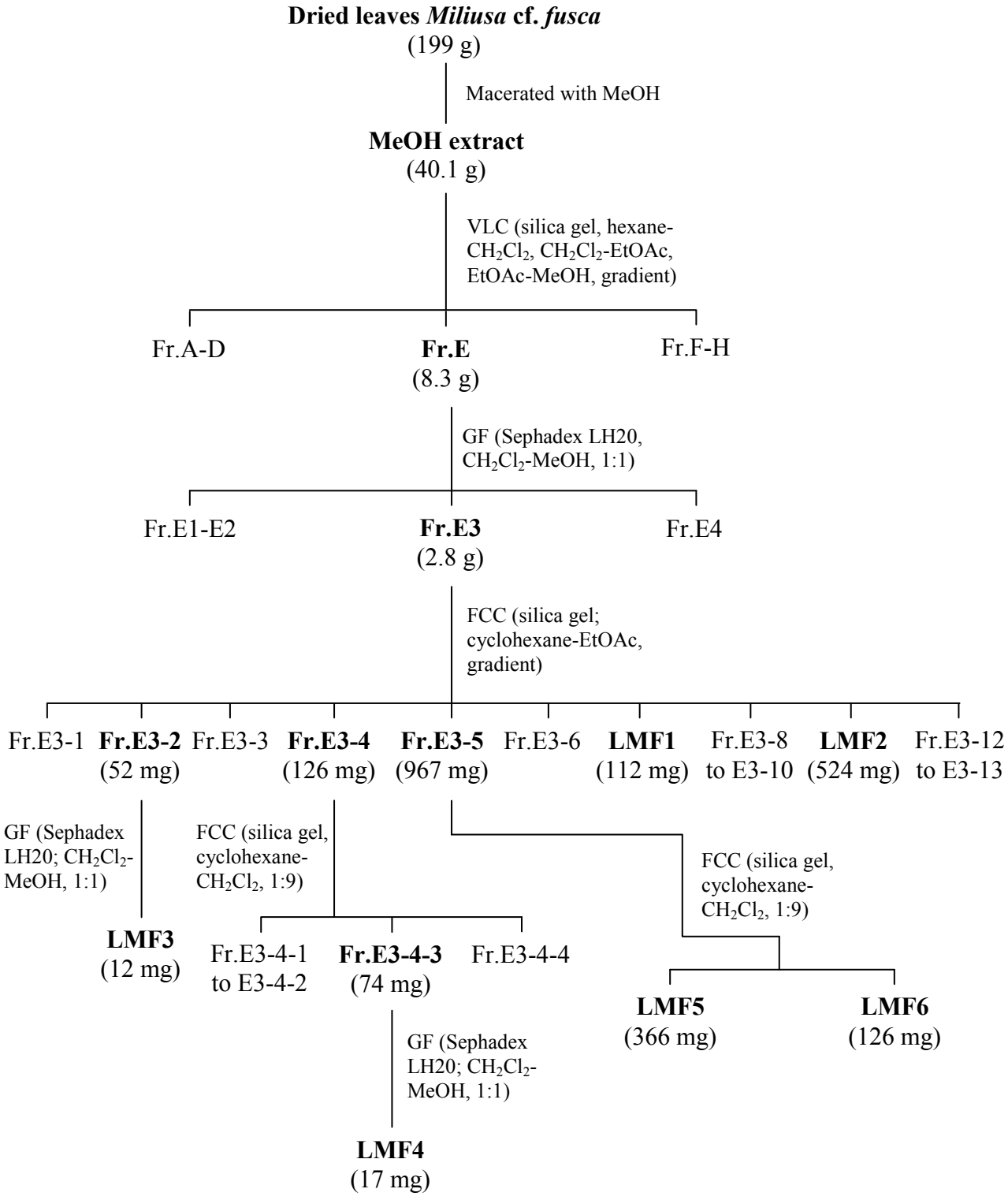

Scheme 3 Extraction and chromatographic separation of *M.* cf. *fusca* leaves

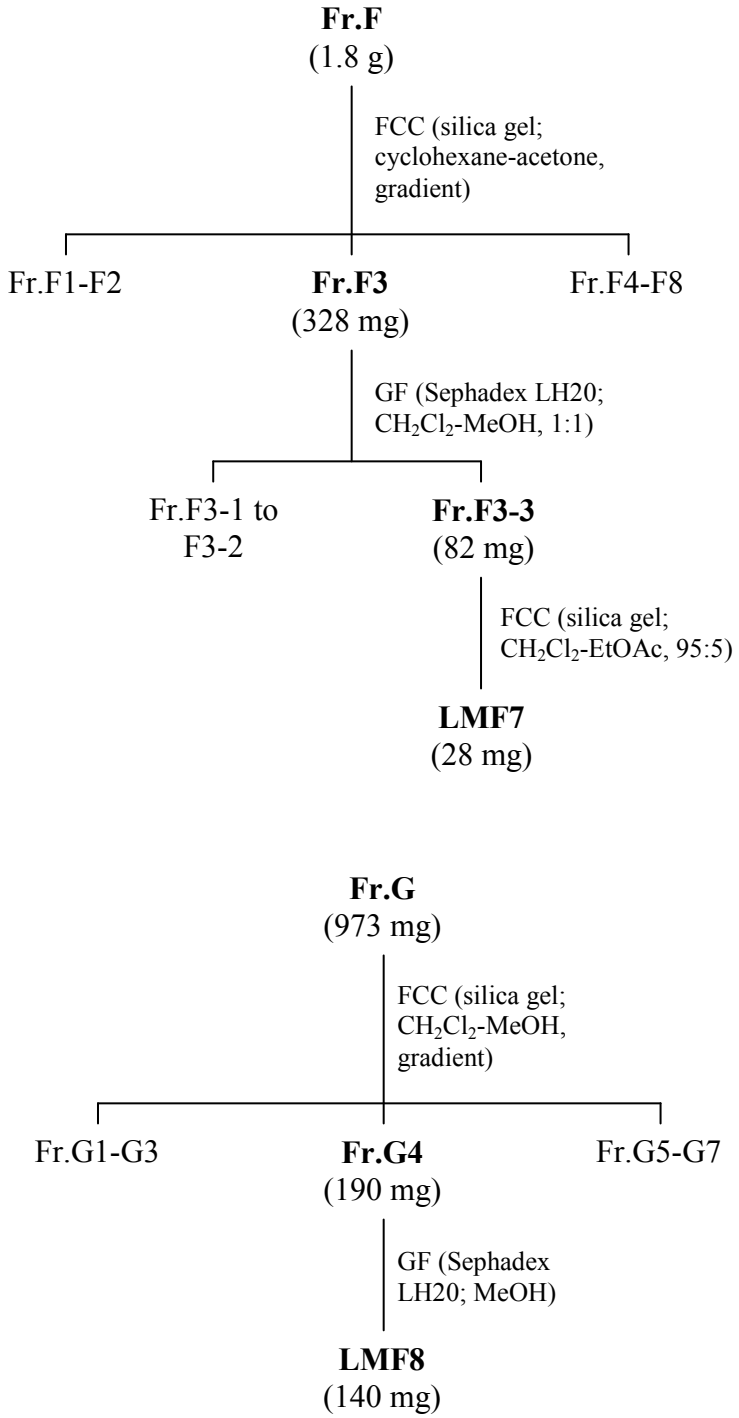

Scheme 3 Extraction and chromatographic separation of *M.* cf. *fusca* leaves (continued)

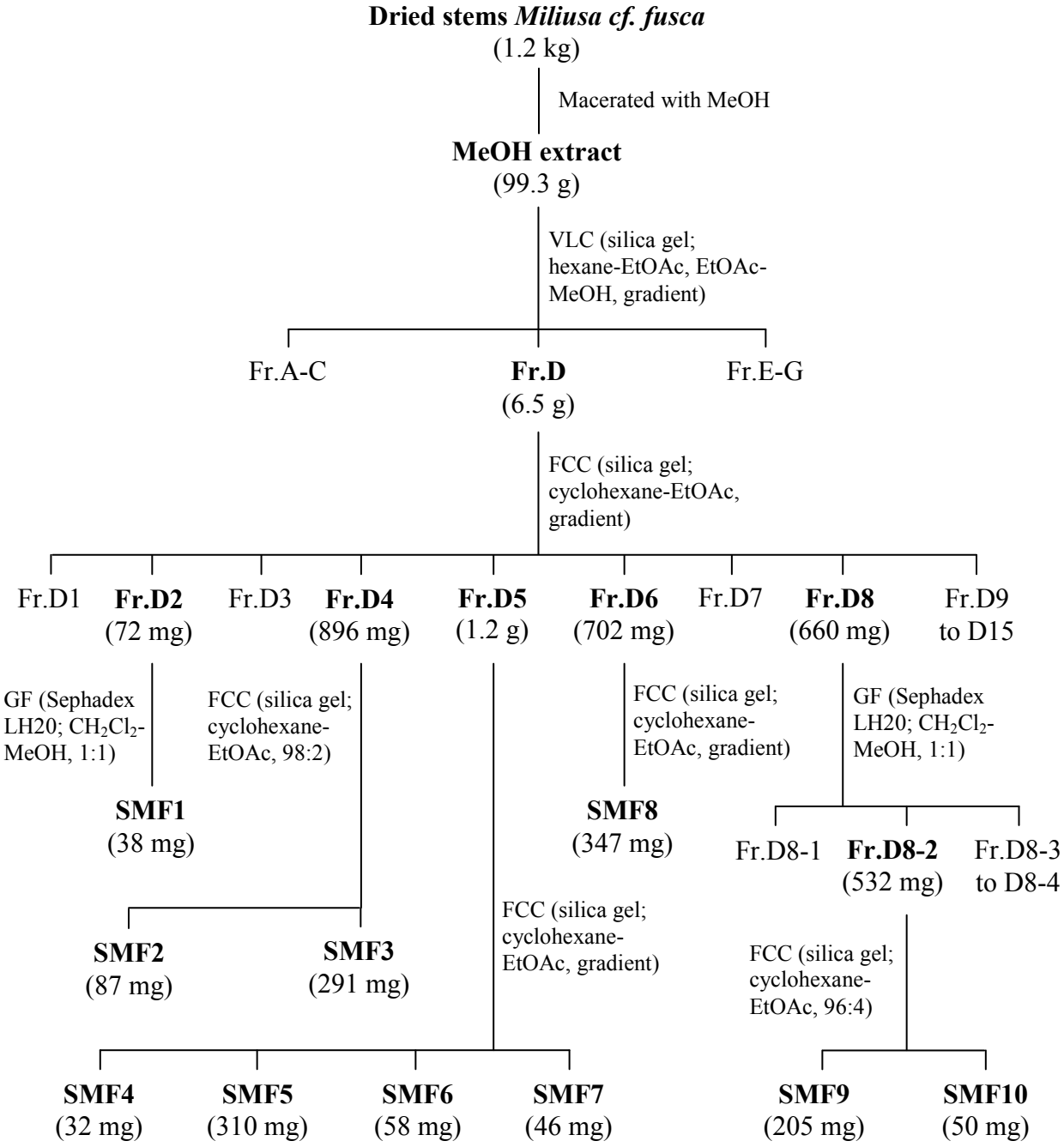

Scheme 4 Extraction and chromatographic separation of *M.* cf. *fusca* stems

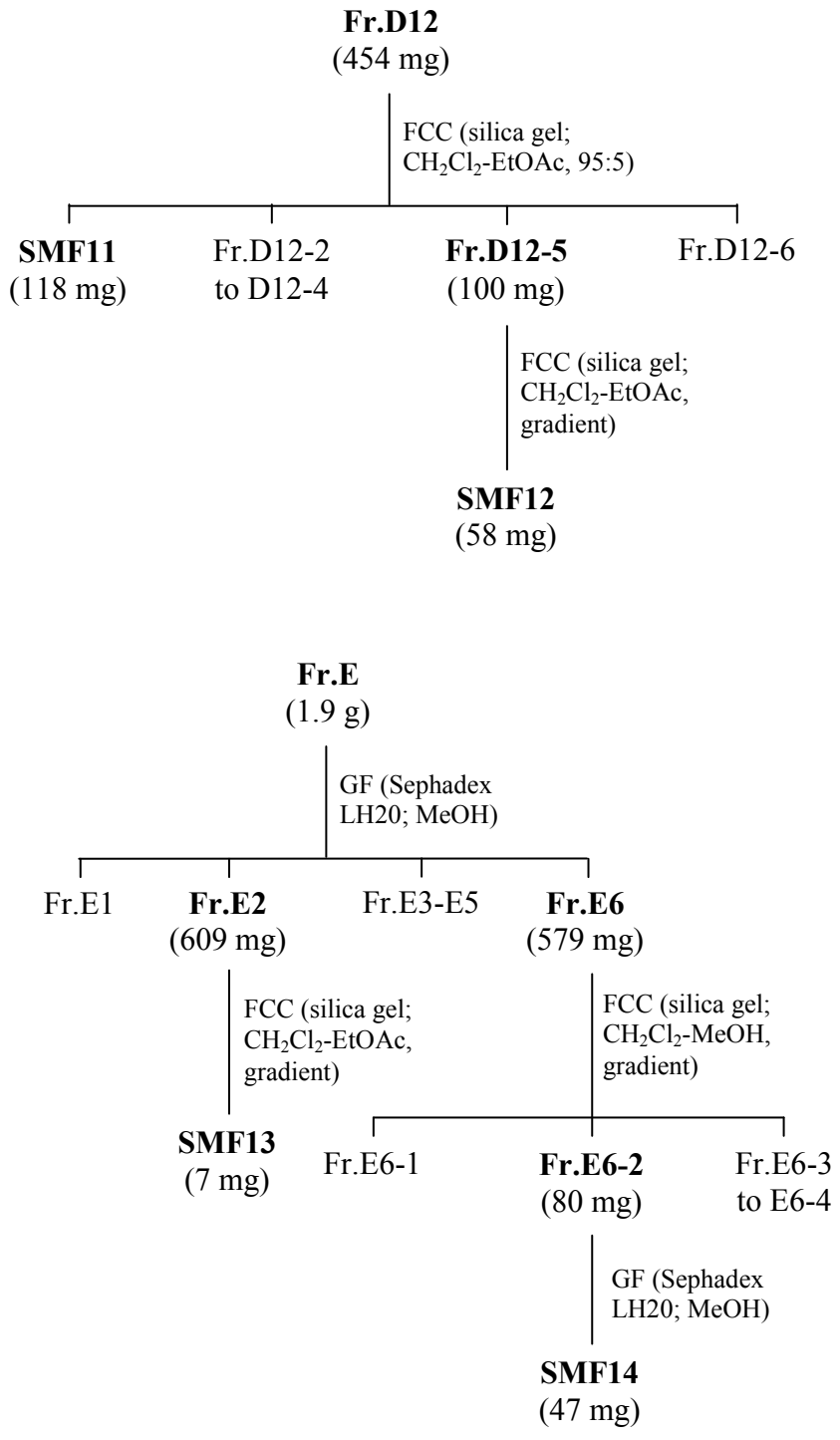

Scheme 4 Extraction and chromatographic separation of *M.* cf. *fusca* stems (continued)

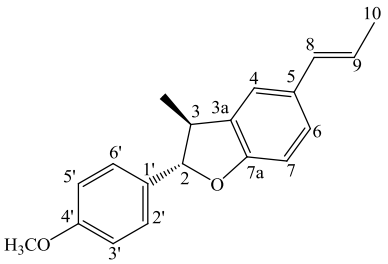

TMM1 (2*S*,3*S*)-2,3-dihydro-2-(4-methoxyphenyl)-3-methyl-5-(*E*)-propenylbenzo furan [**87**]

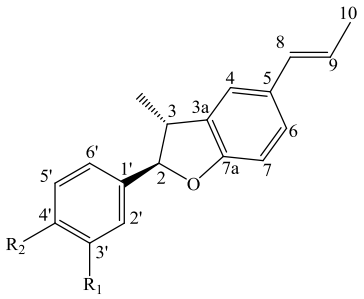

TMM2 (2*R*,3*R*)-2,3-dihydro-2-(4-hydroxy-3-methoxyphenyl)-3-methyl-5-(*E*)-propenylbenzofuran [**88**]; $R_1 = OCH_3$, $R_2 = OH$

TMM4 conocarpan [**90**]; $R_1 = H$, $R_2 = OH$

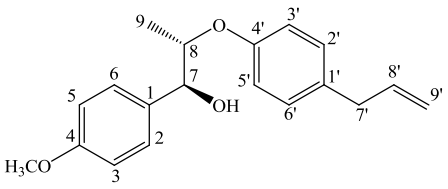

TMM3 (7*S*,8*S*)- *threo*-$\Delta^{8'}$-4-methoxy-8.O.4′-neolignan [**89**]

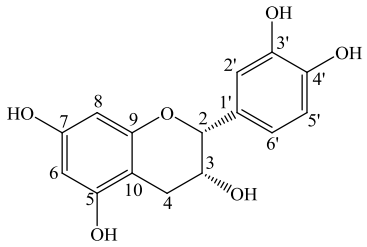

TMM5 (−)-epicatechin [**91**]

Figure 8 Structures of compounds isolated from the twigs of *M. mollis*

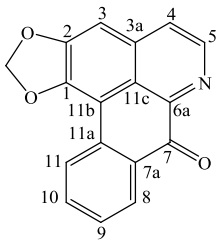

TMM6 liriodenine [**34**]

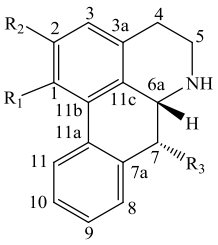

TMM7 asimilobine [**92**]

$R_1 = OCH_3$; $R_2 = OH$; $R_3 = H$

TMM8 (–)-norushinsunine [**93**]

R_1-$R_2 = OCH_2O$; $R_3 = OH$

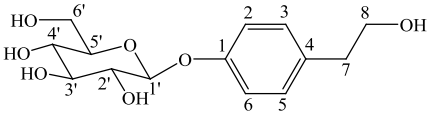

TMM9 icariside D_2 [**94**]

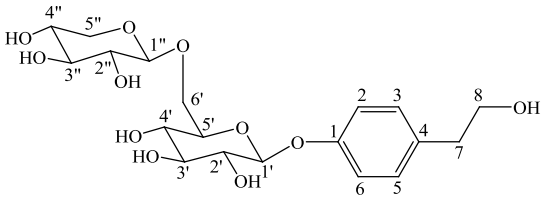

TMM10 tyrosol-1-*O*-*β*-xylopyranosyl-(1→6)-*O*-*β*-glucopyranoside [**95**]

Figure 8 Structures of compounds isolated from the twigs of *M. mollis* (continued)

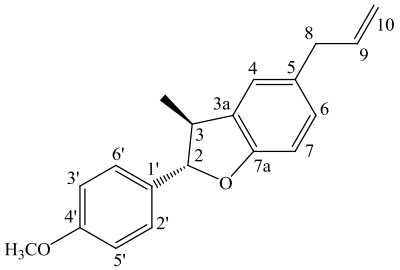

LMM1 (2*S*,3*S*)-5-allyl-2-(4-methoxyphenyl) -3-methyl-2,3-dihydrobenzofuran [**96**]

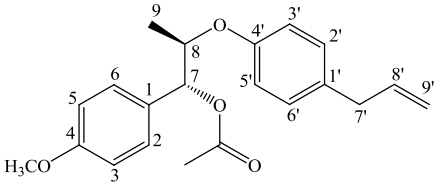

LMM2 (7*R*,8*R*)-*threo* $\Delta^{8'}$-7-acetoxy-4-methoxy-8.O.4′-neolignan [**97**]

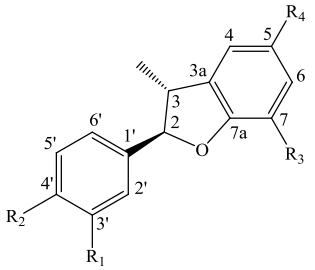

LMM3 (2*R*,3*R*)-5-allyl-2-(4-hydroxy-3-methoxyphenyl)-3-methyl-2,3-dihydro-benzofuran [**98**]

$R_1 = OCH_3$; $R_2 = OH$; $R_3 = H$; $R_4 = CH_2\text{-}CH{=}CH_2$

LMM4 (2*R*,3*R*)-5-allyl-2-(4-hydroxyphenyl)-3-methyl-2,3-dihydrobenzofuran [**99**]

$R_1 = H$; $R_2 = OH$; $R_3 = H$; $R_4 = CH_2\text{-}CH{=}CH_2$

LMM5 (2*R*,3*R*)-5-allyl-2-(4-hydroxyphenyl)-7-methoxy-3-methyl-2,3-dihydrobenzo-furan [**100**]; $R_1 = H$; $R_2 = OH$; $R_3 = OCH_3$; $R_4 = CH_2\text{-}CH{=}CH_2$

LMM6 decurrenal [**101**]; $R_1 = H$; $R_2 = OH$; R3 = H; $R_4 = CHO$

LMM7 (2*R*,3*R*)-2-(4-hydroxyphenyl)-3-methyl-5-(2-oxopropyl)-2,3-dihydrobenzo-furan [**102**]; $R_1 = H$; $R_2 = OH$; $R_3 = H$; $R_4 = CH_2\text{-}CO\text{-}CH_3$

Figure 9 Structures of compounds isolated from the leaves of *M. mollis*

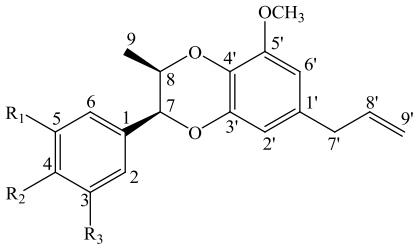

LMF1 (7*S*,8*R*)-$\Delta^{8'}$-5-hydroxy-3,4,5′-trimethoxy-7.O.3′,8.O.4′-neolignan [**103**]

R_1 = OH, R_2 = OCH_3, R_3 = OCH_3

LMF2 (7*S*,8*R*)-$\Delta^{8'}$-4-hydroxy-3,5,5′-trimethoxy-7.O.3′,8.O.4′-neolignan [**104**]

R_1 = OCH_3, R_2 = OH, R_3 = OCH_3

LMF6 eusiderin D [**108**]; R_1 = H, R_2 = OCH_3, R_3 = OCH_3

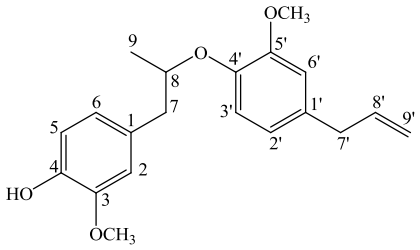

LMF3 2-methoxy-4-[2-[2-methoxy-4-(2-propen-1-yl)phenoxy]propyl]phenol [**105**]

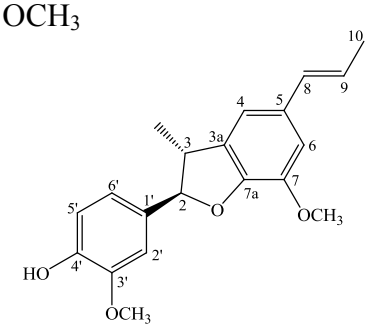

LMF4 licarin A [**106**]

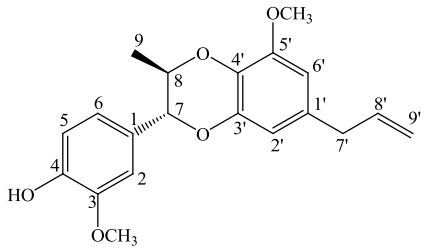

LMF5 (7*R*,8*R*)-$\Delta^{8'}$-4-hydroxy-3,5′-dimethoxy-7.O.3′,8.O.4′-neolignan [**107**]

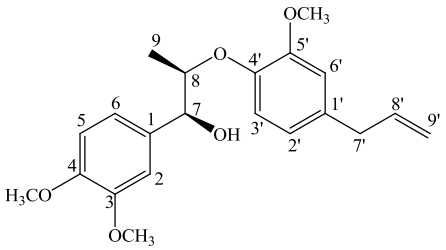

LMF7 (7*S*,8*R*)-*erythro*-7-hydroxy-3,4,3′-trimethoxy-$\Delta^{1,3,5,1',3',5',8'}$-8.O.4′-neolignan [**109**]

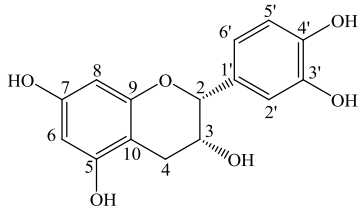

LMF8 (–)-epicatechin [**91**]

Figure 10 Structures of compounds isolated from the leaves of *M.* cf. *fusca*

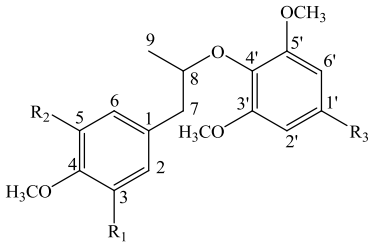

SMF1 2-(4-allyl-2,6-dimethoxyphenoxy)-1-(3,4-dimethoxyphenyl)propane [**110**]

$R_1 = CH_3O$, $R_2 = H$, $R_3 = CH\text{-}CH{=}CH_2$

SMF7 virolongin B [**114**]; $R_1 = CH_3O$, $R_2 = CH_3O$, $R_3 = CH_2\text{-}CH{=}CH_2$

SMF13 $\Delta^{7'}$-9′-hydroxy-4,5,3′,5′-tetramethoxy-8.O.4′-neolignan [**119**]

$R_1 = CH_3O$, $R_2 = H$, $R_3 = CH{=}CH\text{-}CH_2OH$

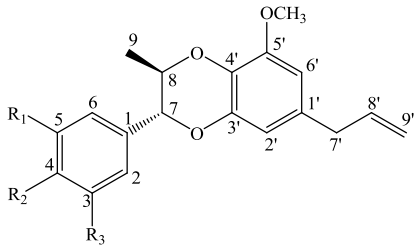

SMF2 (7*R*,8*R*)-$\Delta^{8'}$-3,4,5′-trimethoxy-7.O.3′,8.O.4′-neolignan [**111**]

$R_1 = H$, $R_2 = OCH_3$, $R_3 = OCH_3$

SMF4 (7*R*,8*R*)-$\Delta^{8'}$-4-hydroxy-3,5′-dimethoxy-7.O.3′,8.O.4′-neolignan [**107**]

$R_1 = H$, $R_2 = OH$, $R_3 = OCH_3$

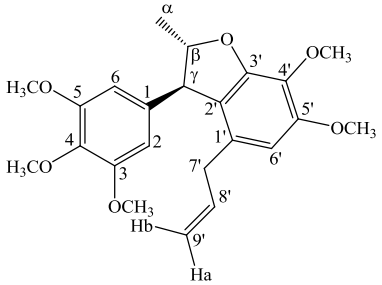

SMF3 3,4,5,4′,5′-pentamethoxy-3′,β-epoxy-γ,2′-neolign-8′-ene [**112**]

Figure 11 Structures of compounds isolated from the stem of *M.* cf. *fusca*

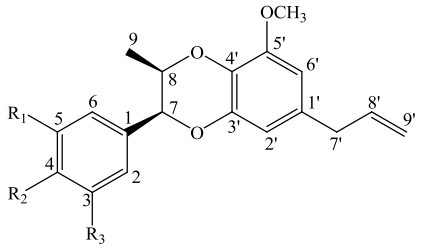

SMF5 eusiderin D [**108**]; R_1 = H, R_2 = OCH_3, R_3 = OCH_3

SMF8 eusiderin C [**115**]; R_1 = OCH_3, R_2 = OCH_3, R_3 = OCH_3

SMF11 (7*S*,8*R*)-$\Delta^{8'}$-4-hydroxy-3,5,5′-trimethoxy-7.O.3′,8.O.4′-neolignan [**104**]

R_1 = OCH_3, R_2 = OH, R_3 = OCH_3

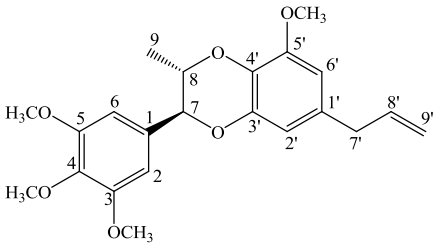

SMF6 (7*S*,8*S*)-$\Delta^{8'}$-3,4,5,5′-tetramethoxy-7.O.3′,8.O.4′-neolignan [**113**]

R_1 = OCH_3, R_2 = OCH_3, R_3 = OCH_3

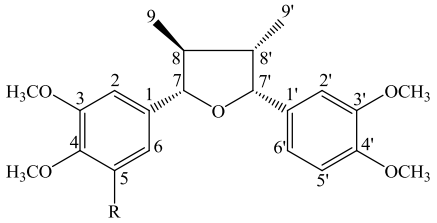

SMF9 (+)-veraguensin [**116**]; R = H

SMF10 (7*S*,8*S*, 7′*R*, 8′*S*)-3,4,5,3′,4′-pentamethoxy-7,7′-epoxylignan [**117**]; R = OCH_3

SMF12 *rel*-(7*S*,8*S*,7′*R*,8′*S*)-5-hydroxy-3,4,3′,4′-tetramethoxy-7,7′-epoxylignan [**118**]; R = OH

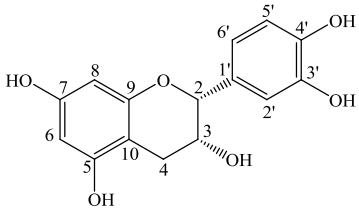

SMF14 (−)-epicatechin [**91**]

Figure 11 Structures of compounds isolated from the stem of *M.* cf. *fusca* (continued)

4. Physical and spectral data of isolated compounds

4.1 Compound TMM1

Compound TMM1 was obtained as a colorless oil, soluble in CH_2Cl_2 (22 mg, 5.79 x 10^{-3} % based on dried weight of twigs).

HRESIMS : $[M+Na]^+$ at *m/z* 303.1280 (calcd. for $C_{19}H_{20}O_2Na$, 303.1361); Figure 12

UV : λ_{max} (MeOH) nm (log ε) 228 (3.76), 274 (3.26) nm; Figure 13

IR : υ_{max} (film) 2962, 2931, 2837, 1515, 1486, 1243 cm^{-1}; Figure 14

[α] $_D^{20}$: –13.22 (*c* 0.42 g/100 ml, MeOH)

CD : $[\theta]_{300}$ –401, $[\theta]_{264}$ –2,296, $[\theta]_{226}$ +1,791; (*c* 0.001 M, MeOH); Figure 21

^{1}H MMR : δ ppm, 300 MHz, in $CDCl_3$; see Table 7, Figure 15

^{13}C MMR : δ ppm, 75 MHz, in $CDCl_3$; see Table 7, Figure 16

4.2 Compound TMM2

Compound TMM2 was obtained as a white amorphous solid, soluble in CH_2Cl_2 (100 mg, 2.64 x 10^{-2} % based on dried weight of twigs).

EIMS : *m/z* (% relative intensity); Figure 22
296 ($[M]^+$, 100), 281 (51), 267 (6), 253 (23), 171 (7), 159 (3), 151 (16), 150 (7), 137 (11), 131 (9), 115 (10), 103 (4), 91 (8).

UV : λ_{max} (MeOH) nm (log ε) 222 (3.91), 267 (3.88) nm; Figure 23

[α] $_D^{20}$: +18.39 (*c* 0.35 g/100 ml, MeOH)

CD : $[\theta]_{304}$ +187, $[\theta]_{260}$ +3,635, $[\theta]_{228}$ –3,676; (*c* 0.005 M, MeOH); Figure 21

^{1}H MMR : δ ppm, 300 MHz, in $CDCl_3$; see Table 8, Figure 24

^{13}C MMR : δ ppm, 75 MHz, in $CDCl_3$; see Table 8, Figure 25

4.3 Compound TMM3

Compound TMM3 was obtained as a colorless oil, soluble in CH_2Cl_2 (2 mg, 6.58 x 10^{-4} % based on dried weight of twigs).

HRESIMS : $[M+Na]^+$ at *m/z* 321.1375 (calcd. for $C_{19}H_{22}O_3Na$, 321.1468); Figure 27

UV : λ_{max} (MeOH) nm (log ε) 227 (4.18), 275 (3.48) nm; Figure 28

IR : υ_{max}(film) 3448(br), 1509, 1243 cm^{-1}; Figure 29

[α] $^{20}_{D}$: +10.0 (*c* 0.05 g/100 ml, MeOH)

CD : $[\theta]_{276}$ −2,220, $[\theta]_{244}$ −1,128, $[\theta]_{233}$ +2,933, $[\theta]_{228}$ +5,927; (*c* 0.002 M, MeOH); Figure 36

^{1}H MMR : δ ppm, 300 MHz, in $CDCl_3$; see Table 9, Figure 30

^{13}C MMR : δ ppm, 75 MHz, in $CDCl_3$; see Table 9, Figure 31

4.4 Compound TMM4

Compound TMM4 was obtained as a white amorphous solid, soluble in CH_2Cl_2 (339 mg, 8.92 x 10^{-2} % based on dried weight of twigs).

EIMS : *m/z* (% relative intensity); Figure 37

266 ($[M]^+$, 100), 265 (9), 251 (43), 237 (9), 223 (25), 171 (6), 159 (3), 131 (13), 121 (22), 119 (5), 107 (6), 77 (8)

UV : λ_{max} (MeOH) nm (log ε) 223 (4.23), 264 (4.22); Figure 38

[α] $^{20}_{D}$: +65.28 (*c* 0.36 g/100 ml, MeOH)

CD : $[\theta]_{324}$ +542, $[\theta]_{264}$ +3,560, $[\theta]_{226}$ −1,945; (*c* 0.001 M, MeOH); Figure 21

^{1}H MMR : δ ppm, 300 MHz, in $CDCl_3$; see Table 10, Figure 39

^{13}C MMR : δ ppm, 75 MHz, in $CDCl_3$; see Table 10, Figure 40

4.5 Compound TMM5

Compound TMM5 was obtained as a white amorphous powder, soluble in acetone or MeOH (163 mg, 4.28 x 10^{-2} % based on dried weight of twigs).

EIMS : *m/z* (% relative intensity); Figure 42

290 ($[M]^+$, 18), 167 (13), 152 (32), 149 (21), 139 (100), 124 (74), 123 (57), 111 (15)

UV : λ_{max} (MeOH) nm (log ε) 225 (4.19), 280 (3.60) nm; Figure 43

[α] $^{20}_{D}$: −51.18 (*c* 0.03 g/100 ml, MeOH)

^{1}H MMR : δ ppm, 300 MHz, in $CDCl_3$; see Table 11, Figure 44

^{13}C MMR : δ ppm, 75 MHz, in $CDCl_3$; see Table11, Figure 45

4.6 Compound TMM6

Compound TMM6 was obtained as a yellow amorphous powder, soluble in CH_2Cl_2 (2 mg, 6.32 x 10^{-4} % based on dried weight of twigs).

EIMS : *m/z* (% relative intensity); Figure 47
275 ($[M]^+$, 100), 247 (34), 246 (30), 219 (25), 217 (6), 189 (23), 188 (31), 162 (16).

UV : λ_{max} (EtOH) nm (log ε) 248 (4.43), 268 (4.36), 306 (3.90), 411 (4.02) nm; Figure 48

^{1}H MMR : δ ppm, 300 MHz, in $CDCl_3$; see Table 12, Figure 49

^{13}C MMR : δ ppm, 75 MHz, in $CDCl_3$; see Table12, Figure 50

4.7 Compound TMM7

Compound TMM7 was obtained as a light brownish viscous residue, soluble in CH_2Cl_2 (3 mg, 8.16 x 10^{-4} % based on dried weight of twigs).

EIMS : *m/z* (% relative intensity); Figure 52
267 ($[M]^+$, 31), 266 (100), 252 (26), 236 (14), 207 (4)

UV : λ_{max} (EtOH) nm (log ε) 213 (4.22), 272 (4.11), 307 (3.41) nm; Figure 53

$[\alpha]_D^{20}$: –89.74 (*c* 0.20 g/100 ml, EtOH)

^{1}H MMR : δ ppm, 300 MHz, in $CDCl_3$; see Table 13, Figure 54

^{13}C MMR : δ ppm, 75 MHz, in $CDCl_3$; see Table13, Figure 55

4.8 Compound TMM8

Compound TMM8 was obtained as a brown powder, soluble in CH_2Cl_2 (4 mg, 1.18 x 10^{-3} % based on dried weight of twigs).

EIMS : *m/z* (% relative intensity); Figure 57
281 ($[M]^+$, 53), 280 (100), 262 (44), 252 (25), 232 (40), 222 (8), 204 (37), 194 (20).

UV : λ_{max} (EtOH) nm (log ε) 214 (3.45), 271 (3.28), 316 (2.76) nm; Figure 58

$[\alpha]_D^{20}$: –25.00 (*c* 0.09 g/100 ml, CH_2Cl_2)

^{1}H MMR : δ ppm, 300 MHz, in $CDCl_3$; see Table 14, Figure 59

^{13}C MMR : δ ppm, 75 MHz, in $CDCl_3$; see Table 14, Figure 61

4.9 Compound TMM9

Compound TMM9 was obtained as a white amorphous powder, soluble in MeOH (10 mg, 2.63 x 10^{-3} % based on dried weight of twigs).

HRESIMS : $[M+Na]^+$ at *m/z* 323.1036 (calcd. for $C_{14}H_{20}O_7Na$, 323.1107); Figure 65

UV : λ_{max} (MeOH) nm (log ε) 225 (3.37), 273 (2.96) nm; Figure 66

[α] $^{20}_{D}$: –28.98 (*c* 0.25 g/100 ml, MeOH)

^{1}H MMR : δ ppm, 300 MHz, in CD_3OD; see Table 15, Figure 67

^{13}C MMR : δ ppm, 75 MHz, in CD_3OD; see Table15, Figure 68

4.10 Compound TMM10

Compound TMM10 was obtained as a colorless amorphous powder, soluble in DMSO (3 mg, 8.16 x 10^{-4} % based on dried weight of twigs).

HRESIMS : $[M+Na]^+$ at *m/z* 455.1619 (calcd. for $C_{19}H_{28}O_{11}Na$, 455.1529); Figure 70

UV : λ_{max} (MeOH) nm (log ε) 223 (3.51), 273 (2.77) nm; Figure 71

IR : υ_{max}(film) 3366 (br), 1510, 1071, 1043 cm^{-1}; Figure 72

[α] $^{20}_{D}$: –48.75 (*c* 0.08 g/100 ml, MeOH)

^{1}H MMR : δ ppm, 500 MHz, in DMSO-d_6; see Table 16, Figure 73

^{13}C MMR : δ ppm, 125 MHz, in DMSO-d_6; see Table 16, Figure 74

4.11 Compound LMM1

Compound LMM1 was obtained as a colorless oil, soluble in CH_2Cl_2 (13 mg, 6.82 x 10^{-3} % based on dried weight of leaves).

HRESIMS : $[M+H]^+$ at *m/z* 281.1593 (calcd. for $C_{19}H_{20}O_2$, 281.1542); Figure 78

UV : λ_{max} (MeOH) nm (log ε) 212 (3.95), 229 (4.09), 283 (3.63) nm; Figure 79

IR : υ_{max} (film) 1513, 1484, 1237 cm^{-1}; Figure 80

[α] $^{20}_{D}$: –25.00 (*c* 0.12 g/100 ml, $CHCl_3$)

CD : $[\theta]_{304}$ –1,378, $[\theta]_{284}$ +863, $[\theta]_{238}$ –25,323, $[\theta]_{226}$ –11,374; (*c* 0.0009 M, MeOH); Figure 87

^{1}H MMR : δ ppm, 300 MHz, in $CDCl_3$; see Table 17, Figure 81

^{13}C MMR : δ ppm, 75 MHz, in $CDCl_3$; see Table 17, Figure 82

4.12 Compound LMM2

Compound LMM2 was obtained as a colorless oil, soluble in CH_2Cl_2 (11 mg, 2.79 x 10^{-3} % based on dried weight of leaves).

HRESIMS : $[M+Na]^+$ at *m/z* 363.1578 (calcd. for $C_{21}H_{24}O_4Na$, 363.1572); Figure 88

UV : λ_{max} (MeOH) nm (log ε) 228 (4.31), 273 (3.84) nm; Figure 89

IR : υ_{max} (film) 1734, 1507, 1227 cm^{-1}; Figure 90

[α] $^{20}_{D}$: –55.38 (*c* 0.20 g/100 ml, $CHCl_3$)

CD : $[\theta]_{278}$ –2,366, $[\theta]_{230}$ –13,098; (*c* 0.0014 M, MeOH); Figure 97

^{1}H MMR : δ ppm, 300 MHz, in $CDCl_3$; see Table 18, Figure 91

^{13}C MMR : δ ppm, 75 MHz, in $CDCl_3$; see Table 18, Figure 92

4.13 Compound LMM3

Compound LMM3 was obtained as a colorless oil, soluble in CH_2Cl_2 (161 mg, 8.16 x 10^{-2} % based on dried weight of leaves).

HRESIMS : $[M+Na]^+$ at *m/z* 319.1321 (calcd. for $C_{19}H_{20}O_3Na$, 319.1310); Figure 98

UV : λ_{max} (MeOH) nm (log ε) 208 (4.46), 233 (4.22), 283 (3.95) nm; Figure 99

IR : υ_{max} (film) 3431 (br), 1515, 1484, 1234 cm^{-1}; Figure 100

[α] $^{20}_{D}$: +8.57 (*c* 0.18 g/100 ml, $CHCl_3$)

CD : $[\theta]_{290}$ –2,751, $[\theta]_{240}$ +4,197, $[\theta]_{230}$ +2,745; (*c* 0.0017 M, MeOH); Figure 87

^{1}H MMR : δ ppm, 300 MHz, in $CDCl_3$; see Table 19, Figure 101

^{13}C MMR : δ ppm, 75 MHz, in $CDCl_3$; see Table 19, Figure 102

4.14 Compound LMM4

Compound LMM4 was obtained as a colorless oil, soluble in CH_2Cl_2 (8 mg, 8.16 x 10^{-2} % based on dried weight of leaves).

HRESIMS : $[M-H]^-$ at *m/z* 265.1225 (calcd. for $C_{18}H_{17}O_2$, 265.1229); Figure 107

UV : λ_{max} (MeOH) nm (log ε) 209 (4.30), 230 (4.31), 285 (3.82) nm; Figure 108

IR : υ_{max} (film) 3392, 1517, 1485, 1237 cm^{-1}; Figure 109

[α] $^{20}_{D}$: +32.35 (*c* 0.17 g/100 ml, $CHCl_3$)

CD : $[\theta]_{290}$ –6,930, $[\theta]_{236}$ +22,491; (*c* 0.0005 M, MeOH); Figure 87

^{1}H MMR : δ ppm, 300 MHz, in $CDCl_3$; see Table 20, Figure 110

^{13}C MMR : δ ppm, 75 MHz, in $CDCl_3$; see Table 20, Figure 111

4.15 Compound LMM5

Compound LMM5 was obtained as a colorless oil, soluble in CH_2Cl_2 (6 mg, 3.08 x 10^{-3} % based on dried weight of leaves).

HRESIMS : $[M+Na]^+$ at *m/z* 319.1304 (calcd. for $C_{19}H_{20}O_3Na$, 319.1310); Figure 116

UV : λ_{max} (MeOH) nm (log ε) 211 (4.46), 228 (4.30), 280 (3.82) nm; Figure 117

IR : υ_{max} (film) 3408, 1516, 1494, 1205, 1138 cm^{-1}; Figure 118

$[\alpha]_D^{20}$: +15.71 (*c* 0.07 g/100 ml, $CHCl_3$)

CD : $[\theta]_{286}$ −4,440, $[\theta]_{242}$ +17,023, $[\theta]_{228}$ −14,231; (*c* 0.0004 M, MeOH); Figure 87

^{1}H MMR : δ ppm, 300 MHz, in $CDCl_3$; see Table 21, Figure 119

^{13}C MMR : δ ppm, 75 MHz, in $CDCl_3$; see Table 21, Figure 120

4.16 Compound LMM6

Compound LMM6 was obtained as a colorless oil, soluble in CH_2Cl_2 (64 mg, 3.22 x 10^{-2} % based on dried weight of leaves).

ESIMS : $[M-H]^-$ at *m/z* 253; Figure 125

UV : λ_{max} (MeOH) nm (log ε) 209 (4.31), 229 (4.33), 294 (4.21) nm; Figure 126

$[\alpha]_D^{20}$: +77.00 (*c* 0.10 g/100 ml, $CHCl_3$)

CD : $[\theta]_{288}$ −6,167, $[\theta]_{236}$ +24,435; (*c* 0.0005 M, MeOH); Figure 87

^{1}H MMR : δ ppm, 300 MHz, in $CDCl_3$; see Table 22, Figure 127

^{13}C MMR : δ ppm, 75 MHz, in $CDCl_3$; see Table 22, Figure 128

4.17 Compound LMM7

Compound LMM7 was obtained as a white amorphous powder, soluble in CH_2Cl_2 (27 mg, 1.36 x 10^{-2} % based on dried weight of leaves).

HRESIMS : $[M+Na]^+$ at *m/z* 305.1158 (calcd. for $C_{18}H_{18}O_3Na$, 305.1154); Figure 130

UV : λ_{max} (MeOH) nm (log ε) 207 (4.35), 229 (4.34), 284 (3.90) nm; Figure 131

IR : υ_{max} (film) 3378, 1704, 1517, 1485, 1237 cm^{-1}; Figure 132

[α] $^{20}_{D}$: +22.96 (*c* 0.14 g/100 ml, $CHCl_3$)

CD : $[\theta]_{290}$ −7,913, $[\theta]_{236}$ +23,272; (*c* 0.0004 M, MeOH); Figure 87

^{1}H MMR : δ ppm, 300 MHz, in $CDCl_3$; see Table 23, Figure 133

^{13}C MMR : δ ppm, 75 MHz, in $CDCl_3$; see Table 23, Figure 134

4.18 Compound LMF1

Compound LMF1 was obtained as a colorless oil, soluble in CH_2Cl_2 (112 mg, 5.64 x 10^{-2} % based on dried weight of leaves).

HRESIMS : $[M+Na]^+$ at *m/z* 395.1456 (calcd. for $C_{21}H_{24}O_6Na$, 395.1471); Figure 139

UV : λ_{max} (MeOH) nm (log ε) 220 (4.51), 275 (3.63) nm; Figure 140

IR : υ_{max} (film) 3438 (br), 2937, 2841, 1597, 1506, 1454, 1432, 1211, 1121 cm^{-1}; Figure 141

[α] $^{20}_{D}$: +65.54 (*c* 0.46 g/100 ml, $CHCl_3$)

CD : $[\theta]_{286}$ +795, $[\theta]_{246}$ −9,662; (*c* 0.0005 M, MeOH); Figure 148

^{1}H MMR : δ ppm, 300 MHz, in $CDCl_3$; see Table 24, Figure 142

^{13}C MMR : δ ppm, 75 MHz, in $CDCl_3$; see Table 24, Figure 143

4.19 Compound LMF2

Compound LMF2 was obtained as a colorless oil, soluble in CH_2Cl_2 (524 mg, 2.65 x 10^{-1} % based on dried weight of leaves).

HRESIMS : $[M+Na]^+$ at *m/z* 395.1473 (calcd. for $C_{21}H_{24}O_6Na$, 395.1471): Figure 149

UV : λ_{max} (MeOH) nm (log ε) 215 (4.59), 276.0 (4.43) nm; Figure 150

IR : υ_{max} (film) 3436 (br), 2937, 1598, 1506, 1455, 1213, 1117 cm^{-1}; Figure 151

[α] $^{20}_{D}$: +96.88 (*c* 0.16 g/100 ml, $CHCl_3$)

CD : $[\theta]_{284}$ +2,404, $[\theta]_{248}$ −5,969, $[\theta]_{234}$ +7,670, $[\theta]_{222}$ +7,670; (*c* 0.0013 M, MeOH); Figure 148

^{1}H MMR : δ ppm, 300 MHz, in $CDCl_3$; see Table 25, Figure 152

^{13}C MMR : δ ppm, 75 MHz, in $CDCl_3$; see Table 25, Figure 153

4.20 Compound LMF3

Compound LMF3 was obtained as a colorless oil, soluble in CH_2Cl_2 (12 mg, 6.23 x 10^{-3} % based on dried weight of leaves).

HRESIMS : $[M+Na]^+$ at *m/z* 351.1568 (calcd. for $C_{20}H_{24}O_4Na$, 351.1572); Figure 158

UV : λ_{max} (MeOH) nm (log ε) 210 (4.20), 229 (4.07), 281 (3.70) nm; Figure 159

IR : υ_{max} (film) 3441 (br), 2967, 2936, 1514, 1464, 1268, 1232 cm^{-1}; Figure 160

[α] $_D^{20}$: –20.0 (*c* 0.11 g/100 ml, $CHCl_3$)

CD : $[\theta]_{276}$ −1,185, $[\theta]_{240}$ −6,575; (*c* 0.0019 M, MeOH); Figure 166

^{1}H MMR : δ ppm, 300 MHz, in $CDCl_3$; see Table 26, Figure 161

^{13}C MMR : δ ppm, 75 MHz, in $CDCl_3$; see Table 26, Figure 162

4.21 Compound LMF4

Compound LMF4 was obtained as a white solid, soluble in CH_2Cl_2 (17 mg, 8.44 x 10^{-3} % based on dried weight of leaves).

ESIMS : $[M+Na]^+$ at *m/z* 349.03; Figure 167

UV : λ_{max} (MeOH) nm (log ε) 211 (4.39), 278 (3.91) nm; Figure 168

[α] $_D^{20}$: +22.2 (*c* 0.14 g/100 ml, $CHCl_3$)

CD : $[\theta]_{286}$ +589, $[\theta]_{266}$ +445, $[\theta]_{238}$ –2,376, $[\theta]_{214}$ –2111; (*c* 0.0011 M, MeOH); Figure 172

^{1}H MMR : δ ppm, 300 MHz, in $CDCl_3$; see Table 27, Figure 169

^{13}C MMR : δ ppm, 75 MHz, in $CDCl_3$; see Table 27, Figure 170

4.22 Compound LMF5

Compound LMF5 was obtained as a white solid, soluble in CH_2Cl_2 (366 mg, 1.84 x 10^{-1} % based on dried weight of leaves).

HRESIMS : $[M-H]^-$ at *m/z* 341.1392 (calcd. for $C_{20}H_{21}O_5$, 341.1389); Figure 173

UV : λ_{max} (MeOH) nm (log ε) 215 (4.42), 281 (3.73) nm; Figure 174

IR : υ_{max} (film) 3440 (br), 2936, 1560, 1509, 1453, 1433, 1225, 1149, 1103 cm^{-1}; Figure 175

[α] $_D^{20}$: –23.64 (*c* 0.33 g/100 ml, $CHCl_3$)

CD : $[\theta]_{288}$ −1824, $[\theta]_{238}$ −7940; (*c* 0.0009 M, MeOH); Figure 148

^{1}H MMR : δ ppm, 300 MHz, in $CDCl_3$; see Table 28, Figure 176

^{13}C MMR : δ ppm, 75 MHz, in $CDCl_3$; see Table 28, Figure 177

4.23 Compound LMF6

Compound LMF6 was obtained as a colorless oil, soluble in CH_2Cl_2 (126 mg, 6.33 x 10^{-2} % based on dried weight of leaves).

ESIMS : $[M+Na]^+$ at *m/z* 379.06; Figure 183

UV : λ_{max} (MeOH) nm (log ε) 215 (4.50), 279 (3.79) nm; Figure 184

$[\alpha]_D^{20}$: +80.00 (*c* 0.15 g/100 ml, $CHCl_3$)

CD : $[\theta]_{284}$ +2491, $[\theta]_{246}$ −7338, $[\theta]_{228}$ +3,917; (*c* 0.0010 M, MeOH); Figure 148

^{1}H MMR : δ ppm, 300 MHz, in $CDCl_3$; see Table 29, Figure 185

^{13}C MMR : δ ppm, 75 MHz, in $CDCl_3$; see Table 29, Figure 186

4.24 Compound LMF7

Compound LMF7 was obtained as a colorless oil, soluble in CH_2Cl_2 (28 mg, 1.40 x 10^{-2} % based on dried weight of leaves).

ESIMS : $[M+Na]^+$ at *m/z* 381.13; Figure 187

UV : λ_{max} (MeOH) nm (log ε) 209 (4.15), 230 (4.02), 279 (3.62) nm; Figure 188

$[\alpha]_D^{20}$: –24.21 (*c* 0.01 g/100 ml, $CHCl_3$)

CD : $[\theta]_{276}$ −2,253, $[\theta]_{240}$ −7,253; (*c* 0.0007 M, MeOH); Figure 193

^{1}H MMR : δ ppm, 300 MHz, in $CDCl_3$; see Table 30, Figure 189

^{13}C MMR : δ ppm, 75 MHz, in $CDCl_3$; see Table 30, Figure 190

4.25 Compound LMF8

Compound LMF8 was obtained as a white amorphous powder, soluble in acetone or MeOH (140 mg, 7.05 x 10^{-2} % based on dried weight of leaves). It has physical and spectra data identical with those of compound TMM5.

4.26 Compound SMF1

Compound SMF1 was obtained as a colorless oil, soluble in CH_2Cl_2 (38 mg, 3.20 x 10^{-3} % based on dried weight of stem).

ESIMS : $[M+Na]^+$ at *m/z* 395.10; Figure 194

UV : λ_{max} (MeOH) mm (log ε) 214 (4.68), 279 (3.80); Figure 195

[α] $^{20}_{D}$: –7.55 (*c* 0.28 g/100 ml, $CHCl_3$)

CD : $[\theta]_{278}$ –1,357, $[\theta]_{244}$ –4,518, $[\theta]_{224}$ +1,324; (*c* 0.0011 M, MeOH); Figure 198

^{1}H MMR : δ ppm, 300 MHz, in $CDCl_3$; see Table 31, Figure 196

^{13}C MMR : δ ppm, 75 MHz, in $CDCl_3$; see Table 31, Figure 197

4.27 Compound SMF2

Compound SMF2 was obtained as a colorless oil, soluble in CH_2Cl_2 (87 mg, 7.23 x 10^{-3} % based on dried weight of stem).

HRESIMS : $[M+Na]^+$ at *m/z* 379.1514 (calcd. for $C_{21}H_{24}O_5Na$, 379.1521); Figure 199

UV : λ_{max} (MeOH) nm (log ε) 215 (4.97), 278 (4.09) nm; Figure 200

IR : υ_{max} (film) 2936, 2838, 1599, 1509, 1453, 1263, 1225, 1148, 1104, 1028 cm^{-1}; Figure 201

[α] $^{20}_{D}$: –15.27 (*c* 0.28 g/100 ml, $CHCl_3$)

CD : $[\theta]_{284}$ –1,166, $[\theta]_{238}$ –7,707; (*c* 0.0007 M, MeOH); Figure 209

^{1}H MMR : δ ppm, 300 MHz, in $CDCl_3$; see Table 32, Figure 202

^{13}C MMR : δ ppm, 75 MHz, in $CDCl_3$; see Table 32, Figure 203

4.28 Compound SMF3

Compound SMF3 was obtained as a colorless oil, soluble in CH_2Cl_2 (291 mg, 2.43 x 10^{-2} % based on dried weight of stem).

HRESIMS : $[M+Na]^+$ at *m/z* 423.1776 (calcd. for $C_{23}H_{28}O_6Na$, 423.1784); Figure 210

UV : λ_{max} (MeOH) nm (log ε) 216 (4.85), 276 (3.64) nm; Figure 211

IR : υ_{max} (film) 2967, 2936, 2838, 1589, 1506, 1462, 1423, 1233, 1126 cm^{-1}; Figure 212

[α] $^{20}_{D}$: +15.00 (*c* 0.20 g/100 ml, $CHCl_3$)

CD : $[\theta]_{282}$ –850, $[\theta]_{242}$ +1,311, $[\theta]_{230}$ +208; (*c* 0.0050 M, MeOH); Figure 219

^{1}H MMR : δ ppm, 300 MHz, in $CDCl_3$; see Table 33, Figure 213

^{13}C MMR : δ ppm, 75 MHz, in $CDCl_3$; see Table 33, Figure 214

4.29 Compound SMF4

Compound SMF4 was obtained as a white solid, soluble in CH_2Cl_2 (32 mg, 2.70 x 10^{-3} % based on dried weight of stem). It has physical and spectra data identical with those of compound LMF5.

4.30 Compound SMF5

Compound SMF5 was obtained as a colorless oil, soluble in CH_2Cl_2 (310 mg, 2.59 x 10^{-2} % based on dried weight of stem). It has physical and spectra data identical with those of compound LMF6.

4.31 Compound SMF6

Compound SMF6 was obtained as a white solid, soluble in CH_2Cl_2 (38 mg, 3.20 x 10^{-3} % based on dried weight of stem).

HRESIMS : $[M+Na]^+$ at *m/z* 409.1629 (calcd. for $C_{22}H_{26}O_6Na$, 395.1622); Figure 220

UV : λ_{max} (MeOH) nm (log ε) 215 (4.77), 273 (3.60) nm; Figure 221

IR : υ_{max} (film) 2,938, 2,840, 1,597, 1,508, 1,463, 1,226, 1,148, 1,127, 1,105 cm^{-1}; Figure 222

[α] $_D^{20}$: +13.64 (*c* 0.33 g/100 ml, $CHCl_3$)

CD : $[\theta]_{294}$ −1,409, $[\theta]_{238}$ +3,787; (*c* 0.0008 M, MeOH); Figure 209

^{1}H MMR : δ ppm, 300 MHz, in $CDCl_3$; see Table 34, Figure 223

^{13}C MMR : δ ppm, 75 MHz, in $CDCl_3$; see Table 34, Figure 224

4.32 Compound SMF7

Compound SMF7 was obtained as a colorless oil, soluble in CH_2Cl_2 (46 mg, 3.83 x 10^{-3} % based on dried weight of stem).

ESIMS : $[M+Na]^+$ at *m/z* 425.12; Figure 225

UV : λ_{max} (MeOH) nm (log ε) 211 (4.52), 271 (3.28) nm; Figure 226

[α] $_D^{20}$: −8.00 (*c* 0.13 g/100 ml, $CHCl_3$)

CD : $[\theta]_{276}$ −937, $[\theta]_{244}$ −2,305, $[\theta]_{230}$ −1,181; (*c* 0.0008 M, MeOH); Figure 198

^{1}H MMR : δ ppm, 300 MHz, in $CDCl_3$; see Table 35, Figure 227

^{13}C MMR : δ ppm, 75 MHz, in $CDCl_3$; see Table 35, Figure 228

4.33 Compound SMF8

Compound SMF8 was obtained as a colorless oil, soluble in CH_2Cl_2 (347 mg, 2.89 x 10^{-2} % based on dried weight of stem).

ESIMS : $[M+Na]^+$ at *m/z* 409.03; Figure 229

UV : λ_{max} (MeOH) nm (log ε) 215 (4.68), 255 (3.33), 273 (3.48) nm; Figure 230

$[\alpha]_D^{20}$: +52.86 (*c* 0.07 g/100 ml, $CHCl_3$)

CD : $[\theta]_{298}$ +617, $[\theta]_{248}$ −6,328; (*c* 0.0009 M, MeOH); Figure 209

^{1}H MMR : δ ppm, 300 MHz, in $CDCl_3$; see Table 36, Figure 231

^{13}C MMR : δ ppm, 75 MHz, in $CDCl_3$; see Table 36, Figure 232

4.34 Compound SMF9

Compound SMF9 was obtained as a colorless crystalline solid, soluble in CH_2Cl_2 (205 mg, 1.71 x 10^{-2} % based on dried weight of stem).

ESIMS : $[M+Na]^+$ at *m/z* 395.12; Figure 235

UV : λ_{max} (MeOH) nm (log ε) 210 (4.06), 232 (4.06), 279 (3.58) nm; Figure 236

$[\alpha]_D^{20}$: +34.12 (*c* 0.09 g/100 ml, $CHCl_3$)

CD : $[\theta]_{294}$ −881, $[\theta]_{280}$ +409, $[\theta]_{260}$ −209, $[\theta]_{240}$ +1,721, $[\theta]_{226}$ +6,310, $[\theta]_{222}$ -130; (*c* 0.0027 M, MeOH); Figure 240

^{1}H MMR : δ ppm, 300 MHz, in $CDCl_3$; see Table 37, Figure 237

^{13}C MMR : δ ppm, 75 MHz, in $CDCl_3$; see Table 37, Figure 238

4.35 Compound SMF10

Compound SMF10 was obtained as a colorless oil, soluble in CH_2Cl_2 (205 mg, 1.71 x 10^{-2} % based on dried weight of stem).

ESIMS : $[M+Na]^+$ at *m/z* 425.15; Figure 241

UV : λ_{max} (MeOH) nm (log ε) 215 (4.30), 229 (4.18), 277 (3.54) nm; Figure 242

$[\alpha]_D^{20}$: +30.00 (*c* 0.11 g/100 ml, $CHCl_3$)

CD : $[\theta]_{296}$ −1,036, $[\theta]_{272}$ +375, $[\theta]_{254}$ −133, $[\theta]_{228}$ +7,371, $[\theta]_{222}$ +8,424; (*c* 0.0021 M, MeOH); Figure 240

^{1}H MMR : δ ppm, 300 MHz, in $CDCl_3$; see Table 37, Figure 243

^{13}C MMR : δ ppm, 75 MHz, in $CDCl_3$; see Table 37, Figure 244

4.36 Compound SMF11

Compound SMF11 was obtained as a colorless oil, soluble in CH_2Cl_2 (118 mg, 9.80 x 10^{-3} % based on dried weight of leaves). It has physical and spectra data identical with those of compound LMF2.

4.37 Compound SMF12

Compound SMF12 was obtained as a colorless oil, soluble in CH_2Cl_2 (291 mg, 2.43 x 10^{-2} % based on dried weight of stem).

HRESIMS : $[M+Na]^+$ at *m/z* 411.1770 (calcd. for $C_{22}H_{28}O_6Na$, 411.1784); Figure 247

UV : λ_{max} (MeOH) nm (log ε) 216 (4.30), 233 (4.25), 279 (3.67) nm; Figure 248

IR : υ_{max} (film) 3422 (br), 2958, 2933, 1593, 1513, 1463, 1258, 1234, 1136, 1102, 1028, 1005 cm^{-1}; Figure 249

$[\alpha]_D^{20}$: +37.65 (*c* 0.17 g/100 ml, $CHCl_3$)

CD : $[\theta]_{292}$ −1,240, $[\theta]_{276}$ +655, $[\theta]_{256}$ -100, $[\theta]_{236}$ +4,828, $[\theta]_{228}$ +9,107, $[\theta]_{218}$ +1,378 ; (*c* 0.0017 M, MeOH); Figure 240

^{1}H MMR : δ ppm, 300 MHz, in $CDCl_3$; see Table 39, Figure 250

^{13}C MMR : δ ppm, 75 MHz, in $CDCl_3$; see Table 39, Figure 251

4.38 Compound SMF13

Compound SMF13 was obtained as a colorless oil, soluble in CH_2Cl_2 (291 mg, 2.43 x 10^{-2} % based on dried weight of stem).

HRESIMS : $[M+Na]^+$ at *m/z* 411.1768 (calcd. for $C_{22}H_{28}O_6Na$, 411.1784); Figure 256

UV : λ_{max} (MeOH) nm (log ε) 215 (3.67), 277 (3.16) nm; Figure 257

IR : υ_{max} (film) 3521 (br), 2934, 1515, 1463, 1264, 1236, 1126 cm^{-1}; Figure 258

$[\alpha]_D^{20}$: −18.67 (*c* 0.17 g/100 ml, $CHCl_3$)

CD : $[\theta]_{284}$ −453, $[\theta]_{244}$ −1,458, $[\theta]_{228}$ −799; (*c* 0.0019 M, MeOH); Figure 198

^{1}H MMR : δ ppm, 300 MHz, in $CDCl_3$; see Table 40, Figure 259

^{13}C MMR : δ ppm, 75 MHz, in $CDCl_3$; see Table 40, Figure 260

4.39 Compound SMF14

Compound SMF14 was obtained as a white amorphous powder, soluble in acetone or MeOH (47 mg, 3.93 x 10^{-3} % based on dried weight of stem). It has physical and spectra data identical with those of compound TMM5.

5. Determination of free radical scavenging activity

5.1 TLC screening assay

The samples were loaded as spots on TLC plate and developed with suitable developing solvent. After drying, the TLC plate was sprayed with 0.2% solution of 1,1-diphenyl-2-picrylhydrazyl (DPPH) in methanol. After 30 min, active compounds appeared as yellow spots on the purple background (Takao *et al*., 1994**)**.

5.2 Free radical scavenging activity assay

5.2.1 Preparation of test sample

The test compound (0.5 mg) was dissolved in 1 mL of methanol (or suitable solvent) and diluted with methanol until a suitable range of concentration (mg/mL) was obtained. The final concentration was expressed as μM. For example, TMM1 (MW 280) at 0.5 mg/1 mL was equal to 1786 μM [(0.5 mg x 10^3 x 1000 mL)/376)]. For each well, 20 μL of test solution was added to the reaction mixture to furnish the total volume of 200 μL. The final concentration was calculated by the formula below (Braca *et al*., 2002).

$$N_1V_1 = N_2V_2$$

N_1 = Beginning concentration (μM)

V_1 = Beginning volume (μL)

N_2 = Final concentration (μM)

V_2 = Final volume (μL)

Thus, the final concentration of TMM1 solution = 1786 μM x 20 μL/ 200 μL

= 132.9 μM

5.2.2 Preparation of DPPH solution (100 μM)

DPPH (2 mg) was dissolved in 100 mL of methanol, and the solution was stirred for 30 min.

5.2.3 Measurement of activity

The test sample (20 μL) was added to 180 μL of DPPH solution (100 μM) in 96-well plate. The solution mixture was incubated at 37ºC for 30 min and then the absorbance of each well was measured at 510 nm on a SpectraMax M5 Microplate reader (Pharmaceutical Research Instrument Center, Faculty of Pharmaceutical Sciences, Chulalongkorn University). The DPPH solution (180 μL) mixed with methanol (20 μL) was used as negative control and quercetin was used as a reference compound.

5.2.4 Calculation of percent inhibition of DPPH scavenging activity

The percentage of DPPH reduction was calculated as follows.

$$\% \text{ DPPH reduction} = (A-B) \times 100 / A$$

A = The absorbance of DPPH solution after incubation at 510 nm

B = The absorbance of the reaction mixture after incubation at 510 nm

For IC_{50} evaluation of pure compounds, a graph showing concentration versus % DPPH reduction was plotted. The IC_{50} was calculated from the graph.

6. Determination of cytotoxic activity

6.1 Resazurin microplate assay (REMA)

Three human cancer cell lines were used in this study, including oral cavity (KB), breast (MCF-7) and lung (NCI-H187). This assay was performed using the method described by Brien *et al*., 2000. In brief, cells at a logarithmic growth phase were harvested and diluted to $7x10^4$ cells/mL for KB and $9x10^4$ cells/mL for MCF-7 and NCI-H187, in fresh medium. Successively, 5 μL of test sample diluted in 5% DMSO, and 45 μL of cell suspension were added to 384 well-plates, incubated at 37^oC in 5% CO_2 incubator. After the incubation period (3 days for KB and MCF-7, and 5 days for NCI-H187), 12.5 μL of 62.5 μg/mL resazurin solution were added to each well, and the plates were then incubated at 37^oC for 4 hours. Fluorescence signal were measured using SpectraMax M5 multi-detection microplate reader (Moleecular Devices, USA) at the excitation and emission wavelengths of 530 nm and 590 nm. Percent inhibition of cell growth was calculated by the following equation.

$$\% \text{ inhibition} = [1-(FU_T/FU_C)] \times 100$$

FU_T = The mean fluorescence unit from treated conditions

FU_C = The fluorescence unit from untreated conditions

The dose response curves were plotted from 6 conditions of 2-fold serially diluted test compounds and the sample concentrations that inhibit cell growth by 50% (IC_{50}) can be derived using the SOFTMax Pro software (Mollecular Devices, USA). Ellipticine, doxorubicin and tamoxifen were used as positive controls, and 0.5% DMSO was used as a negative control.

6.2 Green fluorescent protein (GFP) detection

The GFP-expressing Vero cell line was generated by stably transfecting the African green monkey kidney cell line (Vero, ATCC CCL-81), with pEGFP-N1 plasmid (Clontech). The cell line is maintained in minimal essential medium supplemented with 10% heat-inactivated fetal bovine serum, 2 mM L-glutamine, 1 mM sodium pyruvate, 1.5 g/L sodium bicarbonate and 0.8 mg/mL geneticin, at 37°C in a humidified incubator with 5% CO_2. The assay is carried out by adding 45 μL of cell suspension at 3.3 x 10^4 cells/mL to each well of 384-well plates containing 5 μL of test compounds previously diluted in 0.5% DMSO, and then incubating for 4 days in 37°C incubator with 5% CO_2. Fluorescence signals are measured by using SpectraMax M5 microplate reader (Molecular Devices, USA) in the bottom-reading mode with excitation and emission wavelengths of 485 and 535 nm. Fluorescence signal at day 4 is substracted with background fluorescence at day 0. The percentage of cytotoxicity is calculated by the following equation, where FU_T and FU_C represent the fluorescence units of cells treated with test compound and untreated cells, respectively (Hunt *et al*., 1999):

$$\% \text{ cytotoxicity} = [1-(FU_T/FU_C)] \times 100$$

IC_{50} values are derived from dose-response curves, using 6 concentrations of 2-fold serially diluted samples, by the SOFTMax Pro software (Molecular device). Ellipticine and 0.5% DMSO are used as a positive and negative control, respectively.

7. Determination of anti-herpes simplex virus activity

7.1 Viruses and cells

HSV strains used were HSV-1 (KOS) and HSV-2 (Baylor186). Vero cells (ATCC CCL81) were grown and maintained in Eagle's minimum medium supplemented with 10% fetal bovine serum.

7.2 Plaque reduction assay

Anti-HSV activity of the compound was determined by the plaque reduction assay modified from the previously reported method (Chansriniyom *et al*., 2009; Lipipun *et al*., 2003). Briefly, in the post-treatment assay, Vero cells, in 96-well tissue culture plate, were infected with 30 plaque forming units of HSV-1 (KOS) or HSV-2 (Baylor186). After 1 hr incubation at room temperature for virus adsorption, the cells were added with overlay media containing various concentrations of the compound. The infected cultures were incubated at 37 °C for 2 days. The infected cells were fixed and stained, and then the number of plaques was counted. The 50% effective concentration (EC_{50}) was determined from the curve relating the plaque number to the concentration of the compound. Acyclovir was used as a positive control. In the inactivation assay, each of 30 plaque forming units of HSV-1 or HSV-2 was mixed with various concentrations of compound and incubated for 1 hour, and then the mixture was added to Vero cells in 96-well tissue culture plate. After 1 hour incubation for virus adsorption, the overlay media were added. The infected cultures were incubated at 37 °C for 2 days. The infected cells were fixed, stained, and the plaques were counted. The 50% effective concentration (EC_{50}) was determined.

CHAPTER IV

RESULTS AND DISCUSSION

Phytochemical investigations of *Miliusa mollis*, and *Miliusa* cf. *fusca* led to the isolation of thirty-nine pure compounds.

The structure determinations of all isolates were carried out by interpretation of their UV, MS and NMR data, and for known structures, were confirmed by comparison with previously reported values. Furthermore, the DPPH radical scavenging, cytotoxic and anti-herpes simplex virus activities of the isolated compounds were evaluated.

1. Structure determination of isolated compounds

1.1 Structure determination of compound TMM1

Compound TMM1 was obtained as a colorless oil. The positive HRESI mass spectrum (Figure 12) exhibited an $[M+Na]^+$ ion at *m/z* 303.1280 (calcd. for $C_{19}H_{20}O_2Na$, 303.1361), suggesting the molecular formula $C_{19}H_{21}O_2$. The UV spectrum (Figure 13) showed two absorption maxima at 228 and 274 nm, and the IR spectrum (Figure 14) exhibited absorption bands for aliphatic protons (2962, 2931 and 2837 cm^{-1}), conjugated unsaturation (1515 and 1486 cm^{-1}), and ether (1243 cm^{-1}) functionalities.

The ^1H NMR spectrum (Figure 15, Table 7) of compound TMM1 showed signals for seven aromatic and two olefinic protons at δ 7.35 (2H, d, *J* = 8.7 Hz, H-2′, H-6′), 7.14 (1H, br s, H-4), 7.12 (1H, d, *J* = 8.1 Hz, H-6), 6.91 (2H,d, *J* = 8.7 Hz, H-3′, H-5′), 6.76 (1H, d, *J* = 8.1 Hz, H-7), 6.37 (1H, d, *J* = 15.8 Hz, H-8) and 6.09 (1H, dq, *J* = 15.8, 6.3 Hz, H-9), two methine protons at δ 5.09 (1H, d, *J* = 9.0 Hz, H-2) and 3.39 (1H, m, H-3), a methoxy group at δ 3.81 (3H, s), and two methyl groups at δ 1.86 (3H, d, *J* = 6.3 Hz, H-10) and 1.39 (3H, d, *J* = 6.6 Hz, CH_3-3). The ^{13}C-NMR (Figure 16, Table 7), DEPT (Figure 17) and HMQC spectra (Figure 18) of compound TMM1 display 19 carbon signals, corresponding to a methoxyl, two methyls, eleven methines and five quaternary carbons. The ^1H-NMR signals at δ 5.09, 3.39 and 1.39 and the ^{13}C-NMR resonances at δ 92.6 (C-2), 45.2 (C-3), and 17.8 (CH_3-3) are

characteristic features of the *trans*-2-aryl-3-methyl-2,3-dihydrobenzofuran system (Achenbach, H. *et al*., 1987). This was supported by the NOESY (Figure 19) interactions of CH_3-3 protons with H-2. In the structure of TMM1, a methoxy group [δ_H 3.81 (3H, s); δ_C 55.3] was present at C-4′, as indicated from the HMBC (Figure 20) correlations from the protons at δ 3.81 to C-4′ (δ 158.3), and from H-2′ and H-6′ (δ 7.35, 2H, d, J = 8.7 Hz) to C-2 (δ 92.6) and C-4′. In addition, a 2-propenyl moiety [δ_H 6.37 (1H, d, J = 15.8 Hz, H-8), 6.09 (1H, dq, J = 15.8, 6.3 Hz, H-9), 1.86 (3H, d, J = 6.3 Hz, Me-10); δ_C 130.8 (C-8), 122.9 (C-9), 18.3 (C-10)] was located at C-5 (δ 131.2), as evidenced by the ^3J-coupling from C-5 to H-9 (δ 6.09). These spectral data appeared to be superimposable on those reported for synthetic (±)-*trans*-2,3-dihydro-2-(4-methoxyphenyl)-3-methyl-5-(*E*)-propenylbenzofuran [**121**] (Snider, Han and Xie, 1997). It is known that a *trans*-2-aryl-3-methyl-2,3-dihydrobenzofuran structure with 2*R*,3*R* configuration shows a positive Cotton effect at about 260 nm or shows a negative Cotton effect at about 281 nm and positive Cotton effect at about 233 nm in the CD spectrum, whereas the reverse is true for the 2*S*,3*S*-isomer (Achenbach, H. *et al*., 1987). Since compound TMM1 showed a negative optical rotation ($[\alpha]_D^{20}$ −13.22) and its CD curve exhibited a negative Cotton effect at 264 nm, the structure of compound TMM1 was determined as (2*S*,3*S*)-2,3-dihydro-2-(4-methoxyphenyl)-3-methyl-5-(*E*)-propenylbenzofuran [**87**], which is a new dihydrobenzofuran neolignan. Figure 21 shows the CD curve of compound TMM1, in contrast with that of compound TMM2 and compound TMM4, which are in the 2*R*,3*R* series. It should be noted that although the antipodal isomer of compound TMM1 was earlier mentioned (Achenbach *et al*., 1991; Achenbach *et al*., 1995), its spectroscopic data were not provided.

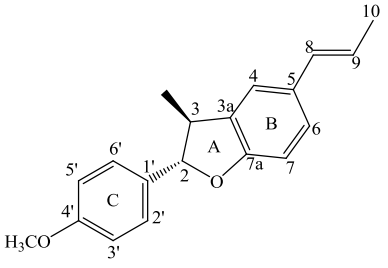

[**87**]

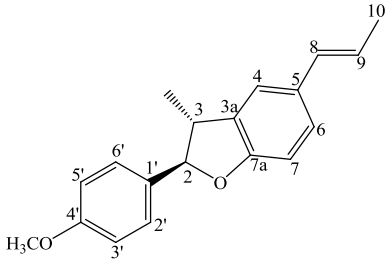

[**121**]

Table 7 NMR spectral data of compound TMM1 ($CDCl_3$) as compared with (±)-*trans*-2,3-dihydro-2-(4-methoxyphenyl)-3-methyl-5-(*E*)-propenylbenzo-furan ($CDCl_3$)

Position	Compound TMM1		(±)-*trans*-2,3-Dihydro-2-(4-methoxyphenyl)-3-methyl-5-(*E*)-propenylbenzofuran*	
	^1H (mult., *J* in Hz)	^{13}C	^1H (mult., *J* in Hz)	^{13}C
2	5.09 (d, 9.0)	92.6	5.09 (d, 8.8)	92.6
3	3.39 (m)	45.2	3.40 (dq, 8.8, 6.8)	45.2
3a	-	132.7	-	132.6
4	7.14 (br s)	120.7	7.14 (s)	120.7
5	-	131.2	-	131.2
6	7.12 (d, 8.1)	126.3	7.12 (d, 8.1)	126.3
7	6.76 (d, 8.1)	109.2	6.76 (d, 8.1)	109.3
7a	-	159.6	-	159.6
8	6.37 (d, 15.8)	130.8	6.36 (dd, 15.7, 1.5)	130.7
9	6.09 (dq, 15.8, 6.3)	122.9	6.09 (dq, 15.7, 6.6)	123.0
10	1.86 (d, 6.3)	18.3	1.86 (dd, 6.6, 1.6)	18.4
1′	-	132.4	-	132.4
2′	7.35 (d, 8.7)	127.6	7.35 (dt, 8.7, 2.0)	127.6
3′	6.91 (d, 8.7)	114.0	6.91 (dt, 8.7, 2.0)	114.0
4′	-	158.3	-	158.3
5′	6.91 (d, 8.7)	114.0	6.91 (dt, 8.7, 2.0)	114.0
6′	7.35 (d, 8.7)	127.6	7.35 (dt, 8.7, 2.0)	127.6
CH_3-3	1.39 (d, 6.6)	17.8	1.39 (d, 6.8)	17.8
CH_3O	3.81 (3H, s)	55.3	3.81 (3H, s)	55.3

* (Snider, Han and Xie, 1997)

1.2 Structure determination of compound TMM2

Compound TMM2 was obtained as a white amorphous solid. The EI mass spectrum revealed a molecular ion peak at *m/z* 296, suggesting the molecular formula $C_{19}H_{20}O_3$ (Figure 22). The UV spectrum showed three absorption maxima at 222 and 267 nm (Figure 23).

The ^{1}H NMR data of compound TMM2 (Figure 24, Table 8) are similar to those of compound TMM1, (2*S*,3*S*)-2,3-dihydro-2-(4-methoxyphenyl)-3-methyl-5-(*E*)-propenylbenzofuran [**87**], except for the absence of the proton signal for H-3′. Furthermore, the difference in the molecular weights of compound TMM1 and compound TMM2 indicated that compound TMM2 had a hydroxyl and a methoxyl group whereas TMM1 had only a methoxyl group. This was supported by the ^{13}C NMR (Figure 25, Table 8) and DEPT spectra (Figure 26), which showed quaternary carbons at δ 146.7 and 145.7 for C-3′ and C-4′, respectively.

The absolute configuration of compound TMM2 was determined by CD measurement. This compound showed a positive optical rotation ($[\alpha]_D^{20}$ +18.39) and its CD curve (Figure 21) showed a positive Cotton effect at 260 nm. These suggested that compound TMM2 has 2*R*,3*R* configuration (Achenbach, H. *et al*., 1987).

Through comparison of its ^{1}H NMR, ^{13}C NMR and MS data with those reported in the literature (Achenbach, H. *et al*., 1987), compound TMM2 was identified as (2*R*,3*R*)-2,3-dihydro-2-(4-hydroxy-3-methoxyphenyl)-3-methyl-5-(*E*)-propenylbenzofuran [**88**], which was first isolated from the roots of *Krameria cystisoides*.

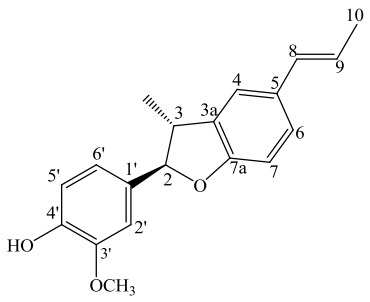

[**88**]

Table 8 NMR spectral data of compound TMM2 ($CDCl_3$) as compared with (2*R*, 3*R*)-2,3-dihydro-2-(4-hydroxy-3-methoxyphenyl)-3-methyl-5-(*E*)-propenylbenzofuran ($CDCl_3$)

Position	Compound TMM2		(2*R*,3*R*)-2,3-Dihydro-2-(4-hydroxy-3-methoxyphenyl)-3-methyl-5-(*E*)-propenylbenzofuran*	
	^1H (mult., *J* in Hz)	^{13}C	^1H (mult., *J* in Hz)	^{13}C
2	5.07 (d, 9.0)	93.0	5.08 (d, 9.3)	93.02
3	3.40 (m)	45.2	3.35 (m)	45.27
3a	-	132.3	-	132.54
4	7.15 (br s)	120.7	7.24 (br s)	120.79
5	-	131.3	-	131.40
6	7.14 (d, 8.1)	126.2	7.13 (dd, 8.3, 1.5)	126.28
7	6.79 (d, 8.1)	109.2	6.70 (d, 8.3)	109.27
7a	-	158.2	-	158.33
8	6.38 (d, 15.6)	130.7	6.38 (dd, 15.7, 2.0)	130.91
9	6.10 (dq, 15.6, 6.6)	123.0	6.10 (dq, 15.7, 6.4)	122.91
10	1.87 (d, 5.7)	18.3	1.83 (dd, 6.4, 2.0)	18.28
1′	-	132.3	-	132.38
2′	6.97 (d, 3.6)	108.5	7.09 (d, 2.0)	108.78
3′	-	146.7	-	146.87
4′	-	145.7	-	145.89
5′	6.91 (br s)	114.2	6.84 (d, 8.5)	114.37
6′	6.91 (br s)	119.6	6.91 (dd, 8.5)	119.58
CH_3-3	1.40 (d, 6.6)	17.6	1.37 (d, 7.1)	17.76
CH_3O	3.86 (s)	55.9	3.85 (s)	55.96

* Achenbach, H. *et al*., 1987

1.3 Structure determination of compound TMM3

Compound TMM3 gave an $[M+Na]^+$ ion at *m/z* 321.1375 in the HRESI mass spectrum (Figure 27), indicating a molecular formula of $C_{19}H_{22}O_3$. The UV spectrum (Figure 28) showed absorption maxima at 227 and 275 nm, and the IR spectrum (Figure 29) demonstrated absorption bands for hydroxyl (3,448 cm^{-1}), conjugated unsaturation (1509 cm^{-1}), and ether (1243 cm^{-1}) functionalities.

The ^{1}H-NMR spectrum (Figure 30, Table 9) showed two pairs of doublets appearing at δ 7.32 (2H, d, *J* = 8.6 Hz, H-2 and H-6) and 6.88 (2H, d, *J* = 8.6 Hz, H-3 and H-5), and at δ 7.09 (2H, d, *J* = 8.4 Hz, H-2′ and H- 6′) and 6.87 (2H, d, *J* = 8.4 Hz, H-3′ and H-5′). In support of this, the ^{13}C-NMR (Figure 31, Table 9) and DEPT spectra (Figure 32) showed a nineteen-carbon structure with two *p*-disubstituted benzene rings. In the HMQC spectrum, two tertiary oxygenated carbon signals appearing at δ 77.7 (C-7) and 79.3 (C-8) showed direct coupling with protons at δ 4.62 (1H, d, *J* = 7.7 Hz, H-7) and 4.34 (1H, dq, *J* = 7.7, 6.2 Hz, H-8), respectively (Figure 33). These two methine protons constituted an ABX coupling system with the CH_3 protons at δ 1.07 (3H, d, *J* = 6.2 Hz, CH_3-9) in the ^{1}H-^{1}H COSY spectrum (Figure 34).

Moreover, H-2 and H-6 exhibited 3-bond coupling with C-7, whereas H-8 showed HMBC connectivity to C-4′ (δ 156.1) through an ether linkage (Figure 35, Table 9). These spectral data of compound TMM3 were similar to those of previously reported 8.O.4′ neolignans (Braga *et al*., 1984). Compound TMM3 should have a methoxy group (δ_H 3.79, 3H, s; δ_C 55.3) at C-4 (δ 159.6) and an allyl moiety [(δ_H 3.32 (2H, br d, *J* = 6.6 Hz), 5.03 (1H, d, *J* = 10.2 Hz), 5.04 (1H, d, *J* = 16.8 Hz) and 5.93 (1H, m); δ_C 39.3, 115.5 and 137.7)] at C-1′ (δ 133.1). The placement of the CH_3O group at C-4 was supported by the HMBC correlation from the CH_3O-4 protons (δ 3.79) to C-4, which in turn showed ^3J-coupling with H-2 and H-6. In accordance with this proposed structure, HMBC correlations were observed from C-1′ to H-3′ and H-5′ and H-7′ (Figure 35, Table 9). It is known that for neolignans of this skeleton, the large coupling constant (*J* = 7.7 Hz) for H-7 and H-8, which was due to the intramolecular hydrogen bonding of the benzyllic hydroxyl and the aryloxyl group, suggested a *threo* relative configuration (Morais *et al*., 2009; Huo *et al*., 2008). On the

basis of the negative and positive peaks at 276 and 233 nm, respectively in the CD spectrum (Figure 36), the absolute configurations at C-7 and C-8 of compound TMM3 were both assigned to be *S* (Huo *et al*., 2008).

Based on the above evidences, the structure of compound TMM3 was determined to be (7*S*,8*S*)-*threo*-$\Delta^{8'}$-4-methoxy-8.O.4′-neolignan [**89**], which is a new 8.O.4′ neolignan.

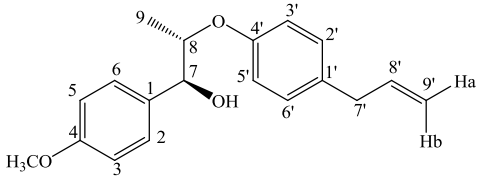

[**89**]

Table 9 NMR spectral data of compound TMM3 ($CDCl_3$)

Position	Compound TMM3		HMBC (correlation with ^1H)
	^1H (mult., *J* in Hz)	^{13}C	
1	-	132.0	3, 5, 7*
2	7.32 (d, 8.6)	128.5	6, 7
3	6.88 (d, 8.6)	113.9	5
4	-	159.6	2, 6, CH_3O
5	6.88 (d, 8.6)	113.9	3
6	7.32 (d, 8.6)	128.5	2, 7
7	4.62 (d, 7.7)	77.7	9
8	4.34 (dq, 7.7, 6.2)	79.3	9*
9	1.07 (d, 6.2)	15.7	-
1′	-	133.1	3′, 5′, 7′*
2′	7.09 (d, 8.4)	129.7	6′, 7′
3′	6.87 (d, 8.4)	116.4	-
4′	-	156.1	8, 2′, 6′
5′	6.87 (d, 8.4)	116.4	-

* Two-bond coupling

Table 9 NMR spectral data of compound TMM3 ($CDCl_3$) (continued)

Position	Compound TMM3		HMBC (correlation with ^1H)
	^1H (mult., *J* in Hz)	^{13}C	
6′	7.09 (d, 8.4)	129.7	2′, 7′
7′	3.32 (br d, 6.6)	39.3	-
8′	5.93 (m)	137.7	7′*
$9'_a$	5.03 (br d, 10.2)	115.5	7′
$9'_b$	5.04 (br d, 16.8)	-	-
CH_3O	3.79 (s)	55.3	-

* Two-bond coupling

1.4 Structure determination of compound TMM4

Compound TMM4 was obtained as a white amorphous solid. The EI mass spectrum revealed a molecular ion peak at *m/z* 266, corresponding to the molecular formula $C_{18}H_{18}O_2$ (Figure 37). The UV spectrum showed three absorption maxima at 223 and 264 nm (Figure 38).

The ^1H NMR spectrum (Figure 39, Table 10) showed characteristic features of the *trans*-2-aryl-3-methyl-2,3-dihydrobenzofuran system (Achenbach *et al*., 1987) at δ 5.07 (1H, d, *J* = 8.0 Hz, H-2), 3.37 (1H, quint, *J* = 8.0 Hz, H-3) and 1.39 (3H, d, *J* = 6.6 Hz). Ring B showed the presence of an ABM spin system at δ 7.13 (1H, s, H-4), 7.11 (1H, d, *J* = 8.3 Hz, H-6) and 6.77 (1H, d, *J* = 8.3 Hz, H-7), and an allyl moiety at δ 6.36 (1H, br d, *J* = 15.8 Hz, H-8), 6.10 (1H, dq, *J* = 15.8, 6.6 Hz, H-9) and 1.85 (3H, d, *J* = 6.6 Hz, H-10). The *ortho*-coupled doublets (*J* = 8.4 Hz) at δ 7.28 (2H, H-2′ and H-6′) and 6.80 (2H, H-3′ and H-5′) indicated the presence of *p*-substitued benzene ring. From the above observations, it appears that compound TMM4 should have a structure similar to that of compound TMM1, (2*S*,3*S*)-2,3-dihydro-2-(4-methoxyphenyl)-3-methyl-5-(*E*)-propenylbenzofuran [**87**] except for the absence of the methoxy signal. The ^{13}C-NMR (Figure 40, Table 10) and DEPT spectra (Figure 41) showed the presence of a methoxy, two methyl, ten methine and six quaternary carbons.

TMM4 exhibited positive optical rotation ($[\alpha]_D^{20}$ +65.28) and a positive Cotton effect at 264 nm in CD spectrum (Figure 21), which were similar to those of TMM2 [**88**]. This indicated that compound TMM4 should have a 2*R*,3*R* configuration.

From all of the above data, it was concluded that compound TMM4 was identical with conocarpan [**90**]. This was confirmed by comparison of its ^{1}H NMR, ^{13}C NMR and MS data with previously reported valued for **90**, which was isolated from the leaves of *Piper decurrens* (Chauret *et al*., 1996).

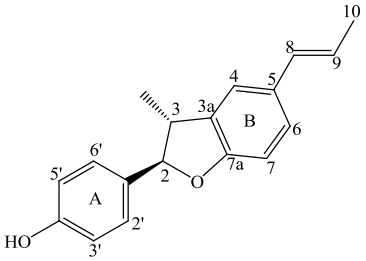

[**90**]

Table 10 NMR spectral data of compound TMM4 ($CDCl_3$) as compared with conocarpan ($CDCl_3$)

Position	Compound TMM4		Conocarpan*	
	^{1}H (mult., *J* in Hz)	^{13}C	^{1}H (mult., *J* in Hz)	^{13}C
2	5.07 (d, 8.0)	92.6	5.09 (d, 8.8)	92.68
3	3.37 (quint, 8.0)	45.2	3.40 (quint, 7.3)	45.17
3a	-	132.8	-	132.73
4	7.13 (s)	120.7	7.14 (s)	120.76
5	-	131.3	-	131.32
6	7.11 (d, 8.3)	126.3	7.13 (d, 8.2)	126.31
7	6.77 (d, 8.3)	109.3	6.77 (d, 8.2)	109.30
7a	-	158.2	-	158.22
8	6.36 (br d, 15.8)	130.8	6.37 (dd, 15.7, 1.5)	130.77
9	6.10 (dq, 15.8, 6.6)	123.0	6.45 (dq, 15.7, 6.5)	123.08
10	1.85 (d, 6.6)	18.3	1.87 (dd, 6.6, 1.5)	18.39
1′	-	132.3	-	132.37

* Chauret *et al*., 1996

Table 10 NMR spectral data of compound TMM4 ($CDCl_3$) as compared with conocarpan ($CDCl_3$) (continued)

Position	Compound TMM4		Conocarpan*	
	^1H (mult., *J* in Hz)	^{13}C	^1H (mult., *J* in Hz)	^{13}C
2′	7.28 (d, 8.4)	127.8	7.30 (d, 8.5)	127.87
3′	6.80 (d, 8.4)	115.5	6.83 (d, 8.5)	115.75
4′	-	155.7	-	155.75
5′	6.80 (d, 8.4)	115.5	6.83 (d, 8.5)	115.75
6′	7.28 (d, 8.4)	127.8	7.30 (d, 8.5)	127.87
CH_3-3	1.39 (d, 6.6)	17.8	1.40 (d, 6.8)	17.82

* Chauret *et al*., 1996

1.5 Structure determination of compound TMM5

Compound TMM5 was obtained as a white amorphous powder. The EI mass spectrum displayed a molecular ion at *m/z* 290, suggesting the molecular formula $C_{15}H_{14}O_6$ (Figure 42). The UV spectrum showed two absorption maxima at 225 and 280 nm (Figure 43), suggesting a catechin skeleton.

The ^1H NMR (Figure 44, Table 11) spectral data showed signals for methylene protons at δ 2.86 (1H, dd, *J* = 16.5, 4.4 Hz, H-4*α*), at δ 2.73 (1H, dd, *J* = 16.5, 3.3 Hz, H-4*β*), and methines at δ 4.87 (1H, s, H-2) and at δ 4.20 (1H, br d, *J* = 3.6 Hz, H-3). The doublet signals (*J* = 2.1 Hz) at δ 6.01 and 5.91 could be assigned to the *meta* coupled protons H-6 and H-8 of ring A. An ABM spin system at δ 7.04 (1H, d, *J* = 1.4 Hz), 6.78 (1H, d, *J* = 8.4 Hz) and 6.83 (1H, dd, *J* = 8.4, 1.4 Hz) could be assigned to H-2′, H-5′ and H-6′, respectively. The ^{13}C-NMR (Figure 45, Table 11) and DEPT spectra (Figure 46) exhibited signals for a methylene, seven methine and seven quaternary carbons. The sign of the optical rotation of compound TMM5 was negative ($[\alpha]_D^{20}$ −51.18).

The ^1H NMR, ^{13}C NMR, MS and optical rotation data of compound TMM5 were in excellent agreement with previously reported values for (–)-epicatechin [**91**] (Shahat, 2006).

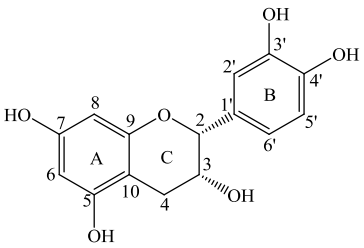

[**91**]

Table 11 NMR spectral data of compound TMM5 (acetone-d_6) as compared with (–)-epicatechin (acetone-d_6)

Position	Compound TMM5		(–)-Epicatechin*	
	^{1}H (mult., *J* in Hz)	^{13}C	^{1}H (mult., *J* in Hz)	^{13}C
2	4.87 (s)	79.4	4.81 (s)	79.85
3	4.20 (br d, 3.6)	66.9	4.17 (br s)	67.74
4α	2.86 (dd, 16.5, 4.4)	28.9	2.85 (dd, 16.5, 4.5)	29.22
4β	2.73 (dd, 16.5, 3.3)	-	2.73 (dd, 16.7, 2.5)	-
5	-	157.5	-	157.95
6	6.01 (d, 2.1)	96.2	5.94 (d, 2.2)	96.46
7	-	157.5	-	157.61
8	5.91 (d, 2.1)	95.7	5.91 (d, 2.2)	95.92
9	-	157.1	-	157.34
10	-	99.8	-	100.09
1′	-	132.2	-	132.30
2′	7.04 (d, 1.4)	115.2	6.97 (d, 1.7)	115.34
3′	-	145.4	-	145.89
4′	-	145.2	-	145.72
5′	6.78 (d, 8.4)	115.5	6.74 (d, 7.5)	115.92
6′	6.83 (dd, 8.4, 1.4)	119.4	6.78 (dd, 7.5, 1.7)	119.12

* Shahat, 2006

1.6 Structure determination of compound TMM6

Compound TMM6 was obtained as a yellow amorphous powder. The EI mass spectrum revealed a molecular ion peak at *m/z* 275, corresponding to the molecular formula $C_{17}H_9NO_3$ (Figure 47). The UV spectrum showed the absorption maxima at 248, 268, 306 and 411 nm (Figure 48), a typical of 7-oxoaphorphine skeleton.

The ^{1}H NMR spectrum (Figure 49, Table 12) showed aromatic protons at δ 8.86 (1H, d, *J* = 5.3 Hz) for H-5, 8.58 (1H, d, *J* = 7.8) for -11, 8.53 (1H, d, *J* = 7.8 Hz) for H-8, 7.73 (1H, d, *J* = 5.3 Hz) for H-4, 7.71 (1H, t, *J* = 7.8) for H-10, 7.54 (1H, t, *J* = 7.8 Hz) for H-9 and 7.14 (1H, s) for H-3. The signal at δ 6.35 (2H, s) represented methylene protons of O-CH_2-O.

The ^{13}C NMR (Figure 50, Table 12) and DEPT (Figure 51) spectra exhibited seventeen signals that were two methylene, seven methine and eight quarternary carbons, in which one of quaternary carbons was a carbonyl of ketone group (δ 182.3, C-7). Through comparison of these data with previously published data, compound TMM6 was identified as previously reported liriodenine [**34**] (Pang *et al.,* 2007; Zhang *et al*., 2002).

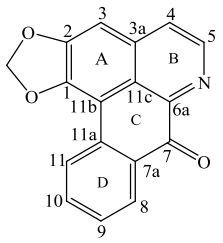

[**34**]

Table 12 NMR spectral data of compound TMM6 ($CDCl_3$) as compared with liriodenine (δ_H, CD_3OD and δ_C, $CDCl_3$: CD_3OD (3:1))

Position	Compound TMM6		Liriodenine	
	^{1}H (mult., *J* in Hz)	^{13}C	^{1}H* (mult., *J* in Hz)	^{13}C**
1	-	148.1	-	148.6
2	-	151.8	-	152.3
3	7.14 (s)	103.2	7.16 (s)	103.5

* Pang *et al.,* 2007; ** Zhang *et al*., 2002

Table 12 NMR spectral data of compound TMM6 ($CDCl_3$) as compared with liriodenine (δ_H, CD_3OD and δ_C, $CDCl_3$: CD_3OD (3:1)) (continued)

Position	Compound TMM6		Liriodenine*	
	^1H (mult., *J* in Hz)	^{13}C	^1H (mult., *J* in Hz)	^{13}C
3a	-	145.2	-	145.1
4	7.73 (d, 5.3)	124.2	7.74 (d, 5.2)	124.9
5	8.86 (d, 5.3)	144.7	8.90 (d, 5.2)	144.6
6a	-	135.8	-	136.3
7	-	182.3	-	182.8
7a	-	131.2	-	131.3
8	8.53 (d, 7.8)	128.6	8.57 (d, 8.0)	128.8
9	7.54 (t, 7.8)	128.8	7.57 (dt, 8.0, 1.1)	128.9
10	7.71 (t, 7.8)	135.9	7.72 (dt, 8.0, 1.1)	134.4
11	8.58 (d, 7.8)	127.3	8.65 (d, 8.0)	127.7
11a	-	132.8	-	133.2
11b	-	108.1	-	108.1
11c	-	123.2	-	123.5
O-CH_2-O	6.35 (s)	102.5	6.36 (s)	103.0

* Pang *et al.,* 2007; ** Zhang *et al*., 2002

1.7 Structure determination of compound TMM7

Compound TMM7 was obtained as a light brownish viscous residue. The EI mass spectrum displayed a molecular ion peak at *m/z* 267, corresponding to the molecular formula $C_{17}H_{17}NO_2$ (Figure 52). The UV absorptions at 213, 272 and 307 nm (Figure 53) were characteristics of 1,2-disubstituted aporphine (Likhitwitayawuid *et al*., 1993)

The ^1H NMR spectrum (Figure 54, Table 13) exhibited five aromatic signals at δ 8.27 (1H, d, *J* = 7.8 Hz, H-11), 7.19-7.32 (3H, m, H-8, H-9, H-10) and 6.70 (1H, s, H-3), a methoxy signal at δ 3.57 (3H, s) and a methine signal at δ 3.95 (1H, dd, *J* = 13.2, 4.5 Hz, H-6a). Three pairs of methylene protons were found at δ 3.51 (1H, m,

H-5_{eq}), 2.74 (1H, br d, J = 13.5 Hz, H-4_{eq}) and 3.20-2.94 (4H, m, H-4_{ax}, H-5_{ax} and H-7). The ^{1}H NMR spectrum of compound TMM7 is similar to that of compound TMM6, liriodenine [**34**], except for the presence of three pairs of methylene protons (H-4_{ax}, H-4_{eq}, H-5_{ax}, H-5_{eq}, and H_2-7) and one methine proton (H-6a).

The ^{13}C NMR (Figure 55, Table 13) and DEPT spectra (Figure 56) displayed seventeen signals, including one methyl carbon, three methylene carbons, six methine carbons and eight quaternary carbons. This compound exhibited a negative sign of optical rotation ($[\alpha]_D^{20}$ –89.74).

This compound was identified as asimilobine **[92]** by comparison of the above data with previously reported values (Fischer *et al*., 1999; Zanin and Lordello, 2007).

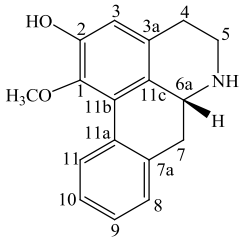

[**92**]

Table 13 NMR spectral data of compound TMM7 ($CDCl_3$) compared with asimilobine (δ_H, $CDCl_3$ and δ_C, DMSO-d_6)

Position	Compound TMM7		Asimilobine*	
	^{1}H (mult., J in Hz)	^{13}C	^{1}H* (mult., J in Hz)	^{13}C**
1	-	143.2	-	143.2
2	-	148.9	-	148.9
3	6.70 (s)	114.6	6.50 (s)	115.7
3a	-	125.7	-	126.8
4_{ax}	3.20-2.94 (m)	27.5	2.46-2.78 (m)	28.5
4_{eq}	2.74 (br d, 13.5)	-	2.46-2.78 (m)	-
5_{ax}	3.20-2.94 (m)	42.6	2.46-2.78 (m)	42.6
5_{eq}	3.51 (m)	-	3.19-3.21 (m)	-
6a	3.95 (dd, 13.2, 4.5)	53.4	3.62-3.68 (dd, 13.2, 4.8)	53.2

* Fischer *et al*., 1999; ** Zanin and Lordello, 2007

Table 13 NMR spectral data of compound TMM7 ($CDCl_3$) compared with asimilobine (δ_H, $CDCl_3$ and δ_C, DMSO-d_6) (continued)

Position	Compound TMM7		Asimilobine*	
	^1H (mult., *J* in Hz)	^{13}C	^1H* (mult., *J* in Hz)	^{13}C**
7	3.20-2.94 (m)	36.1	2.46-2.78 (m)	36.9
7a	-	135.0	-	136.3
8	7.19-7.32 (m)	128.2	7.01-7.12 (m)	127.7
9	7.19-7.32 (m)	127.9	7.01-7.12 (m)	127.5
10	7.19-7.32 (m)	127.5	7.01-7.12 (m)	127.2
11	8.27 (d, 7.8)	127.4	8.06-8.08 (d, 6.0)	126.5
11a	-	131.6	-	132.1
11b	-	125.6	-	125.1
11c	-	128.8	-	129.3
CH_3O	3.57 (s)	60.4	3.58 (s)	59.3

* Fischer *et al*., 1999; ** Zanin and Lordello, 2007

1.8 Structure determination of compound TMM8

Compound TMM8 was obtained as a brown powder. It has a molecular formula of $C_{17}H_{15}NO_3$, as indicated by the molecular ion peak at *m/z* 281 in the EI mass spectrum (Figure 57). The UV spectrum showed absorption maxima at 214, 271 and 316 nm (Figure 58), suggesting an aporphine structure.

The ^1H NMR spectrum (Figure 59, Table 14) showed five aromatic signals at δ 8.13 (1H, d, *J* = 7.2 Hz) for H-11, 7.42 (1H, d, *J* = 7.2 Hz) for H-8, 7.37 (1H, t, *J* = 7.2 Hz) for H-10, 7.29 (1H, t, *J* = 7.2 Hz) for H-9 and 6.55 (1H, s) for H-3, and three methylene protons at δ 6.07 (1H, br s) and 5.92 (1H, br s) for O-CH_2-O, 3.37 (1H, *J* = dd, *J* = 12.0, 5.7 Hz) for H-5_{eq}, 3.11 (1H, td, *J* = 12.0, 3.9 Hz) for 5_{ax}, 2.93 (1H, m) for H-4_{ax} and 2.62 (1H, br d, *J* = 16.2 Hz) for H-4_{eq}. Two methine signals at δ 4.59 (1H, d, *J* = 1.8 Hz) and 4.03 (1H, br s) were due to the *cis* protons H-7 and H-6a, which was confirmed by the correlation peak in the NOESY spectrum (Figure 60). From the above ^1H NMR data, it appeared that compound TMM8 should have a structure

similar to that of compound TMM7, asimilobine [**92**] except for the presence of hydroxyl group at C-7, and methylene dioxide (-O-CH_2-O-)

The ^{13}C NMR, DEPT and HMQC spectra (Figures 61-63) exhibited signals for three methylene carbons, seven methine carbons and seven quaternary carbons. Based on the above spectral data, compound TMM8 was identified as (–)-norushinsunine [**93**]. This compound has been isolated from the stems of *Michelia compressa* (Lo, 2004). The complete ^{13}C NMR assignments of compound TMM8 were obtained from the HMBC correlation (Figure 64). The H-C long range correlations observed in the HMBC spectrum of compound TMM8 are summarized in Table 14.

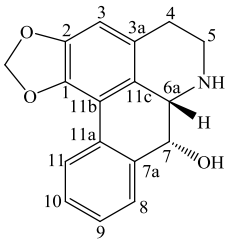

[**93**]

Table 14 NMR spectral data of compound TMM8 ($CDCl_3$) as compared with (–)-norushinsunine ($CDCl_3$)

Position	Compound TMM8		(–)-Norushinsunine*	HMBC
	^1H (mult., *J* in Hz)	^{13}C	^1H (mult., *J* in Hz)	(correlation with ^1H)
1	-	142.7	-	3, O-CH_2-O
2	-	147.2	-	3, O-CH_2-O
3	6.55 (s)	108.4	6.55 (s)	4
3a	-	128.6	-	5_{eq}
4_{ax}	2.93 (m)	29.1	2.95 (m)	3, 5_{eq}
4_{eq}	2.62 (br d, 16.2)	-	2.62 (dd, 16.0, 3.6)	-
5_{ax}	3.11 (td, 12.0, 3.9)	43.0	3.08 (td, 12.4, 4.0)	-
5_{eq}	3.37 (dd, 12.0, 5.7)	-	3.20 (m)	-
6a	4.03 (br s)	57.2	4.00 (d, 2.8)	5_{ax}, 5_{eq}, 7**
7	4.59 (d, 1.8)	71.0	4.61 (d, 2.8)	8

* Lo, 2004
** Two-bond coupling

Table 14 NMR spectral data of compound TMM8 ($CDCl_3$) as compared with (–)-norushinsunine ($CDCl_3$) (continued)

Position	Compound TMM8		(–)-Norushinsunine*	HMBC (correlation with ^1H)
	^1H (mult., *J* in Hz)	^{13}C	^1H (mult., *J* in Hz)	
7	4.59 (d, 1.8)	71.0	4.61 (d, 2.8)	8
7a	-	135.4	-	7**, 9, 11
8	7.42 (d, 7.2)	129.4	7.41 (dd, 8.0, 1.2)	7, 10
9	7.29 (t, 7.2)	127.9	7.29 (td, 8.0, 1.2)	11
10	7.37 (t, 7.2)	129.4	7.39 (td, 8.0, 1.2)	8
11	8.13 (d, 7.2)	127.6	8.14 (dd, 8.0, 1.2)	9
11a	-	130.3	-	8, 10
11b	-	115.1	-	11
11c	-	123.4	-	3, 7
O-CH_2-O	5.92 (br s) 6.07 (br s)	100.8	5.91 (d, 1.2) 6.07 (d, 1.2)	-

* Lo, 2004
** Two-bond coupling

1.9 Structure determination of compound TMM9

Compound TMM9 was obtained as a white amorphous powder. The HRESI mass spectrum (Figure 65) revealed a $[M+Na]^+$ at *m/z* 323.1036, corresponding to the molecular formula $C_{14}H_{20}O_7$. The UV spectrum showed absorption maxima at 225 and 273 nm (Figure 66).

The ^1H NMR (Figure 67, Table 15) spectrum showed two pairs of *ortho* coupled protons at δ 7.10 (2H, d, *J* = 8.4 Hz, H-3, H-5) and 7.00 (2H, d, *J* = 8.4 Hz, H-2, H-6), indicating the presence of a *p*-substituted benzene ring. One of the substituents was hydroxyethyl group [δ 3.67 (3H, m, H-8) and 2.72 (2H, t, *J* = 7.2 Hz, H-7)]. The other was sugar unit (*β*-glucopyranose), as evidenced by an anomeric proton at δ 4.82 (1H, d, *J* = 7.5 Hz, H-1′) and other proton signals at δ 3.85 (1H, br d, *J* = 11.4 Hz, H-6′$_a$), 3.67 (1H, m, H-6′$_b$) and 3.39 (4H, m, H-2′, H-3′, H-4′, H-5′).

The ^{13}C NMR (Figure 68, Table 15) and DEPT (Figure 69) spectra showed fourteen signals, including three methylene carbons, nine methine carbons and two quaternary carbons. Compound TMM9 was identified as icariside D_2 [**94**] by comparison of its NMR data with previously reported values (Miyase *et al*., 1989)

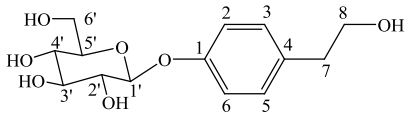

[**94**]

Table 15 NMR spectral data of compound TMM9 (CD_3OD) as compared with icariside D_2 (pyridine -d_6)

Position	Compound TMM9		Icariside D_2*	
	^1H (mult., *J* in Hz)	^{13}C	^1H (mult., *J* in Hz)	^{13}C
1	-	157.7	-	157.2
2	7.00 (d, 8.4)	117.8	7.29 (s)	117.0
3	7.10 (d, 8.4)	130.9	7.29 (s)	130.5
4	-	134.3	-	133.9
5	7.10 (d, 8.4)	130.9	7.29 (s)	130.5
6	7.00 (d, 8.4)	117.8	7.29 (s)	117.0
7	2.72 (t, 7.2)	39.4	2.96 (t, 7.0)	39.6
8	3.67 (m)	64.4	4.03 (t, 7.0)	63.7
1′	4.82 (d, 7.5)	102.6	not reported	102.5
2′	3.39 (m)	75.0		75.0
3′	3.39 (m)	78.1		78.8
4′	3.39 (m)	71.4		71.4
5′	3.39 (m)	78.0		78.6
$6'_a$	3.85 (br d, 11.4)	62.6		62.5
$6'_b$	3.67 (m)	-		-

* Miyase *et al*., 1989

1.10 Structure determination of compound TMM10

Compound TMM10 was obtained as a colorless amorphous powder. It has a molecular formula of $C_{19}H_{28}O_{11}$, as indicated by the $[M+Na]^+$ ion peak at *m/z* 455.1619 in the HRESI mass spectrum (Figure 70). The compound showed UV absorptions at 223 and 273 nm (Figure 71), and IR bands at 3,366 (hydroxyl), 1,510 (conjugated unsaturation), and 1071 and 1043 (ether) cm^{-1} (Figure 72).

The ^1H NMR spectrum (Figure 73, Table 16) of compound TMM10 resembled that of compound TMM9, except for the presence of *β*-xylopyranosyl-(1→6)-*O*-*β*-glucopyranose instead of a *β*-glucopyranose as in compound TMM9. The aglycon of this compound showed signals for aromatic proton resonances at δ 7.10 (2H, d, *J* = 8.6 Hz, H-3 and H-5) and 6.95 (2H, d, *J* = 8.6 Hz, H-2 and H-6), and aliphatic proton signals at δ 2.64 (2H, t, *J* = 6.5 Hz, H-7) and 3.54 (2H, t, *J* = 6.5 Hz, H-8). This was supported by the ^{13}C-NMR signals (Figure 74, Table 16) at δ 155.7 (C-1), 132.7 (C-4), 129.7 (C-3, C-5), 116.2 (C-2, C-6), 38.2 (C-7) and 62.4 (C-8). Compound TMM10 possessed two sugar units, as evidenced by two anomeric protons at δ 4.73 (1H, d, *J* = 7.3 Hz, H-1′) and 4.17 (1H, d, *J* = 7.6 Hz, H-1″), which were correlated to the carbons at δ 100.7 (C-1′) and 103.8 (C-1″), respectively, in the HMQC spectrum (Figure 75). The inner sugar was *β*-glucopyranose [δ_H 4.73 (1H, d, *J* = 7.3 Hz, H-1′), 3.22 (2H, m, H-2′ and H-3′), 3.14 (1H, t, *J* = 8.8 Hz, H-4′), 3.48 (1H, dd, *J* = 8.8, 6.6 Hz, H-5′), 3.55 (1H, dd, *J* = 10.9, 6.6 Hz, H-6′$_a$) and 3.93 (1H, dd, *J* = 10.9, 8.8 Hz, H-6′$_b$); δ_C δ 100.7 (C-1′), 73.2 (C-2′), 76.5 (C-3′), 69.6 (C-4′), 75.8 (C-5′) and 68.2 (C-6′)] (Agrawal, 1992), and its connection to the aglycon through an arylether bond was demonstrated by the HMBC (Figure 76, Table 15) correlation from H-1′ to C-1 (δ 155.7) and the NOESY (Figure 77) interaction of H-1′ with H-2 and H-6. The other sugar unit was *β*-xylopyranose [δ_H 4.17 (1H, d, *J* = 7.6 Hz, H-1″), 2.96 (1H, dd, *J* = 8.7, 7.6 Hz, H-2″), 3.06 (1H, t, *J* = 8.7 Hz, H-3″), 3.22 (1H, m, H-4″), 3.65 (1H, dd, *J* = 11.3, 5.3 Hz, H-5″$_b$), 2.94 (1H, t, *J* = 11.3 Hz, H-5″$_a$); δ_C δ 103.8 (C-1″), 73.4 (C-2″), 76.5 (C-3″), 69.6 (C-4″), 65.6 (C-5″)], with its anomeric carbon linked to C-6′ of the glucose moiety through an ether bridge (Hua *et al*., 2008; Schroeder, Lutterbach and Stöckigt, 1996). This linkage was further confirmed by the HMBC correlations between C-1″ and H_2-6′, and between C-6′ and H-1″. Thus, the

structure of TMM10 was determined to be tyrosol-1-*O*-*β*-xylopyranosyl-(1→6)-*O*-*β*-glucopyranoside, which is a new phenolic glycoside.

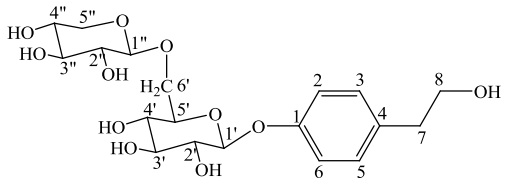

[**95**]

Table 16 NMR spectral data of compound TMM10 (DMSO-d_6)

Position	Compound TMM10		HMBC (correlation with ^{1}H)
	^{1}H (mult., *J* in Hz)	^{13}C	
1	-	155.7	2, 3*, 5*, 6, 1′
2	6.95 (d, 8.6)	116.2	3*, 6
3	7.10 (d, 8.6)	129.7	2*, 5, 7
4	-	132.7	2, 6, 7*, 8
5	7.10 (d, 8.6)	129.7	3, 6*, 7
6	6.95 (d, 8.6)	116.2	2, 5*
7	2.64 (t, 6.5)	38.2	3, 5, 8*
8	3.54 (t, 6.5)	62.4	7*
1′	4.73 (d, 7.3)	100.7	5′
2′	3.22 (m)	73.2	3′*
3′	3.22 (m)	76.5	1′
4′	3.14 (t, 8.8)	69.6	2′, 3′*, 5′*, 6′$_b$
5′	3.48 (dd, 8.8, 6.6)	75.8	1′, 6′$_a$*
6′$_a$	3.55 (dd, 10.9, 6.6)	68.2	-
6′$_b$	3.93 (dd, 10.9, 8.8)	-	5′*, 1″
1″	4.17 (d, 7.6)	103.8	5″$_a$, 5″$_b$, 6′$_a$, 6′$_b$
2″	2.96 (dd, 8.7, 7.6)	73.4	1″*, 3″*
3″	3.06 (t, 8.7)	76.5	2″*, 5″$_a$, 5″$_b$

* Two-bond coupling

Table 16 NMR spectral data of compound TMM10 (DMSO-d_6) (continued)

Position	Compound TMM10		HMBC (correlation with ^{1}H)
	^{1}H (mult., *J* in Hz)	^{13}C	
4″	3.22 (m)	69.6	2″, 3″*, 5″$_a$*, 5″$_b$*
5″$_a$	2.94 (t, 11.3)	65.6	-
5″$_b$	3.65 (dd, 11.3, 5.3)	-	1″

* Two-bond coupling

1.11 Structure determination of compound LMM1

Compound LMM1 was obtained as a colorless oil. The positive HRESI mass spectrum (Figure 78) exhibited an $[M+H]^+$ ion at *m/z* 281.1593, suggesting the molecular formula $C_{19}H_{20}O_2$. The UV spectrum (Figure 79) showed three absorption maxima at 212, 229 and 283 nm, and the IR spectrum (Figure 80) exhibited absorption bands for conjugated unsaturation (1513 and 1484 cm^{-1}), and ether (1237 cm^{-1}) functionalities.

The ^{1}H-NMR (Figure 81, Table 17) and the ^{13}C-NMR (Figure 82, Table 17) spectral data exhibited signals similar to those of TMM1 [**87**], except for the presence of allyl group instead of (*E*)-propenyl group at C-5 (δ 132.2). The ^{1}H-NMR spectrum showed signals for ring C of the *trans*-2-aryl-3-methyl-2,3-dihydrobenzofuran system (Achenbach *et al*., 1987) at δ 5.11 (1H, d, *J* = 9.1 Hz, H-2), 3.43 (1H, apparent quint, *J* = 7.9 Hz, H-3) and 1.41 (3H, d, *J* = 6.8 Hz, CH_3-3). This was supported by the proton correlations in ^{1}H-^{1}H COSY spectrum (Figure 83) and the NOE interaction of CH_3-3 protons with H-2 in the NOESY spectrum (Figure 84). There was an ABM spin system of ring B at 7.00 (1H, br d, *J* = 9.3 Hz, H-6), 6.98 (1H, br s, H-4) and 6.80 (1H, d, *J* = 9.3 Hz, H-7), and a pair of doublets for ring A protons appeared at δ 7.38 (2H, d, *J* = 8.7 Hz, H-2′, H-6′) and 6.94 (2H, d, *J* = 8.7 Hz, H-3′, H-5′). The signals for the allyl moiety showed at δ 6.00 (1H, ddt, *J* = 16.9, 9.3, 6.7 Hz, H-9), 5.11 (1H, br dd, *J* = 16.9, 1.7 Hz, H-10b), 5.08 (1H, br dd, *J* = 9.3, 1.7 Hz, H-10a) and 3.38 (2H, br d, *J* = 6.7 Hz, H_2-8).

The ^{13}C-NMR spectrum showed the presence of two methyl, two methylene, ten methine carbons. HSQC (Figure 85) and HMBC (Figure 86, Table 17) experiments were carried out to establish the structure. The quaternary carbon at C-1′ (δ 132.4) was correlated to the proton H-2; C-3a (δ 132.7) was correlated to H-2, H-3, CH_3-3; C-7a (δ 157.6) was correlated to H-2 and C-5 was correlated to H-8 and H-9. Thus, compound LMM1 was identified as 5-allyl-2-(4-methoxyphenyl)-3-methyl-2,3-dihydrobenzofuran.

The value of the optical rotation of compound LMM1 was similar to that of compound TMM1, i.e. the negative ($[\alpha]_D^{20}$ –25.0). It is known that a *trans*-2-aryl-3-methyl-2,3-dihydrobenzofuran structure with 2*R*,3*R* configuration shows a positive Cotton effect at about 260 nm or shows a negative Cotton effect at about 281 nm and positive Cotton effect at about 233 nm in the CD spectrum (Achenbach *et al*., 1987). In this study, compound LMM1 showed a positive Cotton effect at 284 nm and negative Cotton effect at 238 nm (Figure 87), indicating the 2*S*,3*S* absolute configuration.

Hence, compound LMM1 was identified as a new dihydrobenzofuran neolignan, and its structure was characterized as (2*S*,3*S*)-5-allyl-2-(4-methoxy-phenyl)-3-methyl-2,3-dihydrobenzofuran [**96**].

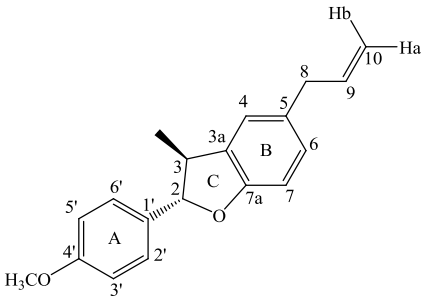

[**96**]

Table 17 NMR spectral data of compound LMM1 ($CDCl_3$)

Position	Compound LMM1		HMBC (correlation with ^1H)
	^1H (mult., *J* in Hz)	^{13}C	
2	5.11 (d, 9.1)	92.6	3*, CH_3-3, 2′, 6′
3	3.43 (apparent quint, 7.9)	45.4	CH_3-3*, 2*, 4
3a	-	132.7	2, 3*, CH_3-3, 7
4	6.98 (br s)	123.7	6, 8
5	-	132.2	7, 8*, 9
6	7.00 (br d, 9.3)	128.3	4, 7*, 8
7	6.80 (d, 9.3)	109.2	6*
7a	-	157.6	2, 4, 6, 7*
8	3.38 (br d, 6.7)	39.8	4, 6, 9*, 10
9	6.00 (ddt, 16.9, 9.3, 6.7)	138.1	8*
10_a	5.08 (br dd, 9.3, 1.7)	115.4	8
10_b	5.11 (br dd, 16.9, 1.7)	-	-
1′	-	132.4	3′, 5′
2′	7.38 (d, 8.7)	127.7	2, 3′*, 6′
3′	6.94 (d, 8.7)	114.0	2′*, 5′
4′	-	159.6	2′, 3′*, 5′*, 6′, CH_3O
5′	6.94 (d, 8.7)	114.0	3′, 6′*
6′	7.38 (d, 8.7)	127.7	2, 2′, 5′*
CH_3-3	1.41 (d, 6.8)	17.7	2, 3*
CH_3O	3.84 (s)	55.3	-

* Two-bond coupling

1.12 Structure determination of compound LMM2

Compound LMM2 gave an $[M+Na]^+$ ion at *m/z* 363.1578 in the HRESI mass spectrum (Figure 88), indicating a molecular formula of $C_{21}H_{24}O_4$. The UV spectrum (Figure 89) showed absorption maxima at 228 and 273 nm, and the IR spectrum (Figure 90) demonstrated absorption bands for carbonyl (1734 cm^{-1}), conjugated unsaturation (1507 cm^{-1}), and ether (1227 cm^{-1}) functionalities.

The ^{1}H-NMR spectrum (Figure 91, Table 18) showed two pairs of doublets appearing at δ 7.33 (2H, d, *J* = 8.7 Hz, H-2 and H-6) and 6.91 (2H, d, *J* = 8.7 Hz, H-3 and H-5), and at δ 7.12 (2H, d, *J* = 8.7 Hz, H-2′ and H- 6′) and 6.91 (2H, d, *J* = 8.7 Hz, H-3′ and H-5′). The ^{13}C-NMR spectrum of LMM2 (Figure 92, Table 18) showed a twenty-one carbon structure with two *p*-disubstituted benzene rings. In the HSQC spectrum (Figure 93), two tertiary oxygenated carbon signals at δ 77.7 (C-7) and 76.2 (C-8) showed direct coupling with protons at δ 5.89 (1H, d, *J* = 7.2 Hz, H-7) and 4.61 (1H, apparent quint, *J* = 6.5 Hz, H-8), respectively. These two methine protons (H-7 and H-8) constituted an ABX coupling system with the CH_3 protons at δ 1.15 (3H, d, *J* = 6.4 Hz, CH_3-9) in the ^{1}H-^{1}H COSY spectrum (Figure 94).

In the HMBC spectrum, H-7 exhibited 3-bond coupling with C-2/6 (δ 128.9) and the carbonyl of the acetoxy moiety [(δ_C 170.2 (OO<u>C</u>CH_3) and 21.2 (OOC<u>CH_3</u>); δ_H 2.02 (3H, s, OOC<u>CH_3</u>)], whereas H-8 showed HMBC connectivity to C-4′ (δ 156.7) through an ether linkage (Figure 95, Table 18). Compound LMM2 possessed a methoxy group (δ_H 3.83, 3H, s; δ_C 55.3) at C-4 (δ 159.6) and an allyl moiety [(δ_H 3.35 (2H, br d, *J* = 6.7 Hz, H-7′), 5.07 (1H, br dd, *J* = 10.1, 1.7 Hz, H-9′a), 5.09 (1H, br dd, *J* = 17.0, 1.7 Hz, H-9′b) and 5.97 (1H, ddt, *J* = 17.0, 10.1, 6.7 Hz, H-8′); δ_C 39.4, 115.5 and 137.8)] at C-1′ (δ_C 132.7). The HMBC showed the correlation of CH_3O protons to C-4, which in turn showed ^{3}J-coupling with H-2 and H-6. In accordance with this proposed structure, HMBC correlations were observed from C-1′ to H-3′/5′ and H-7′. The above spectral data suggested that LMM2 was an acetyl derivative of TMM3 [**89**]. It is known that for neolignans of this skeleton, the large coupling constant (*J* = 7.2 Hz) for H-7 and H-8 suggests a *threo* relative configuration (Braga *et al*., 1984). The relative configuration of this compound was indicated from the NOESY interaction of H-7 with H-8 (Figure 96). The absolute configuration was then determined by comparison the CD data with those of ligraminol C (Kim *et al*., 2011). The CD spectrum (Figure 97) exhibited negative peaks at 278 and 230 nm, respectively. Based on the above evidences, the structure of compound LMM2 was identified as (7*R*,8*R*)-*threo*-$\Delta^{8'}$-7-acethoxy-4-methoxy-8.O.4′-neolignan [**97**]. It is a new 8.O.4′ neolignan.

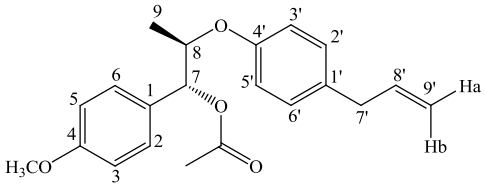

[**97**]

Table 18 NMR spectral data of compound LMM2 ($CDCl_3$)

Position	Compound LMM2		HMBC (correlation with ^1H)
	^1H (mult., *J* in Hz)	^{13}C	
1	-	129.3	3, 5, 8
2	7.33 (d, 8.7)	128.9	6
3	6.91 (d, 8.7)	113.9	5
4	-	159.6	2, 3*, 5*, 6, CH_3O
5	6.91 (d, 8.7)	113.9	3
6	7.33 (d, 8.7)	128.9	2
7	5.89 (d, 7.2)	77.7	2, 6, 8, 9, COO
8	4.61 (apparent quint, 6.5)	76.2	7*, 9*
9	1.15 (d, 6.5)	16.4	7, 8*
1′	-	132.7	3′, 5′, 7′
2′	7.12 (d, 8.7)	129.6	3′*, 6′, 7′
3′	6.91 (d, 8.7)	116.2	2′*, 5′
4′	-	156.7	8, 2′, 3′, 5′, 6′
5′	6.91 (d, 8.7)	116.2	3′, 6′*
6′	7.12 (d, 8.7)	129.6	2′, 5′*, 7′
7′	3.35 (br d, 6.7)	39.4	2′, 6′, 9′
8′	5.97 (ddt, 17.0, 10.1, 6.7)	137.8	7′*
$9'_a$	5.07 (br dd, 10.1, 1.7)	115.5	7′*
$9'_b$	5.09 (br dd, 17.0, 1.7)	-	-
COO	-	170.2	7, $OOCCH_3$*
$OOCCH_3$	2.02 (s)	21.2	-
CH_3O	3.83 (s)	55.3	-

* Two-bond coupling

1.13 Structure determination of compound LMM3

Compound LMM3 gave an $[M+Na]^+$ ion at *m/z* 319.1321 in the HRESI mass spectrum (Figure 98), indicating a molecular formula of $C_{19}H_{20}O_3$. The UV spectrum (Figure 99) showed absorption maxima at 208, 233 and 283 nm, and the IR spectrum (Figure 100) demonstrated absorption bands for hydroxyl (3431 cm^{-1}), conjugated unsaturation (1515 and 1484 cm^{-1}), and ether (1234 cm^{-1}) functionalities.

The ^{1}H-NMR (Figure 101, Table 19) and ^{13}C-NMR (Figure 102, Table 19) spectra of compound LMM3 exhibited the signals similar to that of compound TMM2 [**88**], except for presence of an allyl moiety in place of (*E*)-propenyl moiety. The *trans*-2-aryl-3-methyl-2,3-dihydrobenzofuran system (Achenbach *et al*., 1987) was supported by the NOESY (Figure 103) interactions of CH_3-3 protons with H-2. The allyl group [δ_H 5.98 (1H, ddt, *J* = 17.8, 11.6, 6.8 Hz, H-9), 5.09 (1H, br dd, *J* = 17.8, 1.8 Hz, H-10b), 5.03 (1H,br dd, *J* = 11.6, 1.8 Hz, H-10a) and 3.35 (2H, br d, *J* = 6.8 Hz, H-8); δ_C 138.5 (C-9), 114.6 (C-10) and 39.5 (C-8)] was located at C-5 (δ 132.2). This was supported by the HMBC correlation from H-4 [δ 7.03 (1H, br s)] and H-6 [δ 6.99 (1H, br d, *J* = 8.1 Hz)] to C-8, and C-5 to H-7, H-8 and H-9. In addition, the ^{1}H-^{1}H COSY, HSQC and HMBC correlations (Figures 104-106) were consistent with the proposed structure. Compound LMM3 exhibited a positive optical rotation ($[\alpha]_D^{20}$+8.57), and the CD spectrum (Figure 87) of LMM3 showed a negative and a positive Cotton effect at 290 nm and 240 nm, respectively, indicating the *2R,3R* configuration (Achenbach *et al*., 1987). The structure of compound LMM3 was characterized as (*2R,3R*)-5-allyl-2-(4-hydroxy-3-methoxyphenyl)-3-methyl-2,3-dihydrobenzofuran [**98**], which is a new dihydrobenzofuran neolignan.

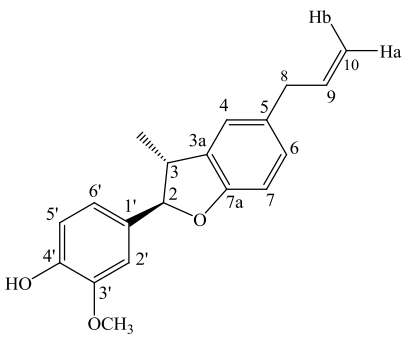

[**98**]

Table 19 NMR spectral data of compound LMM3 (acetone-d_6)

Position	Compound LMM3		HMBC (correlation with ^{1}H)
	^{1}H (mult., *J* in Hz)	^{13}C	
2	5.07 (d, 9.1)	92.8	3*, CH_3-3, 2′, 6′
3	3.41 (apparent quint, 7.9)	45.3	2*, 4, CH_3-3*
3a	-	132.5	2, 3*, CH_3-3, 7
4	7.03 (br s)	123.8	3, 6, 8
5	-	132.2	7, 8*, 9
6	6.99 (br d, 8.1)	128.1	4, 8
7	6.73 (d, 8.1)	108.8	6*
7a	-	157.8	2, 4, 6, 7*
8	3.35 (br d, 6.8)	39.5	4, 6, 9*, 10
9	5.98 (ddt, 17.8, 11.6, 6.8)	138.5	8*
10_a	5.03 (br dd, 11.6, 1.8)	114.6	8
10_b	5.09 (br dd, 17.8, 1.8)	-	-
1′	-	132.2	2*, 3, 2′*, 5′
2′	7.10 (d, 1.7)	109.7	2, 6′
3′	-	147.6	2′, CH_3O
4′	-	146.7	2′, 5′*, 6′
5′	6.87 (d, 8.1)	114.8	-
6′	6.92 (dd, 8.1, 1.7)	119.4	2, 2′
CH_3-3	1.37 (d, 6.8)	17.0	2, 3*
CH_3O	3.84 (s)	55.4	-

* Two-bond coupling

1.14 Structure determination of compound LMM4

Compound LMM4 was obtained as a colorless oil. The negative HRESI mass spectrum (Figure 107) exhibited an $[M\text{-}H]^-$ ion at *m/z* 265.1225, suggesting the molecular formula $C_{18}H_{18}O_2$. The UV spectrum (Figure 108) showed three absorption maxima at 209, 230 and 285 nm, and the IR spectrum (Figure 109) demonstrated

absorption bands for hydroxyl (3392 cm^{-1}), conjugated unsaturation (1517 and 1485 cm^{-1}) and ether (1237 cm^{-1}) functionalities.

The ^{1}H-NMR (Figure 110, Table 20) and ^{13}C-NMR (Figure 111, Table 20) spectral data showed characteristic features of the *trans*-2-aryl-3-methyl-2,3-dihydrobenzofuran system (Achenbach *et al*., 1987): H-2 [δ_H 5.10 (1H, d, J = 8.8 Hz); δ_C 92.5], H-3 [δ_H 3.43 (1H, apparent quint, J = 7.7 Hz); δ_C 45.3] and CH_3-3 [δ_H 1.41 (3H, d, J = 6.8 Hz); δC 17.7], two pairs of *ortho*-coupled signals for H-2′/H-6′ [δ_H 7.32 (2H, d, J = 8.7 Hz); δ_C 127.9] and H-3′/H-5′ [δ_H 6.85 (2H, d, J = 8.7 Hz); δ_C 115.4], an ABM aromatic spin system of H-6 [δ_H 7.00 (1H, br d, J = 9.2 Hz); δ_C 128.2], H-4 [δ_H 6.99 (1H, br s); δ_C 123.7] and H-7 [δ_H 6.79 (1H, d, J = 9.2 Hz); δ_C 109.1], and an allyl moiety [H-10_b [δ_H 5.11 (1H, br dd, J = 16.9, 1.7 Hz); δ_C 115.4], H-10_a [δ_H 5.04 (1H,br dd, J = 9.9, 1.7 Hz); δ_C 115.4], H-9 [δ_H 6.00 (1H, ddt, J = 16.9, 9.9, 6.8 Hz); δ_C 138.1] and H-8 [δ_H 3.38 (2H, br d, J = 6.8 Hz); δ_C 39.8]]. The above spectral data of compound LMM4 were closely similar to those of compound LMM1, except for the absence of methoxy signals. The placement of the hydroxyl group in compound LMM4 was confirmed by HMBC correlation from H-2′/H-6′ [δ 7.32 (1H, d, J = 8.7 Hz)] and H-3′/H-5′ [δ 6.85 6.85 (1H, d, 8.7)] to C-4′ (δ 155.7) as shown in Figure 112 and Table 20. In addition, the ^{1}H-^{1}H COSY (Figure 113), HSQC (Figure 114) and the other HMBC (Figure 112, Table 20) correlations supported the proposed structure.

The relative configuration at C-2 (δ 92.8) and C-3 (δ 45.3) was determined as *trans* due to the large coupling constant (J = 9.1 Hz) between H-2 (1H, d, J = 9.1 Hz) and H-3 (1H, apparent quint, J = 7.9 Hz). These data were supported by the correlation peak between H-2 [δ 5.07 (1H, d, J = 9.1 Hz)] and CH_3-3 [δ 1.37 (3H, d, 6.8)] in the NOESY spectrum (Figure 115). Compound LMM4 showed optical and CD properties (Figure 87) similar to those of compound LMM3. It exhibited a positive optical rotation ($[\alpha]_D^{20}$+32.35). The CD spectrum showed a negative Cotton effect at 290 nm and a positive Cotton effect at 236 nm, indicating the *2R,3R* absolute configuration (Achenbach *et al*., 1987). The structure of compound LMM4 was identified to be (*2R,3R*)-5-allyl-2-(4-hydroxyphenyl)-3-methyl-2,3-dihydrobenzofuran [**99**], which is a new dihydrobenzofuran neolignan.

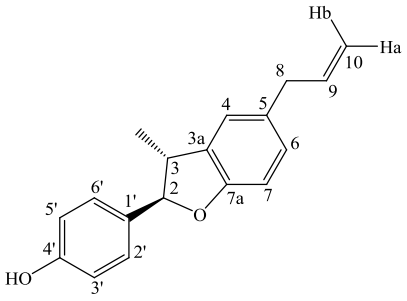

[**99**]

Table 20 NMR spectral data of compound LMM4 ($CDCl_3$)

Position	Compound LMM4		HMBC (correlation with ^1H)
	^1H (mult., *J* in Hz)	^{13}C	
2	5.10 (d, 8.8)	92.5	3*, CH_3-3, 2′, 6′
3	3.43 (apparent quint, 7.7)	45.3	2*, 4*, CH_3-3*
3a	-	132.7	2, 3*, CH_3-3, 7
4	6.99 (br s)	123.7	3, 6, 8
5	-	132.2	7, 8*, 9
6	7.00 (br d, 9.2)	128.2	4, 7*, 8
7	6.79 (d, 9.2)	109.1	4, 6*
7a	-	157.5	4, 6, 7*
8	3.38 (br d, 6.8)	39.8	4, 6, 9*, 10
9	6.00 (ddt, 16.9, 9.9, 6.8)	138.1	8*
10_a	5.04 (br dd, 9.9, 1.7)	115.4	8
10_b	5.11 (br dd, 16.9, 1.7)	-	-
1′	-	132.4	2*, 3′, 5′
2′	7.32 (d, 8.7)	127.9	2, 3′*, 6′
3′	6.85 (d, 8.7)	115.4	5′
4′	-	155.7	2′, 3′*, 5′*, 6′
5′	6.85 (d, 8.7)	115.4	3′
6′	7.32 (d, 8.7)	127.9	2, 2′, 5′*
CH_3-3	1.41 (d, 6.8)	17.7	2, 3*

*Two-bond coupling

1.15 Structure determination of compound LMM5

Compound LMM5 obtained as a colorless oil. The positive HRESI mass spectrum (Figure 116) exhibited an $[M+Na]^+$ ion at *m/z* 319.1304 which accorded to the molecular formula $C_{19}H_{20}O_3$. The UV spectrum (Figure 117) showed three absorption maxima at 211, 228 and 280 nm, and the IR spectrum (Figure 118) demonstrated absorption bands for hydroxyl (3408 cm^{-1}), conjugated unsaturation (1516 and 1494 cm^{-1}) and ether (1205 and 1138 cm^{-1}) functionalities.

The ^{1}H-NMR (Figure 119, Table 21) and ^{13}C-NMR (Figure 120, Table 21) spectral data showed the *trans*-2-aryl-3-methyl-2,3-dihydrobenzofuran system (Achenbach *et al*., 1987): H-2 [δ_H 5.13 (1H, d, J = 9.6 Hz); δ_C 93.2], H-3 [δ_H 3.46 (1H, apparent quint, J = 7.5 Hz); δ_C 45.8] and CH_3-3 [δ_H 1.39 (3H, d, J = 6.8 Hz); δC 17.7], two pairs of *ortho*-coupled signals for H-2′/H-6′ [δ_H 7.32 (2H, d, J = 8.6 Hz); δ_C 128.2] and H-3′/H-5′ [δ_H 6.83 (2H, d, J = 8.6 Hz); δ_C 115.3] indicating the *p*-substituted benzene ring, two methine protons of H-6 [δ_H 6.64 (1H, br s); δ_C 111.8] and H-4 [δ_H 6.62 (1H, br s); δ_C 115.7] suggesting the presence of the 1,3,4,5-tetrasubstituted ring, a methoxyl group [δ_H 3.89 (3H,s); δ_C 56.0], and an allyl moiety [H-10_b [δ_H 5.13 (1H, br dd, J = 16.7, 1.7 Hz); δ_C 115.6], H-10_a [δ_H 5.08 (1H,br dd, J = 11.4, 1.7 Hz); δ_C 115.4], H-9 [δ_H 6.00 (1H, ddt, J = 16.7, 11.4, 6.8 Hz); δ_C 137.9] and H-8 [δ_H 3.38 (2H, br d, J = 6.8 Hz); δ_C 40.2]]. The spectral data of compound LMM5 were similar to those of compound LMM4, except that compound LMM5 showed two methine signals of H-6 and H-4 instead of an ABM aromatic spin system of compound LMM4. The methoxy group [δ 3.89 (3H, s)] was located at C-7 as indicated from the HMBC correlation from the protons of OCH_3 at δ 3.89 to C-7 (δ 144.0), and from H-6 to C-7 (Figure 121, Table 21). Moreover, the ^{1}H-^{1}H COSY (Figure 122), HSQC (Figure 123) and the other HMBC (Figure 121, Table 21) correlations were in excellent agreement with the proposed structure.

The relative configuration at C-2 (δ 93.2) and C-3 (δ 45.8) was determined as *trans* from the coupling constant (J = 9.1 Hz) between H-2 [δ 5.13 (1H, d, J = 9.6 Hz)] and H-3 [δ 3.46 (1H, apparent quint, J = 7.5 Hz)]. The *trans* correlation were supported by the cross peak of H-2 and CH_3-3 [δ 1.39 (3H, d, J = 6.8 Hz)] in the NOESY spectrum (Figure 124). The absolute configuration of compound LMM5 was

determined from the optical rotation and the CD spectrum. Compound LMM5 showed a positive optical rotation ($[\alpha]_D^{20}$+15.71) and its CD curve (Figure 87) exhibited a negative Cotton effect at 286 nm and a positive Cotton effect at 242 nm, which were similar to those of (2*R*,3*R*)-2,3-dihydro-2-(4-hydroxyphenyl)-7-methoxy-3-methyl-5-(*E*)-propenylbenzofuran (Achenbach *et al*., 1987). The structure of **5** was determined as (2*R*,3*R*)-5-allyl-2-(4-hydroxyphenyl)-7-methoxy-3-methyl-2,3-dihydrobenzofuran [**100**]. It is a new dihydrobenzofuran neolignan.

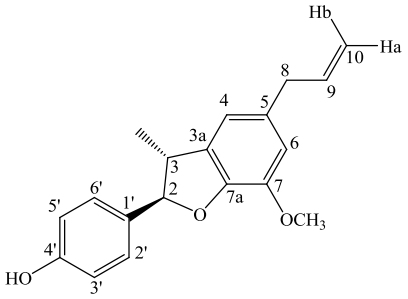

[**100**]

Table 21 NMR spectral data of compound LMM5 ($CDCl_3$)

Position	Compound LMM5		HMBC (correlation with ^1H)
	^1H (mult., *J* in Hz)	^{13}C	
2	5.13 (d, 9.6)	93.2	3*, CH_3-3, 2′, 6′
3	3.46 (apparent quint, 7.5)	45.8	2*, CH_3-3*, 4
3a	-	133.1	3*, CH_3-3, 4*
4	6.62 (br s)	115.7	3, 6, 8
5	-	133.5	8*, 9
6	6.64 (br s)	111.8	4, 8
7	-	144.0	6*, CH_3O
7a	-	145.7	2, 4, 6
8	3.38 (br d, 6.8)	40.2	4, 6, 9*, 10
9	6.00 (ddt, 16.7, 11.4, 6.8)	137.9	8*
10_a	5.08 (br dd, 11.4, 1.7)	115.6	8
10_b	5.13 (br dd, 16.7, 1.7)	-	-

* Two-bond coupling

Table 21 NMR spectral data of compound LMM5 ($CDCl_3$) (continued)

Position	Compound LMM5		HMBC (correlation with ^1H)
	^1H (mult., *J* in Hz)	^{13}C	
1′	-	132.6	2*, 3, 3′, 5′
2′	7.32 (d, 8.6)	128.2	2, 6′
3′	6.83 (d, 8.6)	115.3	5′
4′	-	155.6	2′, 3′*, 5′*, 6′
5′	6.83 (d, 8.6)	115.3	3′
6′	7.32 (d, 8.6)	128.2	2, 2′
CH_3-3	1.39 (d, 6.8)	17.7	2, 3*
CH_3O	3.89 (s)	56.0	-

* Two-bond coupling

1.16 Structure determination of compound LMM6

Compound LMM6 was obtained as colorless oil. The negative ESI mass spectrum (Figure 125) exhibited an $[M-H]^-$ ion at *m/z* 253, suggesting the molecular formula $C_{16}H_{14}O_3$. The UV spectrum (Figure 126) showed absorption maxima at 209, 229 and 294 nm.

The ^1H-NMR spectrum (Figure 127, Table 22) showed signals for the *trans*-2-aryl-3-methyl-2,3-dihydrobenzofuran system (Achenbach *et al*., 1987) at δ 5.24 (1H, d, *J* = 8.7 Hz, H-2), 3.49 (1H, apparent quint, *J* = 7.7 Hz, H-3) and 1.45 (3H, d, *J* = 6.8 Hz, CH_3-3), the *ortho*-coupled doublets (*J* = 8.7 Hz) at δ 7.29 (1H, d, H-2′ and H-6′) and 6.91 (1H, d, H-3′ and H-5′) indicating the presence of *p*-substituted benzene ring, an ABM aromatic spin system at δ 7.75 (1H, br d, *J* = 8.4 Hz, H-6) 7.74 (1H, d, *J* = 1.3 Hz, H-4) and 6.95 (1H, d, *J* = 8.4 Hz, H-7), and an aldehyde proton at δ 9.87 (1H, s, C<u>H</u>O). The ^{13}C-NMR spectrum (Figure 128, Table 22) showed sixteen signals, which included one methyl carbon, ten methine carbons and five quaternary carbons.

The relative *trans* configuration at C-2 (δ 94.0) and C-3 (δ 44.3) was determined from the coupling constant (*J* = 8.7 Hz) between H-2 and H-3. These data were supported by the cross peak of H-2 and CH_3-3 in the NOESY spectrum (Figure 129). The absolute configuration of compound LMM6 was determined from the

optical rotation and the CD spectrum. Compound LMM6 showed a positive optical rotation ($[\alpha]_D^{20}$ +77.0) and its CD curve (Figure 87) exhibited a negative Cotton effect at 288 nm and a positive Cotton effect at 236 nm, which indicated 2*R*,3*R* configuration (Achenbach *et al*., 1987).

The above data of compound LMM6 were in excellent agreement with previously reported values for decurrenal [**101**] (Chauret *et al*., 1996).

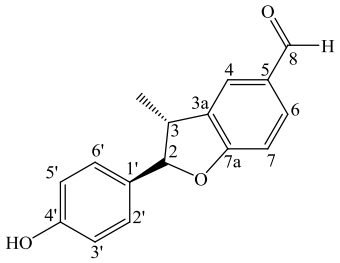

[**101**]

Table 22 NMR spectral data of compound LMM6 ($CDCl_3$) as compared with decurrenal (pyridine-d_6)

Position	Compound LMM6		Decurrenal*	
	^1H (mult., *J* in Hz)	^{13}C	^1H (mult., *J* in Hz)	^{13}C
2	5.24 (d, 8.7)	94.0	4.85 (d, 8.7)	93.65
3	3.49 (apparent quint, 7.7)	44.3	3.01 (apparent quint, 7.4)	44.32
3a	-	133.8	-	133.61
4	7.74 (d, 1.3)	124.7	7.54 (d, 1.2)	124.42
5	-	130.5	-	131.08
6	7.75 (d, 8.4)	133.8	7.36 (dd, 8.2, 1.2)	133.37
7	6.95 (d, 8.4)	109.9	6.67 (d, 8.2)	109.49
7a	-	164.9	-	164.70
8	9.87 (s)	191.3	9.65 (s)	189.93
1′	-	131.4	-	131.69
2′	7.29 (d, 8.7)	127.9	6.98 (d, 8.5)	128.04
3′	6.91 (d, 8.7)	115.7	6.60 (d, 8.5)	115.50
4′	-	156.4	-	156.69

* Chauret *et al*., 1996

Table 22 NMR spectral data of compound LMM6 ($CDCl_3$) as compared with decurrenal (pyridine-d_6) (continued)

Position	Compound LMM6		Decurrenal*	
	^1H (mult., *J* in Hz)	^{13}C	^1H (mult., *J* in Hz)	^{13}C
5′	6.91 (d, 8.7)	115.7	6.60 (d, 8.5)	115.50
6′	7.29 (d, 8.7)	127.9	6.98 (d, 8.5)	128.04
CH_3-3	1.45 (d, 6.8)	17.9	0.91 (d, 6.8)	17.26

1.17 Structure determination of compound LMM7

Compound LMM7 was obtained as a white amorphous powder. The positive HRESI mass spectrum (Figure 130) exhibited an $[M+Na]^+$ ion at *m/z* 305.1158 which corresponded to the molecular formula $C_{18}H_{18}O_3$. The UV spectrum (Figure 131) showed three absorption maxima at 207, 229 and 284 nm, and the IR spectrum (Figure 132) demonstrated absorption bands for hydroxyl (3378 cm^{-1}), carbonyl (1704 cm^{-1}), conjugated unsaturation (1517 and 1485 cm^{-1}) and ether (1237 cm^{-1}) functionalities.

The ^1H-NMR (Figure 133, Table 23) and ^{13}C-NMR (Figure 134, Table 23) spectral data showed characteristic features of the *trans*-2-aryl-3-methyl-2,3-dihydrobenzofuran system (Achenbach *et al*., 1987): H-2 [δ_H 5.09 (1H, d, *J* = 9.2 Hz); δ_C 92.8], H-3 [δ_H 3.40 (1H, apparent quint, *J* = 7.0 Hz); δ_C 45.2] and CH_3-3 [δ_H 1.37 (3H, d, *J* = 6.8 Hz); δC 17.6], two pairs of *ortho*-coupled signals for H-2′/H-6′ [δ_H 7.29 (2H, d, *J* = 8.5 Hz); δ_C 127.9] and H-3′/H-5′ [δ_H 6.84 (2H, d, *J* = 8.5 Hz); δ_C 115.4], and an ABM aromatic spin system of H-6 [δ_H 7.01 (1H, br d, *J* = 7.9 Hz); δ_C 129.3], H-4 [δ_H 6.98 (1H, br s); δ_C 124.6] and H-7 [δ_H 6.81 (1H, d, *J* = 7.9 Hz); δ_C 109.6]. These data of compound LMM7 was similar to those of compound LMM4. In addition, the ^1H and ^{13}C-NMR data suggested an 2-oxopropyl moiety [δ_H 3.69 (2H, s, H-8) and 2.22 (3H, s, H-10); δ_C 208.4 (C-9), 50.5 (C-8) and 29.3 (C-10)] at C-5, which was confirmed by the HMBC correlation from H-8 to C-6 (δ 129.3), C-5(δ 126.3) and C-4 (δ 124.6), and from H-6 [δ 7.01 (1H, d, *J* = 7.9 Hz)] and H-4 [δ 6.98

(1H, br s)] to C-8 (Figure 135, Table 23). Moreover, the ^{1}H-^{1}H COSY (Figure 136), HSQC (Figure 137) and the other HMBC (Figure 135, Table 23) correlations confirmed the proposed structure. However, compound LMM7 showed 2-oxopropyl moiety in place of allyl moiety in compound LMM4.

The structure of compound LMM7 should have relative *trans* configuration at C-2 (δ 92.8) and C-3 (δ 45.2) due to the large coupling constant (J = 9.2 Hz) between H-2 and H-3. These data were supported by the cross-peak of H-2 and CH_3-3 in the NOESY spectrum (Figure 138). The structure of compound LMM7 showed positive optical rotation ($[\alpha]_D^{20}$ +32.35), and showed a negative Cotton effect at 290 nm and a positive Cotton effect at 236 nm in the CD curve (Figure 87). Compound LMM7 was determined as (*2R,3R*)-2-(4-hydroxyphenyl)-3-methyl-5-(2-oxopropyl)-2,3-dihydro-benzofuran [**102**]. It is a new dihydrobenzofuran neolignan.

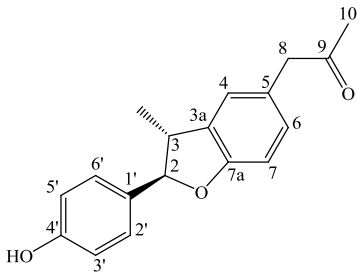

[**102**]

Table 23 NMR spectral data of compound LMM7 ($CDCl_3$)

Position	Compound LMM7		HMBC (correlation with ^{1}H)
	^{1}H (mult., J in Hz)	^{13}C	
2	5.09 (d, 9.2)	92.8	3*, CH_3-3, 2′, 6′
3	3.40 (apparent quint, 7.0)	45.2	2*, CH_3-3*
3a	-	132.8	3*, 7, CH_3-3
4	6.98 (br s)	124.6	3, 6, 8
5	-	126.3	7, 8*
6	7.01 (d, 7.9)	129.3	4, 8
7	6.81 (d, 7.9)	109.6	-

* Two-bond coupling

Table 23 NMR spectral data of compound LMM7 ($CDCl_3$) (continued)

Position	Compound LMM7		HMBC (correlation with ^1H)
	^1H (mult., *J* in Hz)	^{13}C	
7a	-	158.3	4, 6, 7*
8	3.69 (s)	50.5	4, 6
9	-	208.4	8*, 10*
10	2.22 (s)	29.3	-
1′	-	132.2	2*, 3′, 5′
2′	7.29 (d, 8.5)	127.9	2, 6′
3′	6.84 (d, 8.5)	115.5	5′
4′	-	156.1	2′, 3′*, 5′*, 6′
5′	6.84 (d, 8.5)	115.5	3′
6′	7.29 (d, 8.5)	127.9	2, 2′
CH_3-3	1.37 (d, 6.8)	17.6	2, 3*

* Two-bond coupling

1.18 Structure determination of compound LMF1

Compound LMF1 was obtained as a colorless oil. The HRESI mass spectrum (Figure 139) showed a pseudomolecular ion at *m/z* 395.1456 $[M+Na]^+$ $C_{21}H_{24}O_6Na$, which corresponded to the molecular formula $C_{21}H_{24}O_6$. The UV spectrum (Figure 140) showed absorptions at 220 and 275 nm. The IR spectrum (Figure 141) showed absorption bands for hydroxyl (3438 cm^{-1}), conjugated unsaturation (1506 and 1454 cm^{-1}), and ether (1211 and 1121 cm^{-1}) functionalities.

Compound LMF1 showed the characteristic NMR chemical shifts of the benzodioxane neolignan at δ 5.10 (1H, d, *J* = 2.3 Hz, H-7), 4.62 (1H, dq, *J* = 2.3, 6.6 Hz, H-8) and 1.15 (3H, d, *J* = 6.6 Hz, H-9), and δ 76.8 (C-7), 73.1 (C-8) and 12.6 (C-9) in its ^1H-NMR (Figure 142, Table 24) and ^{13}C-NMR (Figure 143, Table 24) spectra (Motter Mogri, Kato and Yoshida 1996). The ^1H-NMR spectrum also exhibited two sets of *meta*-coupled protons at δ 6.65 (1H, d, *J* = 1.8 Hz, H-6), 6.56 (1H, d, *J* = 1.8 Hz, H-2), 6.53 (1H, d, *J* = 1.9 Hz, H-2′) and 6.40 (1H, d, *J* = 1.9 Hz, H-6′), indicating

the presence of two 1,3,4,5-tetrasubstituted aromatic rings. The linkage point of the substituent on the 1,4 dioxane moiety in compound LMF1 was determined by the HMBC correlation (Figure 144, Table 24) from H-7 to C-3′ (δ 143.3) and H-8 to C-4′ (δ 129.5). The presence of three methoxy groups [δ 3.87 (3H, s) and 3.86 (6H, s)] at C-3 (δ 152.5), C-4 (δ 135.1) and C-5′ (δ 149.2) was supported by the HMBC correlation (Figure 144, Table 24). In addition, an allyl moiety [δ_H 3.33 (2H, br d, J = 6.8 Hz, H-7′), 5.98 (1H, ddt, J = 16.1, 10.2, 6.8 Hz, H-8′), 5.10 (1H, br dd, J = 10.2, 1.6 Hz, H-9′a) and 5.13 (1H, br dd, J = 16.1, 1.6 Hz, H-9′b); δ_C 40.0 (C-7′), 137.4 (C-8′) and 115.9 (C-9′)] was located at C-1′ (δ 132.2), which was confirmed by the HMBC correlation between C-1′ to H-7′ (Figure 144, Table 24). Moreover, the ^{1}H-^{1}H COSY and HSQC correlation (Figure 145-146) supported the proposed structure.

The *cis*-arrangement of methyl and aryl groups on the benzodioxane ring was evidenced by the signal of CH_3-9 (δ_H 1.15) and $J_{H7,\ H8}$ (2.3 Hz) (Fernandes *et al*., 1980), and the NOESY spectrum (Figure 147) exhibited a cross peak between H-7 and H-8. The absolute configurations at C-7 and C-8 were determined from the circular dichroism (CD) spectrum. The *cis*-series with *S*,*R* configuration show a negative Cotton effect at about 246 nm, while the other configuration (*R*,*S*) show a positive Cotton effect at about 247 nm. In the case of *trans*-series, compounds with *R*,*R* configuration show a negative Cotton effect at about 242 nm those with and *S*,*S* configuration exhibit a positive Cotton effect at about 242 nm (Silva *et al*., 1989). The structure of compound LMF1 exhibited a negative Cotton effect at 246 nm (Figure 148), which indicated the 7*S*,8*R* configuration. Based on the above data, the structure of compound LMF1 was identified to be (7*S*,8*R*)-$\Delta^{8'}$-5-hydroxy-3,4,5′-trimethoxy-7.O.3′,8.O.4′-neolignan [**103**], which is a new 7.O.3′,8.O.4′-neolignan.

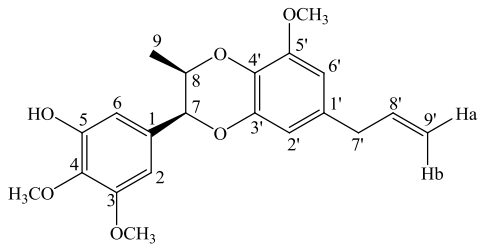

[**103**]

Table 24 NMR spectral data of compound LMF1 ($CDCl_3$)

Position	Compound LMF1		HMBC (correlation with ^1H)
	^1H (mult., *J* in Hz)	^{13}C	
1	-	133.0	7*
2	6.56 (d, 1.8)	101.9	6, 7
3	-	152.5	2*, CH_3O-3
4	-	135.1	2, 6, CH_3O-4
5	-	149.3	-
6	6.65 (d, 1.8)	105.9	2, 7
7	5.10 (d, 2.3)	76.8	2, 6, 9
8	4.62 (dq, 2.3, 6.6)	73.1	7*, 9*
9	1.15 (d, 6.6)	12.6	7
1′	-	132.2	7′*
2′	6.53 (d, 1.9)	109.7	6′, 7′
3′	-	143.3	7, 2′*
4′	-	129.5	8, 2′, 6′
5′	-	149.2	6′*, CH_3O-5′
6′	6.40 (d, 1.9)	104.9	2′, 7′
7′	3.33 (br d, 6.8)	40.1	2′, 6′, 8′*, 9′
8′	5.98 (ddt, 16.1, 10.2, 6.8)	137.4	7′*, 9′*
$9'_a$	5.10 (br dd, 10.2, 1.6)	115.9	7′
$9'_b$	5.13 (br dd, 16.1, 1.6)	-	-
CH_3O-3	3.86 (s)	56.1	-
CH_3O-4	3.87 (s)	61.0	-
CH_3O-5′	3.86 (s)	56.0	-

* Two-bond coupling

1.19 Structure determination of compound LMF2

Compound LMF2 was isolated as a colorless oil. The positive HRESI mass spectrum (Figure 149) exhibited an $[M+Na]^+$ ion at *m/z* 395.1473, indicating the molecular formula $C_{21}H_{24}O_6$, which was same as that of compound LMF1. The UV spectrum (Figure 150) showed absorptions at 215 and 276 nm. The IR spectrum (Figure 151) showed absorption bands for hydroxyl (3436 cm^{-1}), conjugated unsaturation (1506 and 1455 cm^{-1}), and ether (1213 and 1117 cm^{-1}) functionalities.

The ^{1}H-NMR (Figure 152, Table 25) and ^{13}C-NMR (Figure 153, Table 25) spectra of compound LMF2 were very similar to those of compound LMF1, (7*S*,8*R*)-$\Delta^{8'}$-5-hydroxy-3,4,5′-trimethoxy-7.O.3′,8.O.4′-neolignan [**103**], except that H-2 and H-6 had the same chemical shift [δ_H 6.60 (2H, br s); δ_C 102.8]. In addition, the HMBC correlation between each of the methoxy signals [δ_H 3.88 (6H, s); δ_C 56.4] and aromatic carbons at δ 147.1 (C-3/5) indicated the position of the methoxy groups at C-3 and C-5 (Figure 154, Table 25). Moreover, the ^{1}H-^{1}H COSY (Figure 155), HSQC (Figure 156) and the other HMBC (Figure 154, Table 25) correlations confirmed the proposed structure. The spectral data of compound LMF2 appeared to be closely related to those reported for synthetic (±) eusiderin K [**122**] (Jing *et al*., 2001), except for the downfield shift of the *cis*-protons of H-7 [δ 5.08 (1H, d, *J* = 2.4 Hz)] and H-8 [δ 4.56 (1H, dq, *J* = 2.4, 6.6 Hz)]. Additionally, the NOESY spectrum also exhibited a cross-peak between H-7 and H-8 (Figure 157).

The CD spectrum (Figure 148) of compound LMF2 exhibited a negative Cotton effect at 248 nm, which indicated the 7*S*,8*R* configuration, similar to compound LMF1. The structure of compound LMF2 was characterized as (7*S*,8*R*)-$\Delta^{8'}$-4-hydroxy-3,5,5′-trimethoxy-7.O.3′,8.O.4′-neolignan [**104**]. It is a new 7.O.3′,8.O.4′-neolignan.

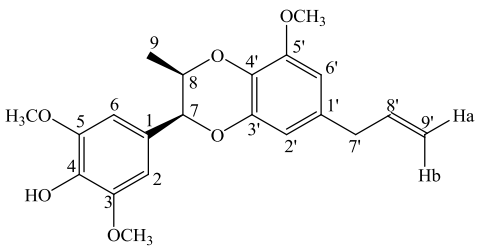

[**104**]

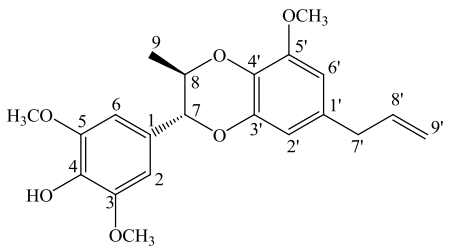

[**122**]

Table 25 NMR spectral data of compound LMF2 ($CDCl_3$)

Position	Compound LMF2		HMBC (correlation with ^1H)
	^1H (mult., *J* in Hz)	^{13}C	
1	-	128.0	2*, 6*, 7*
2	6.60 (br s)	102.8	6, 7
3	-	147.1	2*, CH_3O-3
4	-	134.4	2, 6
5	-	147.1	CH_3O-5, 6*
6	6.60 (br s)	102.8	2, 7
7	5.08 (d, 2.4)	77.0	2, 6, 9
8	4.56 (dq, 2.4, 6.6)	73.4	7*, 9*
9	1.11 (d, 6.6)	12.5	7, 8*
1′	-	132.2	7′*, 8′
2′	6.50 (d, 1.9)	109.7	6′, 7′
3′	-	143.4	7, 2′*
4′	-	129.5	8, 2′, 6′
5′	-	149.2	6′*, CH_3O-5′
6′	6.37 (d, 1.9)	104.9	2′, 7′
7′	3.29 (br d, 6.8)	40.1	2′, 6′, 8′*, 9′
8′	5.94 (ddt, 17.0, 10.0, 6.8)	137.4	7′*, 9′
$9'_a$	5.10 (br dd, 10.0, 1.9)	115.9	7′
$9'_b$	5.12 (br dd, 17.0, 1.9)	-	-
CH_3O-3	3.88 (s)	56.4	-
CH_3O-5	3.88 (s)	56.4	-
CH_3O-5′	3.87 (s)	56.1	-

* Two-bond coupling

1.20 Structure determination of compound LMF3

Compound LMF3 was obtained as a colorless oil. The HRESI mass spectrum (Figure 158) showed an $[M+Na]^+$ ion at *m/z* 351.1568, indicating a molecular formula of $C_{20}H_{24}O_4$. The UV spectrum (Figure 159) showed absorption maxima at 210, 229 and 281 nm, and the IR spectrum (Figure 160) demonstrated absorption bands for hydroxyl (3441 cm^{-1}), conjugated unsaturation (1514 and 1464 cm^{-1}), and ether (1268 and 1232 cm^{-1}) functionalities.

The ^{1}H-NMR (Figure 161Table 26) and the ^{13}C-NMR (Figure 162, Table 26) spectra showed two sets of ABM spin system [H-5 [δ_H 6.85 (1H, d, *J* = 8.2 Hz); δ_C 114.0], H-2 [δ_H 6.83 (1H, d, *J* = 1.9 Hz); δ_C 112.2] and H-6 [6.75 (1H, dd, *J* = 8.2, 1.9 Hz); δ_C 122.1], H-3′ [δ_H 6.80 (1H, br d, *J* = 8.1 Hz); δ_C 116.1], H-6′ [δ_H 6.73 (1H, br s); δ_C 112.6] and H-2′ [δ_H 6.70 (1H, dd, *J* = 8.1, 1.7 Hz); δ_C 120.5]. The ^{1}H-NMR spectrum also exhibited an allyl moiety [δ 5.98 (1H, ddt, *J* = 17.1, 10.0, 6.7 Hz, H-8′), 5.10 (1H, br dd, *J* = 17.1, 1.6 Hz, H-9′b), 5.08 (1H, br dd, *J* = 10.0, 1.6 Hz, H-9′a) and 3.35 (2H, br d, *J* = 6.7 Hz, H-7′)], and two methoxy groups [δ 3.88 (3H, s); and 3.85 (3H, s)]. In the HSQC spectrum (Figure 163), tertiary oxygenated carbon and methylene signals appearing at δ 76.9 (C-8) and 42.4 (C-7) showed direct coupling with protons at δ 4.46 (1H, apparent sext, *J* = 6.2 Hz, H-8), 3.11 (1H, dd, *J* = 13.7, 6.0 Hz, H-7_b) and 2.77 (1H, dd, *J* =13.7, 6.7 Hz, H-7_a), respectively. These methine and methylene protons constituted an ABX coupling system with the CH_3 protons at δ 1.32 (3H, d, *J* = 6.1 Hz, CH_3-9) in the COSY spectrum (Figure 164). The allyl moiety was present at C-1′, which was supported by the HMBC correlations (Figure 165, Table 26) from H-7′ and H-8′ to C-1′ (δ 133.3), and from H-2′ and H-6′ to C-7′ (δ 39.9). In addition, the HMBC correlations (Figure 165, Table 26) between two methoxy signals at δ 3.88 and 3.85, and aromatic carbons at δ 146.2 and 150.4, respectively, indicated the position of methoxy group at C-5′ and C-3. The NMR spectroscopic data of compound LMF3 showed close similarity with those of 2-(4-allyl-2,6-dimethoxyphenoxy)-1-(4-hydroxy-3-methoxyphenyl) propane (Hattori *et al*., 1987) [**123**] except for the absence of the methoxyl group at C-3′. This compound showed a negative optical rotation ($[\alpha]_D^{20}$ –20), and its CD curve (Figure 166) showed negative Cotton effects at 276 and 240 nm. From the above data the structure of

compound LMF3 was identified as 2-methoxy-4-[2-[2-methoxy-4-(2-propen-1-yl)phenoxy]propyl]phenol [**105**]. It had been reported in Scifinder as commercially available, but its isolation has never been reported. Hence, it is a new natural product.

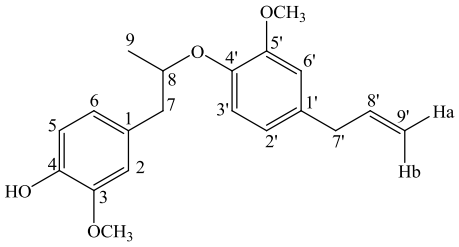

[**105**]

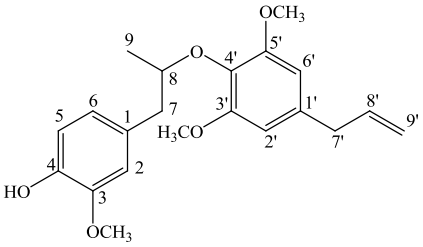

[**123**]

Table 26 NMR spectral data of compound LMF3 ($CDCl_3$)

Position	Compound LMF3		HMBC (correlation with ^1H)
	^1H (mult., *J* in Hz)	^{13}C	
1	-	130.5	5, 7*, 8
2	6.83 (d, 1.9)	112.2	6, 7
3	-	146.2	2*, 5, CH_3O-3
4	-	144.0	2, 5*, 6
5	6.85 (d, 8.2)	114.0	-
6	6.75 (dd, 8.2, 1.9)	122.1	2, 7
7_a	2.77 (dd, 13.7, 6.7)	42.4	2, 6, 8*, 9
7_b	3.11 (dd, 13.7, 6.0)	-	-
8	4.46 (apparent sext, 6.2)	76.9	7*,9 *
9	1.32 (d, 6.1)	19.5	7
1′	-	133.3	3′, 7′*, 8′
2′	6.70 (dd, 8.1, 1.7)	120.5	6′, 7′
3′	6.80 (br d, 8.1)	116.1	-
4′	-	145.6	8, 2′, 3′*, 6′
5′	-	150.4	3′, 6′*, CH_3O-5′
6′	6.73 (br s)	112.6	2′, 7′

* Two-bond coupling

Table 26 NMR spectral data of compound LMF3 ($CDCl_3$) (continued)

Position	Compound LMF3		HMBC (correlation with ^1H)
	^1H (mult., *J* in Hz)	^{13}C	
7′	3.35 (br d, 6.7)	39.9	2′, 6′, 8′*, 9′
8′	5.98 (ddt, 17.1, 10.0, 6.7)	137.2	7′*
$9'_a$	5.08 (br dd, 10.0, 1.6)	116.0	7′
$9'_b$	5.10 (br dd, 17.1, 1.6)	-	-
CH_3O-3	3.88 (s)	55.9	-
CH_3O-5′	3.85 (s)	55.8	-

* Two-bond coupling

1.21 Structure determination of compound LMF4

Compound LMF4 was obtained as a white solid. The positive ESI mass spectrum (Figure 167) exhibited an $[M+Na]^+$ ion at *m/z* 349.03, suggesting the molecular formula $C_{20}H_{22}O_4$. The UV spectrum (Figure 168) showed the absorption maxima at 211 and 278 nm.

The ^1H-NMR spectrum (Figure 169, Table 27) of compound LMF4 showed the *trans*-2-aryl-3-methyl-2,3-dihydrobenzofuran system (Achenbach *et al*., 1987): δ 5.12 (1H, d, *J* = 9.1 Hz, H-2), 3.47 (1H, m, H-3) and 1.40 (3H, d, *J* = 6.8 Hz, CH_3-3), an ABM aromatic spin system at δ 7.00 (1H, br s, H-2′) and 6.92 (2H, br s, H-5′, H-6′), two methine aromatic signals at δ 6.81 (1H, br s, H-6) and 6.79 (1H, br s, H-4). It also showed two methoxy groups at δ 3.91 (3H, s) and 3.90 (3H, s), and the 1(*E*)-propenyl moiety at 6.39 (1H, br d, *J* = 15.8 Hz, H-8), 6.13 (1H, dq, *J* = 15.8, 6.6 HZ, H-9) and 1.89 (3H, d, *J* = 6.6 Hz, H-10).

The ^{13}C-NMR spectrum (Figure 170, Table 27) exhibited twenty carbons, including four methyl carbons, nine methine carbons and seven quarternary carbons.

The structure of compound LMF4 showed the relative *trans* configuration at C-2 (δ 93.8) and C-3 (δ 45.6) due to the large coupling constant (*J* = 9.1 Hz) between H-2 and H-3. These data correlations were supported by the cross-peak of H-2 and CH_3-3 in the NOESY spectrum (Figure 171). The structure of compound LMF4

showed positive optical rotation ($[\alpha]_D^{20}$+22.2), and showed a positive Cotton effect at 266 nm and a negative Cotton effect at 238 nm in the CD curve (Figure 172). This indicated the 2*R*,3*R* configuration (Achenbach *et al*., 1987). Compound LMF4 was determined as licarin A [**106**] by comparison of its NMR data with previously reported values NMR data (Achenbach *et al*., 1987).

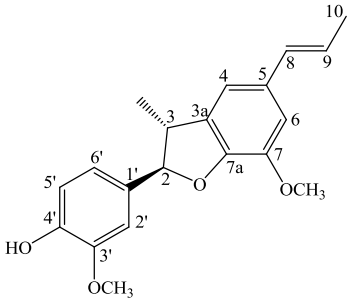

[**106**]

Table 27 NMR spectral data of compound LMF4 ($CDCl_3$) as compared with licarin A ($CDCl_3$)

Position	Compound LMF4		Licarin A*	
	^1H (mult., *J* in Hz)	^{13}C	^1H (mult., *J* in Hz)	^{13}C
2	5.12 (d, 9.1)	93.8	5.05 (d, 9.3)	93.02
3	3.47 (m)	45.6	3.38 (m)	46.25
3a	-	133.3	-	134.41
4	6.79 (br s)	113.3	6.77-7.07 (m)	114.43
5	-	132.2	-	133.00
6	6.81 (br s)	109.1	6.77-7.07 (m)	111.41
7	-	144.2	-	145.10
7a	-	146.6	-	147.86
8	6.39 (br d, 15.8)	130.9	6.31 (br d, 16.0)	132.12
9	6.13 (dq, 15.8, 6.6)	123.5	5.89-6.26 (m)	123.31
10	1.89 (d, 6.6)	18.4	1.81 (br d, 5.1)	18.48
1′	-	132.1	-	132.94
2′	7.00 (br s)	108.9	6.77-7.07 (m)	110.83

* Achenbach *et al*., 1987

Table 27 NMR spectral data of compound LMF4 ($CDCl_3$) as compared with licarin A ($CDCl_3$) (continued)

Position	Compound LMF4		Licarin A*	
	^1H (mult., *J* in Hz)	^{13}C	^1H (mult., *J* in Hz)	^{13}C
3′	-	146.7	-	148.44
4′	-	145.8	-	147.60
5′	6.92 (br s)	114.1	6.77-7.07 (m)	114.37
6′	6.92 (br s)	120.0	7.30 (d, 8.5)	119.58
CH_3-3	1.40 (d, 6.8)	17.5	1.33 (d, 6.8)	18.03
CH_3O-7	3.91 (s)	55.9	3.81 (s)	56.43
CH_3O-3′	3.90 (s)	56.0	3.81 (s)	56.53

* Achenbach *et al*., 1987

1.22 Structure determination of compound LMF5

Compound LMF5 gave an $[M-H]^-$ ion at *m/z* 341.1392 in the HRESI mass spectrum (Figure 173), indicating a molecular formula of $C_{20}H_{21}O_5$. The UV spectrum (Figure 174) showed absorption maxima at 215 and 281 nm, and the IR spectrum (Figure 175) demonstrated absorption bands for hydroxyl (3440 cm^{-1}), conjugated unsaturation (1509 and 1453 cm^{-1}), and ether (1225, 1149 and 1103cm^{-1}) functionalities.

The ^1H-NMR (Figure 176, Table 28) and the ^{13}C-NMR (Figure 177, Table 28) spectra of compound LMF5 showed signals for a 1,3,4-trisubstituted benzene ring [δ_H 6.96 (1H, d, *J* = 8.6 Hz, H-5), 6.89 (1H, dd, *J* = 8.6, 1.7 Hz, H-6) and 6.88 (1H, br s, H-2); δ_C 114.5 (C-5), 121.0 (C-6), 109.5 (C-2)], and two *meta*-coupled signals [δ_H 6.58 (1H, d, *J* = 1.7 Hz, H-2′) and 6.40 (1H, d, *J* = 1.7 Hz, H-6′); δ_C 109.6 (C-2′), 104.5 (C-6′)]. In the HSQC spectrum (Figure 178), two tertiary oxygenated carbon signals appearing at δ 80.9 (C-7) and 74.2 (C-8) showed direct coupling with protons at δ 4.59 (1H, d, *J* = 7.9 Hz, H-7) and 4.12 (1H, dq, *J* = 7.9, 6.4 Hz, H-8), respectively. These two methine protons constituted an ABX coupling system with

the CH_3 protons at δ 1.25 (3H, d, J = 6.4 Hz, CH_3-9) in the ^1H-^1H COSY spectrum (Figure 179).

The HMBC spectrum (Figure 180, Table 28) was examined to confirm the structure but it was not useful in identifying which substituents are located at the C-7 and C-8 positions on the 1,4-benzodioxane ring since there was no HMBC correlation from H-7 or H-8 to C-3′ (δ 144.5) or C-4′ (δ 131.3). This drawback of HMBC had been earlier observed in neolignans (Takahasi *et al*., 2003). In order to overcome this problem, NMR measurement techniques, such as the long-range selective proton-decoupling (LSPD) technique (Takahasi *et al*., 2003) and change of the NMR solvent (Kim *et al*., 2005) had to be used to elucidate the structure of the neolignan. The linkage point of the substituent on the 1,4-dioxane moiety in compound LMF5 was verified unequivocally from HMBC spectrum taken in acetone-d_6 (Figure 181, Table 28) in place of $CDCl_3$ (Figure 180, Table 28), which demonstrated a clear correlation from H-7 to C-3′ (Figure 181, Table 28). In addition, the HMBC experiment indicated the methoxyl groups (δ 3.88 and 3.81) at C-5′ and C-3, respectively by the observation of correlations of C$\underline{H}_3$O (δ 3.88) to C-5′ (δ 148.6), and from H-6′ to C-5′. The C$\underline{H}_3$O (δ 3.81) protons exhibited long-range correlation to C-3 (δ 146.9), and HMBC connectivities was observed from H-2 and H-5 to C-3 (Figure 180, Table 28). The allyl moiety was present at C-1′, which was supported by the HMBC correlation from H-7′ and H-8′ to C-1′ (δ 132.4), from H-2′ and H-6′ to C-7′ (δ 40.0), and from H-7′ to C-2′ (δ 109.5) and C-6′ (δ 104.5) (Figure 180, Table 28).

The *trans* relationship between H-7 and H-8 was determined by the large coupling constant (J = 7.9 Hz) and the NOESY interaction between H-7/CH_3-9 (Figure 182). The absolute configuration at C-7 and C-8 were determined from a negative Cotton effect at 238 nm (Figure 148), which suggested the *R*,*R* configuration (Silva *et al*., 1989). From the above data, compound LMF5 showed a different from (7*S*,8*R*)-4-hydroxy-3,5′-dimethoxy-Δ:1,3,5,1′,3′,5′,7′-7.O.3′,8.O.4′-neolignan [**124**] (Motter Mogri, Kato and Yoshida 1996) in the *trans*-orientation of H-7/H-8. This structure of compound LMF5 was characterized as (7*R*,8*R*)-$\Delta^{8'}$-4-hydroxy-3,5′-dimethoxy-7.O.3′,8.O.4′-neolignan [**107**]. It is a new benzodioxane neolignan.

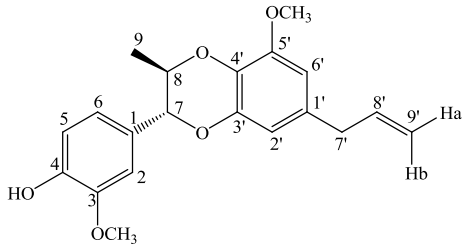

[**107**]

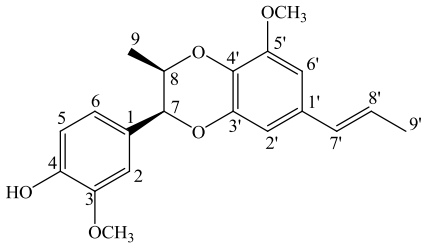

[**124**]

Table 28 NMR spectral data of compound LMF5 ($CDCl_3$ and acetone-d_6)

Position	Compound LMF5				HMBC (correlation with ^1H)
	$^1H^a$ (mult., *J* in Hz)	$^1H^b$ (mult., *J* in Hz)	$^{13}C^a$	$^{13}C^b$	
1	-	-	128.9	128.9	2^c*, 5^c, 6^c*, 7^c*, 8^c
2	6.88 (br s)	7.07 (d, 1.4)	109.5	110.8	6^c, 7^c
3	-	-	146.9	147.7	CH_3O-3^c, 5^c
4	-	-	146.2	147.1	2^c, 6^c
5	6.96 (d, 8.6)	6.90 (br s)	114.5	114.9	-
6	6.89 (dd, 8.6, 1.7)	6.90 (br sd, 1.7)	121.0	120.7	2^c, 7^c
7	4.59 (d, 7.9)	4.58 (d, 7.9)	80.9	80.7	2^c, 6^c, 8^c*, 9^c
8	4.12 (dq, 7.9, 6.4)	4.10 (dq, 7.9, 6.4)	74.2	73.7	7^c*, 9^c*
9	1.25 (d, 6.4)	1.15 (d, 6.4)	17.3	16.7	7^c, 8^c*
1′	-	-	132.4	131.9	$7'^c$*, 8′
2′	6.58 (d, 1.7)	6.38 (d, 1.8)	109.6	109.3	$6'^c$, $7'^c$
3′	-	-	144.5	144.7	$2'^c$*, 7^c
4′	-	-	131.3	131.7	8^a, $2'^c$, $6'^c$
5′	-	-	148.6	148.9	$6'^c$, CH_3O-$5'^c$
6′	6.40 (d, 1.7)	6.45 (d, 1.8)	104.5	104.9	$2'^c$, $7'^c$

* Two-bond coupling

[a] Observed in $CDCl_3$, [b] Observed in acetone-d_6, [c] Observed in $CDCl_3$ and acetone-d_6

Table 28 NMR spectral data of compound LMF5 ($CDCl_3$ and acetone-d_6) (continued)

Position	Compound LMF5				HMBC (correlation with ^1H)
	$^1H^a$ (mult., *J* in Hz)	$^1H^b$ (mult., *J* in Hz)	$^{13}C^a$	$^{13}C^b$	
7′	3.31 (br d, 6.8)	3.28 (d, 6.8)	40.0	39.7	2′[c], 6′[c], 8′[c]*, 9′[c]
8′	5.97 (ddt, 16.7, 9.0, 6.8)	5.96 (ddt, 17.0, 10.1, 6.8)	137.4	137.9	7′[c]*, 9′[c]*
9′a	5.08 (br dd, 9.5, 1.6)	5.02 (br dd, 10.0, 2.1)	115.8	114.9	7′[c], 8′[c]
9′b	5.12 (br dd, 16.7, 1.6)	5.09 (br dd, 17.0, 2.1)	-	-	-
CH_3O-3	3.81 (s)	3.81 (s)	56.1	55.5	-
CH_3O-5′	3.88 (s)	3.88 (s)	56.0	55.4	-

* two-bond coupling
[a] Observed in $CDCl_3$, [b] Observed in acetone-d_6, [c] Observed in $CDCl_3$ and acetone-d_6

1.23 Structure determination of compound LMF6

Compound LMF6 was isolated as a colorless oil. The positive ESI mass spectrum (Figure 183) exhibited an $[M+Na]^+$ ion at *m*/*z* 379.06, indicating the molecular formula $C_{21}H_{24}O_5$. The UV spectrum (Figure 184) showed absorptions at 215 and 279 nm.

The ^{1}H-NMR (Figure 185, Table 29) and the ^{13}C-NMR (Figure 186, Table 29) spectra of compound LMF1 showed the characteristic signals for a benzodioxane neolignan at δ 5.14 (1H, d, *J* = 2.3 Hz, H-7), 4.61 (1H, dq, *J* = 2.3, 6.6 Hz, H-8) and 1.15 (3H, d, *J* = 6.6 Hz, H-9); and δ 77.0 (C-7), 73.2 (C-8) and 12.7 (C-9) (Motter Mogri, Kato and Yoshida 1996), similar to those of compounds LMF1, LMF2 and LMF5. Additional NMR data included an ABM aromatic spin system of H-2 [δ_H 6.95 (1H, br s); δ_C 111.0], H-6 [δ_H 6.94 (1H, br d, *J* = 8.9 Hz); δ_C 118.6] and H-5 [δ_H 6.88 (1H, d, *J* = 8.9 Hz); δ_C 109.3], a pair of meta-coupled protons of H-2′ [δ 6.52 (1H, d, *J*

= 1.7 Hz)] and H-6′ [δ 6.40 (1H, d, *J* = 1.7 Hz)], three methoxy groups [δ 3.91 (3H, s), 3.90 (3H, s) and 3.89 (3H, s)], and allyl moiety [H-8′ at δ_H 5.98 (1H, ddt, *J* = 16.3, 10.0, 6.8 Hz); δ_C 137.4, H-9′b at 5.11 (1H, br dd, *J* = 16.3, 1.7 Hz); δC 115.8, H-9′a at δ_H 5.09 (1H, br dd, *J* = 10.0, 1.7 Hz); δ_C 115.8, and H-7′ at δ_H 3.32 (2H, d, *J* = 6.8 Hz); δ_C 40.1].

The *cis*-arrangement of the methyl and the aryl group on the benzodioxane ring was evidenced by the signal of CH_3-9 (δ_H 1.15) and $J_{H7, H8}$ (2.3 Hz) (Fernandes *et al*., 1980). The absolute configurations at C-7 and C-8 were determined from the CD spectrum, which exhibited a negative Cotton effect at 246 nm (Figure 147) (Silva *et al*., 1989) and indicated to be 7*S*,8*R* configuration.

Based on the above data, compound LMF6 was identified as eusiderin D [**108**], and confirmed by the comparison with previously reported data (Fernandes *et al*., 1980).

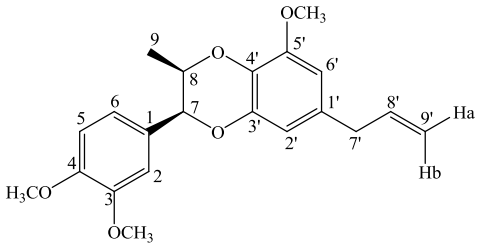

[**108**]

Table 29 NMR spectral data of compound LMF6 ($CDCl_3$) as compared with eusiderin D ($CDCl_3$)

Position	Compound LMF6		Eusiderin D*	
	^1H (mult., *J* in Hz)	^{13}C	^1H (mult., *J* in Hz)	^{13}C
1	-	129.4	-	129.5
2	6.95 (br s)	111.0	6.94 (d, 1.5)	111.2
3	-	149.0	-	149.1
4	-	148.7	-	148.9
5	6.88 (d, 8.9)	109.3	6.87 (d, 8.5)	109.5
6	6.94 (br d, 8.9)	118.6	6.93 (d, 8.5)	118.7

* Fernandes *et al*., 1980

Table 29 NMR spectral data of compound LMF6 ($CDCl_3$) as compared with eusiderin D ($CDCl_3$) (continued)

Position	Compound LMF6		Eusiderin D*	
	^1H (mult., *J* in Hz)	^{13}C	^1H (mult., *J* in Hz)	^{13}C
7	5.14 (d, 2.3)	77.0	5.10 (d, 2.0)	77.1
8	4.61 (dq, 2.3, 6.6)	73.2	4.59 (dq, 2.5, 6.5)	73.2
9	1.15 (d, 6.6)	12.7	1.15 (d, 6.5)	12.7
1′	-	132.2	-	132.5
2′	6.52 (d, 1.7)	109.7	6.52 (d, 1.5)	109.8
3′	-	143.5	-	143.5
4′	-	129.6	-	132.3
5′	-	149.1	-	149.2
6′	6.40 (d, 1.7)	104.8	6.40 (d, 1.5)	105.1
7′	3.32 (d, 6.8)	40.1	3.31 (d, 7.0)	40.1
8′	5.98 (ddt, 16.3, 10.0, 6.8)	137.4	5.98 (ddt, 17.0, 10.6, 6.5)	137.5
$9'_a$	5.09 (br dd, 10.0, 1.7)	115.8	5.20-5.10 (m)	115.9
$9'_b$	5.11 (br dd, 16.3, 1.7)	-	-	-
CH_3O-3	3.90 (s)	56.0	3.98 (s)	56.0
CH_3O-4	3.89 (s)	55.9	3.98 (s)	56.0
CH_3O-5′	3.91 (s)	56.1	3.89 (s)	56.1

* Fernandes *et al*., 1980

1.24 Structure determination of compound LMF7

Compound LMF7 was obtained as a colorless oil. The positive ESI mass spectrum (Figure 187) of compound LMF7 showed a pseudomolecular ion at *m*/*z* 381.13 $[M+Na]^+$ $C_{21}H_{26}O_5Na$, which corresponded to the molecular formula $C_{21}H_{26}O_5$. The UV spectrum (Figure 188) showed absorption maxima at 209, 230 and 279 nm. The ^1H-NMR spectrum (Figure 189, Table 30) showed two sets of ABM aromatic protons spin system [δ 6.84 (1H, br s, H-2), 6.99 (1H, br s, H-5), 6.77 (1H, d, *J* = 5.8 Hz, H-6); 6.99 (1H, d, *J* = 8.5 Hz, H-2′), 6.84 (1H, br s, H-3′) and 6.78 (1H,

br s, H-6′). In addition, the ^{1}H-NMR spectrum suggested three methoxyl groups [δ 3.90 (3H, s), 3.89 (3H, s) and 3.88 (3H, s)], and an allyl moiety [δ 5.99 (1H, ddt, *J* = 16.9, 10.2, 6.7 Hz, H-8′), 5.14 (1H, br dd, *J* = 16.9, 1.7 Hz, H-9′$_b$), 5.10 (1H,br dd, *J* = 10.2, 1.7 Hz, H-9′a) and 3.38 (2H, br d, *J* = 6.7 Hz, H-7′)]. The ^{13}C-NMR spectrum (Figure 190, Table 30) showed twenty-one carbons including four methyl carbons, two methylene carbons, nine methine carbons and six quaternary carbons. The HSQC correlation (Figure 191) also supported the correlation between the protons and carbons in the structure.

The small coupling constant value (*J* = 3.1 Hz) for H-7 [δ 4.85 (2H, d, *J* = 3.1 Hz)] and H-8 [δ 4.34 (1H, dq, *J* = 3.1, 6.4 Hz)], suggested an *erytho* relative configuration (Braga *et al*., 1984, Huo *et al*., 2008). The NOESY spectrum (Figure 192) also showed the correlation peak between H-7 and H-8. On the basis of the negative peaks at 240 and 276 nm in the CD spectrum (Figure 193), the absolute configurations at C-7 and C-8 of compound LMF7 were established as 7*S*,8*R* (Huo *et al*., 2008).

From the above data, the structure of compound LMF7 was determined as (7*S*,8*R*)-*erythro*-hydroxy-3,4,3′-trimethoxy-$\Delta^{1,3,5,1',3',5',8'}$-8.O.4′-neolig- nan [**109**], which had been earlier reported as *rel*-(7*S*,8*R*)-*erythro*-7-hydroxy-3,4,3′-trimethoxy-$\Delta^{1,3,5,1',3',5',8'}$-8.O.4′-neolignan (Morais *et al*., 2009).

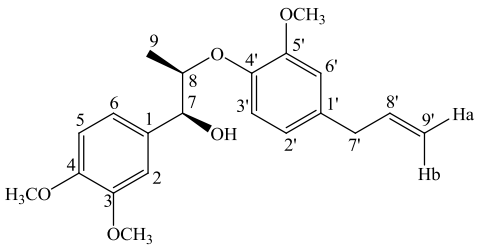

[**109**]

Table 30 NMR spectral data of compound LMF7 ($CDCl_3$) as compared with *rel*-(7*S*,8*R*)-*erythro*-7-hydroxy-3,4,3′-trimethoxy-$\Delta^{1,3,5,1',3',5',8'}$-8.O.4′-neo-lignan ($CDCl_3$)

Position	Compound LMF7		*rel*-(7*S*,8*R*)-*erythro*-7-hydroxy-3,4,3′-trimethoxy-$\Delta^{1,3,5,1',3',5',8'}$-8.O.4′-neolignan*	
	^{1}H (mult., *J* in Hz)	^{13}C	^{1}H (mult., *J* in Hz)	^{13}C
1	-	132.5	-	132.5
2	6.84 (br s)	110.7	7.00-6.75 (m)	110.7
3	-	148.1	-	148.1
4	-	151.4	-	151.4
5	6.99 (br s)	109.4	7.00-6.75 (m)	109.4
6	6.77 (d, 5.8)	121.1	7.00-6.75 (m)	121.1
7	4.85 (d, 3.1)	73.4	4.84 (d, 2.6)	73.4
8	4.34 (dq, 3.1, 6.4)	82.6	4.33 (m)	82.5
9	1.19 (d, 6.4)	13.5	1.18 (d, 6.6)	13.5
1′	-	135.6	-	135.5
2′	6.99 (d, 8.5)	120.0	7.00-6.75 (m)	119.9
3′	6.84 (br s)	118.4	7.00-6.75 (m)	118.4
4′	-	144.8	-	144.7
5′	-	148.8	-	148.8
6′	6.78 (br s)	112.4	7.00-6.75 (1H, m)	112.4
7′	3.38 (br d, 6.7)	40.0	3.37 (d, 7.0)	39.9
8′	5.99 (ddt, 16.9, 10.2, 6.7)	137.3	5.98 (ddt, 6.6, 10.3, 16.6)	137.2
$9'_a$	5.10 (br dd, 10.2, 1.7)	116.0	5.16-5.07 (m)	115.9
$9'_b$	5.14 (br dd, 16.9, 1.7)	-	-	-

* Morais *et al*., 2009

Table 30 NMR spectral data of compound LMF7 ($CDCl_3$) as compared with *rel*-(7*S*,8*R*)-*erythro*-7-hydroxy-3,4,3′-trimethoxy-$\Delta^{1,3,5,1',3',5',8'}$-8.O.4′-neolignan ($CDCl_3$) (continued)

Position	Compound LMF7		*rel*-(7*S*,8*R*)-*erythro*-7-hydroxy-3,4,3′-trimethoxy-$\Delta^{1,3,5,1',3',5',8'}$-8.O.4′-neolignan*	
	^1H (mult., *J* in Hz)	^{13}C	^1H (mult., *J* in Hz)	^{13}C
CH_3O-3	3.90 (s)	55.9	3.90 (s)	55.8
CH_3O-4	3.88 (s)	55.8	3.88 (s)	55.8
CH_3O-5′	3.89 (s)	55.9	3.89 (s)	55.8

* Morais *et al*., 2009

1.25 Structure determination of compound LMF8

Compound LMF8 showed spectroscopic properties (^1H, ^{13}C NMR, Mass and UV data) identical with those of compound TMM5. Therefore, it was identified as (−)-epicatechin [**91**].

1.26 Structure determination of compound SMF1

Compound SMF1 was obtained as a colorless oil. The positive ESI mass spectrum (Figure 194) exhibited an $[M+Na]^+$ ion at *m/z* 395.10, suggesting the molecular formula $C_{22}H_{28}O_5$. The UV spectrum (Figure 195) showed absorption maxima at 214 and 279 nm.

The ^1H-NMR spectrum (Figure 196, Table 31) showed signals for an ABM aromatic spin system [δ 6.80 (1H, d, *J* = 9.0 Hz, H-5), 6.79 (1H, dd, *J* = 1.8, 9.0 Hz, H-6) and 6.78 (1H, d, *J* = 1.8 Hz, H-2)], two aromatic methine signals [δ 6.42 (2H, br s, H-2′, H-6′)], an oxygenated aliphatic methine [δ 4.36 (1H, m, H-8)], methylene proton signals [δ 3.15 (1H, dd, J = 5.1, 13.5 Hz, H-7b) and 2.76 (1H, dd, J = 8.3, 13.5 Hz, H-7a), a sec-methyl [δ 1.22 (3H, d, *J* = 6.2 Hz, H-9)], four methoxyl groups [3.88 (3H, s), 3.87 (3H, s) and 3.81 (6H, s)], and an allyl group [δ 5.99 (1H, ddt, *J* = 17.8,

10.1, 6.8 Hz, H-8′) 5.13 (1H, br dd, *J* = 17.8, 1.7 Hz, H-9′b), 5.11 (1H, br dd, *J* = 10.1, 1.7 Hz, H-9′a) and 3.36 (2H, br d, *J* = 6.8 Hz, H-7′)].

The ^{13}C-NMR spectrum (Figure 197, Table 31) exhibited twenty-two carbons containing five methyl carbons, three methylene carbons, seven methine carbons and seven quaternary carbons. In addition, this compound showed a negative optical rotation ($[\alpha]_D^{20}$ −7.55), and its CD curve (Figure 198) showed negative Cotton effects at 278 and 244 nm. Through comparison of these data with previously reported values, compound SMF1 was identified as 2-(4-allyl-2,6-dimethoxyphenoxy)-1-(3,4-dimethoxyphenyl)propane [**110**] (Yang, Huang and Ahmat, 2008).

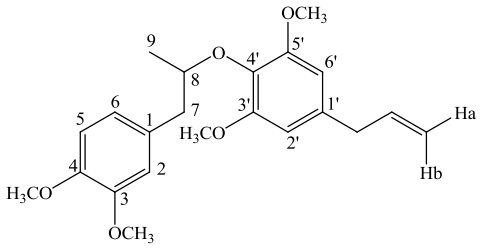

[**110**]

Table 31 NMR spectral data of compound SMF1 ($CDCl_3$) as compared with 2-(4-allyl-2,6-dimethoxyphenoxy)-1-(3,4-dimethoxyphenyl)propane ($CDCl_3$)

Position	Compound SMF1		2-(4-allyl-2,6-dimethoxy phenoxy)-1-(3,4-dimethoxyphe-nyl)propane*	
	^{1}H (mult., *J* in Hz)	^{13}C	^{1}H (mult., *J* in Hz)	^{13}C
1	-	131.7	-	131.7
2	6.78 (d, 1.8)	110.9	6.79 (d, 2.0)	110.9
3	-	148.5	-	148.5
4	-	147.3	-	147.2
5	6.80 (d, 9.0)	112.8	6.84 (d, 8.0)	112.7
6	6.79 (dd, 1.8, 9.0)	121.4	6.76 (dd, 2.0, 8.0)	121.4
7_a	2.76 (dd, 8.3, 13.5)	42.8	2.74 (dd, 8.0, 13.5)	42.8
7_b	3.15 (dd, 5.1, 13.5)	-	3.12 (dd, 5.0, 13.5)	-
8	4.36 (m)	80.0	4.34 (m)	79.9

* Yang, Huang and Ahmat, 2008

Table 31 NMR spectral data of compound SMF1 ($CDCl_3$) as compared with 2-(4-allyl-2,6-dimethoxyphenoxy)-1-(3,4-dimethoxyphenyl)propane ($CDCl_3$) (continued)

Position	Compound SMF1		2-(4-allyl-2,6-dimethoxy phenoxy)-1-(3,4-dimethoxyphe-nyl)propane*	
	^1H (mult., *J* in Hz)	^{13}C	^1H (mult., *J* in Hz)	^{13}C
9	1.22 (d, 6.2)	19.6	1.20 (d, 6.0)	19.5
1′	-	134.2	-	134.2
2′	6.42 (br s)	105.5	6.40 (s)	105.4
3′	-	153.6	-	153.6
4′	-	135.5	-	135.4
5′	-	153.6	-	153.6
6′	6.42 (br s)	105.5	6.40 (s)	105.4
7′	3.36 (br d, 6.8)	40.6	3.34 (d, 7.0)	40.5
8′	5.99 (ddt, 17.8, 10.1, 6.8)	137.3	5.96 (m)	137.3
$9'_a$	5.11 (br dd, 10.1, 1.7)	116.0	5.09 (m)	115.9
$9'_b$	5.13 (br dd, 17.8, 1.7)	-	-	-
CH_3O-3	3.88 (s)	55.8	3.86 (s)	56.0
CH_3O-4	3.87 (s)	55.9	3.85 (s)	56.3
CH_3O-3′	3.81 (s)	56.0	3.79 (s)	55.8
CH_3O-5′	3.81 (s)	56.0	3.79 (s)	55.8

* Yang, Huang and Ahmat, 2008

1.27 Structure determination of compound SMF2

Compound SMF2 was obtained as a colorless oil. The HRESI mass spectrum (Figure 199) showed an $[M+Na]^+$ ion at *m/z* 379.1514, indicating a molecular formula of $C_{21}H_{24}O_5$. The UV spectrum (Figure 200) showed absorption maxima at 215 and 278 nm, and the IR spectrum (Figure 201) demonstrated absorption bands for

conjugated unsaturation (1509 and 1453 cm^{-1}), and ether (1263, 1225, 1148, 1104 and 1028 cm^{-1}) functionalities.

The ^{1}H-NMR (Figure 202, Table 32) and ^{13}C-NMR (Figure 203, Table 32) spectra of compound SMF2 showed a 1,3,4-trisubstituted benzene ring [δ_H δ 6.95 (1H, dd, *J* = 8.1, 1.7 Hz, H-6), 6.93 (1H, d, *J* = 8.1 Hz, H-5) and 6.88 (1H, d, *J* = 1.7 Hz, H-2); δ_C 120.3 (C-6), 111.1 (C-5), 110.0 (C-2)], two *meta*-coupled signals [δ_H 6.50 (1H, d, *J* = 1.7 Hz, H-2′) and 6.39 (1H, d, *J* = 1.7 Hz, H-6′); δC 109.6 (C-2′), 104.5 (C-6′)]. In the HSQC spectrum (Figure 204), two tertiary oxygenated carbon signals at δ 80.8 (C-7) and 74.2 (C-8) showed direct coupling with protons at δ 4.61 (1H, d, *J* = 7.9 Hz, H-7) and 4.13 (1H, dq, *J* = 6.4, 7.9 Hz, H-8), respectively. These two methine protons constituted an ABX coupling system with the CH_3 protons at δ 1.26 (3H, d, J = 6.4 Hz, CH_3-9) in the ^{1}H-^{1}H COSY spectrum (Figure 205). The ^{1}H and ^{13}C-NMR data also suggested three methoxyl groups [δ 3.92 (6H, s) and 3.91 (3H, s)] at C-3 (δ 149.5), C-4 (δ 149.3) and C-5′(δ 148.5), which were supported by the HMBC correlations (Figure 203, Table 31). The allyl moiety [δ 5.97 (1H, ddt, *J* = 16.7, 9.9, 6.8 Hz, H-8′), 5.11 (1H, br dd, *J* = 16.7, 1.6 Hz, H-9′b), 5.08 (1H, br dd, *J* = 9.9, 1.6 Hz, H-9′a) and 3.31 (2H, br d, *J* = 6.8 Hz, H-7′)] should be located at C-1′. The HMBC spectrum (Figure 206, table 32) showed correlations from H-7′/H-8′ to C-1′ (δ 132.4), and from H-2′/H-6′ to C-7′ (δ 40.1).

The HMBC spectrum ($CDCl_3$) was not useful in determining which substituents are located at the C-7 and C-8 positions on the 1,4-benzodioxane ring since there was no HMBC correlation between H-7 or H-8 and C-3′ (δ 144.4) or C-4′ (δ 131.3). This drawback of HMBC ($CDCl_3$) had been observed in several neolignans (Takahasi *et al*., 2003; Kim *et al*., 2005). This problem was solved by using other NMR measurement techniques, such as the long-range selective proton-decoupling (LSPD) technique (Takahasi *et al*., 2003) or changing the NMR solvent (Kim *et al*., 2005). The linkage point of the substituent on the 1,4-dioxane moiety in compound SMF2 was determined clearly from HMBC spectrum using acetone-d_6 (Figure 207, Table 32) as the solvent. This HMBC (acetone-d_6) spectrum showed clear correlation from H-7 to C-3′. From the above data, the structure SMF2 was closely similar to that of eusiderin D [**108**] (Fernandes *et al*., 1980) except for the large coupling constant (*J*

= 7.9 Hz) between H-7 and H-8, in contrast with the small coupling constant in eusiderin D.

The *trans* relationship between H-7 and H-8 was supported by the cross-peak in the NOESY interaction between H-7 and CH_3-9 (Figure 208). The *trans* orientation between H-7 and H-8 with *R*,*R* configuration show a negative Cotton effect at about 242 nm and *S*,*S* configuration exhibit a positive Cotton effect at about 242 nm in CD spectrum (Silva *et al*., 1989). Compound SMF2 showed a negative Cotton effect at 238 nm in the CD spectrum (Figure 209), suggesting *R*,*R* configuration. The structure of compound SMF2 was established as (7*R*,8*R*)-$\Delta^{8'}$-3,4,5′-trimethoxy-7.O.3′,8.O.4′-neolignan [**111**]. It is a new 7.O.3′,8.O.4′-neolignan.

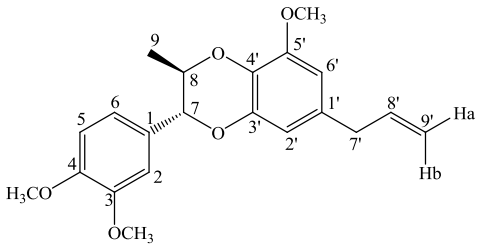

[**111**]

Table 32 NMR spectral data of compound SMF2 ($CDCl_3$ and acetone-d_6)

Position	Compound SMF2				HMBC (correlation with ^1H)
	$^1H^a$ (mult., *J* in Hz)	$^1H^b$ (mult., *J* in Hz)	$^{13}C^a$	$^{13}C^b$	
1	-	-	129.5	129.9	2^c*, 5^c, 6^c*, 7^c*, 8^b
2	6.88 (d, 1.7)	7.07 (br s)	110.0	111.0	6^c, 7^c
3	-	-	149.5	149.9	2^b*, 5^c, CH_3O-3^c
4	-	-	149.3	149.6	2^c, 5^b*, 6^c, CH_3O-4^c
5	6.93 (d, 7.3)	7.00 (br s)	111.1	111.5	6^b*
6	6.95(dd, 7.3, 1.7)	7.00 (br s)	120.3	120.2	2^c, 5^b*, 7^c

* Two-bond coupling
[a] Observed in $CDCl_3$, [b] Observed in acetone-d_6, [c] Observed in $CDCl_3$ and acetone-d_6

Table 32 NMR spectral data of compound SMF2 ($CDCl_3$ and acetone-d_6) (continued)

Position	Compound SMF2				HMBC (correlation with 1H)
	$^1H^a$ (mult., *J* in Hz)	$^1H^b$ (mult., *J* in Hz)	$^{13}C^a$	$^{13}C^b$	
7	4.61 (d, 7.9)	4.61 (d, 7.8)	80.8	80.5	2^c, 6^c, 8^c*, 9^c
8	4.13 (dq, 6.4, 7.9)	4.12 (dq, 6.5, 7.5)	74.2	73.6	7^c*, 9^c*
9	1.26 (d, 6.4)	1.15 (d, 6.3)	17.3	16.6	7^c, 8^c*
1′	-	-	132.4	132.0	$7'^c$*, 8′
2′	6.50 (d, 1.7)	6.39 (br s)	109.6	109.3	$6'^c$, $7'^c$
3′	-	-	144.4	144.6	7^b, $2'^c$
4′	-	-	131.3	131.7	$2'^c$, $6'^c$
5′	-	-	148.5	148.9	$6'^c$*, CH_3O-$5'^c$
6′	6.39 (d, 1.7)	6.46 (br s)	104.5	105.0	$2'^c$, $7'^c$
7′	3.31 (br d, 6.8)	3.29 (d, 6.8)	40.1	39.7	$2'^c$, $6'^c$, $8'^c$*, $9'^c$
8′	5.97 (ddt, 16.7, 9.9, 6.8)	5.96 (ddt, 17.0, 10.1, 6.9)	137.4	137.9	$7'^c$*, $9'^b$*
$9'_a$	5.08 (br dd, 9.9, 1.6)	5.02 (br d, 10.1)	115.9	114.8	$7'^c$, $8'^b$*
$9'_b$	5.11 (br dd, 16.7, 1.6)	5.09 (br d, 17.0)	-	-	-
CH_3O-3	3.92 (s)	3.84 (s)	56.0	55.3	-
CH_3O-4	3.92 (s)	3.84 (s)	56.0	55.2	-
CH_3O-5′	3.91 (s)	3.81 (s)	56.1	55.3	-

* Two-bond coupling,
[a] Observed in $CDCl_3$, [b] Observed in acetone-d_6, [c] Observed in $CDCl_3$ and acetone-d_6

1.28 Structure determination of compound SMF3

Compound SMF3 was obtained as a colorless oil. The positive HRESI mass spectrum (Figure 210) of SMF3 showed a pseudomolecular ion at *m*/*z* 423.1776 $[M+Na]^+$ $C_{23}H_{28}O_6Na$, which corresponded to the molecular formula $C_{23}H_{28}O_6$. The UV spectrum (Figure 211) showed absorption maxima at 216 and 276 nm, and the IR spectrum (Figure 212) demonstrated absorption bands for conjugated unsaturation (1506 and 1462 cm^{-1}), and ether (1233 and 1126 cm^{-1}) functionalities.

The ^{1}H-NMR spectrum (Figure 213, Table 33) showed signals for a methine proton attached to a carbinol carbon at δ 4.72 (1H, quin, *J* = 6.4 Hz, H-β), a methine proton at δ 4.03 (1H, d, *J* = 6.4 Hz, H-γ) and *sec*-methyl protons at δ 1.52 (3H, d, *J* = 6.4 Hz, H-α), which were correlated to the ^{13}C-NMR resonances (Figure 214, Table 33) at δ 89.4 (C-β), 55.8 (C-γ) and 21.0 (C-α), in the HSQC spectrum (Figure 215), respectively. Moreover, the ^{1}H-^{1}H COSY spectrum (Figure 216) showed correlations between H-β and H-γ, between H-β and H-α. These data seemed to suggest *trans*-2-aryl-3-methyl-2,3-dihydrobenzofuran system (Achenbach *et al*., 1987). However, the *trans*-2-aryl-3-methyl-2,3-dihydrobenzofuran system such as compound LMF4 (licarin A [**106**]) showed an upfield shift for CH_3 (or C-α) (δ_C 17.5) as compared with its counterpart in compound SMF3 (δ_C 21.0) due to *γ*-gauche effect (Silverstein and Webster, 1996). C-3 (or C-β) in LMF4 (δ_C 45.6) was also found to be upfield shifted as compared with C-β in SMF3 (δ_C 89.5). Moreover, LMF4 showed C-2 (or C-γ) (δ_C 93.8) at a more downfield position when compared with C-γ in SMF3 (δ_C 55.8). These data indicated a 3′,β-epoxy-γ,2′-neolignan system for compound SMF3. The arrangement of this stucture was confirmed by the HMBC correlation (Figure 217, Table 33) from H-β to C-2′ (δ 122.3) and C-3′ (δ 151.8); H-γ to C-1′ (δ 131.3), C-2′ and C-3′; H-6′ to C-2′, C-4′ (δ 131.7) and C-5′ (δ 152.9). The ^{1}H-NMR spectrum also showed five methoxy groups [δ 3.96 (3H, s), 3.86 (3H, s), 3.84 (3H, s) and 3.81 (6H, s)], and an allyl moiety at δ 5.69 (1H, ddt, *J* = 16.8, 10.2, 7.1 Hz, H-8′), 4.96 (1H, br dd, *J* = 10.2, 1.8 Hz, H-9′$_a$), 4.85 (1H, br dd, *J* = 16.8, 1.8 Hz, H-9′$_b$) and 2.93 (2H, br dd, *J* = 7.1, 1.4 Hz, H-7′). The allyl group was located at C-1′, which was supported by the correlation from H-7′ to C-1′ and C-2′, and from H-γ to C-1′. In addition, the ^{1}H-NMR spectrum exhibited a pair of *meta*-coupled aromatic protons at δ 6.36 (2H,

br s, H-2, H-6), indicating the presence of a 1,3,4,5-tetrasubstituted aromatic ring, which was attached to the dihydrofuran ring at C-γ due to correlations between H-2/H-6 and C-γ, and between H-β/H-γ and C-1 (δ 138.5) in the HMBC spectrum. The relative configuration was determined by the cross-peak between H-γ and H-α in the NOESY spectrum (Figure 218). The CD spectrum (Figure 219) showed a negative Cotton effect at 282 nm and a positive Cotton effect at 242 nm. From the above data, the structure of SMF3 was proposed as 3,4,5,4′,5′-pentamethoxy-3′,β-epoxy-γ,2′-neolign-8′-ene [**112**].

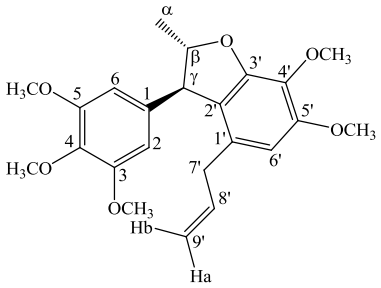

[**112**]

Table 33 NMR spectral data of compound SMF3 ($CDCl_3$)

Position	Compound SMF3		HMBC (correlation with ^1H)
	^1H (mult., *J* in Hz)	^{13}C	
1	-	138.5	β, γ*
2	6.36 (br s)	104.6	6, γ
3	-	153.4	2*, CH_3O-3
4	-	136.8	2, 6, CH_3O-4
5	-	153.4	6*, OCH_3-5
6	6.36 (br s)	104.6	2, γ
α	1.52 (d, 6.3)	21.0	γ
β	4.72 (quint, 6.3)	89.5	α*, γ*
γ	4.03 (d, 6.4)	55.8	β*, α*, 2, 6
1′	-	131.3	γ, 6′*, 7′*, 8′
2′	-	122.3	β, γ*, 6′, 7′
3′	-	151.8	β

* Two-bond coupling

Table 33 NMR spectral data of compound SMF3 ($CDCl_3$) (continued)

Position	Compound SMF3		HMBC (correlation with ^1H)
	^1H (mult., *J* in Hz)	^{13}C	
4′	-	131.7	6′, CH_3O-4′
5′	-	152.9	6′*, CH_3O-5′
6′	6.25 (s)	105.4	7′
7′	2.93 (br dd, 7.5, 1.4)	36.6	6′, 8′*, 9′
8′	5.69 (ddt, 16.6, 10.2, 6.6)	136.1	7′*
$9'_a$	4.96 (br dd, 10.1, 1.8)	115.7	7′
$9'_b$	4.85 (br dd, 17.0, 1.8)	-	-
CH_3O-3	3.81 (s)	56.2	-
CH_3O-4	3.84 (s)	60.9	-
CH_3O-5	3.81 (s)	56.2	-
CH_3O-4′	3.96 (s)	60.8	-
CH_3O-5′	3.86 (s)	56.2	-

* Two-bond coupling

1.29 Structure determination of compound SMF4

Compound SMF4 had physical and spectra data (^1H, ^{13}C NMR, Mass, UV and IR data) identical with those of compound LMF5. Therefore, it was identified as (7*R*,8*R*)-$\Delta^{8'}$-5-hydroxy-3,4,5′-trimethoxy-7.O.3′,8.O.4′-neolignan [**107**].

1.30 Structure determination of compound SMF5

Compound SMF5 showed spectroscopic properties (^1H, ^{13}C NMR, Mass, UV and IR data) identical with those of compound LMF6. Therefore, it was identified as eusiderin D [**108**].

1.31 Structure determination of compound SMF6

Compound SMF6 was obtained as a white solid. The HRESI mass spectrum (Figure 220) showed an $[M+Na]^+$ ion at *m/z* 409.1629, indicating a molecular formula

of $C_{22}H_{26}O_6$. The UV spectrum (Figure 221) showed absorption maxima at 215 and 273 nm. The IR spectrum (Figure 222) demonstrated absorption bands for conjugated unsaturation (1597, 1508 and 1463 cm^{-1}), and ether (1226, 1148, 1127 and 1105 cm^{-1}) functionalities.

The ^{1}H-NMR (Figure 223, Table 34) and ^{13}C-NMR (Figure 224, Table 34) spectra of compound SMF6 showed two sets of *meta*-coupled protons [δ_H H-2/H-6 [δ_H 6.59 (2H, s); δ_C 104.4], H-2′ [δ_H 6.50 (1H, d, J = 1.8 Hz); δ_C 109.6] and H-6′ [δ_H 6.40 (1H, d, J = 1.8 Hz); δ_C 104.6]. These spectra also showed signals for methine carbinol carbons [δ_H 4.58 (1H, d, J = 7.9 Hz, H-7) and 4.11 (1H, dq, 6.4, 7.9, H-8); δ_C 81.1 (C-7) and 74.1 (C-8)] and one *sec* methyl carbon [δ_H 1.23 (3H, d, J = 6.3 Hz, CH_3-9); δ_C 17.3], similar to SMF2, [**111**]. In addition, resonances for four methoxy groups [δ_H 3.91 (3H, s), 3.90 (6H, s) and 3.87 (3H, s); δ_C 60.9, 56.2 and 56.1] and an allyl group [H-8′ [δ_H 5.96 (1H, ddt, J = 16.9, 10.0, 6.8 Hz); δC 137.3], H-9′$_b$ [δ_H 5.10 (1H, br dd, J = 16.9, 1.6 Hz); δ_C 115.9], H-9′$_a$ [δ_H 5.08 (1H, br dd, J = 9.6, 1.6 Hz); 115.9] and H-7′ [δ_H 3.31 (2H, br d, J = 6.8 Hz); δ_C 40.0]] also showed in these spectra. These spectral data appeared to be superimposable on those reported for eusiderin A (Silva *et al*., 1989).

The absolute configurations at C-7 and C-8 were determined by the CD spectrum, which showed a positive Cotton effect at 238 nm (Figure 206) suggesting the *S*,*S* configuration (Silva *et al*., 1989). This configuration was opposite to eusiderin A, which indicated that compound SMF6 was an enantiomer of eusiderin A.

The structure of compound SMF6 was characterized as (7*S*,8*S*)-$\Delta^{8'}$-3,4,5,5′-tetramethoxy-7.O.3′,8.O.4′-neolignan [**113**]. It is a new 7.O.3′,8.O.4′-neolignan.

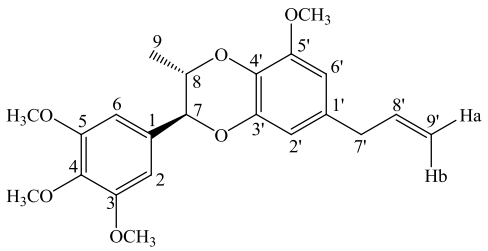

[**113**]

Table 34 NMR spectral data of compound SMF6 ($CDCl_3$) as compared with eusiderin A ($CDCl_3$)

Position	Compound SMF6		Eusiderin A*	
	^1H (mult., *J* in Hz)	^{13}C	^1H (mult., *J* in Hz)	^{13}C
1	-	132.5	-	132.4
2	6.59 (s)	104.4	6.60 (s)	104.7
3	-	153.5	-	153.6
4	-	138.4	-	138.4
5	-	153.5	-	153.6
6	6.59 (s)	104.4	6.60 (s)	104.7
7	4.58 (d, 7.9)	81.1	4.40 (d, 8.0)	81.1
8	4.11 (dq, 6.4, 7.9)	74.1	3.80-4.20 (m)	74.1
9	1.23 (d, 6.3)	17.3	1.25 (d, 6.0)	17.3
1′	-	132.5	-	132.6
2′	6.50 (d, 1.8)	109.6	6.40 (d, 2.0)	109.7
3′	-	144.3	-	144.4
4′	-	131.3	-	131.5
5′	-	148.6	-	148.7
6′	6.40 (d, 1.8)	104.6	6.30 (d, 2.0)	104.8
7′	3.31 (br d, 6.8)	40.0	3.25 (d, 6.0)	40.0
8′	5.96 (ddt, 16.9, 10.0, 6.8)	137.3	5.70-6.20 (m)	137.4
$9'_a$	5.08 (br dd, 10.0, 1.6)	115.9	4.90-5.90 (m)	115.8
$9'_b$	5.10 (br dd, 16.9, 1.6)	-	-	-
CH_3O-3	3.90 (s)	56.2	3.85 (s)	56.2
CH_3O-4	3.87 (s)	60.9	3.75 (s)	60.8
CH_3O-5	3.90 (s)	56.2	3.85 (s)	56.3
CH_3O-5′	3.91 (s)	56.1	3.80 (s)	56.0

* Silva *et al*., 1989

1.32 Structure determination of compound SMF7

Compound SMF7 was obtained as a colorless oil. The ESI mass spectrum (Figure 225) showed an $[M+Na]^+$ ion at *m/z* 425.12, indicating a molecular formula of $C_{23}H_{30}O_6$. The UV spectrum (Figure 226) showed absorption maxima at 211 and 271 nm.

The ^{1}H-NMR spectrum (Figure 227, Table 35) showed four aromatic protons at δ 6.48 (2H, s, H-2′, H-6′) and δ 6.42 (2H, s, H-2, H-6)], an allyl moiety at δ 5.99 (1H, ddt, *J* = 16.9, 10.1, 6.8 Hz, H-8′), 5.13 (1H, br dd, *J* = 16.8, 1.7 Hz, H-9′b), 5.11 (1H, br dd, *J* = 10.1, 1.7 Hz, H-9′a) and 3.36 (2H, br d, *J* = 6.8 Hz, H-7′), a methine proton attached to a carbinol carbon at δ 4.39 (1H, m, H-8), methylene protons at δ 3.14 (1H, dd, *J* = 13.5, 5.4 Hz, H-7$_b$) and 2.76 (1H, dd, *J* = 13.5, 7.8 Hz, H-7*a*), five methoxy groups at δ 3.85 (6H, s), 3.81 (6H, s) and 3.83 (3H, s), and a *sec*-methyl protons at δ 1.24 (3H, d, *J* = 6.2 Hz).

The ^{13}C-NMR spectrum (Figure 228, Table 35) exhibited twenty three carbons including six methyl carbons, three methylene carbons, six methine carbons and eight quaternary carbons.

Optical rotation of this compound was negative ($[\alpha]_D^{20}$ −7.55). The CD spectrum (Figure 198) showed negative Cotton effects at 276 and 244 nm.

Based on the above evidence data, and comparison with previously reported data (Barbosa-Filho *et al*., 1989), compound SMF7 was determined as virolongin B [**114**].

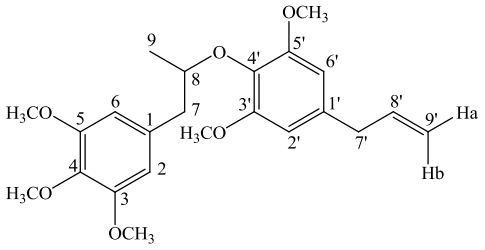

[**114**]

Table 35 NMR spectral data of compound SMF7 ($CDCl_3$) as compared with virolongin B ($CDCl_3$)

Position	Compound SMF7		Virolongin B*	
	^1H (mult., *J* in Hz)	^{13}C	^1H (mult., *J* in Hz)	^{13}C
1	-	134.9	-	134.8
2	6.42 (s)	106.4	6.40 (s)	106.6
3	-	153.6	-	153.6
4	-	136.2	-	136.5
5	-	153.6	-	153.6
6	6.42 (s)	106.4	6.40 (s)	106.6
7_a	2.76 (dd, 13.5, 7.8)	43.7	2.70 (dd, 16.0, 8.0)	43.6
7_b	3.14 (dd, 13.5, 5.4)	-	3.10 (dd, 14.0, 6.0)	-
8	4.39 (m)	79.7	4.20-4.60 (m)	79.5
9	1.24 (d, 6.2)	19.8	1.20 (d, 6.0)	19.6
1′	-	134.2	-	134.5
2′	6.48 (br s)	105.4	6.50 (s)	105.7
3′	-	152.8	-	152.8
4′	-	135.5	-	135.3
5′	-	152.8	-	152.8
6′	6.48 (br s)	105.4	6.50 (s)	105.7
7′	3.36 (br d, 6.8)	40.6	3.30 (d, 7.0)	40.5
8′	5.99 (ddt, 16.9, 10.1, 6.8)	137.3	5.80-6.30 (m)	137.2
$9'_a$	5.11 (br dd, 10.1, 1.7)	116.0	5.00-5.30 (m)	115.8
$9'_b$	5.13 (br dd, 16.9, 1.7)	-	-	-
CH_3O-3	3.81 (s)	56.0	3.85 (s)	56.0
CH_3O-4	3.83 (s)	60.9	3.85 (s)	60.6
CH_3O-5	3.81 (s)	56.0	3.85 (s)	56.0
CH_3O-3′	3.85 (s)	56.0	3.80 (s)	56.0
CH_3O-5′	3.85 (s)	56.0	3.80 (s)	56.0

* Barbosa-Filho *et al*., 1989

1.33 Structure determination of compound SMF8

Compound SMF8 was obtained as a colorless oil. The ESI mass spectrum (Figure 229) showed an $[M+Na]^+$ ion at *m/z* 409.03, indicating a molecular formula of $C_{22}H_{26}O_6$. The UV spectrum (Figure 230) showed absorption maxima at 215, 255 and 273 nm.

The ^{1}H-NMR (Figure 231, Table 36) and ^{13}C-NMR (Figure 232, Table 36) spectra of compound SMF8 showed the characteristic features of a benzodioxane neolignan by the presence of the proton signals at δ 5.12 (1H, d, *J* = 2.4 Hz, H-7), 4.62 (1H, dq, *J* = 2.4, 6.6 Hz, H-8) and 1.16 (3H, d, *J* = 6.6 Hz, H-9); the carbon signals at δ 77.0 (C-7), 73.2 (C-8) and 12.6 (C-9) (Motter Mogri, Kato and Yoshida, 1996), which were similar to those of LMF1, LMF2 and LMF6. These spectra showed four aromatic signals for H-2/H-6 [δ_H 6.62 (2H, s); δ_C 103.0], H-2′ [δ_H 6.54 (1H, d, *J* = 1.5 Hz); δ_C 109.7] and H-6′ [δ_H 6.40 (1H, d, *J* = 1.5 Hz); δ_C 105.0]. Furthermore, four methoxy groups [δ_H 3.90 (3H, s), 3.89 (6H, s) and 3.86 (3H, s); δ_C 60.9, 56.2 and 56.1] and an allyl group [H-8′ [δ_H 5.98 (1H, ddt, *J* = 16.7, 10.0, 6.8 Hz); δC 137.4], H-9′b [δ_H 5.10 (1H, br dd, *J* = 16.7, 1.4 Hz); δ_C 115.9], H-9′a [δ_H 5.09 (1H, br dd, *J* = 10.0, 1.4 Hz); δ_C 115.9] and H-7′ [δ_H 3.33 (2H, br d, *J* = 6.8 Hz); δ_C 40.0]] were observed in these spectra.

From the above data, compound SMF 8 was determined as eusiderin C [**115**] (Fernandes *et al*., 1980). However, the NMR assignments of C-1, C-1′ and C-4′ of compound SMF8 were revised in this study through an HMBC experiment (Figure 233). The assignment of C-1 was supported by the long-range correlation from C-1 (δ_C 132.5) to H-7. The position of C-1′ was assigned from the HMBC correlation between C-1′ (δ_C 132.2) and H-8′, H-7′. C-4′ (δ_C 129.5) showed HMBC correlation to H-8′.

The NOESY spectrum (Figure 234) exhibited a correlation peak between H-7 and H-8. The absolute configurations of 7.O.3′,8.O.4′-neolignan at C-7 and C-8 were determined by a negative Cotton effect at 248 nm in CD spectrum (Figure 209), indicating 7*S*,8*R* configuration (Silva *et al*., 1989).

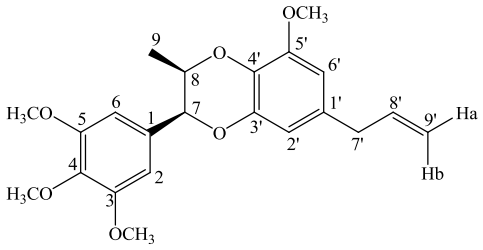

[**115**]

Table 36 NMR spectral data of compound SMF8 ($CDCl_3$) as compared with eusiderin C ($CDCl_3$)

Position	Compound SMF8		Eusiderin C*	
	^1H (mult., *J* in Hz)	^{13}C	^1H (mult., *J* in Hz)	^{13}C
1	-	132.5	-	129.6
2	6.62 (s)	103.0	6.62 (s)	103.2
3	-	153.4	-	153.5
4	-	137.6	-	137.8
5	-	153.4	-	153.5
6	6.62 (s)	103.0	6.62 (s)	103.2
7	5.12 (d, 2.4)	77.0	5.10 (d, 2)	77.1
8	4.62 (dq, 2.4, 6.6)	73.2	4.61 (dq, 2.5, 6.5)	73.2
9	1.16 (d, 6.6)	12.6	1.15 (d, 6.5)	12.6
1′	-	132.2	-	132.5
2′	6.54 (d, 1.5)	109.7	6.52 (d, 1.5)	109.8
3′	-	143.3	-	143.4
4′	-	129.5	-	132.3
5′	-	149.2	-	149.2
6′	6.40 (d, 1.5)	105.0	6.40 (d, 1.5)	105.1
7′	3.33 (br d, 6.8)	40.0	3.31 (d, 7.0)	40.0
8′	5.98 (ddt, 16.7, 10.0, 6.8)	137.4	5.98 (ddt, 6.5, 10.6, 17.0)	137.5
$9'_a$	5.09 (br dd, 10.0, 1.4)	115.9	5.20-5.10 (m)	115.9

* Fernandes *et al*., 1980

Table 36 NMR spectral data of compound SMF8 ($CDCl_3$) as compared with eusiderin C ($CDCl_3$) (continued)

Position	Compound SMF8		Eusiderin C*	
	^1H (mult., *J* in Hz)	^{13}C	^1H (mult., *J* in Hz)	^{13}C
9′b	5.12 (br dd, 16.7, 1.4)	-	-	-
CH_3O-3	3.89 (s)	56.2	3.87 (s)	56.2
CH_3O-4	3.86 (s)	60.9	3.85 (s)	60.9
CH_3O-5	3.89 (s)	56.2	3.87 (s)	56.2
CH_3O-5′	3.90 (s)	56.1	3.88 (s)	56.1

* Fernandes *et al*., 1980

1.34 Structure determination of compound SMF9

Compound SMF9 was obtained as a colorless crystalline solid. The positive ESI mass spectrum (Figure 235) showed an $[M+Na]^+$ ion at *m/z* 395.12, suggesting a molecular formula of $C_{22}H_{28}O_5$. The UV spectrum (Figure 236) showed absorption maxima at 210, 218 and 279 nm.

The ^1H-NMR (Figure 237, Table 37) and the ^{13}C-NMR (Figure 238, Table 37) spectra showed characteristic signals for a tetrahydrofuran lignan which included two methyls at δ_H 1.09 (3H, d, *J* = 6.6 Hz, H-9), 0.68 (3H, d, *J* = 7.0 Hz, H-9′) and δ_C 15.0, 15.0; two methines at δ_H 2.27 (1H, m, H-8′), 1.81 (1H, m, H-8) and δ_C 46.0, 47.9; and two benzylic methines at δ_H 5.16 (1H, d, *J* = 8.6 Hz, H-7′), 4.44 (1H, d, *J* = 9.3 Hz, H-7) and δ_C 83.1, 87.3 (Hada *et al*., 1988). The NOESY interaction (Figure 239) confirmed the relative stereochemistry at the tetrahydrofuran ring as *trans* (H-7/H-8), *trans* (H-8/H-8′), and *cis* (H-8′/H-7′). Additionally, these spectra also showed two ABM aromatic spin systems at δ_H 7.09 (1H, d, *J* = 1.8 Hz, H-2), 7.06 (1H, dd, *J* = 1.8, 8.2 Hz, H-6), 6.90 (1H, d, *J* = 8.2 Hz, H-5), 6.90 (1H, br d, *J* = 8.5 Hz, H-6′), 6.89 (1H, d, *J* = 1.9 Hz, H-2′) and 6.85 (1H, d, *J* = 8.5 Hz, H-5′); δ_C 119.2 (C-6′), 118.6 (C-6), 111.0 (C-5), 110.6 (C-5′), 110.3 (C-2′), 109.9 (C-2), and four methoxy groups [δ_H 3.93 (3H, s), 3.91 (3H, s), 3.90 (3H, s) and 3.88 (3H, s); δ_C 55.9 and 55.8].

The CD spectrum of compound SMF9 showed a negative Cotton effect at 294, 260 and 222, and a positive Cotton effect at 280, 240 and 226 nm (Figure 240).

Based on the above spectral data, this compound was identified as (+)-veraguensin [**116**] (Matcha and Ghosh, 2010).

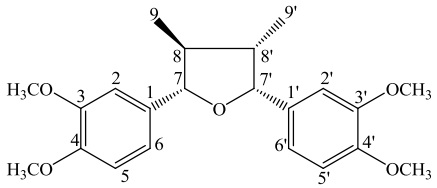

[**116**]

Table 37 NMR spectral data of compound SMF9 ($CDCl_3$) as compared with (+)-veraguensin ($CDCl_3$)

Position	Compound SMF9		(+)-Veraguensin*	
	^1H (mult., *J* in Hz)	^{13}C	^1H (mult., *J* in Hz)	^{13}C
1	-	133.4	-	133.60
2	7.09 (d, 1.8)	109.9	7.07-7.02 (m)	110.10
3	-	148.9	-	149.10
4	-	148.5	-	148.71
5	6.90 (d, 8.2)	111.0	6.89-6.82 (m)	111.10
6	7.06 (dd, 1.8, 8.2)	118.6	7.07-7.02 (m)	119.30
7	4.44 (d, 9.3)	87.3	4.42 (d, 9.2)	87.40
8	1.81 (m)	47.9	1.79 (m)	48.00
9	1.09 (d, 6.6)	15.0	1.07 (d, 6.5)	15.18
1′	-	133.8	-	133.90
2′	6.89 (d, 1.9)	110.3	6.89-6.82 (m)	110.50
3′	-	148.0	-	148.20
4′	-	148.5	-	148.72
5′	6.85 (d, 8.5)	110.6	6.89-6.82 (m)	110.80
6′	6.90 (br d, 8.5)	119.2	6.89-6.82 (m)	118.80
7′	5.16 (d, 8.6)	83.1	5.13 (d, 8.5)	83.10

* Matcha and Ghosh, 2010

Table 37 NMR spectral data of compound SMF9 ($CDCl_3$) as compared with (+)-veraguensin ($CDCl_3$) (continued)

Position	Compound SMF9		(+)-Veraguensin*	
	^1H (mult., *J* in Hz)	^{13}C	^1H (mult., *J* in Hz)	^{13}C
8′	2.27 (m)	46.0	2.25 (m)	46.10
9′	0.68 (d, 7.0)	15.0	0.66 (d, 7.0)	15.11
CH_3O-3	3.93 (s)	55.9	3.90 (s)	55.94
CH_3O-4	3.91 (s)	55.9	3.89 (s)	56.00
CH_3O-3′	3.90 (s)	55.8	3.87 (s)	56.08
CH_3O-4′	3.88 (s)	55.8	3.85 (s)	56.00

* Matcha and Ghosh, 2010

1.35 Structure determination of compound SMF10

Compound SMF10 was obtained as a colorless oil. The positive ESI mass spectrum (Figure 241) showed an $[M+Na]^+$ ion at *m/z* 425.15, suggesting a molecular formula of $C_{23}H_{30}O_6$. The UV spectrum (Figure 242) showed absorption maxima at 215, 229 and 277 nm.

The ^1H NMR (Figure 243, Table 38) and ^{13}C-NMR (Figure 244, Table 38) spectra showed characteristic features for a tetrahydrofuran lignan which included two methyls [H-9 (δ_H 1.12 (3H, d, *J* = 6.5 Hz), δ_C 15.3); H-9′ (δ_H 0.67 (3H, d, *J* = 7.0 Hz), δ_C 15.0), two methines [H-8′ (δ_H 2.27 (1H, m), δ_C 46.0); H-8 (δH 1.80 (1H, m), δ_C 48.1)], and two benzylic methines [H-7′ (δ_H 5.15 (1H, d, *J* = 8.6 Hz), δ_C 83.1); H-7 (δ_H 4.42 (1H, d, *J* = 9.2 Hz), δ_C 87.4)] (Hada *et al*., 1988). The NOESY interaction (Figure 245) supported the relative stereochemistry at the tetrahydrofuran ring as *trans* (H-7/H-8), *trans* (H-8/H-8′), and *cis* (H-8′/H-7′). These NMR spectra showed an ABM aromatic spin system [H-6′ (δ_H 6.91 (1H, dd, *J* = 1.8, 8.8 Hz), δ_C 119.2), H-2′ (δ_H 6.89 (1H, br s), δ_C 110.3), H-5′ (δ_H 6.87 (1H, d, *J* = 8.8 Hz), δ_C 110.6)], two methine aromatic protons [H-2 and H-6 (δ_H 6.76 (2H, s)]. In addition, these spectra showed five methoxy groups [δ_H 3.90 (6H, s), 3.89 (3H, s) and 3.87 (6H, s); δ_C 60.9,

56.1, 55.9 and 55.8]. Compound SMF10 was similar to compound SMF9, (+)-veraguensin, but compound SMF10 had an additional methoxy group.

Based on the above data, compound SMF10 was identified as (7*S*,8*S*,7′*R*,8′*S*)-3,4,5,3′,4′-pentamethoxy-7,7′-epoxylignan [**117**] (Lopes *et al*., 1996). However, the assignment of C-1 and C-1′ of compound SMF10 were revised in this study by examination of the HMBC spectrum (Figure 246). The assignment of C-1 was supported by the long-range correlation from C-1 (δ_C 136.7) to H-7 and H-8. C-1′ (δ 133.7) showed the HMBC correlation to H-7′ and H-8′.

The CD spectrum of compound SMF10 showed negative Cotton effects at 296 and 254 nm, and positive Cotton effects at 272, 228 and 222 nm (Figure 240).

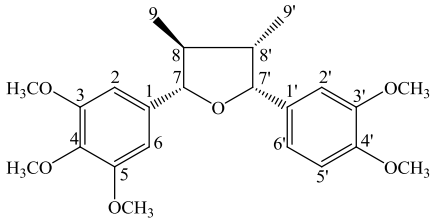

[**117**]

Table 38 NMR spectral data of compound SMF10 ($CDCl_3$) as compared with (7*S*,8*S*,7′*R*,8′*S*)-3,4,5,3′,4′-pentamethoxy-7,7′-epoxylignan **($CDCl_3$)**

Position	Compound SMF10		(7*S*,8*S*,7′*R*,8′*S*)-3,4,5,3′,4′-penta-methoxy-7,7′-epoxylignan*	
	^{1}H (mult., *J* in Hz)	^{13}C	^{1}H (mult., *J* in Hz)	^{13}C
1	-	136.7	-	133.6
2	6.76 (s)	103.3	6.76 (s)	103.3
3	-	153.2	-	153.2
4	-	137.4	-	137.4
5	-	153.2	-	153.2
6	6.76 (s)	103.3	6.73 (s)	103.3
7	4.42 (d, 9.2)	87.4	4.40 (d, 9.1)	88.3
8	1.80 (m)	48.1	1.72 (m)	48.0
9	1.12 (d, 6.5)	15.3	1.09 (d, 6.5)	15.2

* Lopes *et al*., 1996

Table 38 NMR spectral data of compound SMF10 ($CDCl_3$) as compared with (7*S*,8*S*,7′*R*,8′*S*)-3,4,5,3′,4′-pentamethoxy-7,7′-epoxylignan ($CDCl_3$) (continued)

Position	Compound SMF10		(7*S*,8*S*,7′*R*,8′*S*)-3,4,5,3′,4′-penta-methoxy-7,7′-epoxylignan*	
	^1H (mult., *J* in Hz)	^{13}C	^1H (mult., *J* in Hz)	^{13}C
1′	-	133.7	-	136.4
2′	6.89 (br s)	110.3	6.85 (m)	110.3
3′	-	148.5	-	148.5
4′	-	148.1	-	148.0
5′	6.87 (d, 8.5)	110.6	6.85 (m)	110.6
6′	6.91 (dd, 1.8, 8.8)	119.2	6.85 (m)	119.2
7′	5.15 (d, 8.6)	83.1	5.13 (d, 8.6)	83.0
8′	2.27 (m)	46.0	2.23 (m)	45.9
9′	0.67 (d, 7.0)	15.0	0.65 (d, 6.9)	14.9
CH_3O-3	3.90 (s)	56.1	3.88 (s)	56.0
CH_3O-4	3.89 (s)	60.9	3.87 (s)	60.8
CH_3O-5	3.90 (s)	56.1	3.88 (s)	56.0
CH_3O-3′	3.87 (s)	55.9	3.84 (s)	55.8
CH_3O-4′	3.87 (s)	55.8	3.84 (s)	55.7

* Lopes *et al*., 1996

1.36 Structure determination of compound SMF11

Compound SMF11 showed spectroscopic properties (^1H, ^{13}C NMR, Mass and UV data) identical with those of compound LMF2. Therefore, it was identified as (7*S*,8*R*)-$\Delta^{8'}$-4-hydroxy-3,5,5′-trimethoxy-7.O.3′,8.O.4′-neolignan [**104**].

1.37 Structure determination of compound SMF12

Compound SMF12 was obtained as a colorless oil. The HRESI mass spectrum (Figure 247) showed an $[M+Na]^+$ ion at *m/z* 411.1770, indicating a molecular formula of $C_{22}H_{28}O_6$. The UV spectrum (Figure 248) showed absorption maxima at 216, 233 and 279 nm, and the IR spectrum (Figure 249) demonstrated absorption bands for hydroxyl (3422 cm^{-1}), conjugated unsaturation (1514 and 1463 cm^{-1}), and ether (1258, 1234, 1136, 1102, 1028 and 1005 cm^{-1}) functionalities.

The ^{1}H-NMR (Figure 250, Table 39) and the ^{13}C-NMR (Figure 251, Table 39) spectra of compound SMF12 suggested a tetrahydrofuran lignan by signals corresponding to two methyl groups [H-9 (δ_H 1.10 (3H, d, *J* = 6.5 Hz), δC 15.2); H-9′ (δ_H 0.67 (3H, d, *J* = 7.0 Hz), δ_C 15.0)], two aliphatic methines [H-8′ (δ_H 2.25 (1H, m), δ_C 46.0); H-8 (δ_H 1.80 (1H, m), δ_C 47.9)], and two oxybenzyl methines [H-7′ δ_H 5.14 (1H, d, *J* = 8.6 Hz), δ_C 83.2); H-7 (δ_H 4.38 (1H, d, *J* = 9.2 Hz), δ_C 87.3)] (Hada *et al*., 1988). In addition, these NMR spectra showed signals for four methoxyl groups [δ_H 3.91 (3H, s), 3.90 (6H, s) and 3.88 (3H, s); δ_C 61.0, 55.9 and 55.8], an ABM aromatic spin system [H-2′ (δ_H 6.90 (1H, d, *J* = 1.7 Hz), δ_C 110.3); H-6′ (δ_H 6.89 (1H, dd, *J* = 7.9, 1.7 Hz), δ_C 119.2); and H-5′ (δ_H 6.86 (1H, d, *J* = 7.9 Hz), δ_C 110.6)], indicating that the aromatic ring had a 1,3,4-trisubstitution pattern, and a pair *meta*-coupled aromatic protons [H-6 (δ_H 6.78 (1H, d, *J* = 1.8 Hz), δ_C 105.9) and H-2 (δ_H 6.67 (1H, d, *J* = 1.8 Hz), δ_C 102.7)], which suggested that this aromatic ring was tetrasubstituted. The positions of the four methoxyl groups [δ 3.91 (3H, s), 3.90 (6H, s) and 3.88 (3H, s)] at C-3′ (δ 148.5), C-4′ (δ 148.0), C-3 (δ 152.3) and C-4 (δ 134.9) were determined by an HMBC experiment (Figure 252, Table 39). According to the ^{1}H-NMR data, the structure of compound SMF12 was similar to that of compound SMF 10, (7*S*,8*S*,7′*R*,8′*S*)-3,4,5,3′,4′-pentamethoxy-7,7′-epoxylignan [**117**]. However, H-2 and H-6 of compound SMF12 appeared at different chemical shifts whereas H-2 and H-6 of SMF10 appeared at the same chemical shift. The position of attachment of each aromatic ring to the tetrahydrofuran ring was determined from the HMBC spectrum (Figure 252, Table 39). The 1,3,4-trisubstituted ring at C-7′ showed correlation from H-2′ and H-6′ to C-7′ (δ 83.2), and from H-7′ and H-8′ [δ 2.25 (1H, m)] to C-1′ (δ 133.7). In addition, the tetrasubstituted ring was present at C-7, as

supported by the long-range correlation between H-7 and H-8 to C-1 (δ 137.2), and between H-2/H-6 and C-7 (δ 87.3). The ^{1}H-^{1}H COSY and the HSQC spectra (Figure 253-254) supported the proposed structure.

The structure of compound SMF12 has the same configuration as veraguensin (Lopes *et al*., 1996). The NOESY interaction (Figure 255) confirmed the relative stereochemistry as *trans* (H-7/H-8), *trans* (H-8/H-8′), *cis* (H-8′/H-7′), since it showed correlations from H-7 to H-9, H-7′ and H-8′. According to a previous report of veraguensin type tetrahydrofuran lignans (Fonseca *et al*., 1979), the coupling constants of oxybenzylic hydrogens indicate dihedral angles of approximately 150° and 0° between H-7/H-8 and H-7′/H-8′, respectively. This conformation of the tetrahydrofuran ring may be devoid of the steric interaction of the three *cis* substituents at C-7, C-8′ and C-7′ (Fonseca *et al*., 1979).

The CD spectrum of compound SMF12 showed negative Cotton effects at 292 and 256 nm, and positive Cotton effects at 276, 236, 228 and 218 nm (Figure 240).

The structure of compound SMF12 was established as *rel*-(7*S*,8*S*,7′*R*,8′*S*)-5-hydroxy-3,4,3′,4′-tetramethoxy-7,7′-epoxylignan [**118**]. This compound is a new tetrahydrofuran lignan.

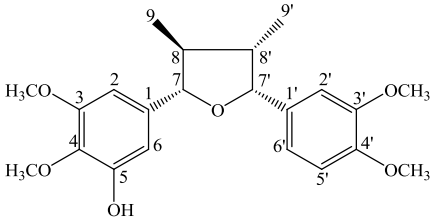

[**118**]

Table 39 NMR spectral data of compound SMF12 ($CDCl_3$)

Position	Compound SMF12		HMBC (correlation with ^{1}H)
	^{1}H (mult., *J* in Hz)	^{13}C	
1	-	137.2	7*, 8
2	6.67 (d, 1.8)	102.7	6, 7
3	-	152.3	2*, CH_3O-3

* Two-bond coupling

Table 39 NMR spectral data of compound SMF12 ($CDCl_3$) (continued)

Position	Compound SMF12		HMBC (correlation with ^1H)
	^1H (mult., *J* in Hz)	^{13}C	
4	-	134.9	2, 6, CH_3O-4
5	-	149.2	6*
6	6.78 (d, 1.8)	105.9	2, 7
7	4.38 (d, 9.2)	87.3	2, 6, 8*, 9, 7′
8	1.80 (m)	47.9	7*, 9*, 7′, 8′*, 9′
9	1.10 (d, 6.5)	15.2	7, 8*, 8′
1′	-	133.7	2′*, 6′*, 7′*, 8′
2′	6.90 (d, 1.7)	110.3	6′, 7′
3′	-	148.5	2′*, 5′, CH_3O-3′
4′	-	148.0	2′, 5′*, 6′, CH_3O-4′
5′	6.86 (d, 7.9)	110.6	-
6′	6.89 (dd, 7.9, 1.7)	119.2	2′, 7′
7′	5.14 (d, 8.6)	83.2	2′, 6′, 8′*, 9′
8′	2.25 (m)	46.0	7, 8*, 9, 7′*, 9′*
9′	0.67 (d, 7.0)	15.0	8, 7′, 8′*
CH_3O-3	3.89 (s)	55.9	-
CH_3O-4	3.91 (s)	61.0	-
CH_3O-3′	3.90 (s)	55.8	-
CH_3O-4′	3.90 (s)	55.8	-

* Two-bond coupling

1.38 Structure determination of compound SMF13

Compound SMF13 was obtained as a colorless oil. The HRESI mass spectrum (Figure 256) showed a pseudomolecular ion at *m*/*z* 411.1768 $[M+Na]^+$ $C_{22}H_{28}O_6Na$, which corresponded to the molecular formula $C_{22}H_{28}O_6$. The UV spectrum (Figure 257) showed absorption maxima at 215 and 277 nm, and the IR spectrum (Figure

258) demonstrated absorption bands for hydroxyl (3521 cm^{-1}), conjugated unsaturation (1515 and 1463 cm^{-1}), and ether (1264, 1236 and 1126 cm^{-1}) functionalities.

The ^{1}H-NMR (Figure 259, Table 40) and the ^{13}C-NMR (Figure 260, Table 40) spectra displayed an ABM aromatic spin system [H-5 (δ_H 6.80 (1H, br d, J = 8.1 Hz), δ_C 110.9); H-2 (δ_H 6.79 (1H, d, J = 2.0 Hz), δ_C 112.8); and H-6 (δ_H 6.77 (1H, br d, J = 8.1 Hz), δ_C 121.4)], aromatic signals for H-2′ and H-6′ [δ_H 6.63 (2H, br s), δ_C 103.6]. In the HSQC spectrum (Figure 261), tertiary oxygenated carbon and methylene signals at δ 80.2 (C-8) and 42.8 (C-7) showed direct coupling with protons at δ 4.40 (1H, m, H-8), 3.14 (1H, dd, J = 13.5, 5.0 Hz, H-7_b) and 2.76 (1H, dd, J = 13.5, 8.2 Hz, H-7_a), respectively. These methine and methylene protons constituted an ABX coupling system with the CH_3 protons at δ 1.23 (3H, d, J = 6.2 Hz, CH_3-9) in the ^{1}H-^{1}H COSY spectrum (Figure 262). Four methoxyl groups [δ 3.87 (6H, s) and 3.84 (6H, s)] were located at C-4 (δ 147.3), C-3 (δ 148.6), C-3′ (δ 153.5) and C-5′ (δ 153.5), as supported by the HMBC spectrum (Figure 263, Table 40). In addition, a 2-propen-1-ol moiety [δ 6.57 (1H, d, J = 15.9 Hz, H-7′), 6.31 (1H, dt, J = 15.9, 5.8 Hz, H-8′) and 4.35 (2H, d, J = 4.7 Hz, H-9′)] was present at C-1′, and this was confirmed by the HMBC correlation form H-8′ to C-1′ (δ 132.1), and from H-2′/H-6′ to C-7′ (δ 131.2). The spectral data of compound SMF13 were closely similar to those of virolongin E [**125**] (Silva *et al*., 1989) except for the presence of an ABM aromatic spin system instead of the singlet proton signal at δ 6.50 for H-2 and H-6 in virolongin E. This compound showed a negative optical rotation ($[\alpha]_D^{20}$ −7.55). The CD spectrum (Figure 198) also showed negative Cotton effects at 276 and 244 nm.

Based on the evidence data the structure of compound SMF13 was established as $\Delta^{7'}$-9′-hydroxy-4,5,3′,5′-tetramethoxy-8.O.4′-neolignan [**119**]. It is a new 8.O.4′-neolignan.

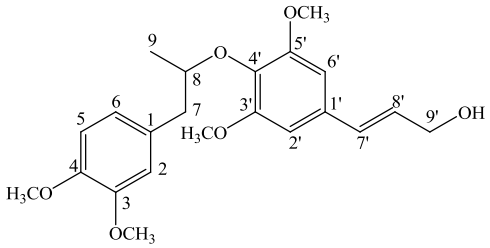

[**119**]

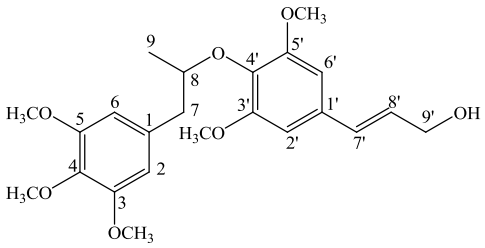

[**125**]

Table 40 NMR spectral data of compound SMF13 ($CDCl_3$)

Position	Compound SMF13		HMBC (correlation with ^1H)
	^1H (mult., *J* in Hz)	^{13}C	
1	-	131.6	2*, 6*, 7*
2	6.79 (d, 2.0)	112.8	3*, 6, 7
3	-	148.6	2*, CH_3O-3
4	-	147.3	2, 6, CH_3O-4
5	6.80 (d, 8.1)	110.9	3, 6*
6	6.77 (br d, 8.1)	121.4	2, 7
7_a	2.76 (dd, 13.5, 8.2)	42.8	2, 6, 8*, 9
7_b	3.14 (dd, 13.5, 5.0)	-	-
8	4.40 (m)	80.2	7*, 9*
9	1.23 (d, 6.2)	19.6	7
1′	-	132.1	8′
2′	6.63 (br s)	103.6	6′, 7′
3′	-	153.8	2′*, CH_3O-3′
4′	-	135.9	8, 2′, 6′
5′	-	153.8	6′*, CH_3O-5′
6′	6.63 (br s)	103.6	2′, 7′
7′	6.57 (d, 15.9)	131.2	2′, 6′, 8′*
8′	6.31 (dt, 15.9, 5.8)	127.8	9′*
9′	4.35 (d, 4.7)	63.7	7′, 8′*
CH_3O-3	3.87 (s)	55.8	-

* Two-bond coupling

Table 40 NMR spectral data of compound SMF13 ($CDCl_3$) (continued)

Position	Compound SMF13		HMBC (correlation with ^1H)
	^1H (mult., *J* in Hz)	^{13}C	
CH_3O-4	3.87 (s)	55.9	-
CH_3O-3′	3.84 (s)	56.0	-
CH_3O-5′	3.84 (s)	56.0	-

* Two-bond coupling

1.39 Structure determination of compound SMF14

Compound SMF14 showed spectroscopic properties (^1H, ^{13}C NMR, Mass and UV data) identical with those of compound TMM5. Therefore, it was identified as (−)-epicatechin [**91**].

2. Free Radical Scavenging Activity

In the TLC bioautographic assays, the methanol extracts from the twigs of *M. mollis*, from the leaves and the stems of *M.* cf. *fusca* showed free radical scavenging activity. Pure compounds isolated from these extracts were initially tested at 100 μg/mL. Compounds showing more than 50% inhibition were evaluated for IC_{50} values. Quercetin was used as positive control. The results are summarized in Tables 41-45.

The isolates *trans*-2-aryl-3-methyl-2,3-dihydrobenzofuran neolignans (**88**) exhibited weak activity against DPPH free radical as compared with quercetin as shown in Table 41. The isolates 8.O.4′ neolignans, the isolates 7.O.3′,8.O.4′ neolignans and the isolates tetrahydrofuran lignans did not show activity against DPPH free radical as shown in Tables 42-44, respectively. In addition, the isolates miscellaneous compounds, **91** and **92** showed weak activity as shown in Table 45.

It can be seen that three active compounds including compound **88**, **91**, and **92** exhibited weak activity against DPPH free radical as compared with quercetin, whereas the other compounds were inactive. It should be noted that the active compounds had an *o*-dioxygen (OH and CH_3O) functionality.

Table 41 Percentage of DPPH reduction of *trans*-2-aryl-3-methyl-2,3-dihydrobenzofuran neolignans

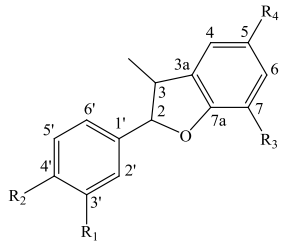

Compounds	Position						% DPPH reduction at 100μg/mL	IC_{50} (μM)
	Ar	CH_3	R_1	R_2	R_3	R_4		
[**87**]	*α*	*β*	H	CH_3O	H	CH=CH-CH_3	20.10	-
[**88**]	*β*	*α*	CH_3O	OH	H	CH=CH-CH_3	91.96	47.46
[**90**]	*β*	*α*	H	OH	H	CH=CH-CH_3	28.62	-
[**96**]	*α*	*β*	H	CH_3O	H	CH_2-CH=CH_2	nt	nt
[**98**]	*β*	*α*	CH_3O	OH	H	CH_2-CH=CH_2	nt	nt
[**99**]	*β*	*α*	H	OH	H	CH_2-CH=CH_2	nt	nt
[**100**]	*β*	*α*	H	OH	CH_3O	CH_2-CH=CH_2	nt	nt
[**101**]	*β*	*α*	H	OH	H	CHO	nt	nt
[**102**]	*β*	*α*	H	OH	H	CH_2-CO-CH_3	nt	nt
[**106**]	*β*	*α*	CH_3O	OH	CH_3O	CH=CH-CH_3	nd	-
quercetin	-						95.47	1.74

nt = not tested due to lack of activity of MeOH extract; nd = not determined due to small amount

Table 42 Percentage of DPPH reduction of 8.O.4′ neolignans

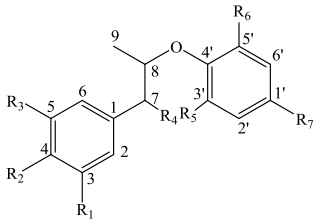

Compounds	Position								% DPPH reduction at 100µg/mL	IC_{50} (µM)
	CH_3	R_1	R_2	R_3	R_4	R_5	R_6	R_7		
[**89**]	*α*	H	CH_3O	H	*β*-OH	H	H	CH_2-CH=CH_2	17.04	-
[**97**]	*β*	H	CH_3O	H	*α*-OAc	H	H	CH_2-CH=CH_2	nt	-
[**105**]	-	CH_3O	OH	H	H	H	CH_3O	CH_2-CH=CH_2	nd	-
[**109**]	*β*	CH_3O	CH_3O	H	*β*-OH	H	CH_3O	CH_2-CH=CH_2	9.95	-
[**110**]	-	CH_3O	CH_3O	H	H	CH_3O	CH_3O	CH_2-CH=CH_2	7.24	-
[**114**]	-	CH_3O	CH_3O	CH_3O	H	CH_3O	CH_3O	CH_2-CH=CH_2	6.73	-
[**119**]	-	H	CH_3O	CH_3O	H	CH_3O	CH_3O	CH=CH-CH2OH	nd	-
quercetin	-								95.47	1.74

nt = not tested due to lack of activity of MeOH extract; nd = not determined due to small amount

Table 43 Percentage of DPPH reduction of 7.O.3′,8.O.4′ neolignans

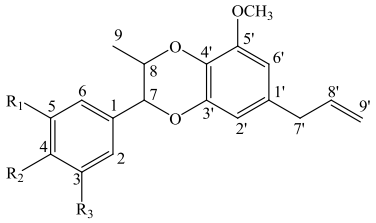

compounds	Position					% DPPH reduction at 100μg/mL	IC_{50} (μM)
	Ar	CH_3	R_1	R_2	R_3		
[**103**]	*β*	*β*	OH	CH_3O	CH_3O	20.08	-
[**104**]	*β*	*β*	CH_3O	OH	CH_3O	48.83	-
[**107**]	*α*	*β*	H	OH	CH_3O	19.48	-
[**108**]	*β*	*β*	H	CH_3O	CH_3O	11.39	-
[**111**]	*α*	*β*	H	CH_3O	CH_3O	9.49	-
[**113**]	*β*	*α*	CH_3O	CH_3O	CH_3O	8.56	-
[**115**]	*β*	*β*	CH_3O	CH_3O	CH_3O	7.84	-
quercetin	-					95.47	1.74

nt = not tested due to lack of activity of MeOH extract; nd = not determined due to small amount

Table 44 Percentage of DPPH reduction of tetrahydrofuran lignans

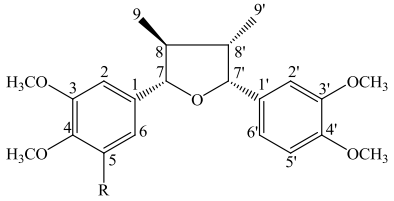

Compounds	R	% DPPH reduction at 100μg/mL	IC_{50} (μM)
[**116**]	H	11.35	-
[**117**]	CH_3O	8.64	-
[**118**]	OH	10.29	-
quercetin	-	95.47	1.74

nt = not tested due to lack of activity of MeOH extract; nd = not determined due to small amount

Table 45 Percentage of DPPH reduction of miscellaneous compounds

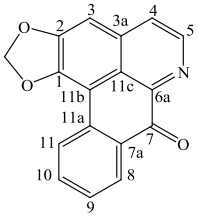

[**34**]

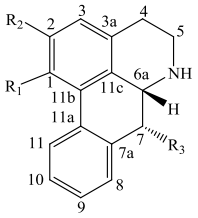

[**92**], [**93**]

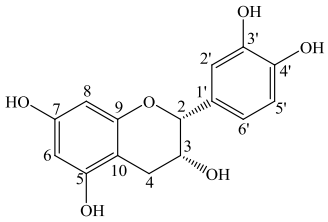

[**91**]

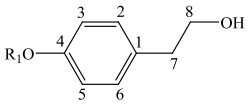

[**94**], [**95**]

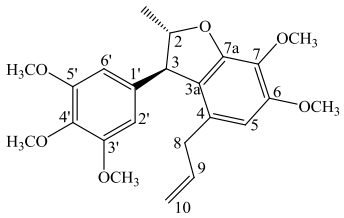

[**112**]

Compounds	Position			% DPPH reduction at 100μg/mL	IC_{50} (μM)
	R_1	R_2	R_3		
[**34**]	-			30.23	-
[**92**]	OCH_3	OH	H	89.07	132.30
[**93**]	$–O–CH_2–O–$		OH	nd	-
[**91**]	-			95.21	82.94
[**94**]	*β*-glc	-	-	24.92	-
[**95**]	*β*-xyl-(1→6)-*O*-*β*-glc	-	-	39.87	-
[**112**]	-			8.05	-
quercetin	-			95.47	1.74

nt = not tested due to lack of activity of MeOH extract; nd = not determined due to small amount

3. Cytotoxic Activity

Compounds obtained from the extracts prepared from the leaves of *M. mollis*, and the leaves of *M.* cf. *fusca* which showed activity against cancer cells were evaluated for cytotoxicity by resazurin microplate assay (REMA) (Brien *et al*., 2000). Ellipticine, doxorubicin and tamoxifen were used as the positive controls, and 0.5% DMSO was used as a negative control. The results are summarized in Table 46-48.

The isolates *trans*-2-aryl-3-methyl-2,3-dihydrobenzofuran neolignans showed moderate to weak cytotoxic activity against KB, MCF7 and NCI-H187 cell lines. Compound **101** and **106** did not show cytotoxic activity against the Vero cell (ATCC CCL-81) as shown in Table 46. The isolates 7.O.3′,8.O.4′ neolignans showed moderate to weak cytotoxic activity against KB, MCF7 and NCI-H187 cancerous cells as shown in Table 47. The 8.O.4′ neolignans (**109**) showed moderate cytotoxic activity against KB, MCF7 and NCI-H187 cell lines, did not show cytotoxicity against the Vero cell (ATCC CCL-81) as shown in Table 48.

Neolignans showed moderate to weak cytotoxic activity against KB, MCF7 and NCI-H187 cell lines. The most active compound was compound **109**, which showed selective toxicity against cancerous cells (KB, MCF7 and NCI-H187) as compared with the Vero cells (ATCC CCL-81). For *trans*-2-aryl-3-methyl-2,3-dihydrobenzofuran neolignans, compound **99** showed stronger cytotoxic activity than compound **101** and **102**. This may suggest that the 2-oxopropyl and the aldehyde groups at C-5 in compound **101** and **102** reduced the activity.

Table 46 IC_{50} values for cytotoxic activity of *trans*-2-aryl-3-methyl-2,3-dihydrobenzofuran neolignans

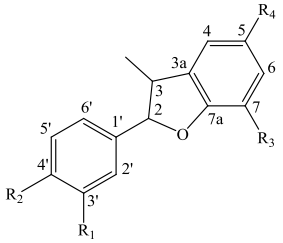

Compounds	Position						IC_{50} in μg/mL (μM)			
	Ar	CH_3	R_1	R_2	R_3	R_4	KB	MCF7	NCI-H187	ATCC CCL-81 (Vero cell)
[**87**]	α	β	H	CH_3O	H	CH=CH-CH_3	nt	nt	nt	nt
[**88**]	β	α	CH_3O	OH	H	CH=CH-CH_3	nt	nt	nt	nt
[**90**]	β	α	H	OH	H	CH=CH-CH_3	nt	nt	nt	nt
[**96**]	α	β	H	CH_3O	H	CH_2-CH=CH_2	nd	nd	nd	nd
[**98**]	β	α	CH_3O	OH	H	CH_2-CH=CH_2	9.28 (31.4)	16.64 (56.2)	18.15 (61.3)	17.05 (57.6)
[**99**]	β	α	H	OH	H	CH_2-CH=CH_2	7.24 (27.2)	19.13 (71.9)	25.35 (95.3)	15.61 (58.7)
[**100**]	β	α	H	OH	CH_3O	CH_2-CH=CH_2	nd	nd	nd	nd
[**101**]	β	α	H	OH	H	CHO	34.89 (137.4)	42.95 (169.1)	24.06 (94.7)	non cytotoxic[a]
[**102**]	β	α	H	OH	H	CH_2-CO-CH_3	27.03 (95.9)	40.23 (142.7)	32.67 (115.9)	36.56 (129.6)
[**106**]	β	α	CH_3O	OH	CH_3O	CH=CH-CH_3	12.90 (39.6)	45.57 (139.8)	16.74 (51.3)	non cytotoxic[a]
Tamoxifen	-						-	9.87 (26.6)	-	-
Doxorubicin	-						0.48 (0.9)	8.63 (15.9)	0.15 (0.3)	-
Ellipticine	-						0.84 (3.4)	-	0.38 (1.5)	0.61 (2.5)

nt = not tested due to lack of activity of MeOH extract; nd = not determined due to small amount; [a] determined at 50 μg/mL

Table 47 IC_{50} values for cytotoxic activity of 7.O.3′,8.O.4′ neolignans

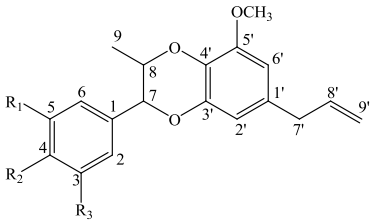

compounds	Position					IC_{50} in μg/mL (μM)			
	Ar	CH_3	R_1	R_2	R_3	KB	MCF7	NCI-H187	ATCC CCL-81 (Vero cell)
[**103**]	*β*	*β*	OH	CH_3O	CH_3O	20.25 (54.4)	22.12 (59.5)	17.06 (45.9)	39.19 (105.3)
[**104**]	*β*	*β*	CH_3O	OH	CH_3O	17.87 (48.0)	28.40 (76.3)	15.89 (42.7)	47.17 (126.8)
[**107**]	*α*	*β*	H	OH	CH_3O	23.82 (69.6)	24.40 (71.3)	16.71 (48.9)	17.21 (50.3)
[**108**]	*β*	*β*	H	CH_3O	CH_3O	18.42 (51.7)	22.61 (63.5)	20.60 (57.9)	17.68 (49.7)
[**111**]	*α*	*β*	H	CH_3O	CH_3O	nt	nt	nt	nt
[**113**]	*β*	*α*	CH_3O	CH_3O	CH_3O	nt	nt	nt	nt
[**115**]	*β*	*β*	CH_3O	CH_3O	CH_3O	nt	nt	nt	nt
Tamoxifen	-					-	9.87 (26.6)	-	-
Doxorubicin	-					0.48 (0.9)	8.63 (15.9)	0.15 (0.3)	-
Ellipticine	-					0.84 (3.4)	-	0.38 (1.5)	0.61 (2.5)

nt = not tested due to lack of activity of MeOH extract; nd = not determined due to small amount; [a] determined at 50 μg/mL

Table 48 IC_{50} values for cytotoxic activity of miscellaneous compounds

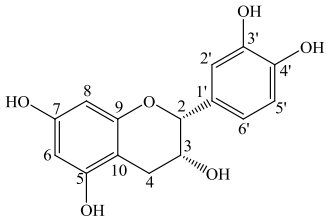

[**91**]

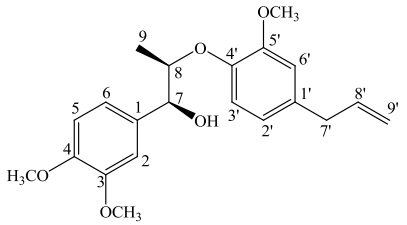

[**109**]

Compounds	IC_{50} in μg/mL (μM)			
	KB	MCF7	NCI-H187	ATCC CCL-81 (Vero cell)
[**91**]	inactive	38.48 (132.7)	inactive	non cytotoxic[a]
[**109**]	14.35 (40.1)	12.95 (36.2)	12.69 (35.4)	non cytotoxic[a]
Tamoxifen	-	9.87 (26.6)	-	-
Doxorubicin	0.48 (0.9)	8.63 (15.9)	0.15 (0.3)	-
Ellipticine	0.84 (3.4)	-	0.38 (1.5)	0.61 (2.5)

nt = not tested due to lack of activity of MeOH extract; nd = not determined due to small amount;
[a] determined at 50 μg/mL

4. Anti-Herpes Simplex Virus Activity

In this study, compounds isolated from extracts prepared from the twigs and leaves of *M. mollis*, and from the leaves and stems of *M.* cf. *fusca* were evaluated for anti-herpes simplex activity (HSV) using the plaque reduction assay (Lipipun *et al*., 2003; Chansriniyom *et al*., 2009). First, pure compounds were tested for anti-HSV activity at the concentration 100 μg/mL. Compounds exhibiting more than 50% inhibition were further evaluated for IC_{50} values. Acyclovir was used as a positive control. The results are summarized in Tables 49-51.

The isolates *trans*-2-aryl-3-methyl-2,3-dihydrobenzofuran neolignans (**102** and **106**) showed weak anti-HSV activity against HSV-1 and HSV-2, in post-treatment assay as shown in Table 49. A new of 7.O.3′,8.O.4′ neolignan, compound **104** showed weak anti-herpes simplex virus activity against HSV-1 and HSV-2, and the CC_{50} against the cells used in assay was 403.2 μM as shown in Table 50. Miscellaneous compounds did not show anti-herpes simplex virus activity as shown in Table 51.

Compounds **102**, **104** and **106** showed weak anti-HSV activity against HSV-1 and HSV-2 with IC_{50} in the range of 155.3-310.3 μM, and the CC_{50} to the cells used in assay in the range of 354.6-460.1 μM in post-treatment assay.

For *trans*-2-aryl-3-methyl-2,3-dihydrobenzofuran neolignans, anti-HSV activity appeared in a compound that has 2-oxopropyl at C-5 and hydroxyl group at C-4′ such as compound **102** as compared with compound **99**. In addition, compound having (*E*)-propenyl at C-5 showed anti-HSV activity when it has three oxegenations at C-7, C-3′ and C-4′ as seen in compound **106** in comparison with **87**, **88** and **90**.

For 7.O.3′,8.O.4′ neolignans, a hydroxyl group at C-4 and two methoxyl groups at C-3 and C-5 may be important for anti-HSV activity as seen in compound **104** in comparison with **103** and **115**.

Table 49 Anti-herpes simplex virus activity of *trans*-2-aryl-3-methyl-2,3-dihydrobenzofuran neolignans

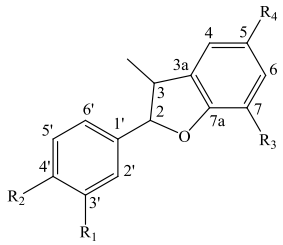

Compounds	Position						Final conc. (μg/mL)	IC_{50} (μg/mL, (μM))				CC_{50}[b] (μg/mL (μM))
	Ar	CH_3	R_1	R_2	R_3	R_4		post-treatment[a]		inactivation-treatment[a]		
								HSV-1	HSV-2	HSV-1	HSV-2	
[**87**]	*α*	*β*	H	CH_3O	H	CH=CH-CH_3	100	inactive	inactive	inactive	inactive	-
[**88**]	*β*	*α*	CH_3O	OH	H	CH=CH-CH_3	100	inactive	inactive	inactive	inactive	-
[**90**]	*β*	*α*	H	OH	H	CH=CH-CH_3	100	inactive	inactive	inactive	inactive	-
[**96**]	*α*	*β*	H	CH_3O	H	CH_2-CH=CH_2	nd	nd	nd	nd	nd	nd
[**98**]	*β*	*α*	CH_3O	OH	H	CH_2-CH=CH_2	100	inactive	inactive	inactive	inactive	-
[**99**]	*β*	*α*	H	OH	H	CH_2-CH=CH_2	100	inactive	inactive	inactive	inactive	-
[**100**]	*β*	*α*	H	OH	CH_3O	CH_2-CH=CH_2	nd	nd	nd	nd	nd	nd
[**101**]	*β*	*α*	H	OH	H	CHO	100	inactive	inactive	inactive	inactive	-
[**102**]	*β*	*α*	H	OH	H	CH_2-CO-CH_3	-	43.8 (155.3)	62.6 (222.0)	87.5 (310.3)	inactive	100 (354.6)
[**106**]	*β*	*α*	CH_3O	OH	CH_3O	CH=CH-CH_3	-	66.7 (204.6)	87.5 (268.4)	66.7 (204.6)	87.5 (268.4)	150.0 (460.1)

nd = not determined due to small amount; [a] IC_{50} (50% inhibition concentration, μg/mL, (μM)) was determined from three independent assays. Maximum concentration tested was 100 mg/mL. The IC_{50} of acyclovir against HSV-1 and HSV-2 were 0.59 μg/mL (1.9 μM) and 0.63 μg/mL (2.1 μM), repectively, in post-treatment and used as positive control. [b] CC_{50} (50% cytotoxic concentration, μg/mL, (μM)), the concentration that was 50% cytotoxic to the cells used in assay, was determined from three independent assays.

Table 50 Anti-herpes simplex virus activity of 7.O.3′,8.O.4′ neolignans

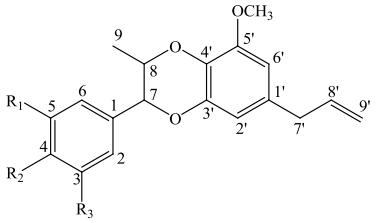

compounds	Position					Final conc. (μg/mL)	IC_{50} (μg/mL, (μM))				CC_{50}[b] (μg/mL (μM))
	Ar	CH_3	R_1	R_2	R_3		post-treatment[a]		inactivation-treatment[a]		
							HSV-1	HSV-2	HSV-1	HSV-2	
[**103**]	*β*	*β*	OH	CH_3O	CH_3O	100	inactive	inactive	inactive	inactive	-
[**104**]	*β*	*β*	CH_3O	OH	CH_3O	-	62.5 (168.0)	87.5 (235.2)	66.7 (179.3)	87.5 (235.2)	150.0 (403.2)
[**107**]	*α*	*β*	H	OH	CH_3O	50	inactive	inactive	inactive	inactive	-
[**108**]	*β*	*β*	H	CH_3O	CH_3O	100	inactive	inactive	inactive	inactive	-
[**111**]	*α*	*β*	H	CH_3O	CH_3O	100	inactive	inactive	inactive	inactive	-
[**113**]	*β*	*α*	CH_3O	CH_3O	CH_3O	100	inactive	inactive	inactive	inactive	-
[**115**]	*β*	*β*	CH_3O	CH_3O	CH_3O	100	inactive	inactive	inactive	inactive	-

[a] IC_{50} (50% inhibition concentration, μg/mL, (μM)) was determined from three independent assays. Maximum concentration tested was 100 mg/mL. The IC_{50} value of acyclovir against HSV-1 and HSV-2 were 0.59 μg/mL (1.9 μM) and 0.63 μg/mL (2.1 μM), repectively, in post-treatment and used as positive control. [b] CC_{50} (50% cytotoxic concentration, μg/mL, (μM)), the concentration that was 50% cytotoxic to the cells used in assay, was determined from three independent assays.

Table 51 Anti-herpes simplex virus activity of miscellaneous compounds

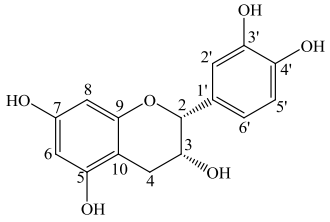

[**91**]

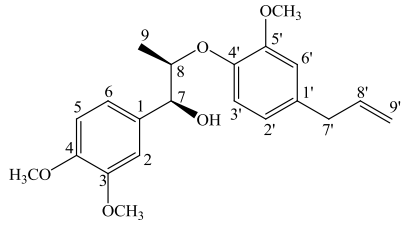

[**109**]

Compounds	Final conc. (μg/mL)	IC_{50} (μg/mL, (μM))				CC_{50}[b] (μg/mL (μM))
		post-treatment[a]		inactivation-treatment[a]		
		HSV-1	HSV-2	HSV-1	HSV-2	
[**91**]	100	inactive	inactive	inactive	inactive	-
[**109**]	100	inactive	inactive	inactive	inactive	-

[a] IC_{50} (50% inhibition concentration, μg/mL, (μM)) was determined from three independent assays. Maximum concentration tested was 100 mg/mL. The IC_{50} value of acyclovir against HSV-1 and HSV-2 were 0.59 μg/mL (1.9 μM) and 0.63 μg/mL (2.1 μM), repectively, in post-treatment and used as positive control. [b] CC_{50} (50% cytotoxic concentration, μg/mL, (μM), the concentration that was 50% cytotoxic to the cells used in assay, was determined from three independent assays.

CHAPTER V

CONCLUSION

In this study, thirty-four compounds were isolated from *Miliusa mollis*, and *Miliusa* cf. *fusca*. These included seventeen new compounds and seventeen known compounds as summarized in Table 52.

Table 52 Chemical constituents obtained from *M. mollis*, and *M.* cf. *fusca*

Part	Plant	Classes of compounds					Total
		neolignans	lignans	Phenolic glycosides	flavans	apor phine alkaloids	
twigs	*M. mollis*	4	-	2	1	3	10
leaves	*M. mollis*	7	-	-	-	-	7
leaves	*M.* cf. *fusca*	7	-	-	1[b]	-	8
stems	*M.* cf. *fusca*	10[a]	3	-	1[b]	-	14
Total		28	3	2	3	3	39

[a] Three neolignans were also isolated from the leaves of *M.* cf. *fusca*.
[b] The flavan was also isolated from the leaves of *M. mollis* and the stem of *M.* cf. *fusca*.

From the twigs of *M. mollis* Pierre, two new neolignans named (2*S*,3*S*)-2,3-dihydro-2-(4-methoxyphenyl)-3-methyl-5-(*E*)-propenylbenzofuran [**87**] and (7*S*,8*S*)-*threo*-$\Delta^{8'}$-4-methoxy-8.O.4′-neolignan [**89**], and a new phenolic glycoside named tyrosol-1-*O*-*β*-xylopyranosyl-(1→6)-*O*-*β*-glucopyranoside [**95**] were isolated along with seven known compounds, including (2*R*,3*R*)-2,3-dihydro-2-(4-hydroxy-3-methoxyphenyl)-3-methyl-5-(*E*)-propenylbenzofuran [**88**], conocarpan [**90**], (–)-epicatechin [**91**], liriodenine [**34**], asimilobine [**92**], (–)-norushinsunine [**93**], and icariside D_2 [**94**]. From the leaves of *M. mollis* Pierre, six new neolignans named (2*S*,3*S*)-5-allyl-2-(4-methoxyphenyl)-3-methyl-2,3-dihydrobenzofuran [**96**], (7*R*,8*R*)-*threo*-$\Delta^{8'}$-7-acethoxy-4-methoxy-8.O.4′-neolignan [**97**], (2*R*,3*R*)-5-allyl-2-(4-hydroxy-

3-methoxyphenyl)-3-methyl-2,3-dihydrobenzofuran [**98**], (2*R*,3*R*)-5-allyl-2-(4-hydroxyphenyl)-3-methyl-2,3-dihydrobenzofuran [**99**], (2*R*,3*R*)-5-allyl-2-(4-hydroxyphenyl)-7-methoxy-3-methyl-2,3-dihydrobenzofuran [**100**], and (2*R*,3*R*)-2-(4-hydroxyphenyl)-3-methyl-5-(2-oxopropyl)-2,3-dihydrobenzofuran [**102**] were isolated along with a known compound, decurrenal [**101**]. From the leaves of *M.* cf. *fusca* Pierre, three new neolignans named (7*S*,8*R*)-$\Delta^{8'}$-5-hydroxy-3,4,5′-trimethoxy-7.O.3′,8.O.4′-neolignan [**103**], (7*S*,8*R*)-$\Delta^{8'}$-4-hydroxy-3,5,5′-trimethoxy-7.O.3′,8.O.4′-neolignan [**104**], and (7*R*,8*R*)-$\Delta^{8'}$-4-hydroxy-3,5′-dimethoxy-7.O.3′,8.O.4′-neolignan [**107**] were isolated along with five known compounds, including (−)-epicatechin [**91**], 2-methoxy-4-[2-[2-methoxy-4-(2-propen-1-yl)phenoxy]propyl]phenol [**105**], licarin A [**106**], eusiderin D [**108**] and (7*S*,8*R*)-*erythro*-7-hydroxy-3,4,3′-trimethoxy-$\Delta^{1,3,5,1',3',5',8'}$-8.O.4′-neolignan [**109**]. From the stems of *M.* cf. *fusca* Pierre, four new neolignans named (7*R*,8*R*)-$\Delta^{8'}$-3,4,5′-trimethoxy-7.O.3′,8.O.4′-neolignan [**111**], 3,4,5,4′,5′-pentamethoxy-3′,β-epoxy-γ,2′-neolign-8′-ene [**112**], (7*S*,8*S*)-$\Delta^{8'}$-3,4,5,5′-tetramethoxy-7.O.3′,8.O.4′-neolignan [**113**], $\Delta^{7'}$-9′-hydroxy-4,5,3′,5′-tetramethoxy-8.O.4′-neolignan [**119**], and a new lignan named *rel*-(7*S*,8*S*,7′*R*,8′*S*)-5-hydroxy-3,4,3′,4′-tetramethoxy-7,7′-epoxylignan [**118**] were isolated along with nine known compounds (two of these compounds were similar to two new compounds in the leaves of *M.* cf. *fusca* Pierre), including (−)-epicatechin [**91**], (7*S*,8*R*)-$\Delta^{8'}$-4-hydroxy-3,5,5′-trimethoxy-7.O.3′,8.O.4′-neolignan [**104**], (7*R*,8*R*)-$\Delta^{8'}$-4-hydroxy-3,5′-dimethoxy-7.O.3′,8.O.4′-neolignan [**107**], eusiderin D [**108**], *erythro*-2-(4-allyl-2,6-dimethoxyphenoxy)-1-(3,4-dimethoxyphenyl)propane [**110**], virolongin B [**114**], eusiderin C [**115**], (+)-veraguensin [**116**] and (7*S*,8*S*,7′*R*,8′*S*)-3,4,5,3′,4′-pentamethoxy-7,7′-epoxylignan [**117**].

The major compounds in *M. mollis* and *M.* cf. *fusca* were neolignans. These neolignans could be divided into 3 classes: (1) dihydrobenzofuran neolignans, (2) 8.O.4′ neolignans and (3) 7.O.4′,8.O.4′ neolignans. The chemical and biological properties of each type of neolignans are summarized as follows.

1. Dihydrobenzofuran neolignans

The UV spectra of dihydrobenzofuran neolignans having (*E*)-propenyl at C-5 [**87-90** and **106**] showed maximum absorptions about 222 and 267 nm whereas the

UV spectra of compounds with an allyl group at C-5 [**96-100**] exhibited maximum absorption about 207, 229 and 284 nm.

This type of neolignans can be separated into 2 systems: (1) *trans*-2-aryl-3-methyl-2,3-dihydrobenzofuran system and (2) 3′,β-epoxy-γ,2′-neolignan system. There are described below.

1.1 *trans*-2-aryl-3-methyl-2,3-dihydrobenzofuran neolignans

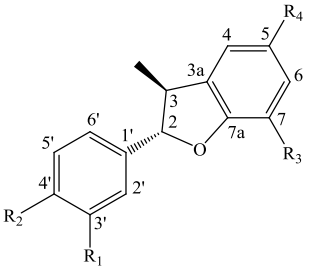

[**87**], [**96**]

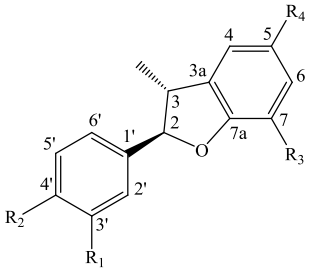

[**88**], [**90**], [**98**], [**99**], [**100**], [**101**], [**102**], [**106**]

Compounds	Position					
	Ar	CH_3	R_1	R_2	R_3	R_4
[**87**]	*α*	*β*	H	CH_3O	H	CH=CH-CH_3
[**88**]	*β*	*α*	CH_3O	OH	H	CH=CH-CH_3
[**90**]	*β*	*α*	H	OH	H	CH=CH-CH_3
[**96**]	*α*	*β*	H	CH_3O	H	CH_2-CH=CH_2
[**98**]	*β*	*α*	CH_3O	OH	H	CH_2-CH=CH_2
[**99**]	*β*	*α*	H	OH	H	CH_2-CH=CH_2
[**100**]	*β*	*α*	H	OH	CH_3O	CH_2-CH=CH_2
[**101**]	*β*	*α*	H	OH	H	CHO
[**102**]	*β*	*α*	H	OH	H	CH_2-CO-CH_3
[**106**]	*β*	*α*	CH_3O	OH	CH_3O	CH=CH-CH_3

The absolute configuration of a *trans*-2-aryl-3-methyl-2,3-dihydrobenzofuran structure could be determined by examination of the CD spectrum. The *R*,*R* configuration compounds showed a positive optical rotation. The CD spectra of these compounds showed a positive Cotton effect about 260 nm or a negative Cotton effect about 281 nm and a positive Cotton effect about 233 nm. On the other hand, the *S*,*S*

configuration compounds exhibited a negative optical rotation and the CD spectra showed a positive Cotton effect about 281 nm and a negative Cotton effect about 233 nm. All CD spectra of *trans*-2-aryl-3-methyl-2,3-dihydrobenzofuran neolignans as shown in Figure 264.

The ^{1}H-NMR signals at δ 5.00 (1H, d, J = 9.0 Hz, H-2), 3.40 (1H, apparent quint, J = 7.0 Hz, H-3) and 1.40 (3H, d, J = 6.6 Hz, CH_3-3), and the ^{13}C-NMR signals at δ 93.0 (C-2), 45.0 (C-3) and 17.5 (CH_3-3) are characteristic features of *trans*-2-aryl-3-methyl-2,3-dihydrobenzofuran system (Achenbach, H. *et al*., 1987). This structure normally had oxygenation at C-4′. For the ^{1}H-NMR spectrum, H-2, CH_3-3, H-4, H-6 and H-7 were downfield shifted when C-5 was substituted with aldehyde group. On the other hand, the upfield shift of H-4, H-6, H-2′ and H-6′ appeared when these protons were located at the *ortho* or *para* with a methoxy group. In the ^{13}C-NMR spectrum, C-2, C-4, C-6, C-7a were downfield shifted due to an aldehyde group at C-5 whereas C-3 was upfield shifted. In addition, C-7 was downfield shifted because of the presence of a methoxy group. Furthermore, C-4, C-6, C-7a, C-2′, C-4′ and C-6′ were upfield shifted if there were oxygenation at the *ortho* or *para* position. The ^{1}H- and the ^{13}C-NMR data for the position 2, 3 and CH_3-3 of *trans*-2-aryl-3-methyl-2,3-dihydrobenzofuran system are summarized in Table 53.

Table 53 ^{1}H- and ^{13}C-NMR data of *trans*-2-aryl-3-methyl-2,3-dihydrobenzofuran system

Compounds	Position					
	2		3		CH_3-3	
	^{1}H (mult., J in Hz)	^{13}C	^{1}H (mult., J in Hz)	^{13}C	^{1}H (mult., J in Hz)	^{13}C
[**87**]	5.09 (d, 9.0)	92.6	3.39 (m)	45.2	1.39 (d, 6.6)	17.8
[**88**]	5.07 (d, 9.0)	93.0	3.40 (m)	45.2	1.40 (d, 6.6)	17.6
[**90**]	5.07 (d, 8.0)	92.6	3.37 (quint, 8.0)	45.2	1.39 (d, 6.6)	17.8
[**96**]	5.11 (d, 9.1)	92.6	3.43 (apparent quint, 7.9)	45.4	1.41 (d, 6.8)	17.7

Table 53 ^{1}H- and ^{13}C-NMR data of *trans*-2-aryl-3-methyl-2,3-dihydrobenzofuran system (continued)

Compounds	Position					
	2		3		CH_3-3	
	^{1}H (mult., *J* in Hz)	^{13}C	^{1}H (mult., *J* in Hz)	^{13}C	^{1}H (mult., *J* in Hz)	^{13}C
[**98**]	5.07 (d, 9.1)	92.8	3.41 (apparent quint, 7.9)	45.3	1.37 (d, 6.8)	17.0
[**99**]	5.10 (d, 8.8)	92.5	3.43 (apparent quint, 7.7)	45.3	1.41 (d, 6.8)	17.7
[**100**]	5.13 (d, 9.6)	93.2	3.46 (apparent quint, 7.5)	45.8	1.39 (d, 6.8)	17.7
[**101**]	5.24 (d, 8.7)	94.0	3.49 (apparent quint, 7.7)	44.3	1.45 (d, 6.8)	17.9
[**102**]	5.09 (d, 9.2)	92.8	3.40 (apparent quint, 7.0)	45.2	1.37 (d, 6.8)	17.6
[**106**]	5.12 (d, 9.1)	93.8	3.47 (m)	45.6	1.40 (d, 6.8)	17.5

1.2 3′,β-epoxy-γ,2′-neolignan

A 3′,β-epoxy-γ,2′-neolignan such as compound **112** can be recognized from the ^{1}H-NMR signal at δ 4.72 (1H, quint, *J* = 6.3 Hz, H-β), 4.03 (1H, d, *J* = 6.4 Hz, H-γ) and 1.52 (3H, d, *J* = 6.3 Hz, H-α), and ^{13}C-NMR resonances at δ 89.5 (C-β), 55.8 (C-γ) and 21.0 (C-α). The ^{1}H- and ^{13}C-NMR spectra of 3′,β-epoxy-γ,2′-neolignan system ([**112**]) and *trans*-2-aryl-3-methyl-2,3-dihydrobenzofuran system ([**98**]) are compared in Table 54.

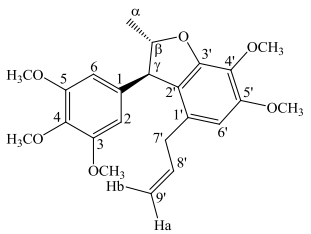

[**112**]

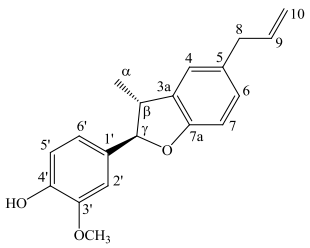

[**98**]

Table 54 ^{1}H- and ^{13}C-NMR data of 3′,β-epoxy-γ,2′-neolignan system and *trans*-2-aryl-3-methyl-2,3-dihydrobenzofuran system

Compounds	Position					
	α		β		γ	
	^{1}H (mult., *J* in Hz)	^{13}C	^{1}H (mult., *J* in Hz)	^{13}C	^{1}H (mult., *J* in Hz)	^{13}C
[**112**]	1.52 (3H, d, 6.3)	21.0	4.72 (1H, quint, 6.3)	89.5	4.03 (3H, d, 6.4)	55.8
[**98**]	1.37 (d, 6.8)	17.0	3.41 (apparent quint, 7.9)	45.3	5.07 (d, 9.1)	92.8

2. 8.O.4′ neolignans

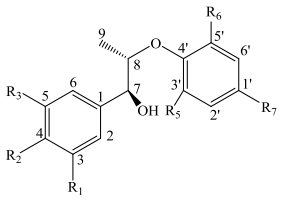

[**89**]

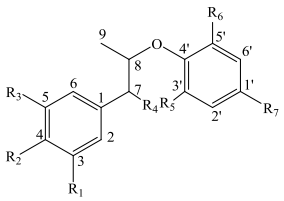

[**105**], [**110**], [**114**], [**119**]

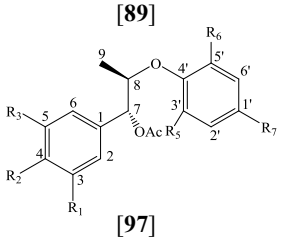

[**97**]

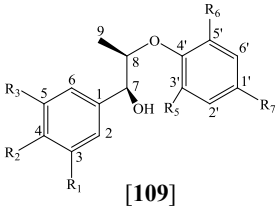

[**109**]

Com pounds	Position							
	CH_3	R_1	R_2	R_3	R_4	R_5	R_6	R_7
[**89**]	*α*	H	CH_3O	H	*β*-OH	H	H	CH_2-CH=CH_2
[**97**]	*β*	H	CH_3O	H	*α*-OAc	H	H	CH_2-CH=CH_2
[**105**]	-	CH_3O	OH	H	H	H	CH_3O	CH_2-CH=CH_2
[**109**]	*β*	CH_3O	CH_3O	H	*β*-OH	H	CH_3O	CH_2-CH=CH_2
[**110**]	-	CH_3O	CH_3O	H	H	CH_3O	CH_3O	CH_2-CH=CH_2
[**114**]	-	CH_3O	CH_3O	CH_3O	H	CH_3O	CH_3O	CH_2-CH=CH_2
[**119**]	-	H	CH_3O	CH_3O	H	CH_3O	CH_3O	CH=CH-CH_2OH

The UV spectra of 8.O.4′ neolignan types commonly showed maximum absorptions about 210 and 275 nm. The maximum absorptions about 230 nm appeared when the aromatic ring had methoxy group at C-5′.

The absolute configuration of 8.O.4′ neolignans with oxygenation at C-7 could be established by the CD spectrum. The *S*,*S* configuration of *threo*-8.O.4′ structures [**89** and **97**] showed a positive optical rotation and the CD spectra of these compounds showed a negative and a positive Cotton effects about 276 and 228 nm, respectively. On the other hand, the *R*,*R* isomers showed a negative optical rotation and the CD curve showed negative Cotton effects about 278 and 230 nm. For *erythro*-8.O.4′ structures [**109**], this structure showed a negative optical rotation, and negative Cotton effects at 276 and 240 nm in the CD curve, indicating the *S*,*R* configuration. The 8.O.4′ neolignans that did not have oxygenation at C-7 showed a negative optical rotation, and the CD spectrum showed negative Cotton effects about 276 and 240 nm. This may be suggesting the same C-8 configuration. These CD spectra are summarized in Figure 265.

The ^{1}H NMR signals of *threo*-8.O.4′ structures [**89** and **97**] exhibited at δ 4.62 (1H, d, *J* = 7.7 Hz, H-7), 4.34 (1H, dq, *J* = 7.7, 6.2 Hz, H-8) and 1.07 (3H, d, *J* = 6.2 Hz, H-9). These protons would be a little downfield shifted because of the presence of OAc at C-7 or changing from *threo* form to *erythro* form. The ^{13}C NMR signals of the *threo* form exhibited at δ 77.7 (C-7), 79.3 (C-8) and 15.7 (C-9). The upfield shift of C-8 appeared when C-7 was substituted with OAc. However, the *erythro* form showed upfield shifts for C-7 and C-9, whereas C-8 was downfield shifted. For 8.O.4′ neolignans without oxygenation at C-7, the ^{1}H NMR spectrum of these structures showed signals at δ 2.77 (1H, dd, *J* = 13.7 Hz, 6.7, H-7$_a$), 3.11 (1H, dd, *J* = 13.7, 6.0 Hz, H-7$_b$), 4.40 (1H, m, H-8) and 1.23 (3H, d, *J* = 6.2 Hz, H-9). The corresponding ^{13}C NMR signals appeared at δ 43.0 (C-7), 80.0 (C-8) and 19.5 (C-9). The 8.O.4′ neolignans were usually oxygenated at C-4. In the ^{1}H NMR spectra, the methine protons (H-2, H-6, H-2′ and H-6′) at the *ortho* or *para* position of an oxygenated group were upfield shifted. In the ^{13}C NMR spectrum, the upfield shifts of C-2 and C-6 occurred when these carbons have oxygenation at the *ortho* or *para* position. The downfield shifts of C-3 and C-5 could happen because of three oxygenations at C-3,

C-4 and C-5. The ^{1}H- and the ^{13}C-NMR data of 8.O.4′ system are summarized in Table 55.

Table 55 ^{1}H- and ^{13}C-NMR data of 8.O.4′ system

Com pounds	Position					
	7		8		9	
	^{1}H (mult., *J* in Hz)	^{13}C	^{1}H (mult., *J* in Hz)	^{13}C	^{1}H (mult., *J* in Hz)	^{13}C
[**89**]	4.62 (d, 7.7)	77.7	4.34 (dq, 7.7, 6.2)	79.3	1.07 (d, 6.2)	15.7
[**97**]	5.89 (d, 7.2)	77.7	4.61 (apparent quint, 6.5)	76.2	1.15 (d, 6.5)	16.4
[**109**]	4.85 (d, 3.1)	73.4	4.34 (dq, 3.1, 6.4)	82.6	1.19 (d, 6.4)	13.5
[**105**]	2.77 (dd, 13.7, 6.7), 7_a 3.11 (dd, 13.7, 6.0), 7_b	42.4	4.46 (apparent sext, 6.2)	76.9	1.32 (d, 6.1)	19.5
[**110**]	2.76 (dd, 8.3, 13.5), 7_a 3.15 (dd, 5.1, 13.5), 7_b	42.8	4.36 (m)	80.0	1.22 (d, 6.2)	19.6
[**114**]	2.76 (dd, 13.5, 7.8), 7_a 3.14 (dd, 13.5, 5.4), 7_b	43.7	4.39 (m)	79.7	1.24 (d, 6.2)	19.8
[**119**]	2.76 (dd, 13.5, 8.2), 7_a 3.14 (dd, 13.5, 5.0), 7_b	42.8	4.40 (m)	80.2	1.23 (d, 6.2)	19.6

3. 7.O.3′,8.O.4′ neolignans

The UV spectra of 7.O.3′,8.O.4′ neolignans showed maximum absorptions about 215 and 275 nm.

The absolute configuration of 7.O.3′,8.O.4′ system was ascertained by CD measurements. *cis*-Compounds with *S*,*R* configuration showed a positive optical rotation. The CD spectrum of these compounds showed a negative Cotton effect about 248 nm. For compounds with *trans* configuration, the *R*,*R* configurational isomers showed a negative optical rotation. They showed a negative Cotton effect at 238 nm in the CD curve. However, the *S*,*S* configurational isomers displayed a positive

optical rotation. The CD spectrum showed a positive Cotton effect at 238 nm. These CD spectra are depicted in Figure 266.

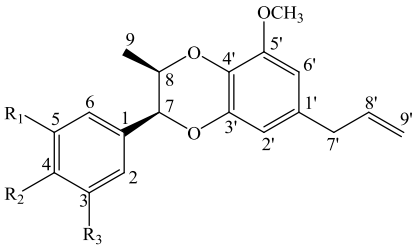

[**103**], [**104**], [**108**], [**115**]

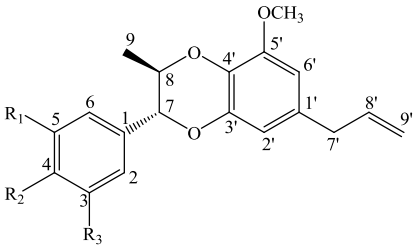

[**107**], [**111**]

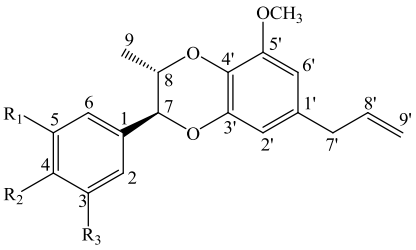

[**113**]

Compounds	Position				
	Ar	CH_3	R_1	R_2	R_3
[**103**]	*β*	*β*	OH	CH_3O	CH_3O
[**104**]	*β*	*β*	CH_3O	OH	CH_3O
[**107**]	*α*	*β*	H	OH	CH_3O
[**108**]	*β*	*β*	H	CH_3O	CH_3O
[**111**]	*α*	*β*	H	CH_3O	CH_3O
[**113**]	*β*	*α*	CH_3O	CH_3O	CH_3O
[**115**]	*β*	*β*	CH_3O	CH_3O	CH_3O

The *cis* 7.O.3′,8.O.4′ neolignans showed ^{1}H NMR signals at δ 5.10 (1H, d, *J* = 2.3 Hz, H-7), 4.62 (1H, dq, *J* = 2.3, 6.6 Hz, H-8) and 1.15 (3H, d, *J* = 6.6 Hz, H-9), and ^{13}C NMR signals at δ 77.0 (C-7), 73.1 (C-8) and 12.6 (C-9) (Motter Mogri, Kato and Yoshida 1996). On the other hand, the ^{1}H NMR signals of the *trans* configuration compounds at H-7 and H-8 were more upfield [4.59 (1H, d, *J* = 7.9 Hz, H-7), 4.12 (1H, dq, *J* = 7.9, 6.4 Hz, H-8)] whereas H-9 was a little downfield shifted [1.25 (3H, d, J = 6.4 Hz, H-9)]. In addition, the coupling constant of H-7 in the *trans*

configuration (J = 7.9 Hz) was larger than in the *cis* configuration (J = 2.3 Hz). The ^{13}C NMR signals of C-7 (80.9), C-8 (74.2) and C-9 (17.3) of the *trans* compounds were more downfield shifted than those in the *cis* configuration compounds. Oxygenation at C-3 and C-4 normally occurred in 7.O.3′,8.O.4′ neolignans. The ^{1}H NMR signals of H-2 and H-6 were upfield shifted when there were oxygenation at the *ortho* or *para* position. In the ^{13}C NMR spectrum, the upfield shift of C-2 and C-6 appeared when there were oxygenation at the *ortho* or *para* position. The downfield shift of C-1 occurred if there was *meta*-oxygenation. The C-3 and C-5 were downfield shifted if the aromatic ring had three oxygenations at C-3, C-4 and C-5. The ^{1}H- and the ^{13}C-NMR data of 7.O.3′,8.O.4′ system are summarized in Table 56.

Table 56 ^{1}H- and ^{13}C-NMR data of 7.O.3′,8.O.4′ system

Compounds	Position						
	Configuration	7		8		9	
		^{1}H (mult., J in Hz)	^{13}C	^{1}H (mult., J in Hz)	^{13}C	^{1}H (mult., J in Hz)	^{13}C
[**103**]	*cis*	5.10 (d, 2.3)	76.8	4.62 (dq, 2.3, 6.6)	73.1	1.15 (d, 6.6)	12.6
[**104**]	*cis*	5.08 (d, 2.4)	77.0	4.56 (dq, 2.4, 6.6)	73.4	1.11 (d, 6.6)	12.5
[**108**]	*cis*	5.14 (d, 2.3)	77.0	4.61 (dq, 2.3, 6.6)	73.2	1.15 (d, 6.6)	12.7
[**115**]	*cis*	5.12 (d, 2.4)	77.0	4.62 (dq, 2.4, 6.6)	73.2	1.16 (d, 6.6)	12.6
[**107**]	*trans*	4.59 (d, 7.9)	80.9	4.12 (dq, 7.9, 6.4)	74.2	1.25 (d, 6.4)	17.3
[**111**]	*trans*	4.61 (d, 7.9)	80.8	4.13 (dq, 6.4, 7.9)	74.2	1.26 (d, 6.4)	17.3
[**113**]	*trans*	4.58 (d, 7.9)	81.1	4.11 (dq, 6.4, 7.9)	74.1	1.23 (d, 6.3)	17.3

Lignans isolated from the stem of *M.* cf. *fusca* in this study were tetrahydrofuran lignans. The structures of these compounds are shown as below

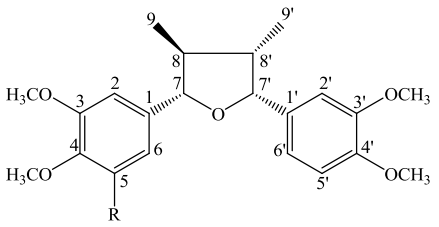

	R
[**116**]	H
[**117**]	CH_3O
[**118**]	OH

The UV spectra of tetrahydrofuran lignans showed maximum absorptions at 215, 232 and 279 nm. Tetrahydrofuran lignans from the stem of *M.* cf. *fusca* showed a positive optical rotation. The CD spectra of these compounds showed negative Cotton effects about 294 and 256, and positive Cotton effects about 276 and 228 nm. The CD spectra of compounds **116** (SMF9), **117** (SMF10) and **118** (SMF12) were illustrated in Figure 240.

The ^{1}H-NMR and the ^{13}C-NMR spectra showed characteristic signals for a tetrahydrofuran lignan which included two methyls at δ_H 1.09 (3H, d, *J* = 6.6 Hz, H-9), 0.68 (3H, d, *J* = 7.0 Hz, H-9′) and δ_C 15.0, 15.0; two methines at δ_H 2.27 (1H, m, H-8′), 1.81 (1H, m, H-8) and δ_C 46.0, 47.9; and two benzylic methines at δ_H 5.16 (1H, d, *J* = 8.6 Hz, H-7′), 4.44 (1H, d, *J* = 9.3 Hz, H-7) and δ_C 83.1, 87.3 (Hada *et al*., 1988). The ^{1}H- and the ^{13}C-NMR data of tetrahydrofuran lignans are summarized in Table 57.

Table 57 ^{1}H- and ^{13}C-NMR data of tetrahydrofuran lignans system

Position	Compounds					
	[**116**]		[**117**]		[**118**]	
	^{1}H (mult., *J* in Hz)	^{13}C	^{1}H (mult., *J* in Hz)	^{13}C	^{1}H (mult., *J* in Hz)	^{13}C
7	4.44 (d, 9.3)	87.3	4.42 (d, 9.2)	87.4	4.38 (d, 9.2)	87.3
8	1.81 (m)	47.9	1.80 (m)	48.1	1.80 (m)	47.9
9	1.09 (d, 6.6)	15.0	1.12 (d, 6.5)	15.3	1.10 (d, 6.5)	15.2
7′	5.16 (d, 8.6)	83.1	5.15 (d, 8.6)	83.1	5.14 (d, 8.6)	83.2
8′	2.27 (m)	46.0	2.27 (m)	46.0	2.25 (m)	46.0
9′	0.68 (d, 7.0)	15.0	0.67 (d, 7.0)	15.0	0.67 (d, 7.0)	15.0

Due to limited amounts of the samples, certain isolated compounds were selected for evaluation for free radical scavenging, cytotoxic, and anti-herpes simplex virus activities. These are summarized in Table 58.

Table 58 Biological activities of isolated compounds from *M. mollis*, and *M.* cf. *fusca*

Activity	numbers of compounds					Total (34)
	Neolignas (25)	Lignans (3)	Phenolic Glycosids (2)	Flavans (1)	aporphine alkaloids (3)	
Free radical scavenging	1	-	-	1	1	3
Cytotoxicity	10	nd	nd	1	nd	11
Anti-HSV	3	-	-	-	-	3

nd = not determined due to small amount

For free radical scavenging activity, compound **88**, **91**, and **92** showed weak activities. For cytotoxic activity, neolignans showed moderate to weak cytotoxic activity against KB, MCF7 and NCI-H187 cell lines. The most active compound was compound **109**, which showed selective toxicity against cancerous cells (KB, MCF7 and NCI-H187) as compared with the Vero cells (ATCC CCL-81). For anti-herpes simplex virus activity, compound **102**, **104** and **106** showed weak anti-HSV activity against HSV-1 and HSV-2.

References

ภาษาไทย

มูลนิธิมหาวิทยาลัยมหิดล. 2548. สารานุกรมสมุนไพร. เล่ม 5. สมุนไพรพื้นบ้านอีสาน. กรุงเทพมหานคร: อมรินทร์พริ้นติ้งแอนด์พับลิชชิ่ง (มหาชน).

ภาษาอังกฤษ

Achenbach, H., Grob, J., Domínguez, X. A., Cano, G., Star, J. V., Brussolo, L. D. C., Munoz, G., Salgado, F., and López, L. 1987. Lignans, neolignans and norneolignans from *Krameria cystisoides*. Phytochemistry 26: 1159–1166.

Achenbach, H., Utz, W., Usubillaga, A., and Rodriguez, H. A. 1991. Lignans from *Krameria ixina*. Phytochemistry 30: 3753–3757.

Achenbach, H., Utz, W., Sánchez, H., Touché, E.M.G., Verde, J., and Dominguez, X.A. 1995. Neolignans, nor-neolignans and other compounds from roots of *Krameria grayi*. Phytochemistry 39: 413–415.

Agrawal, P. K. NMR spectroscopy in the structural elucidation of oligosaccharides and glycosides. 1992. Phytochemistry 31: 3307–3330.

Backer, C. A. and Bakhuizen van der brink, R. C. 1963. Flora of Java. volume I. The Netherlands: The rijksherbarium, Leyden.

Badgujar, V. B., and Surana, S. J. 2011. Comparative investigation on antimicrobial property of *Miliusa tomentosa* leaf oil and leaf extract. Iran. J. Pharmacol. Ther. 10: 7-10.

Bárbosa-Filho, J. M., da silva, M. S., Yoshida, M., and Gottlieb, O. R. 1989. Neolignans from *Licaria aurea*. Phytochemistry 28: 2209-2211.

Braca, A., Sortino, C., Politi, M., Morelli, I., and Mendez, J. 2002. Antioxidant activity of flavonoids from *Licania licaniaeflora*. J. Ethnopharmacology 79: 379-381.

Braga, A. C. H., Zacchino, S., Badano, H., Sierra, M. G., and Rúveda, E. A. 1984. ^{13}C NMR spectral and conformational analysis of 8-*O*-4′ neolignans. Phytochemistry 23: 2025–2028.

Brien, J. O., Wilson, I., Orton, T., and Pognan, F. 2000. Investigation of the alamar blue (resazurin) fluorescent dye for the assessment of mammalian cell cytotoxicity. Eur. J. Biochem. 267: 5421-5426.

Brophy, J. J., Goldsack, R. J., and Forster, P. I. 2004. The leaf oils of the Australian species of *Miliusa* (Annonaceae). J. Essent. Oil Res. 16: 253–255.

Chalermglin, P. 2005. Annonaceae plant. 2nd edition. Bangkok. Amarin printing & publishing.

Chansriniyom, C., Ruangrungsi, N., Lipipun, V., Kumamoto, T., Ishikawa, T. 2009. Isolation of acridone alkaloids and N-[(4-monoterpenyloxy)phenylethyl]-substituted sulfur-containing propanamide derivatives from *Glycosmis parva* and their anti-herpes simplex virus activity. Chem. Pharm. Bull. 57: 1246-1250.

Chaowasku, T. and Keßler, P. J. A. 2006. *Miliusa lanceolata* (Annonaceae), a new species from Papua New Guinea. Blumea 51 : 553-557.

Chaowasku, T., Mols, J. and Van Der Ham, R. W. J. M. 2008. Pollen morphology of *Miliusa* and relatives (Annonaceae). Grana 47: 175–184.

Chaowasku, T., Van Der Brink, L., Keßler, P. J. A. and Chatrou, L. W. A. A synoptic revision of the genus *Miliusa* (Annonaceae), with molecular phylogenetic analyses. Phytotaxa (submitted).

Chauret, D. C., Bernard, C. B., Arnason, J. T., Durst, T., Krishnamurty, H. G., SanchezVindas, P., Moreno, N., San Roman, L., and Poveda, L. 1996. Insecticidal neolignans from *Piper decurrens*. J. Nat. Prod. 59: 152–155.

Chen, B., Ye, Q., Li, B., and Zhang, G. 2002. A new azafluorene alkaloid from *Miliusa balansae*. Indian J. Heterocy. Ch. 12: 81-82.

Chen, B., Feng, C., Li, B. G., and Zhang, G. L. 2003. Two new alkaloids from *Miliusa cuneata*. Nat. Prod. Res. 17: 397–402.

Cragg, G. M., and Newman, D. J. 2005. Plants as a source of anti-cancer agents. J. Ethnopharmacol. 100: 72-79.

Fang, Y. Z., Yang, S., and Wu, G. 2002. Free radicals, antioxidants, and nutrition. Nutrition 18: 872-879.

Fatahzadeh, M., and Schwartz, R. A. 2007. Human herpes simplex virus infections: epidemiology, pathogenesis, symptomatology, diagnosis, and management. J. Am. Acad. Dermatol. 57:737–763.

Fernandes, J. B., Ribeiro, M. N. de S., Gottlieb, O. R., and Gottlieb, H. E. 1980. Eusiderins and 1,3-diarylpropanes from *Virola* species. Phytochemistry 19: 1523-1525.

Fischer, D. C. H., Gonçalves, M. I., Oliveira, F., and Alvarenga, M. A. 1999. Constituents from *Siparuna apiosyce*. Fitoterapia 70: 322-323.

Fonseca, S. F., Barataa, L. E. S., Rúveda, E. A., and Baker, P. M. 1979. ^{13}C neuclear magnetic resonance spectral and conformational analysis of naturally occurring tetrahydrofuran lignans. Can. J. Chem. 57: 441-444.

Gagnepain F. 1907. Annonacées. In: Lecomte, M. H., ed. Flore Generale de L'Indo-Chine, Tome 1 Fasc. 1. p. 111. Paris: Masson et Cie, Editeurs.

Hada, S., Hattori, M., Tesuka, Y., Kikuchi, T., and Namba, T. 1988. New neolignans and lignans from the aril of *Myristica fragrans*. Phytochemistry 27: 563-568.

Harrigan, G. G., Gunatilaka, A. A. L., Kingston, D. G. I., Chan, G. W., and Johnson, R. K. 1994**.** Isolation of bioactive and other oxoaporphine alkaloids from two annonaceous plants, *Xylopia aethiopica* and *Miliusa* cf. *banacea*. J. Nat. Prod. 57: 68–73.

Hattori, M., Hada, S., Shu, Y.Z., Kakiuchi, N., and Namba, T. 1987. New acyclic bis-phenylpropanoids from the aril of *Myristica fragrans*. Chem. Pharm. Bull. 35: 668-674.

Herath, H. T. B., and Priyadarshini, A. M. A. 1996. Two lignans and an aryl alkanone from *Myristica dactyloides*. Phytochemistry 42: 1439-1442.

Hunt, L., Jordan, M., De Jesus, M., Wurm, F. M. 1999. GFP-expressing mammalian cells for fast, sensitive, noninvasive cell growth assessment in a kinetic mode. Biotechnol. Bioeng. 65: 201-205.

Huo, C. H., Liang, H., Zhao, Y. Y., Wang, B., Zhang, Q. Y. 2008. Neolignan glycosides from *Symplocos caudata*. Phytochemistry 69: 788–795.

Huong, D. T., Kamperdick, C., and Van Sung, T. 2004. Homogentisic acid derivatives from *Miliusa balansae*. J. Nat. Prod. 67: 445–447.

Huong, D. T., Luong, D. V., Thao, T. T. P., and Sung, T. V. 2005. A new flavone and cytotoxic activity of flavonoid constituents isolated from *Miliusa balansae* (Annonaceae). Pharmazie 60: 627–629.

Huong, D. T., Van, N. T. H., Kamperdick, C., Anh, N. T. H., and Sung, T. V. 2008. Two new bis-styryl compounds from *Miliusa balansae*. Z. Naturforsch. B. 63: 335–338.

Jemal, A., Bray, F., Center, M. M., Ferlay, J., Ward, E., and Forman, D. 2011. Global cancer statistics. CA Cancer J. Clin. 61: 69-90.

Jing, X., Gu, W., Bie, P., Ren, X., and Pan, X. 2001. Total synthesis of (±)-eusiderin K and (±)-eusiderin J. Synthetic. Commun. 31: 861-867.

Jumana, S., Hasan, C. M., and Rashid, M. A. 2000. Alakaloids from the stem bark of *Miliusa velutina*. Biochem. Syst. Ecol. 28: 483–485.

Jumana, S., Hasan, C. M., and Rashid, M. A. 2000a. Antibacterial activity and cytotoxicity of *Miliusa velutina*. Fitoterapia 71: 559-561.

Kamperdick, C., Hong Van, N., and Van Sung, T. 2002**.** Constituents from *Miliusa balansae* (Annonaceae). Phytochemistry 61: 991–994.

Khan, M. T. H., Ather, A., Thompson, K. D., and Gambari, R. 2005. Extracts and molecules from medicinal plants against herpes simplex viruses. Antivir. Res. 67: 107-119.

Kim, T. H., Ito, H., Hayashi., K., Hasegawa, T., Machiguchi, T., and Yoshida, T. 2005. Aromatic constituents from the heartwood of *Santalum album* L. Chem. Pharm. Bull. 53: 641-644.

Kim, K. H., Kim, H. K., Choi, S. U., Moon, E., Kim, S. Y., and Lee, K. R. 2011. Bioactive lignans from the rhizomes of *Acorus gramineus*. J. Nat. Prod. 74: 2187-2192.

Lei, Y., Wu, L. J., Shi, H. M., and Tu, P. F. 2008. Three new glycosides from the stems of *Miliusa balansae*. Helv. Chim. Acta. 91: 495–500.

Likhitwitayawuid, K., Angerhofer, C. K., Chai, H. Pezzuto, J. M., and Cordell, G. A. 1993. Cytotoxic and antimalarial alkaloids from the tubers of *Stephania pierrei*. J. Nat. Prod. 56: 1468-1478.

Lipipun, V., Kurokawa, M., Suttisri, R., Taweechotipatr, P., Pramyothin, P., Hattori, M., and Shiraki, K. 2003. Efficacy of Thaimedicinal plant extracts against

herpes simplex virus type 1 infection in vitro and in vivo. Antivir. Res. 60: 175–180.

Lo, W. L., Wu, Y. C., Hsieh, T. J., Kuo, S. H., Lin, H. C., and Chen, C. Y. 2004. Chemical constituents from the stems of *Michelia compressa*. Chin. Pharm. J. 56: 69-75.

Lopes, N. M., de Almeida Blumenthal, E. E., Cavalheiro, A. J., Kato, M. J., and Yoshida, M., 1996. Lignans, γ-lactones and propiophenones of *Virola surinamensis*. Phytochemistry. 43: 1089-1092.

Matcha, K. and Ghosh, S. 2010. An asymmetric route to total synthesis of the furano lignan (+)-veraguensin. Tetra. Lett. 51: 6924-6927.

Menon, M. K. and Kar, A. 1970. Analgesic effect of essential oil of *Miliusa tomentosa* (roxb.) J. Sinclair. Ind. J. Exp. Biol. 8: 151-152.

Miyase, T., Ueno, A., Takizawa, N., Kobayashi, H., and Oguchi, H. 1989. Ionone and lignan glycosides from *Epimedium diphyllum*. Phytochemistry. 28: 3483-3485.

Mols, J. B. and Keßler, P. J. A. 2003. The genus *Miliusa* (Annonaceae) in the Austro-Malesian area. Blumea 48 : 421-462.

Morais, S. K. R., Teixeira, A. F., Torres, Z. E. D. S., Nunomura, S. M., Yamashiro-Kanashiro, E. H., Lindoso, J. A. L., and Yoshida, M. 2009. Biological activities of lignoids from amazon Myristicaceae species: *Virola michelii*, *V. mollissima*, *V. pavonis* and *Iryanthera juruensis*. J. Brazil. Chem. Soc. 20: 1110–1118.

Motter Magri, F. M., Kato, M. J., and Yoshida, M. 1996. Butanolides and a neolignan from the fruits of *Iryanthera paraensis* Huber. Phytochemistry 43: 669-671.

Pang, S. Q., Wang, G. Q., Huang, B. K., Zhang, Q. Y., and Qin, L. P. 2007. Isoquinoline alkaloids from *Broussonetia papyrifera* fruits. Chem. Nat. Compd. 43: 100-102.

Pietta, P. G. 2000. Flavonoids as antioxidant. J. Nat. Prod. 63: 1035-1042.

Schroeder, C., Lutterbach, R., and Stöckigt, J. 1996. Preparative biosynthesis of natural glucosides and fluorogenic substrates for β-glucosidases followed by *in vivo* ^{13}C NMR with high density plant cell cultures. Tetrahedron 52: 925–934.

Shahat, A. A. 2006. Procyanidins from *Adansonia digitata*. Pharm. Biol. 44: 445-450.

Silva, M. S. da, Barbosa-Filho, J. M., Yoshida, M., and Gottlieb, O. R. 1989. Benzodioxane and *β*-arylpropane type neolignans from *Licaria chrysophylla*. Phytochemistry 28: 3477-3482.

Silverstein, R. M., and Webster, F. X. 1996. Spectrometric identification of organic compounds. 6th edition. The United state of America. John Wiley & Sons, Inc.

Snider, B. B., Han, L. N., and Xie, C. Y. 1997. Synthesis of 2,3-dihydrobenzofurans by $Mn(OAc)_3$-based oxidative cycloaddition of 2-cyclohexenones with alkenes. Synthesis of (±)-conocarpan. J. Org. Chem. 62: 6978–6984.

Takahasi, H., Yanagi, K., Ueda, M., Nakade, K., and Fukuyama, Y. 2003. Structures of 1,4-benzodioxane derivatives from the seeds of *Phytolacca americana* and their neuritogenic activity in primary cultured rat cortical neurons. Chem. Pharm. Bull. 51: 1377-1381.

Takao, T., Kitatani, F., Watanabe, N., Yaki, A., and Sakata, K. 1994. A simple screening method for antioxidants and isolation of several antioxidants produced by marine bacteria from fish and shellfish. Biosci. Biotech. Biochem. 58: 1780-1783.

Thanh Thuy, T. T., Quan, T. D., Hoang Anh, N. T. and Sung, T. V. 2011. A new hydrochalcone from *Miliusa sinensis*. Nat. Prod. Res. 25: 1361-1365.

Volko, M., Leibfritz, D., Moncol, J., Cronin, M. T. D., Mazur, M. and Telser, J. 2007. Free radicals and antioxidants in normal physiological functions and human diesese. J. Biochem. Cell. Biol. 36: 44-84.

Wu, R., Ye, Q., Chen, N. Y., Zhang, G. L. 2001. A new norditerpene from *Miliusa balansae* Finet *et* Gagnep. Chin. Chem. Lett. 12: 247–248.

Yang, X.W., Huang, X., Ahmat, M. 2008. New neolignan from seed of *Myristica fragrans*. Chin. J. Chin. Mater. Med. 33: 397-402.

Zanin, S. M. W., and Lordello, A. L. L. 2007. Alcalóides aporfinóides do gênero *Ocotea* (Lauraceae). Quim. Nova 30: 92-98.

Zhang, Z., Elsohly, H. N., Jacob, M. R., Pasco, D. S., Walker, L. A., and Clark, A. M. 2002. New sesqiuterpinoids from the root of *Guatteria multivenia*. J. Nat. Prod. 65: 856-859.

Zhang, H. J., Ma, C. Y., Van Hung, N., Cuong, N. M., Tan, G. T., Santarsiero, B. D., Mesecar, A. D., Soejarto, D. D., Pezzuto, J. M., and Fong, H. H. S. 2006.

Miliusanes, a class of cytotoxic agents from *Miliusa sinensis*. J. Med. Chem. 49: 693–708.

APPENDIX

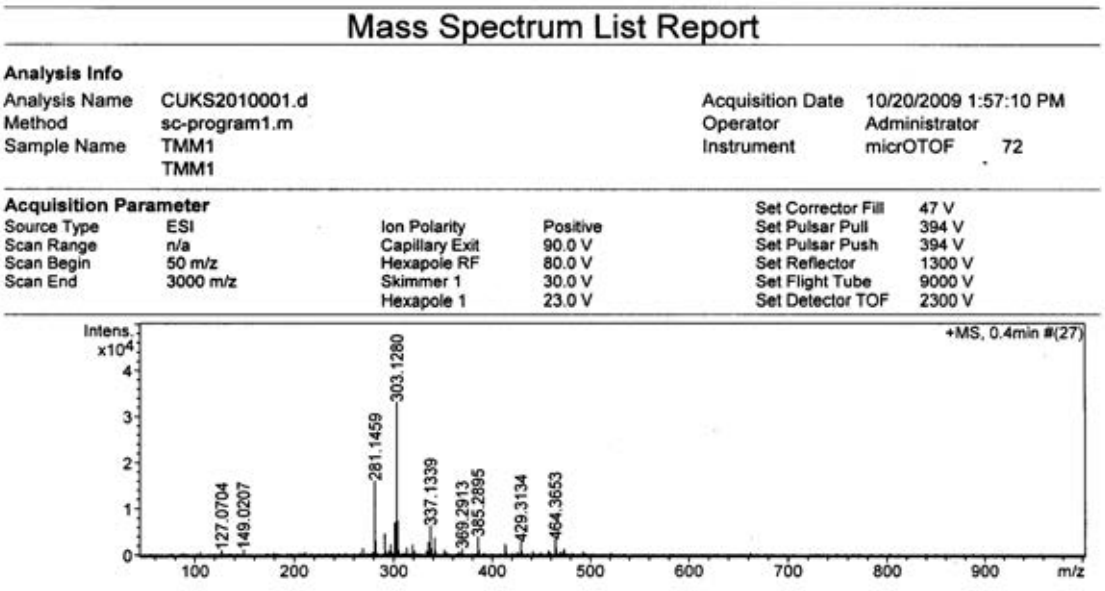

Figure 12 HRESI mass spectrum of compound TMM1 [**87**]

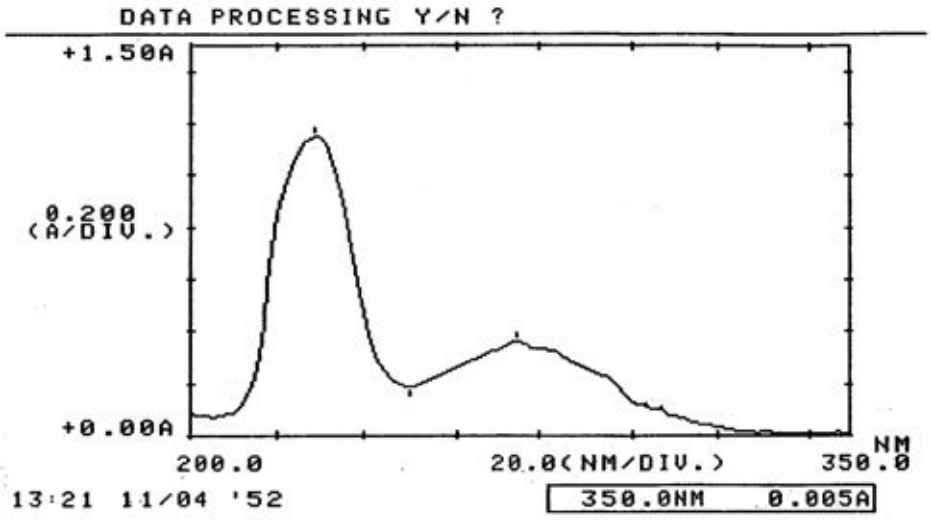

Figure 13 UV spectrum of compound TMM1 [**87**] (MeOH)

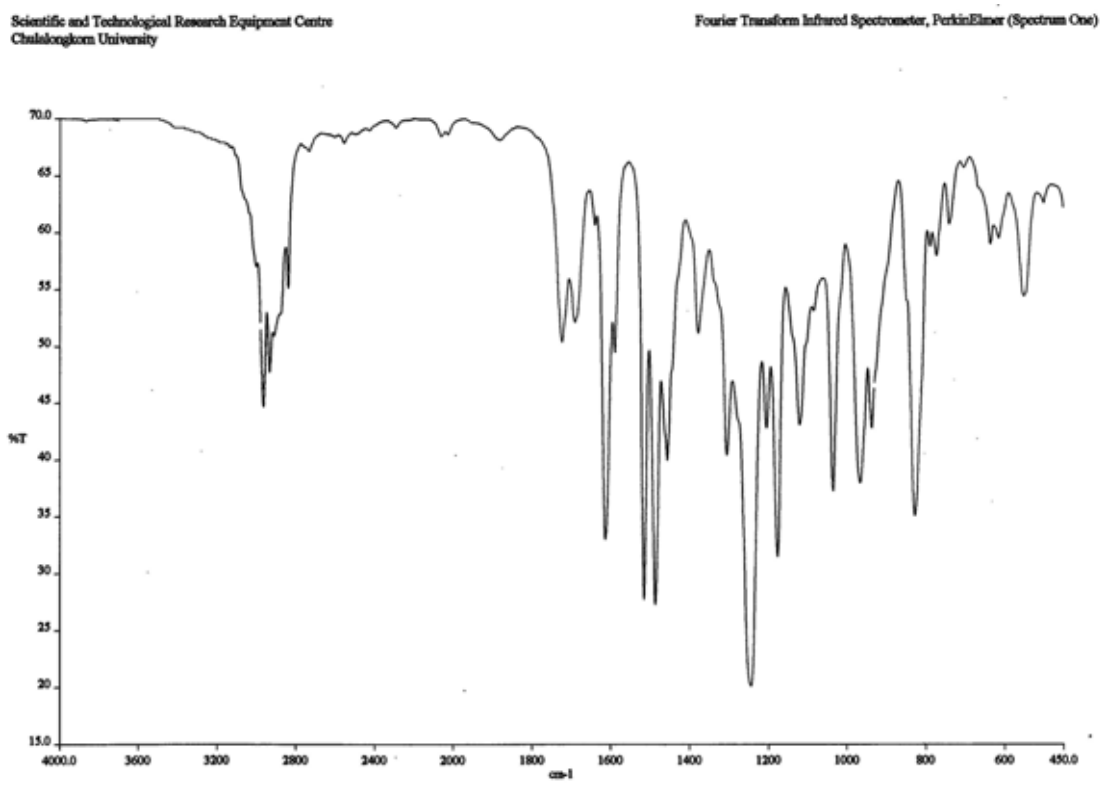

Figure 14 IR spectrum of compound TMM1 [**87**] (film)

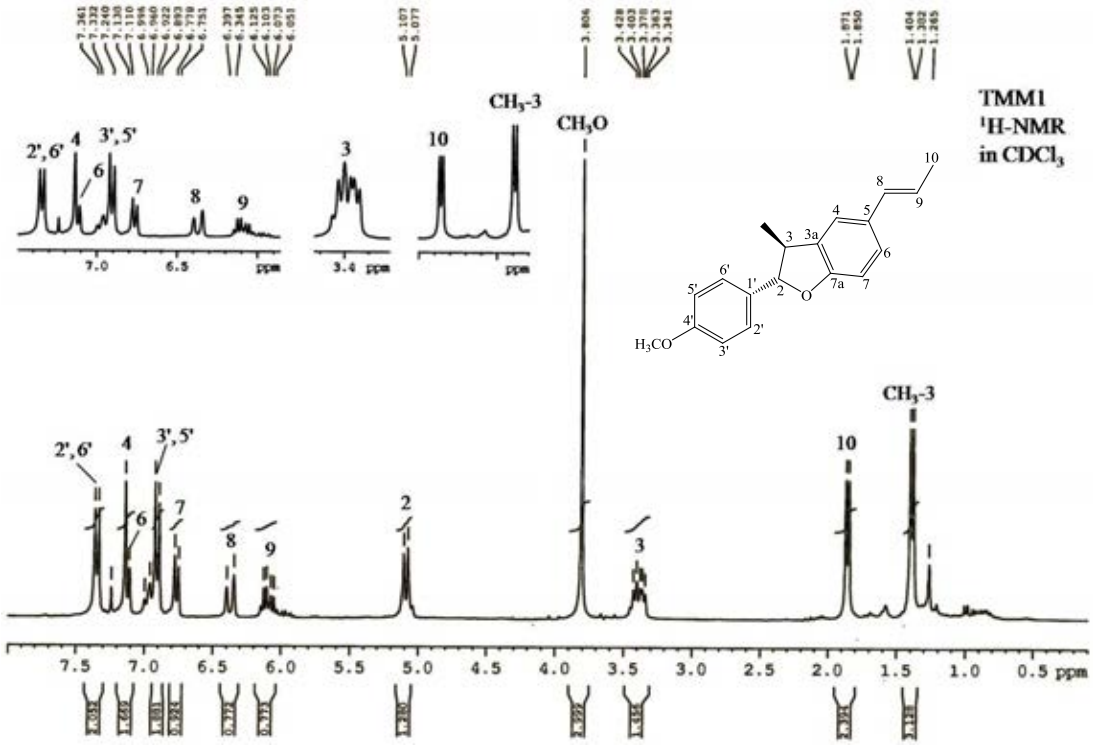

Figure 15 ^{1}H-NMR spectrum of compound TMM1 [**87**] ($CDCl_3$)

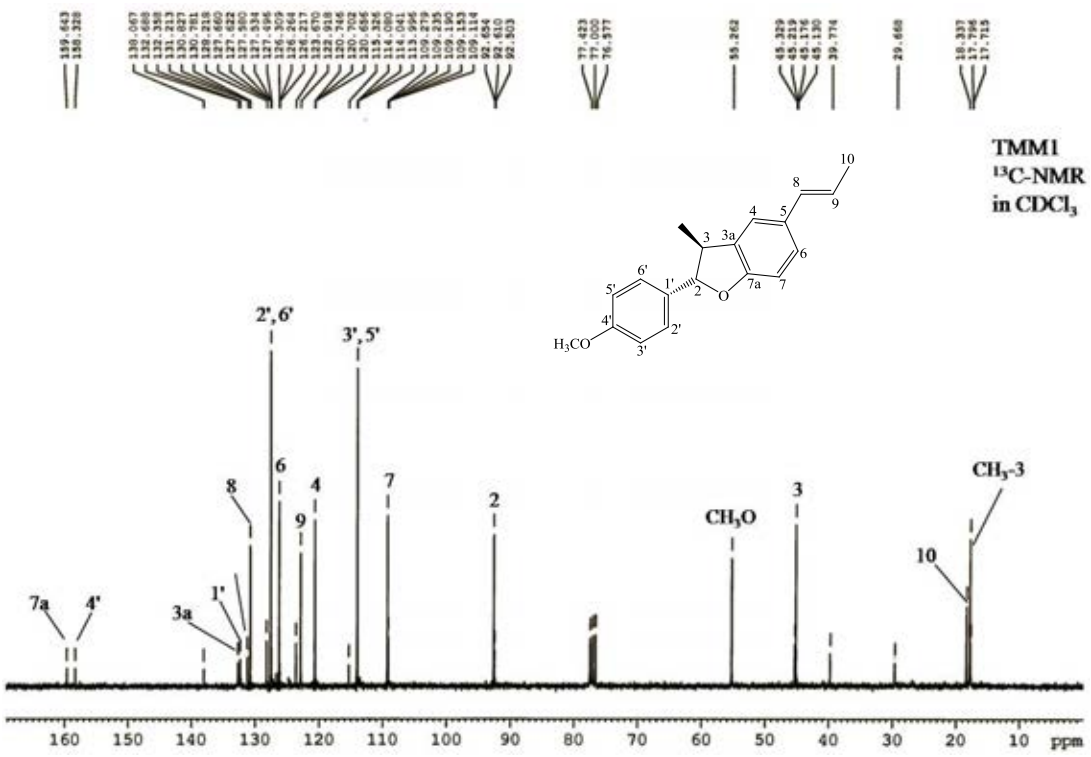

Figure 16 ^{13}C-NMR spectrum of compound TMM1 [**87**] ($CDCl_3$)

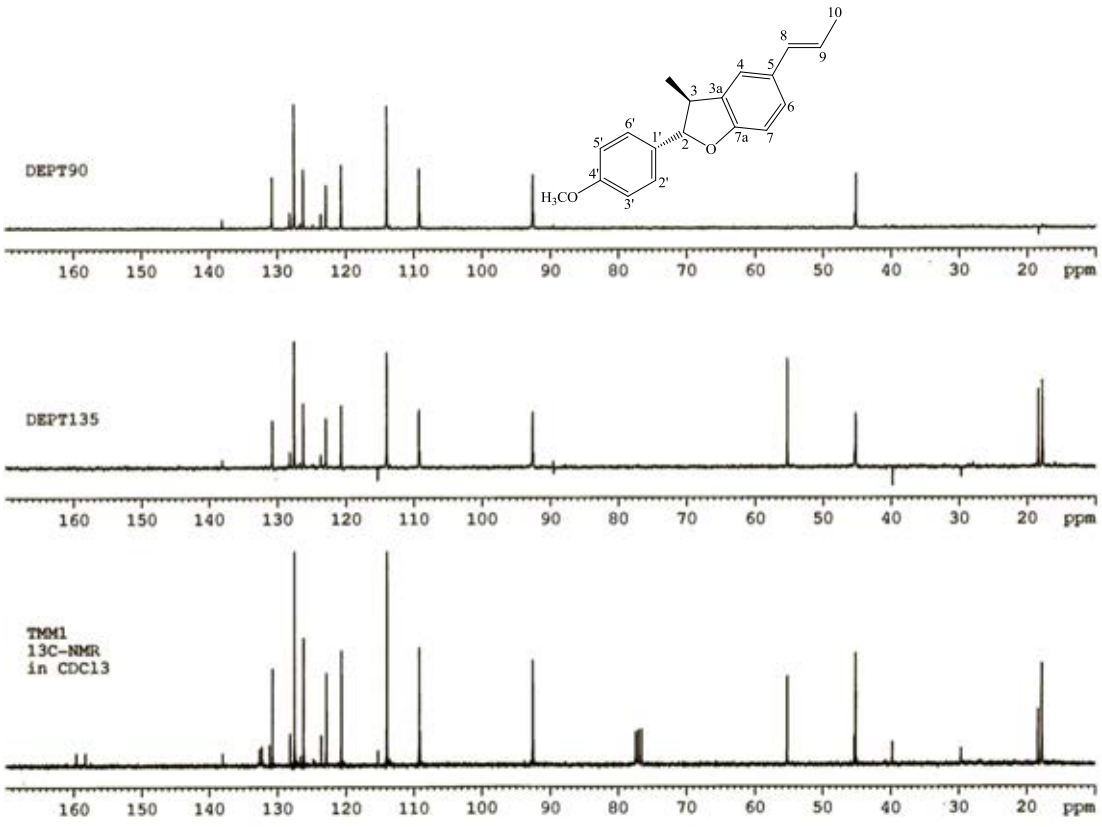

Figure 17 DEPT spectra of compound TMM1 [**87**] ($CDCl_3$)

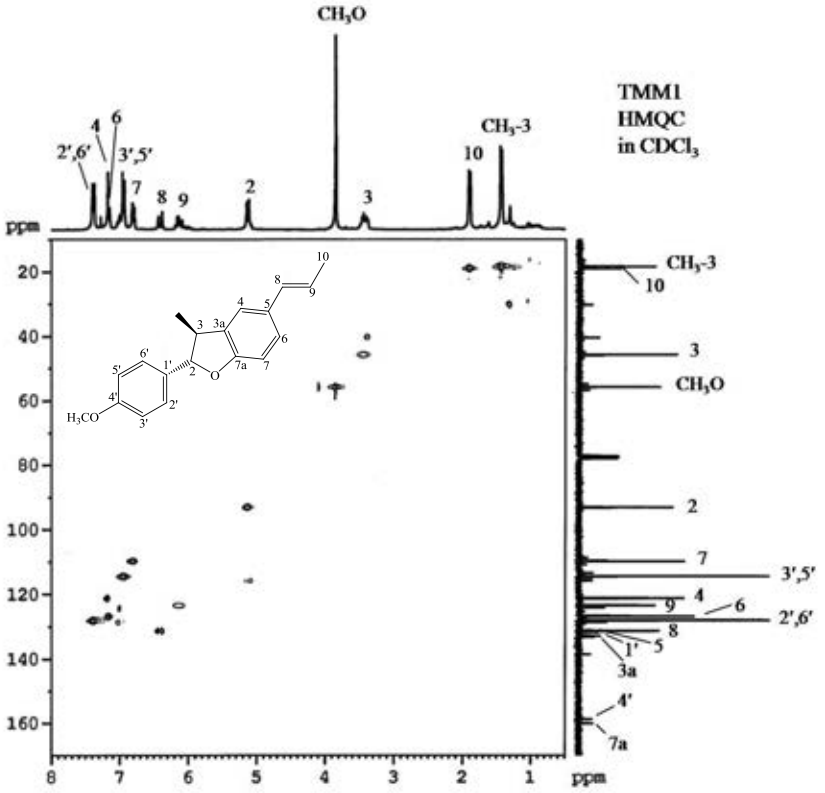

Figure 18 HMQC spectrum of compound TMM1 [**87**] ($CDCl_3$)

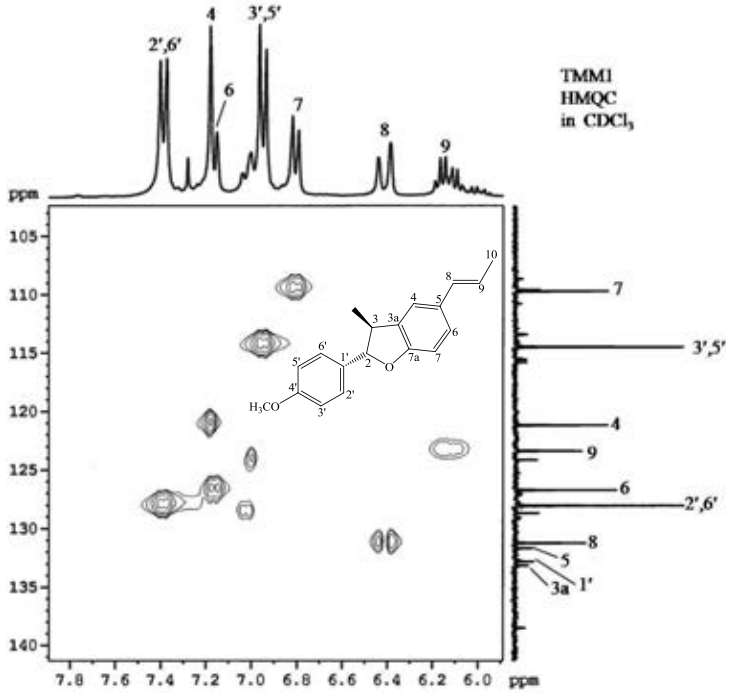

Figure 18a HMQC spectrum of compound TMM1 [**87**] ($CDCl_3$)
[δ_H 7.9-5.9 ppm, δ_C 141-102 ppm]

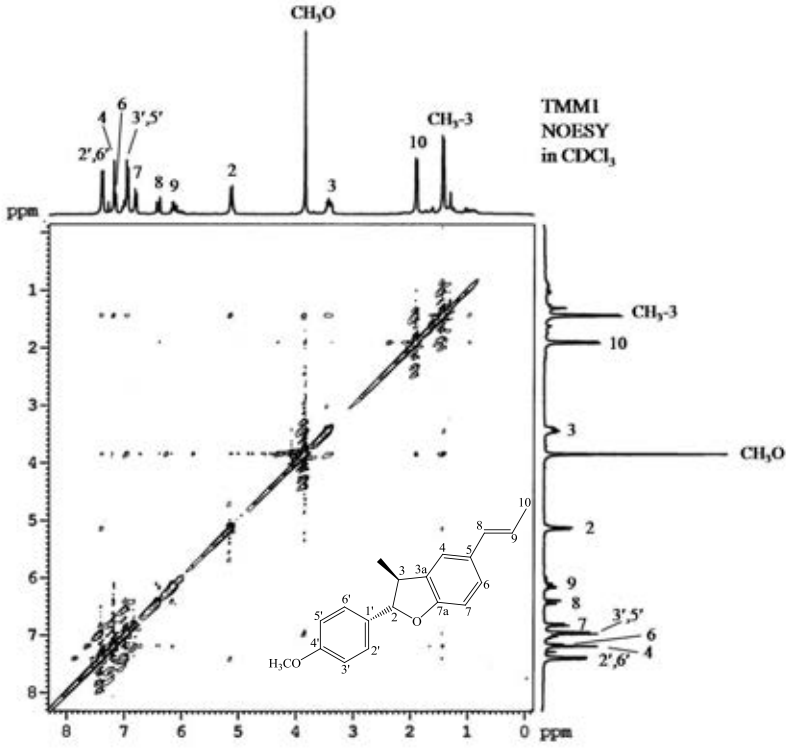

Figure 19 NOESY spectrum of compound TMM1 [**87**] ($CDCl_3$)

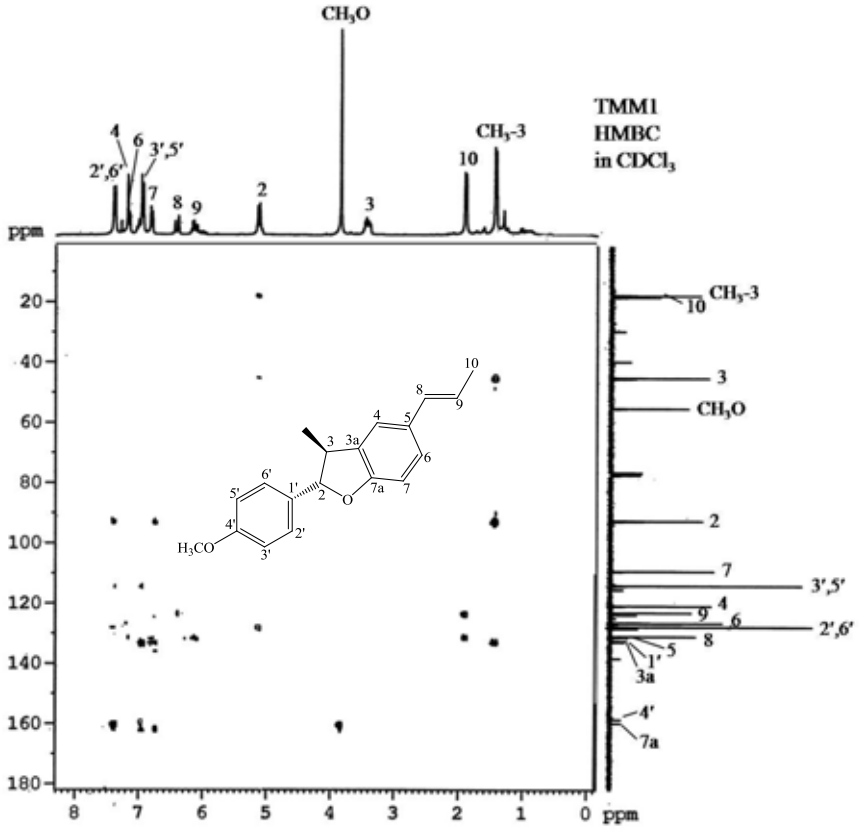

Figure 20 HMBC spectrum of compound TMM1 [**87**] ($CDCl_3$)

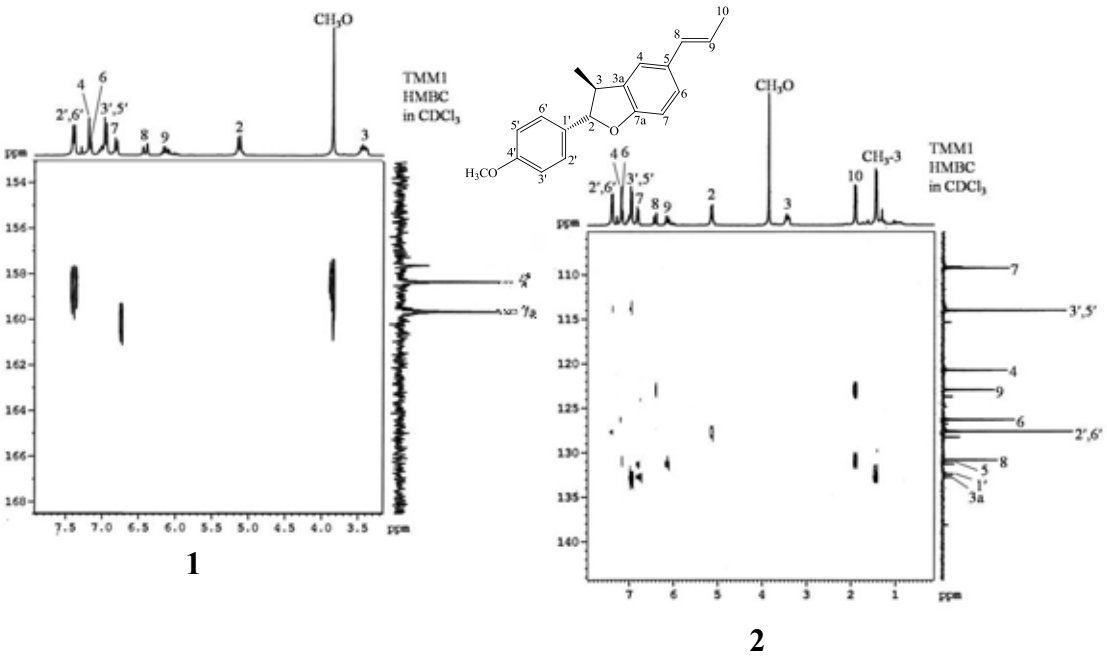

Figure 20a HMBC spectrum of compound TMM1 [**87**] ($CDCl_3$)
[δ_H 7.9-3.2 ppm, δ_C 168.5-153 ppm (1)] and
[δ_H 8-0 ppm, δ_C 144-105 ppm (2)]

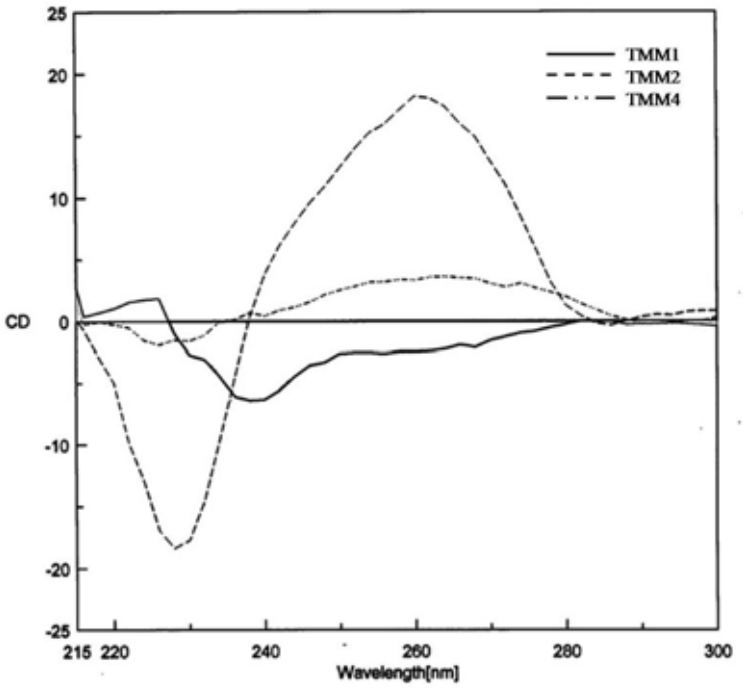

Figure 21 CD spectra (MeOH) of compounds TMM1[**87**], TMM2 [**88**] and TMM4 [**90**]

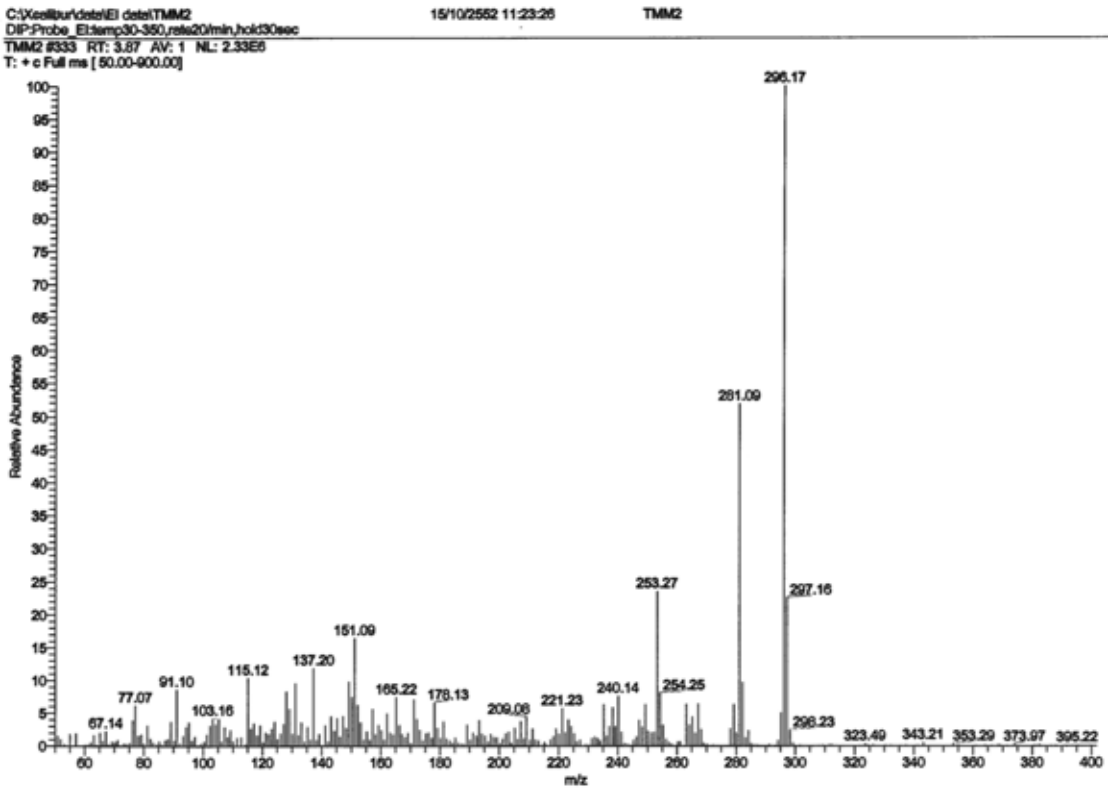

Figure 22 EI mass spectrum of compound TMM2 [**88**]

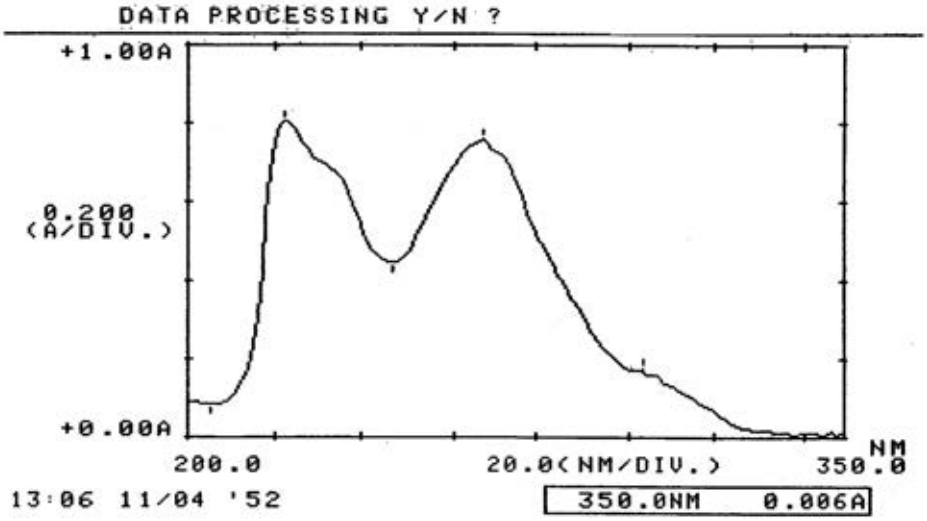

Figure 23 UV spectrum of compound TMM2 [**88**] (MeOH)

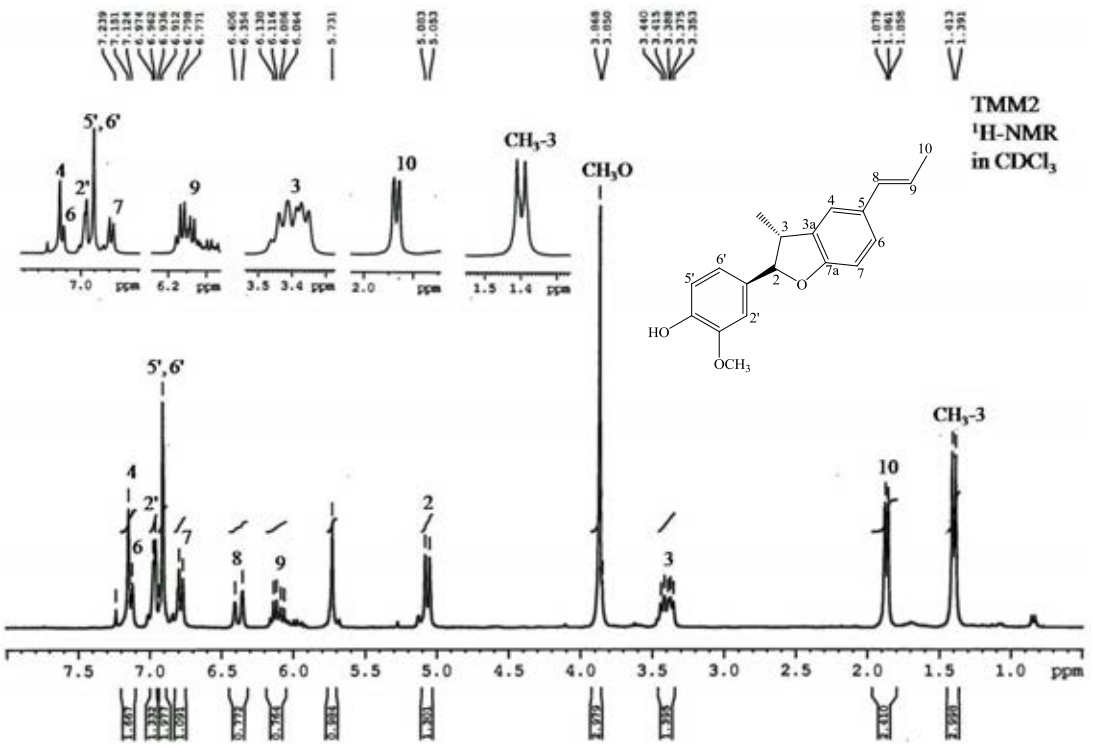

Figure 24 ^{1}H-NMR spectrum of compound TMM2 [**88**] ($CDCl_3$)

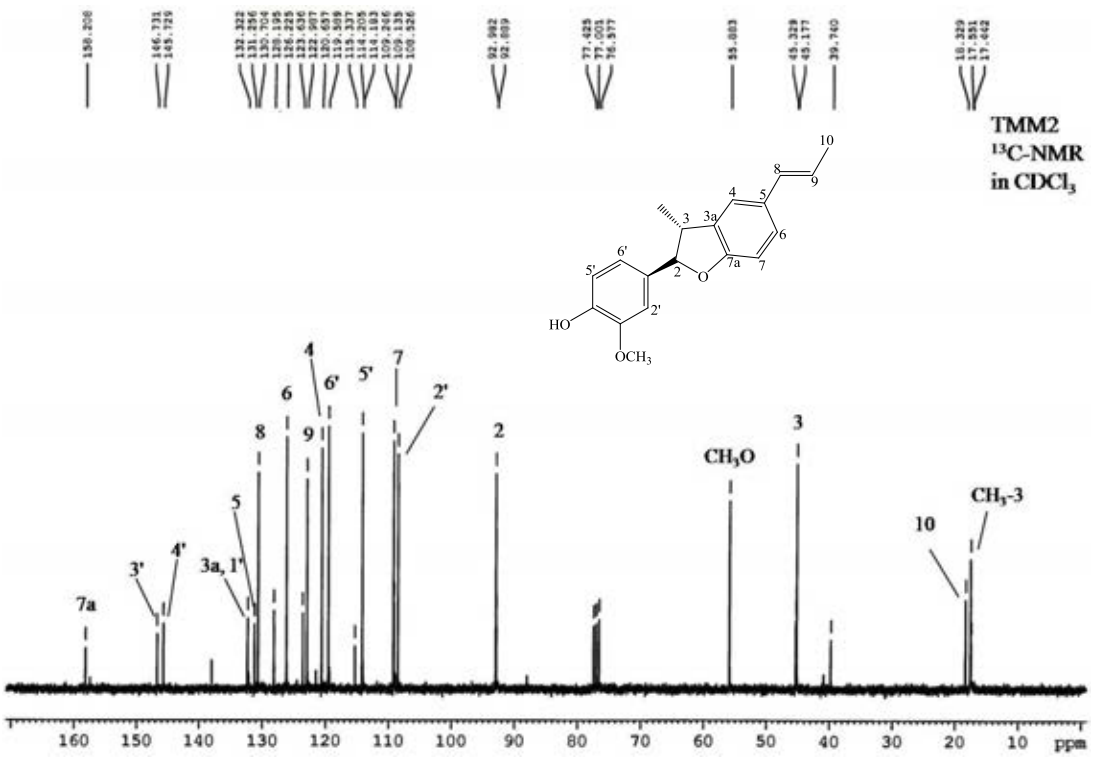

Figure 25 ^{13}C-NMR spectrum of compound TMM2 [**88**] ($CDCl_3$)

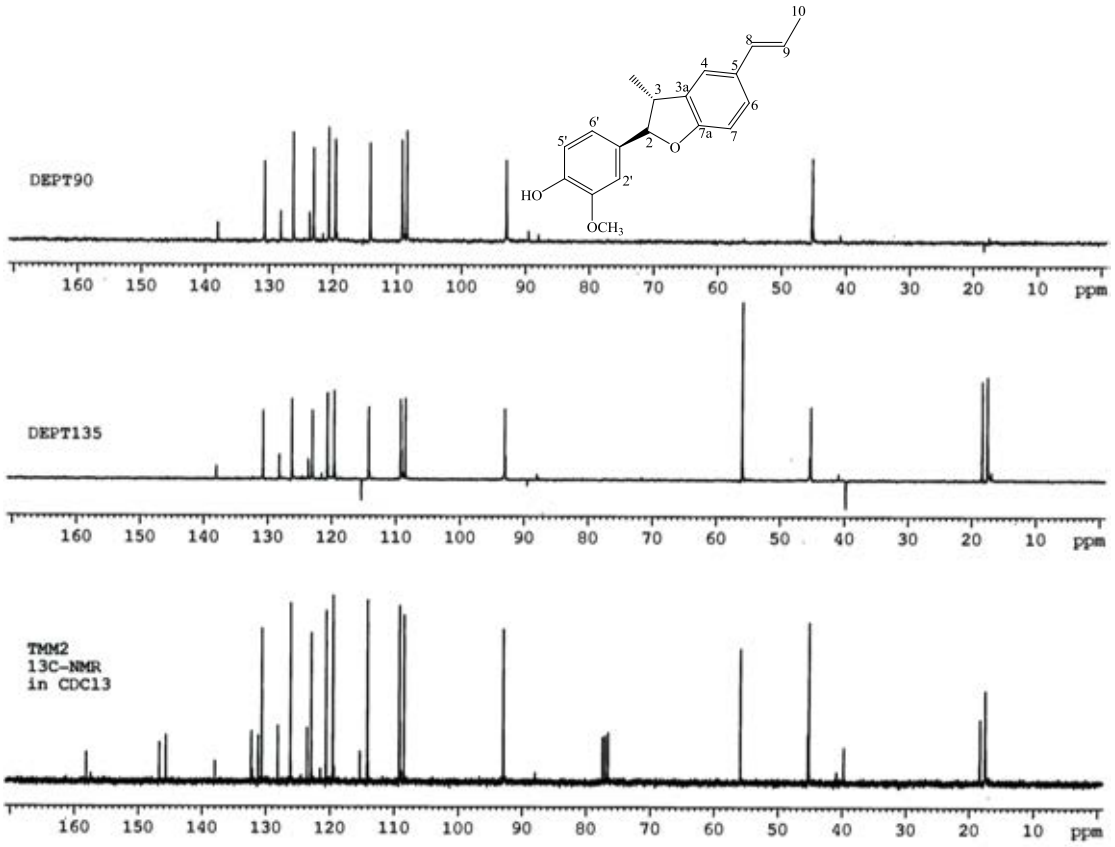

Figure 26 DEPT spectra of compound TMM2 [**88**] ($CDCl_3$)

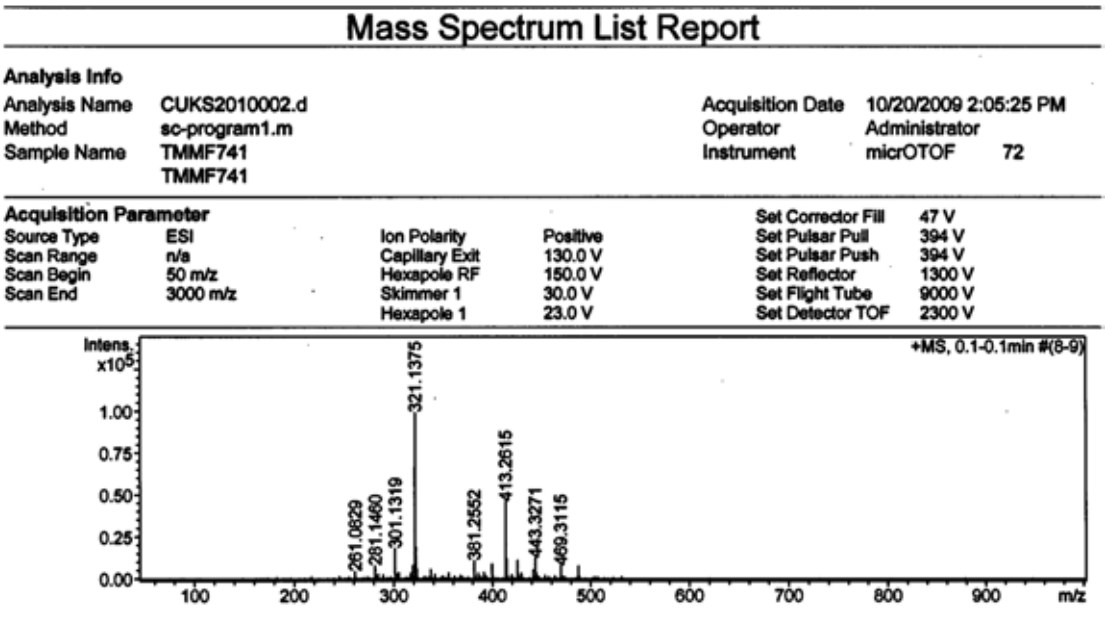

Figure 27 HRESI mass spectrum of compound TMM3 [**89**]

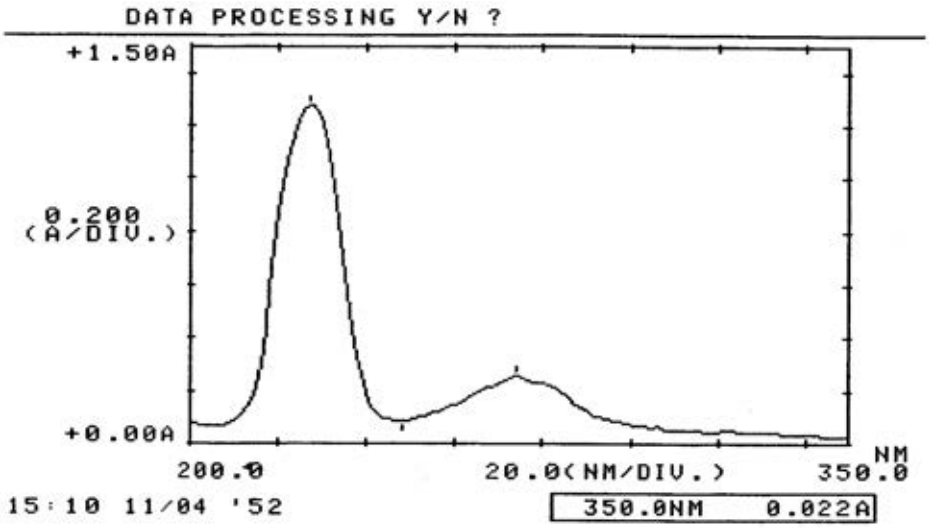

Figure 28 UV spectrum of compound TMM3 [**89**] (MeOH)

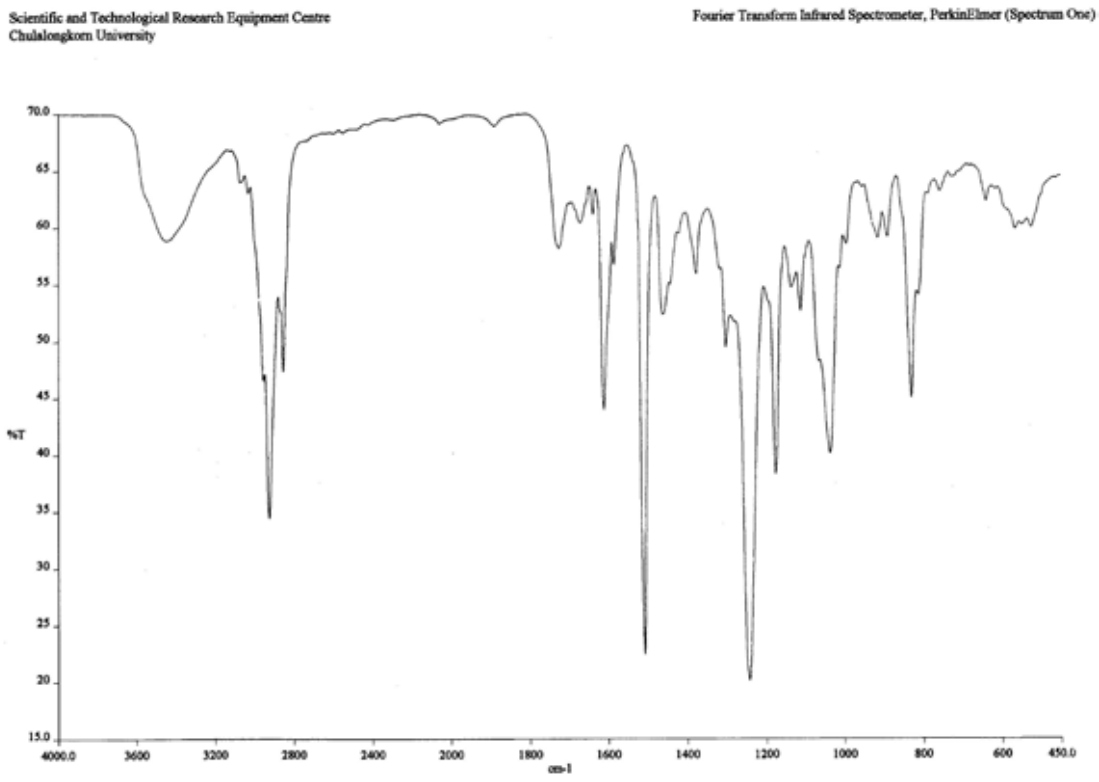

Figure 29 IR spectrum of compound TMM3 [**89**] (film)

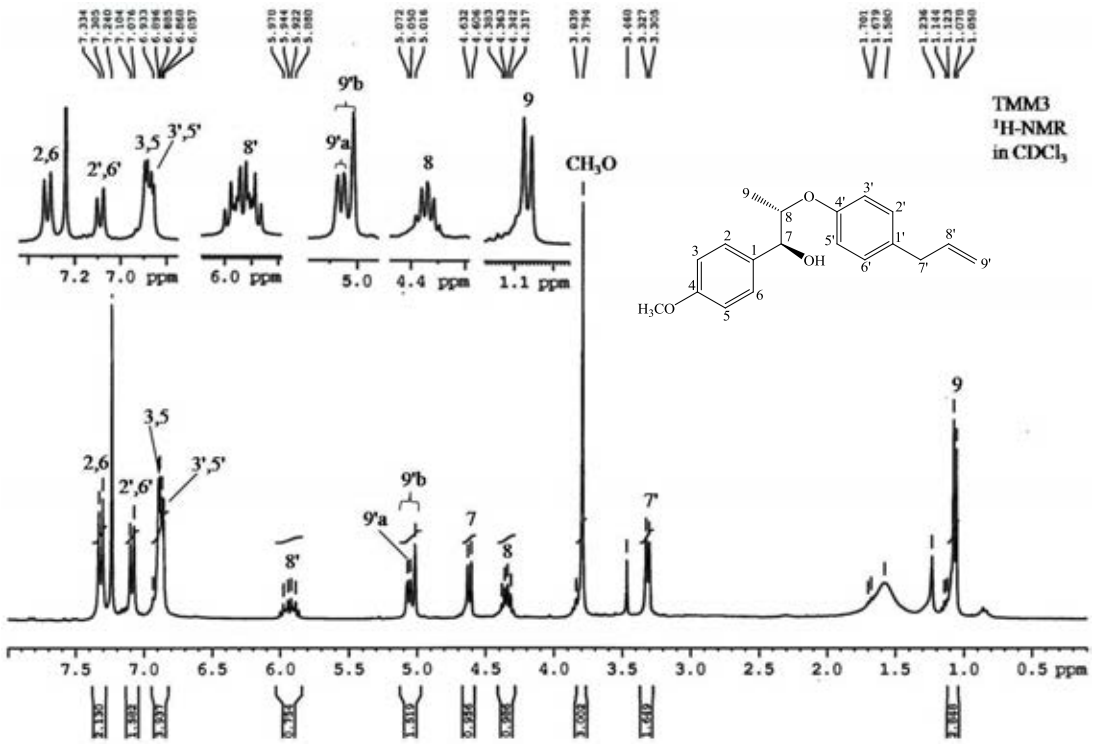

Figure 30 ^{1}H-NMR spectrum of compound TMM3 [**89**] ($CDCl_3$)

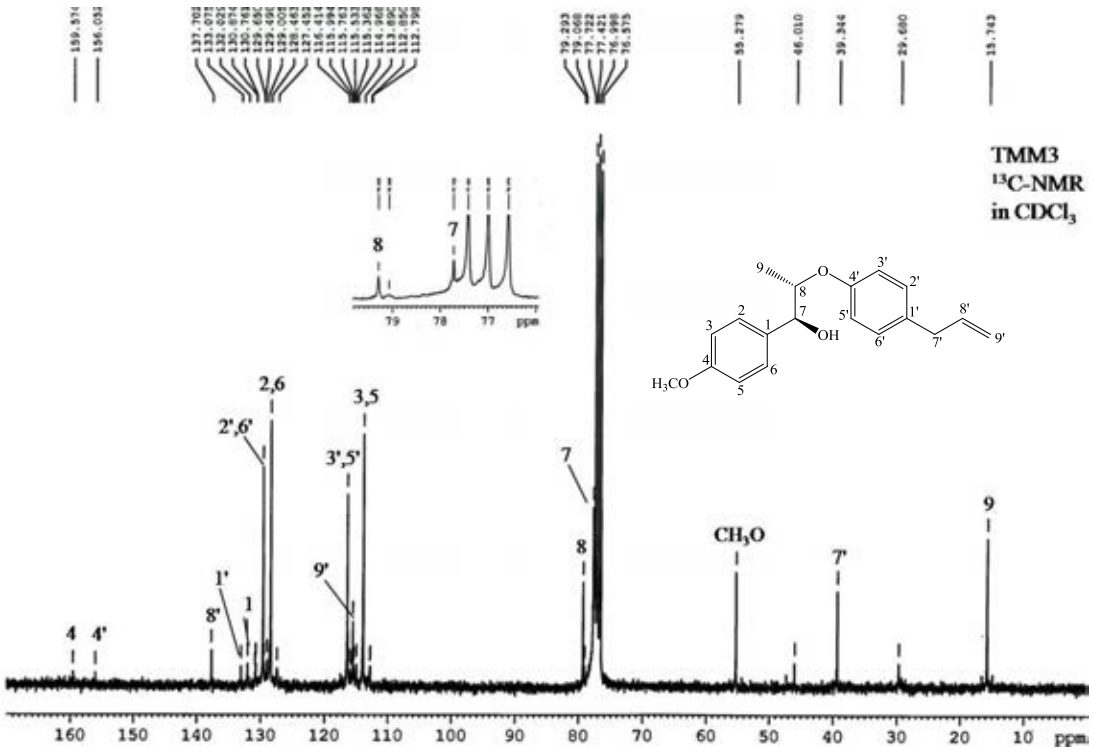

Figure 31 ^{13}C-NMR spectrum of compound TMM3 [**89**] ($CDCl_3$)

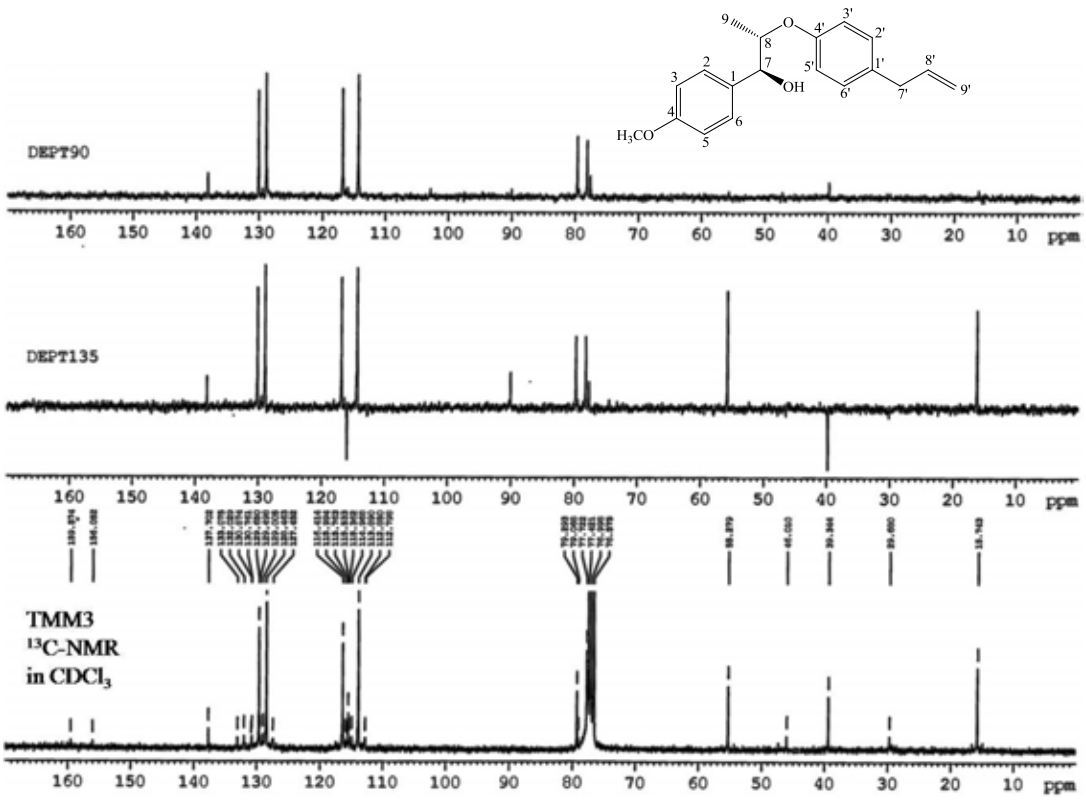

Figure 32 DEPT spectra of compound TMM3 [**89**] ($CDCl_3$)

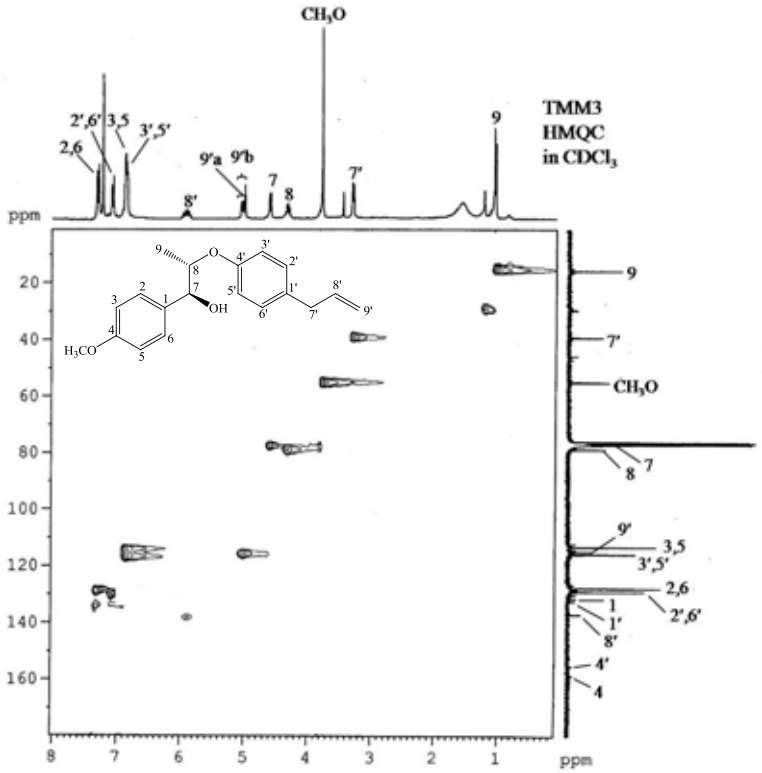

Figure 33 HMQC spectrum of compound TMM3 [**89**] ($CDCl_3$)

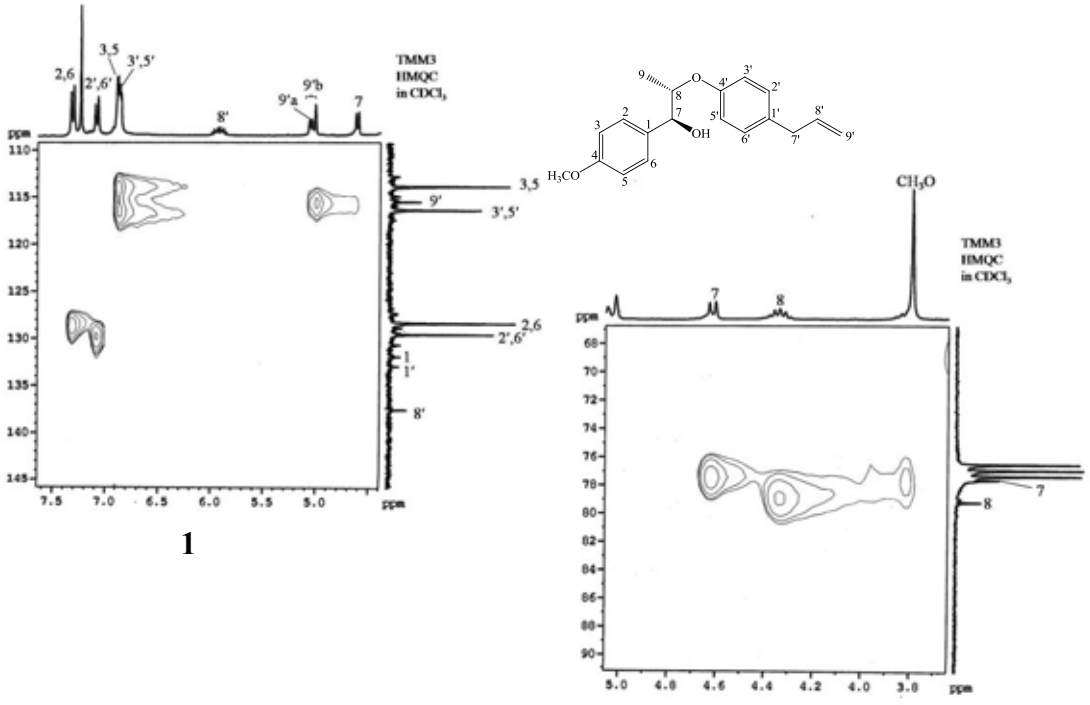

Figure 33a HMQC spectrum of compound TMM3 [**89**] ($CDCl_3$)
[δ_H 7.65-4.9 ppm, δ_C 146-109 ppm (1)] and
[δ_H 5.05-3.65 ppm, δ_C 91-67 ppm (2)]

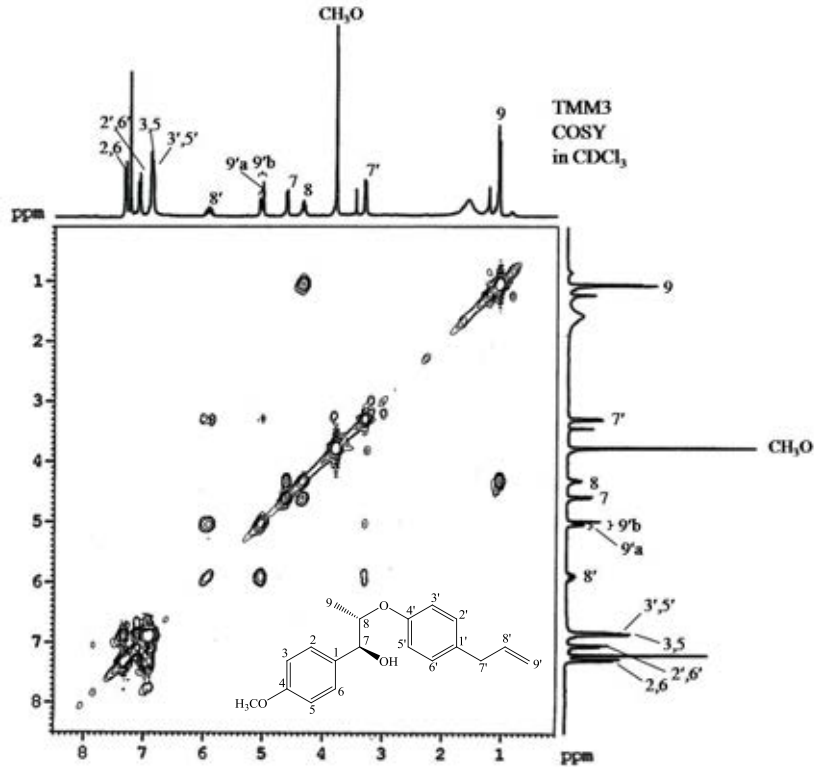

Figure 34 ^1H-^1H COSY spectrum of compound TMM3 [**89**] ($CDCl_3$)

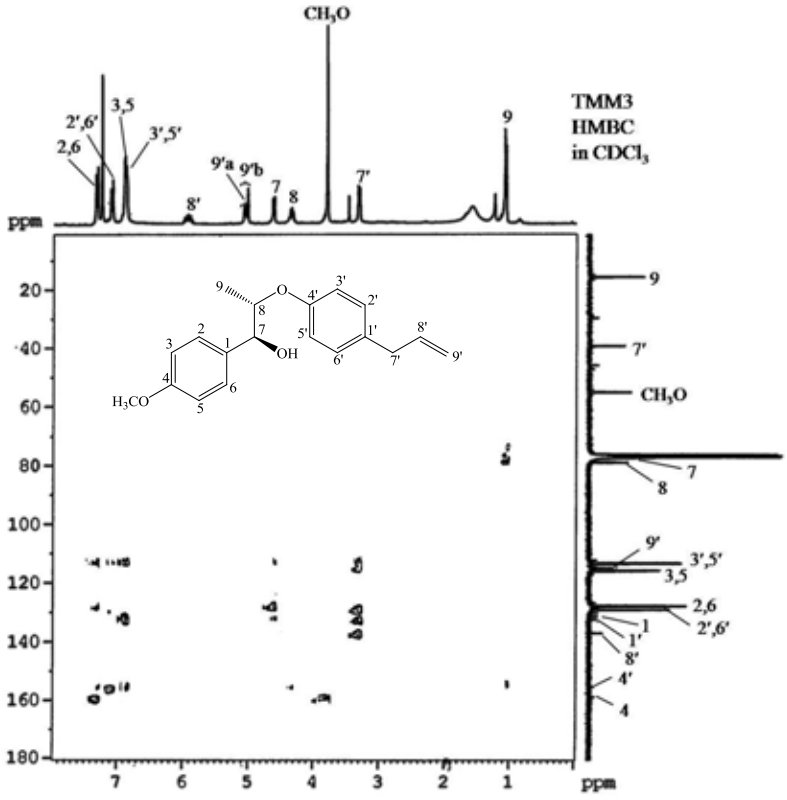

Figure 35 HMBC spectrum of compound TMM3 [**89**] ($CDCl_3$)

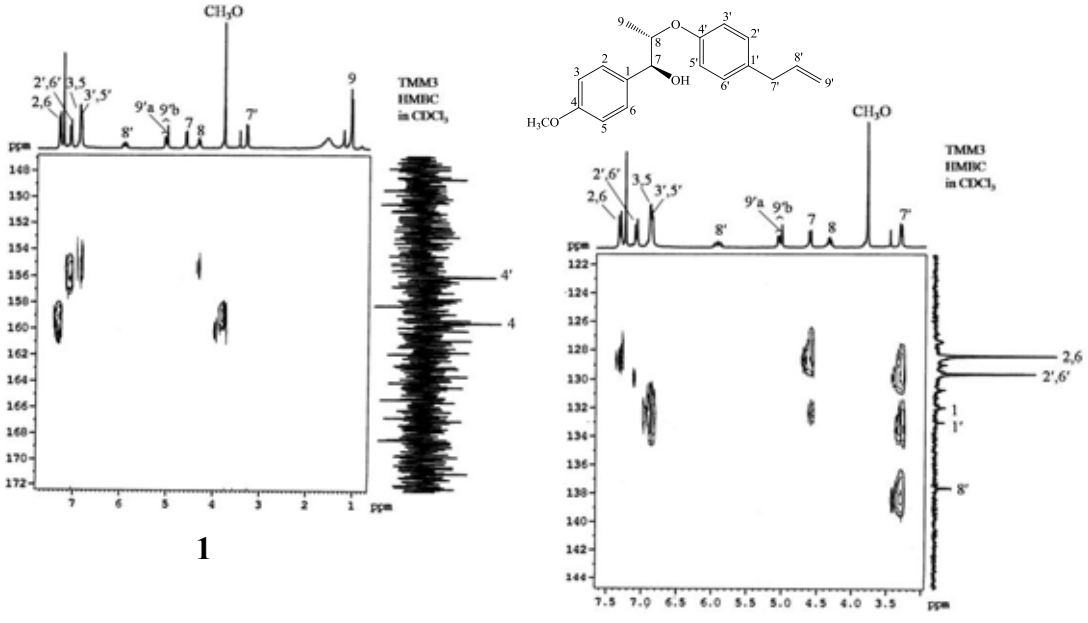

1 **2**

Figure 35a HMBC spectrum of compound TMM3 [89] ($CDCl_3$)
[δ_H 7.8-0.7 ppm, δ_C 172.5-147 ppm (1)] and
[δ_H 7.6-3.4 ppm, δ_C 145-121 ppm (2)]

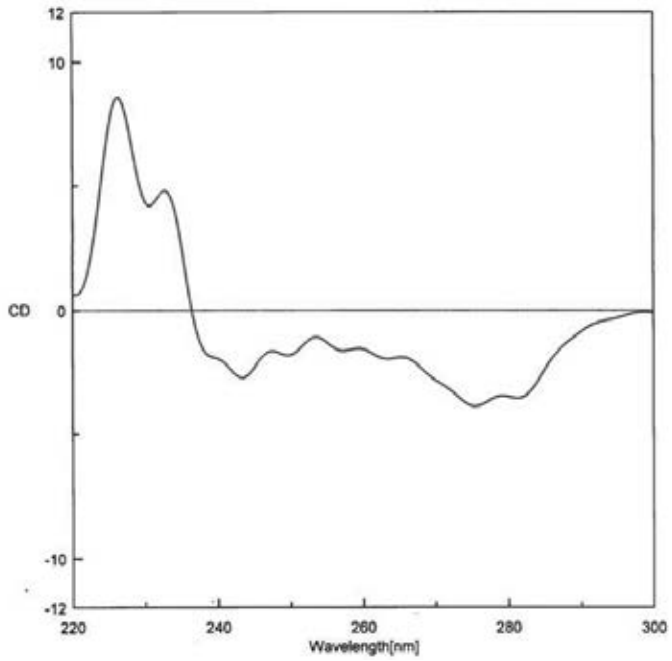

Figure 36 CD spectrum of compound TMM3 [**89**] (MeOH)

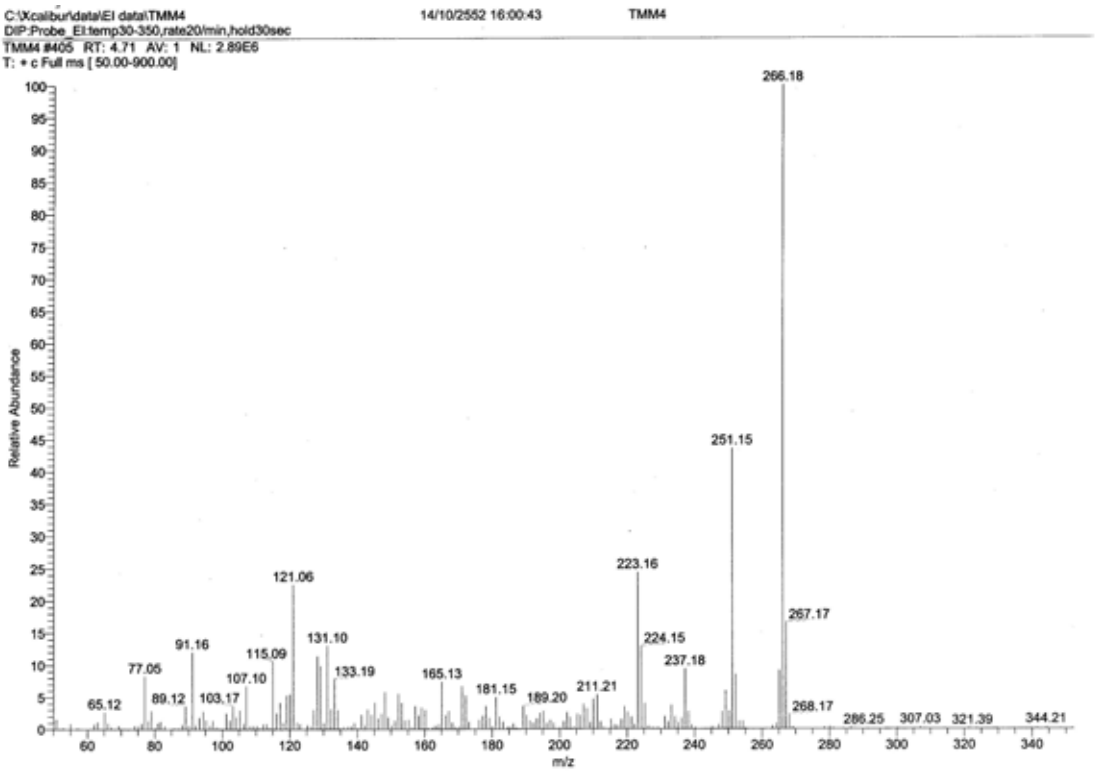

Figure 37 EI mass spectrum of compound TMM4 [**90**]

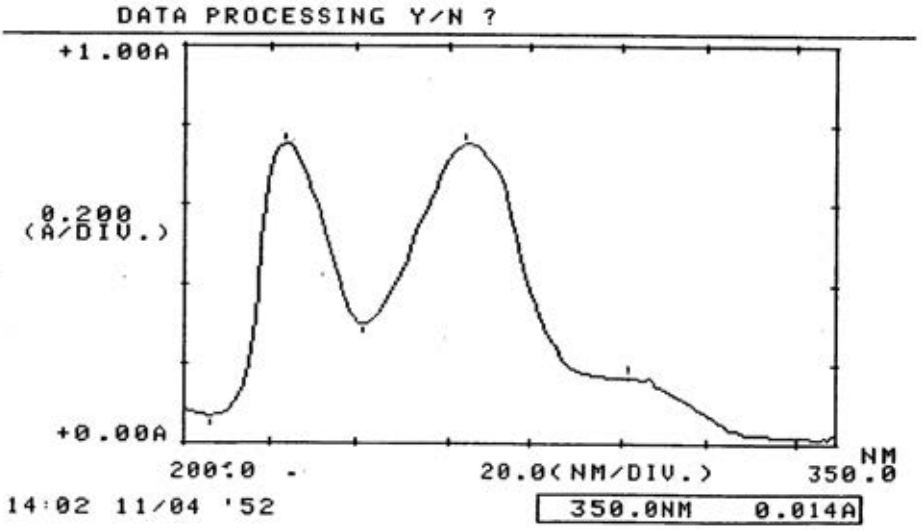

Figure 38 UV spectrum of compound TMM4 [**90**] (MeOH)

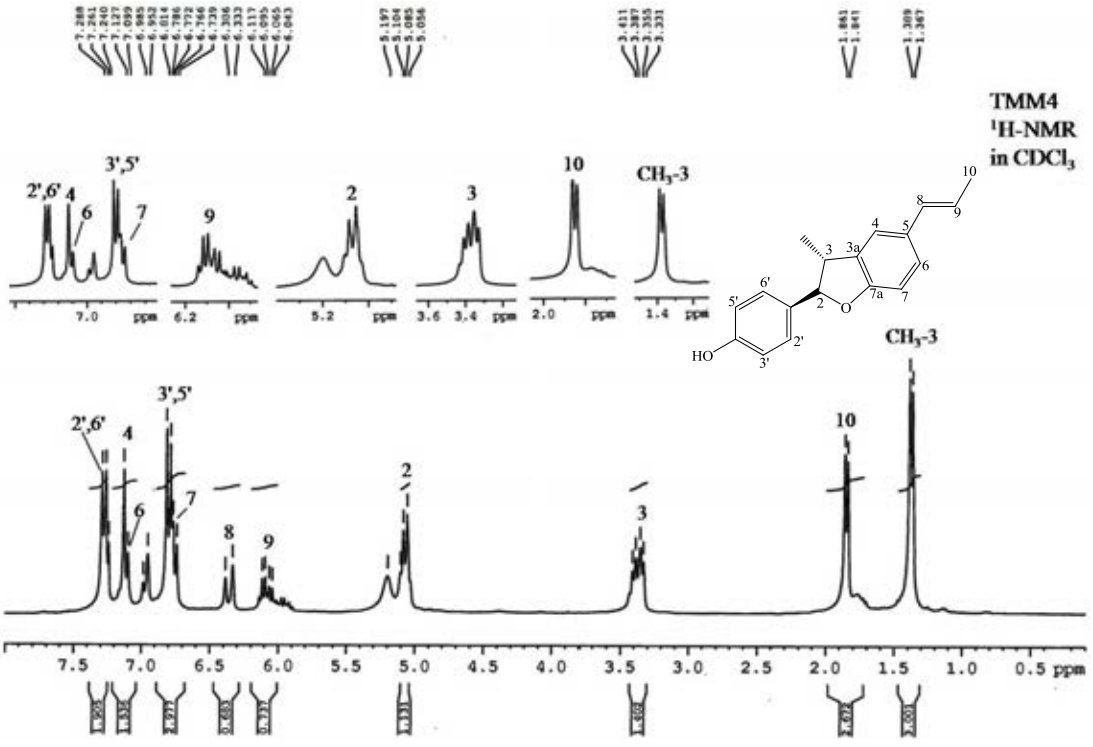

Figure 39 ^{1}H-NMR spectrum of compound TMM4 [**90**] ($CDCl_3$)

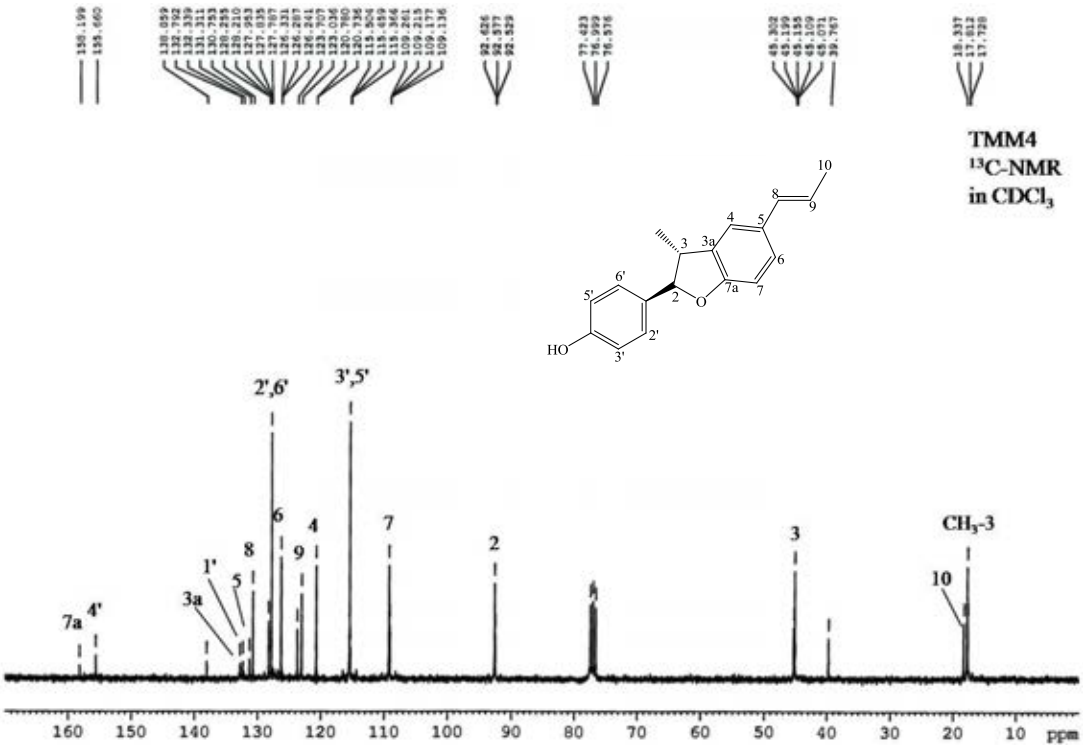

Figure 40 ^{13}C-NMR spectrum of compound TMM4 [**90**] ($CDCl_3$)

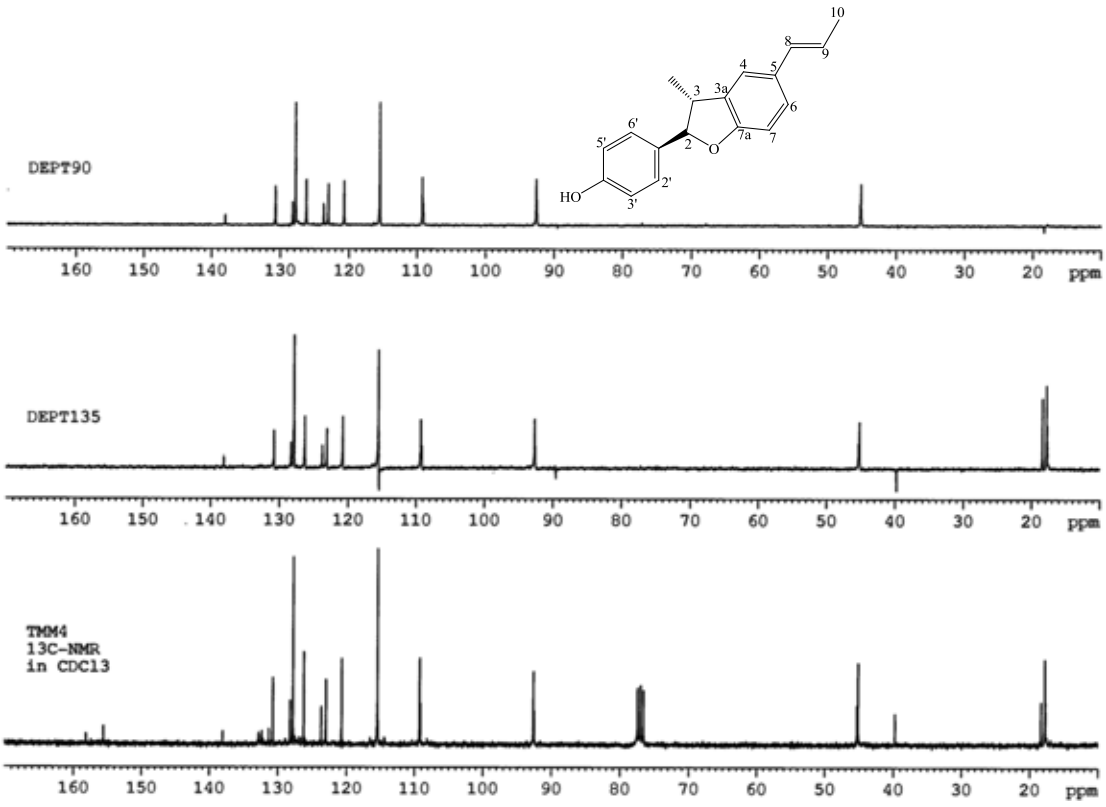

Figure 41 DEPT spectra of compound TMM4 [**90**] ($CDCl_3$)

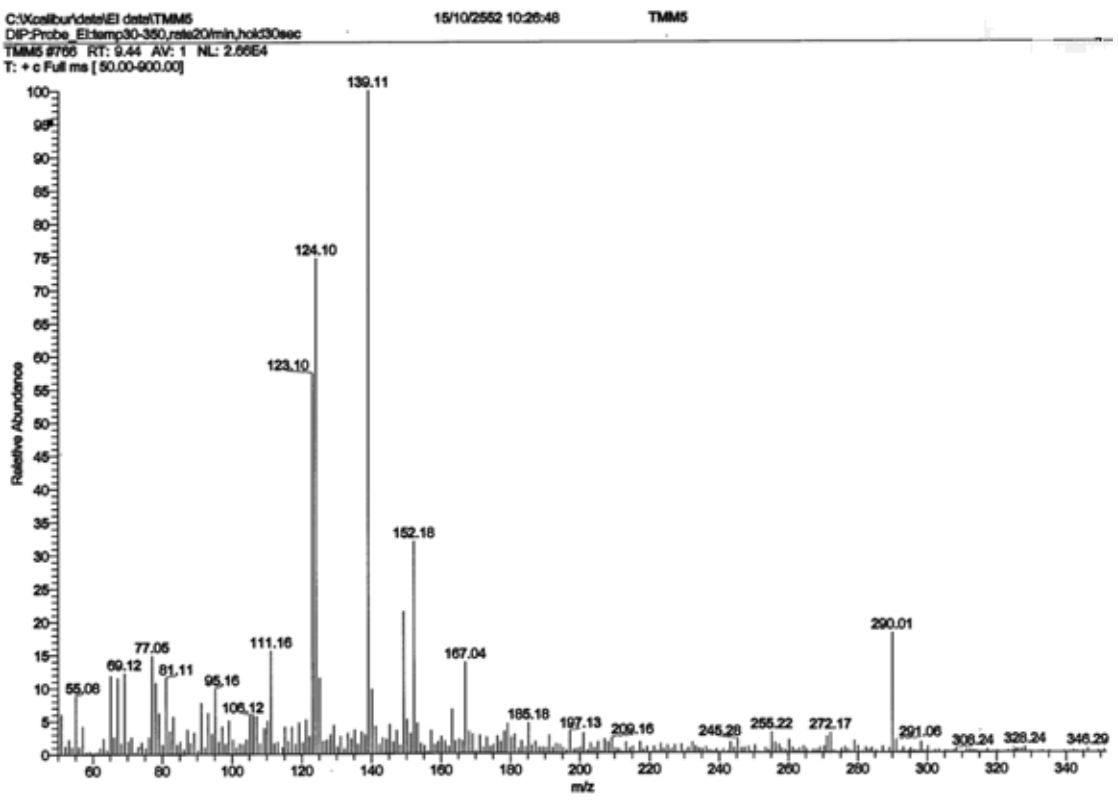

Figure 42 EI mass spectrum of compound TMM5 [**91**]

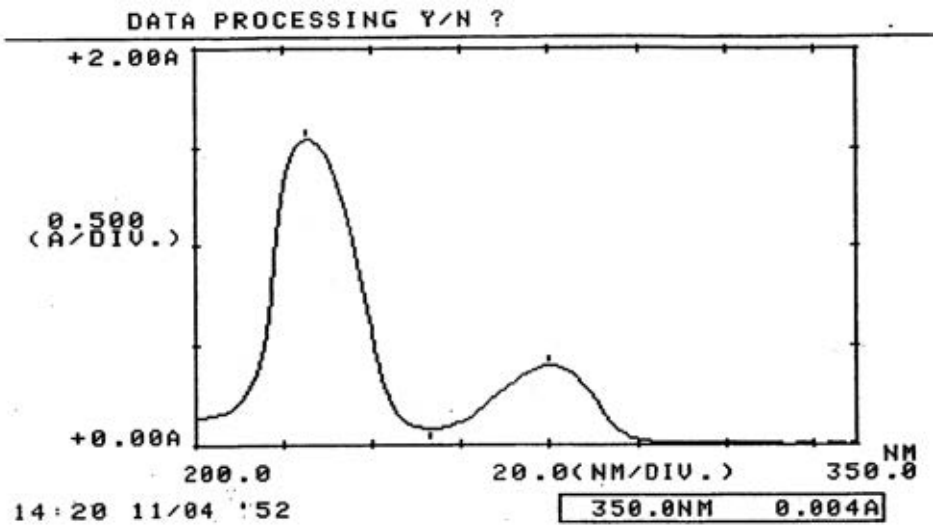

Figure 43 UV spectrum of compound TMM5 [**91**] (film)

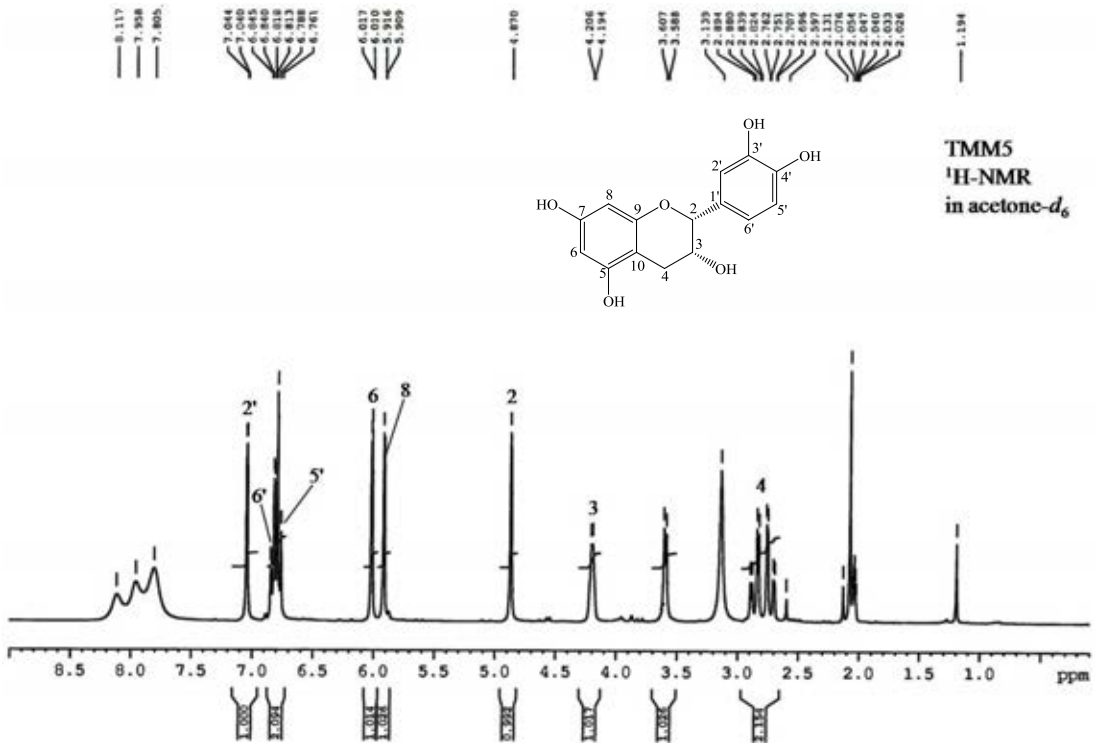

Figure 44 ^{1}H-NMR spectrum of compound TMM5 [**91**] (acetone-d_6)

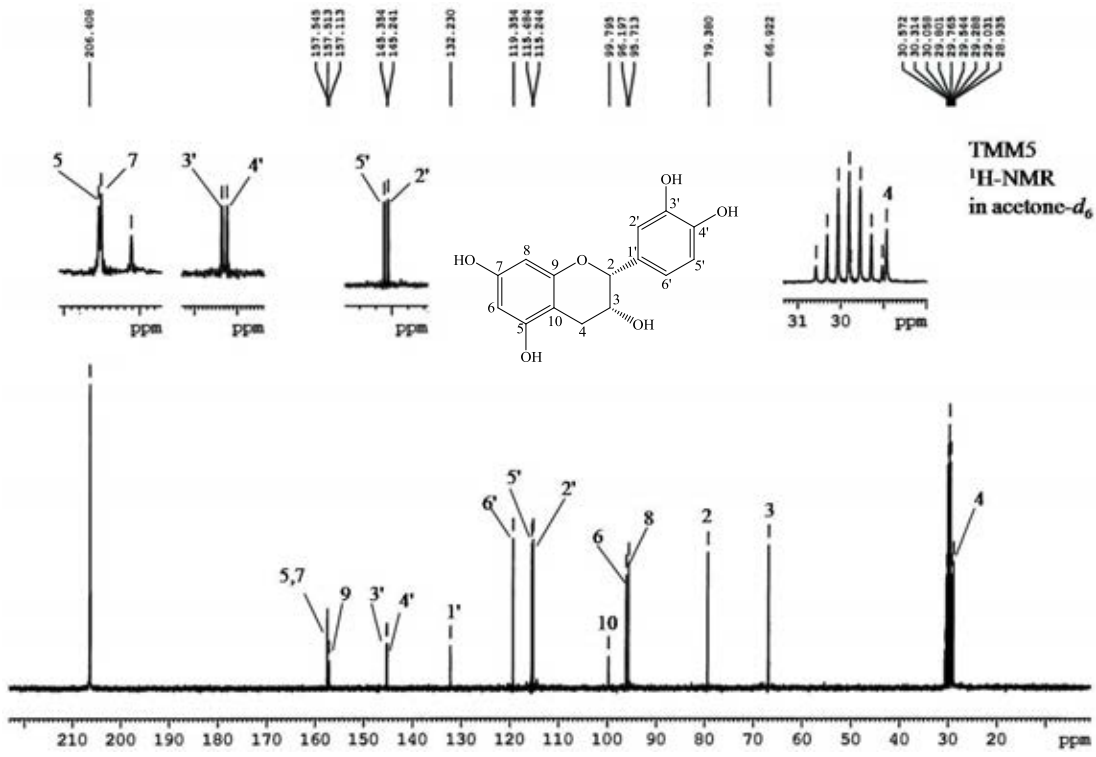

Figure 45 ^{13}C-NMR spectrum of compound TMM5 [**91**] (acetone-d_6)

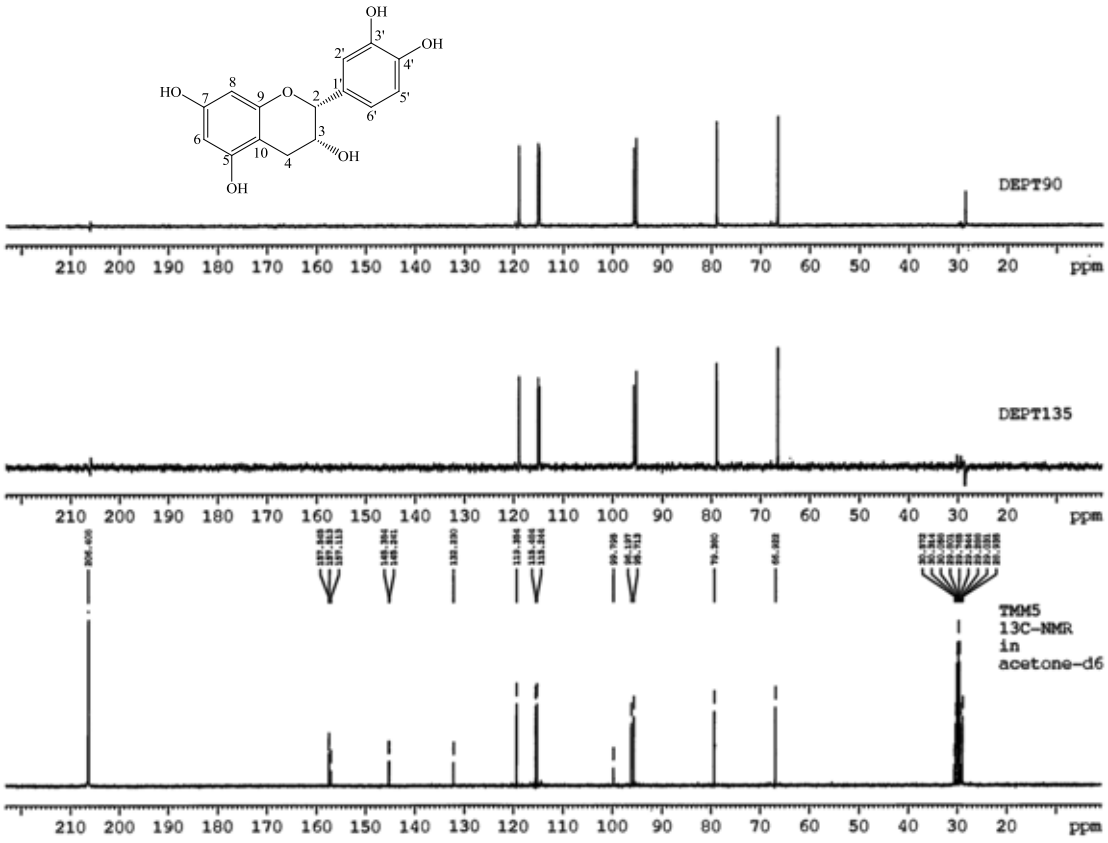

Figure 46 DEPT spectra of compound TMM5 [**91**] (acetone-d_6)

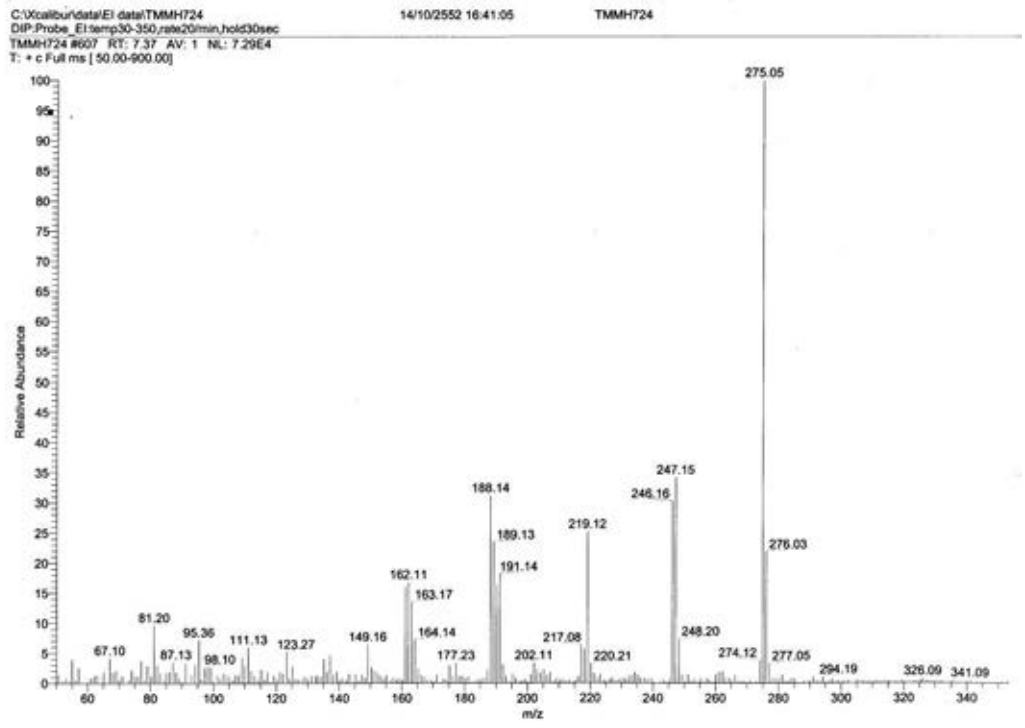

Figure 47 EI mass spectrum of compound TMM6 [**34**]

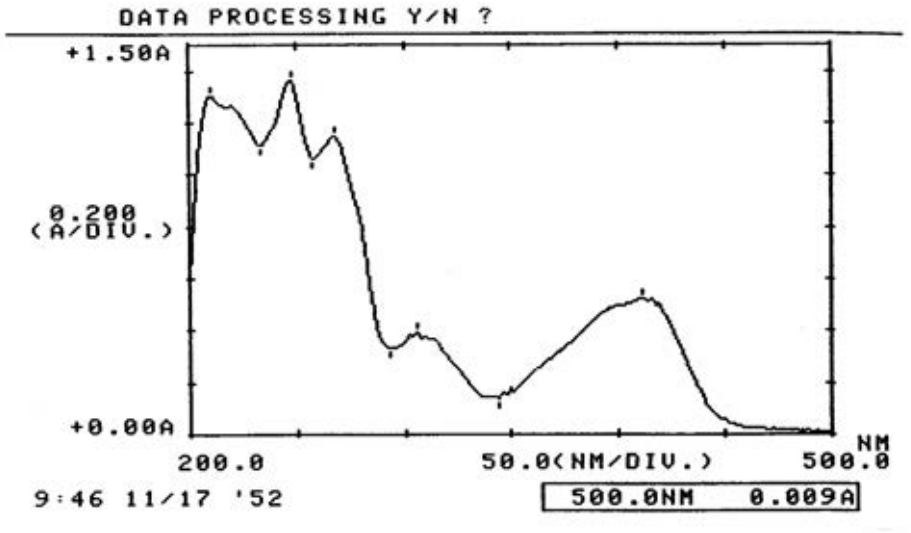

Figure 48 UV spectrum of compound TMM6 [**34**] (MeOH)

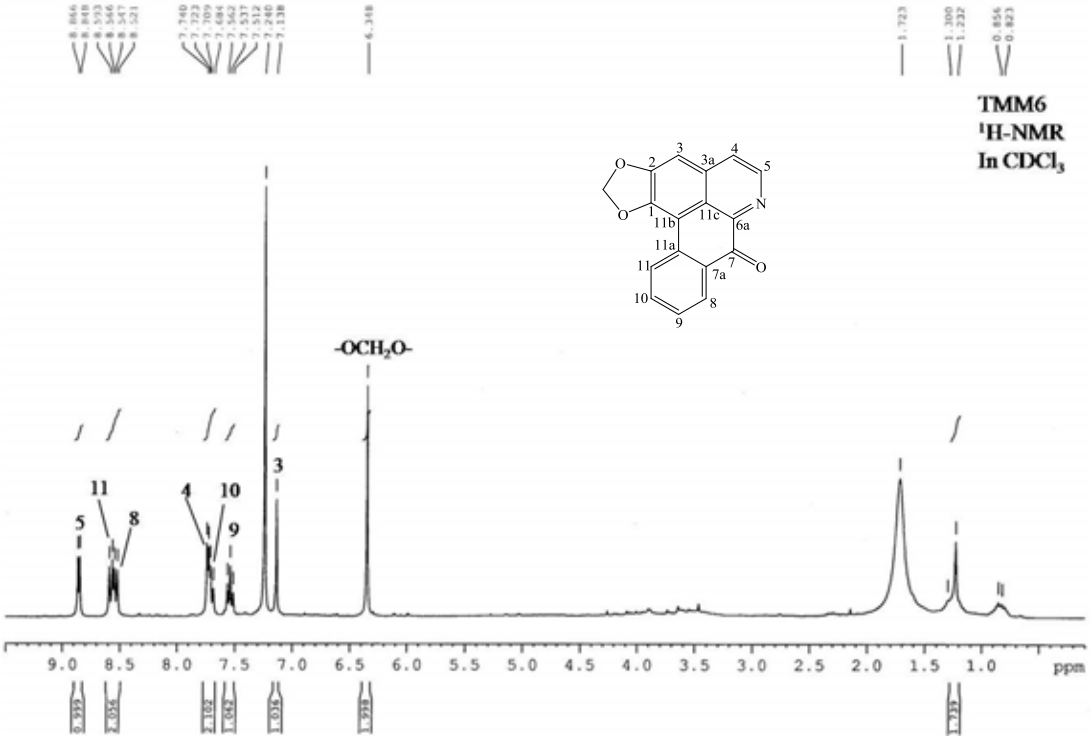

Figure 49 ^{1}H-NMR spectrum of compound TMM6 [**34**] ($CDCl_3$)

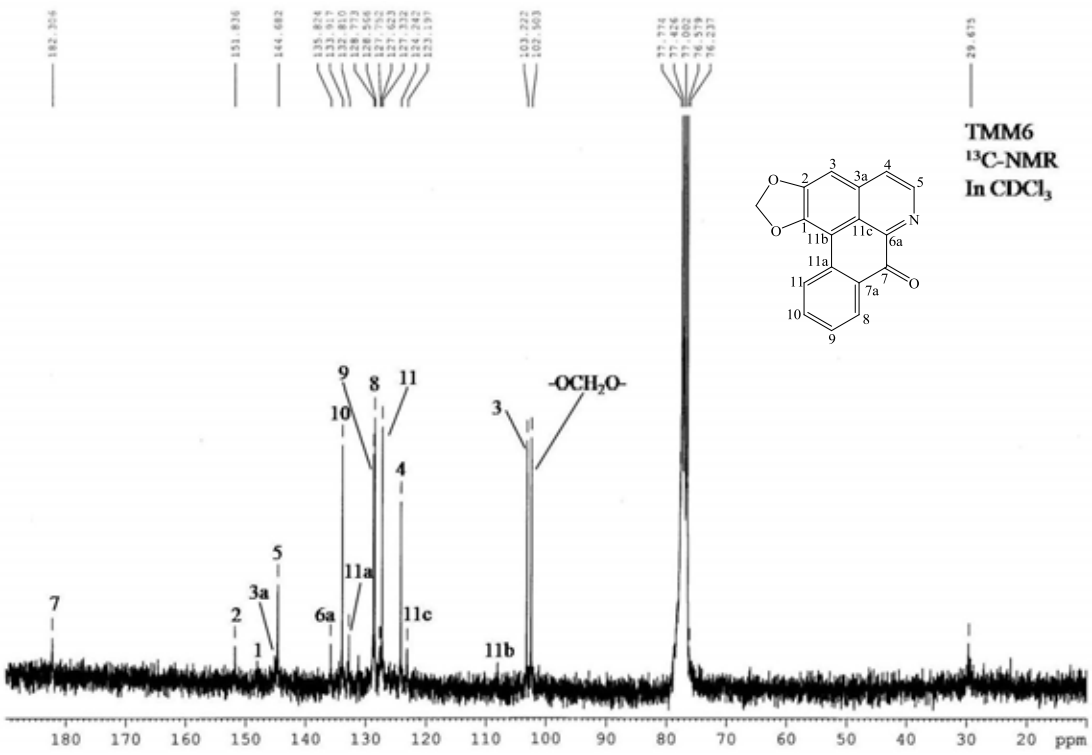

Figure 50 ^{13}C-NMR spectrum of compound TMM6 [**34**] ($CDCl_3$)

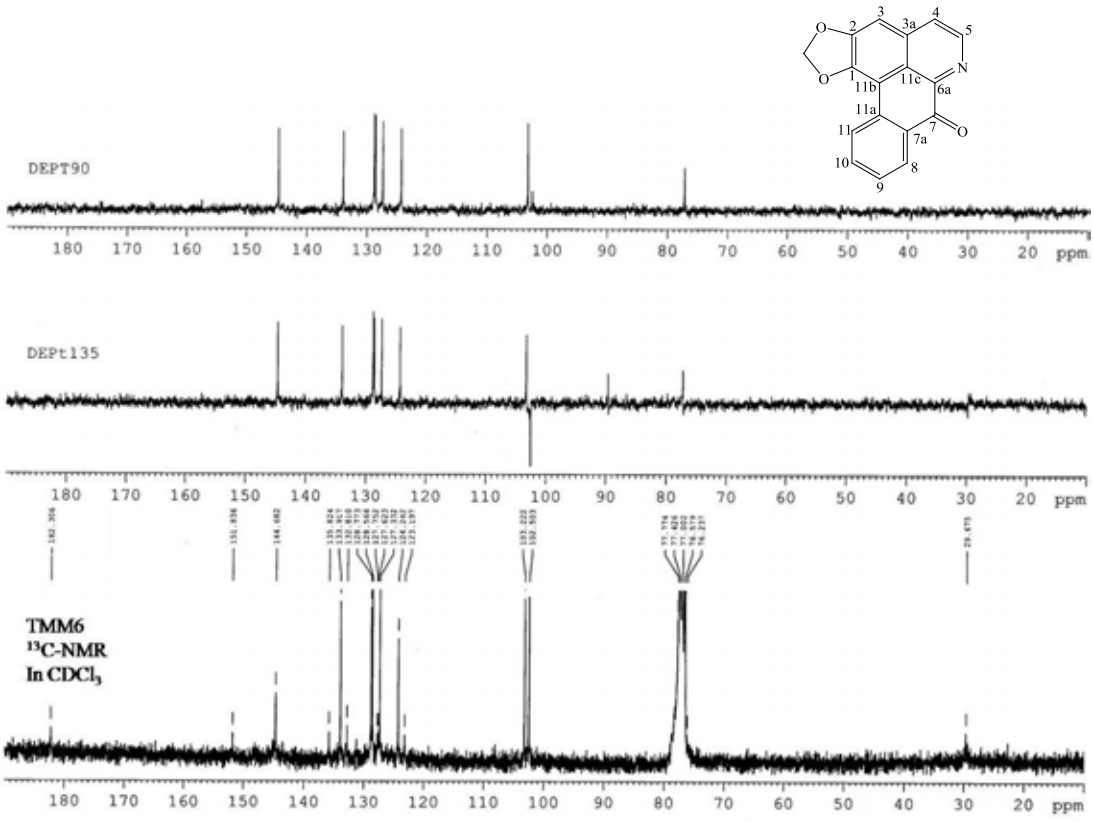

Figure 51 DEPT spectra of compound TMM6 [**34**] ($CDCl_3$)

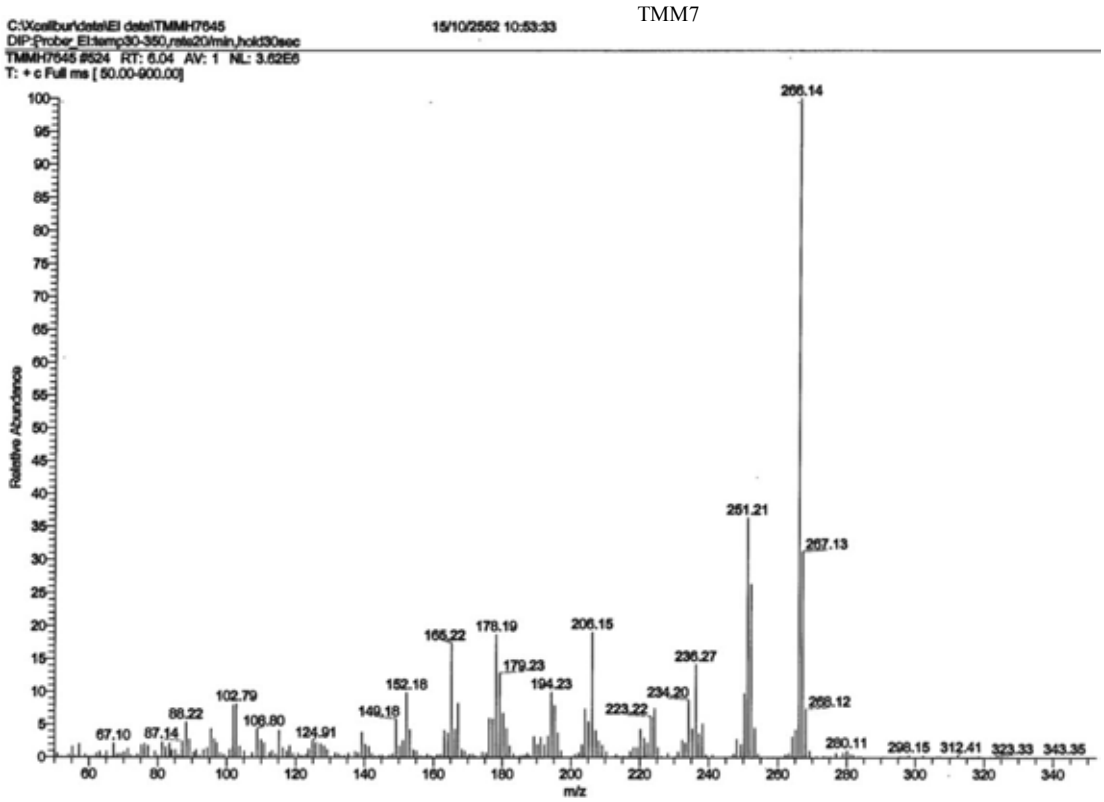

Figure 52 EI mass spectrum of compound TMM7 [**92**]

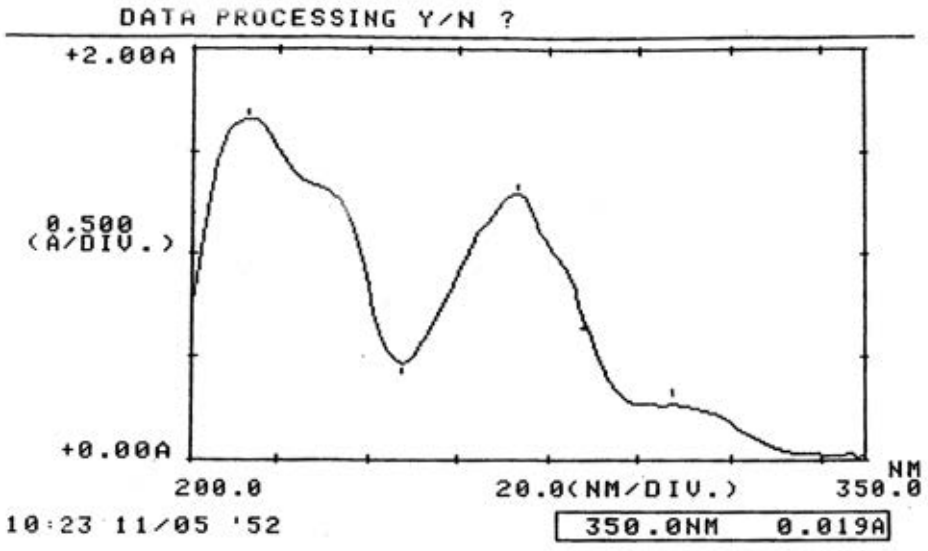

Figure 53 UV spectrum of compound TMM7 [**92**] (MeOH)

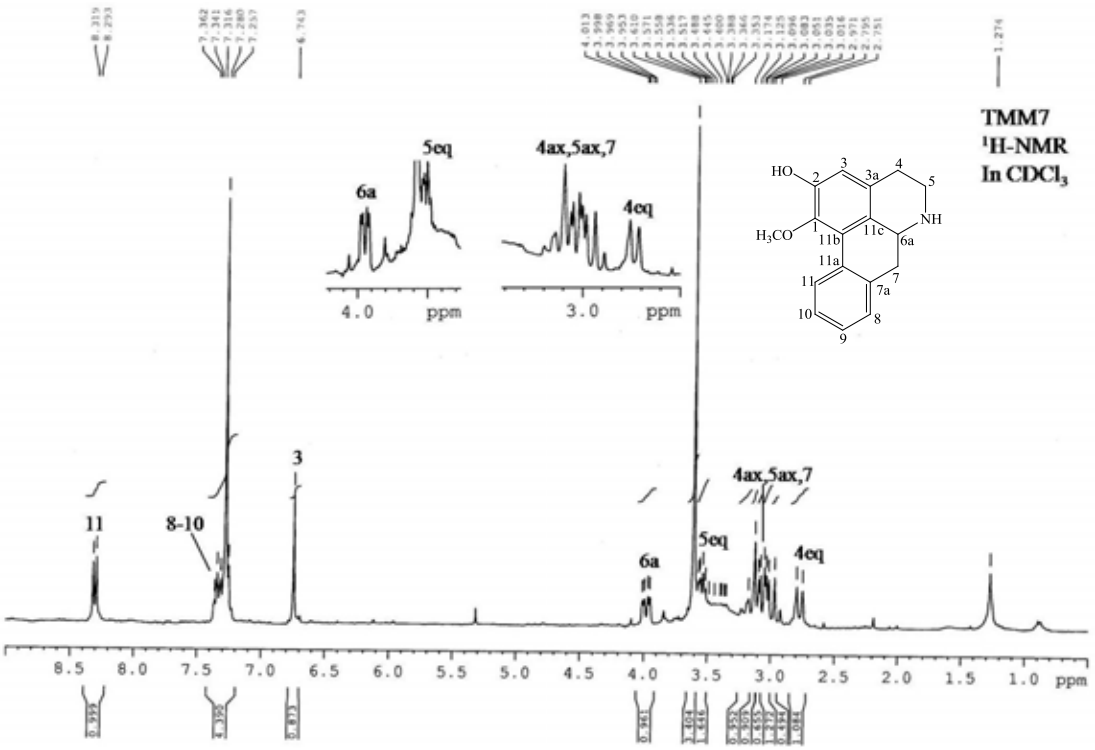

Figure 54 ^{1}H-NMR spectrum of compound TMM7 [**92**] (CDCl3)

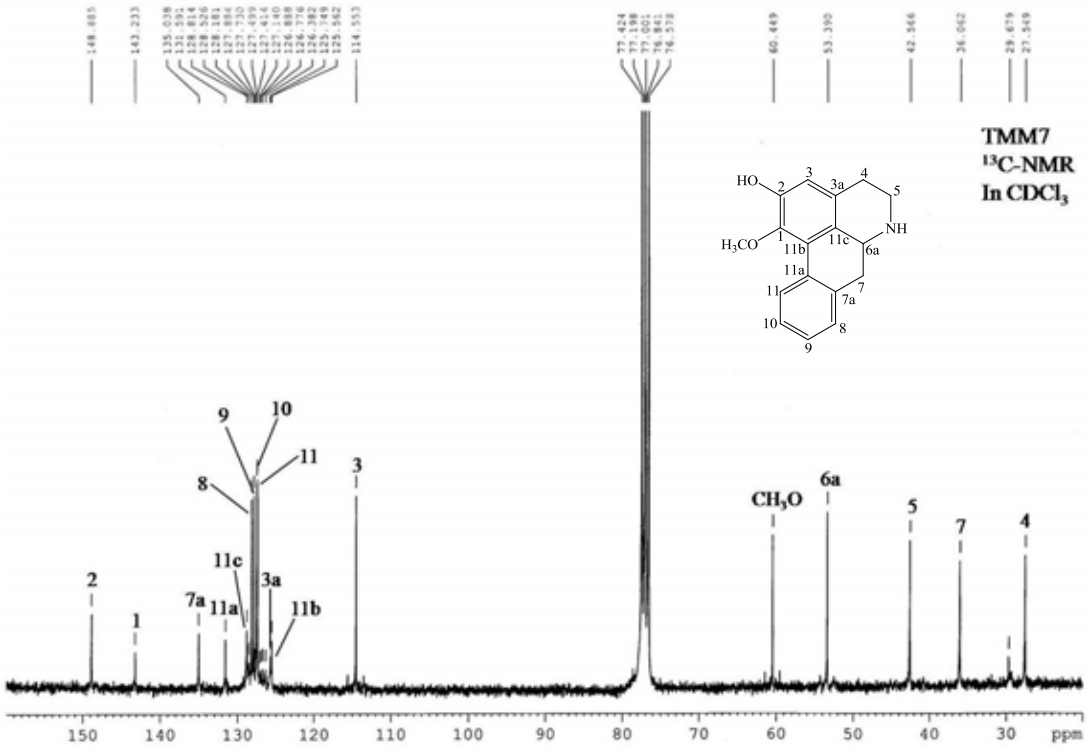

Figure 55 ^{13}C-NMR spectrum of compound TMM7 [**92**] ($CDCl_3$)

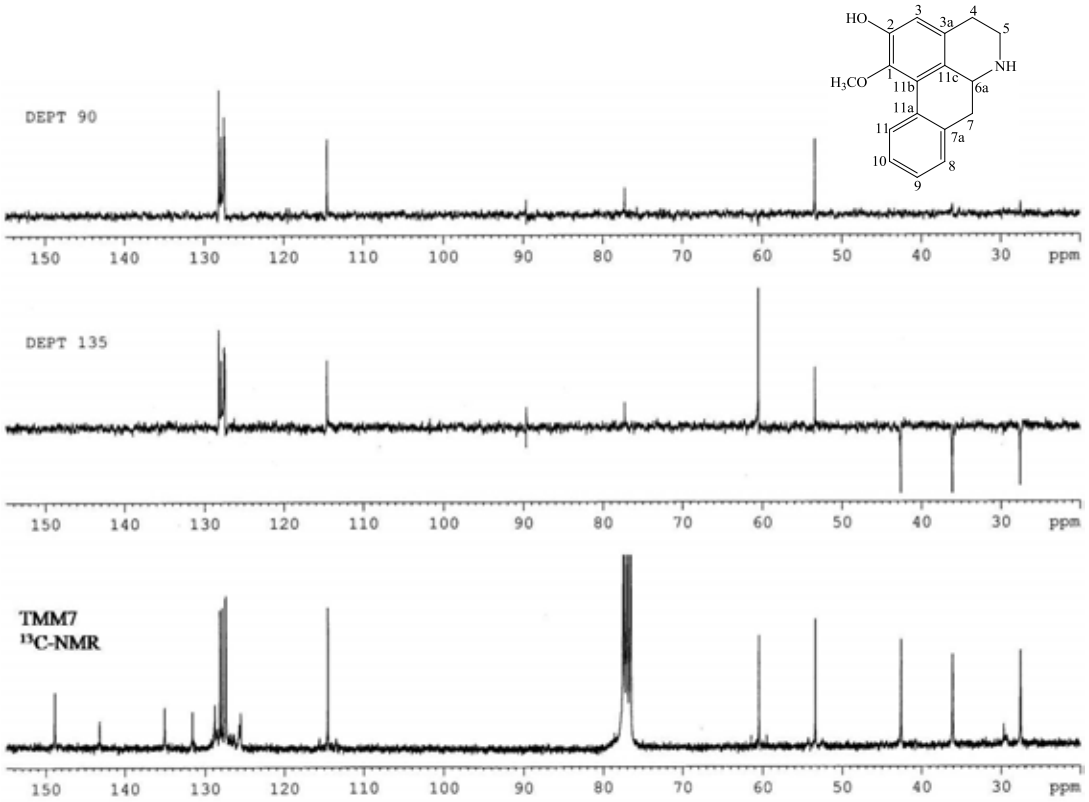

Figure 56 DEPT spectra of compound TMM7 [**92**] ($CDCl_3$)

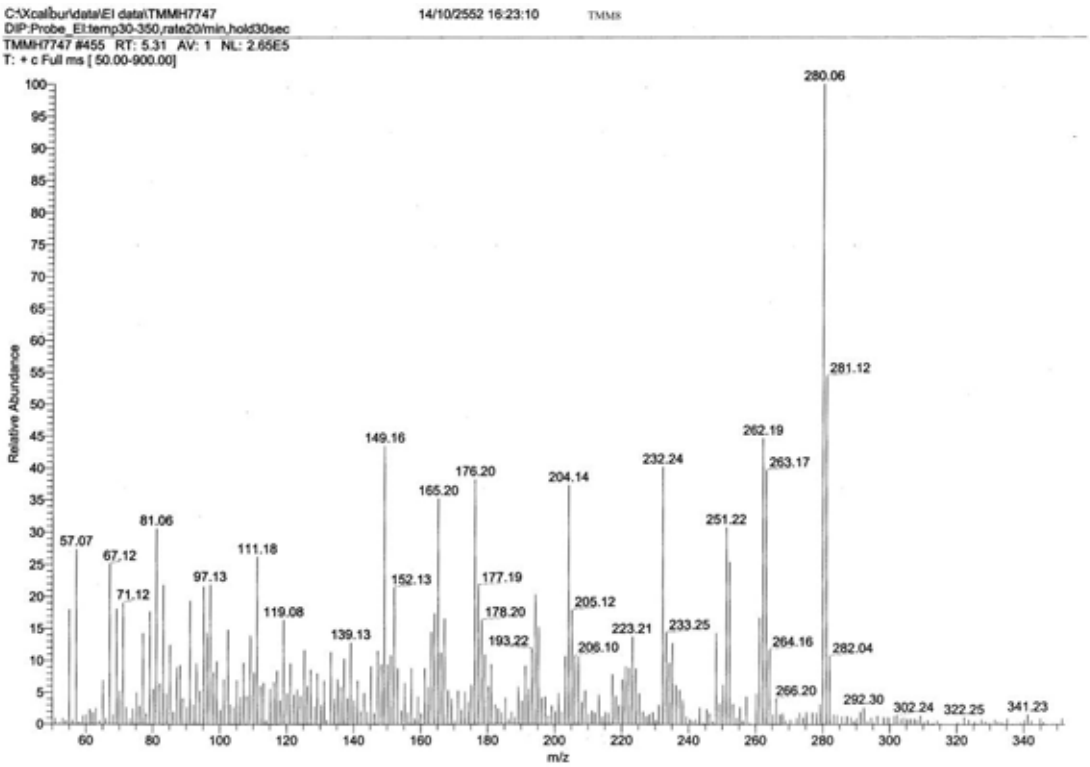

Figure 57 EI mass spectrum of compound TMM8 [**93**]

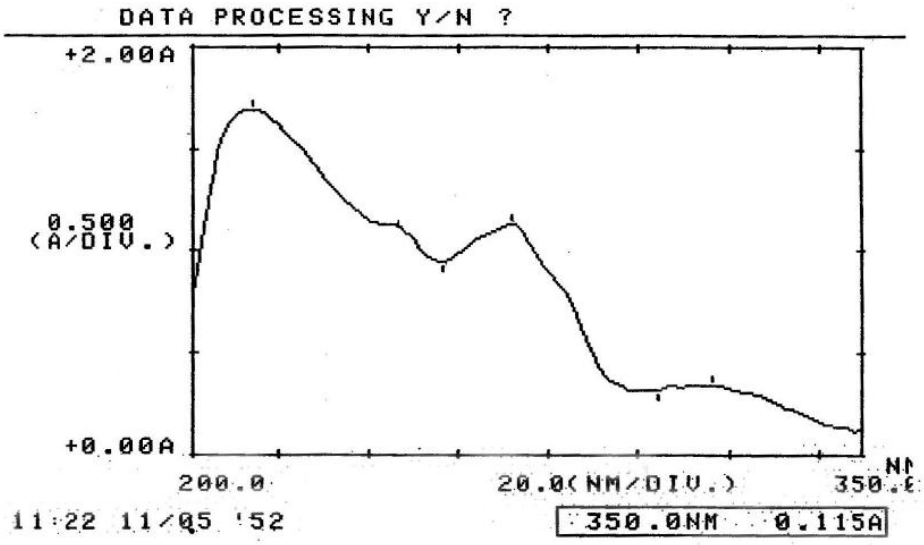

Figure 58 UV spectrum of compound 8 [**93**] (MeOH)

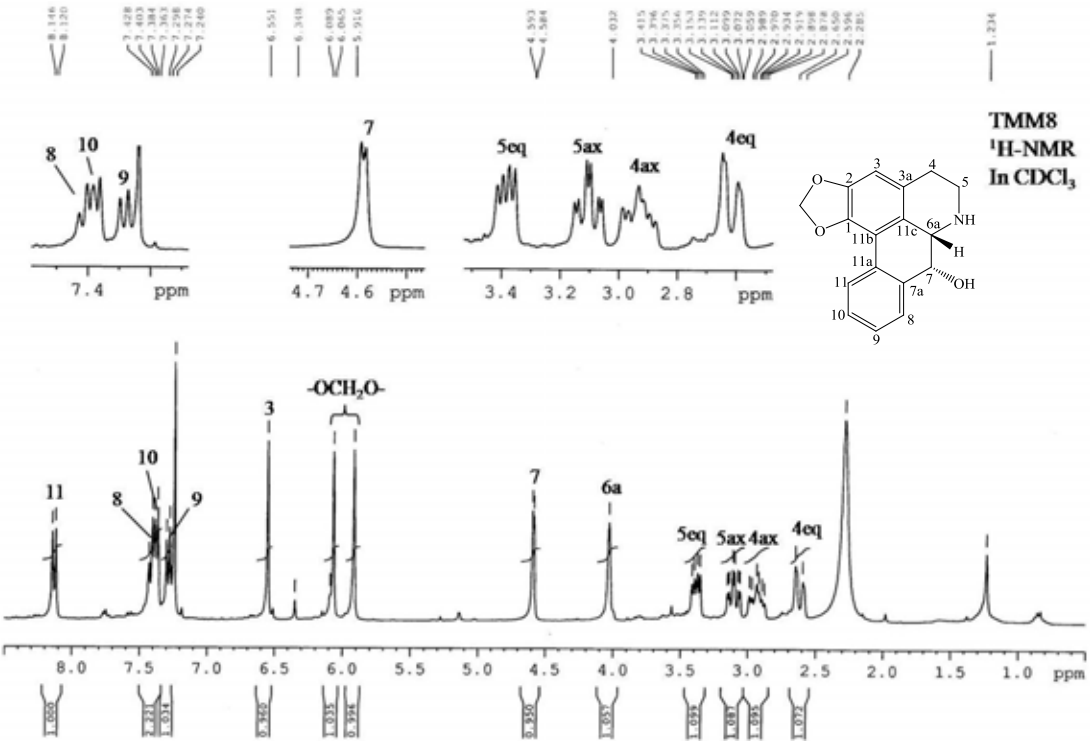

Figure 59 ^{1}H-NMR spectrum of compound TMM8 [**93**] ($CDCl_3$)

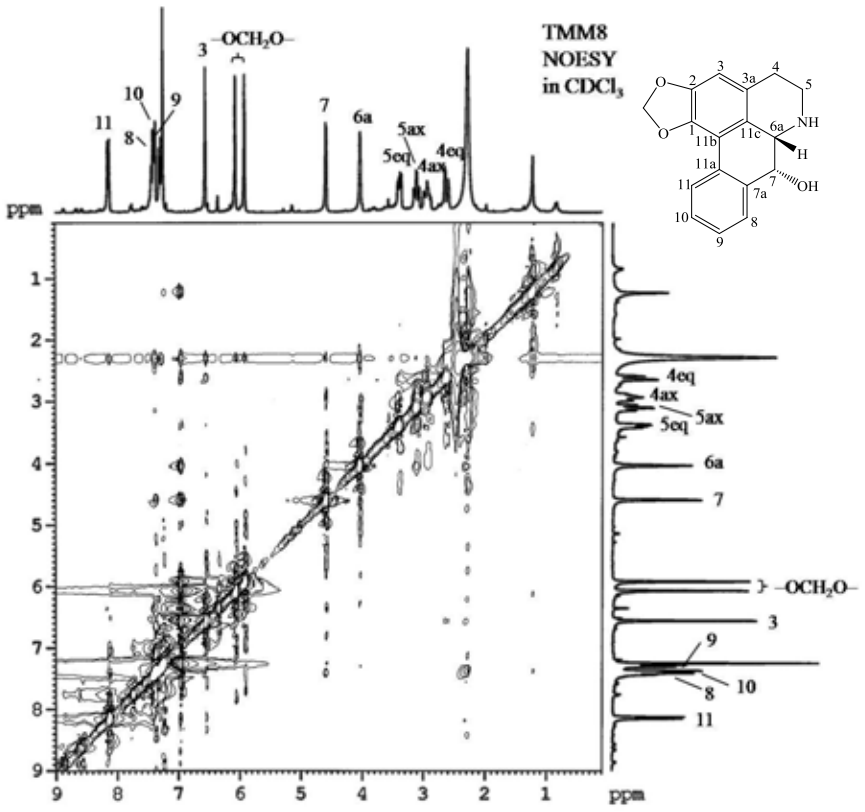

Figure 60 NOESY spectrum of compound TMM8 [**93**] ($CDCl_3$)

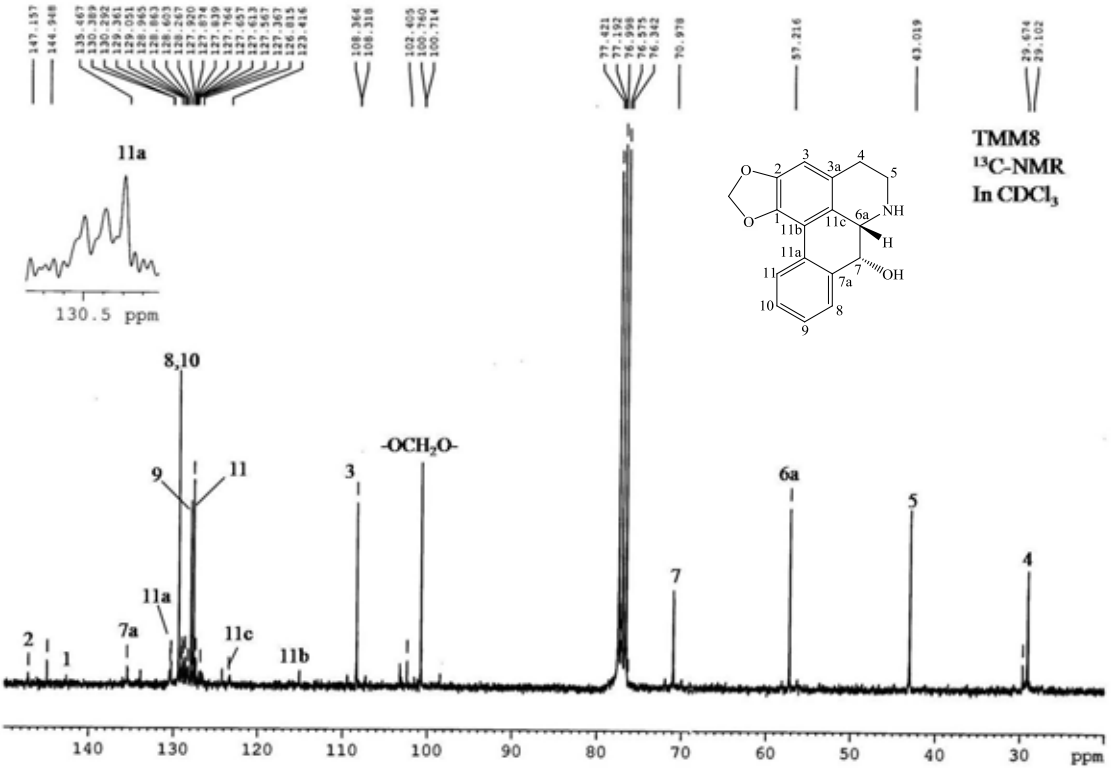

Figure 61 ^{13}C-NMR spectrum of compound TMM8 [**93**] ($CDCl_3$)

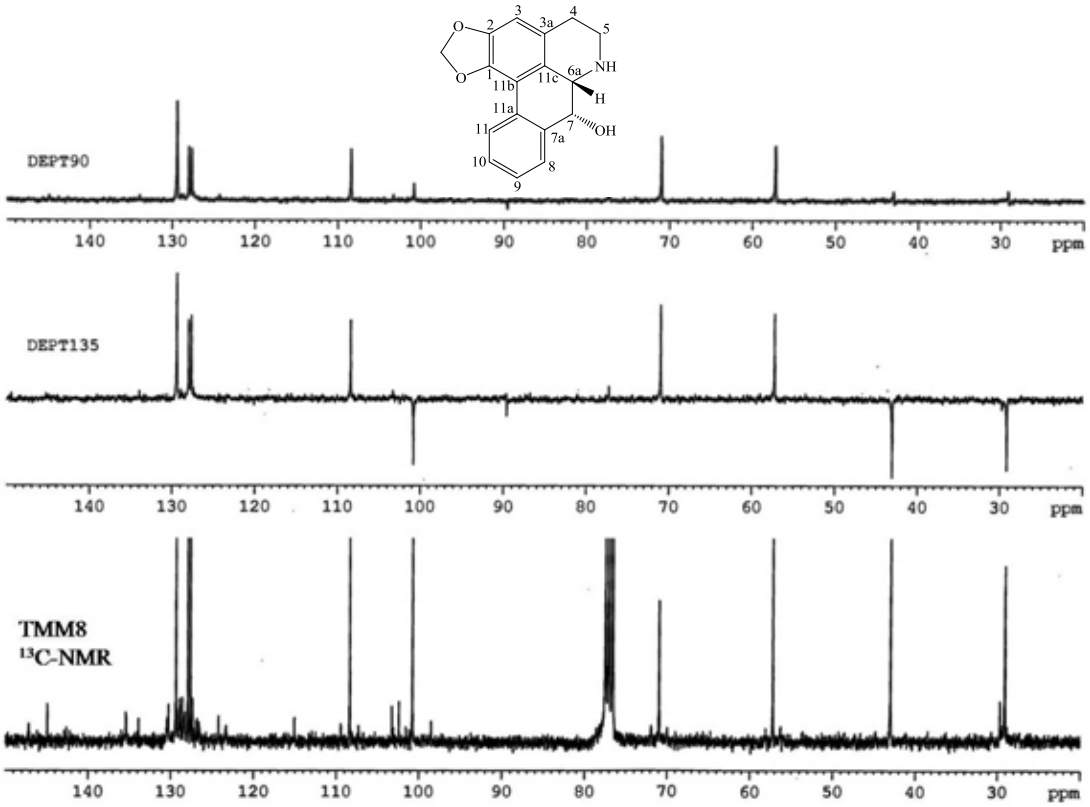

Figure 62 DEPT spectra of compound TMM8 [**93**] ($CDCl_3$)

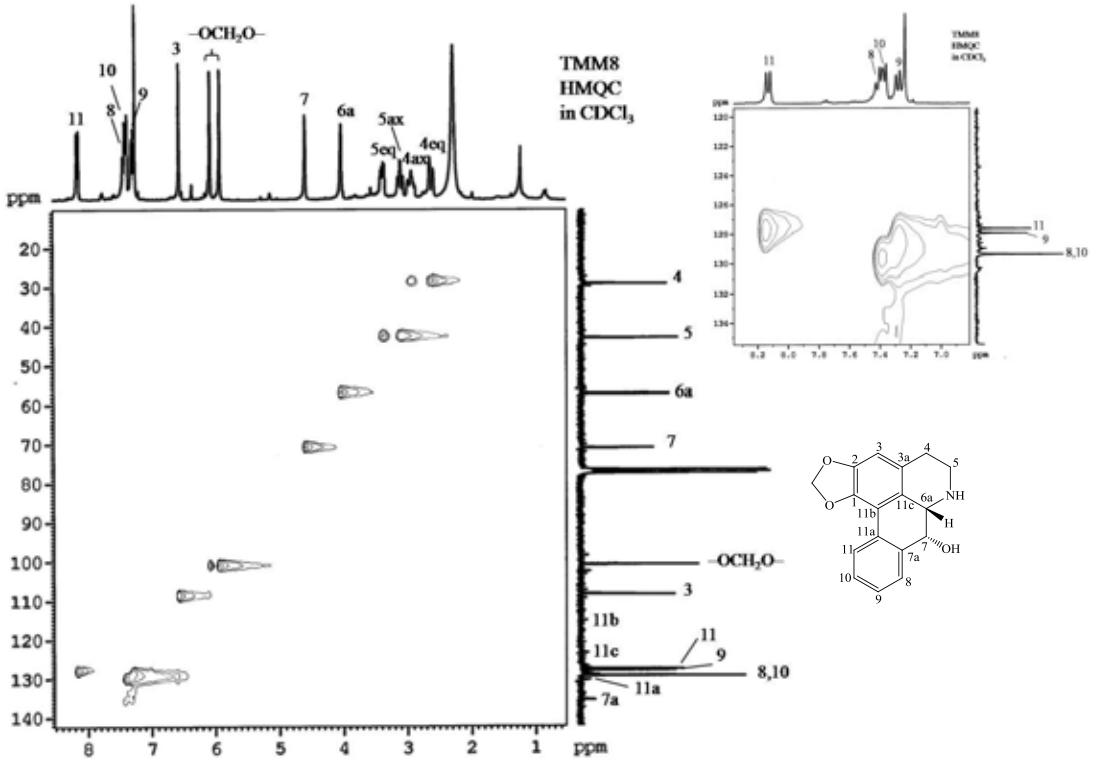

Figure 63 HMQC spectrum of compound TMM8 [**93**] ($CDCl_3$)

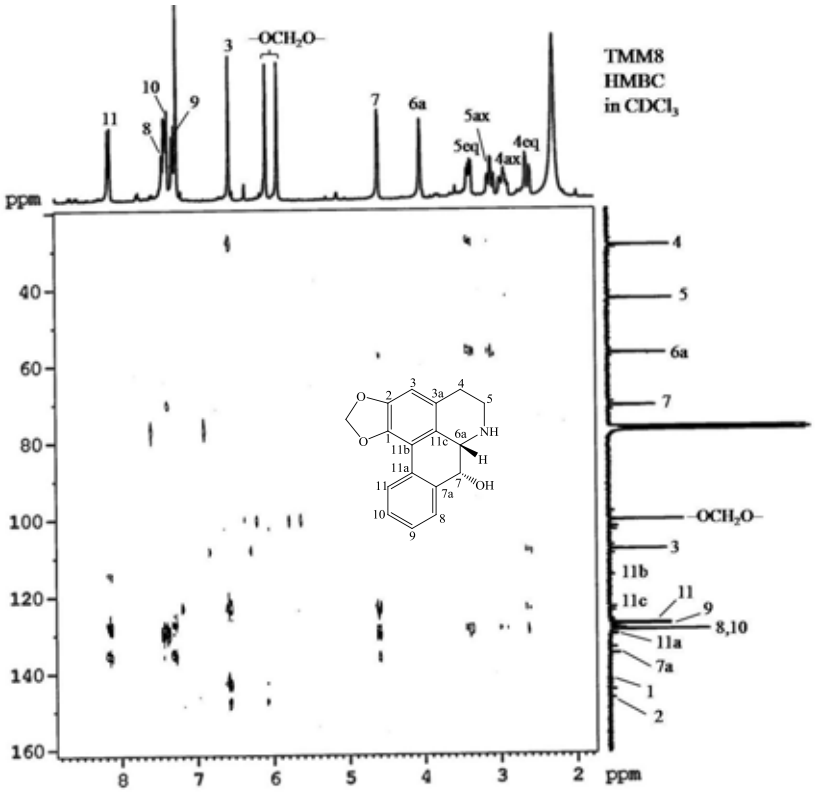

Figure 64 HMBC spectrum of compound TMM8 [**93**] ($CDCl_3$)

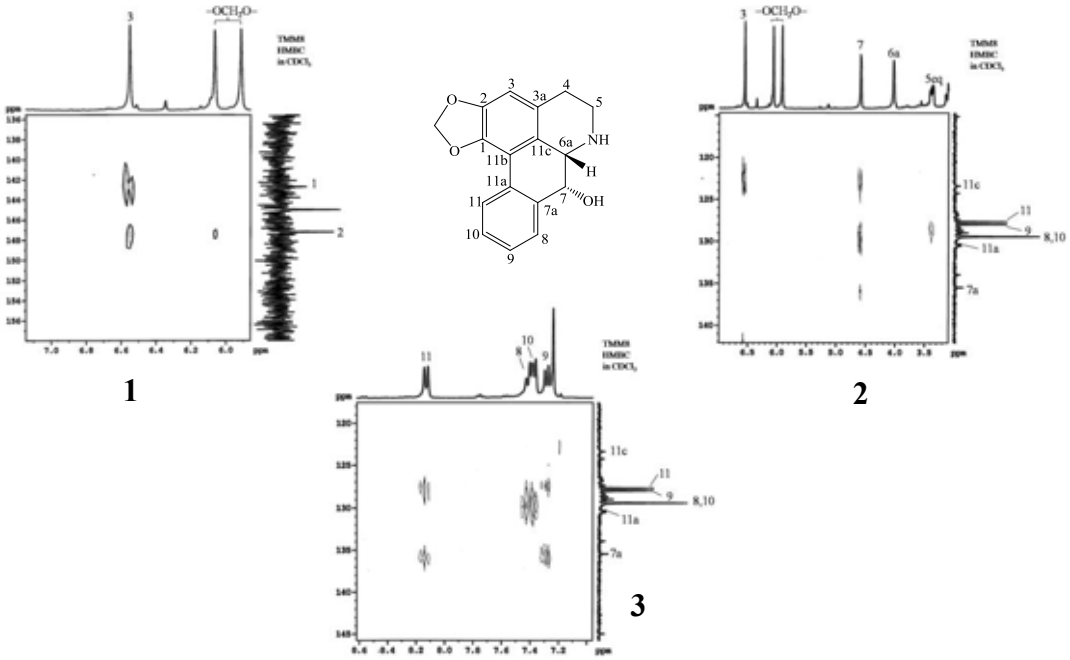

Figure 64a HMBC spectrum of compound TMM8 [**93**] ($CDCl_3$)
[δ_H 7.15-5.9 ppm, δ_C 158-135.5 ppm (1)],
[δ_H 7-3.1 ppm, δ_C 142-115 ppm (2)] and
[δ_H 8.6-7.1 ppm, δ_C 146-118 ppm (3)]

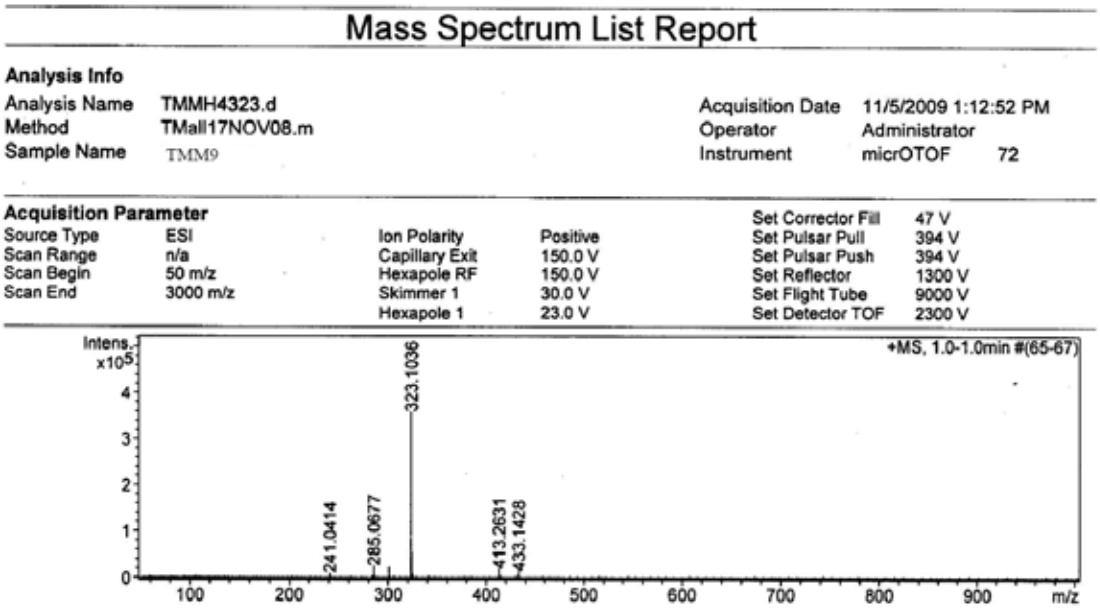

Figure 65 HRESI mass spectrum of compound TMM9 [**94**]

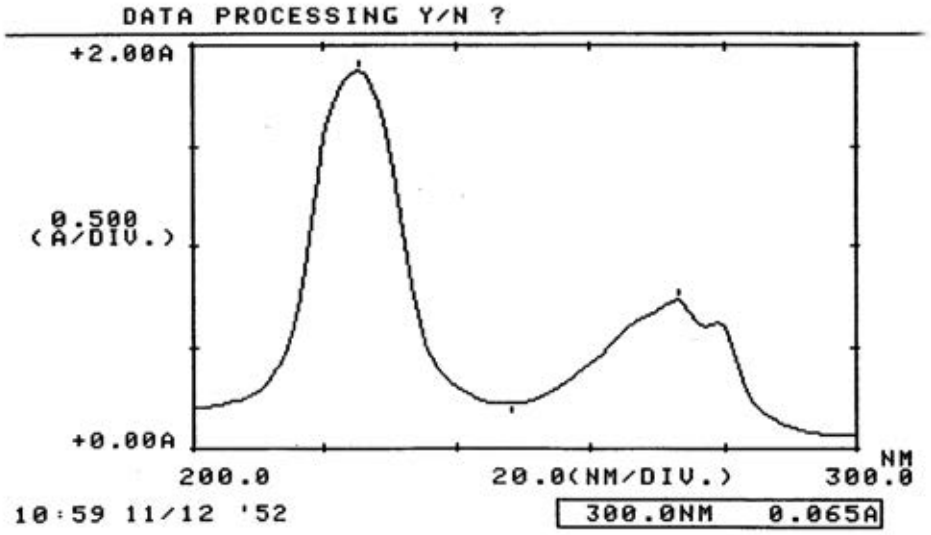

Figure 66 UV spectrum of compound TMM9 [**94**] (MeOH)

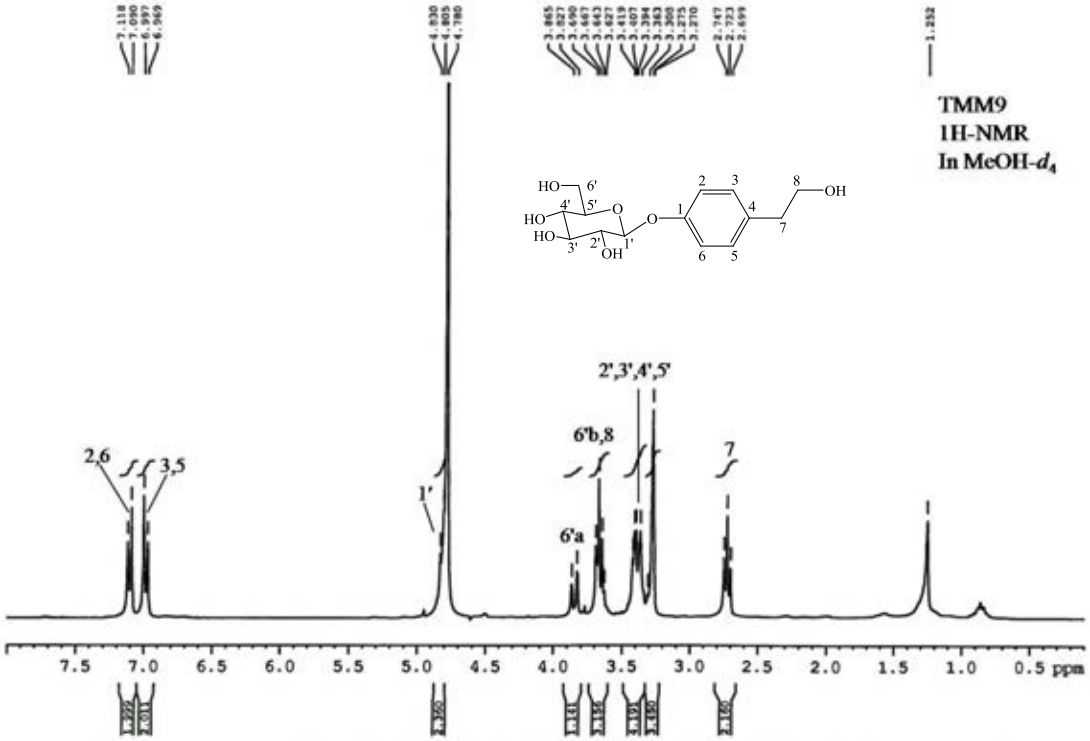

Figure 67 ^{1}H-NMR spectrum of compound TMM9 [**94**] (MeOH-d_4)

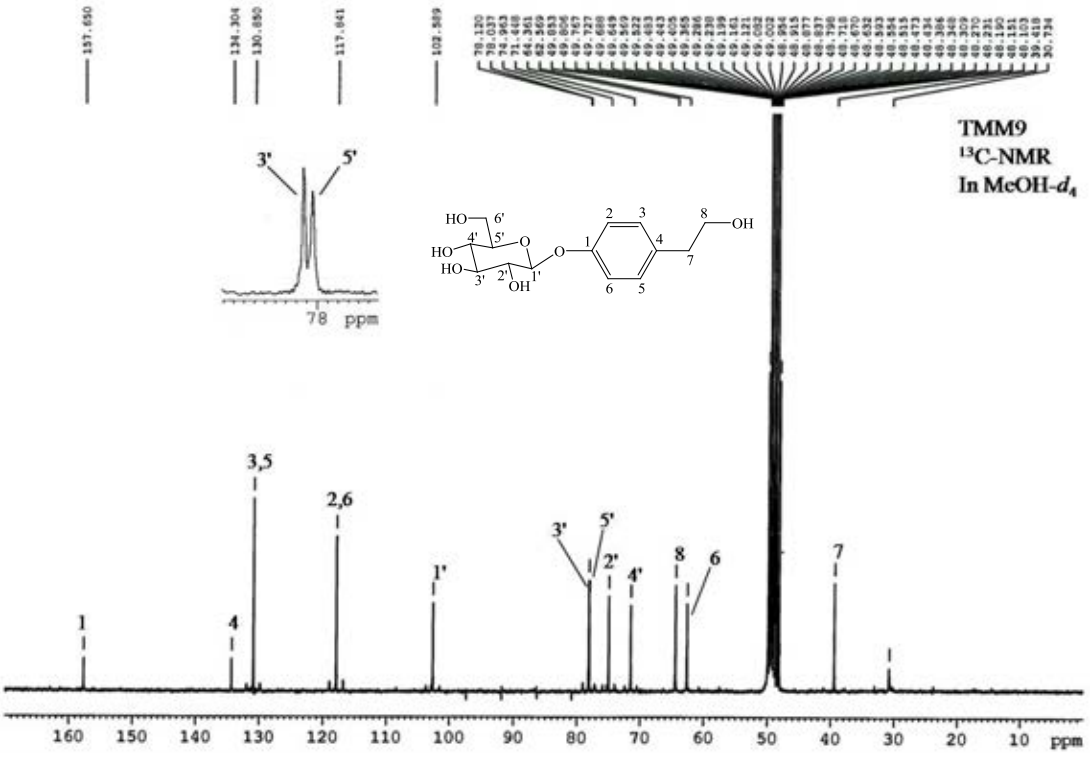

Figure 68 ^{13}C-NMR spectrum of compound TMM9 [**94**] (MeOH-d_4)

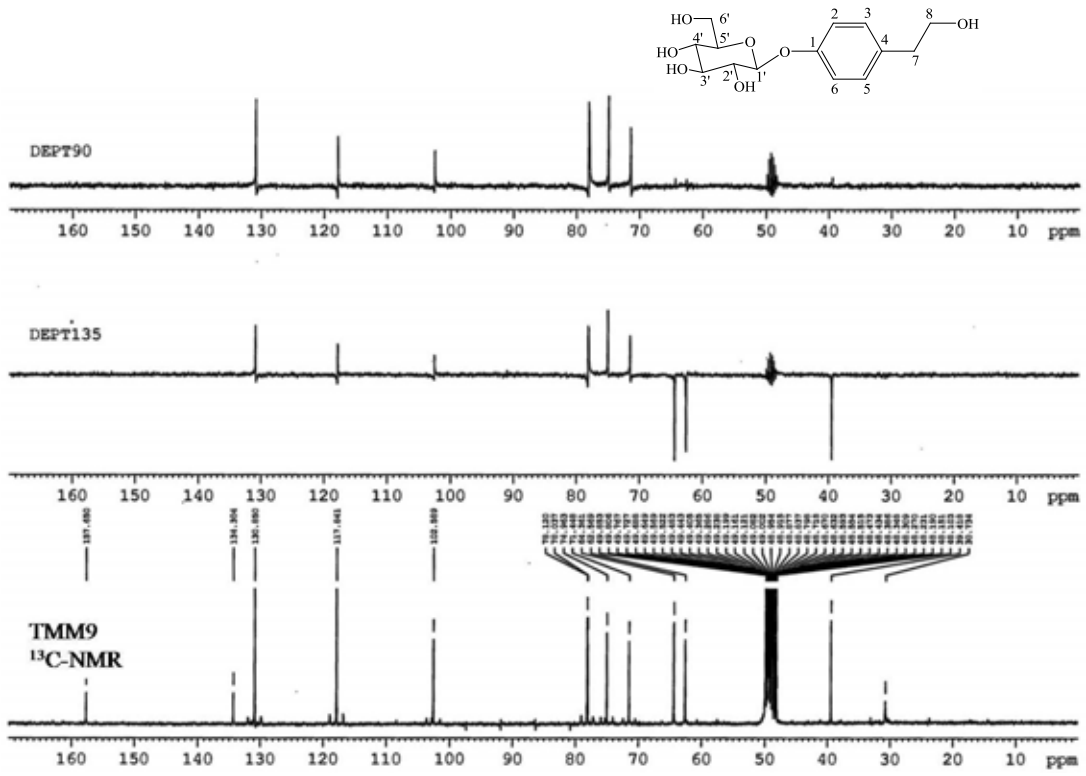

Figure 69 DEPT spectra of compound TMM9 [**94**] (MeOH-d_4)

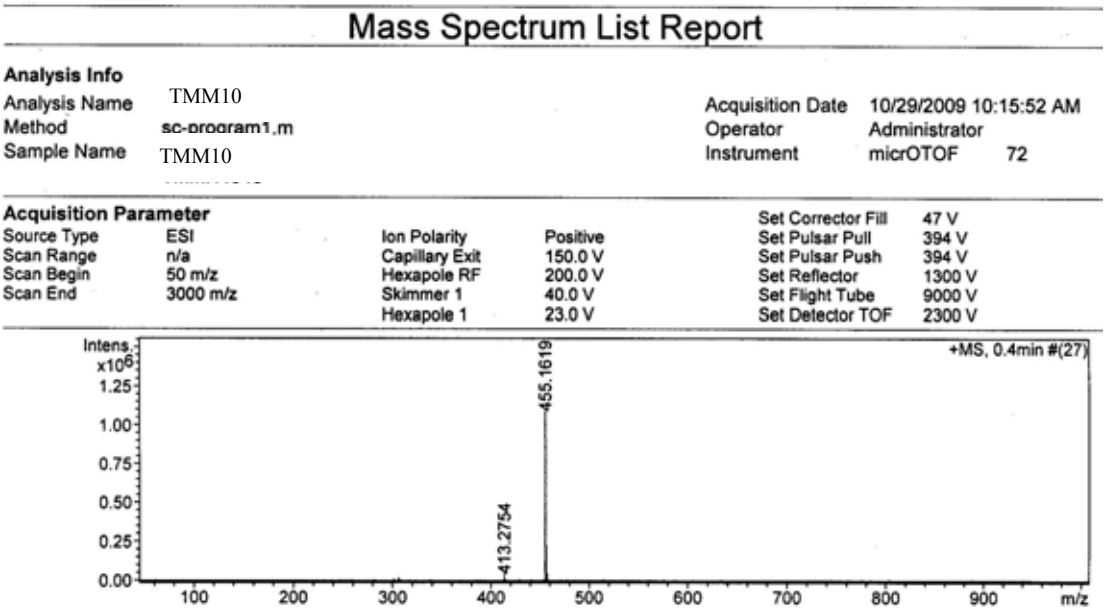

Figure 70 HRESI mass spectrum of compound TMM10 [**95**]

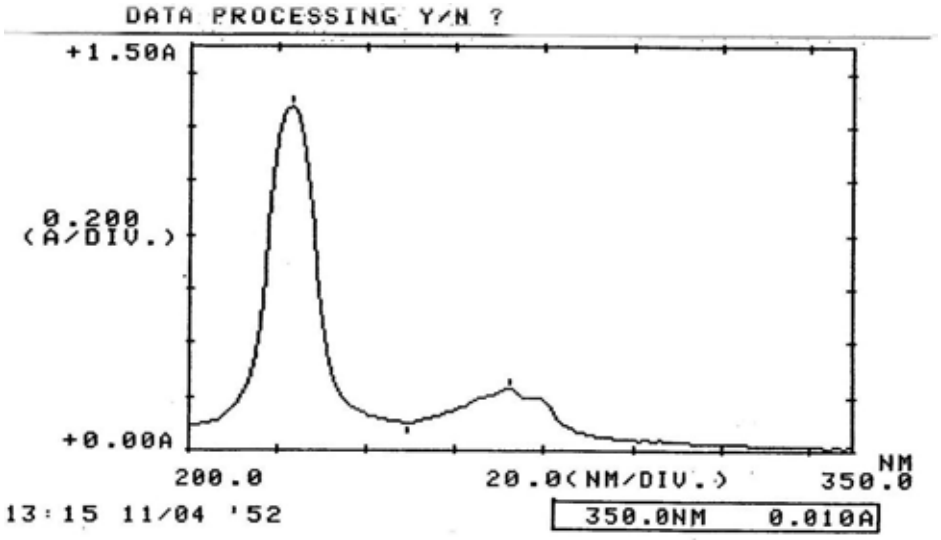

Figure 71 UV spectrum of compound TMM10 [**95**] (MeOH)

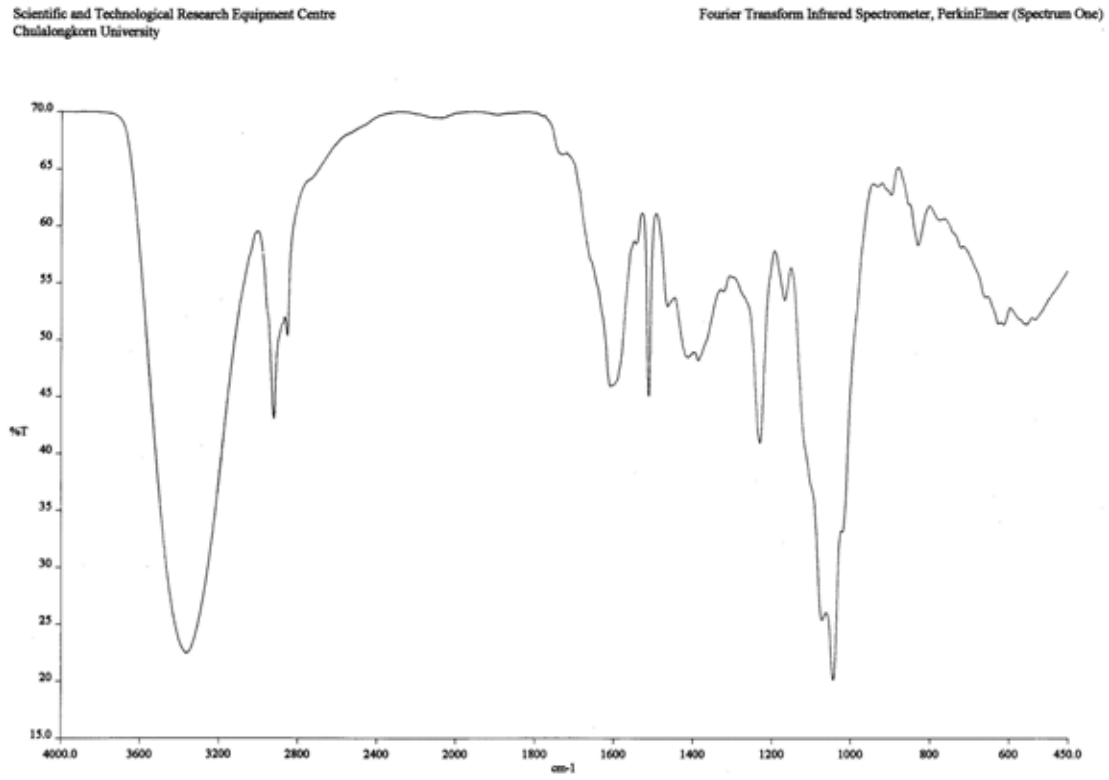

Figure 72 IR spectrum of compound TMM10 [**95**] (film)

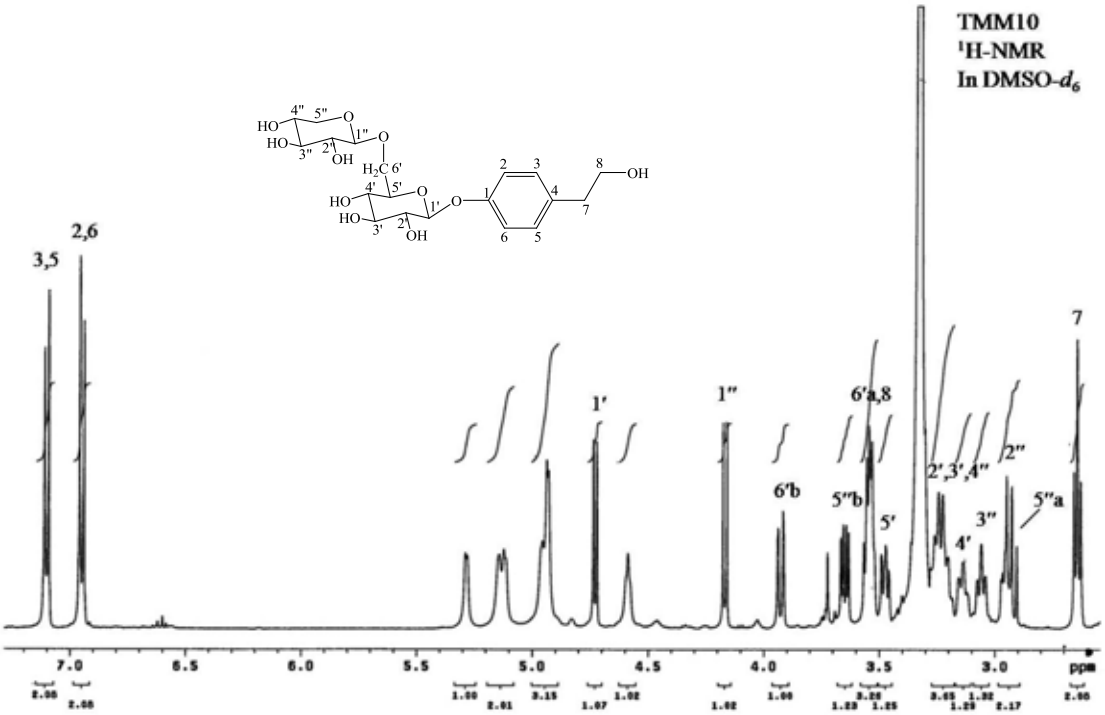

Figure 73 ^{1}H-NMR spectrum of compound TMM10 [**95**] (DMSO-d_6)

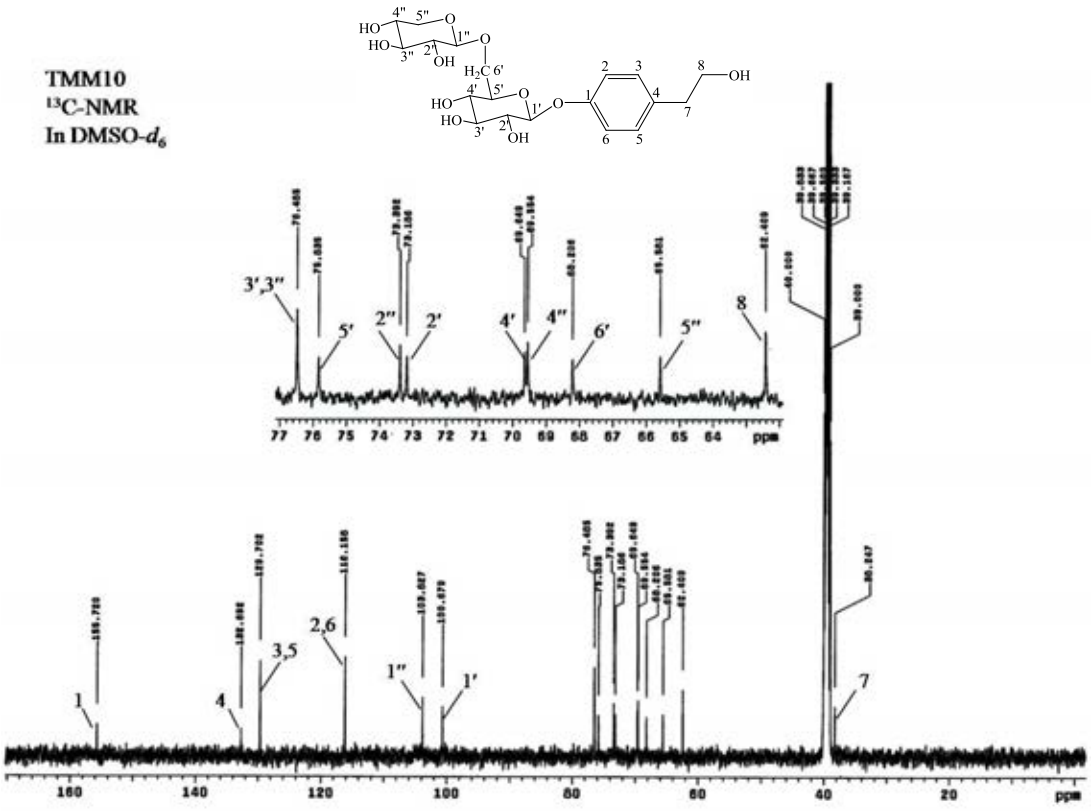

Figure 74 ^{13}C-NMR spectrum of compound TMM10 [**95**] (DMSO-d_6)

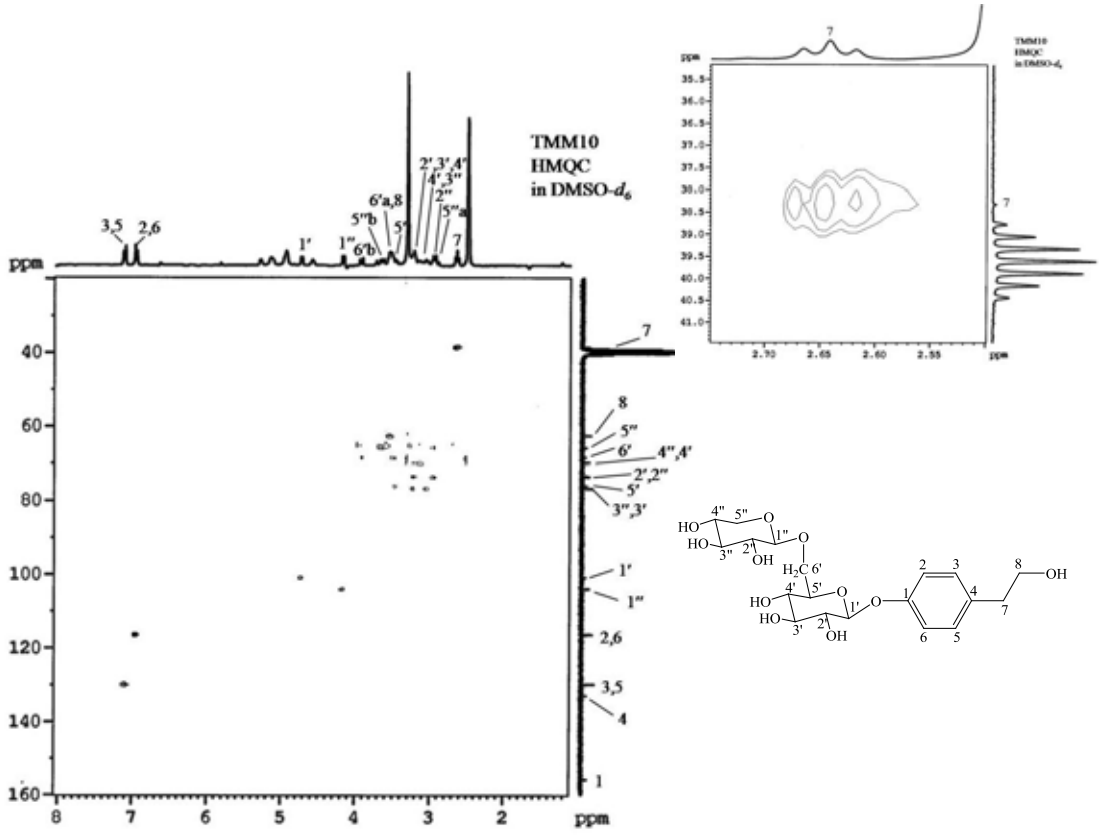

Figure 75 HMQC spectrum of compound TMM10 [**95**] (DMSO-d_6)

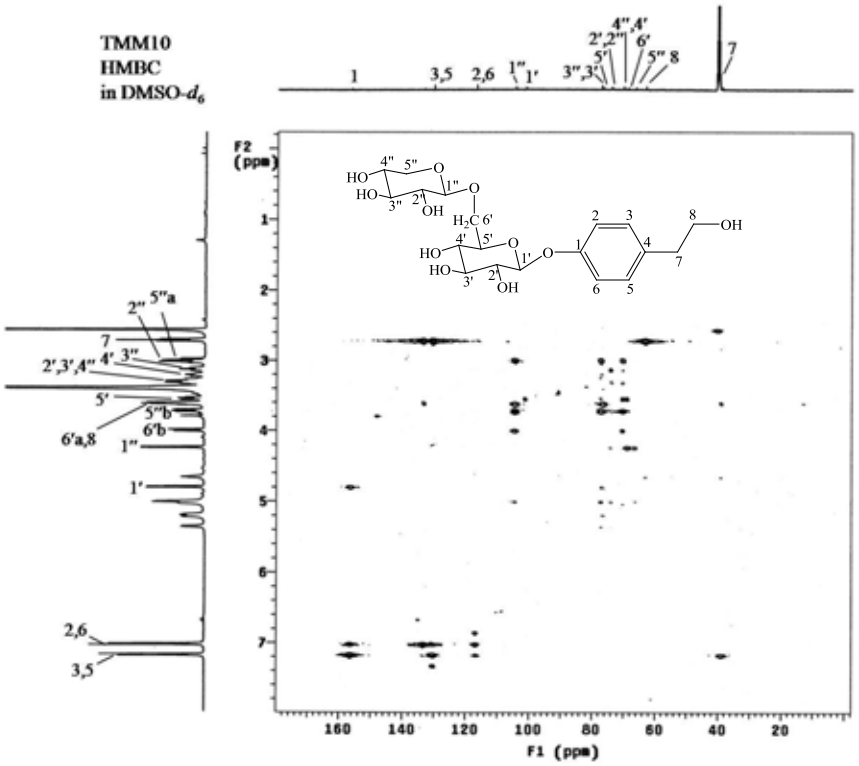

Figure 76 HMBC spectrum of compound TMM10 [**95**] (DMSO-d_6)

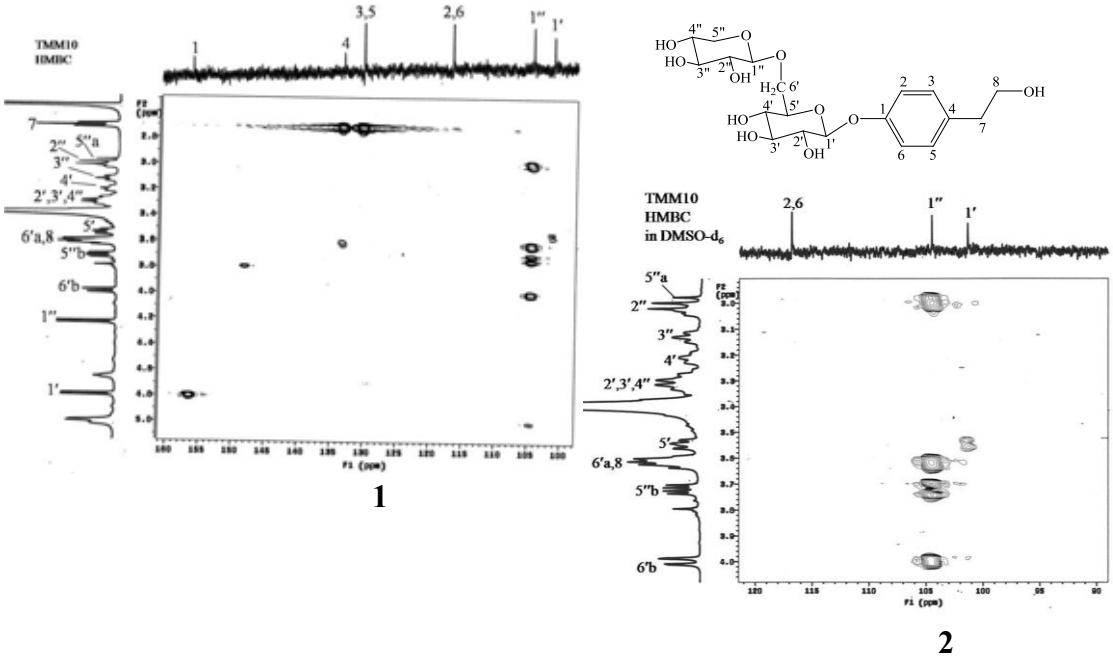

Figure 76a HMBC spectrum of compound TMM10 [**95**] (DMSO-d_6)
[δ_H 5.1-2.4 ppm, δ_C 161-98 ppm (1)] and
[δ_H 4.4-2.5 ppm, δ_C 121.5-89 ppm (2)]

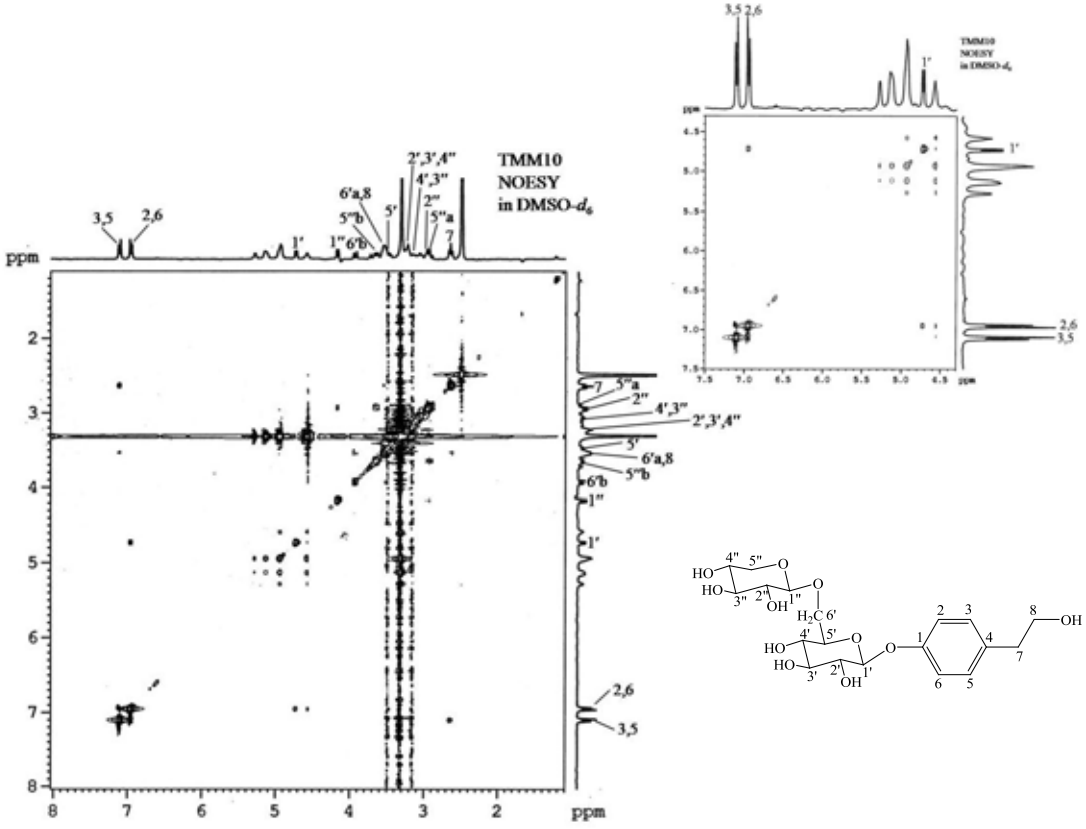

Figure 77 NOESY spectrum of compound TMM10 [**95**] (DMSO-d_6)

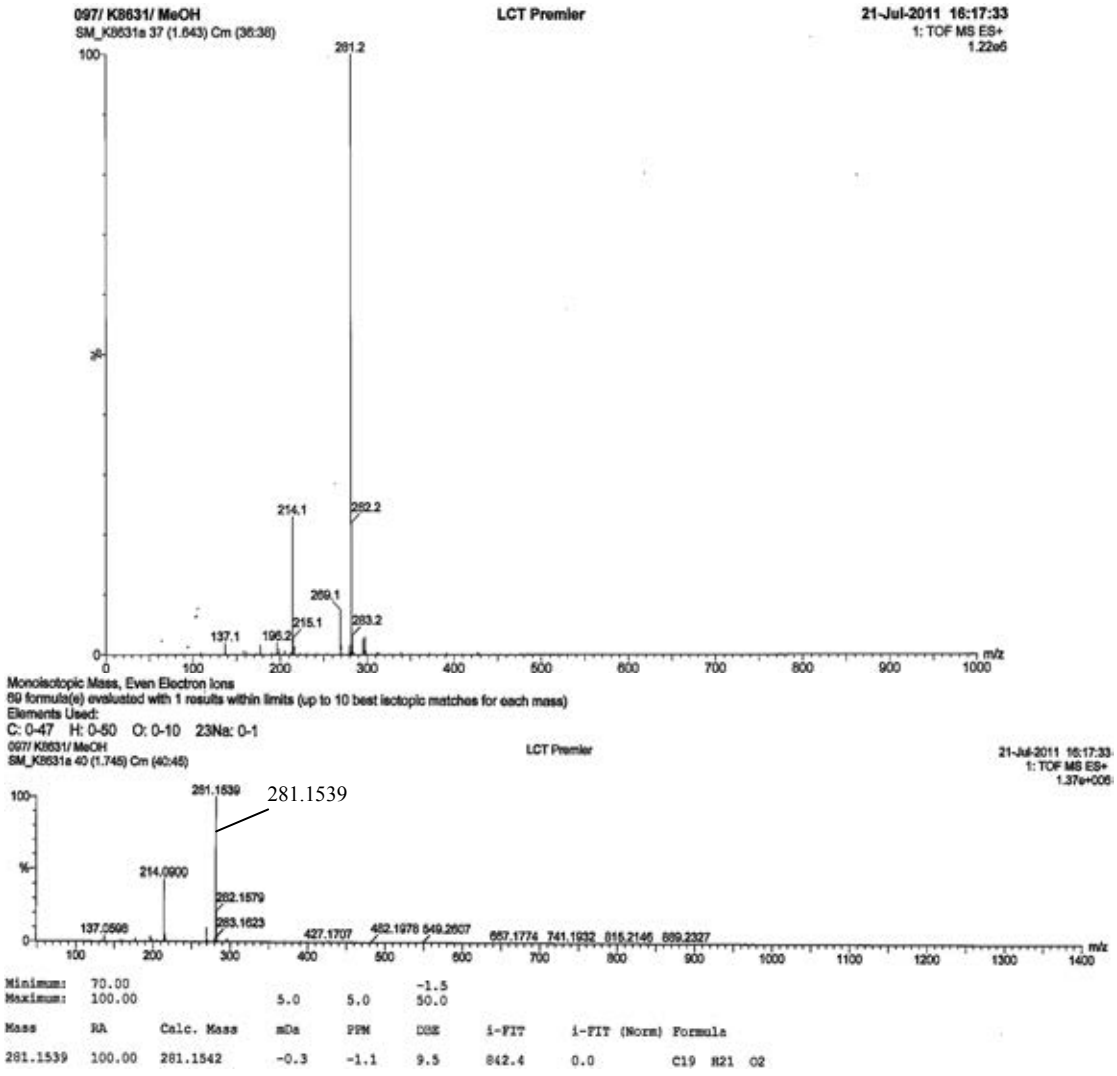

Figure 78 HRESI mass spectrum of compound LMM1 [**96**]

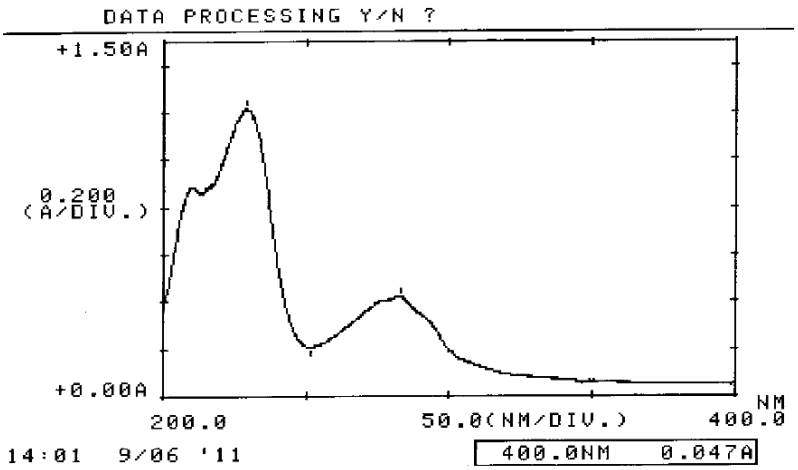

Figure 79 UV spectrum of compound LMM1 [**96**] (MeOH)

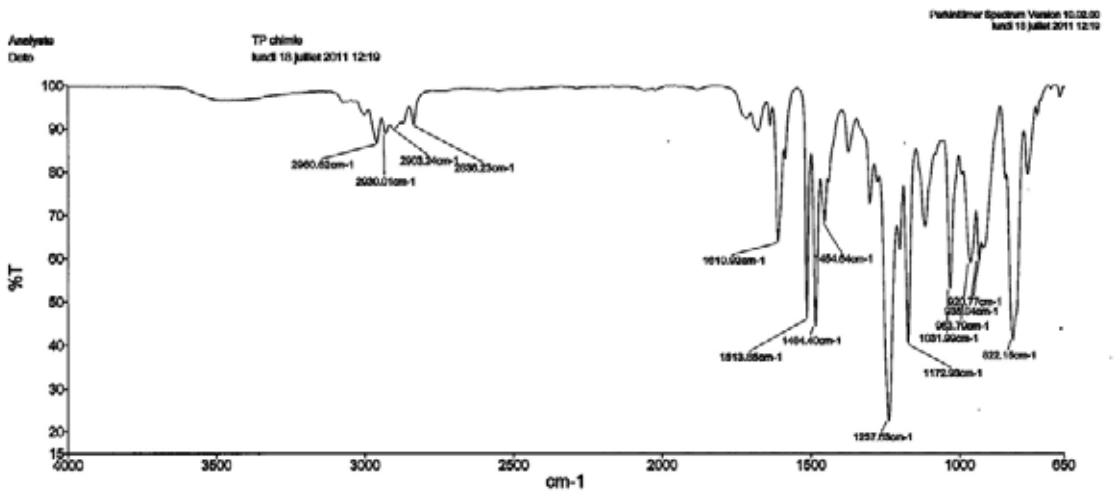

Figure 80 IR spectrum of compound LMM1 [**96**] (film)

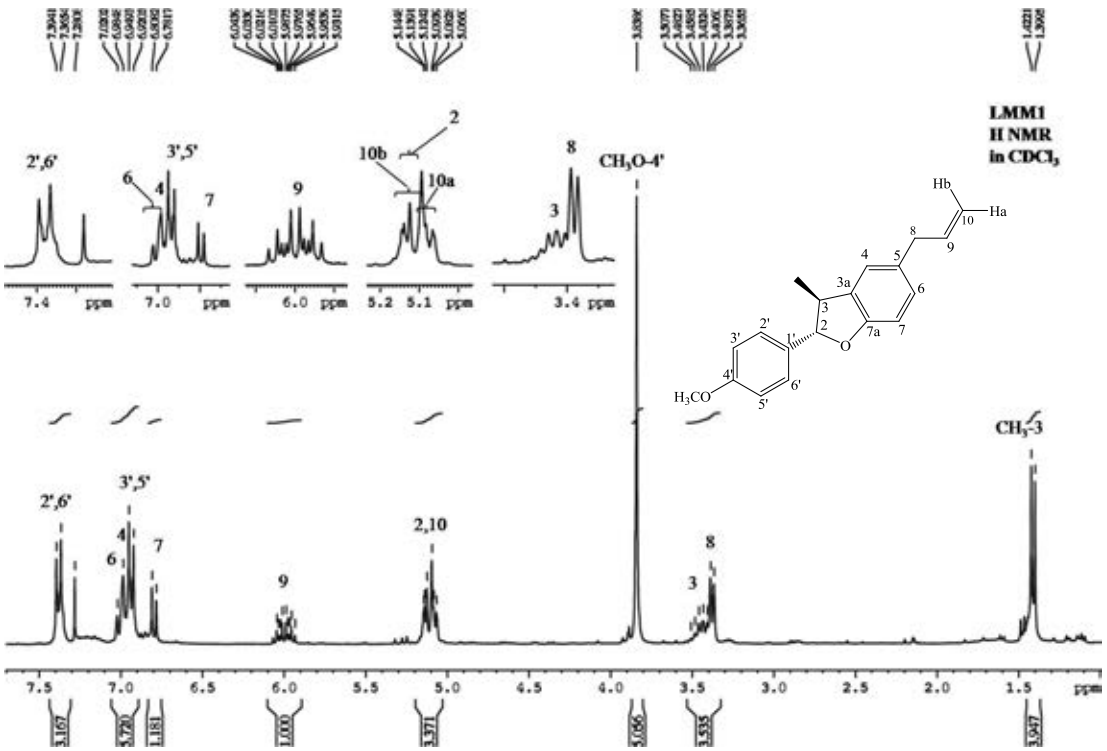

Figure 81 ^{1}H-NMR spectrum of compound LMM1 [**96**] ($CDCl_3$)

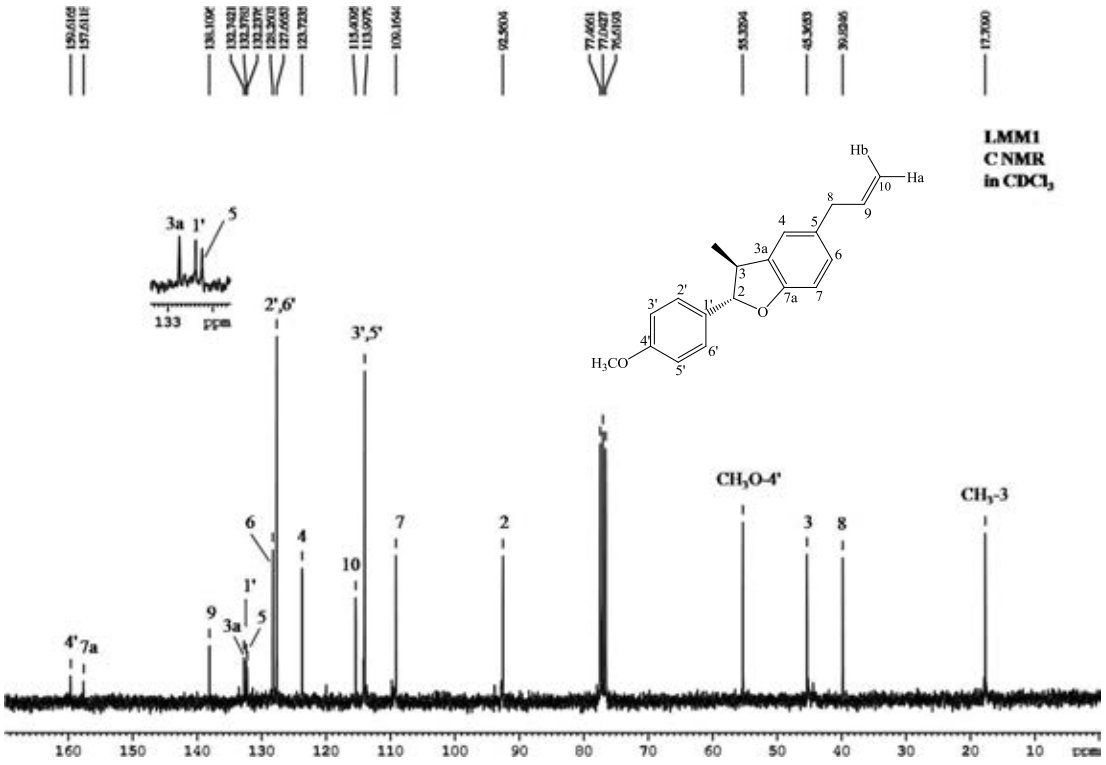

Figure 82 ^{13}C-NMR spectrum of compound LMM1 [**96**] ($CDCl_3$)

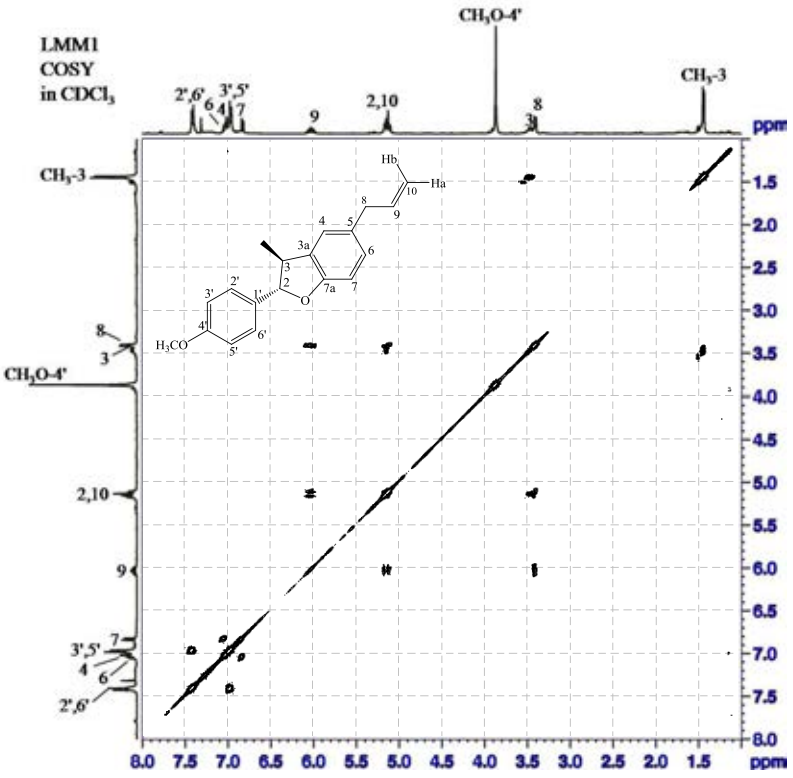

Figure 83 ^{1}H-^{1}H COSY spectrum of compound LMM1 [**96**] ($CDCl_3$)

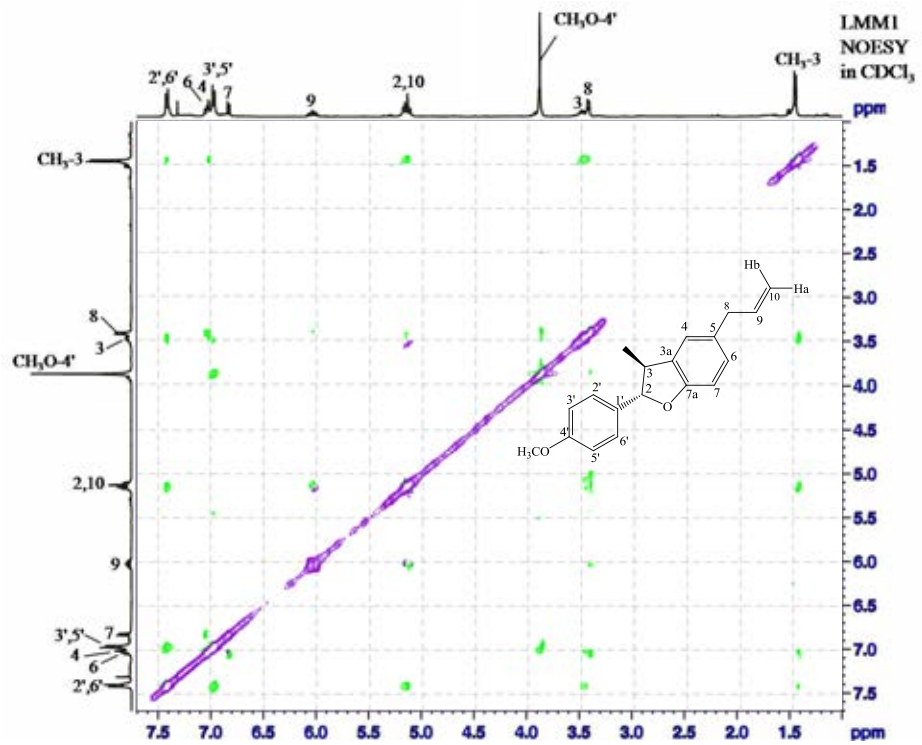

Figure 84 NOESY spectrum of compound LMM1 [**96**] ($CDCl_3$)

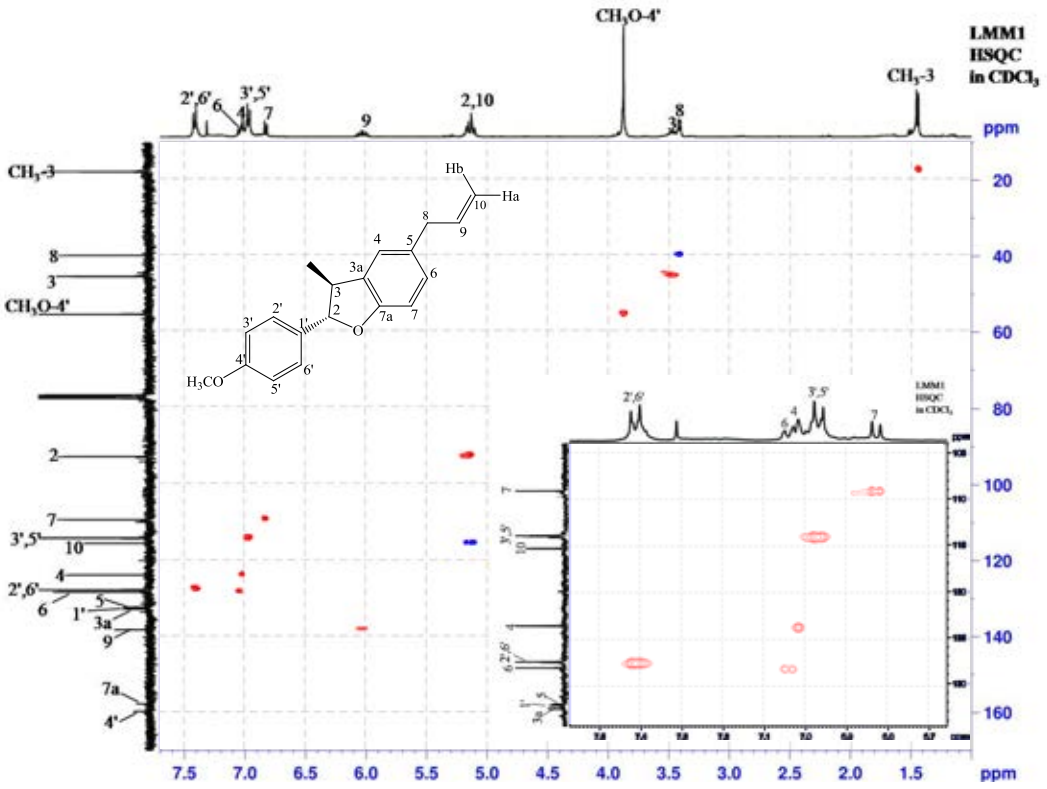

Figure 85 HSQC spectrum of compound LMM1 [**96**] ($CDCl_3$)

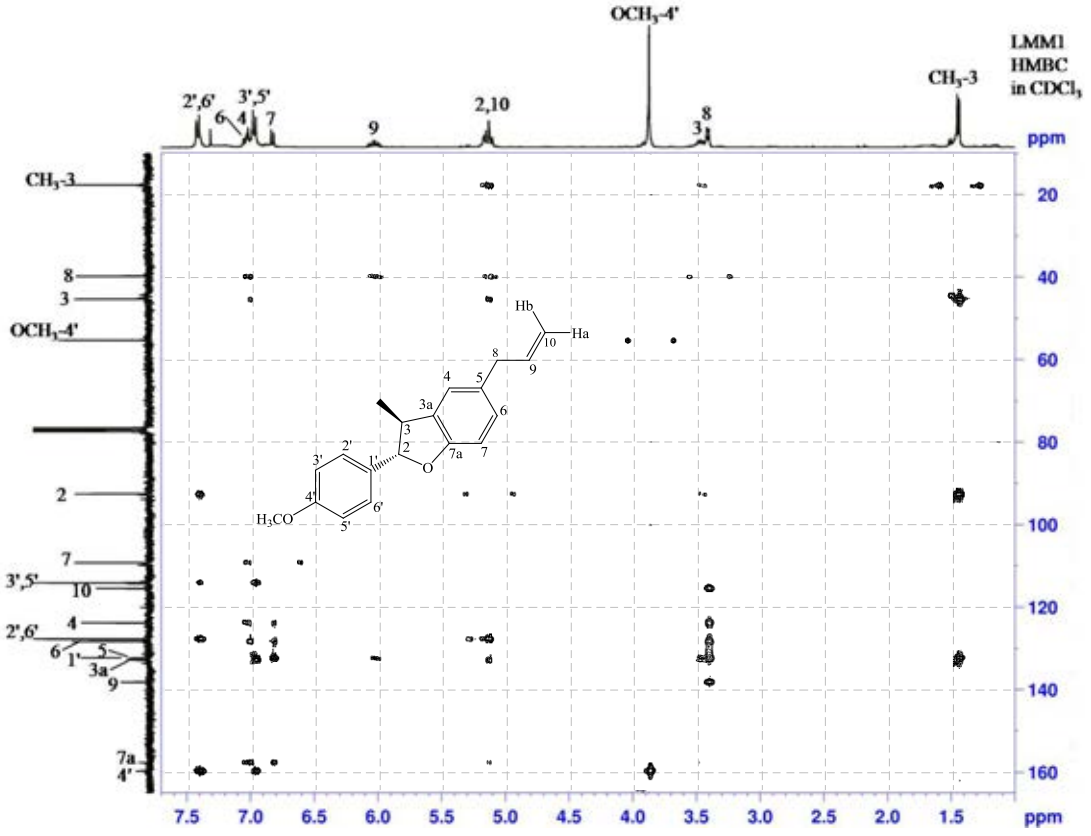

Figure 86 HMBC spectrum of compound LMM1 [**96**] ($CDCl_3$)

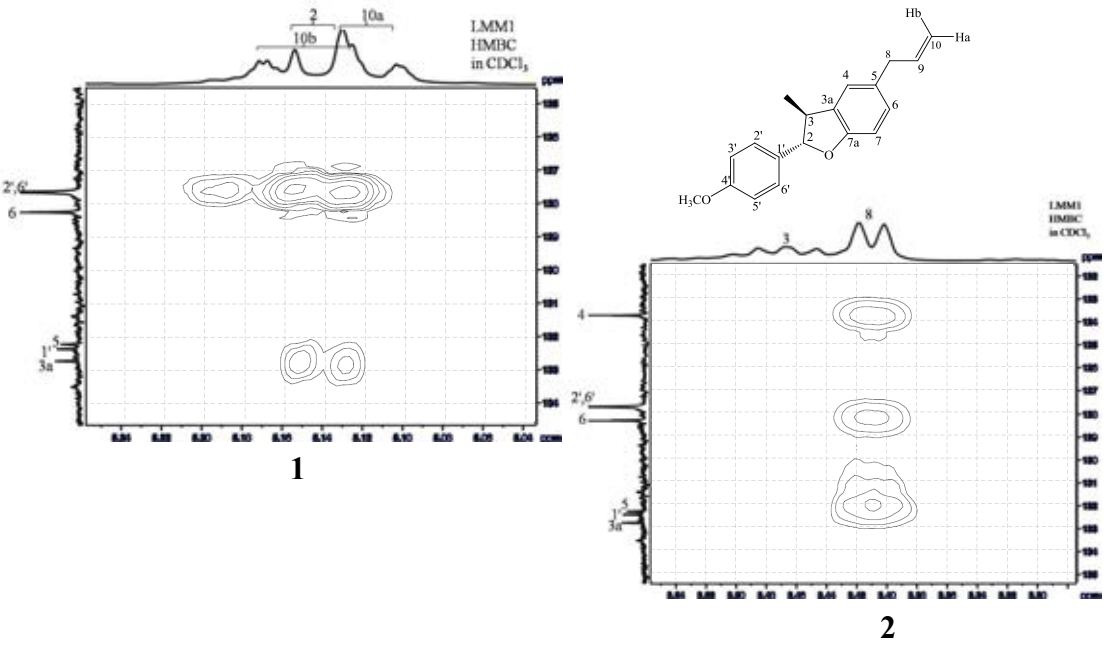

Figure 86a HMBC spectrum of compound LMM1 [**96**] ($CDCl_3$)
[δ_H 5.26-5.03 ppm, δ_C 134.7-124.5 ppm (1)] and
[δ_H 3.56-2.85 ppm, δ_C 135.4-121.5 ppm (2)]

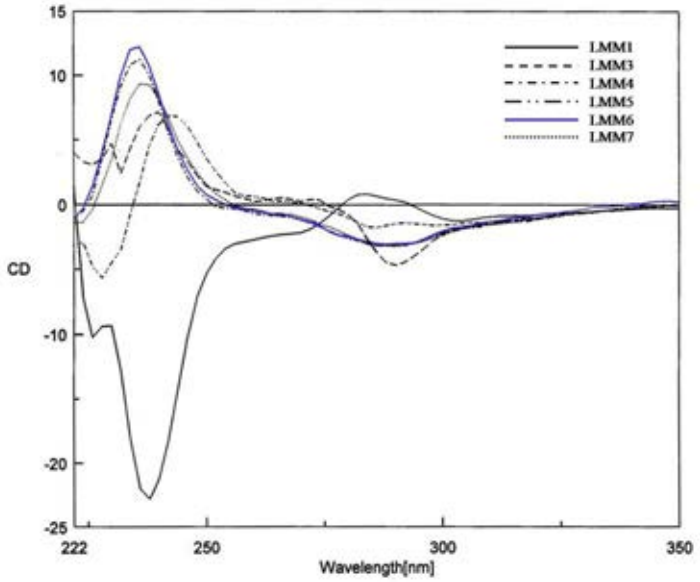

Figure 87 CD spectra (MeOH) of compounds LMM1 [**96**], LMM3 [**98**], LMM4 [**99**], LMM5 [**100**], LMM6 [**101**] and LMM7 [**102**]

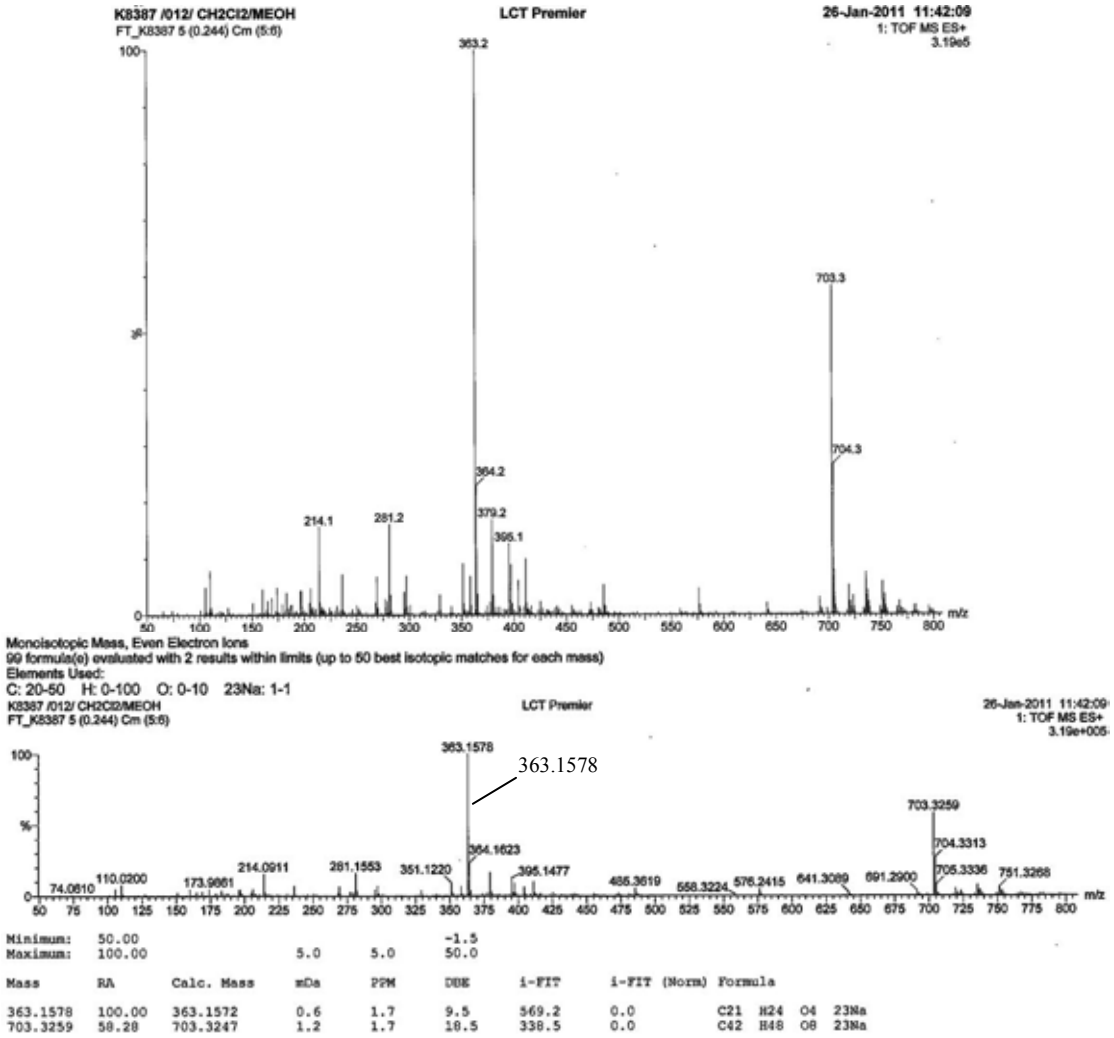

Figure 88 HRESI mass spectrum of compound LMM2 [**97**]

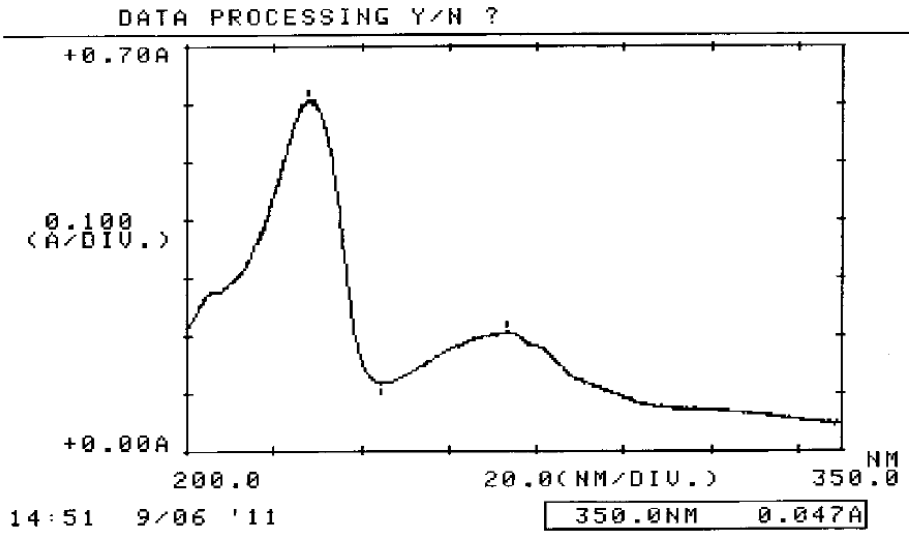

Figure 89 UV spectrum of compound LMM2 [**97**] (MeOH)

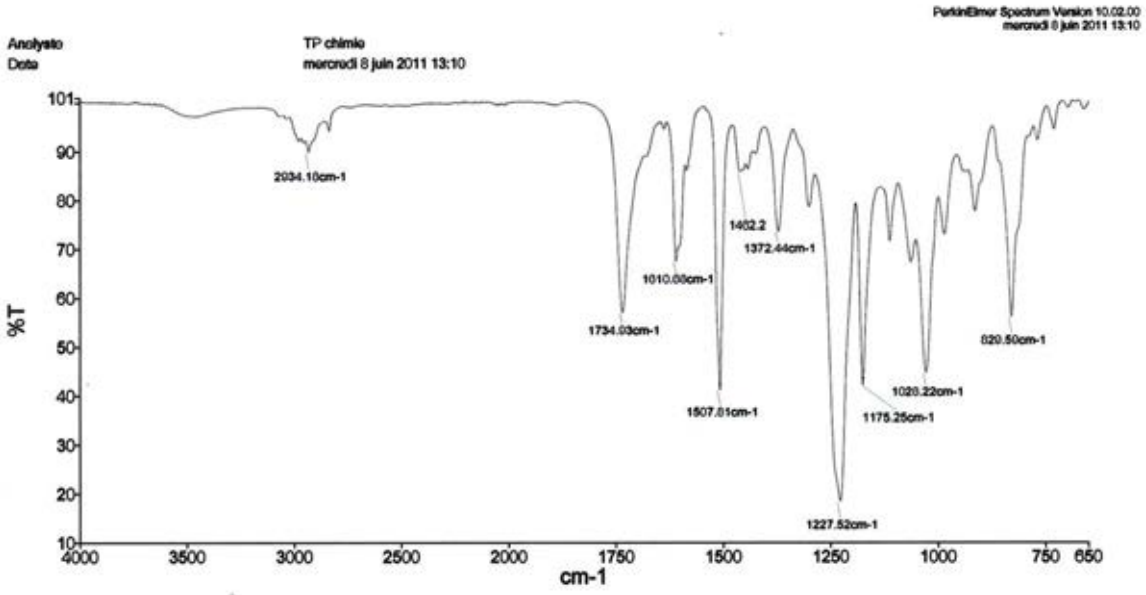

Figure 90 IR spectrum of compound LMM2 [**97**] (film)

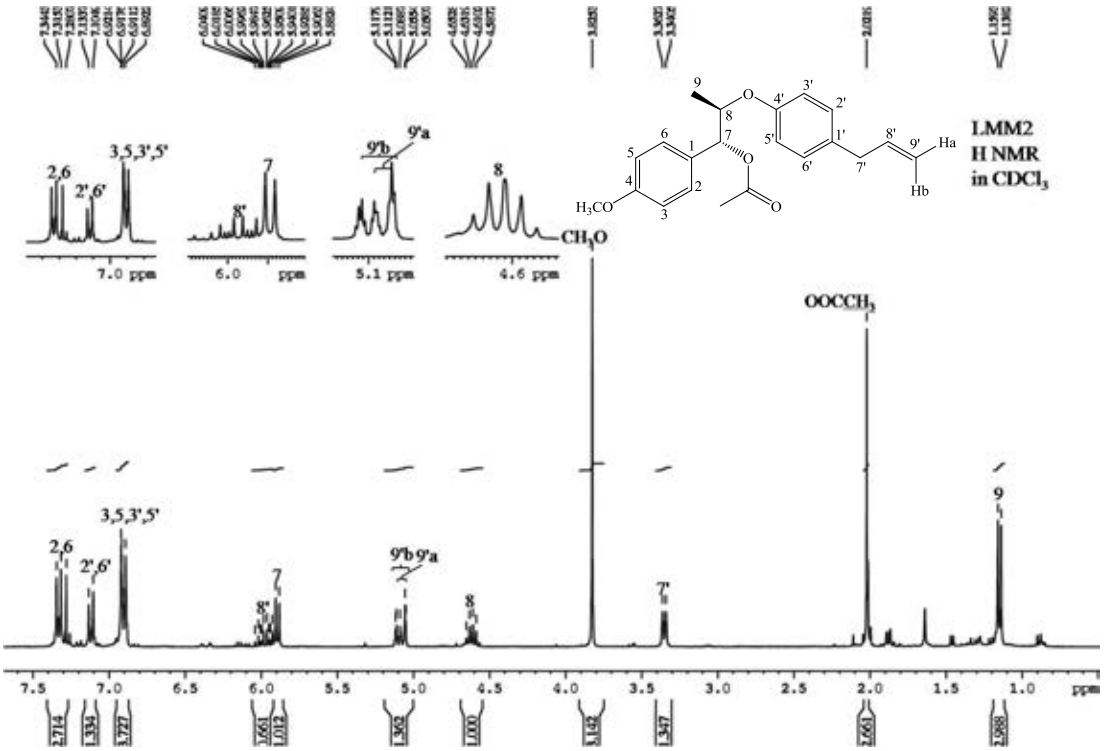

Figure 91 ^{1}H-NMR spectrum of compound LMM2 [**97**] ($CDCl_3$)

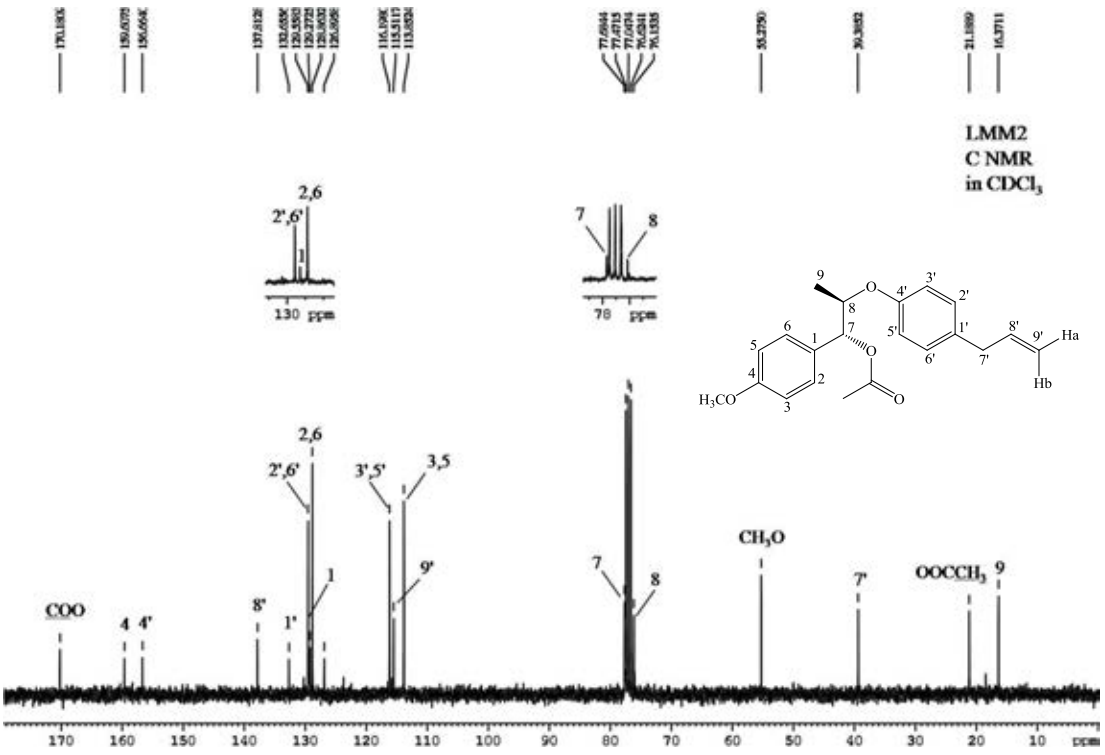

Figure 92 ^{13}C-NMR spectrum of compound LMM2 [**97**] ($CDCl_3$)

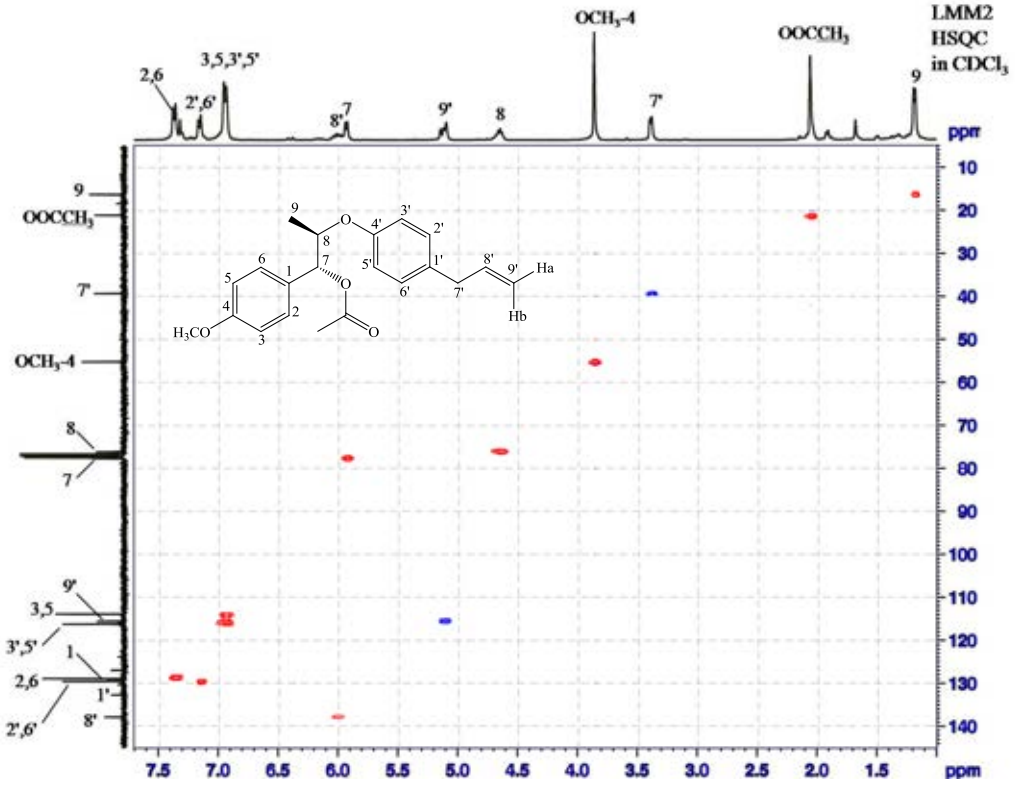

Figure 93 HSQC spectrum of compound LMM2 [**97**] ($CDCl_3$)

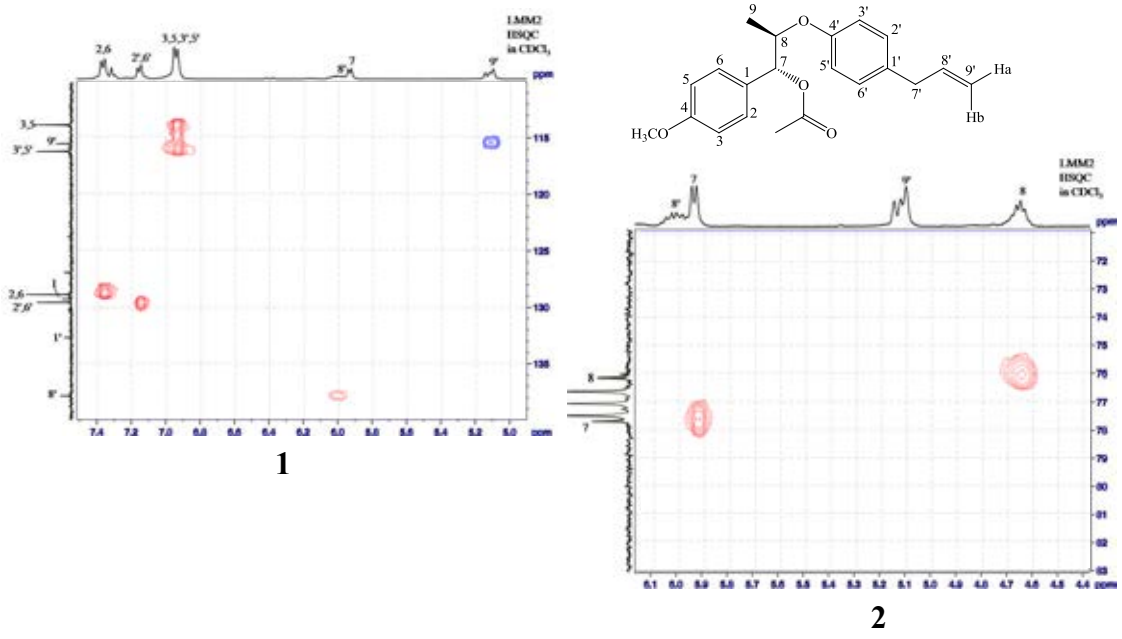

Figure 93a HSQC spectrum of compound LMM2 [**97**] ($CDCl_3$)
[δ_H 7.5-4.9 ppm, δ_C 140-110 ppm (1)] and
[δ_H 6.16-4.37 ppm, δ_C 83-70.9 ppm (2)]

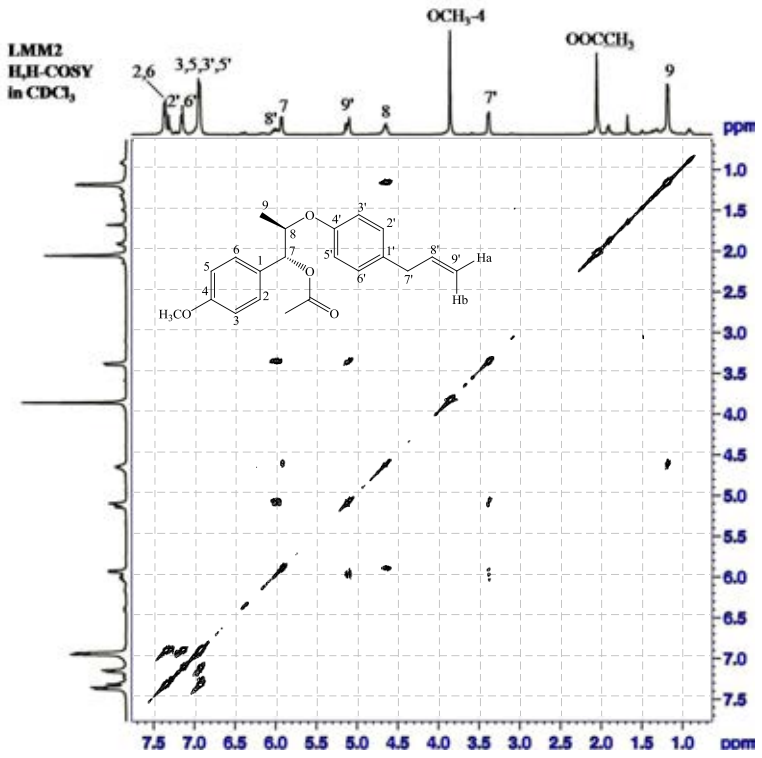

Figure 94 ^{1}H-^{1}H COSY spectrum of compound LMM2 [**97**] ($CDCl_3$)

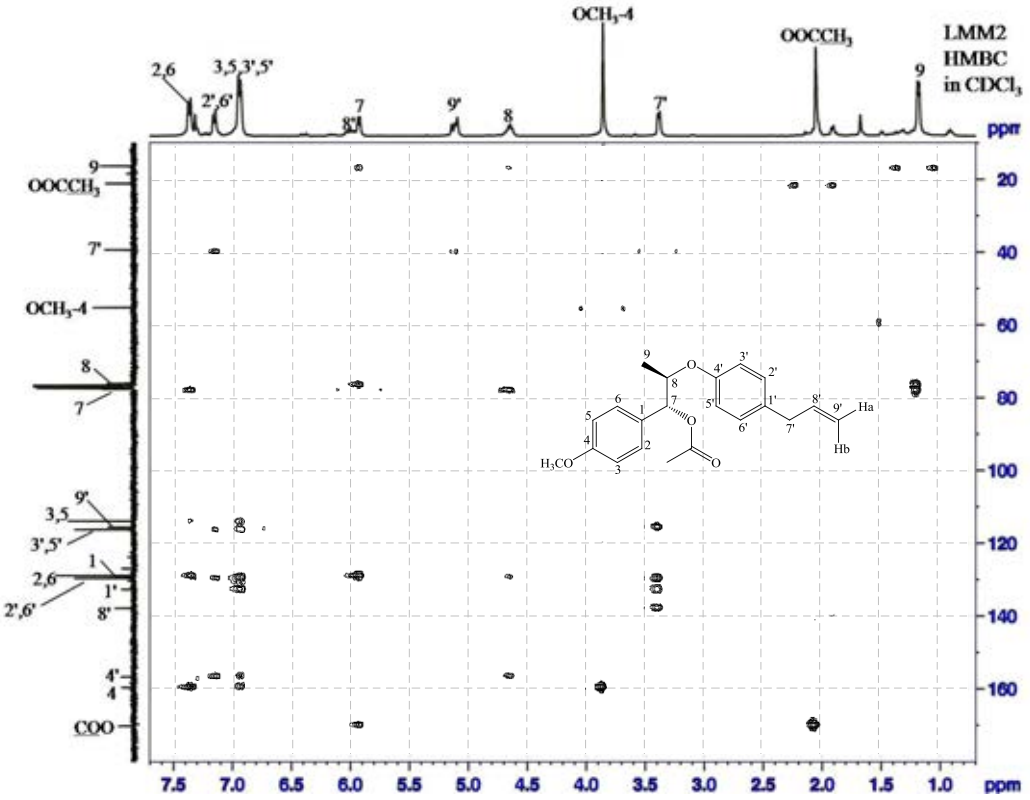

Figure 95 HMBC spectrum of compound LMM2 [**97**] ($CDCl_3$)

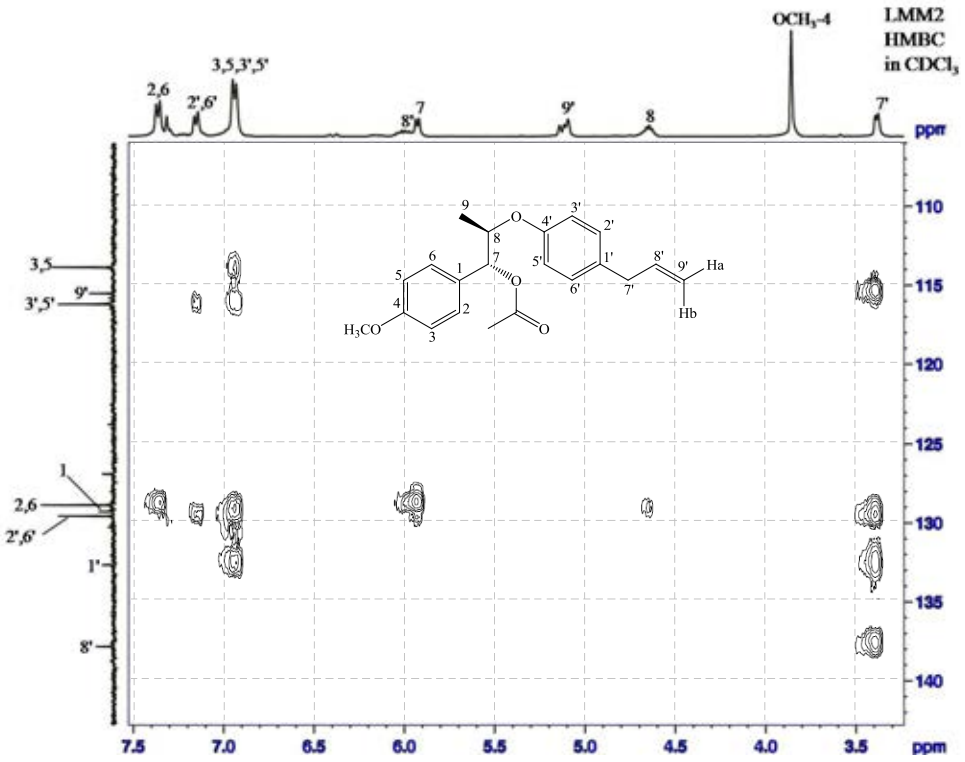

Figure 95a HMBC spectrum of compound LMM2 [**97**] ($CDCl_3$) [δ_H 7.5-3.2 ppm, δ_C 143-106 ppm]

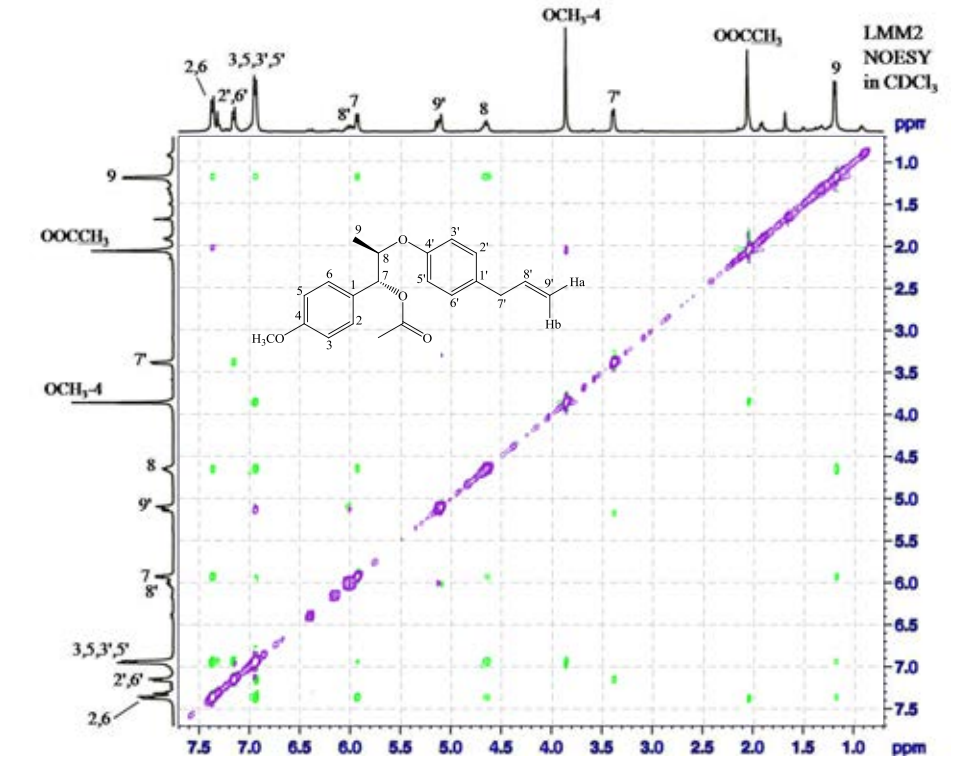

Figure 96 NOESY spectrum of compound LMM2 [**97**] ($CDCl_3$)

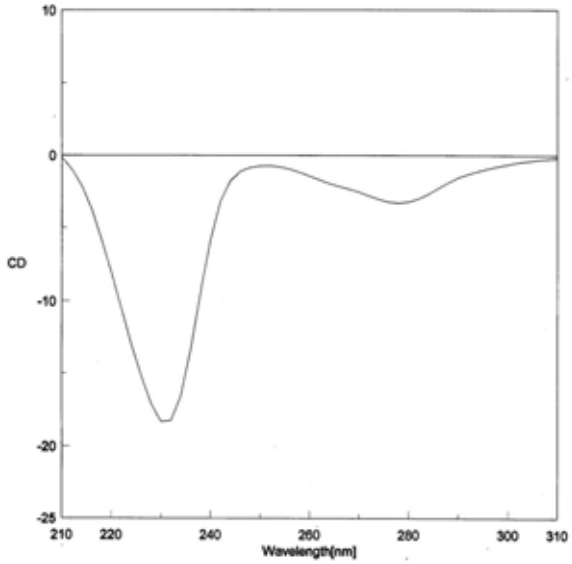

Figure 97 CD spectrum of compound LMM2 [**97**] (MeOH)

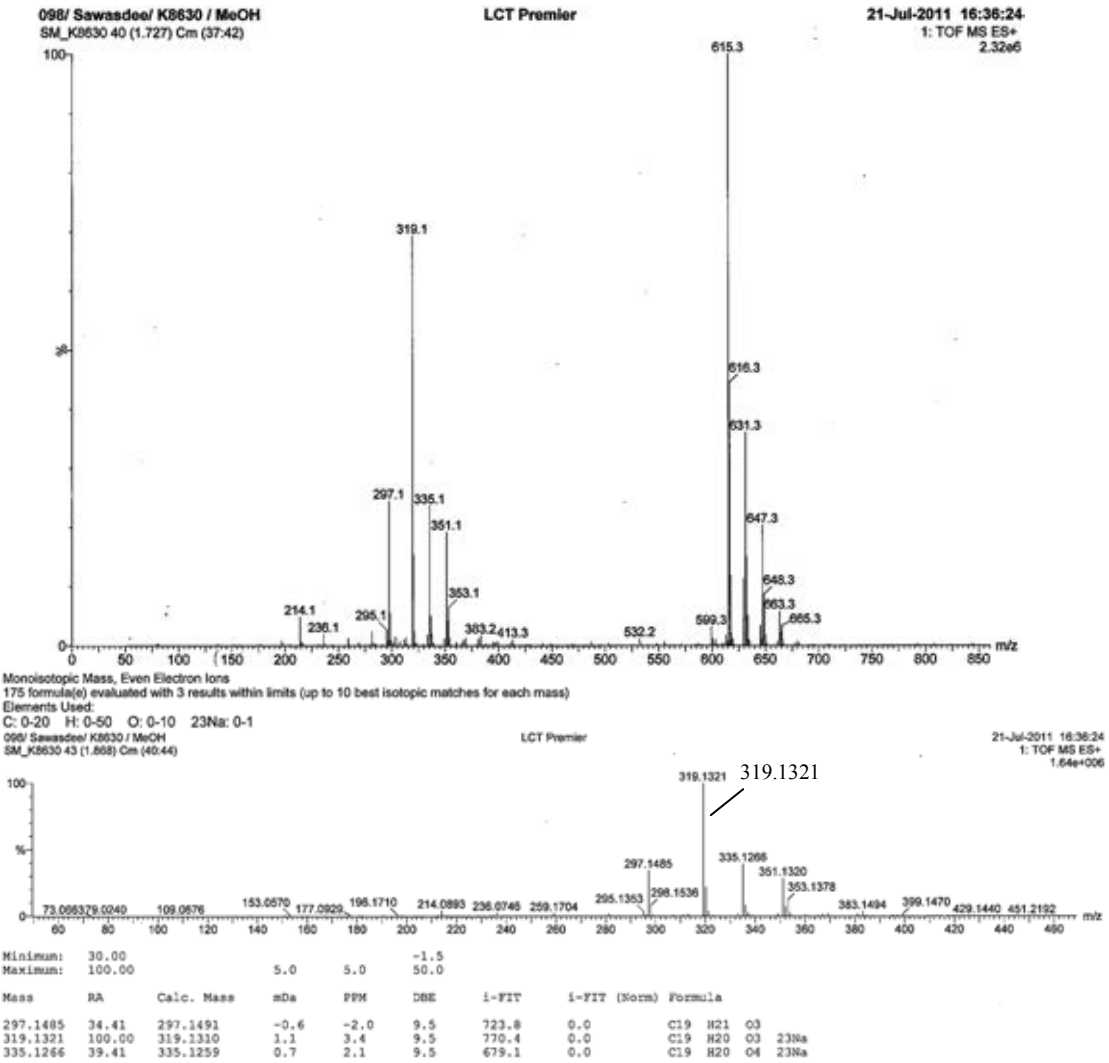

Figure 98 HRESI mass spectrum of compound LMM3 [**98**]

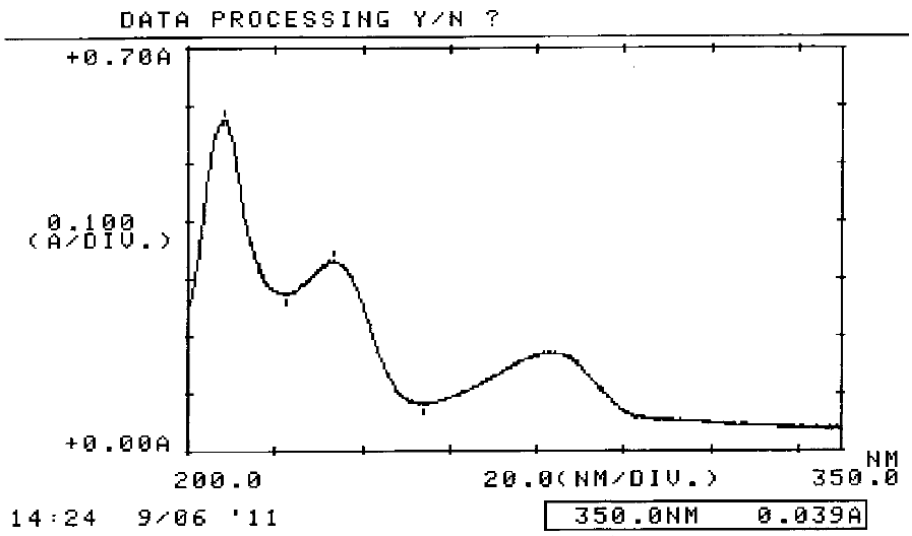

Figure 99 UV spectrum of compound LMM3 [**98**] (MeOH)

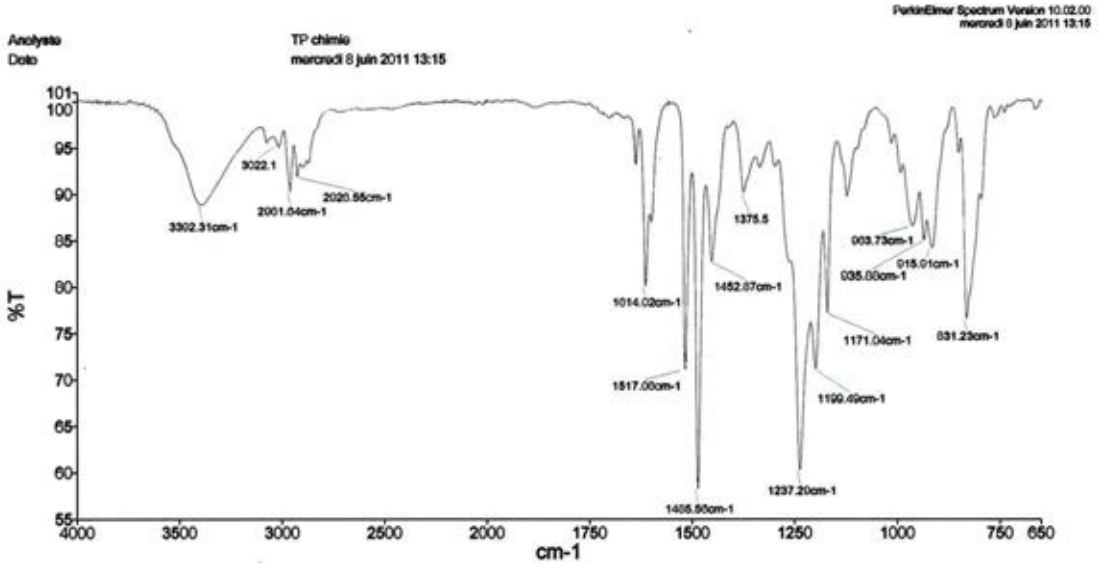

Figure 100 IR spectrum of compound LMM3 [**98**] (film)

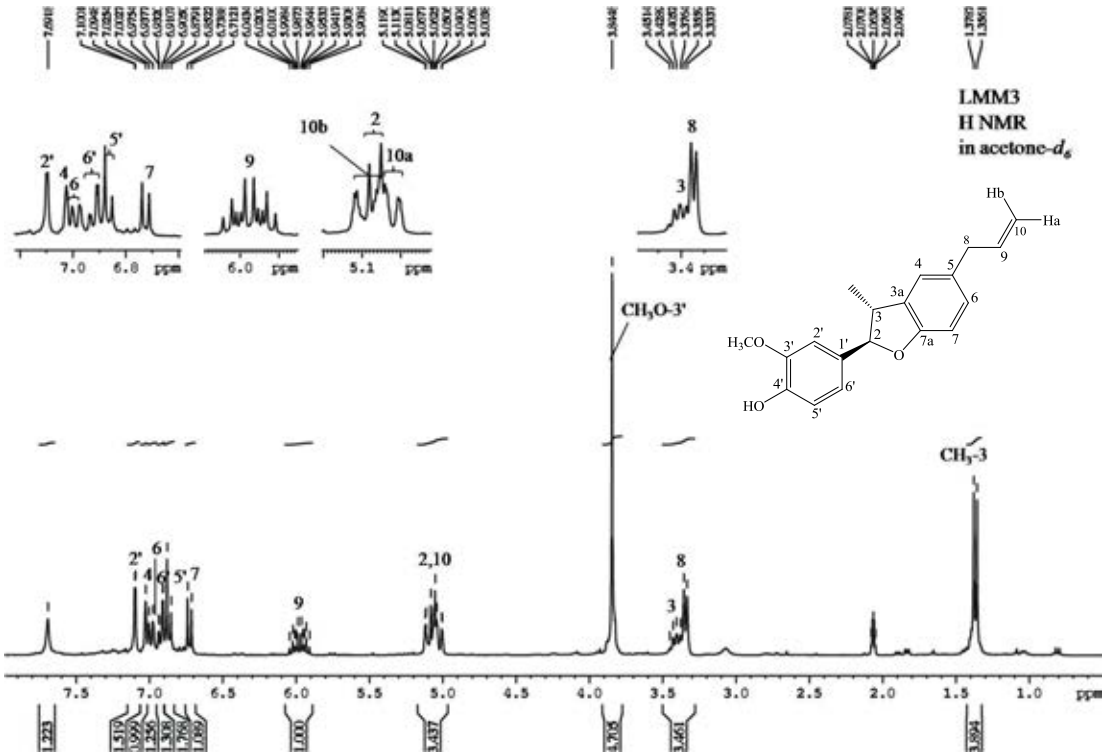

Figure 101 ^{1}H-NMR spectrum of compound LMM3 [**98**] (acetone-d_6)

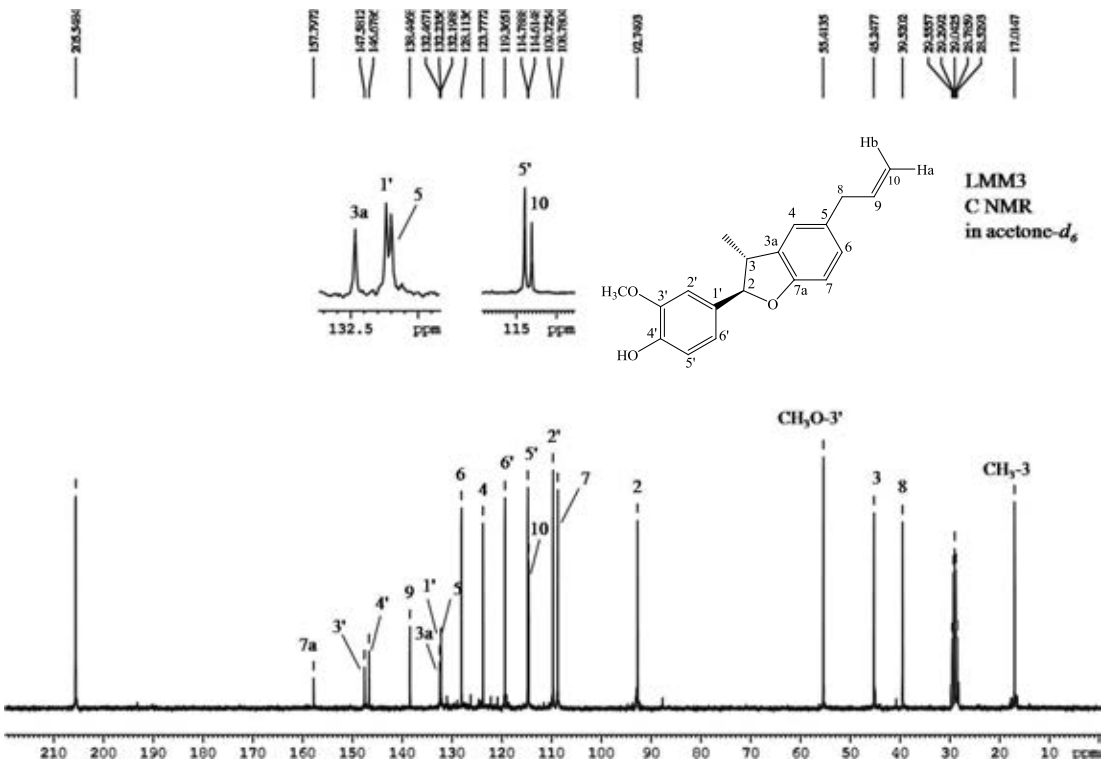

Figure 102 ^{13}C-NMR spectrum of compound LMM3 [**98**] (acetone-d_6)

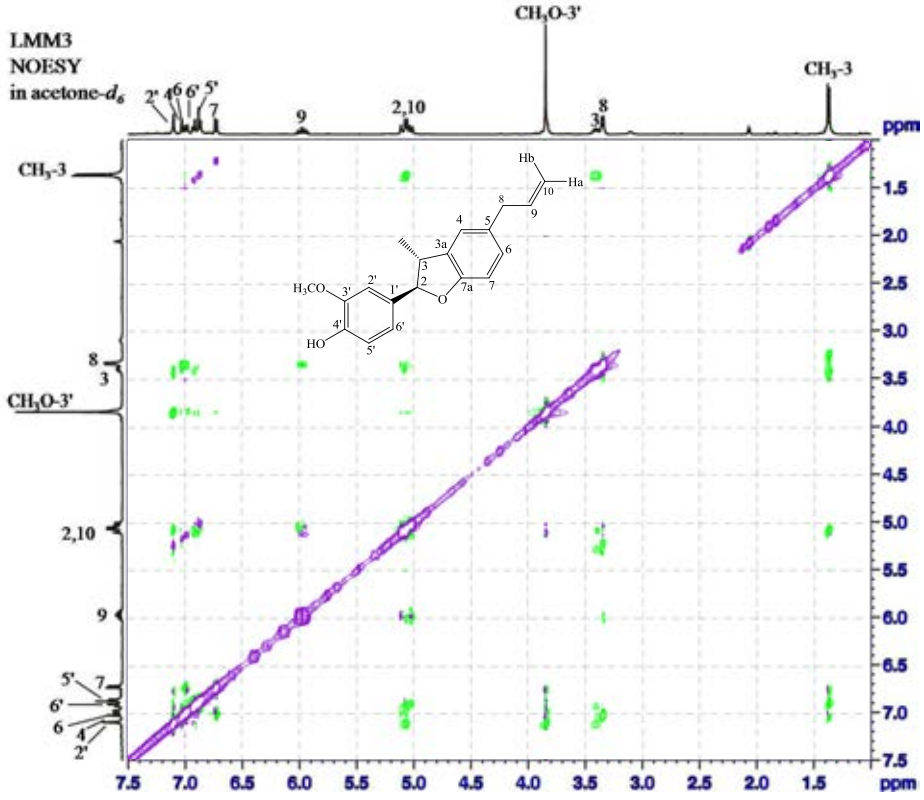

Figure 103 NOESY spectrum of compound LMM3 [**98**] (acetone-d_6)

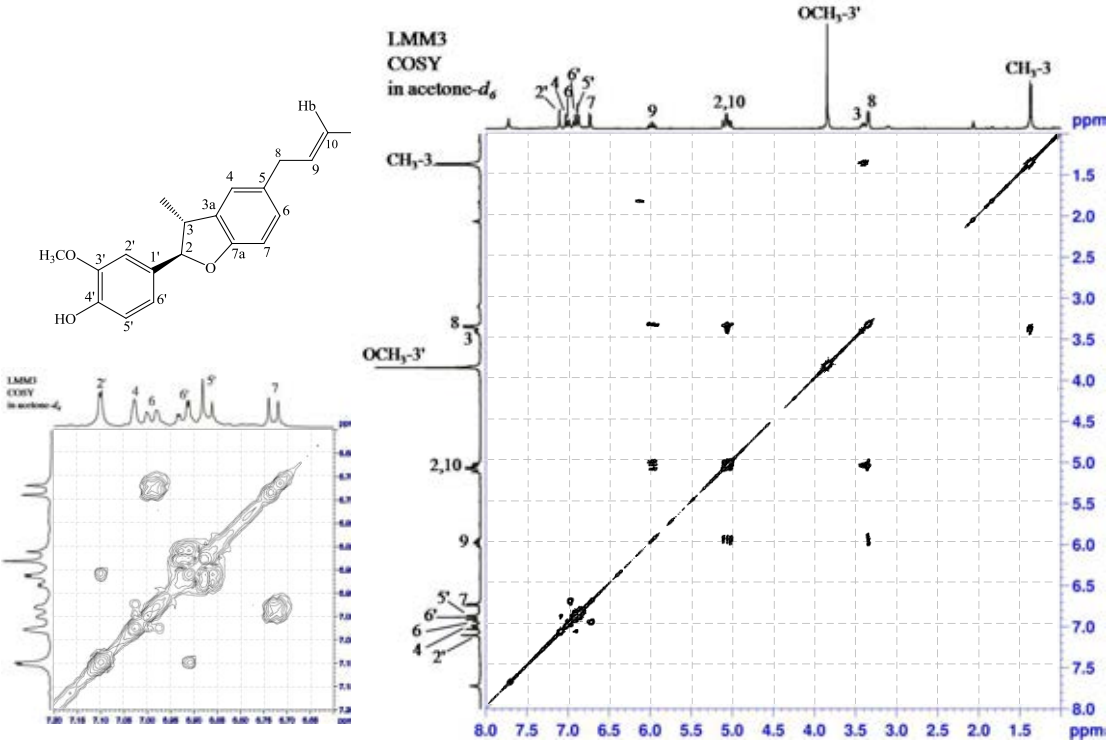

Figure 104 ^{1}H-^{1}H COSY spectrum of compound LMM3 [**98**] (acetone-d_6)

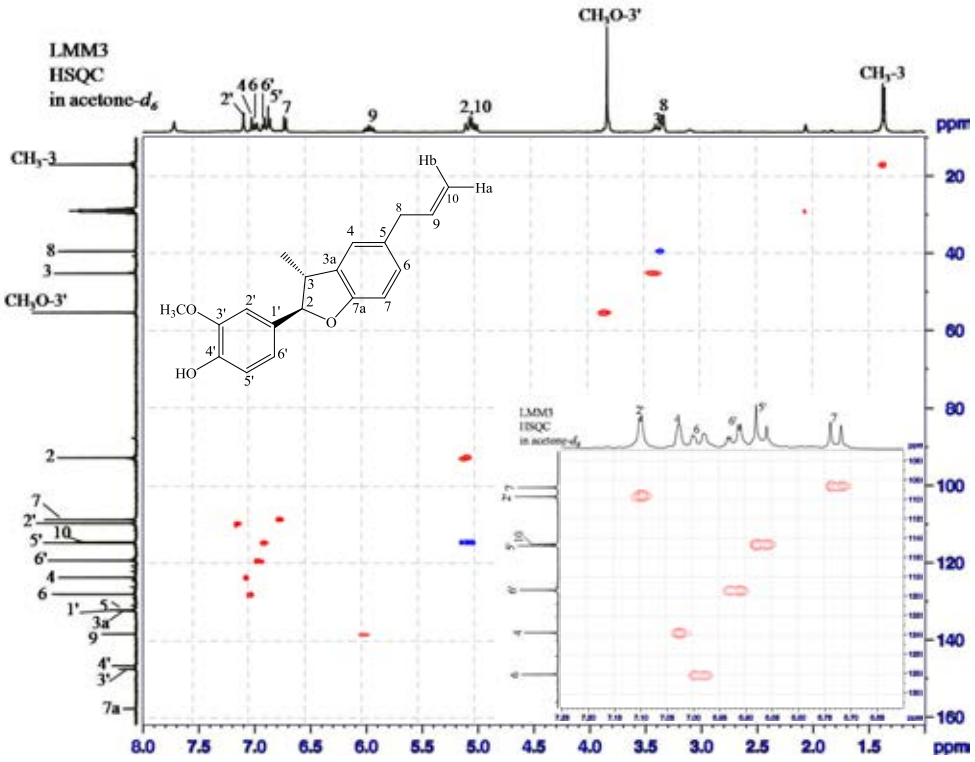

Figure 105 HSQC spectrum of compound LMM3 [**98**] (acetone-d_6)

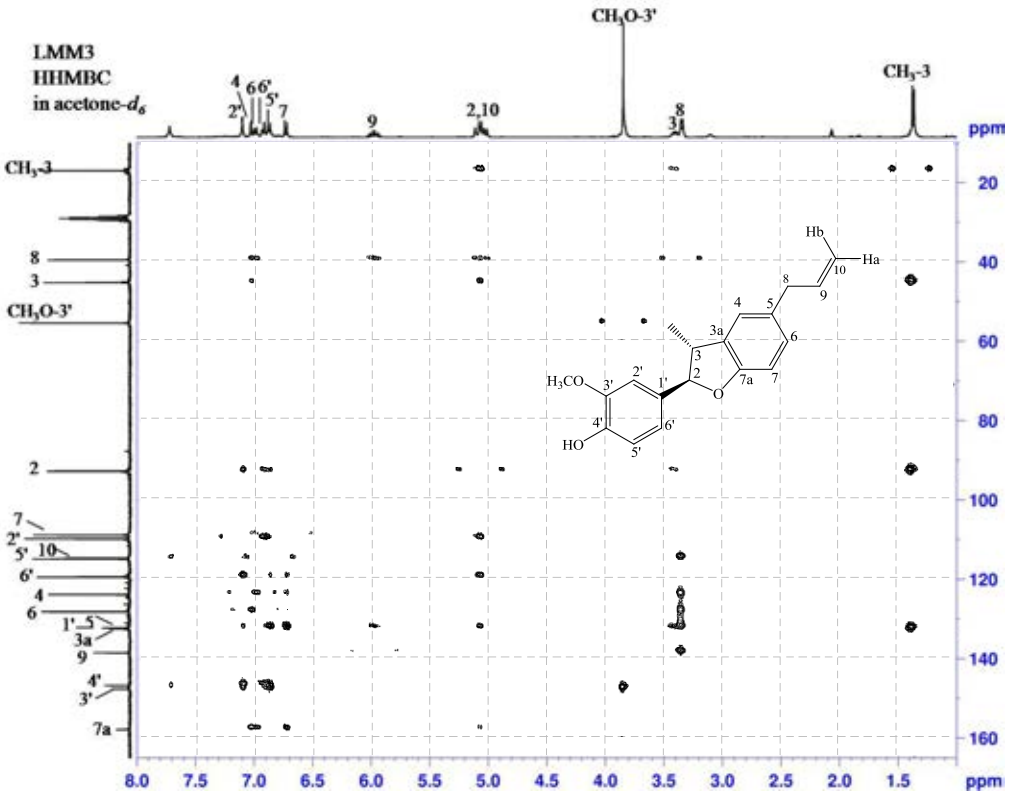

Figure 106 HMBC spectrum of compound LMM3 [**98**] (acetone-d_6)

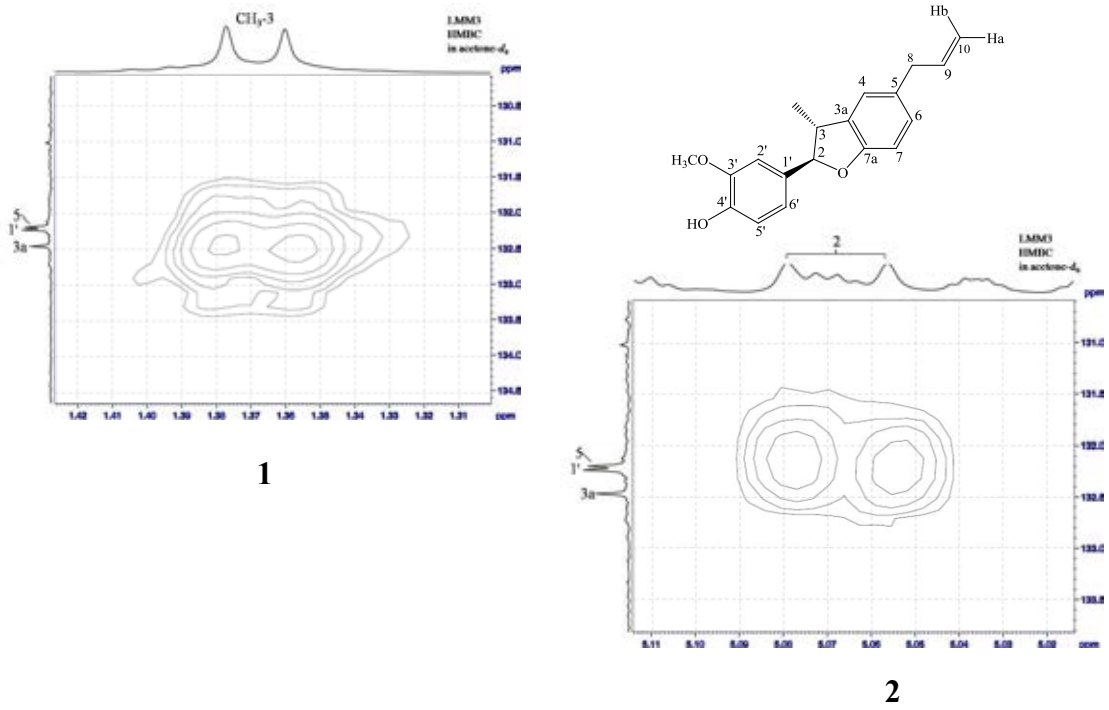

Figure 106a HMBC spectrum of compound LMM3 [**98**] (acetone-d_6)
[δ_H 1.43-1.30 ppm, δ_C 134.7-130.1 ppm (1)] and
[δ_H 5.11-5.01 ppm, δ_C 133.8-130.6 ppm (2)]

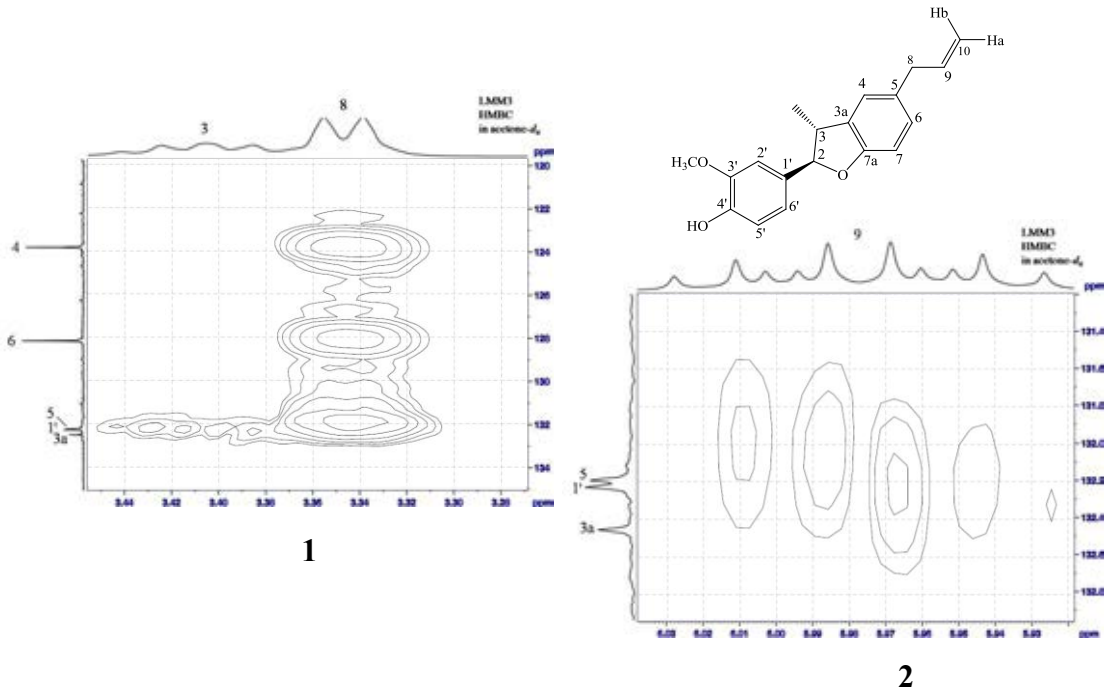

Figure 106b HMBC spectrum of compound LMM3 [**98**] (acetone-d_6)
[δ_H 3.46-3.27 ppm, δ_C 135-120 ppm (1)] and
[δ_H 6.04-5.92 ppm, δ_C 133.0-131.2 ppm (2)]

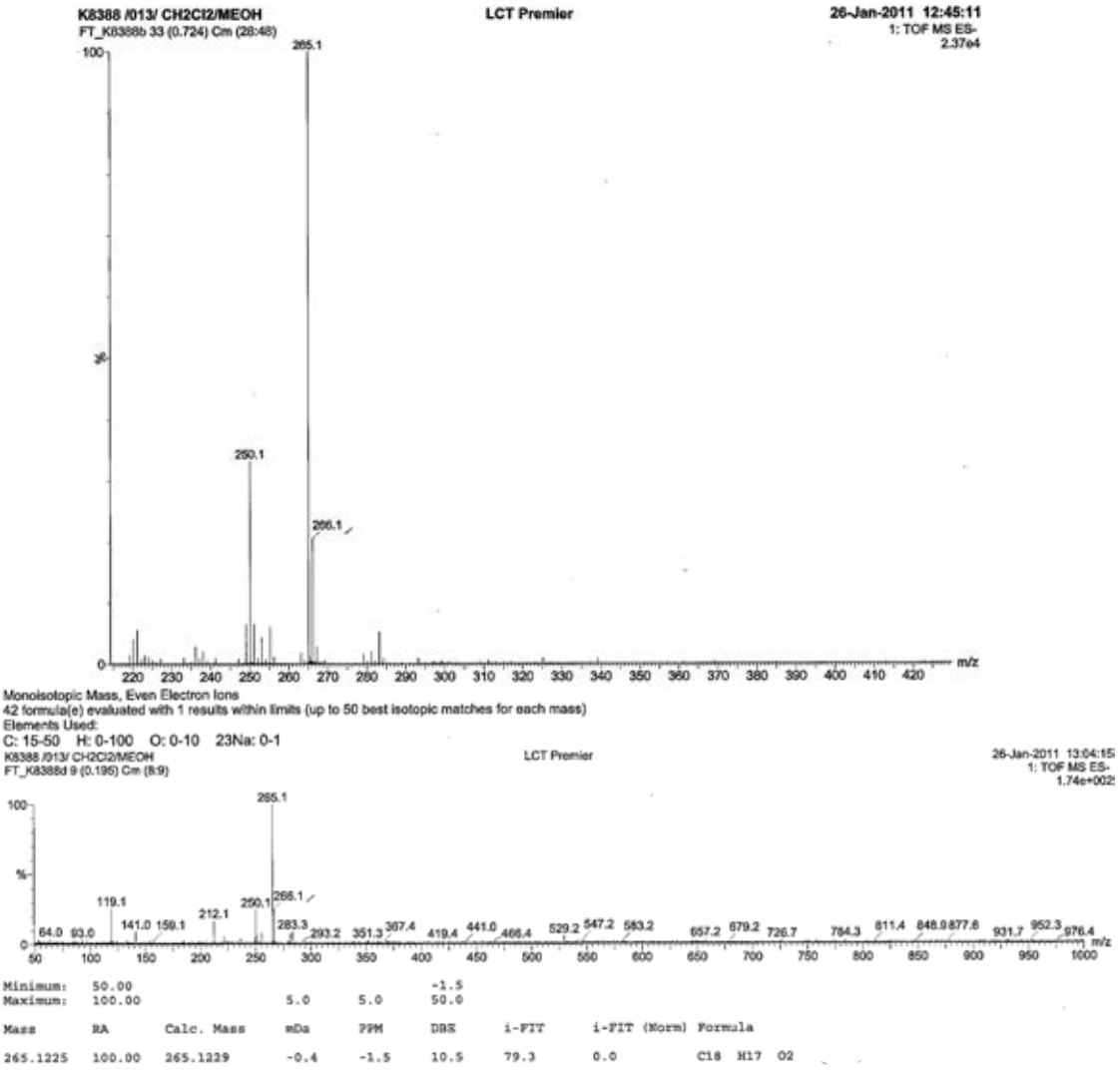

Figure 107 HRESI mass spectrum of compound LMM4 [**99**]

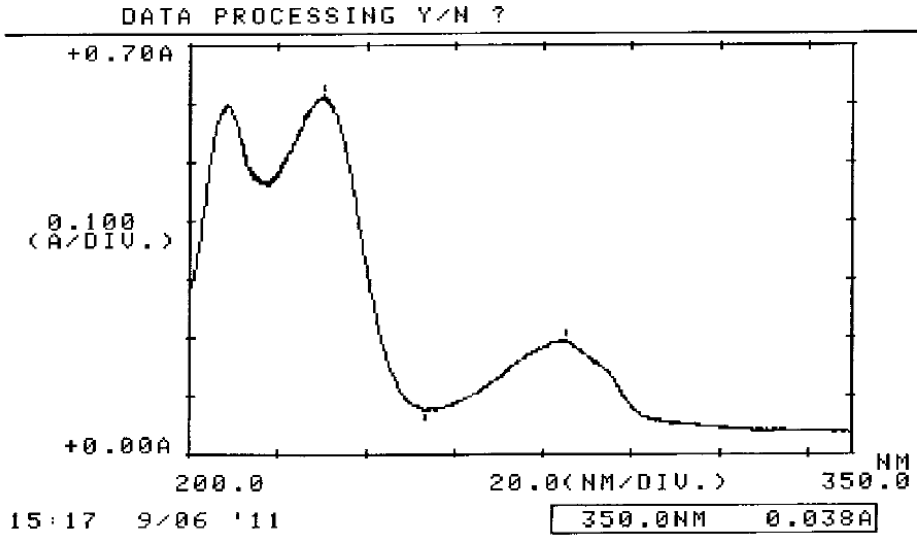

Figure 108 UV spectrum of compound LMM4 [**99**] (MeOH)

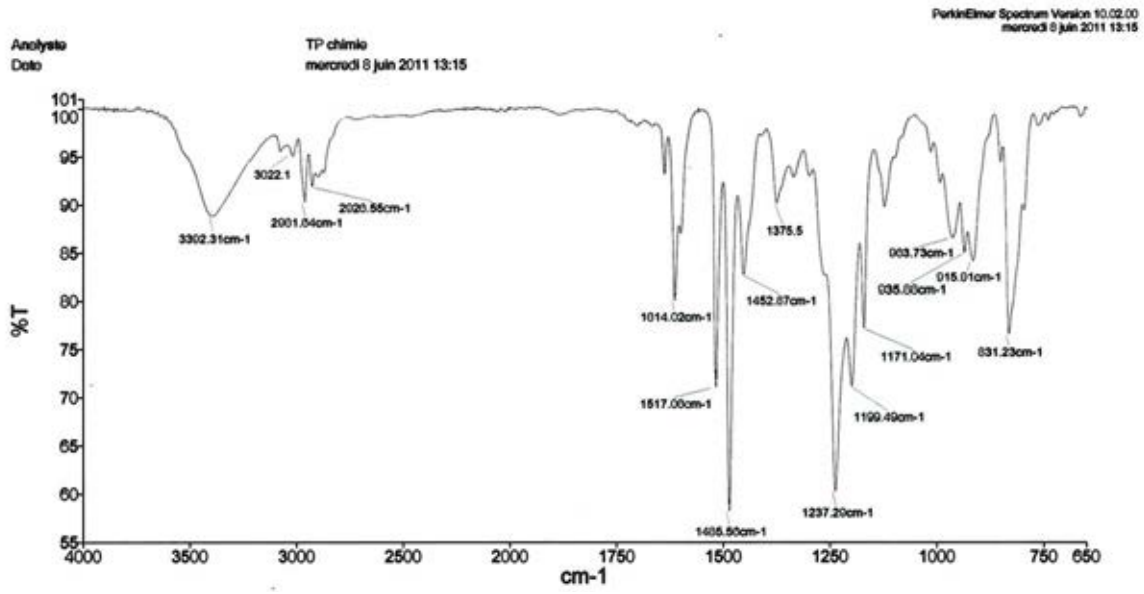

Figure 109 IR spectrum of compound LMM4 [**99**] (film)

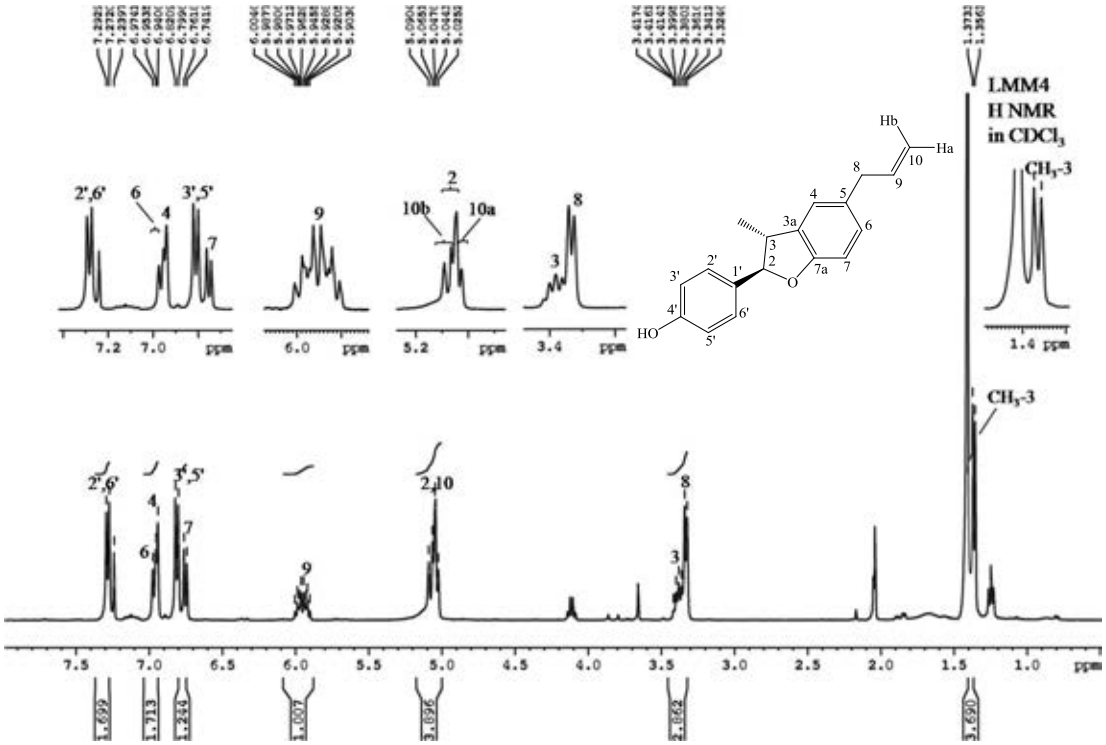

Figure 110 ^{1}H-NMR spectrum of compound LMM4 [**99**] ($CDCl_3$)

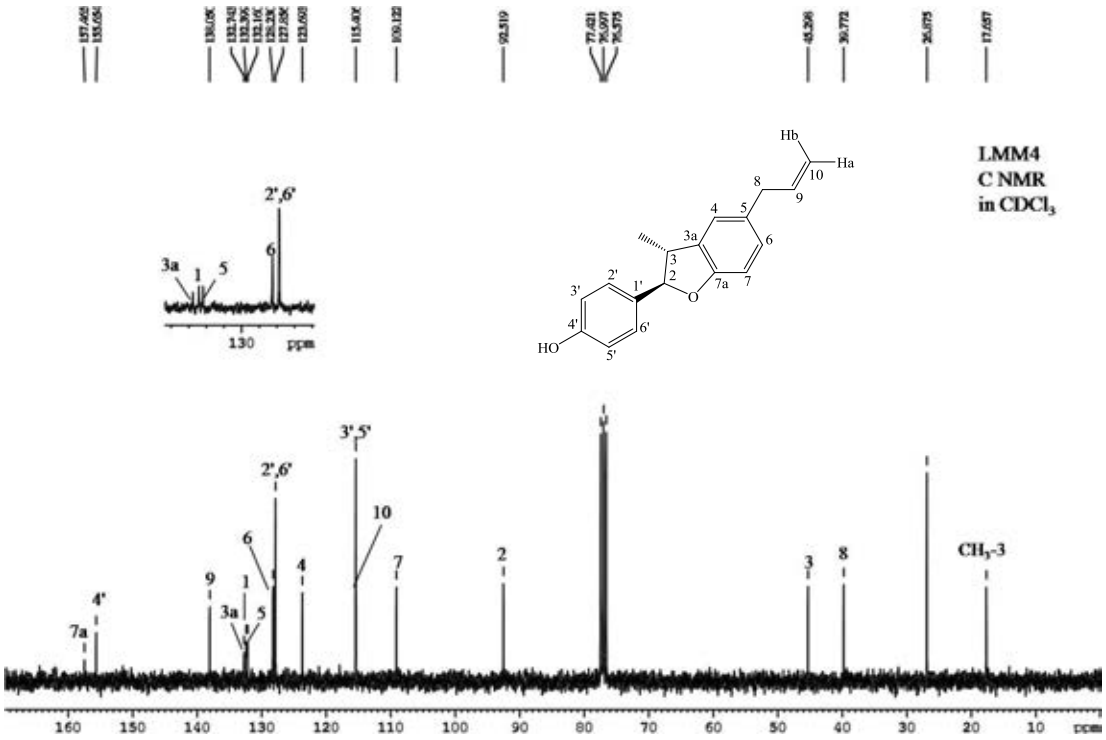

Figure 111 ^{13}C-NMR spectrum of compound LMM4 [**99**] ($CDCl_3$)

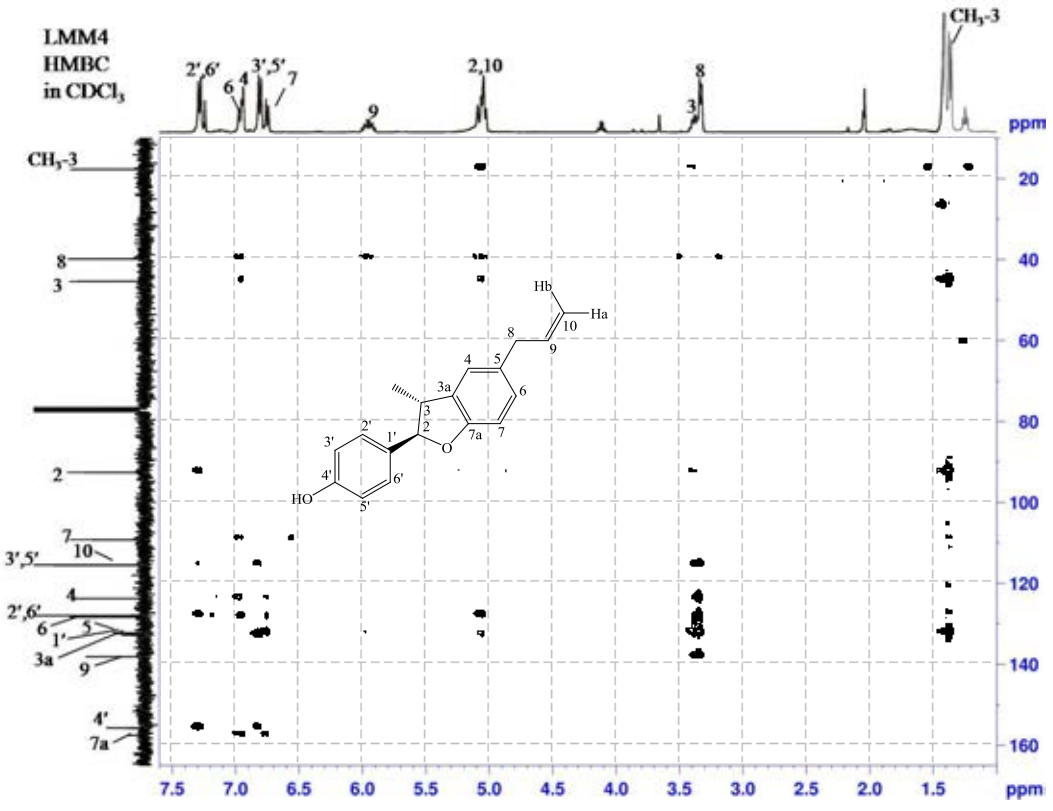

Figure 112 HMBC spectrum of compound LMM4 [**99**] ($CDCl_3$)

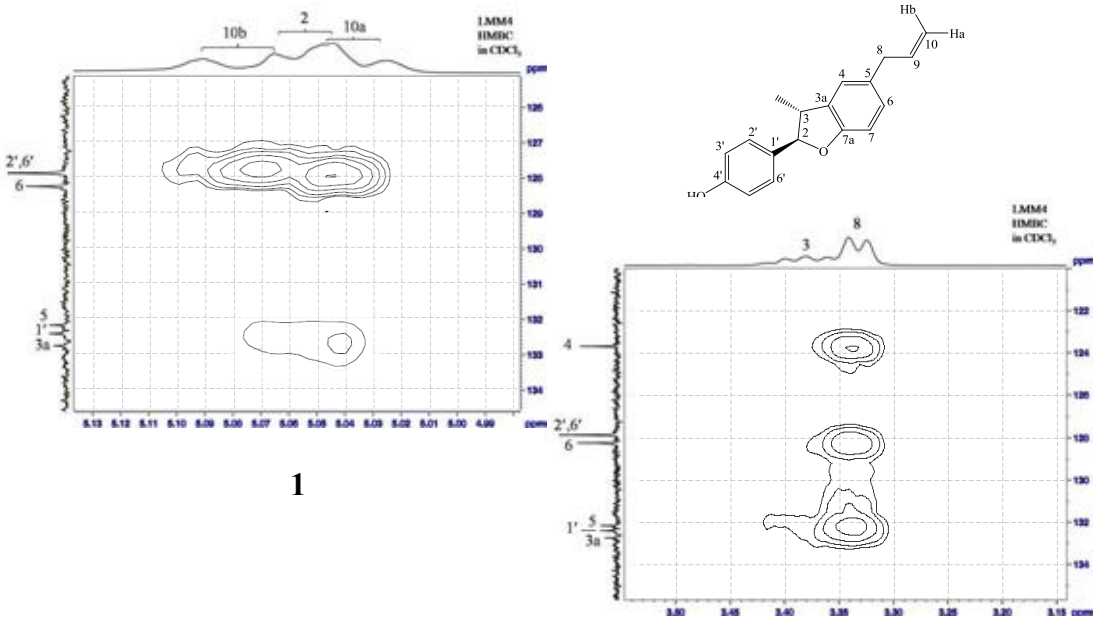

1

2

Figure 112a HMBC spectrum of compound LMM4 [**99**] ($CDCl_3$)
[δ_H 5.14-4.98 ppm, δ_C 135-125 ppm (1)] and
[δ_H 3.55-3.14 ppm, δ_C 135-121 ppm (2)]

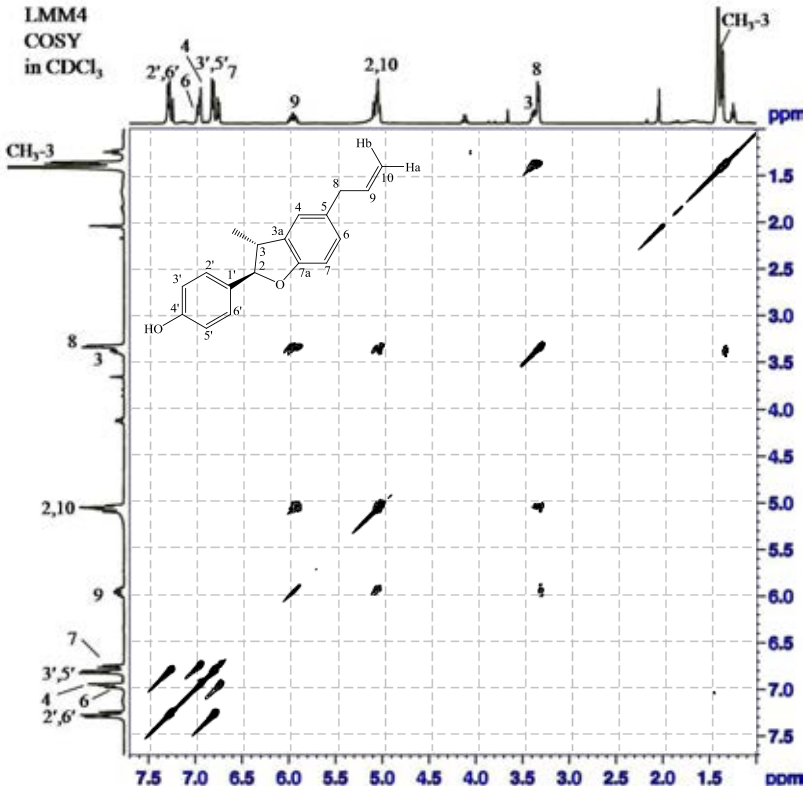

Figure 113 ^1H-^1H COSY spectrum of compound LMM4 [**99**] ($CDCl_3$)

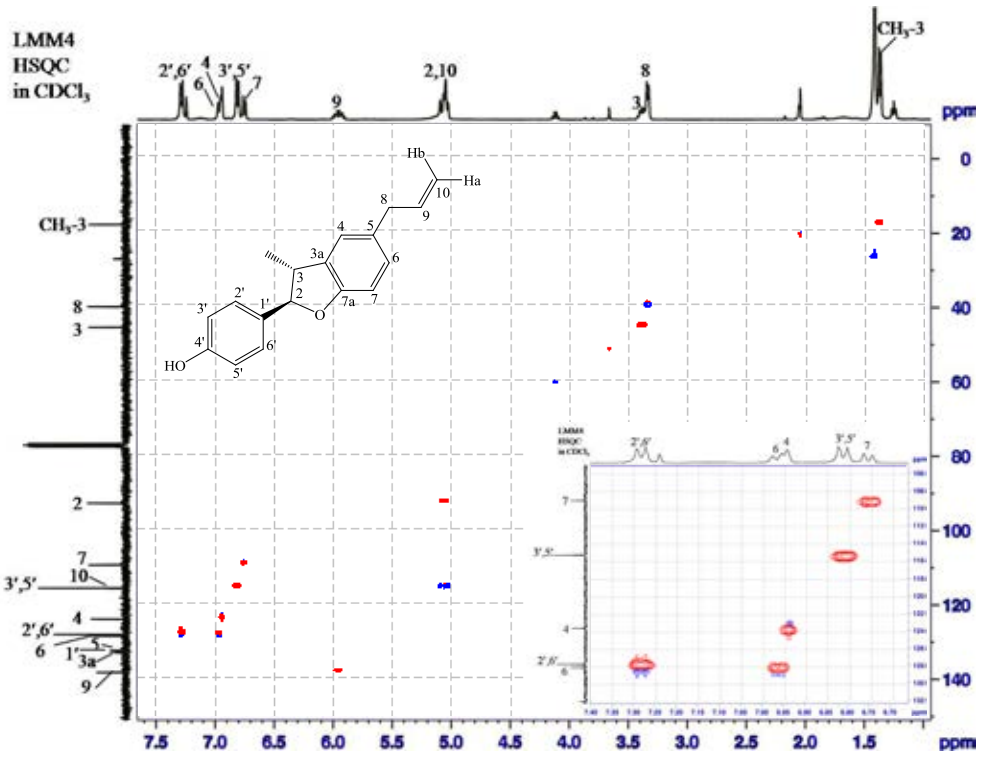

Figure 114 HSQC spectrum of compound LMM4 [**99**] ($CDCl_3$)

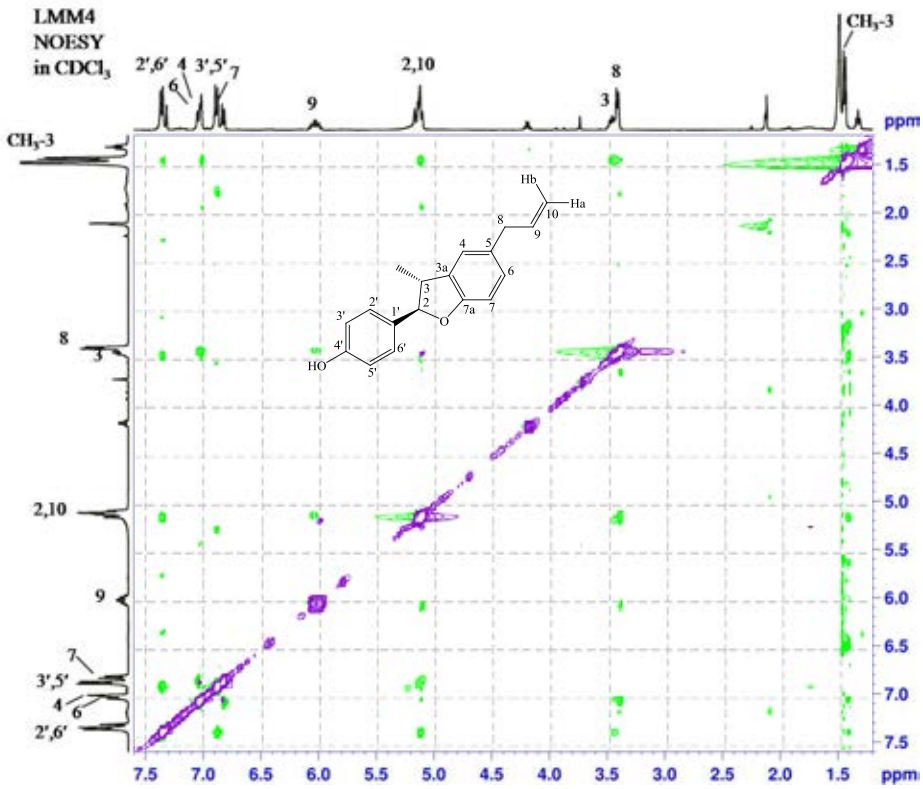

Figure 115 NOESY spectrum of compound LMM4 [**99**] ($CDCl_3$)

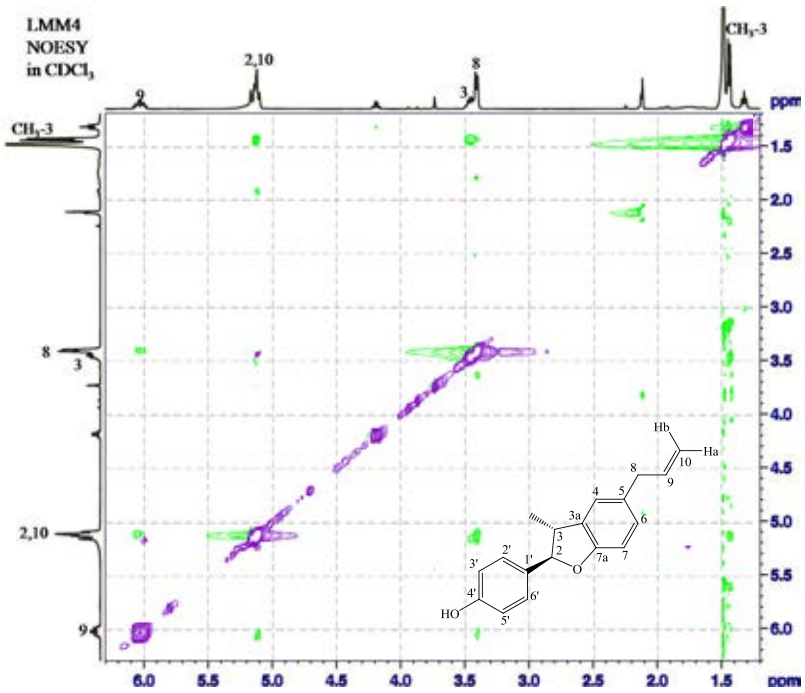

Figure 115a NOESY spectrum of compound LMM4 [**99**] ($CDCl_3$) [δ_H 6.3-1.2 ppm]

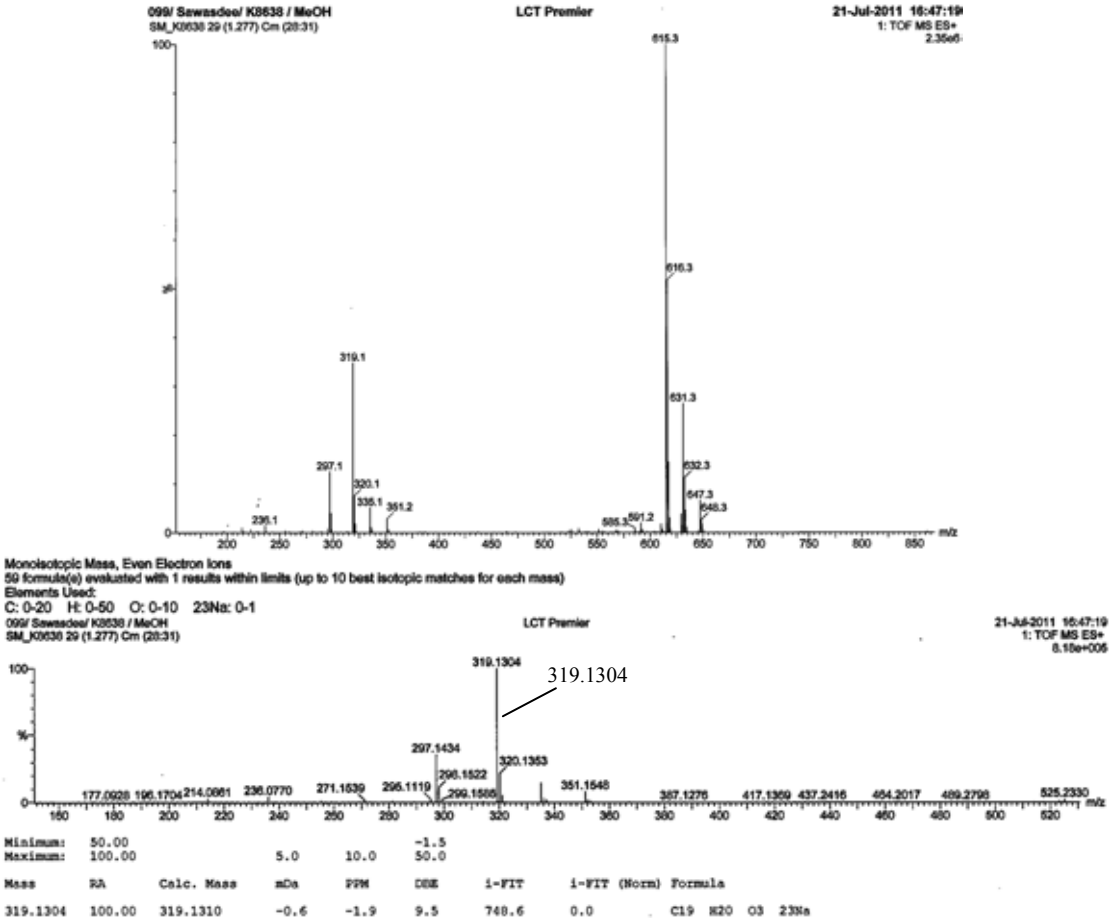

Figure 116 HRESI mass spectrum of compound LMM5 [**100**]

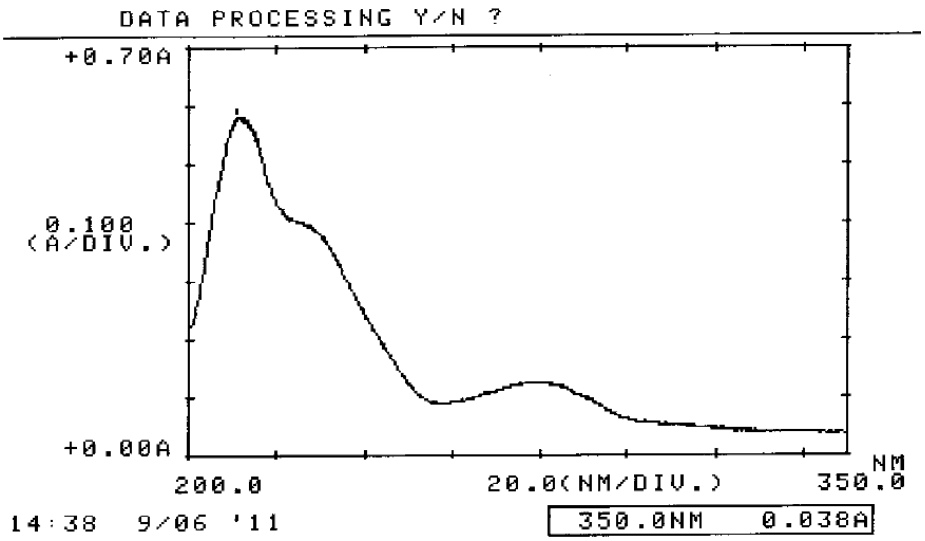

Figure 117 UV spectrum of compound LMM5 [**100**] (MeOH)

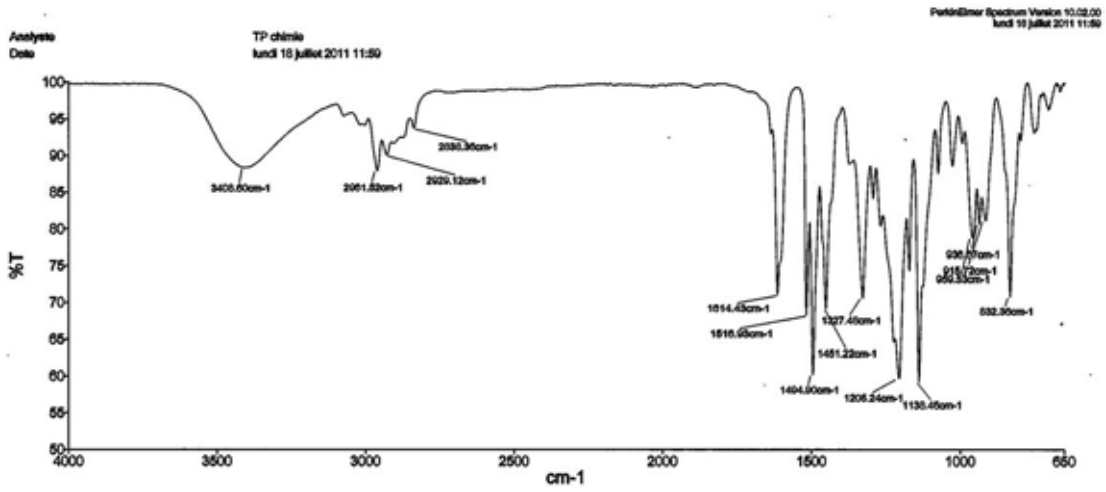

Figure 118 IR spectrum of compound LMM5 [**100**] (film)

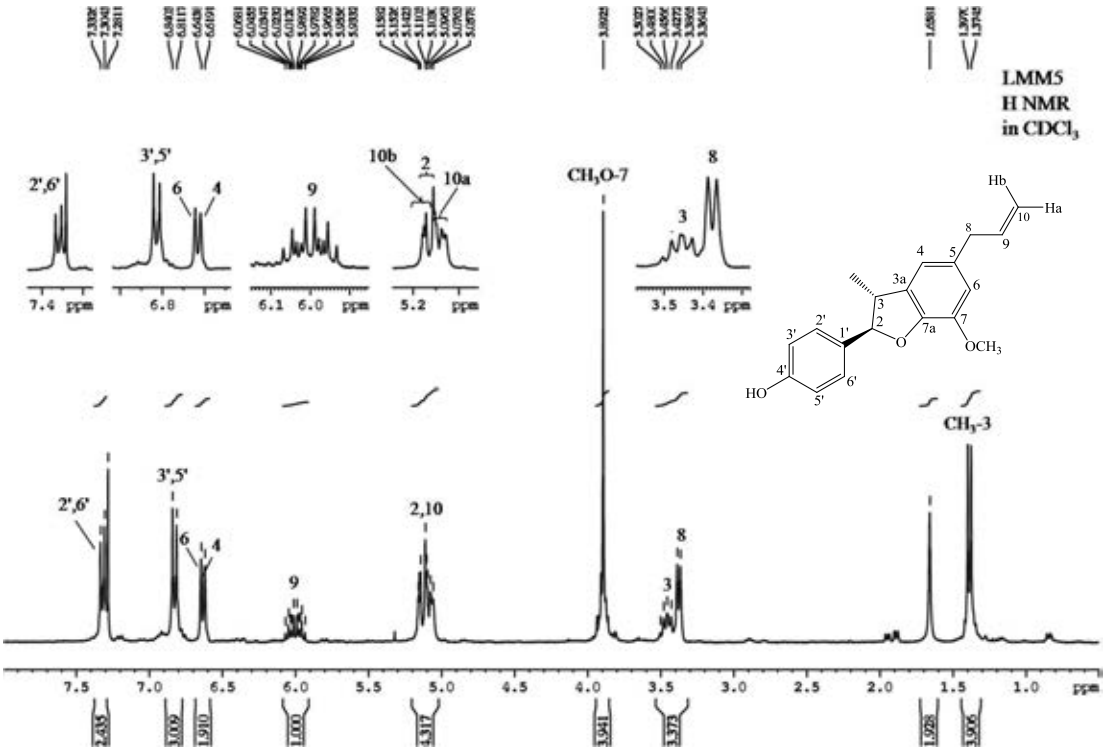

Figure 119 ^{1}H-NMR spectrum of compound LMM5 [**100**] ($CDCl_3$)

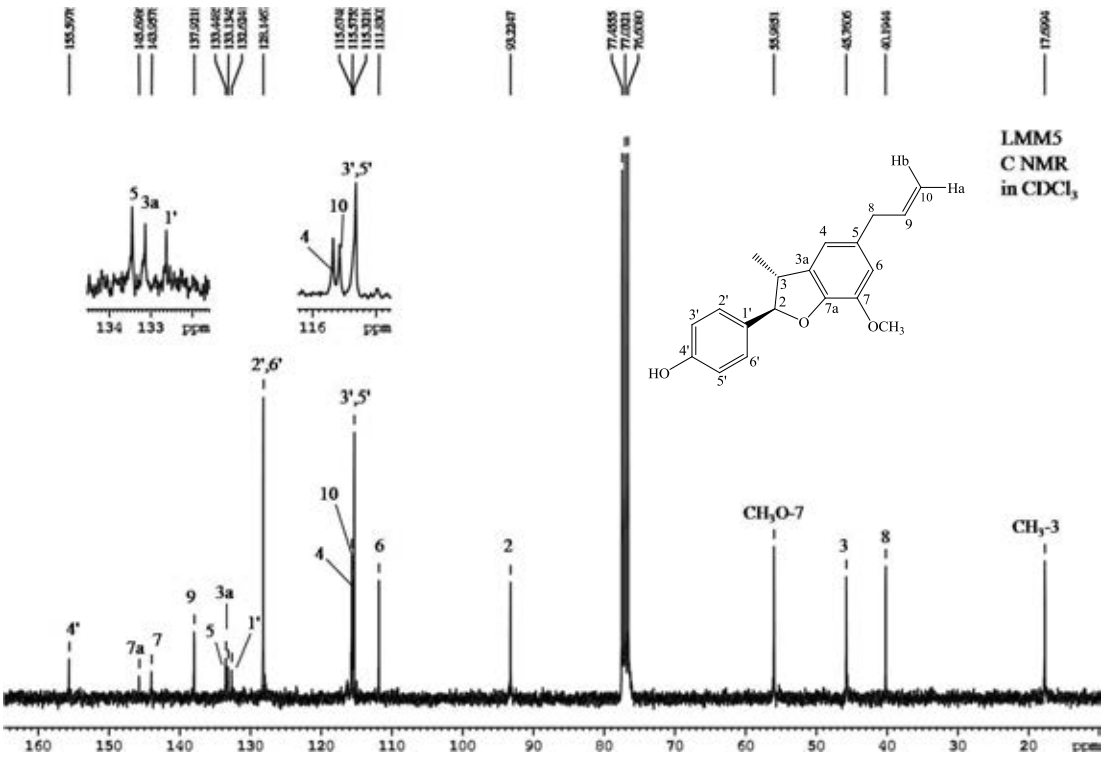

Figure 120 ^{13}C-NMR spectrum of compound LMM5 [**100**] ($CDCl_3$)

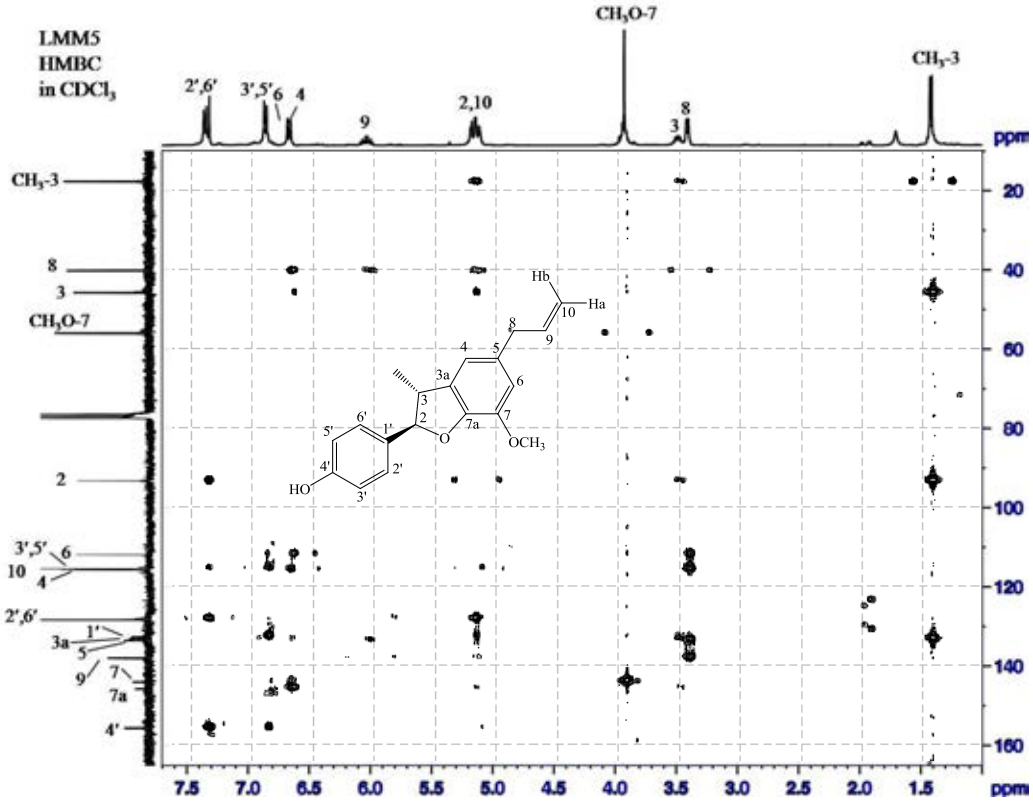

Figure 121 HMBC spectrum of compound LMM5 [**100**] ($CDCl_3$)

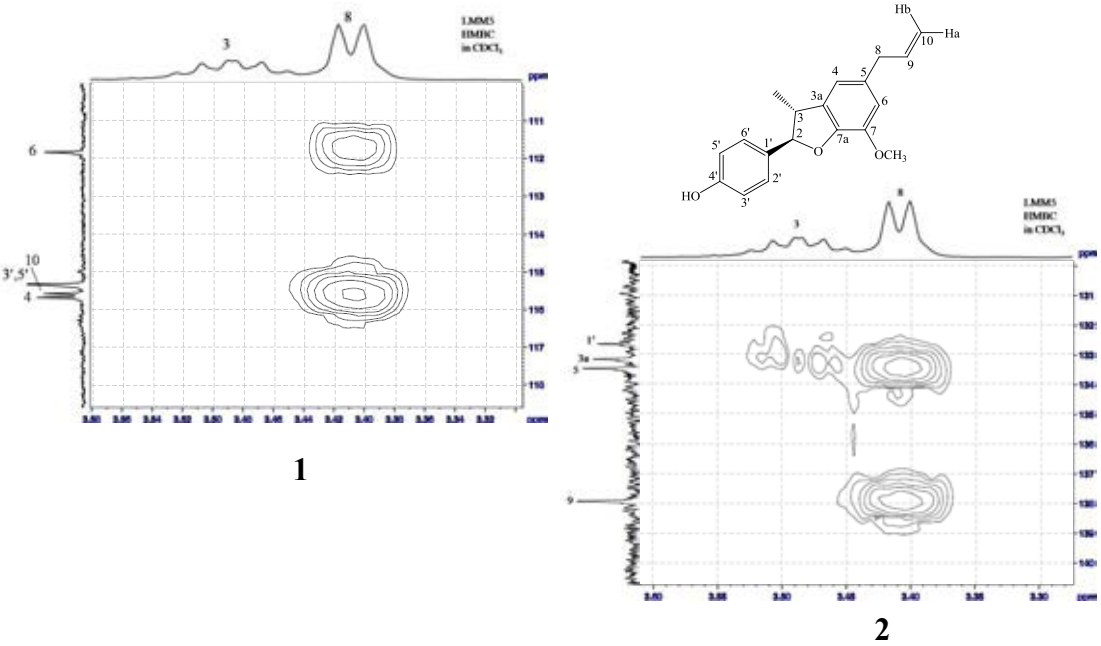

1

2

Figure 121a HMBC spectrum of compound LMM5 [**100**] ($CDCl_3$)
[δ_H 3.58-3.31 ppm, δ_C 118.6-110.0 ppm (1)] and
[δ_H 3.61-3.27 ppm, δ_C 140.7-129.0 ppm (2)]

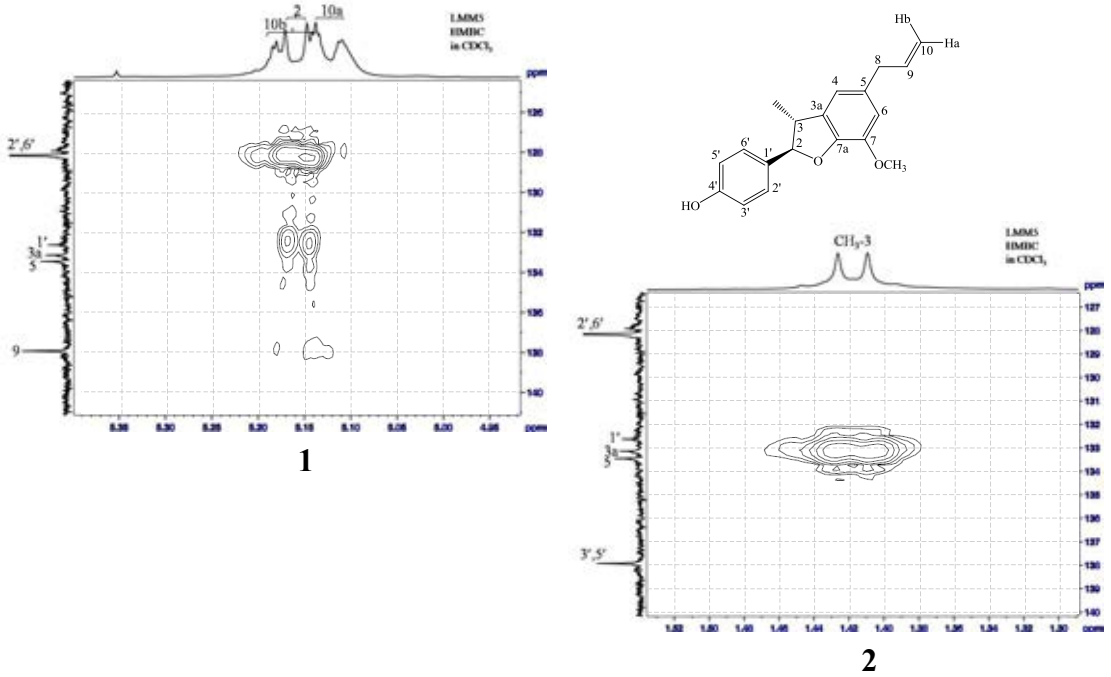

1 **2**

Figure 121b HMBC spectrum of compound LMM5 [**100**] ($CDCl_3$)
[δ_H 5.40-4.92 ppm, δ_C 141-124 ppm (1)] and
[δ_H 1.54-1.29 ppm, δ_C 141.0-126.5 ppm (2)]

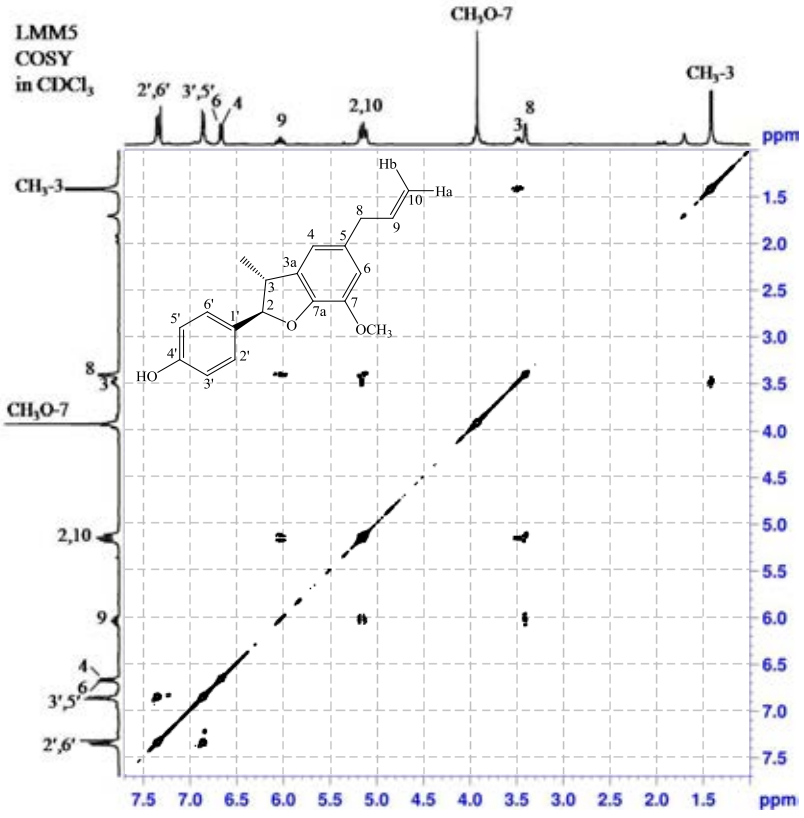

Figure 122 ^1H-^1H COSY spectrum of compound LMM5 [**100**] ($CDCl_3$)

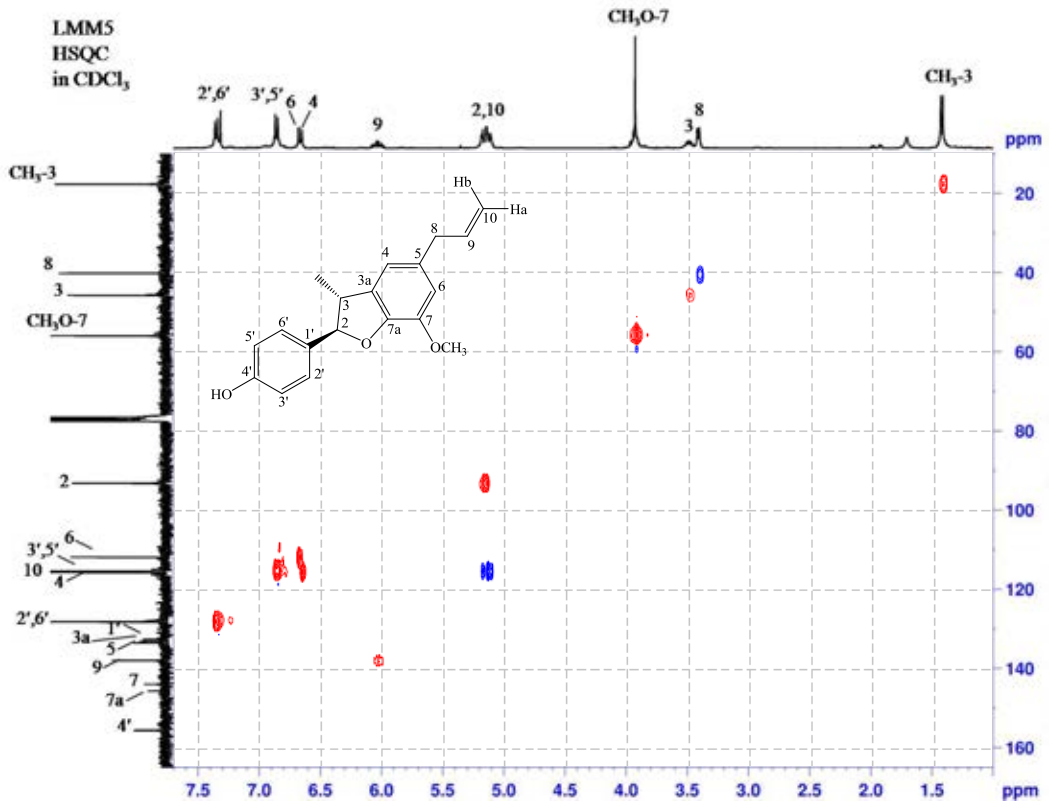

Figure 123 HSQC spectrum of compound LMM5 [**100**] ($CDCl_3$)

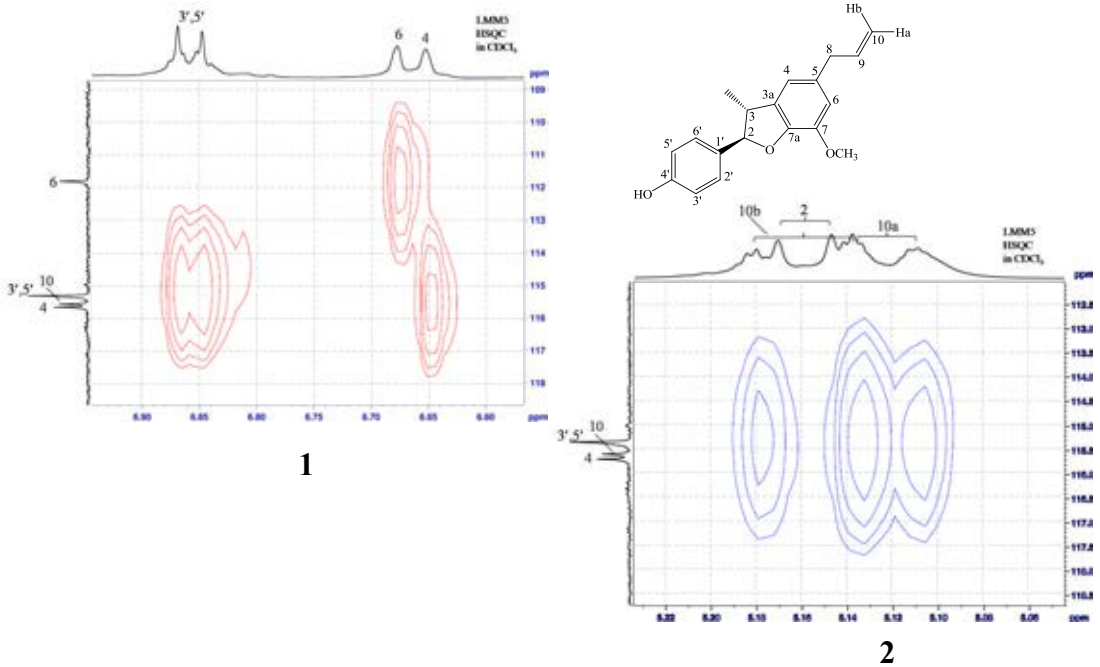

Figure 123a HSQC spectrum of compound LMM5 [**100**] ($CDCl_3$)
[δ_H 6.94-6.57 ppm, δ_C 118.7-108.8 ppm (1)] and
[δ_H 5.24-5.05 ppm, δ_C 118.7-112.0 ppm (2)]

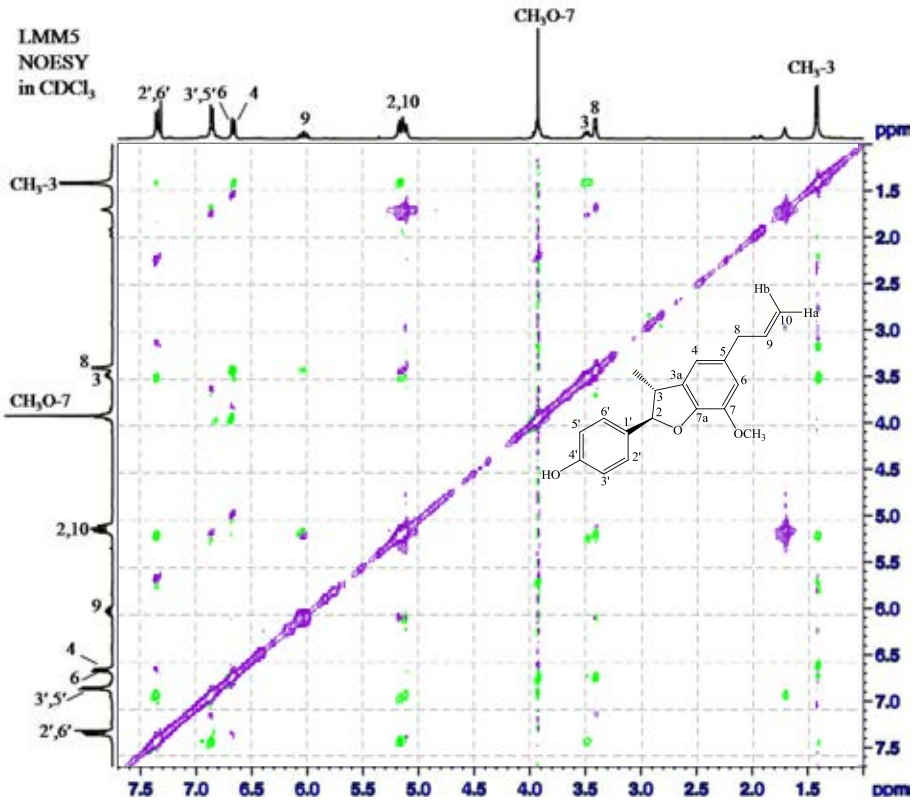

Figure 124 NOESY spectrum of compound LMM5 [**100**] ($CDCl_3$)

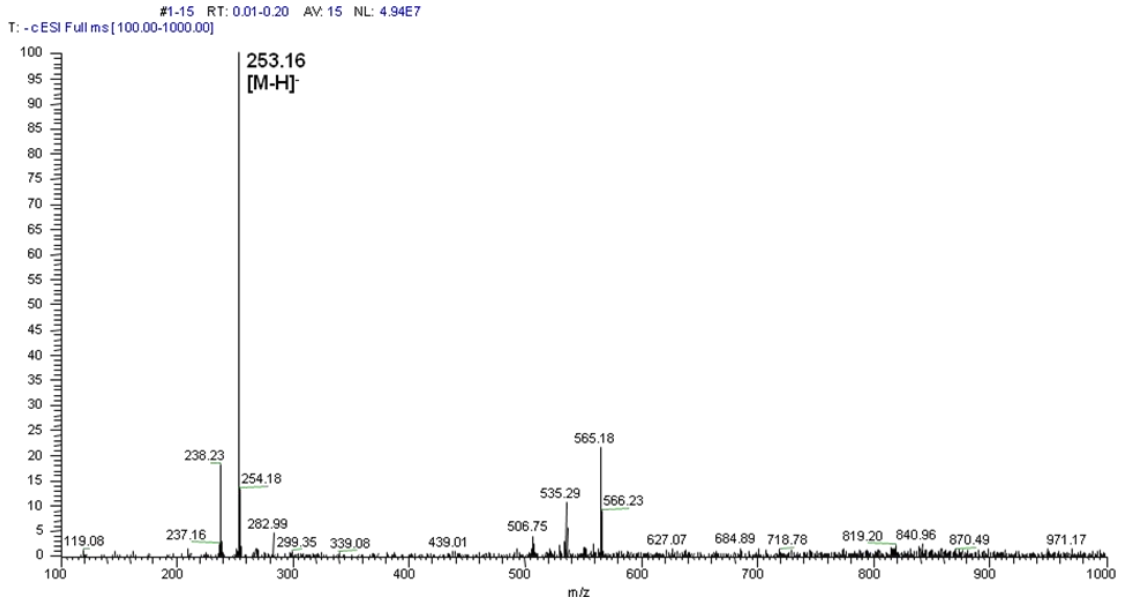

Figure 125 ESI Mass spectrum of compound LMM6 [**101**]

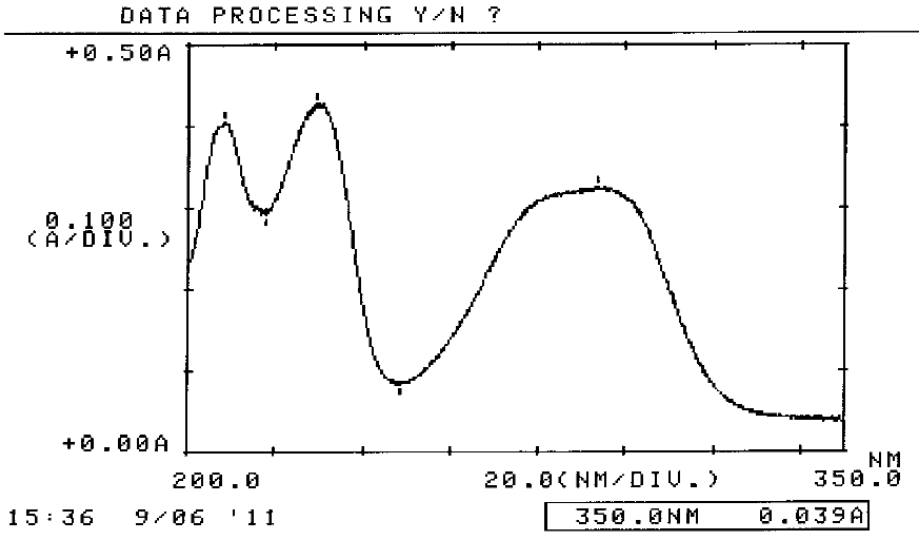

Figure 126 UV spectrum of compound LMM6 [**101**] (MeOH)

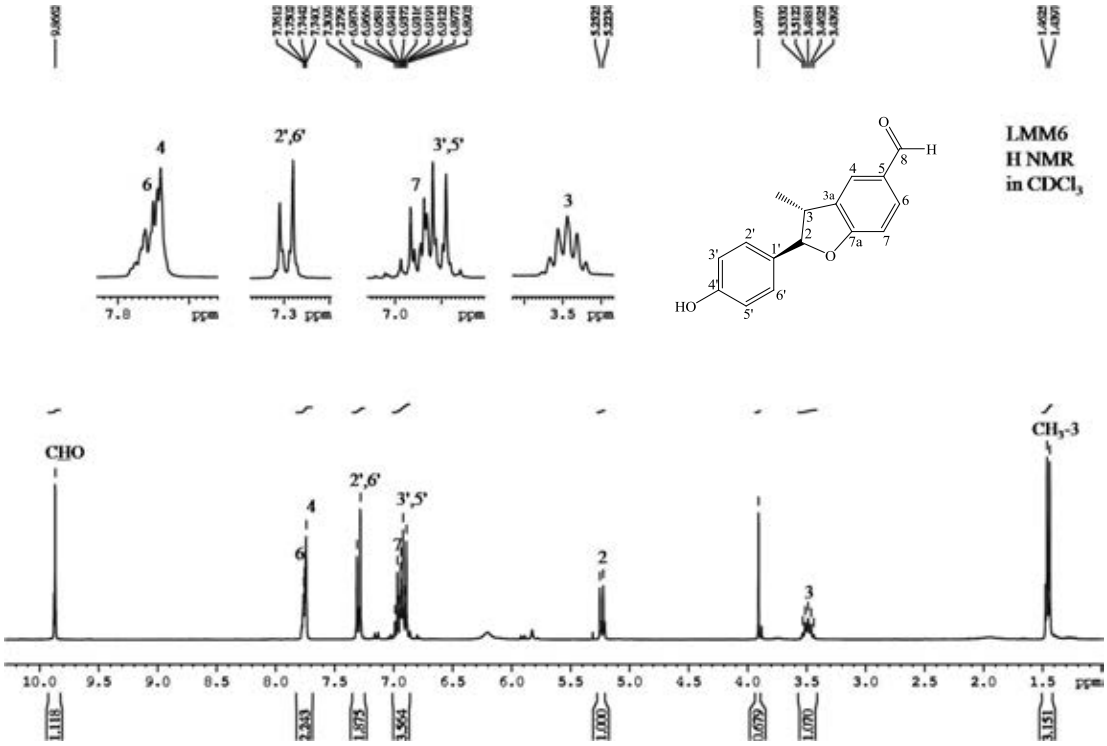

Figure 127 ^{1}H-NMR spectrum of compound LMM6 [**101**] ($CDCl_3$)

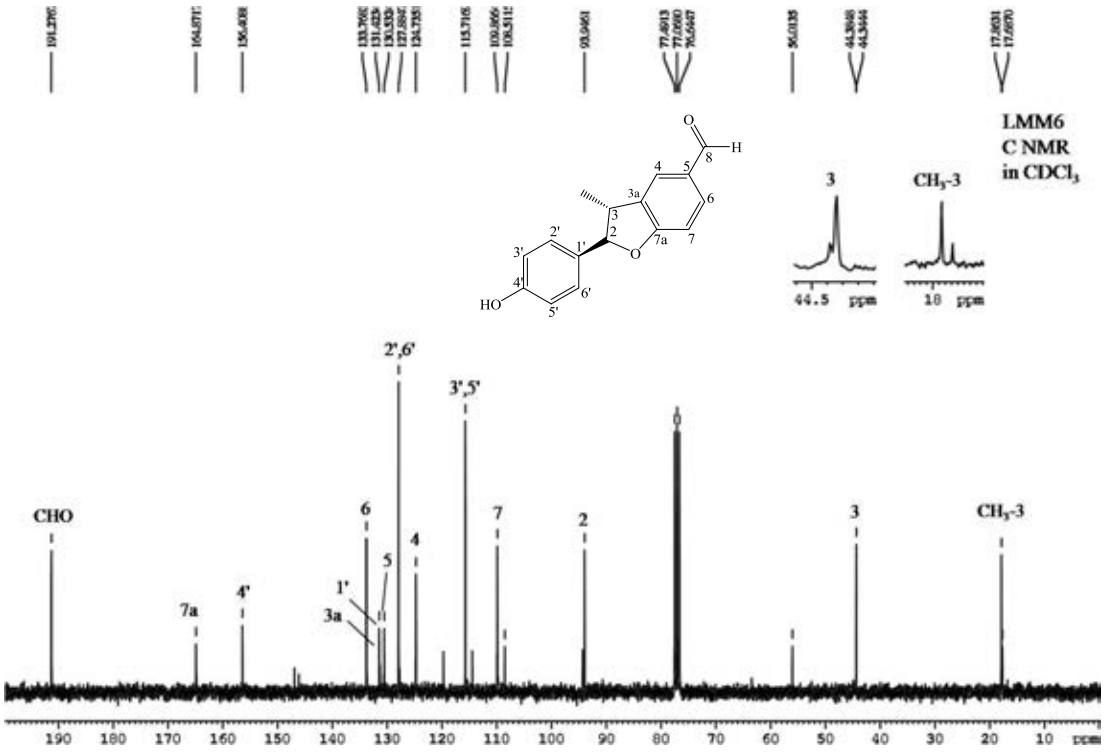

Figure 128 ^{13}C-NMR spectrum of compound LMM6 [**101**] ($CDCl_3$)

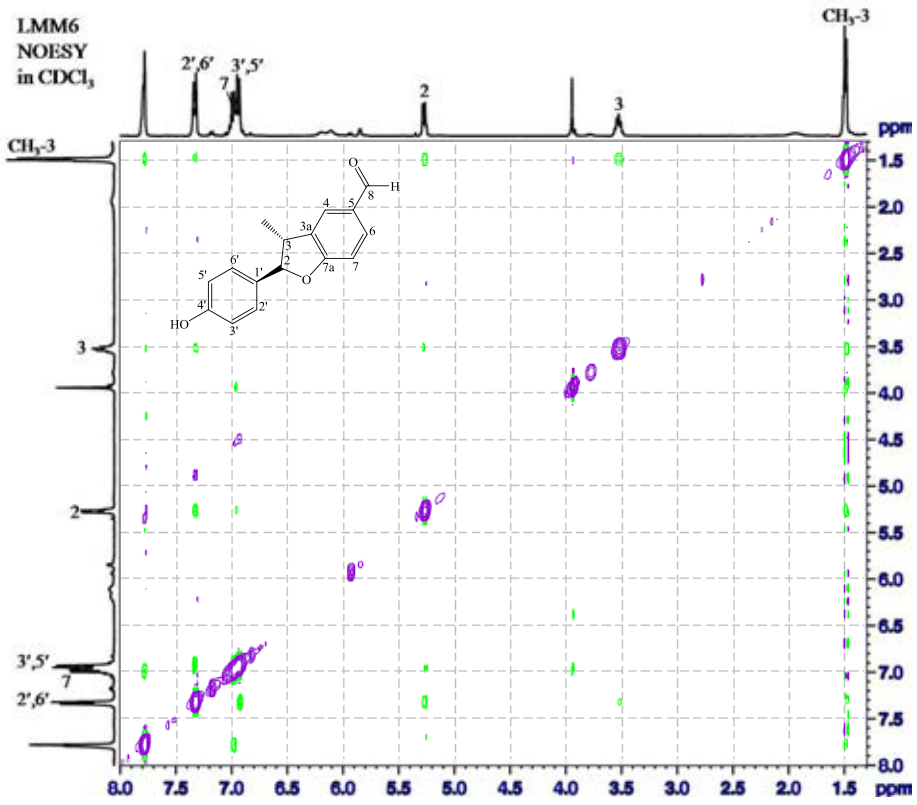

Figure 129 NOESY spectrum of compound LMM6 [**101**] ($CDCl_3$)

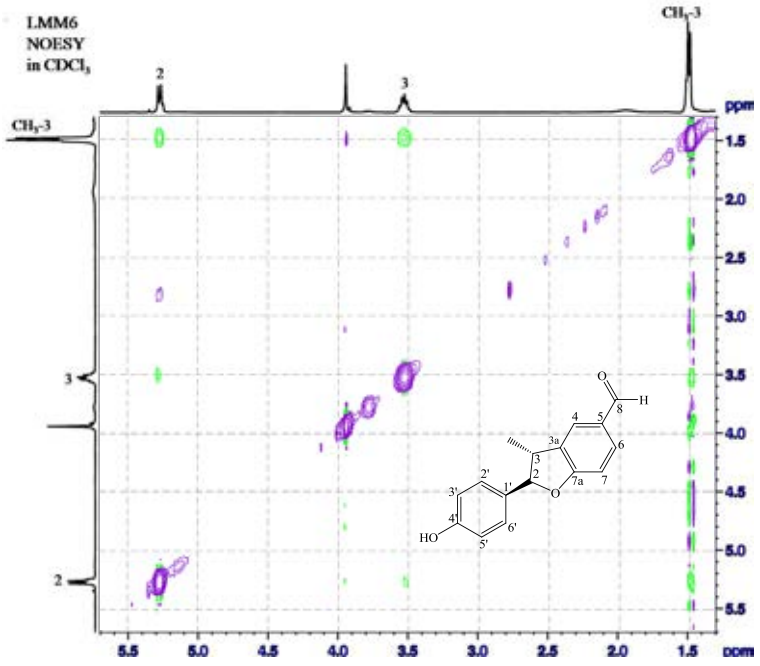

Figure 129a NOESY spectrum of compound LMM6 [**101**] ($CDCl_3$) [δ_H 5.70-1.30 ppm]

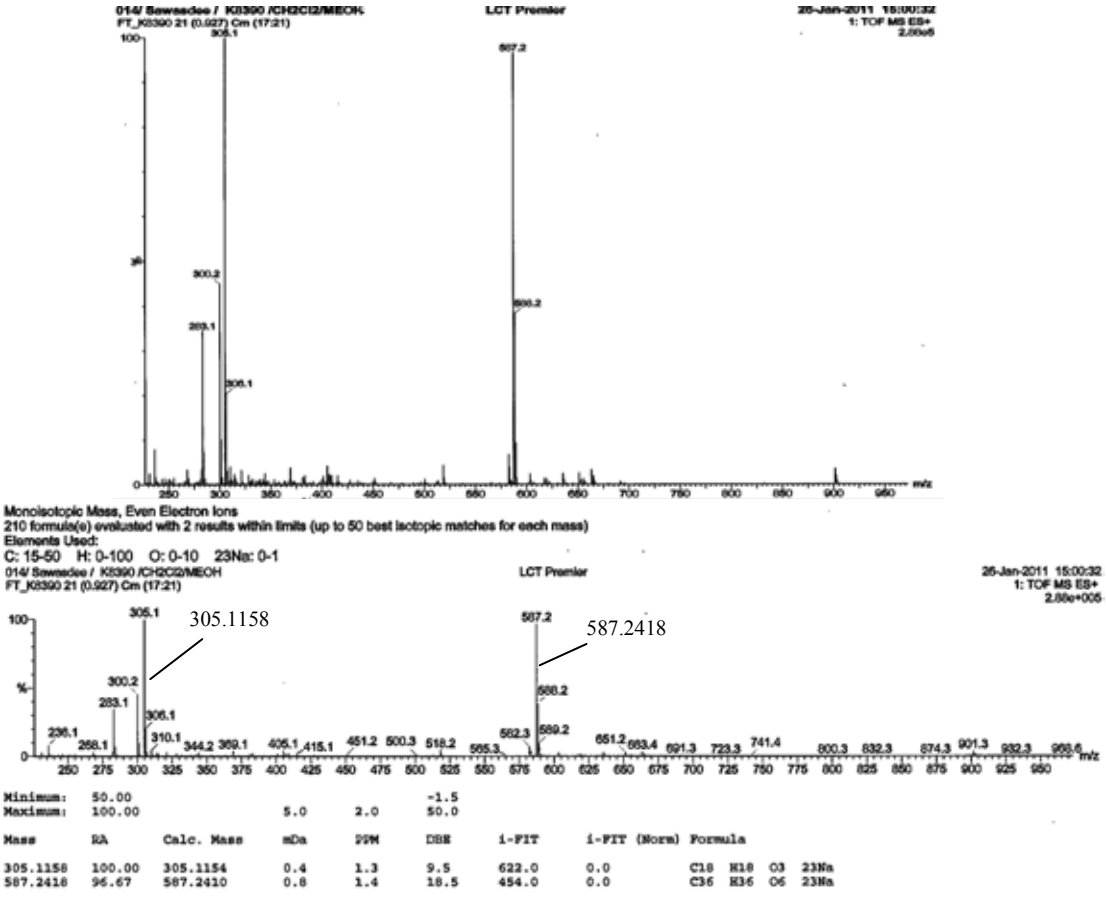

Figure 130 HRESI mass spectrum of compound LMM7 [**102**]

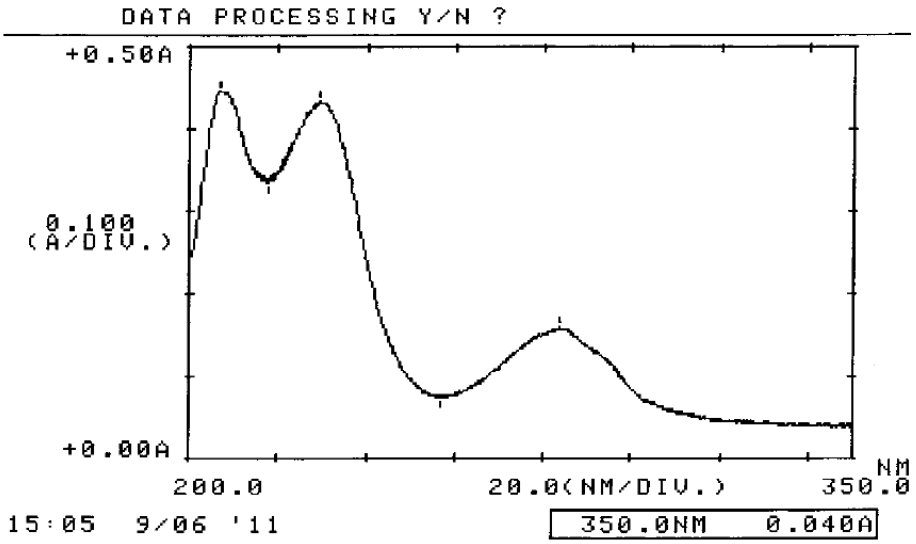

Figure 131 UV spectrum of compound LMM7 [**102**] (MeOH)

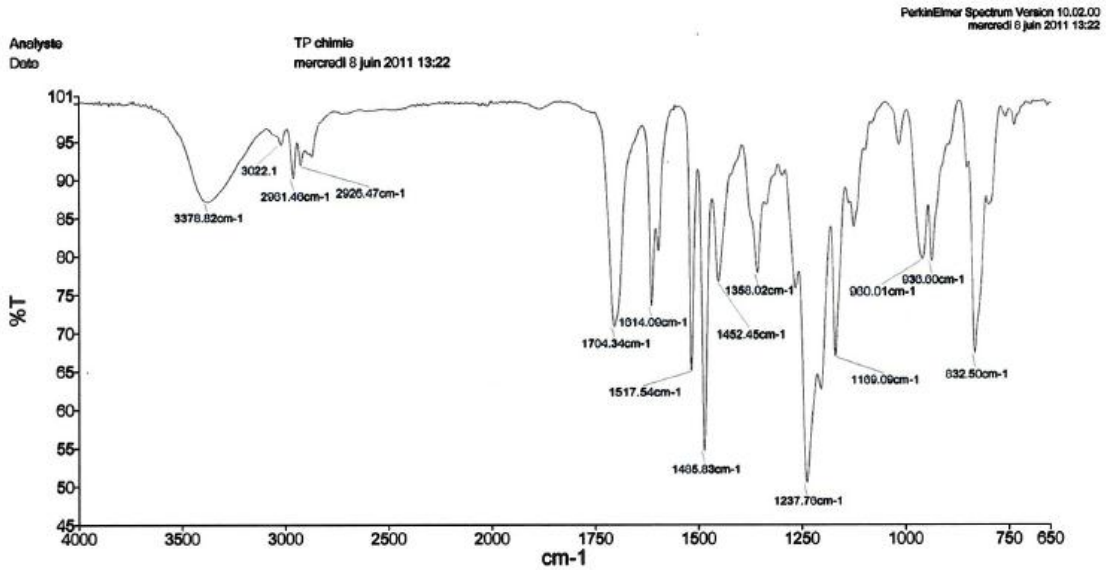

Figure 132 IR spectrum of compound LMM7 [**102**] (film)

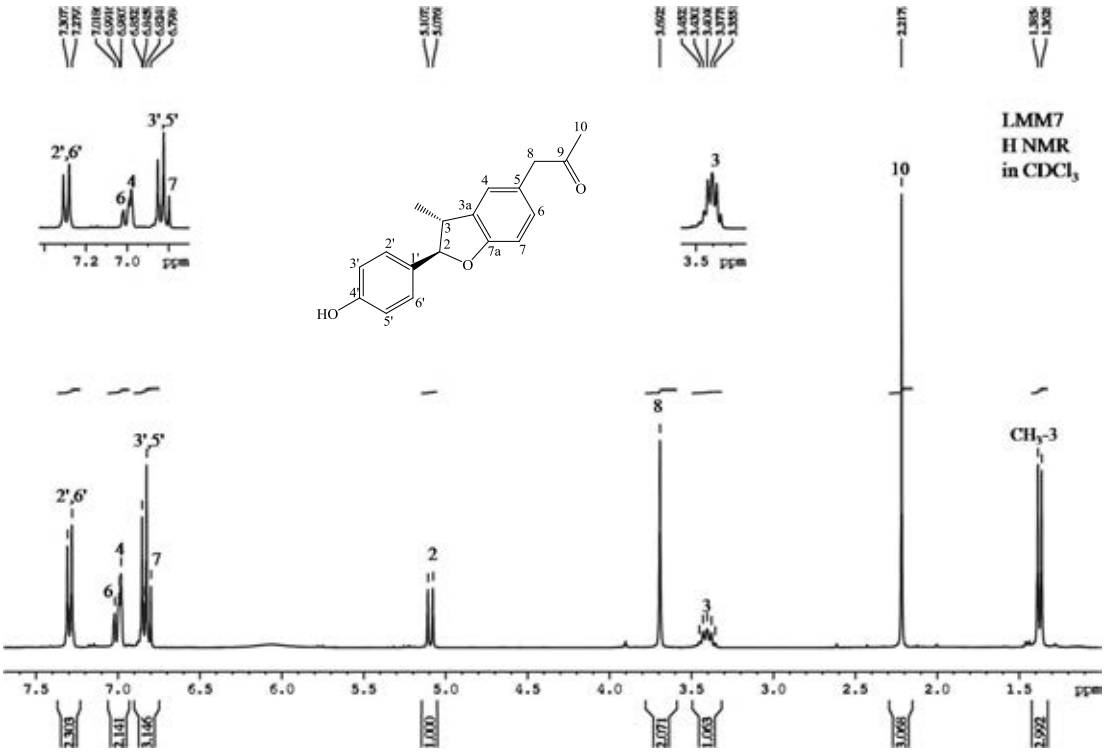

Figure 133 ^{1}H-NMR spectrum of compound LMM7 [**102**] ($CDCl_3$)

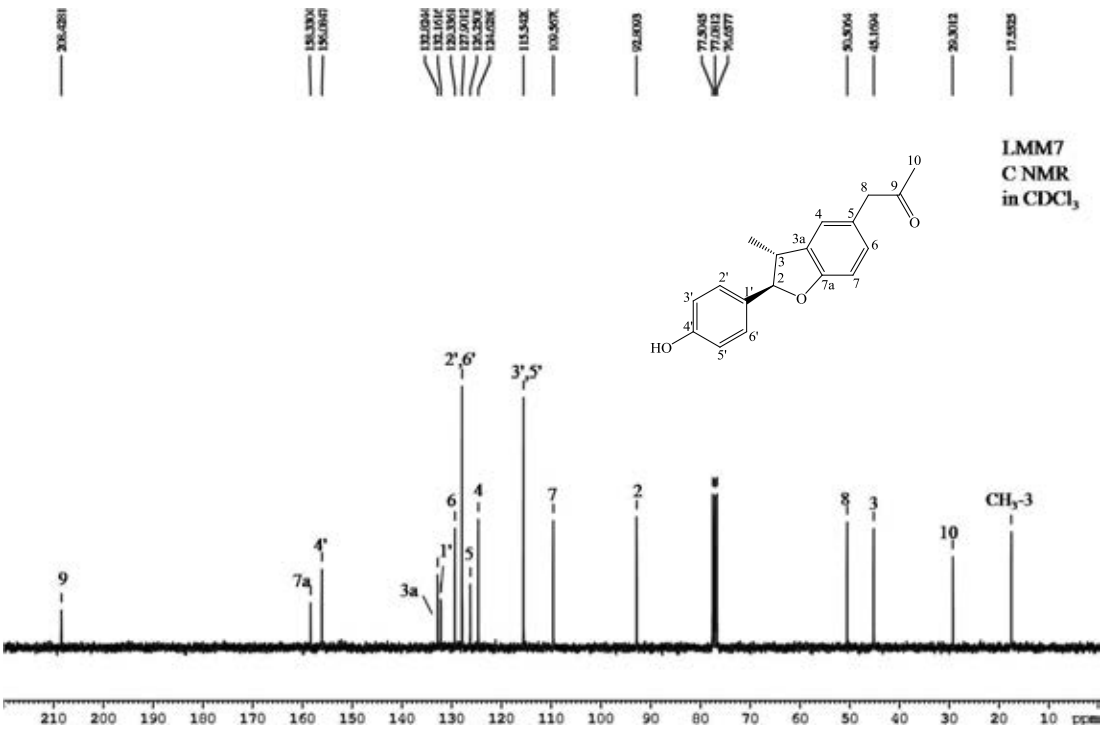

Figure 134 ^{13}C-NMR spectrum of compound LMM7 [**102**] ($CDCl_3$)

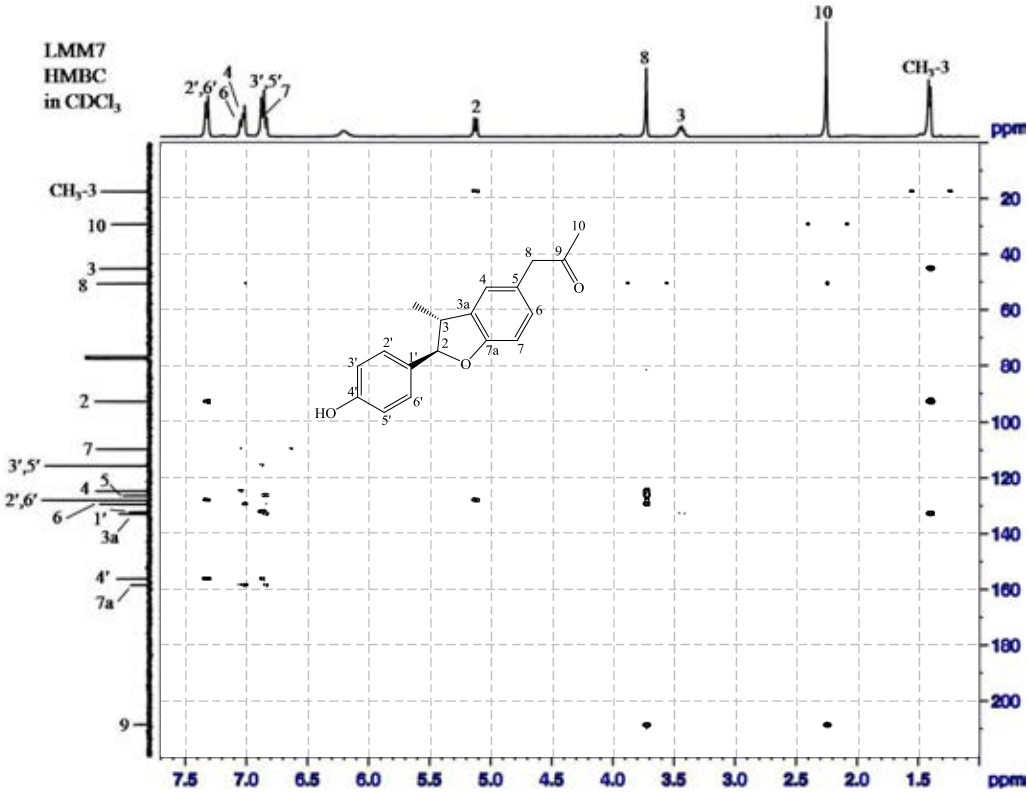

Figure 135 HMBC spectrum of compound LMM7 [**102**] ($CDCl_3$)

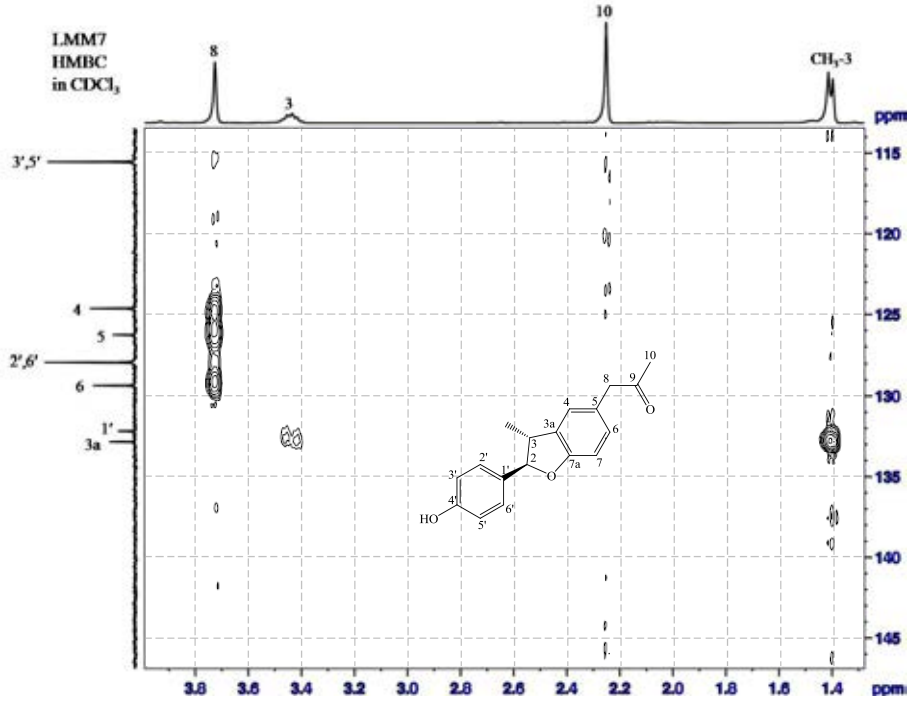

Figure 135a HMBC spectrum of compound LMM7 [**102**] ($CDCl_3$)
[δ_H 3.90-1.30 ppm, δ_C 147.0-113.0 ppm]

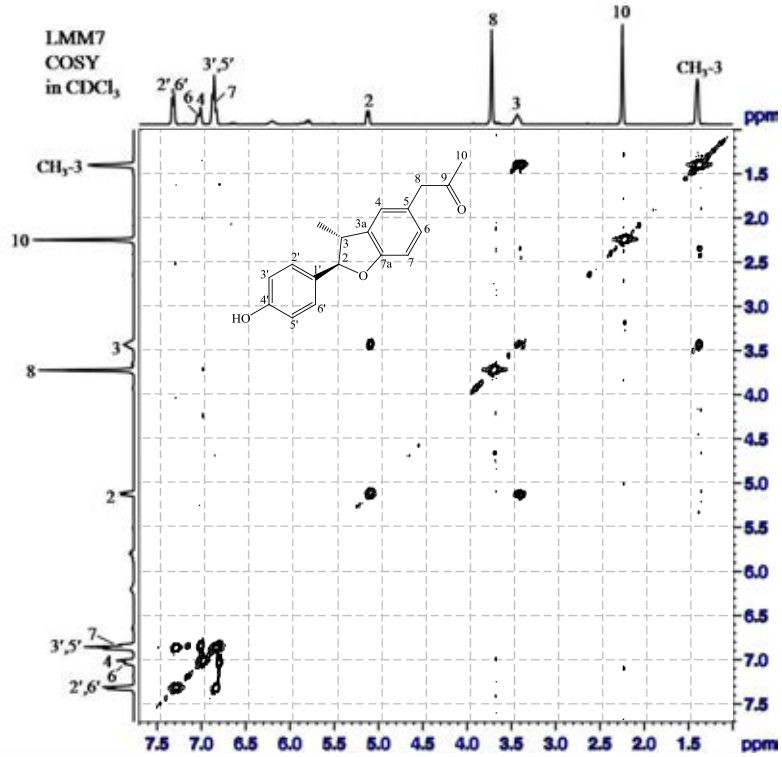

Figure 136 ^{1}H-^{1}H COSY spectrum of compound LMM7 [**102**] ($CDCl_3$)

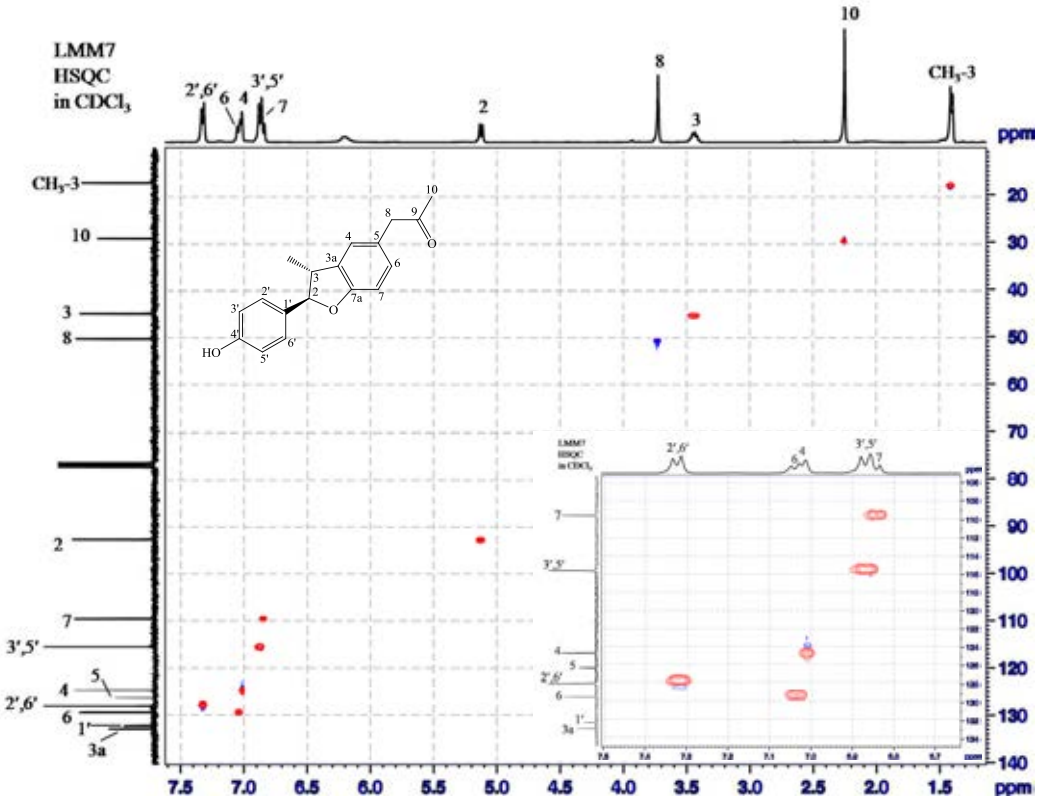

Figure 137 HSQC spectrum of compound LMM7 [**102**] ($CDCl_3$)

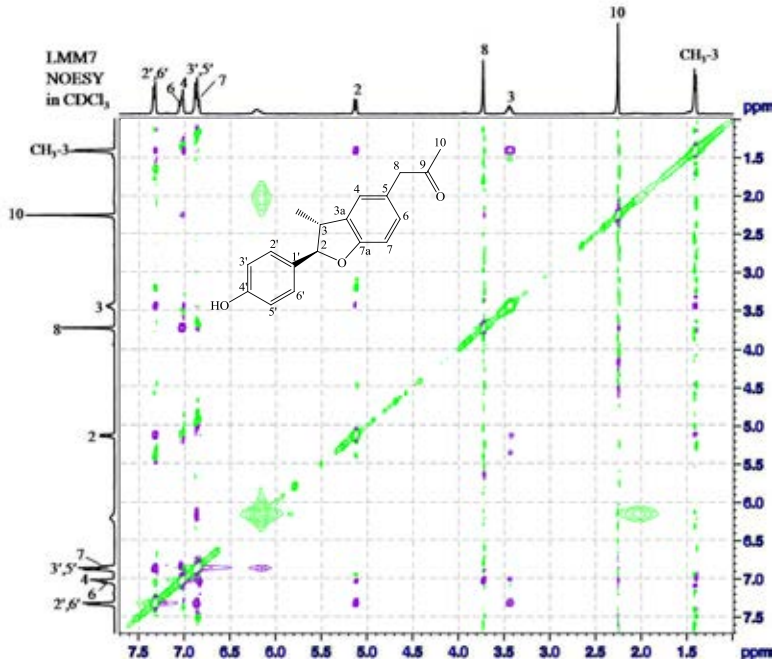

Figure 138 NOESY spectrum of compound LMM7 [**102**] ($CDCl_3$)

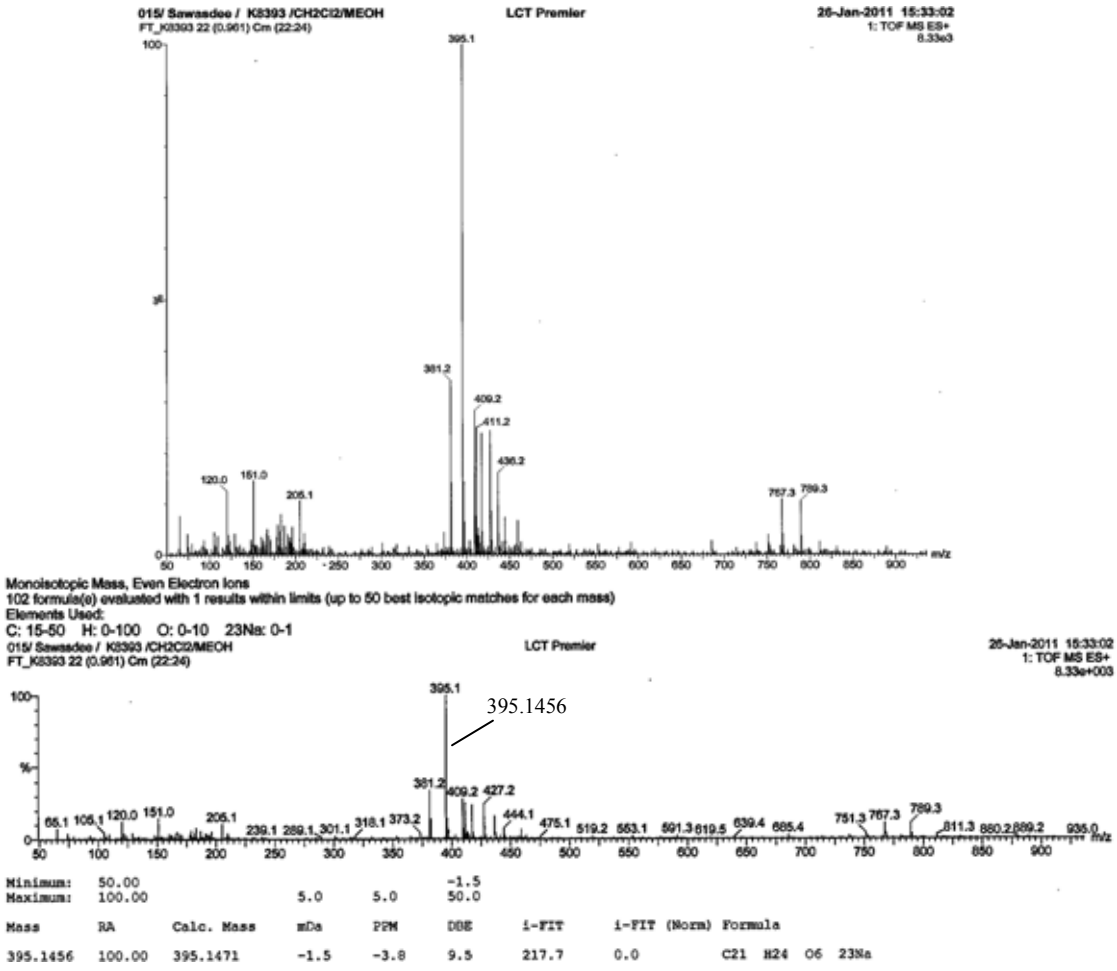

Figure 139 HRESI mass spectrum of compound LMF1 [**103**]

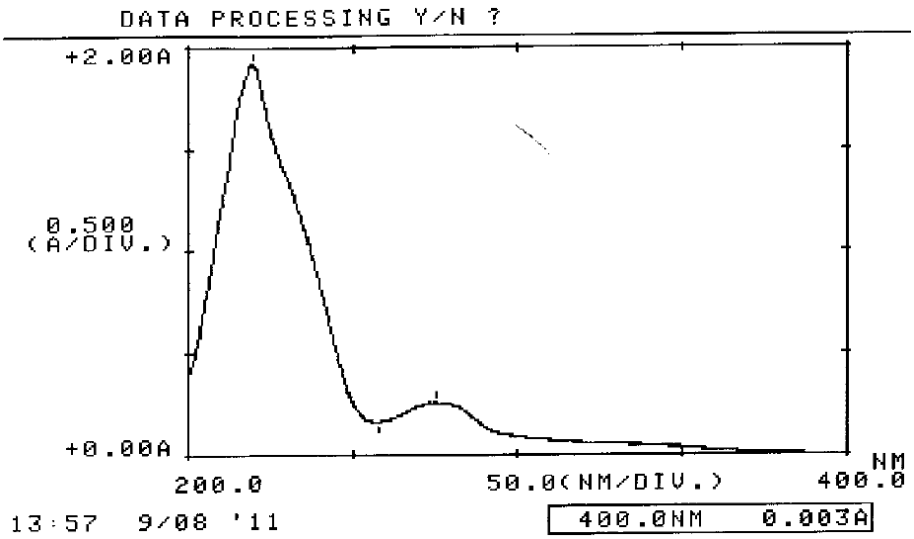

Figure 140 UV spectrum of compound LMF1 [**103**] (MeOH)

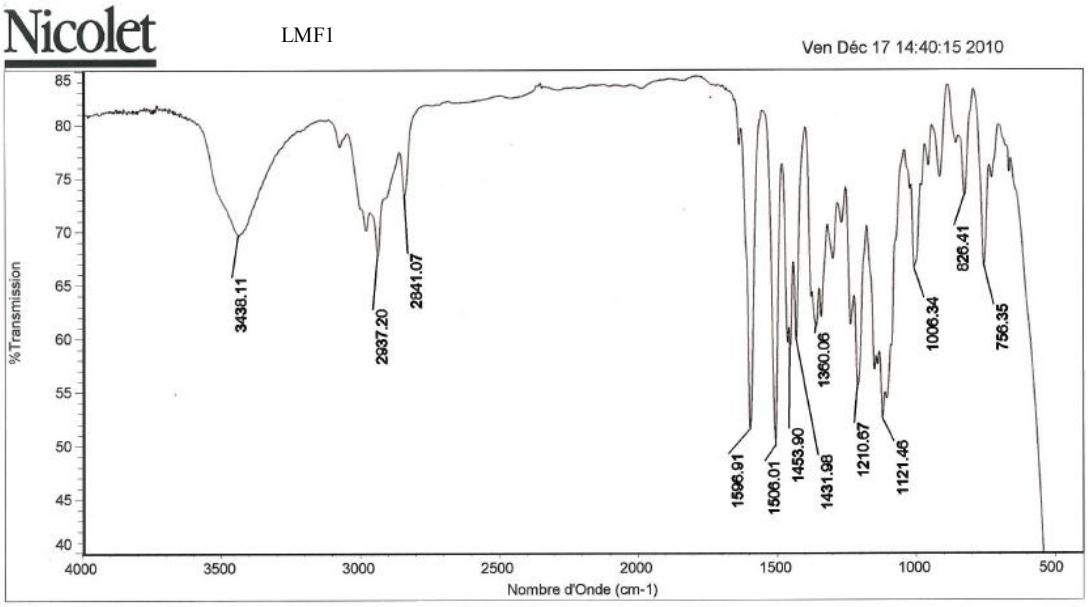

Figure 141 IR spectrum of compound LMF1 [**103**] (film)

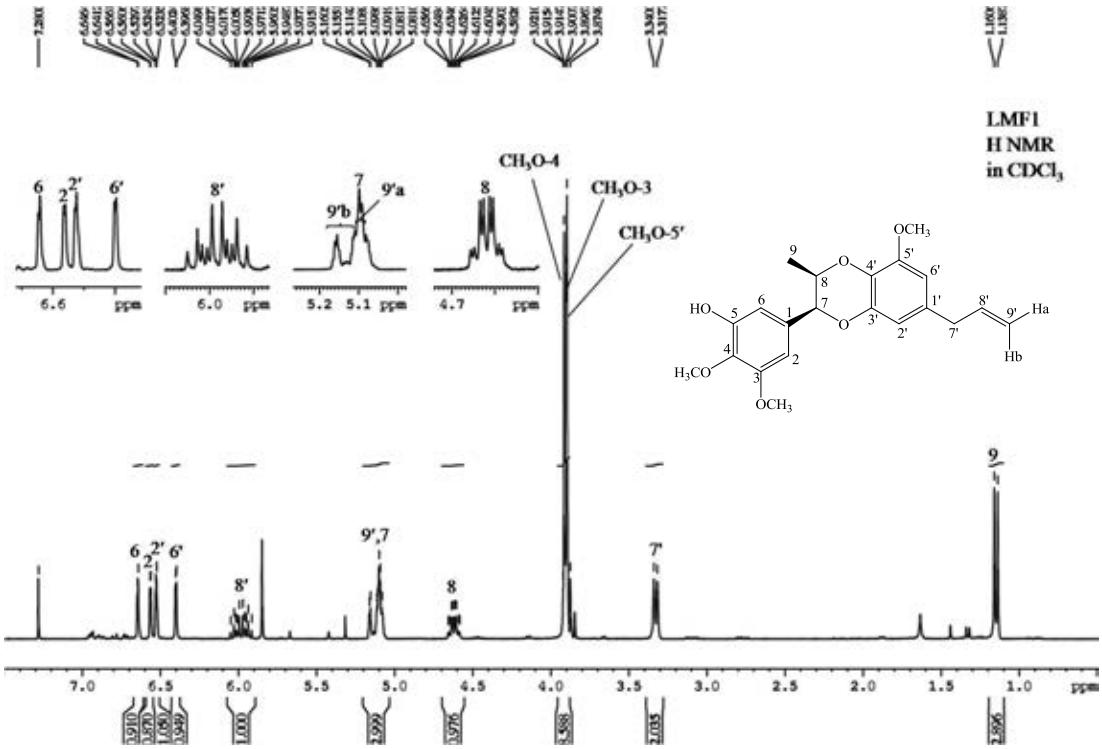

Figure 142 ^{1}H-NMR spectrum of compound LMF1 [**103**] ($CDCl_3$)

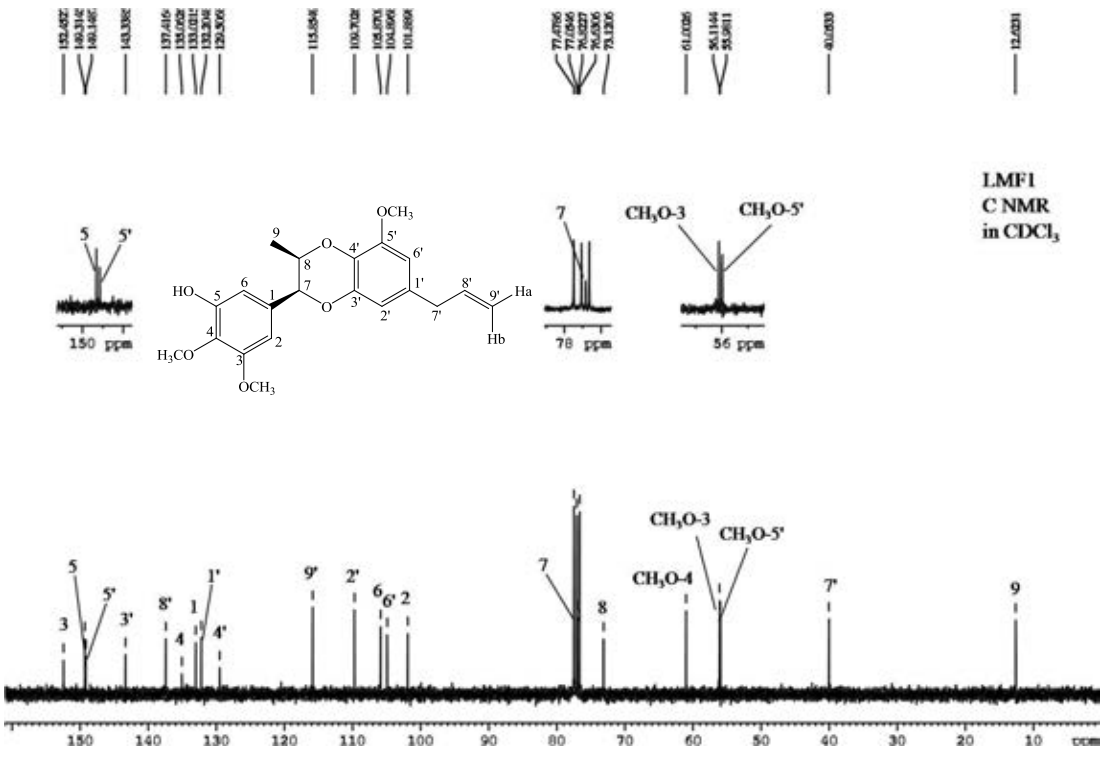

Figure 143 ^{13}C-NMR spectrum of compound LMF1 [**103**] ($CDCl_3$)

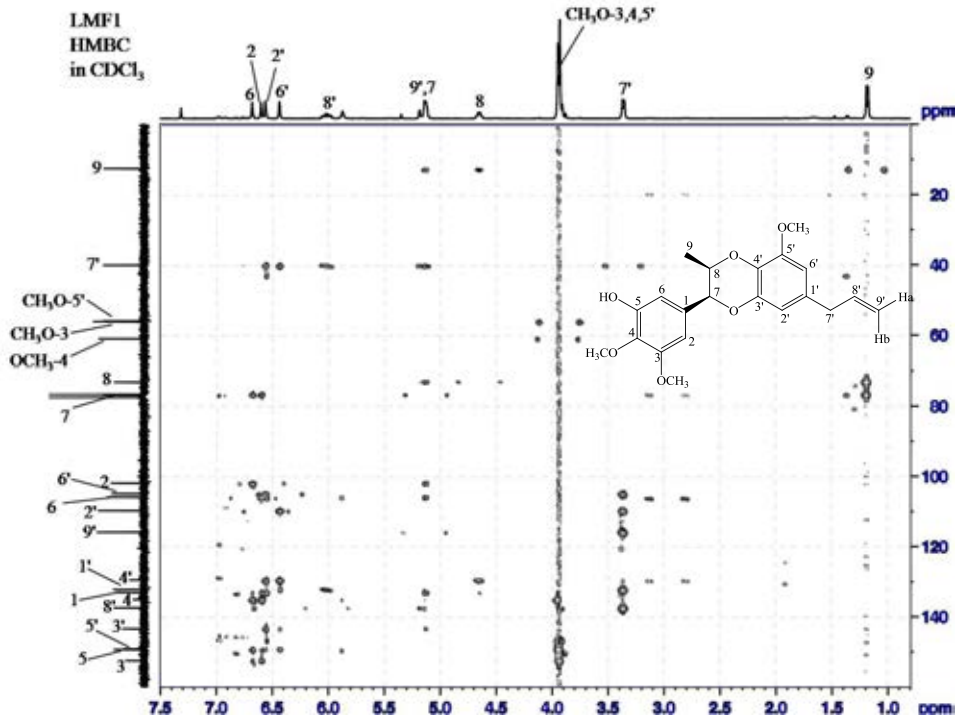

Figure 144 HMBC spectrum of compound LMF1 [**103**] ($CDCl_3$)

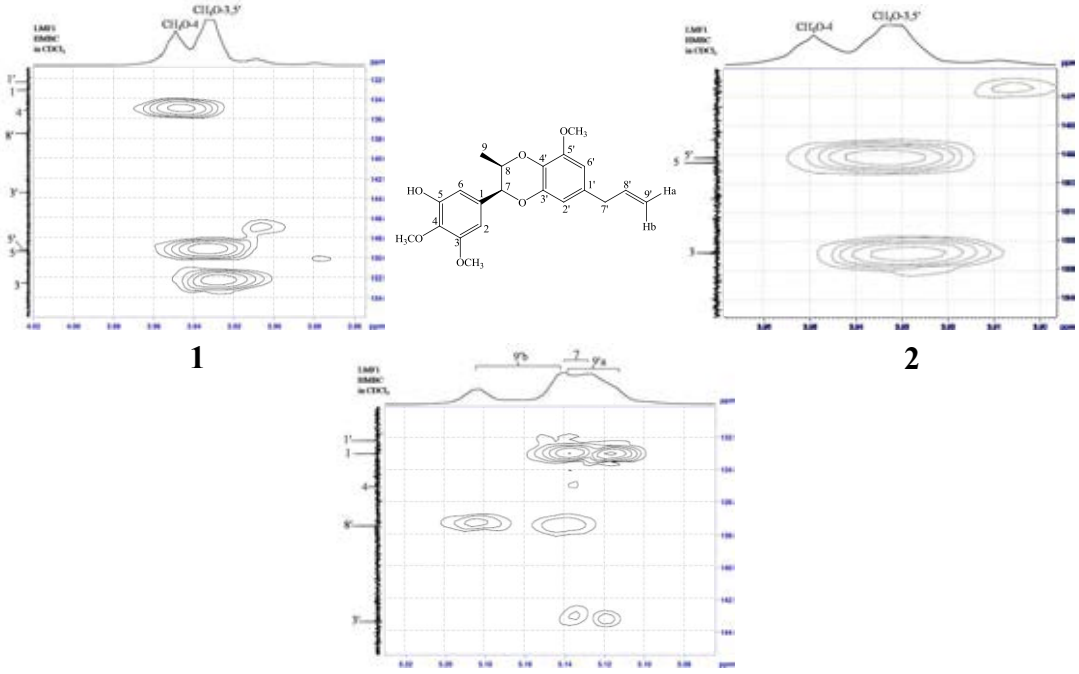

1 **2**

3

Figure 144a HMBC spectrum of compound LMF1 [**103**] ($CDCl_3$)
[δ_H 4.02-3.85 ppm, δ_C 156.0-131.0 ppm (1)],
[δ_H 3.97-3.90 ppm, δ_C 154.7-146.0 ppm (2)] and
[δ_H 5.23-5.06 ppm, δ_C 145.5-130.0 ppm (3)]

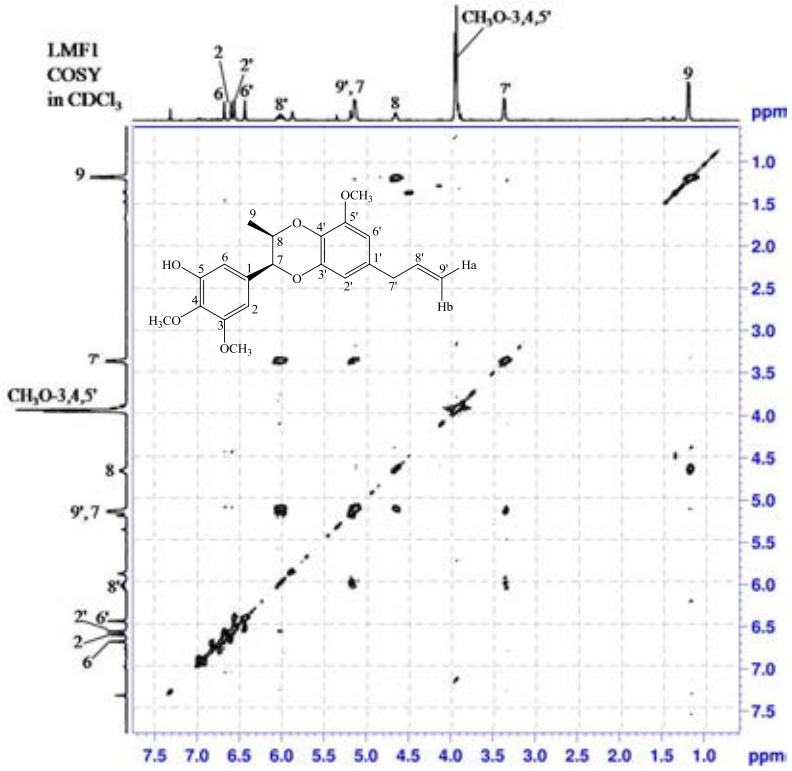

Figure 145 ^{1}H-^{1}H COSY spectrum of compound LMF1 [**103**] ($CDCl_3$)

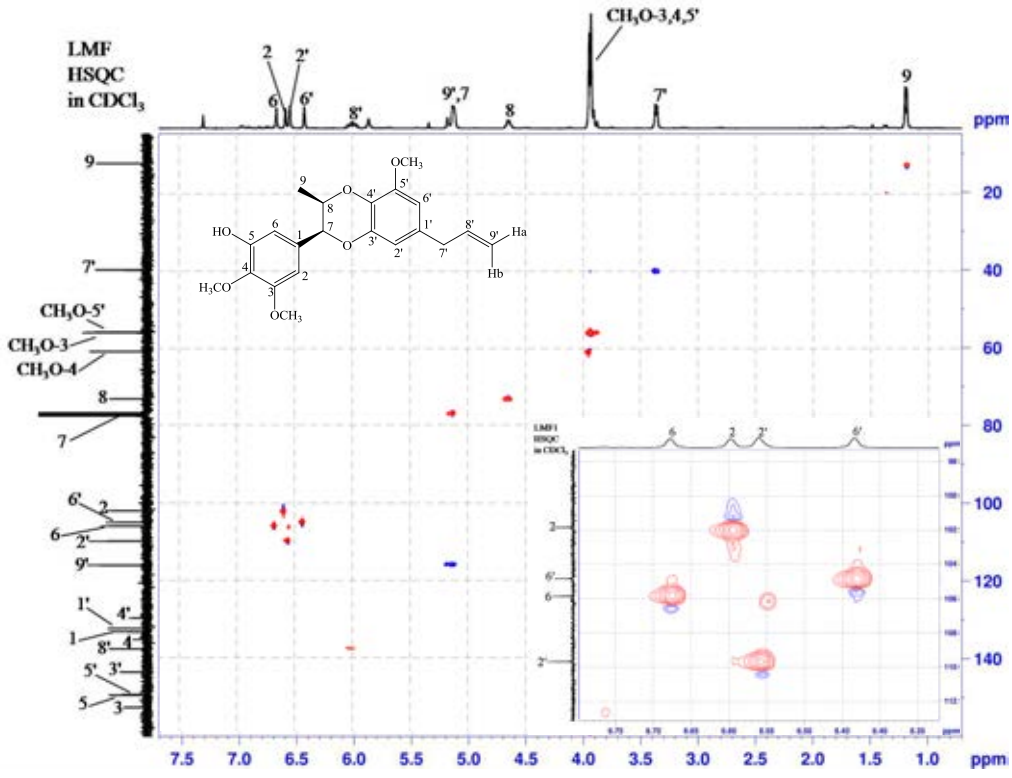

Figure 146 HSQC spectrum of compound LMF1 [**103**] ($CDCl_3$)

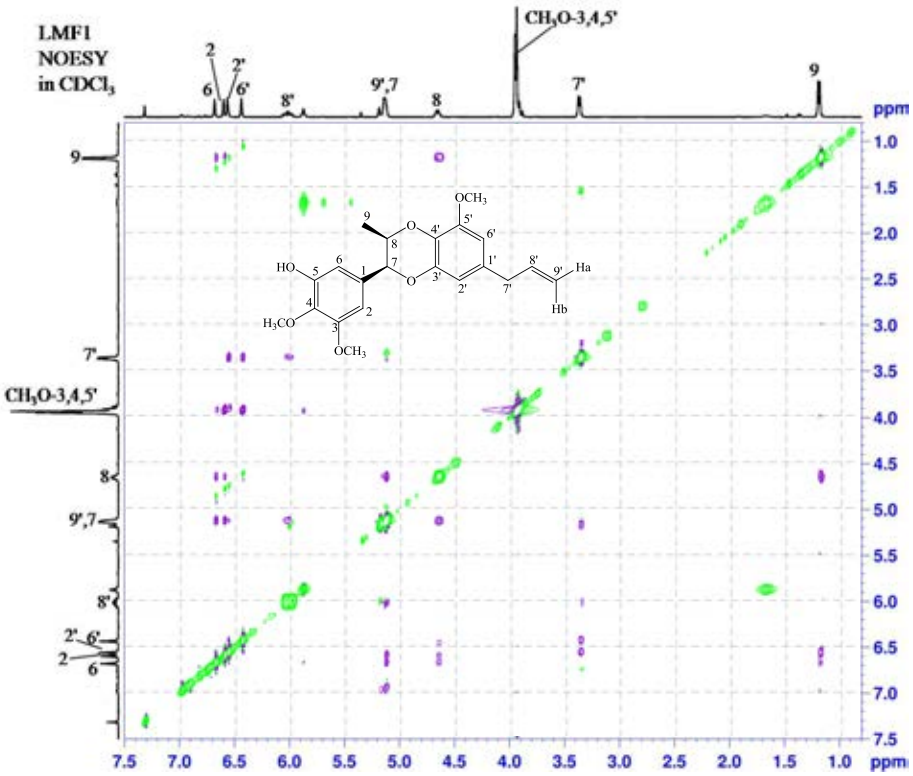

Figure 147 NOESY spectrum of compound LMF1 [**103**] ($CDCl_3$)

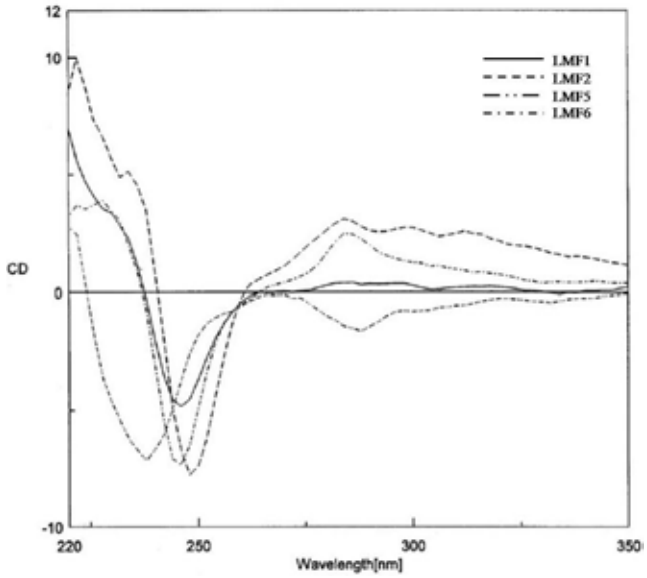

Figure 148 CD spectra (MeOH) of compounds LMF1 [**103**], LMF2 [**104**], LMF5 [**107**] and LMF6 [**108**]

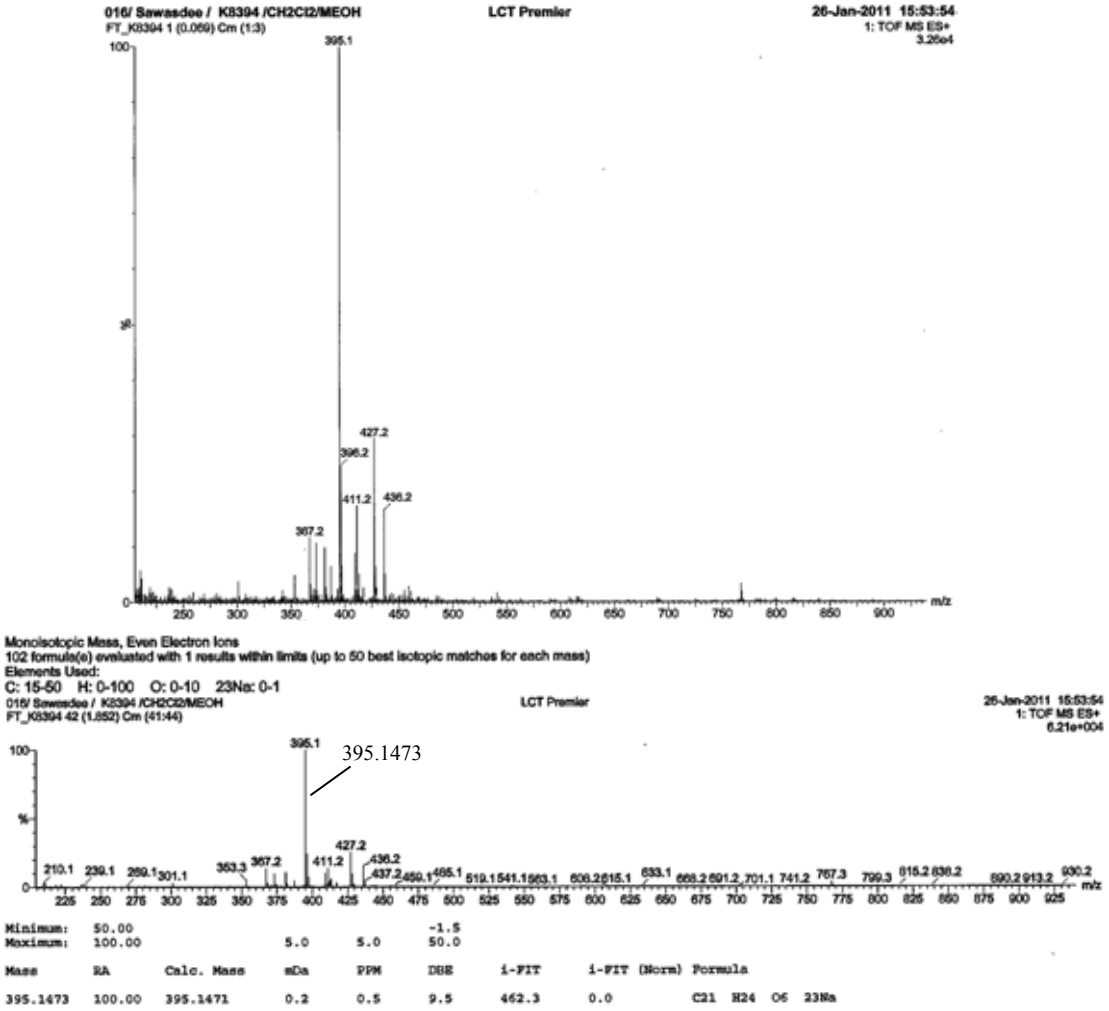

Figure 149 HRESI mass spectrum of compound LMF2 [**104**]

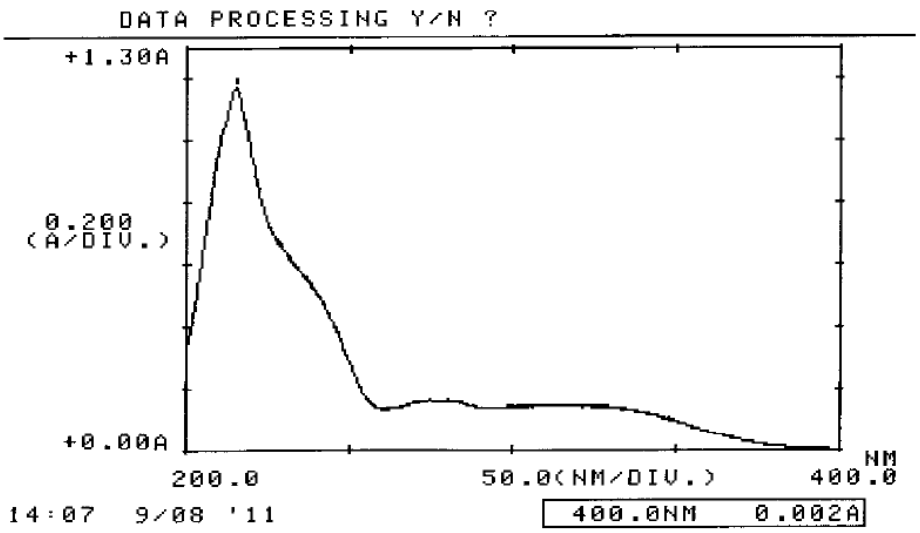

Figure 150 UV spectrum of compound LMF2 [**104**] (MeOH)

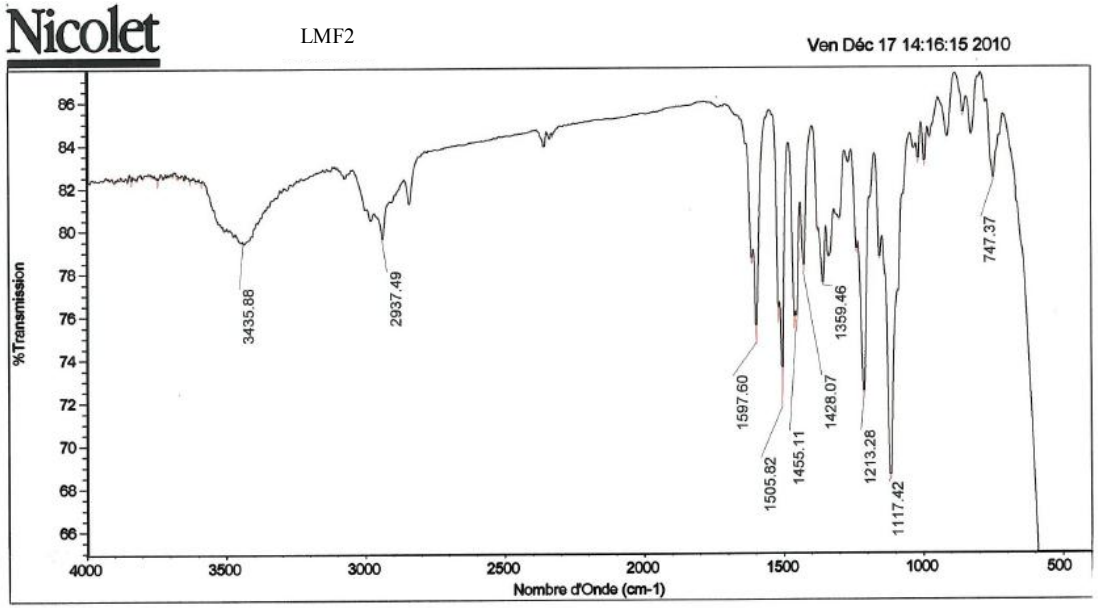

Figure 151 IR spectrum of compound LMF2 [**104**] (film)

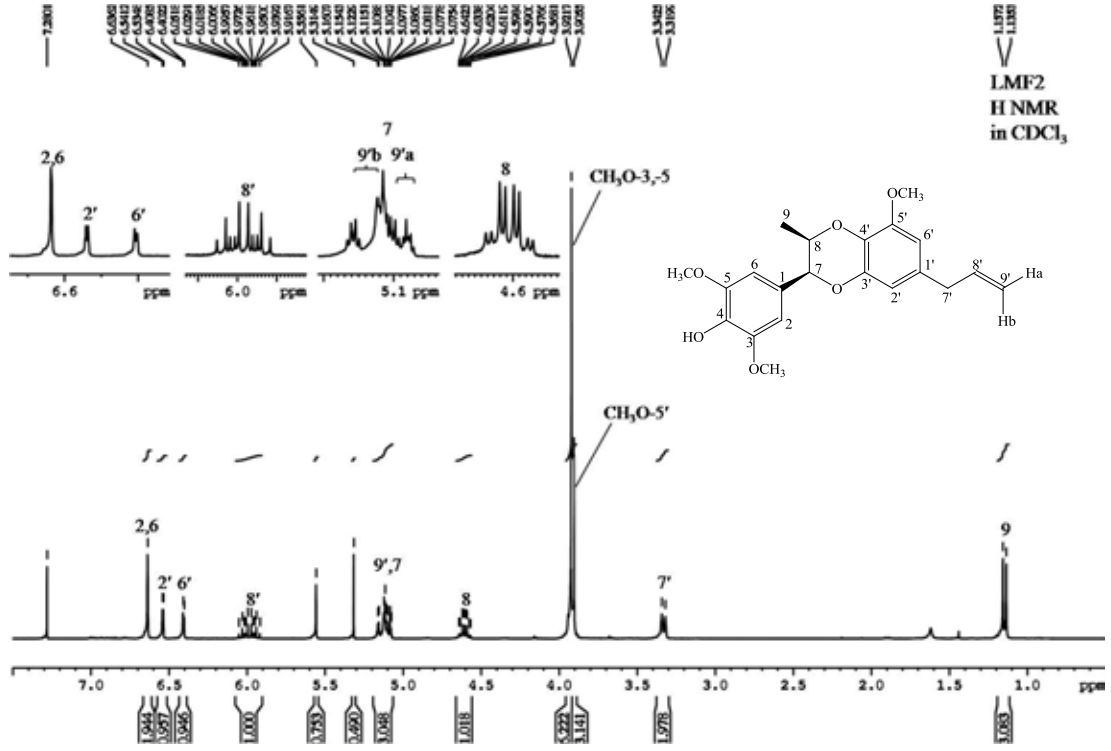

Figure 152 ^{1}H-NMR spectrum of compound LMF2 [**104**] ($CDCl_3$)

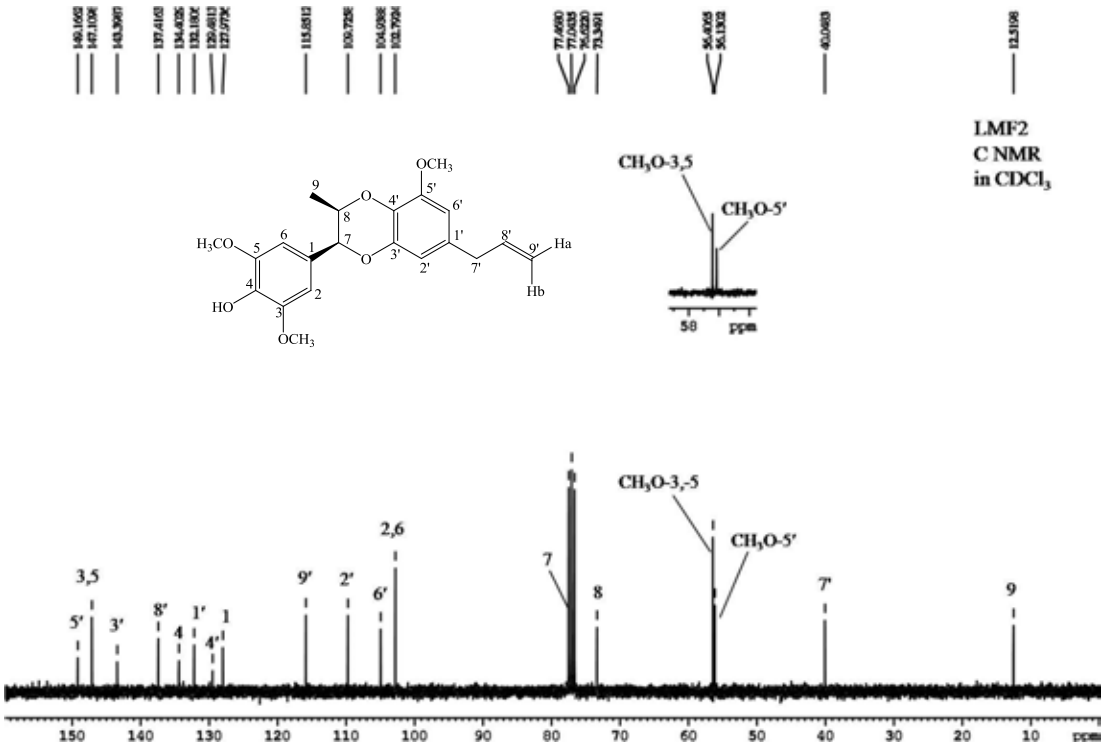

Figure 153 ^{13}C-NMR spectrum of compound LMF2 [**104**] ($CDCl_3$)

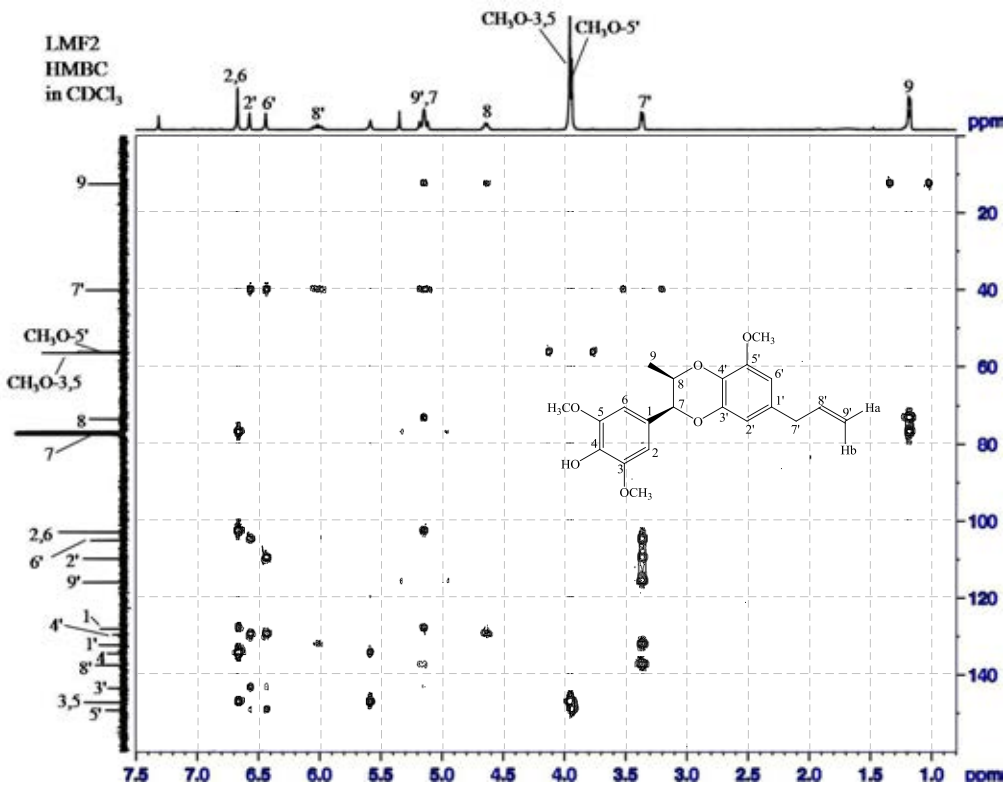

Figure 154 HMBC spectrum of compound LMF2 [**104**] ($CDCl_3$)

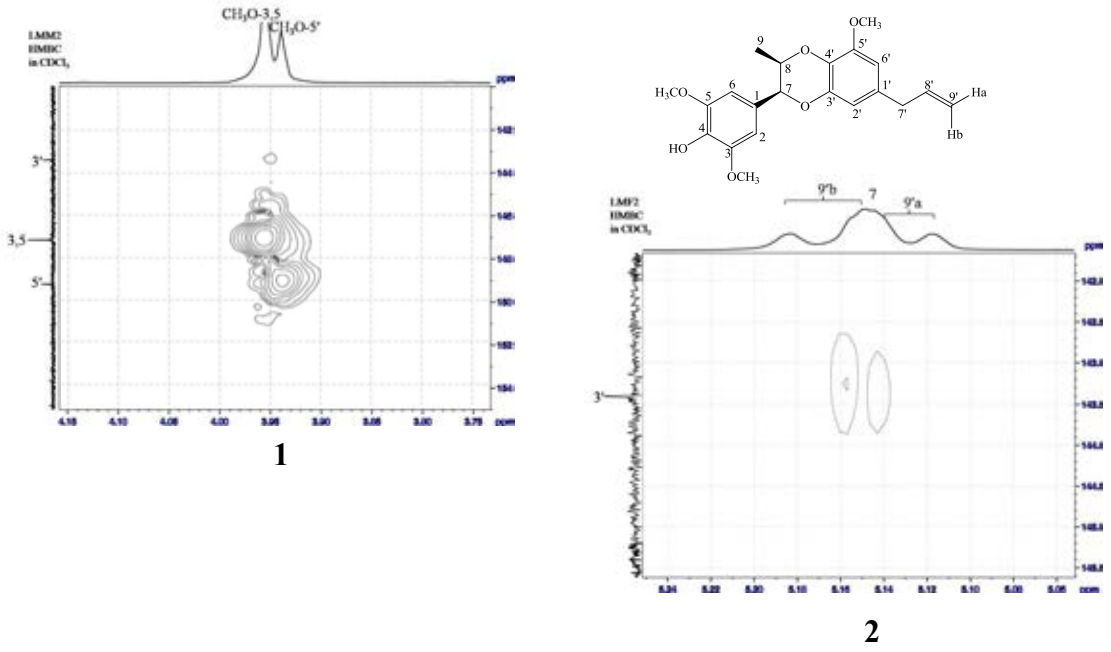

Figure 154a HMBC spectrum of compound LMF2 [**104**] ($CDCl_3$)
[δ_H 4.16-3.73 ppm, δ_C 155.0-140.0 ppm (1)] and
[δ_H 5.25-5.05 ppm, δ_C 145.6-141.6 ppm (2)]

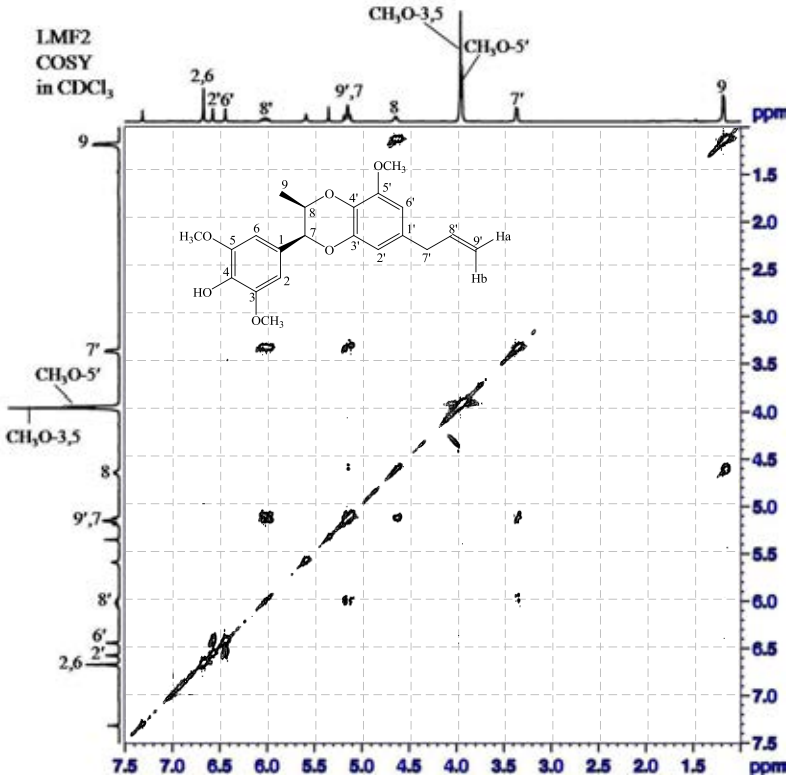

Figure 155 ^1H-^1H COSY spectrum of compound LMF2 [**104**] ($CDCl_3$)

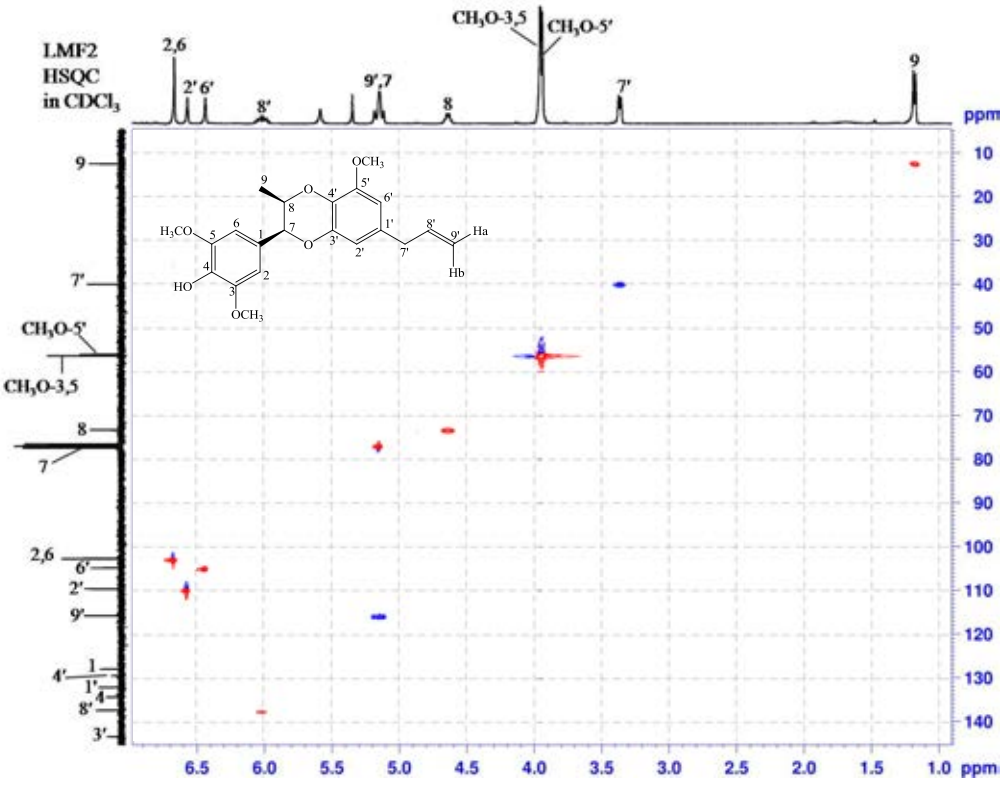

Figure 156 HSQC spectrum of compound LMF2 [**104**] ($CDCl_3$)

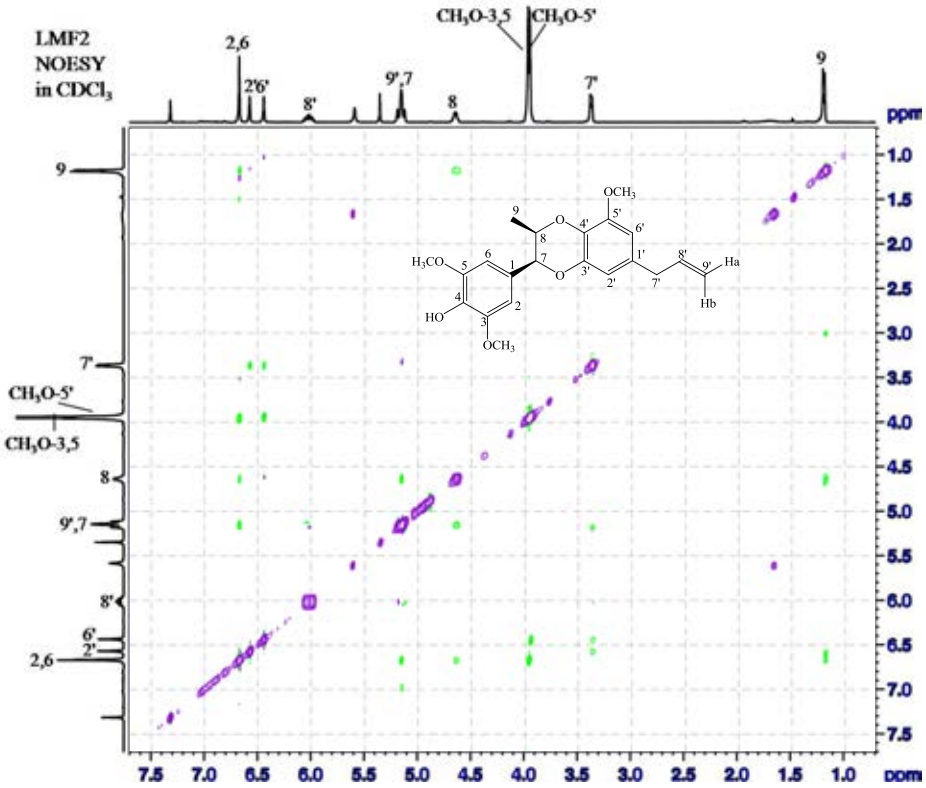

Figure 157 NOESY spectrum of compound LMF2 [**104**] ($CDCl_3$)

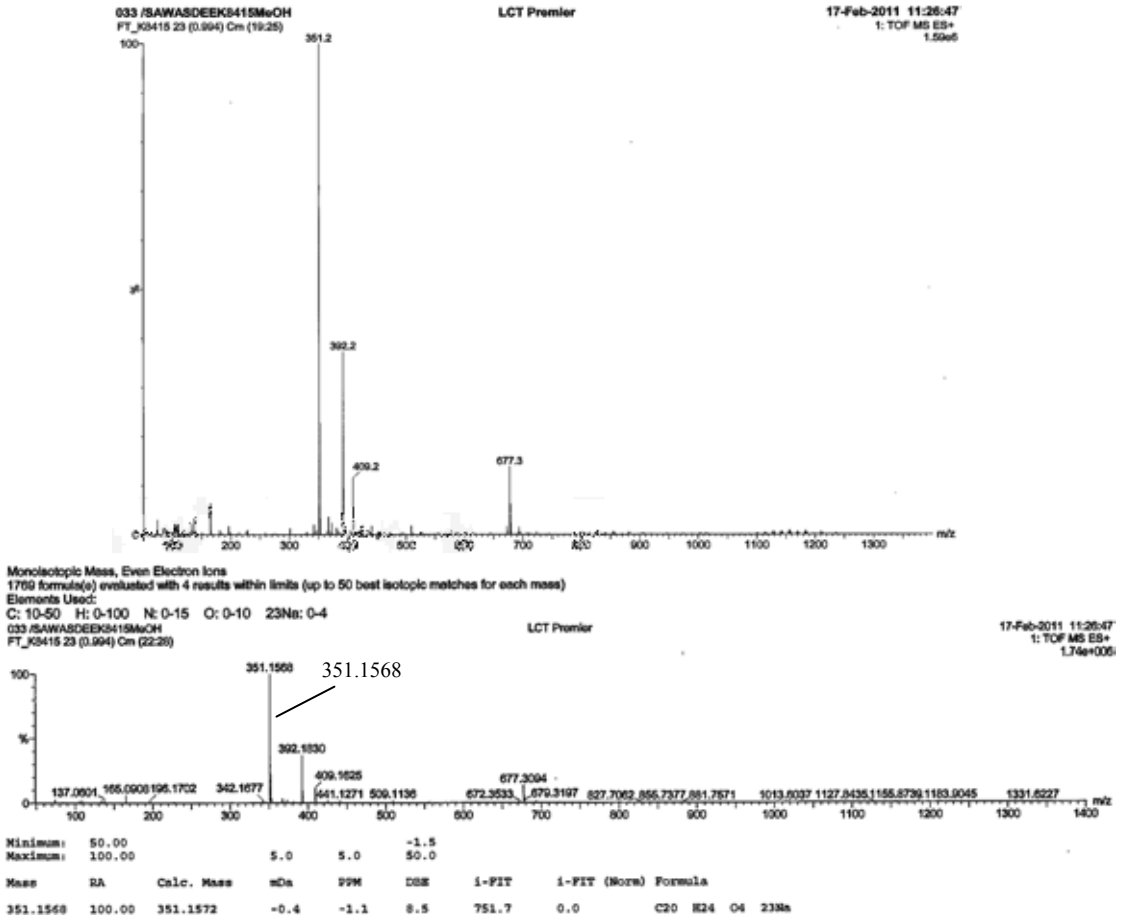

Figure 158 HRESI mass spectrum of compound LMF3 [**105**]

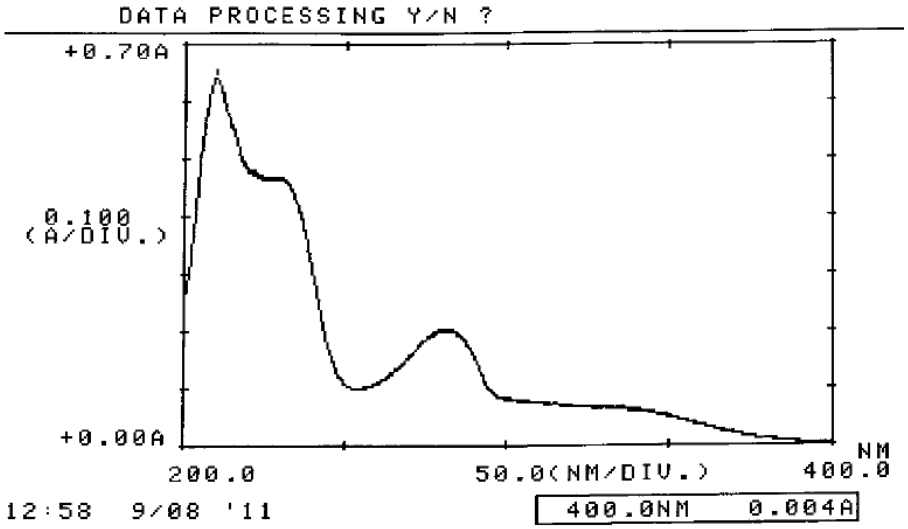

Figure 159 UV spectrum of compound LMF3 [**105**] (MeOH)

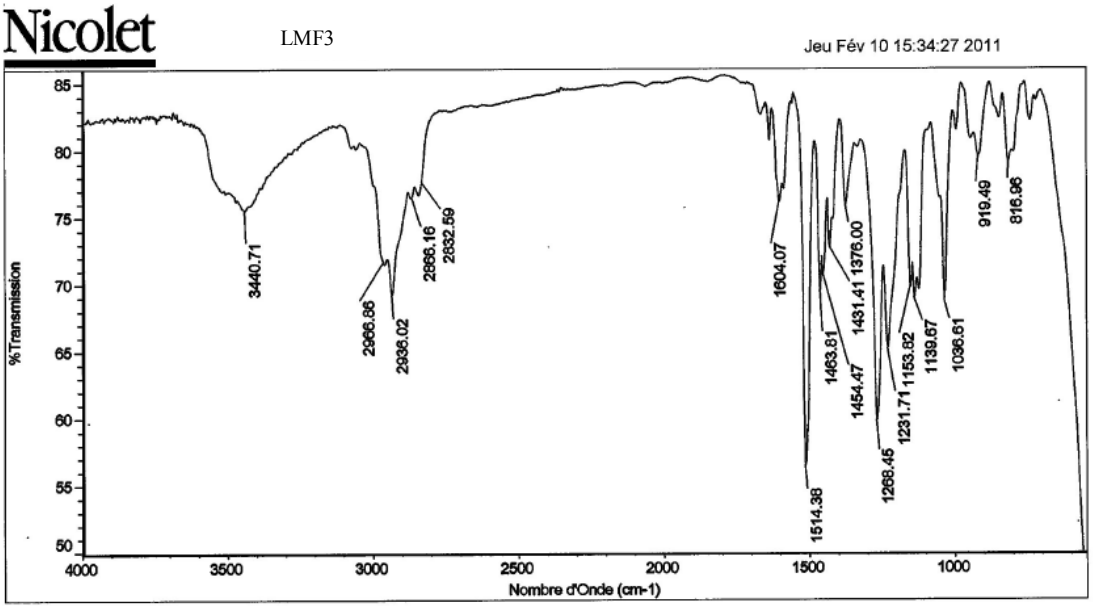

Figure 160 IR spectrum of compound LMF3 [**105**] (film)

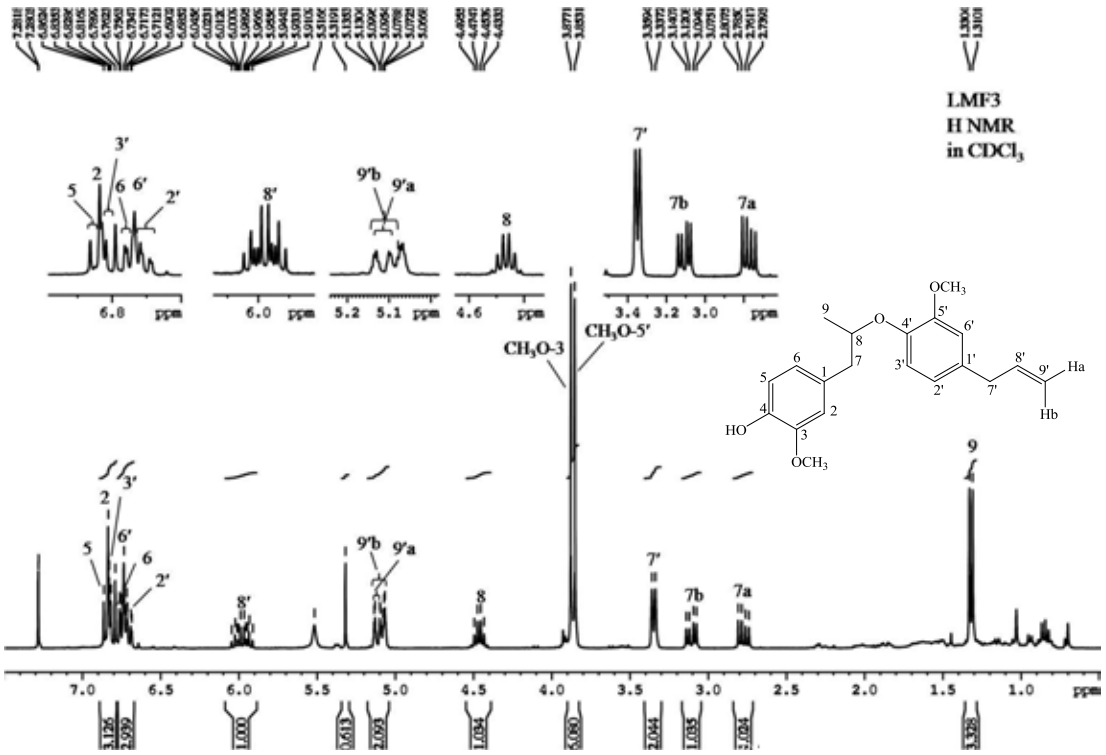

Figure 161 ^{1}H-NMR spectrum of compound LMF3 [**105**] ($CDCl_3$)

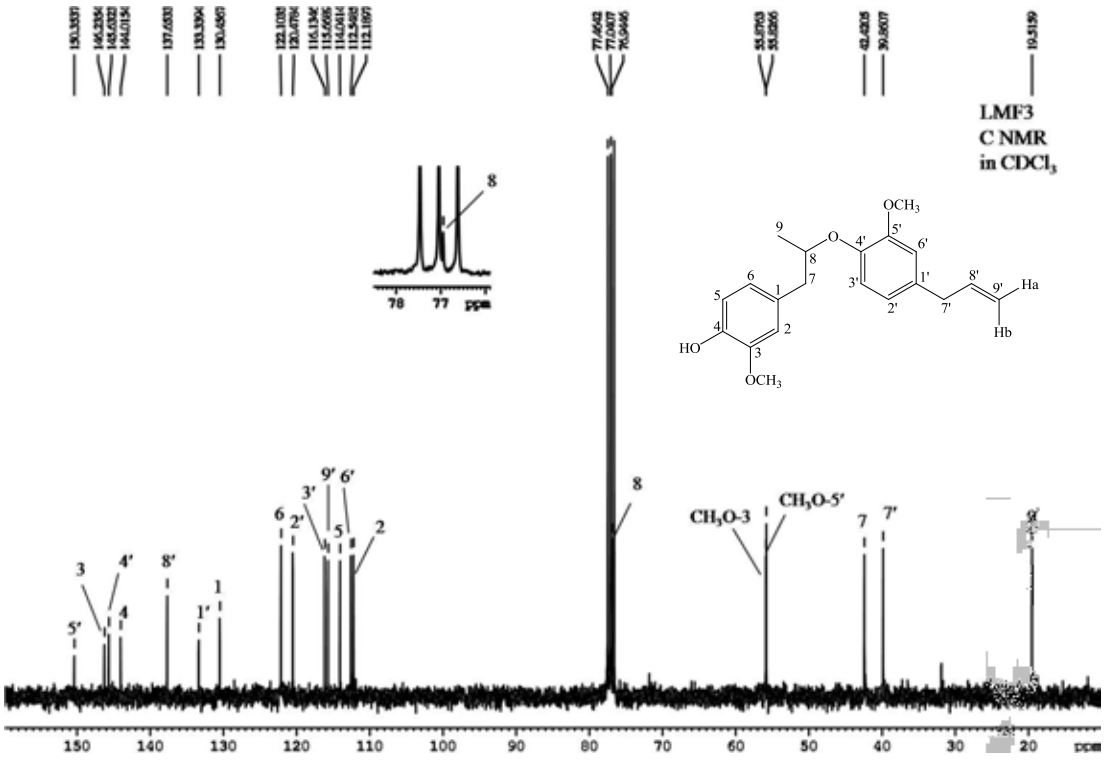

Figure 162 ^{13}C-NMR spectrum of compound LMF3 [**105**] ($CDCl_3$)

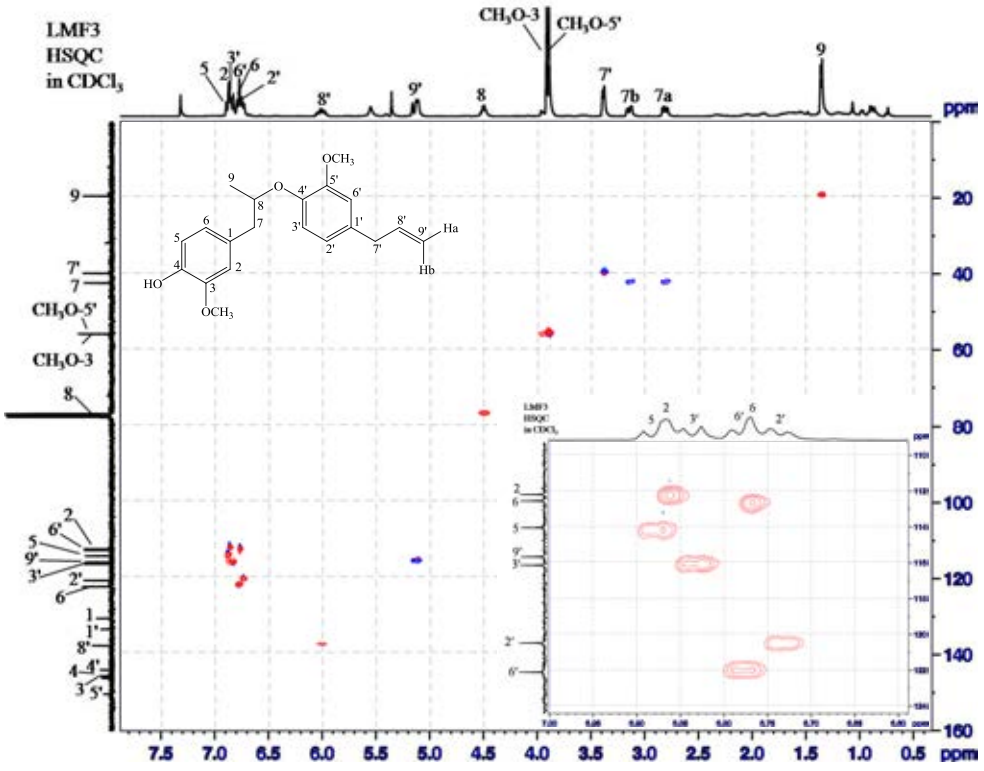

Figure 163 HSQC spectrum of compound LMF3 [**105**] ($CDCl_3$)

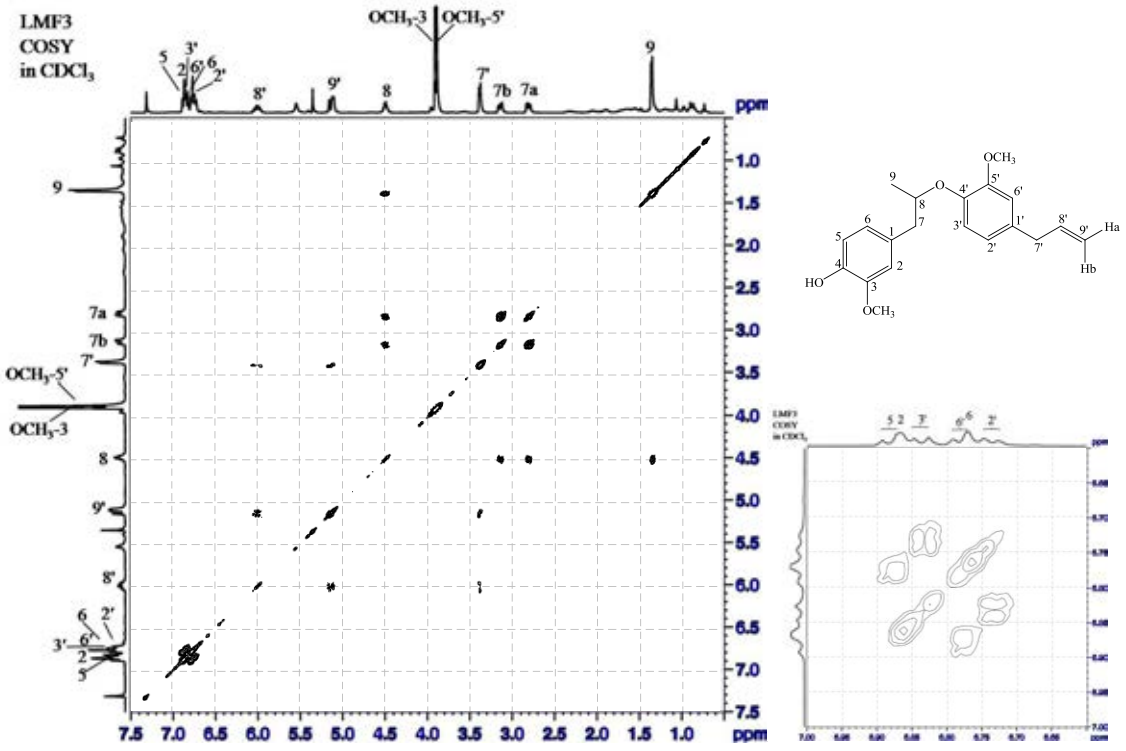

Figure 164 ^{1}H-^{1}H COSY spectrum of compound LMF3 [**105**] ($CDCl_3$)

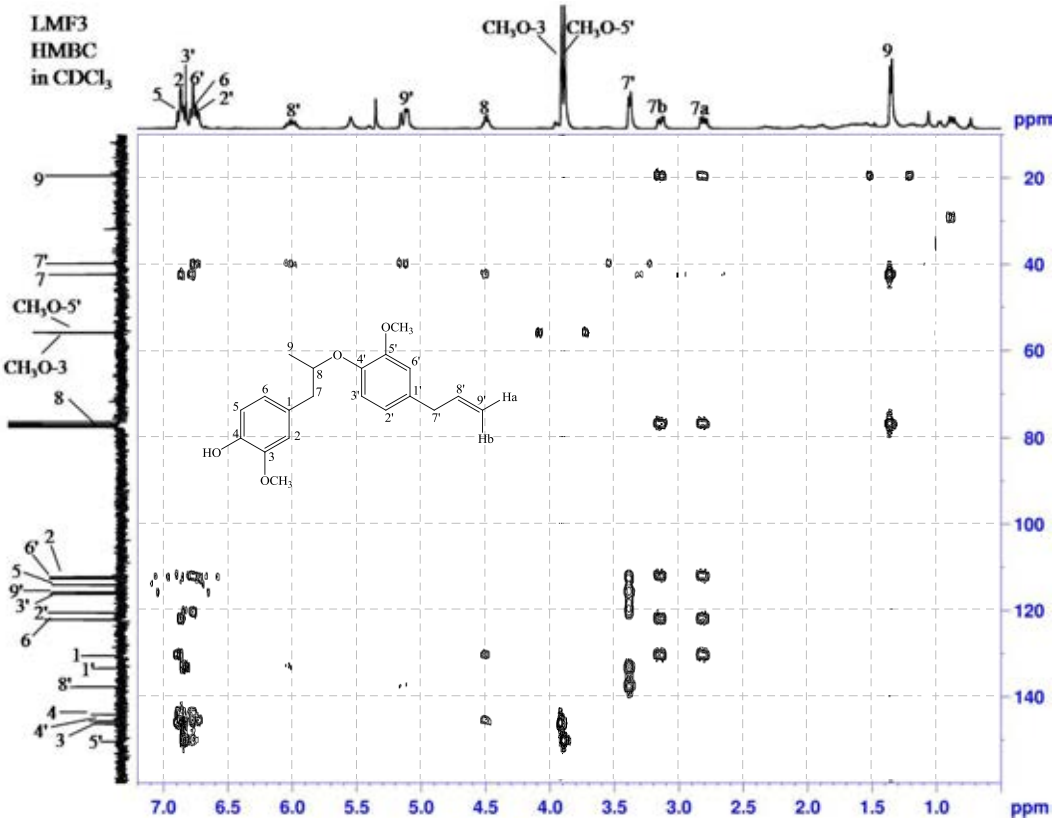

Figure 165 HMBC spectrum of compound LMF3 [**105**] ($CDCl_3$)

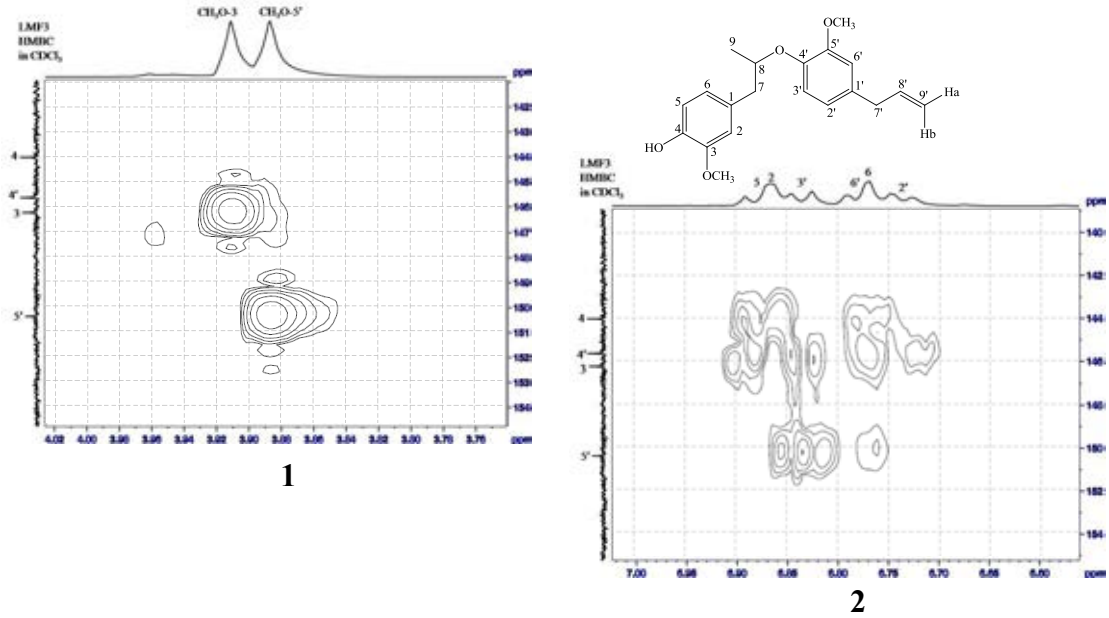

1 **2**

Figure 165a HMBC spectrum of compound LMF3 [**105**] ($CDCl_3$)
[δ_H 4.03-3.74 ppm, δ_C 154.7-141.0 ppm (1)] and
[δ_H 7.02-5.56 ppm, δ_C 155.0-139.0 ppm (2)]

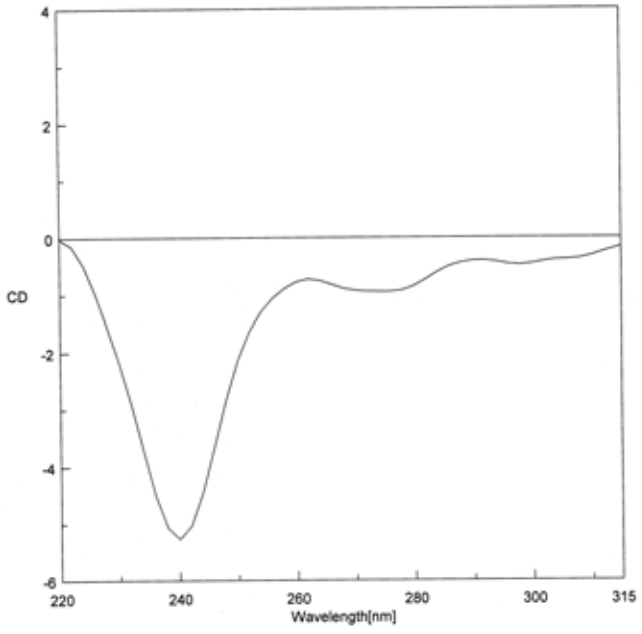

Figure 166 CD spectra of compound LMF3 [**105**] (MeOH)

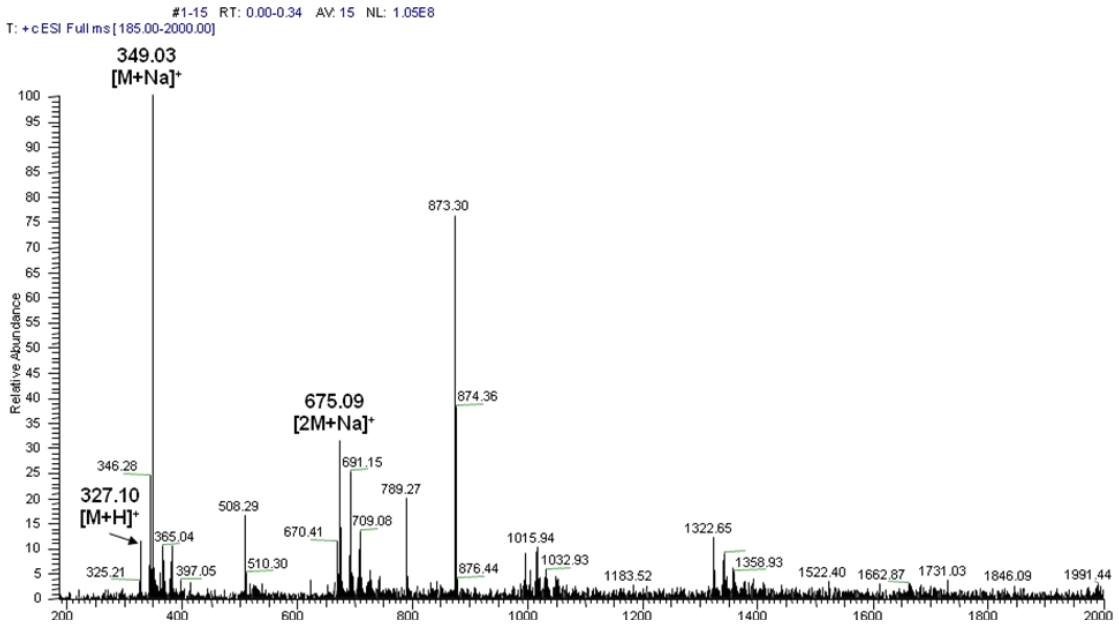

Figure 167 ESI mass spectrum of compound LMF4 [**106**]

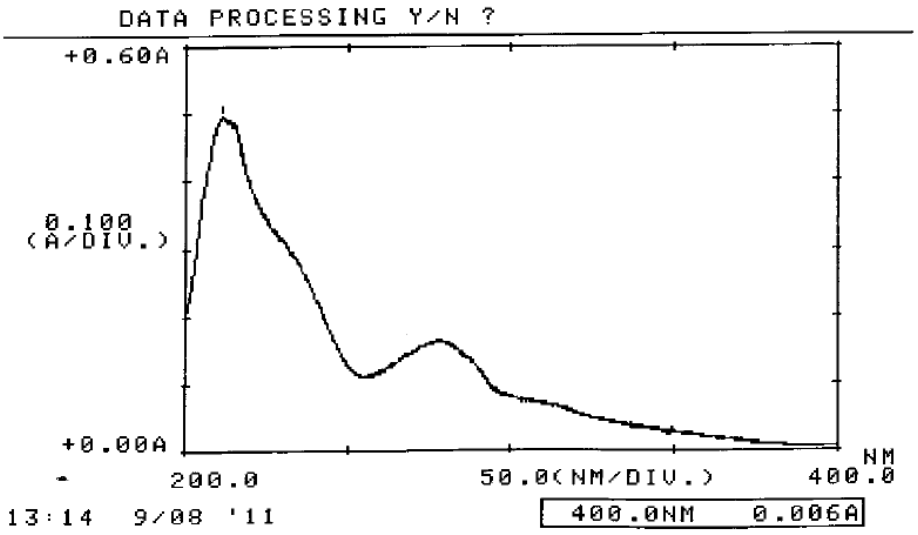

Figure 168 UV spectrum of compound LMF4 [**106**] (MeOH)

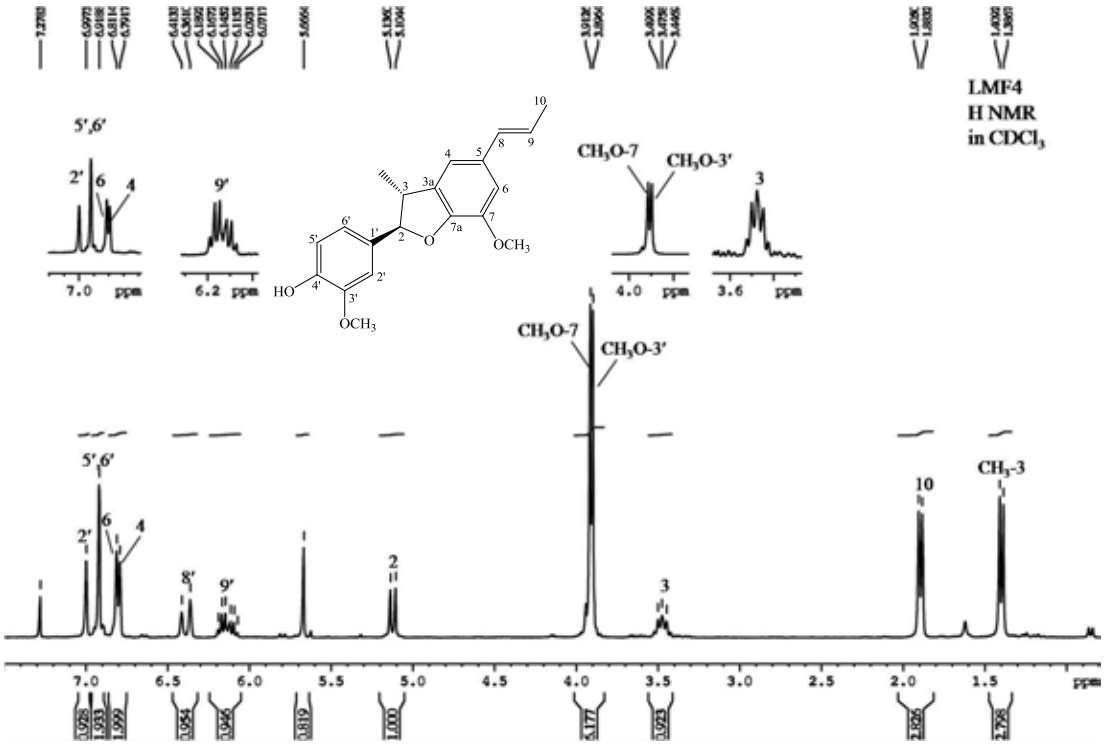

Figure 169 ^{1}H-NMR spectrum of compound LMF4 [**106**] ($CDCl_3$)

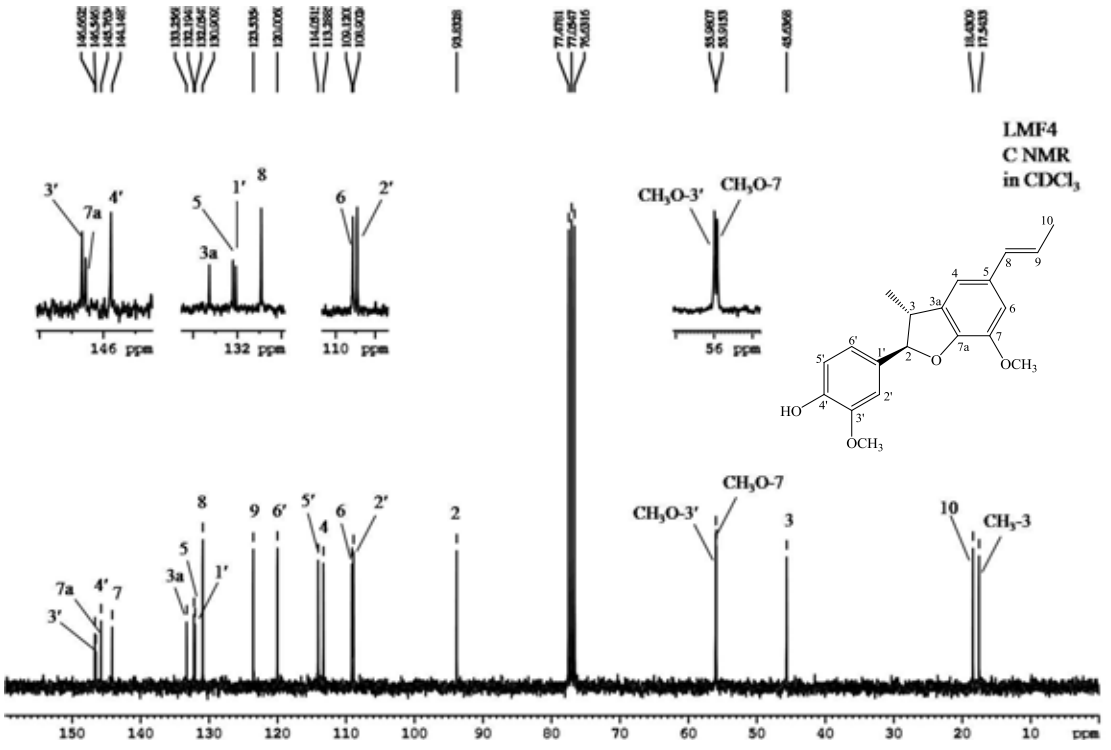

Figure 170 ^{13}C-NMR spectrum of compound LMF4 [**106**] ($CDCl_3$)

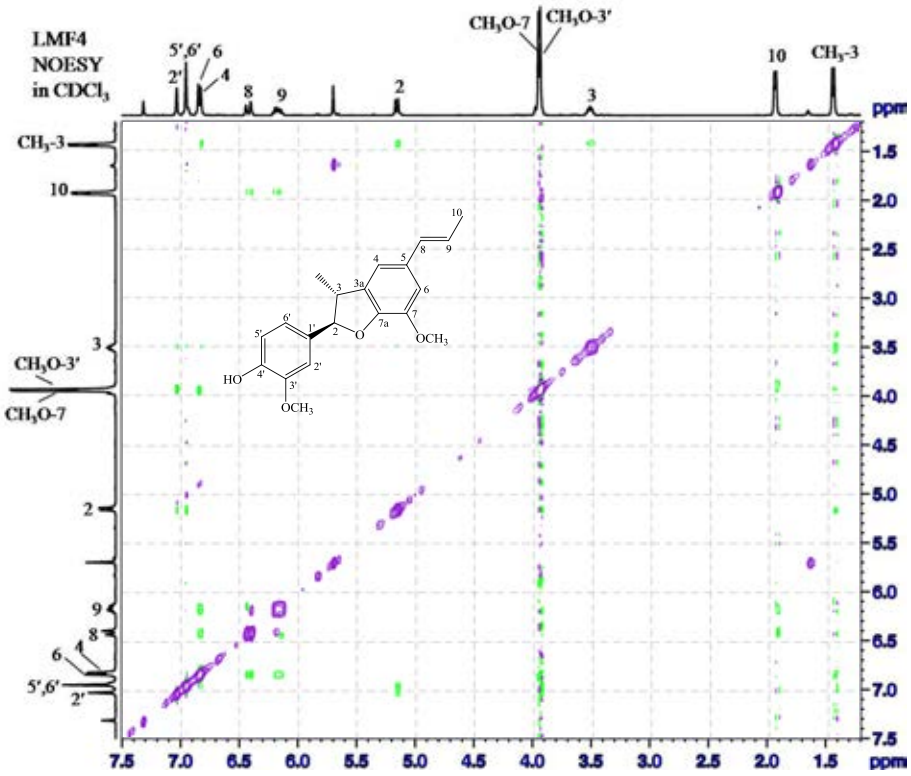

Figure 171 NOESY spectrum of compound LMF4 [**106**] ($CDCl_3$)

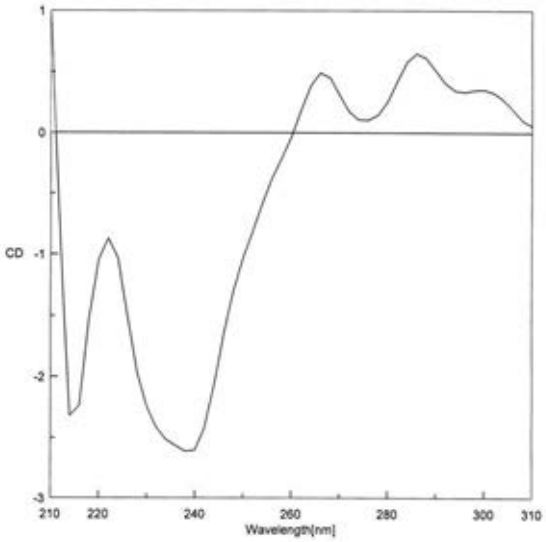

Figure 172 CD spectrum of compound LMF4 [**106**] (MeOH)

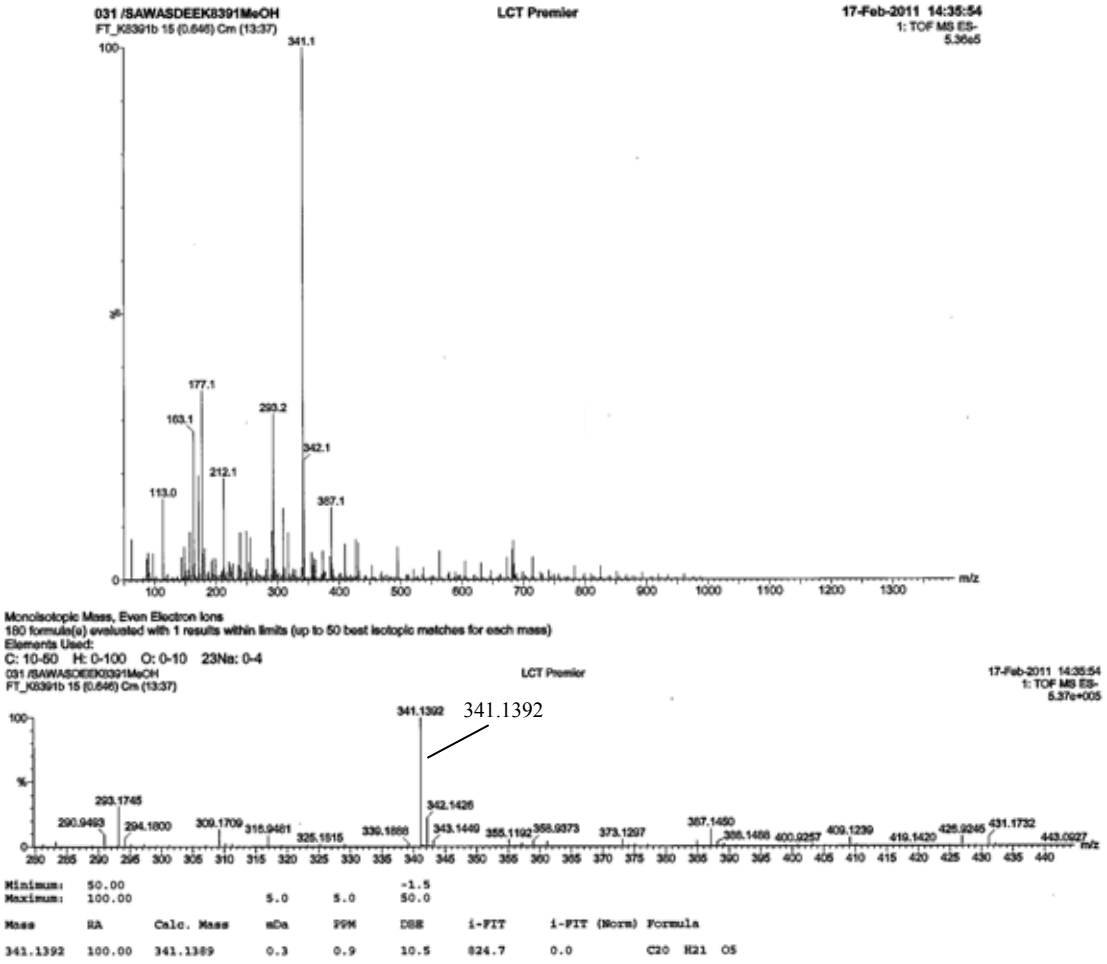

Figure 173 HRESI mass spectrum of compound LMF5 [**107**]

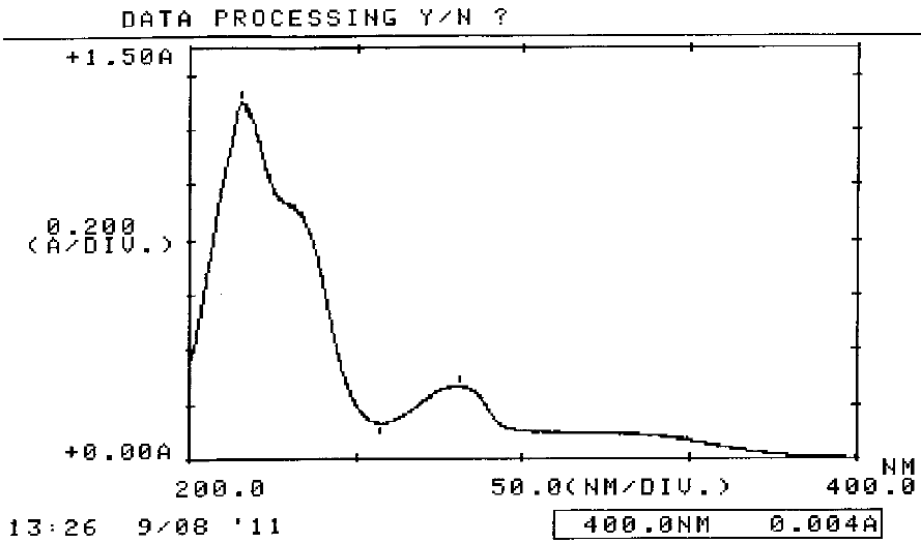

Figure 174 UV spectrum of compound LMF5 [**107**] (MeOH)

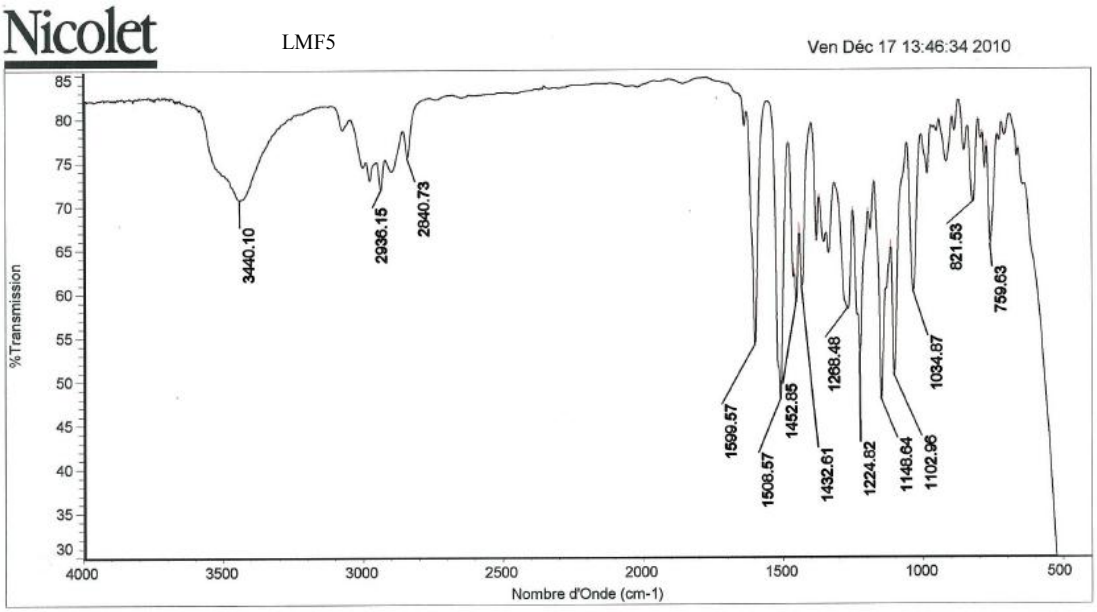

Figure 175 IR spectrum of compound LMF5 [**107**] (film)

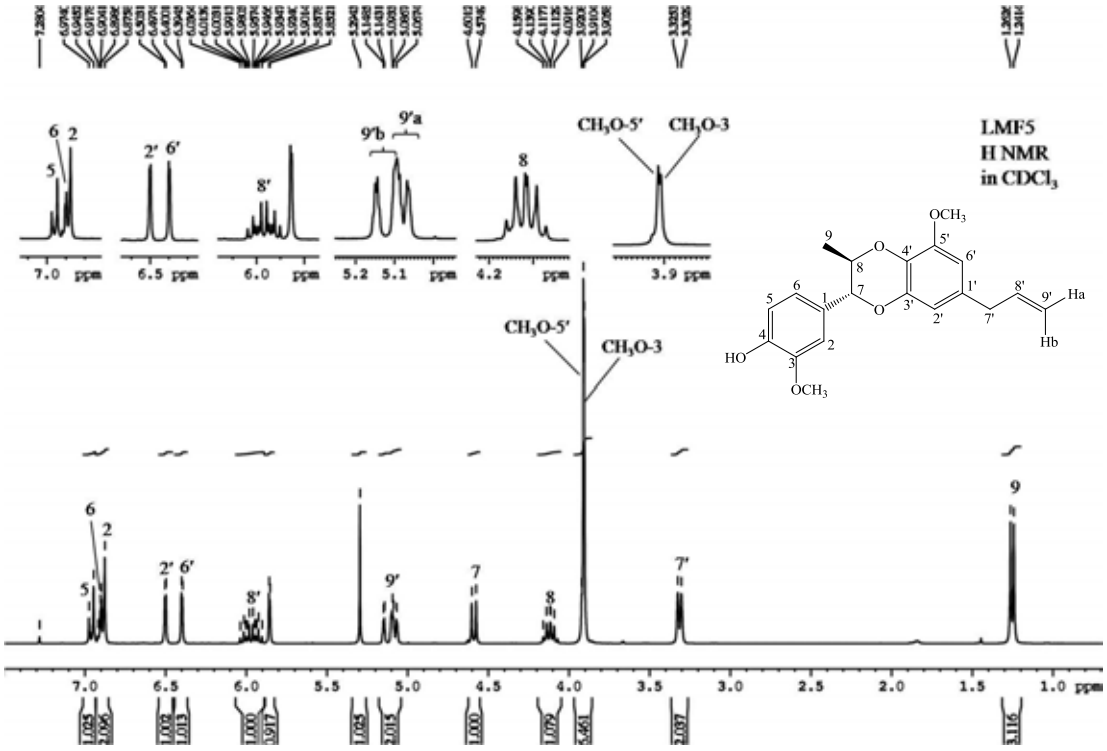

Figure 176 ^{1}H-NMR spectrum of compound LMF5 [**107**] ($CDCl_3$)

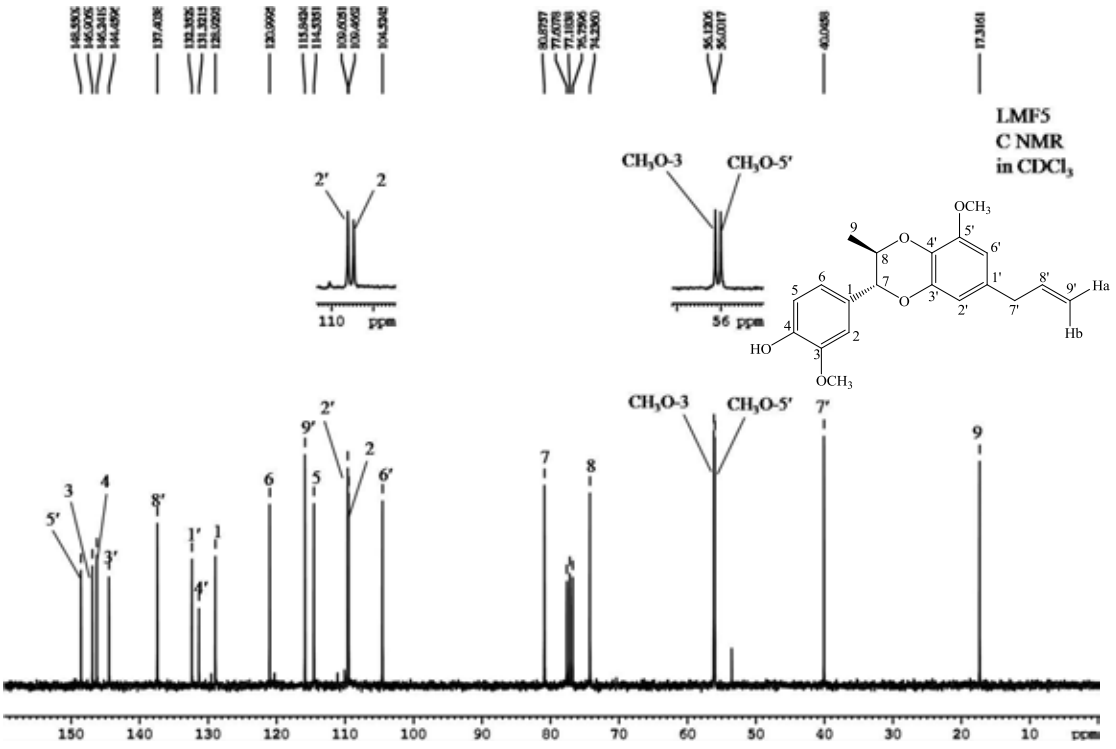

Figure 177 ^{13}C-NMR spectrum of compound LMF5 [**107**] ($CDCl_3$)

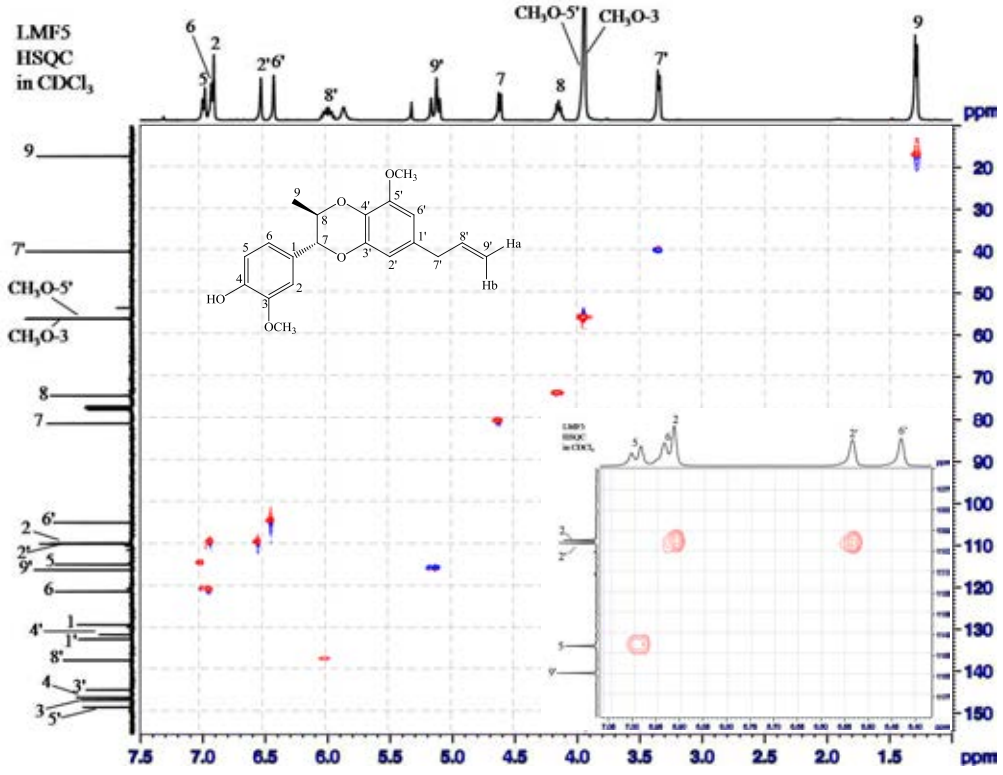

Figure 178 HSQC spectrum of compound LMF5 [**107**] ($CDCl_3$)

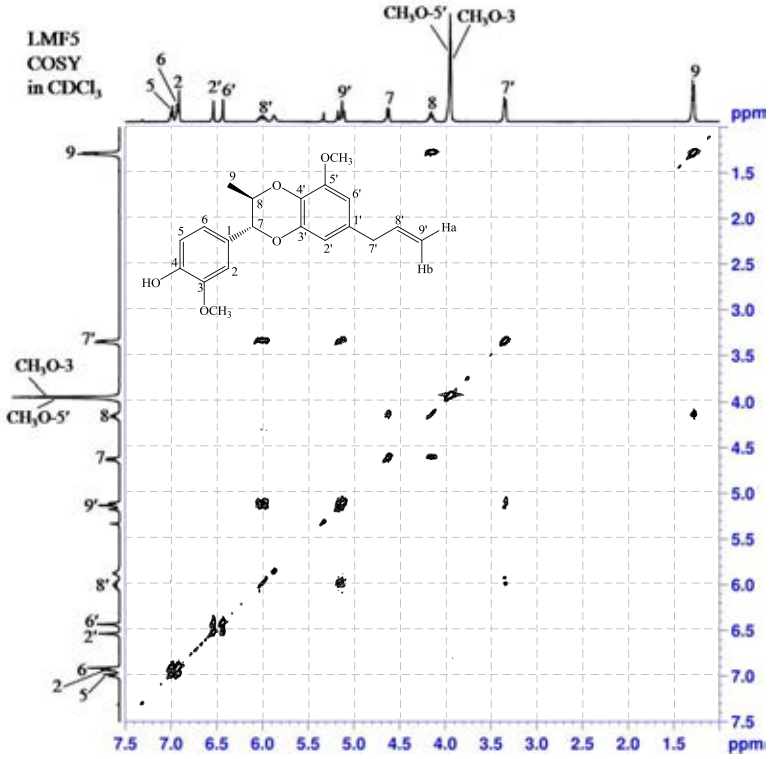

Figure 179 ^{1}H-^{1}H COSY spectrum of compound LMF5 [**107**] ($CDCl_3$)

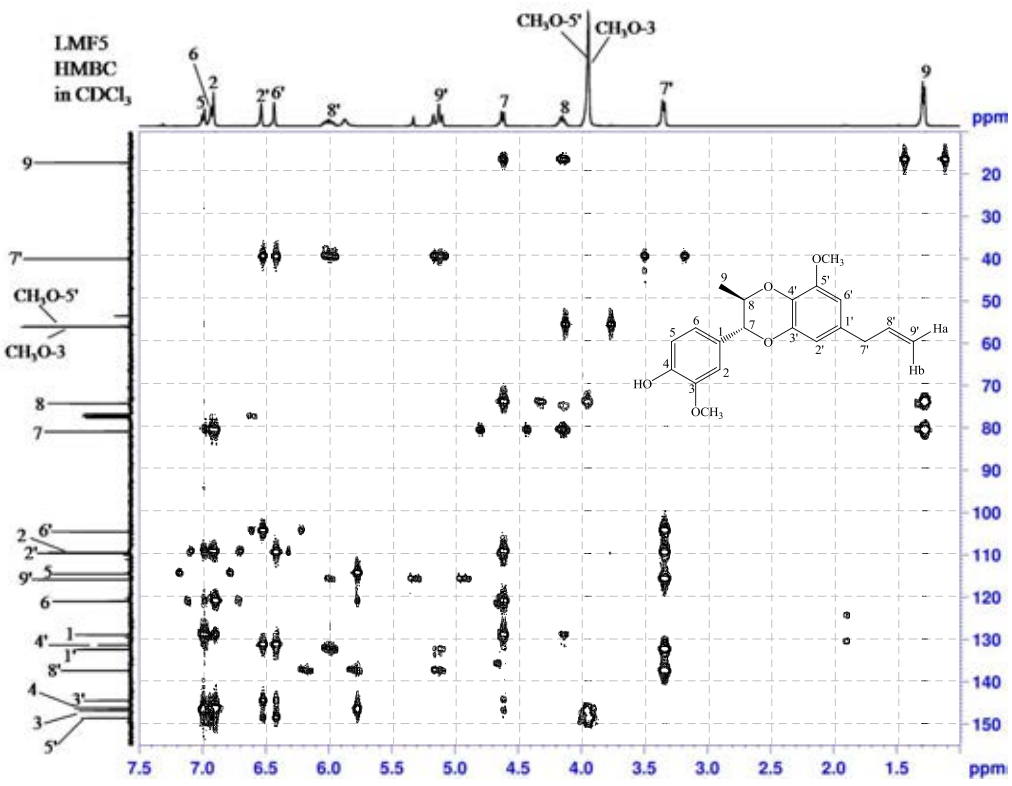

Figure 180 HMBC spectrum of compound LMF5 [**107**] ($CDCl_3$)

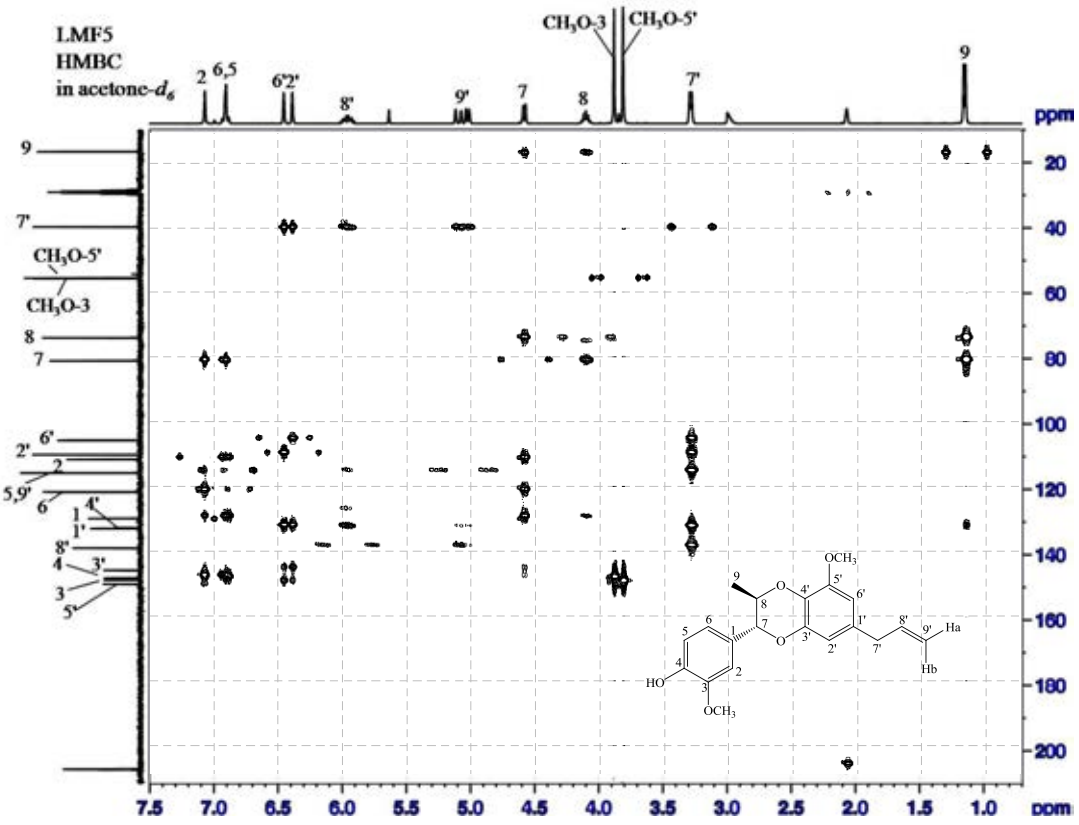

Figure 181 HMBC spectrum of compound LMF5 [**107**] (acetone-d_6)

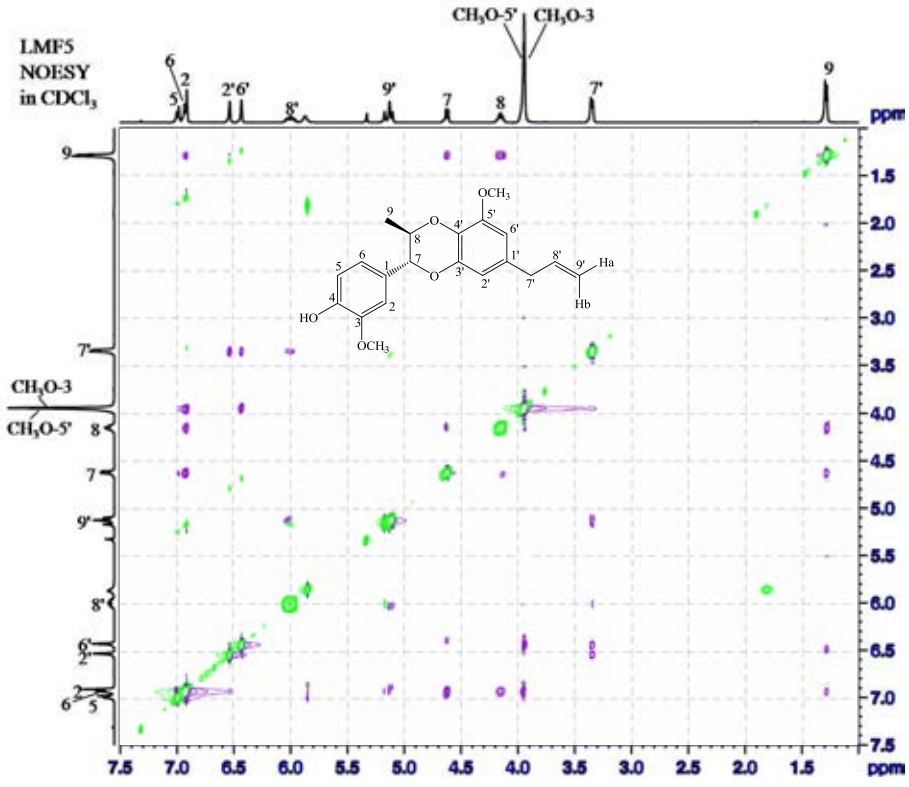

Figure 182 NOESY spectrum of compound LMF5 [**107**] ($CDCl_3$)

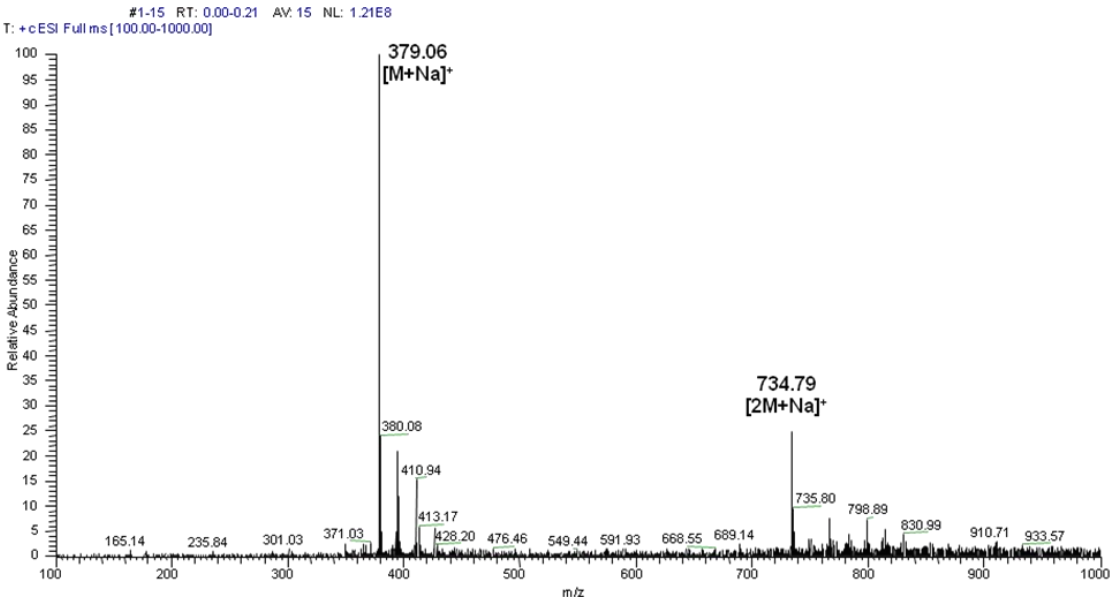

Figure 183 ESI mass spectrum of compound LMF6 [**108**]

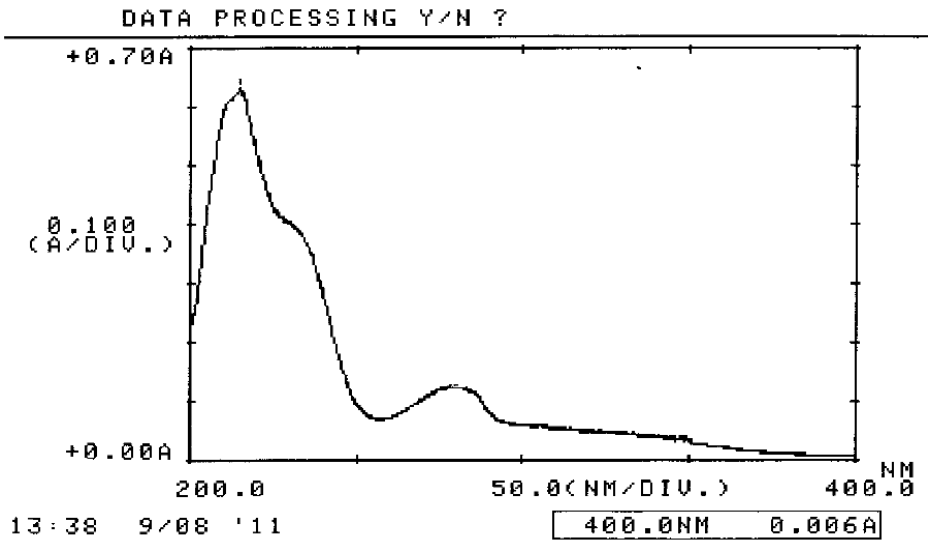

Figure 184 UV spectrum of compound LMF6 [**108**] (MeOH)

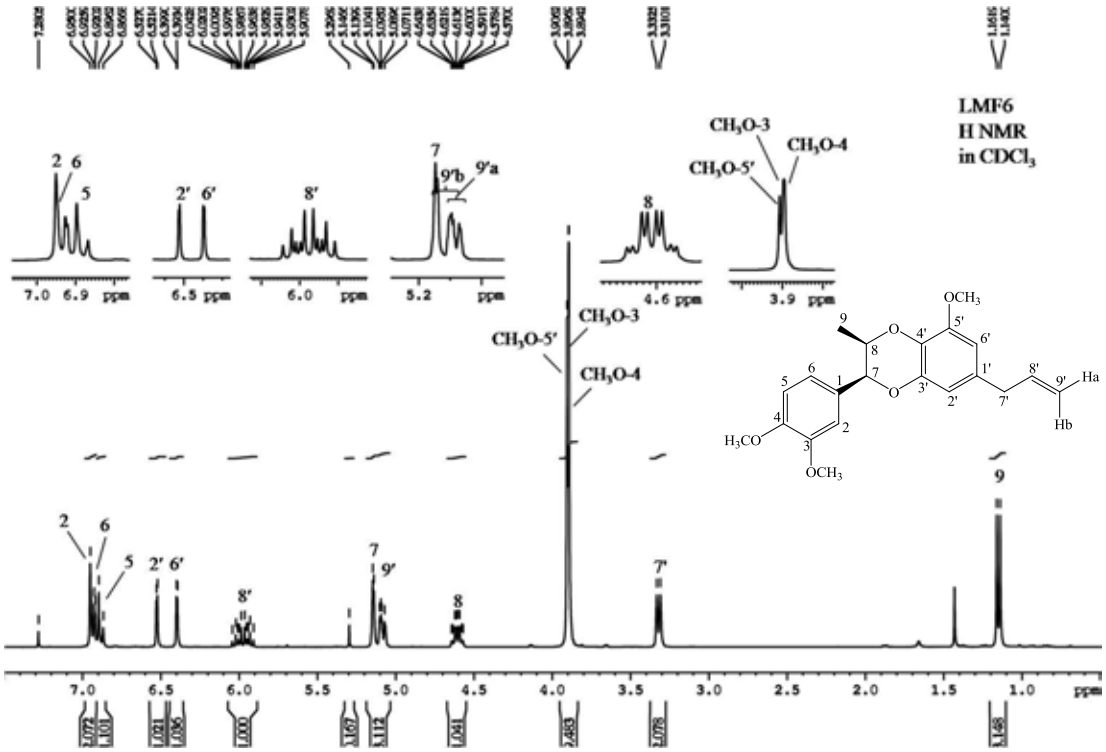

Figure 185 ^{1}H-NMR spectrum of compound LMF6 [**108**] ($CDCl_3$)

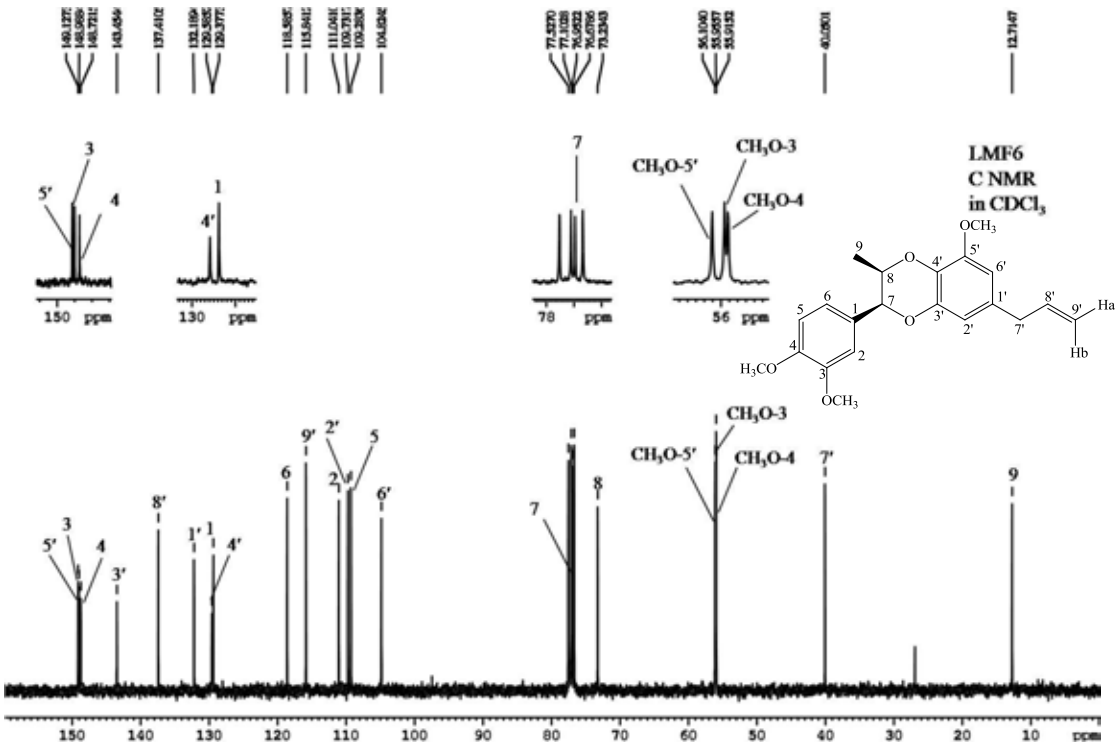

Figure 186 ^{13}C-NMR spectrum of compound LMF6 [**108**] ($CDCl_3$)

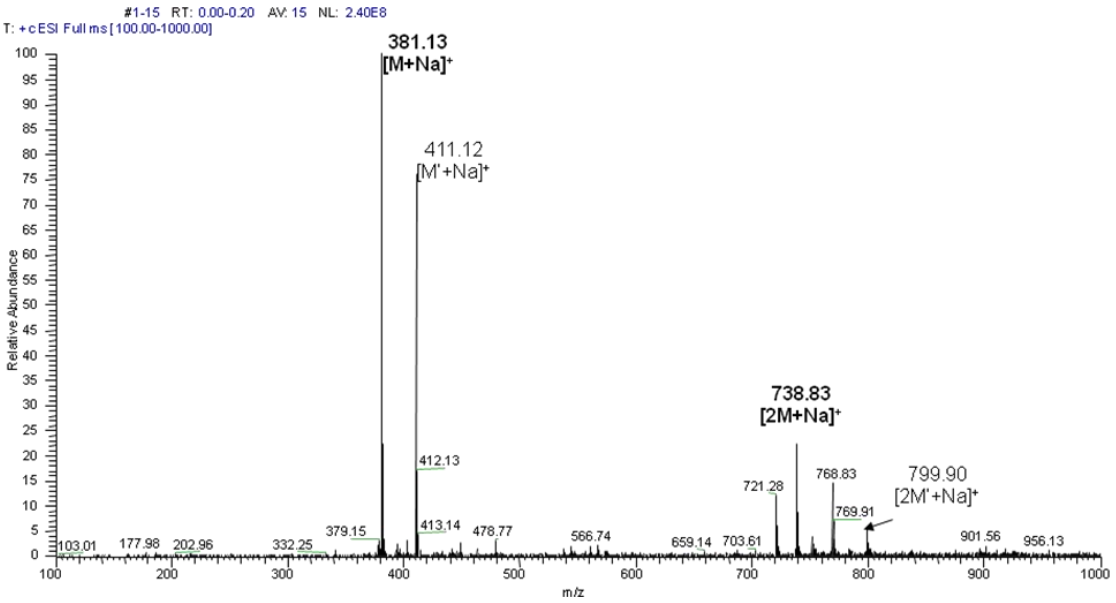

Figure 187 ESI mass spectrum of compound LMF7 [**109**]

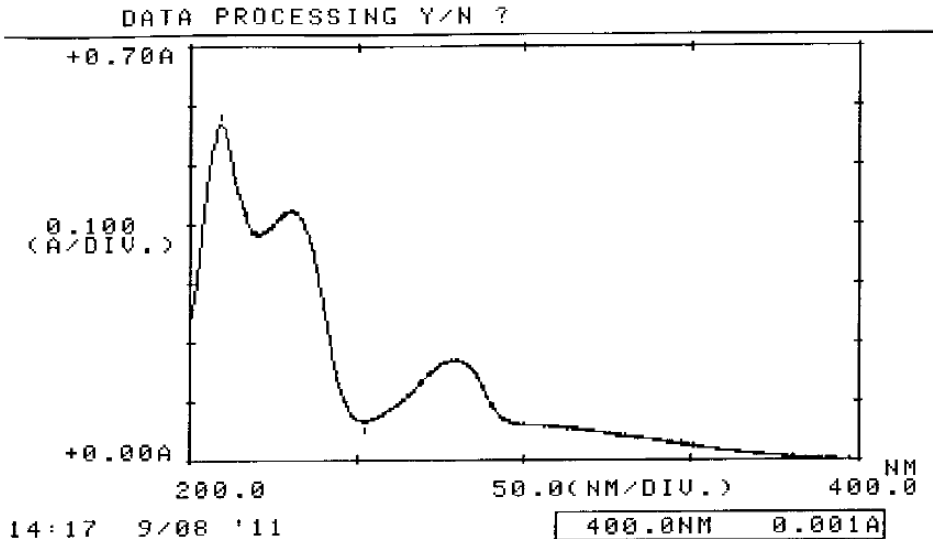

Figure 188 UV spectrum of compound LMF7 [**109**] (MeOH)

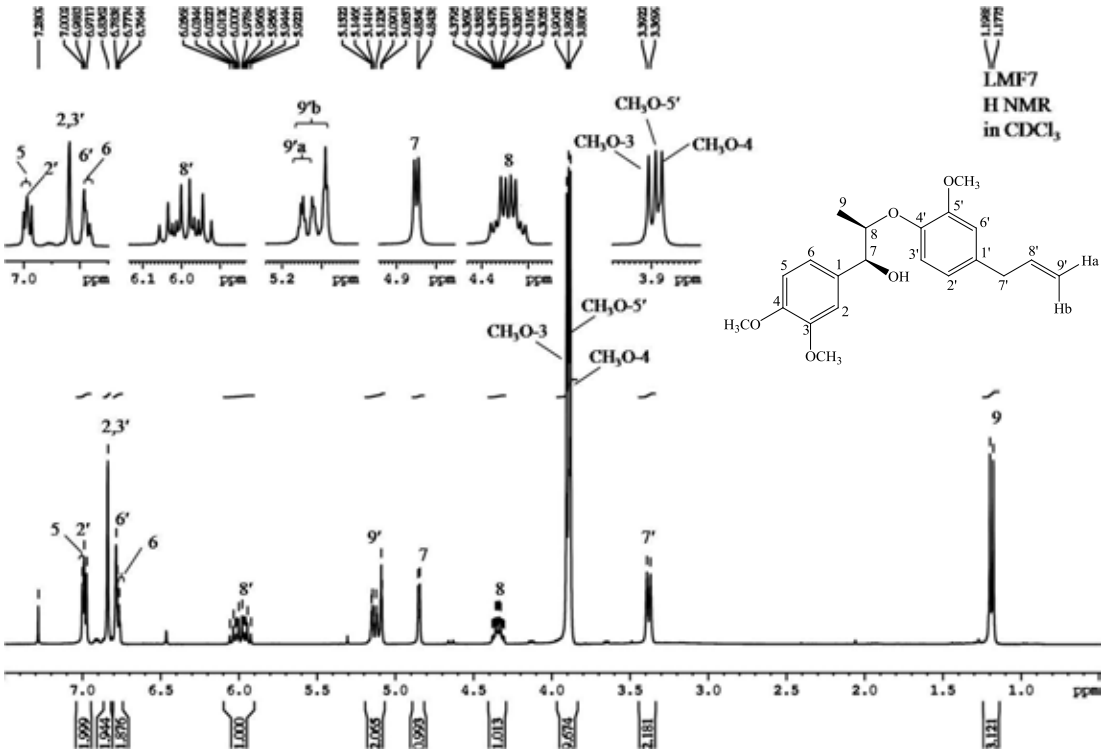

Figure 189 ^{1}H-NMR spectrum of compound LMF7 [**109**] ($CDCl_3$)

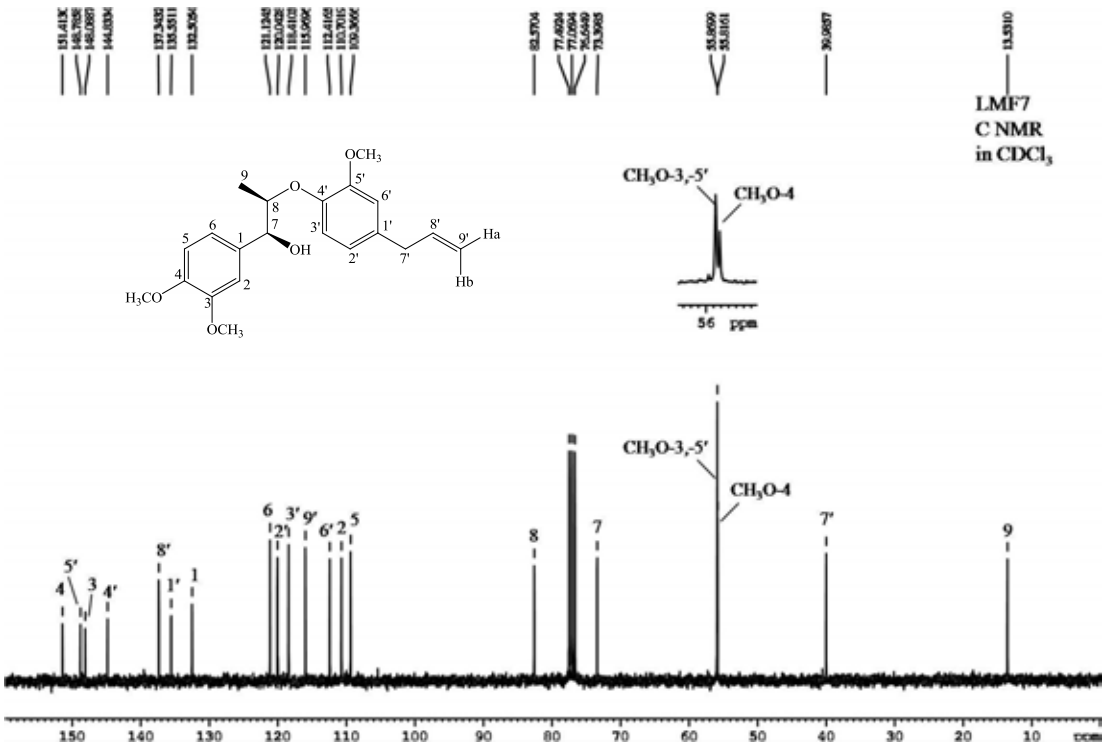

Figure 190 ^{13}C-NMR spectrum of compound LMF7 [**109**] ($CDCl_3$)

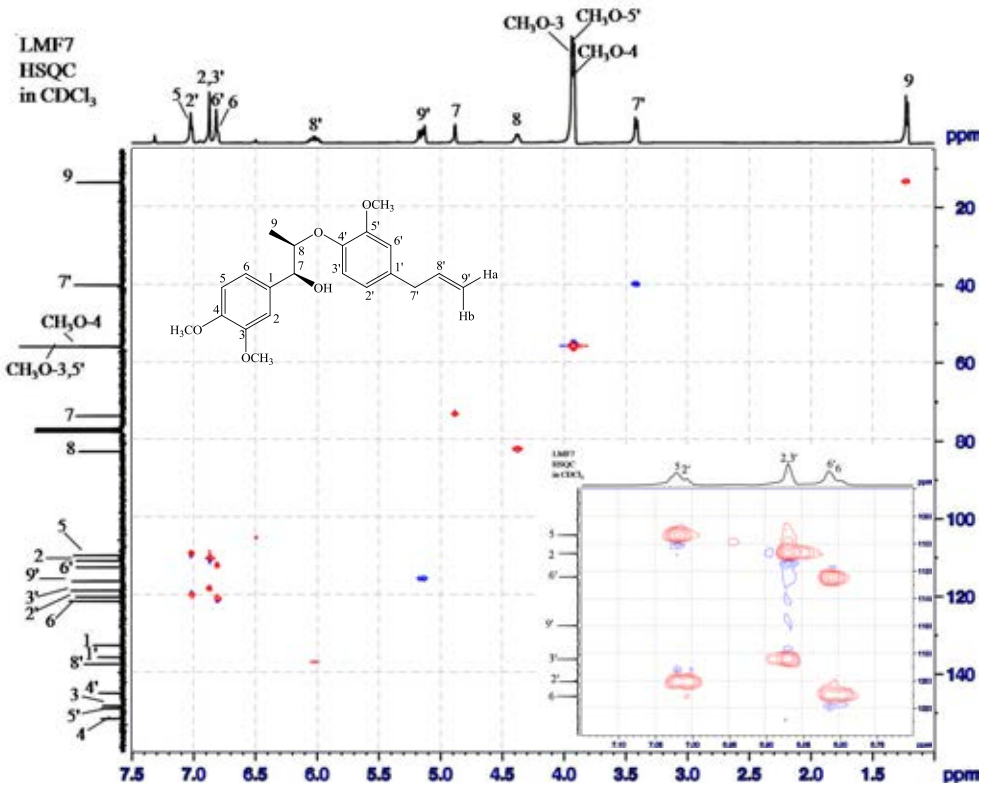

Figure 191 HSQC spectrum of compound LMF7 [**109**] ($CDCl_3$)

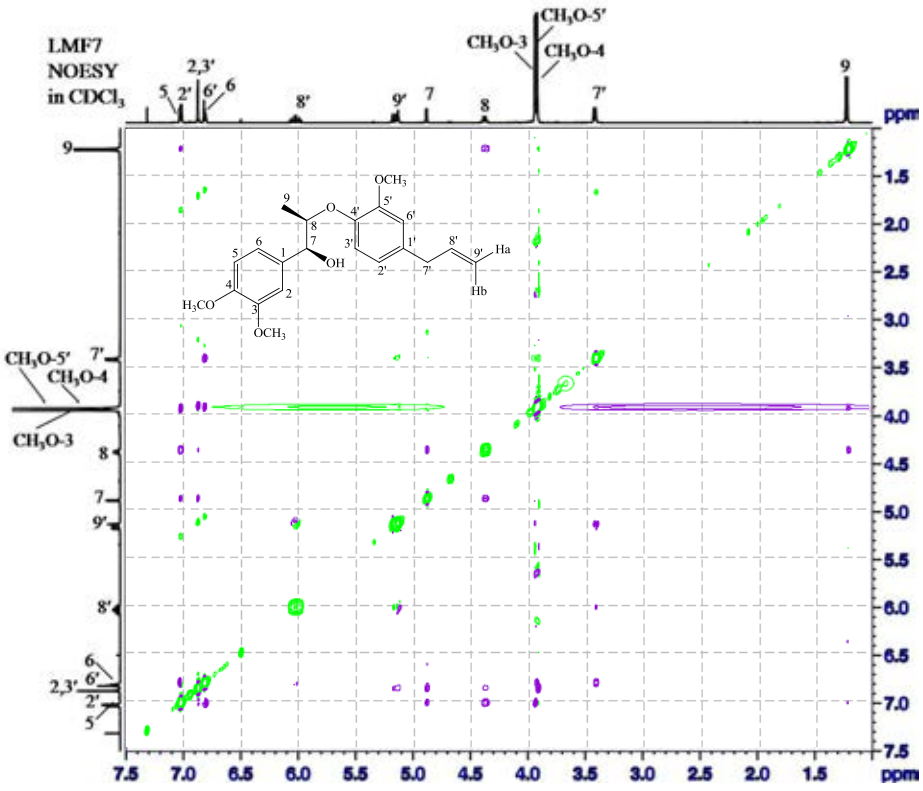

Figure 192 NOESY spectrum of compound LMF7 [**109**] ($CDCl_3$)

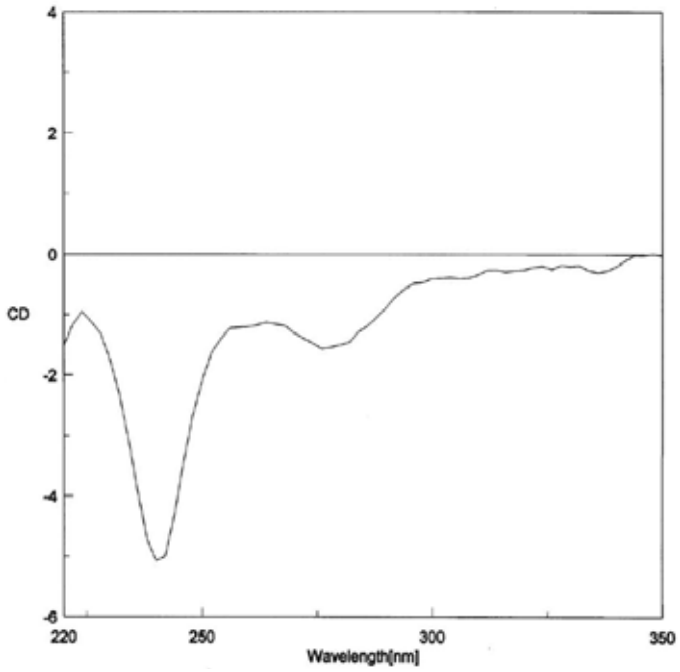

Figure 193 CD spectrum of compound LMF7 [**109**] (MeOH)

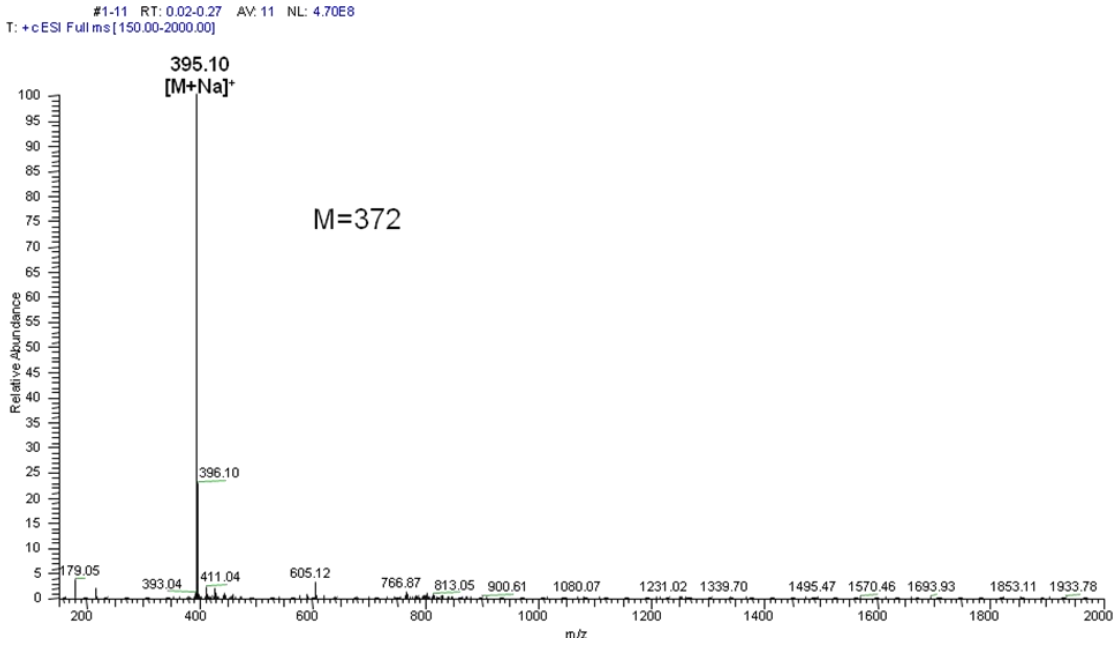

Figure 194 ESI mass spectrum of compound SMF1 [**110**]

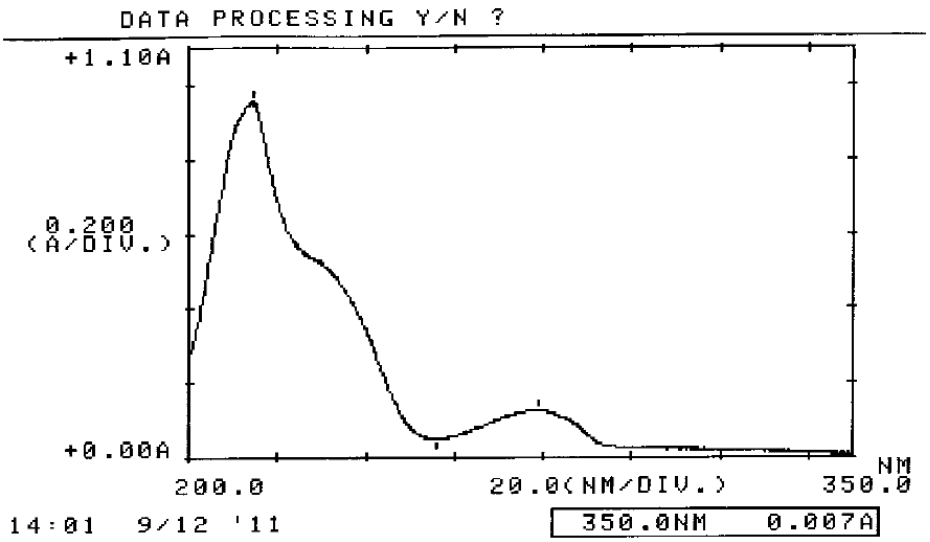

Figure 195 ESI Mass spectrum of compound SMF1 [**110**] (MeOH)

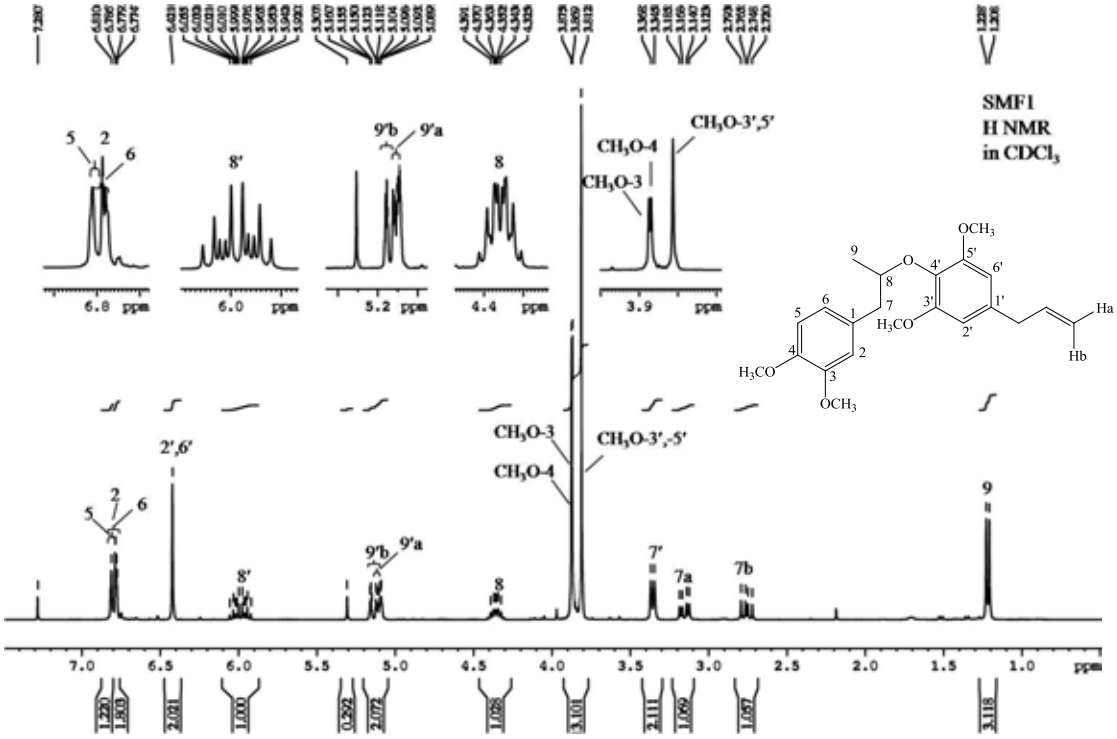

Figure 196 ^{1}H-NMR spectrum of compound SMF1 [**110**] ($CDCl_3$)

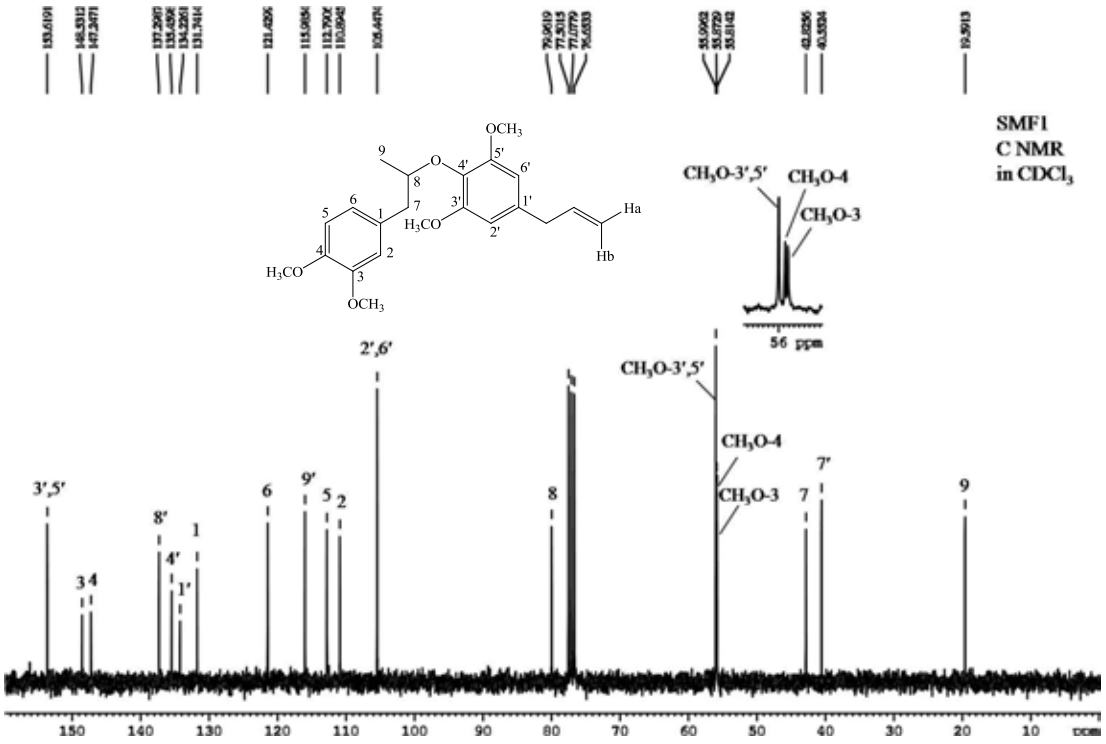

Figure 197 ^{13}C-NMR spectrum of compound SMF1 [**110**] ($CDCl_3$)

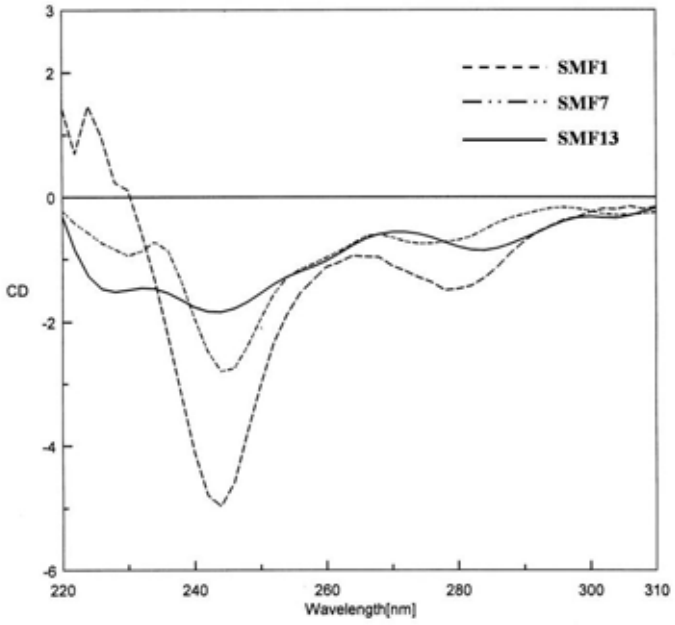

Figure 198 CD spectra (MeOH) of compounds SMF1 [**110**], SMF7 [**114**] and SMF13 [**119**]

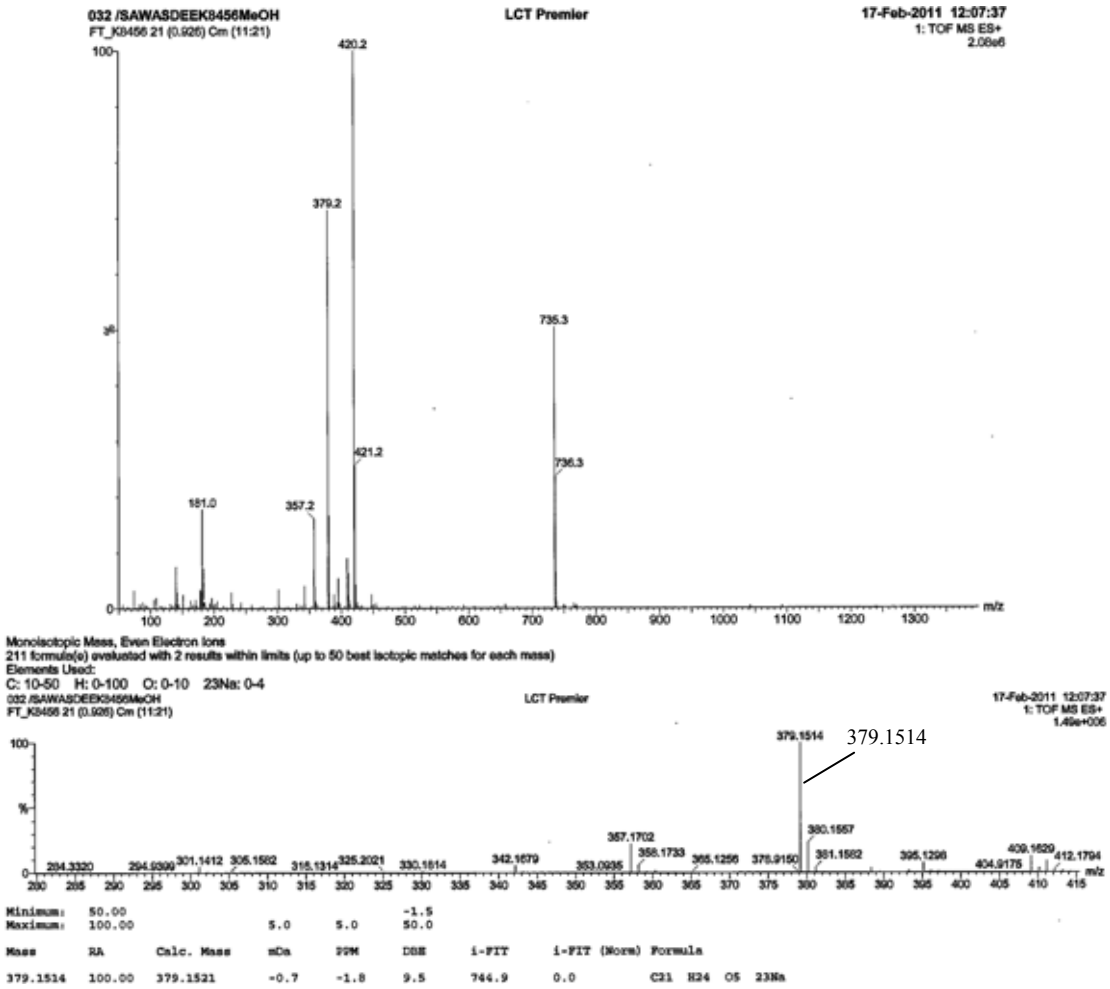

Figure 199 HRESI mass spectrum of compound SMF2 [**111**]

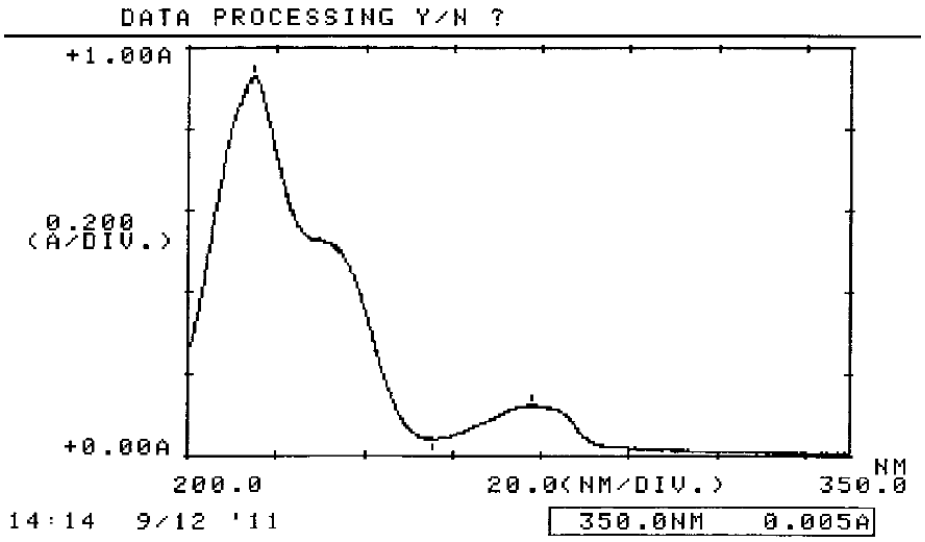

Figure 200 UV spectrum of compound SMF2 [**111**] (MeOH)

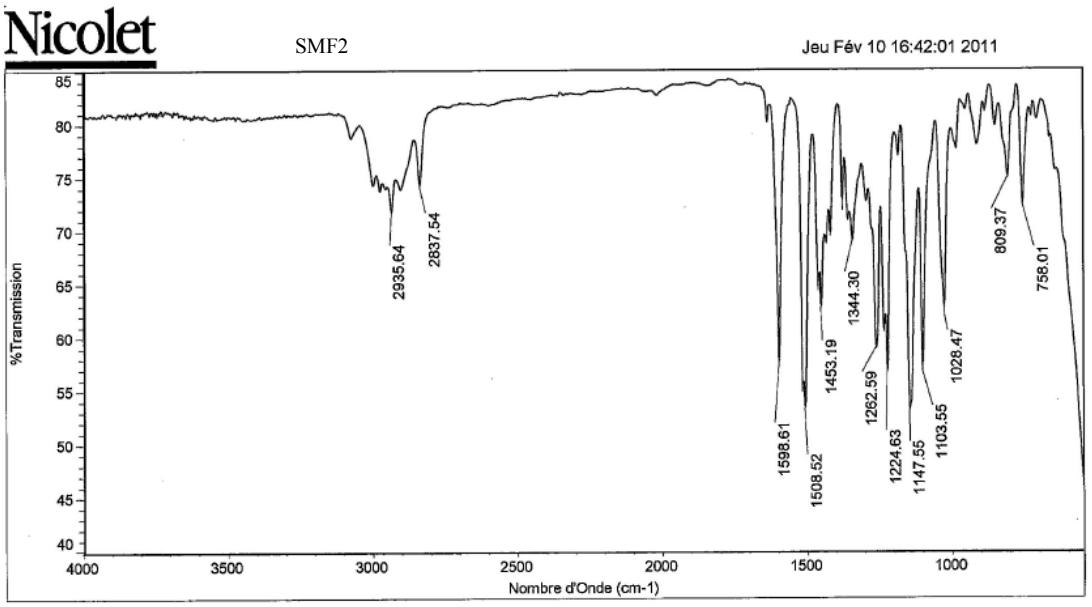

Figure 201 IR spectrum of compound SMF2 [**111**] (film)

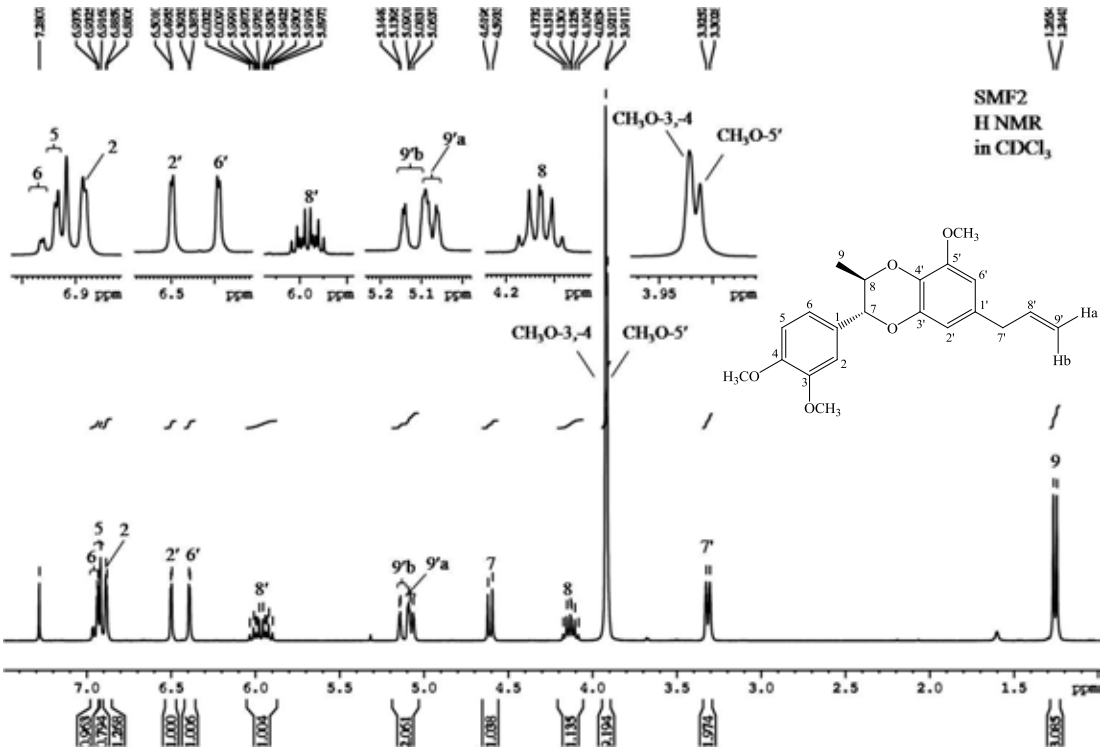

Figure 202 ^{1}H-NMR spectrum of compound SMF2 [**111**] ($CDCl_3$)

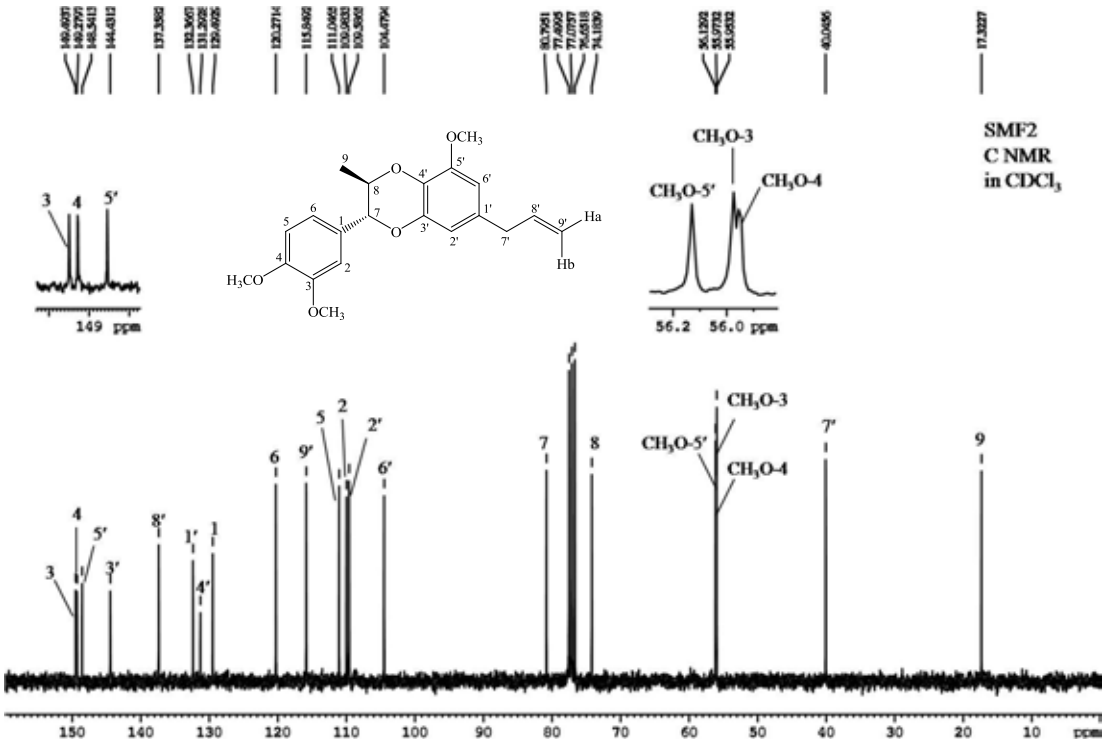

Figure 203 ^{13}C-NMR spectrum of compound SMF2 [**111**] ($CDCl_3$)

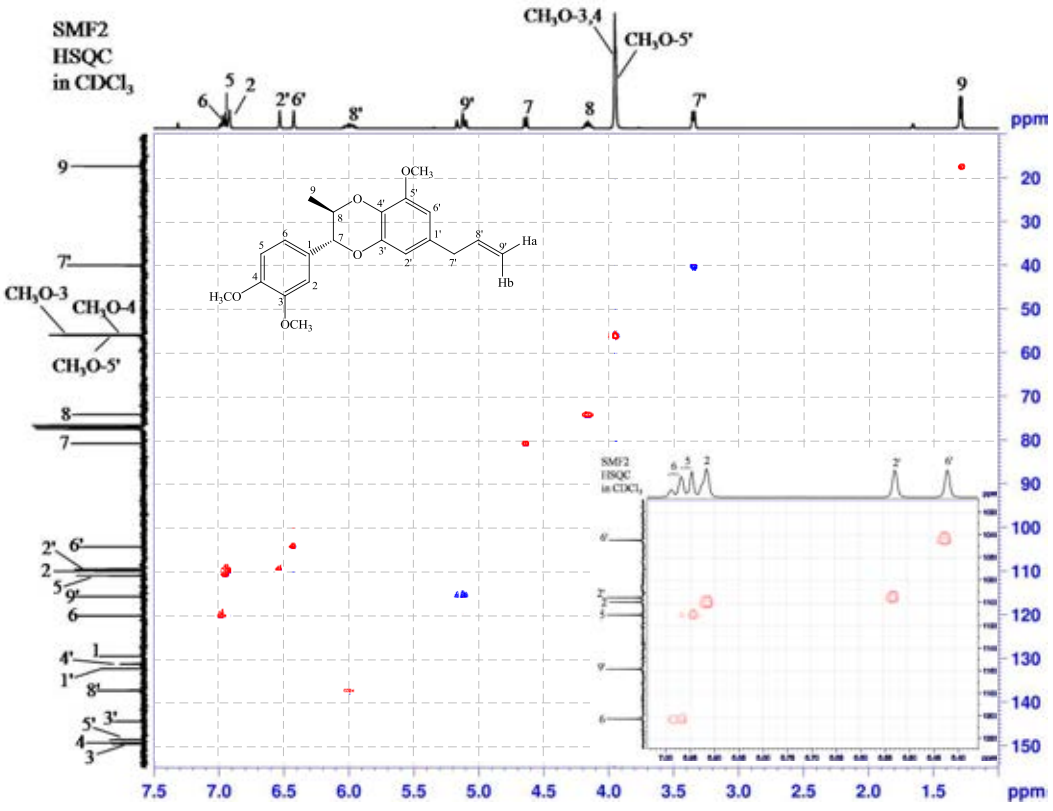

Figure 204 HSQC spectrum of compound SMF2 [**111**] ($CDCl_3$)

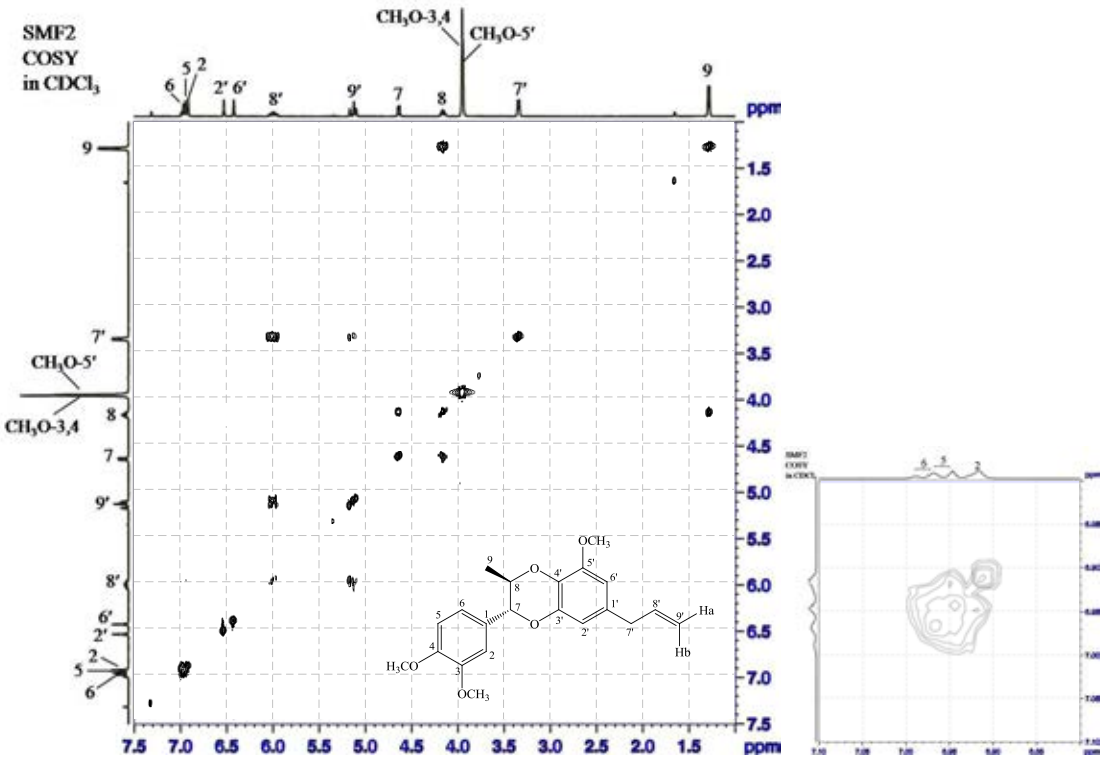

Figure 205 ^{1}H-^{1}H COSY spectrum of compound SMF2 [**111**] ($CDCl_3$)

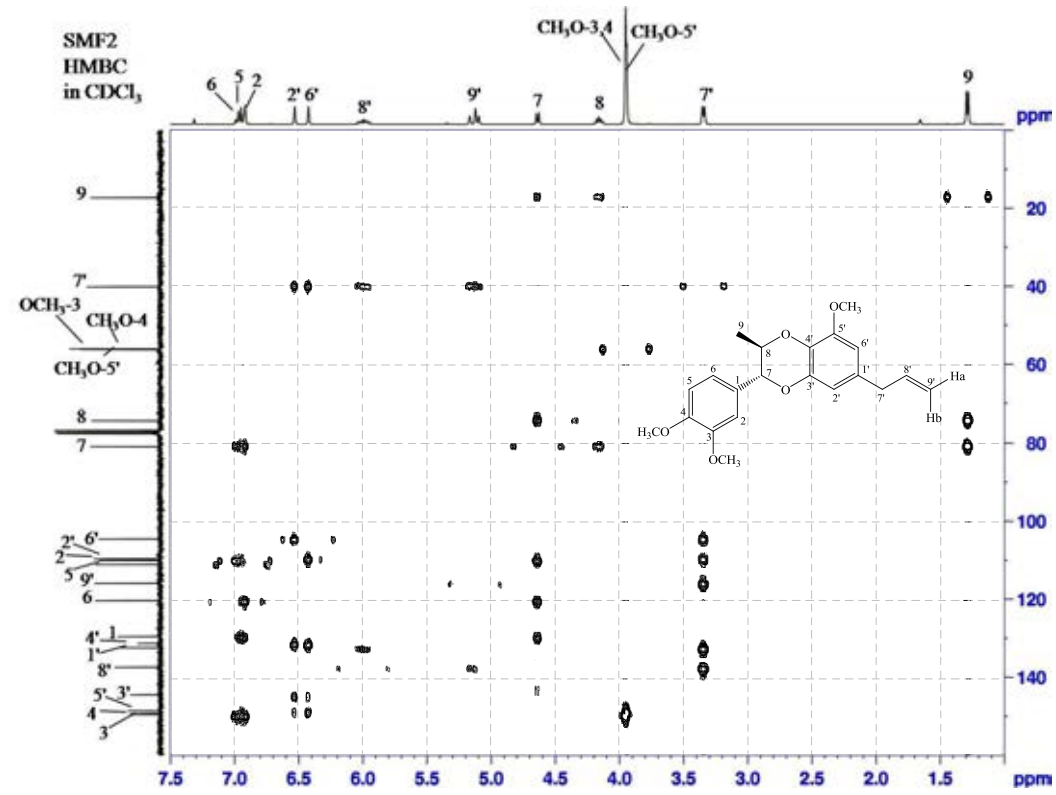

Figure 206 HMBC spectrum of compound SMF2 [**111**] ($CDCl_3$)

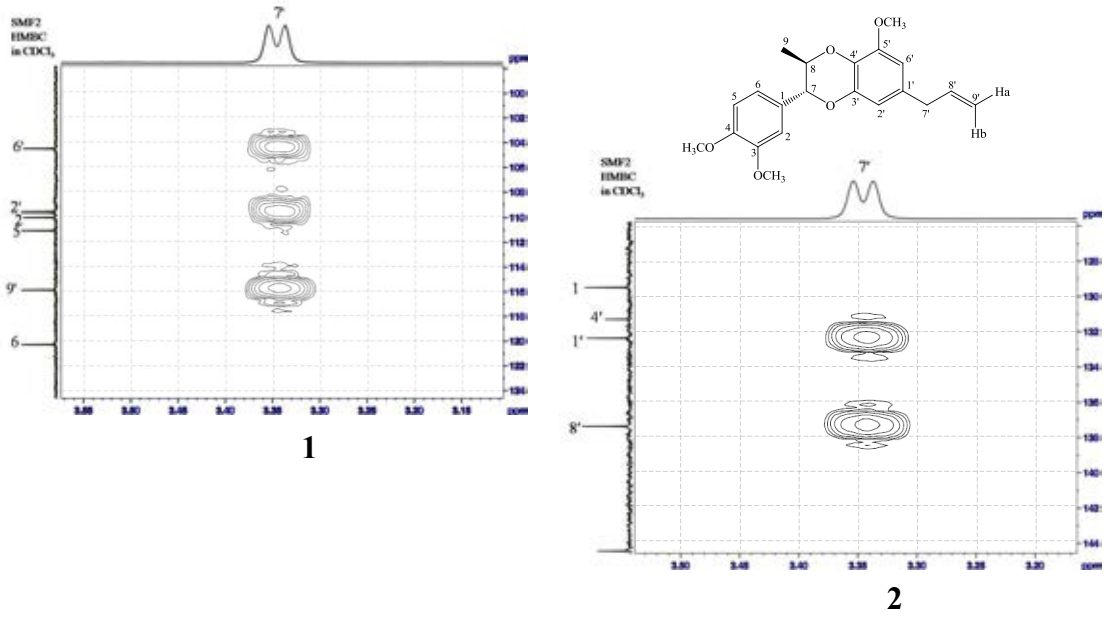

Figure 206a HMBC spectrum of compound SMF2 [**111**] ($CDCl_3$)
[δ_H 3.57-3.11 ppm, δ_C 124.5-98.0 ppm (1)] and
[δ_H 3.54-3.16 ppm, δ_C 144.5-126.0 ppm (2)]

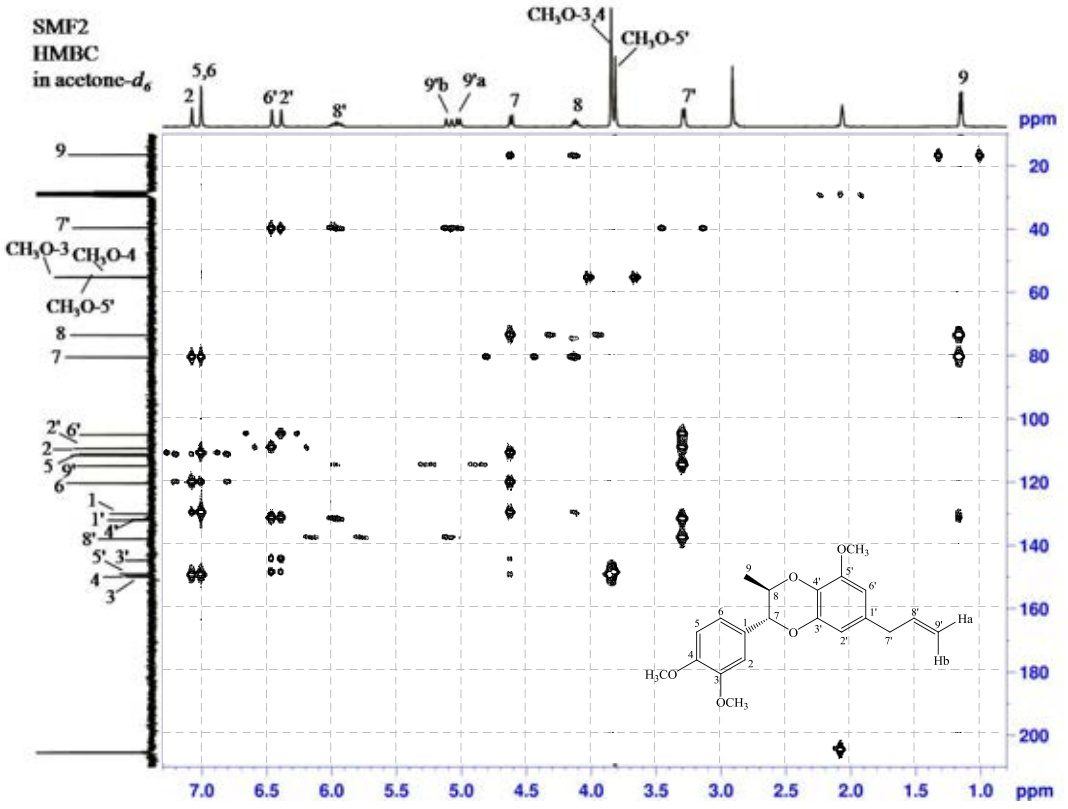

Figure 207 HMBC spectrum of compound SMF2 [**111**] (acetone-d_6)

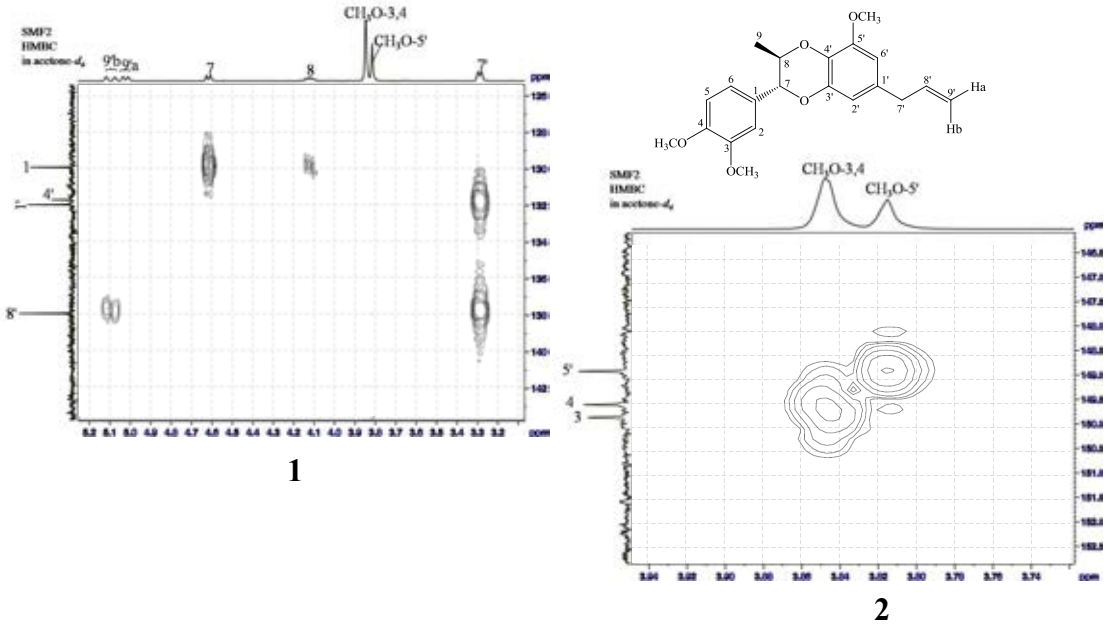

1 **2**

Figure 207a HMBC spectrum of compound SMF2 [**111**] (acetone-d_6)
[δ_H 5.27-3.07 ppm, δ_C 144.0-125.5 ppm (1)] and
[δ_H 3.95-3.72 ppm, δ_C 152.9-146.1 ppm (2)]

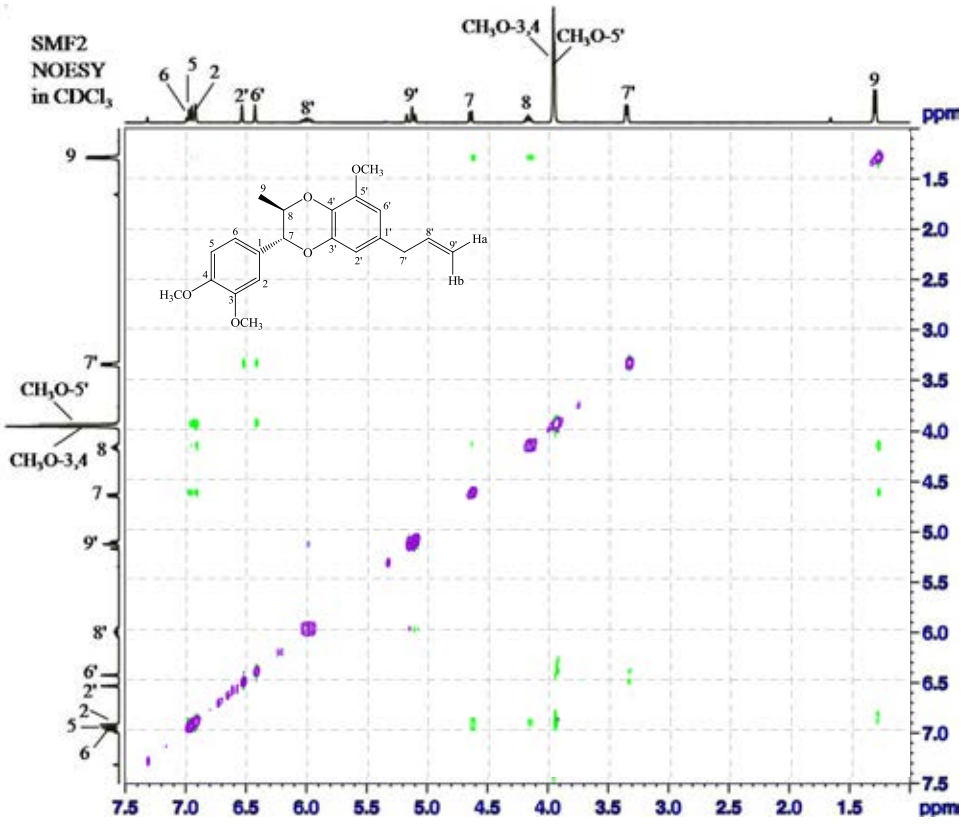

Figure 208 NOESY spectrum of compound SMF2 [**111**] ($CDCl_3$)

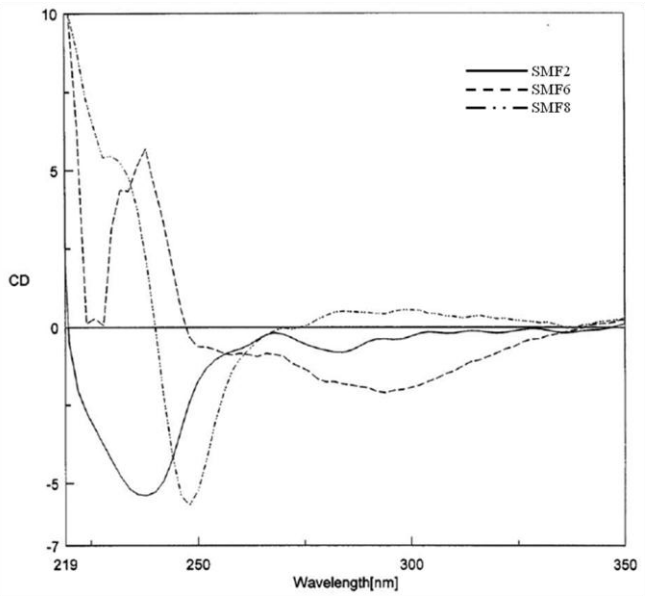

Figure 209 CD spectra (MeOH) of compounds SMF2 [**111**], SMF6 [**113**] and SMF8 [**115**]

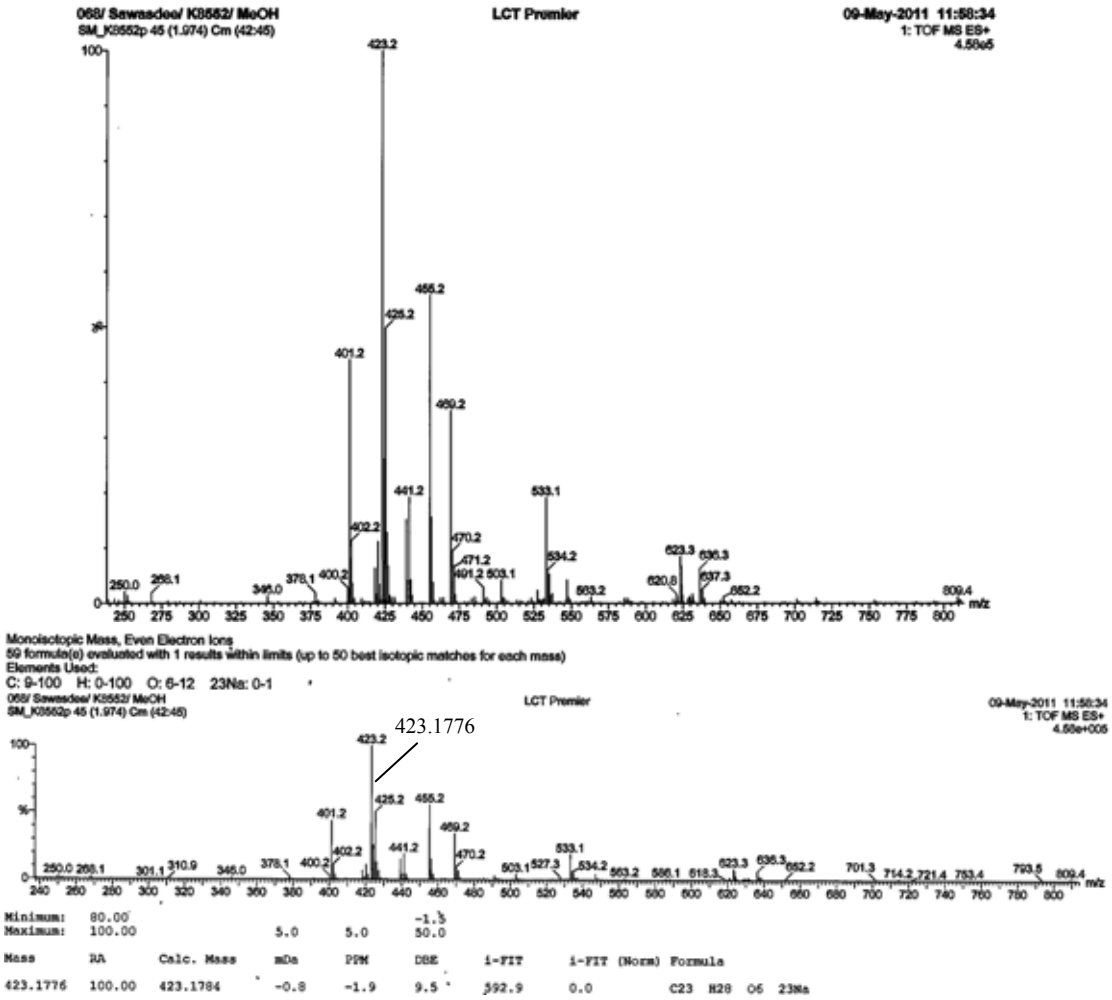

Figure 210 HRESI mass spectrum of compound SMF3 [**112**]

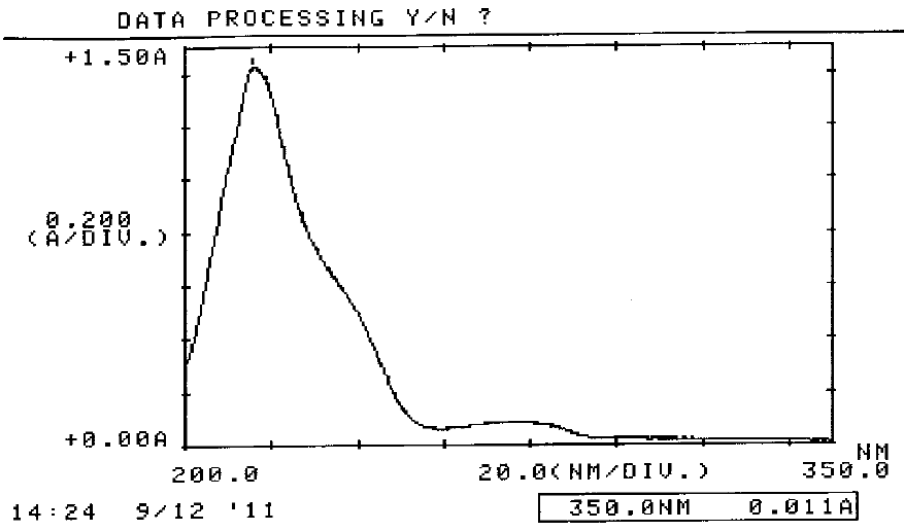

Figure 211 UV spectrum of compound SMF3 [**112**] (MeOH)

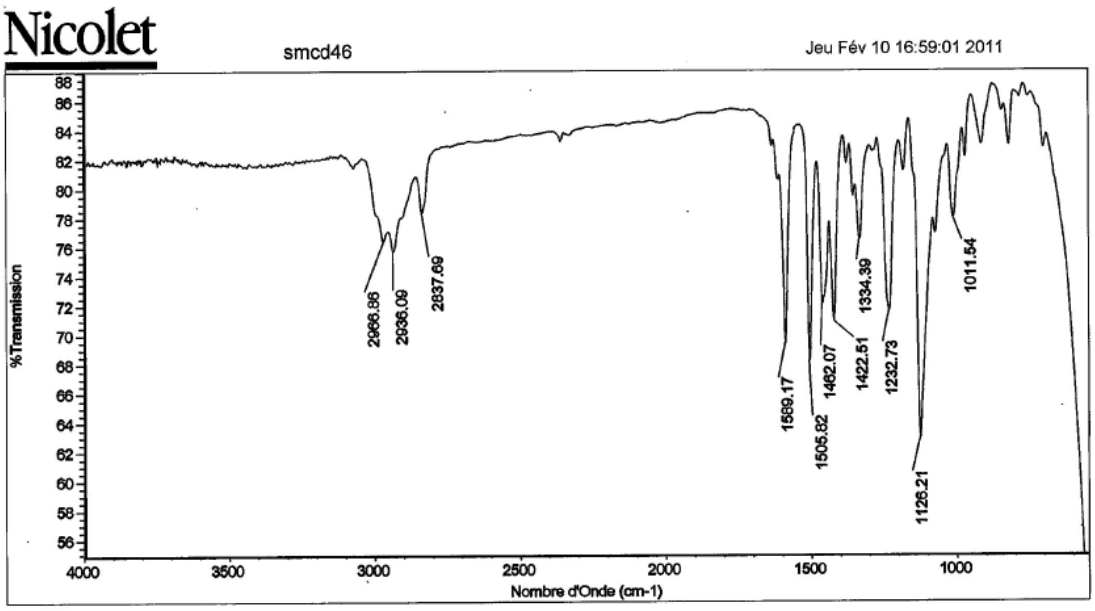

Figure 212 IR spectrum of compound SMF3 [**112**] (film)

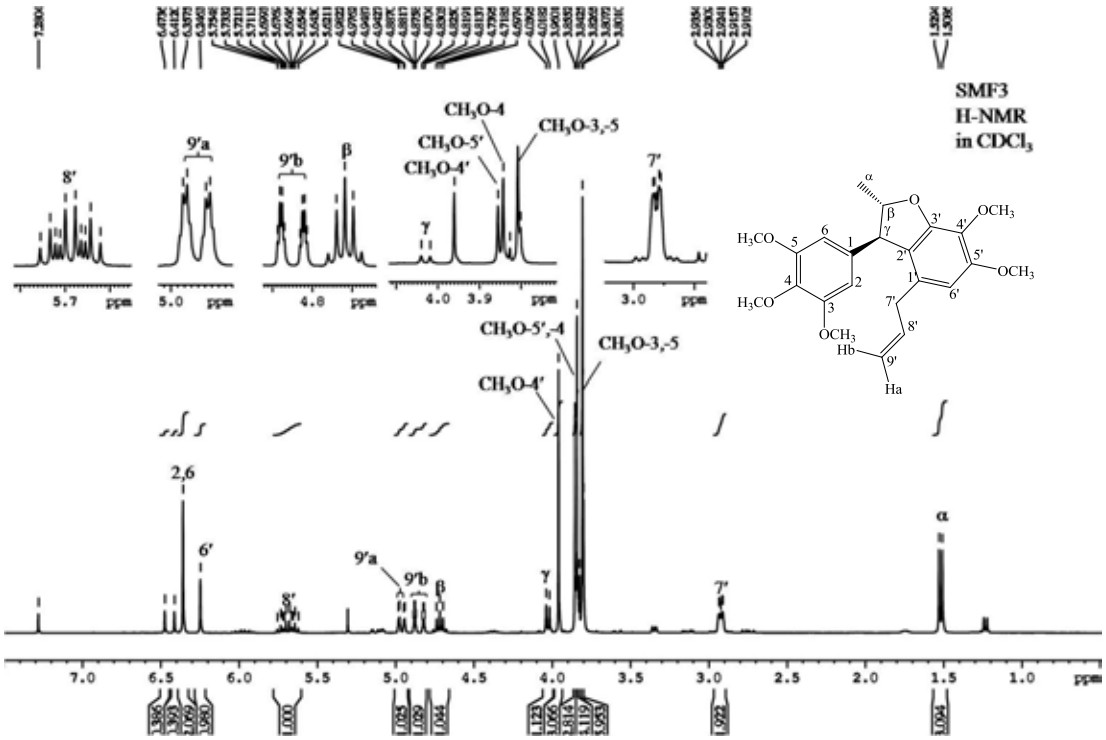

Figure 213 ^{1}H-NMR spectrum of compound SMF3 [**112**] ($CDCl_3$)

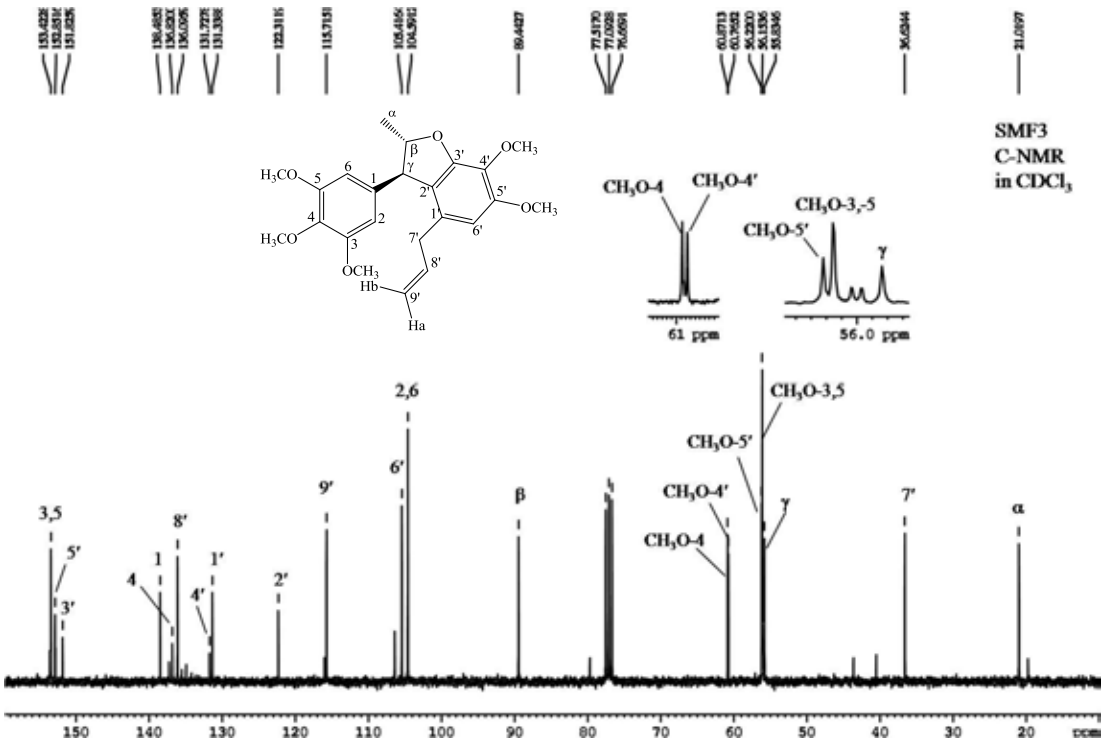

Figure 214 ^{13}C-NMR spectrum of compound SMF3 [**112**] ($CDCl_3$)

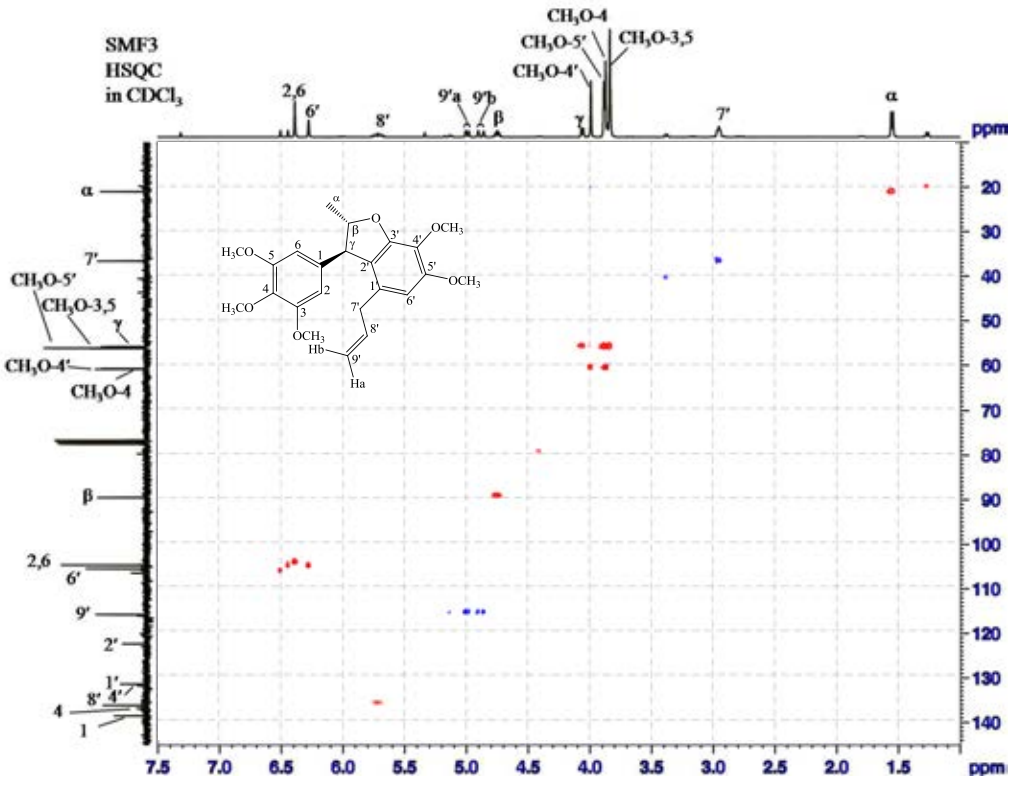

Figure 215 HSQC spectrum of compound SMF3 [**112**] ($CDCl_3$)

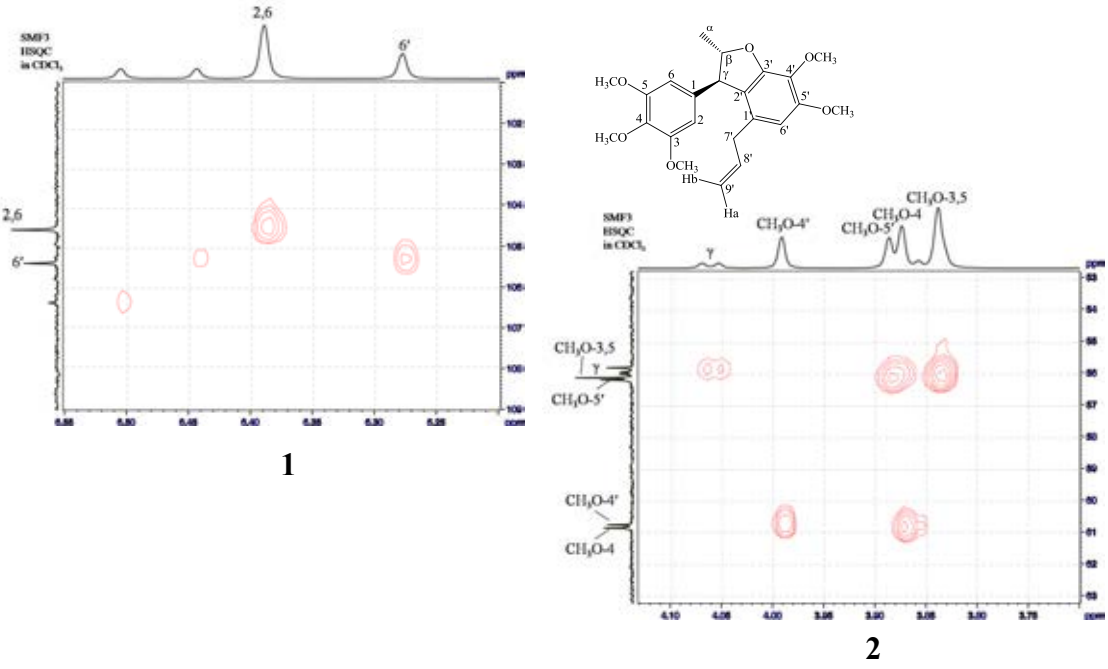

Figure 215a HSQC spectrum of compound SMF3 [**112**] ($CDCl_3$)
[δ_H 6.55-6.20 ppm, δ_C 109.0-101.0 ppm (**1**)] and
[δ_H 4.13-3.70 ppm, δ_C 63.2-52.9 ppm (**2**)]

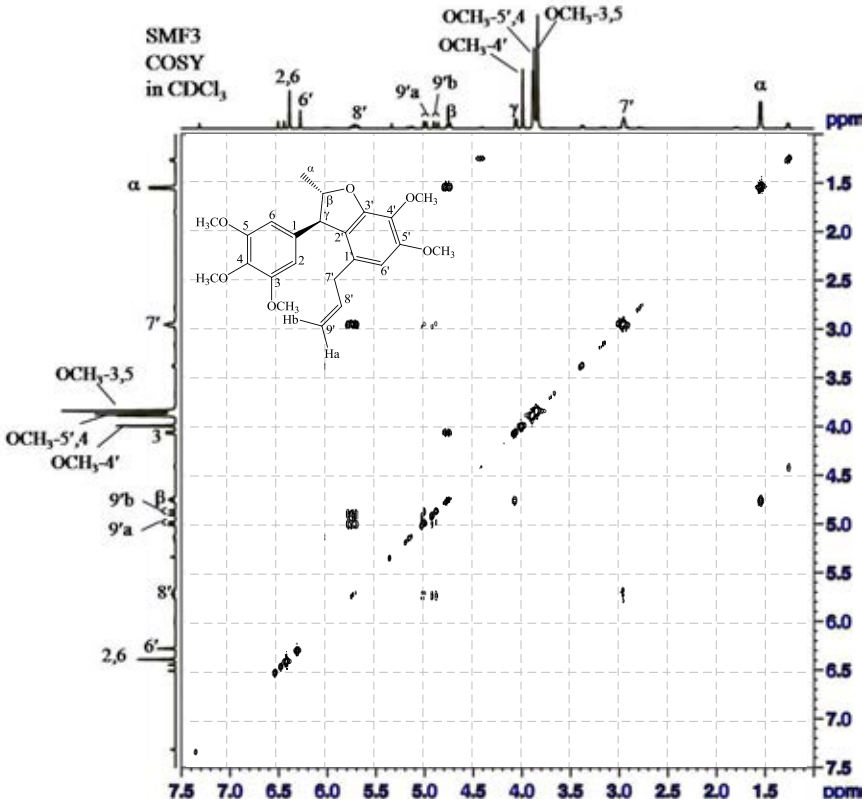

Figure 216 ^{1}H-^{1}H COSY spectrum of compound SMF3 [**112**] ($CDCl_3$)

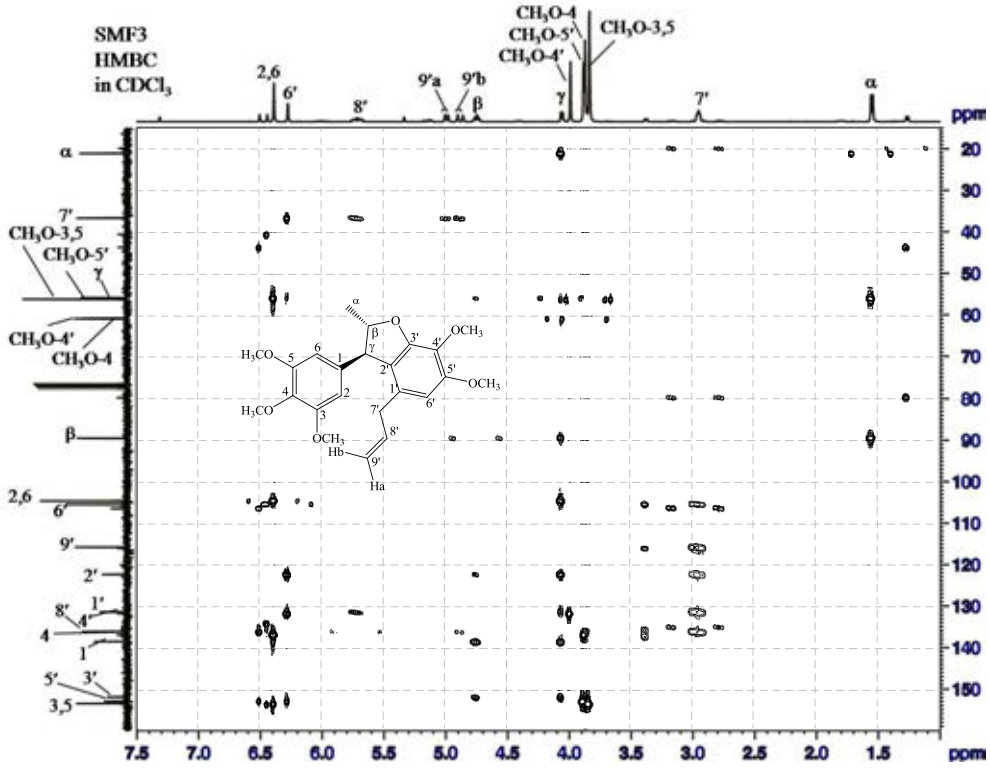

Figure 217 HMBC spectrum of compound SMF3 [**112**] ($CDCl_3$)

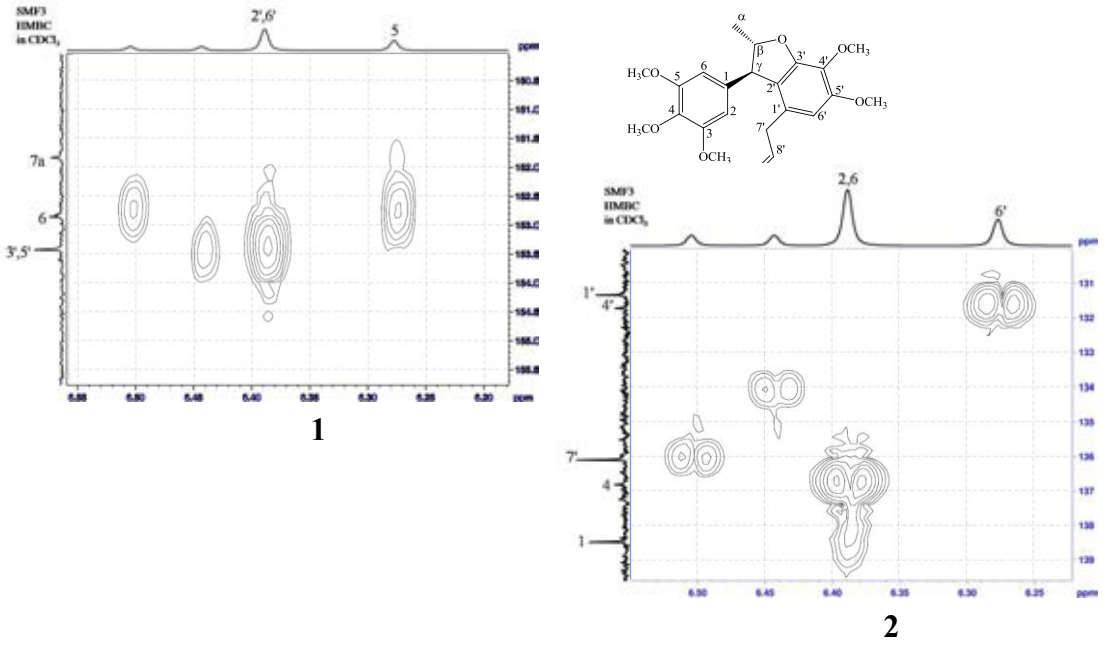

Figure 217a HMBC spectrum of compound SMF3 [**112**] ($CDCl_3$)
[δ_H 6.56-6.18 ppm, δ_C 155.8-150.0 ppm (1)] and
[δ_H 6.55-6.23 ppm, δ_C 139.6-130.0 ppm (2)]

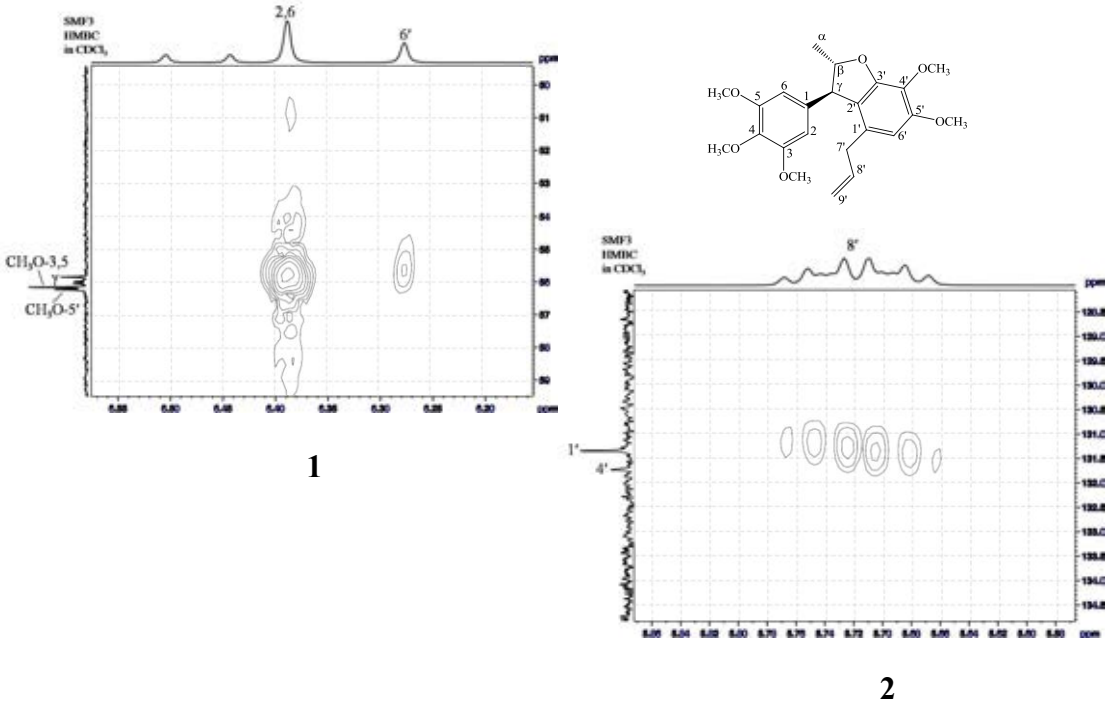

Figure 217b HMBC spectrum of compound SMF3 [**112**] ($CDCl_3$)
[δ_H 6.58-6.16 ppm, δ_C 59.5-50.4 ppm (1)] and
[δ_H 5.87-5.57 ppm, δ_C 134.8-128.0 ppm (2)]

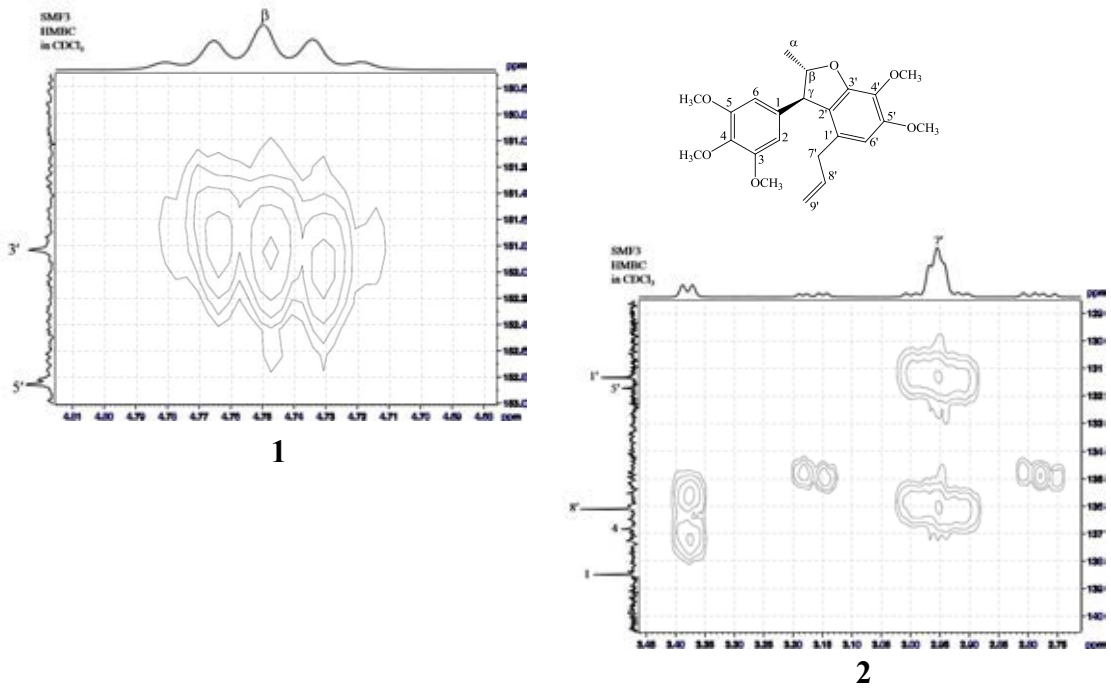

Figure 217c HMBC spectrum of compound SMF3 [**112**] ($CDCl_3$)
[δ_H 4.82-4.68 ppm, δ_C 153.0-150.5 ppm (1)] and
[δ_H 3.46-2.71 ppm, δ_C 140.6-128.5 ppm (2)]

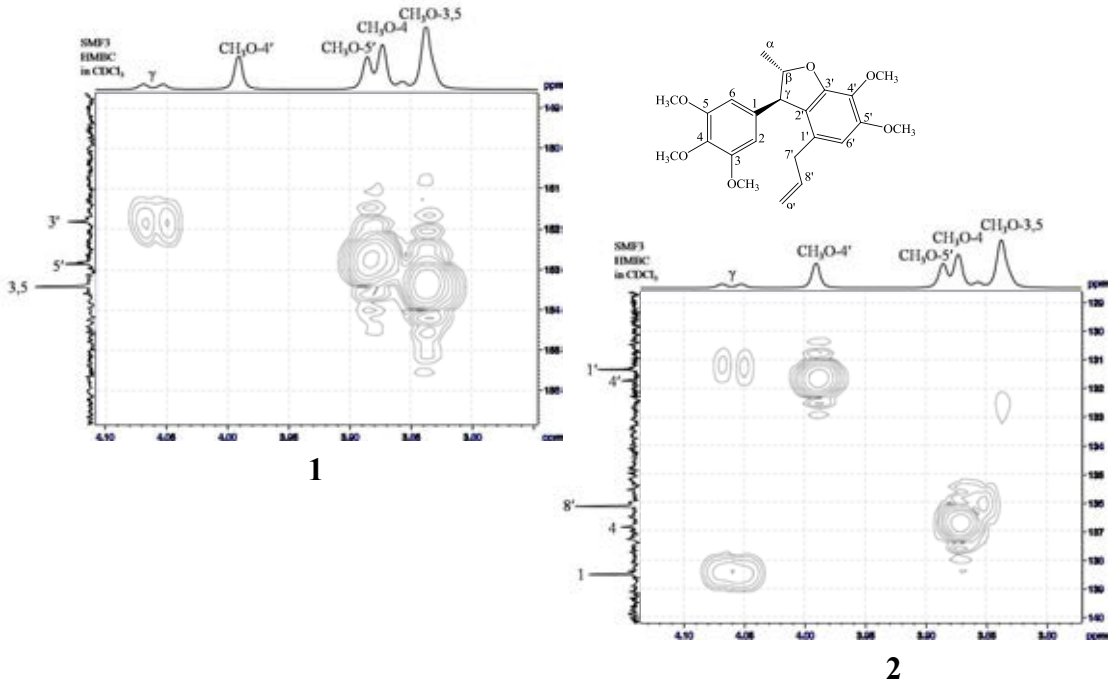

Figure 217d HMBC spectrum of compound SMF3 [**112**] ($CDCl_3$)
[δ_H 4.11-3.75 ppm, δ_C 156.8-148.7 ppm (1)] and
[δ_H 4.14-3.77 ppm, δ_C 140.2-128.6 ppm (2)]

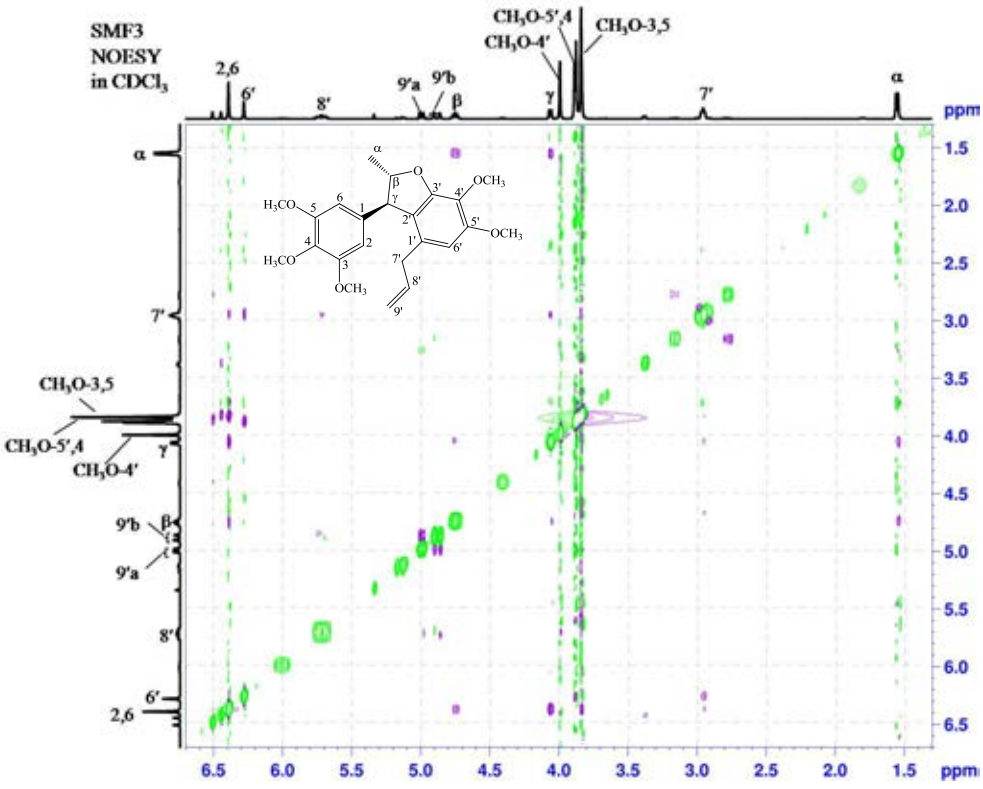

Figure 218 NOESY spectrum of compound SMF3 [**112**] ($CDCl_3$)

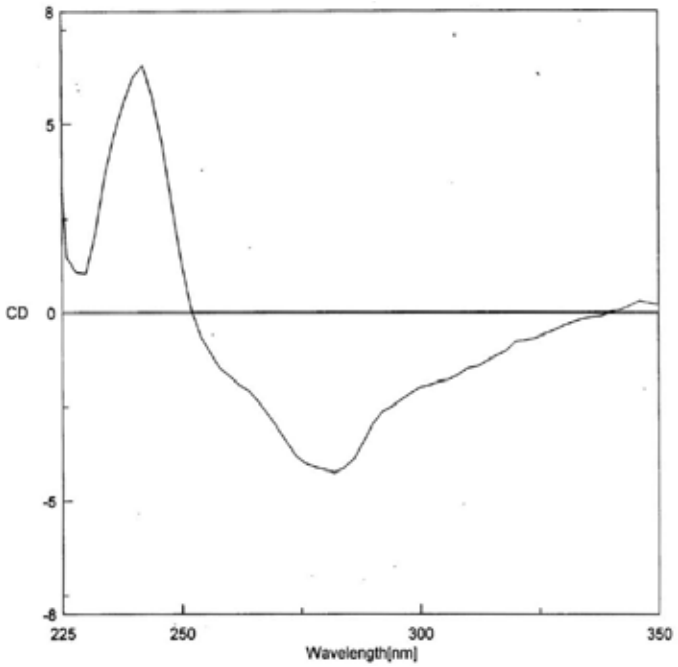

Figure 219 CD spectrum of compound SMF3 [**112**] (MeOH)

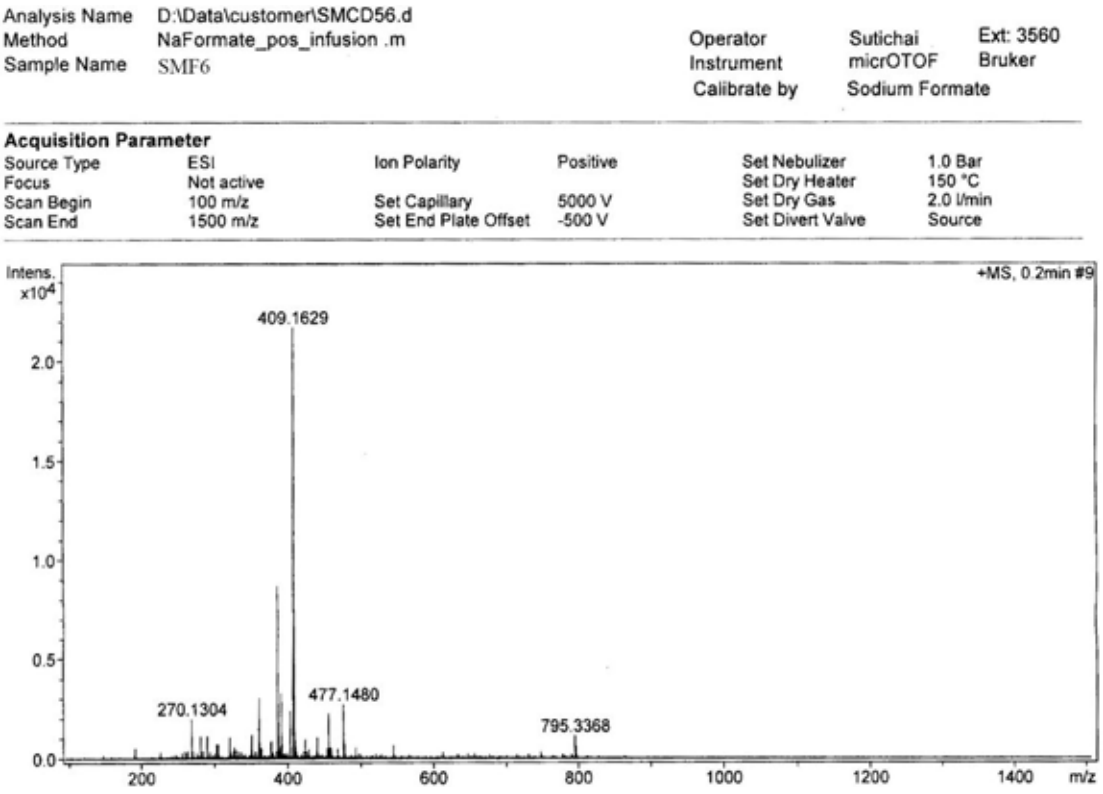

Figure 220 HRESI mass spectrum of compound SMF6 [**112**]

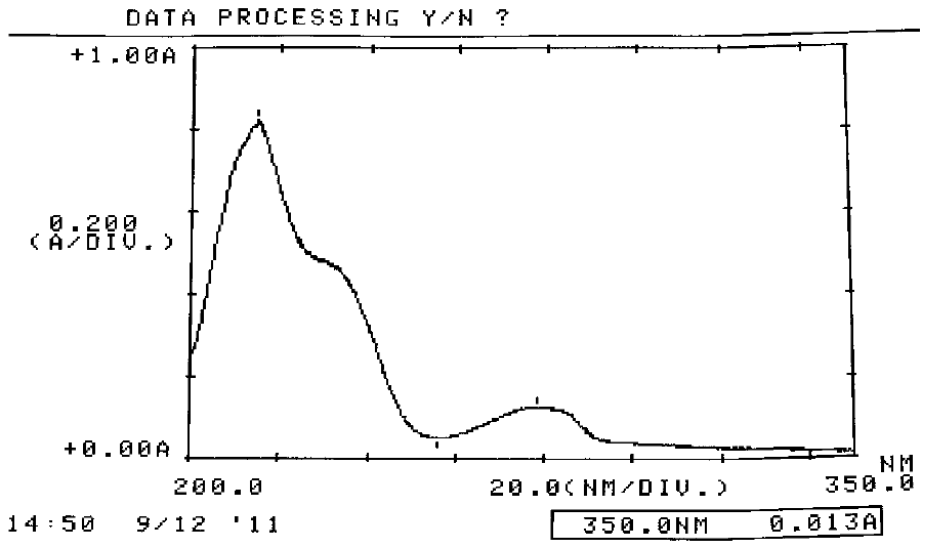

Figure 221 UV spectrum of compound SMF6 [**112**] (MeOH)

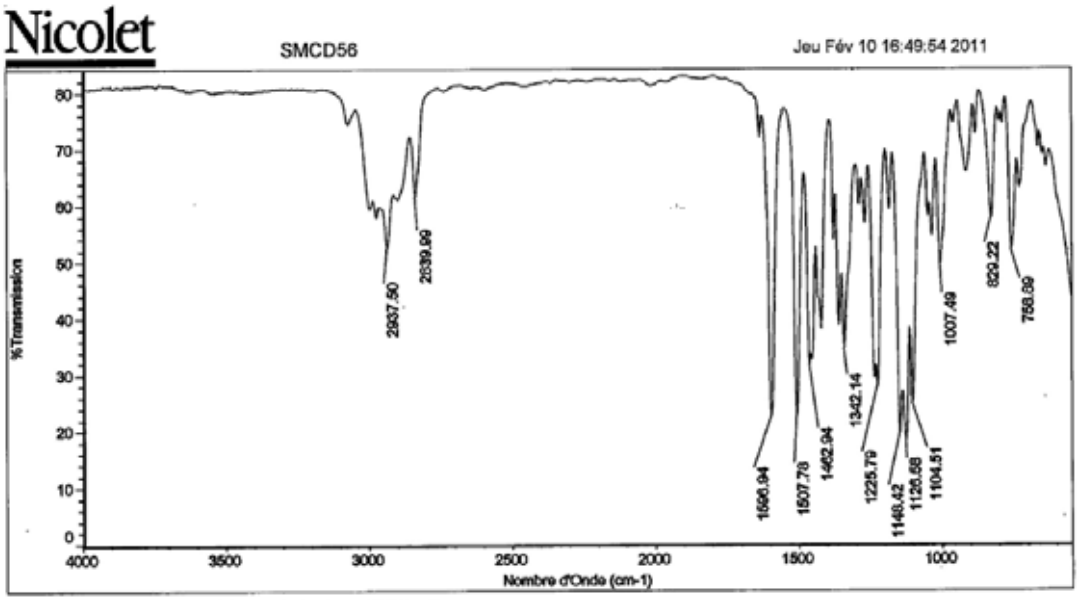

Figure 222 IR spectrum of compound SMF6 [**112**] (film)

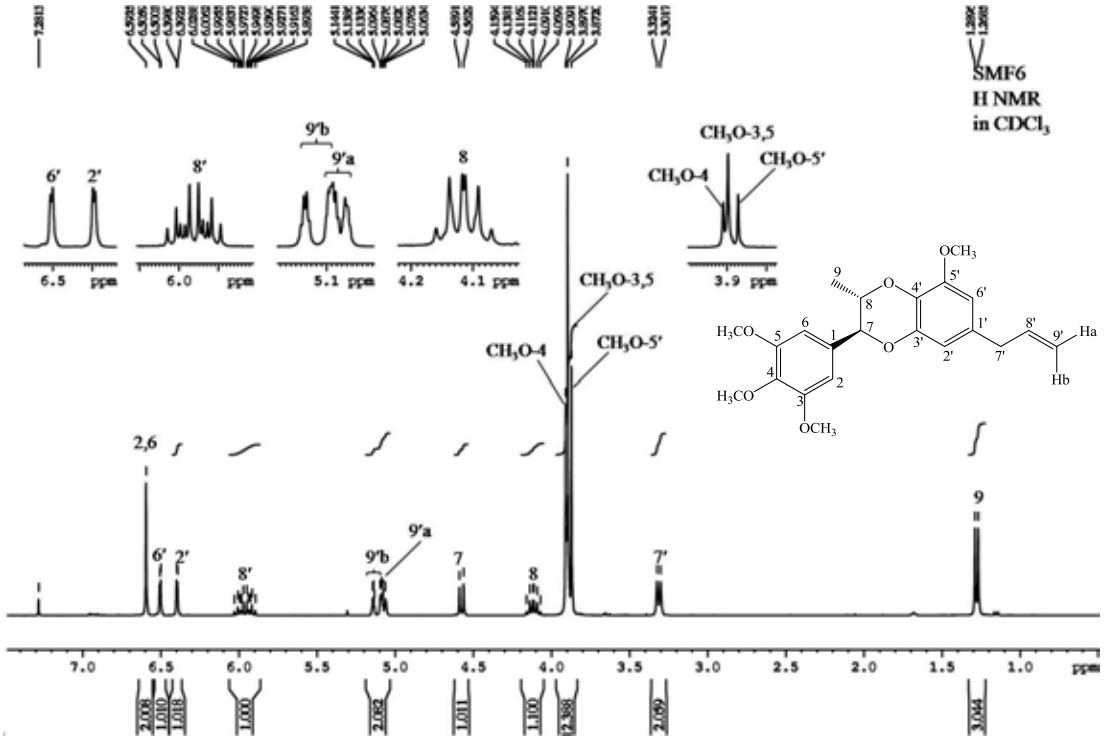

Figure 223 ^{1}H-NMR spectrum of compound SMF6 [**112**] ($CDCl_3$)

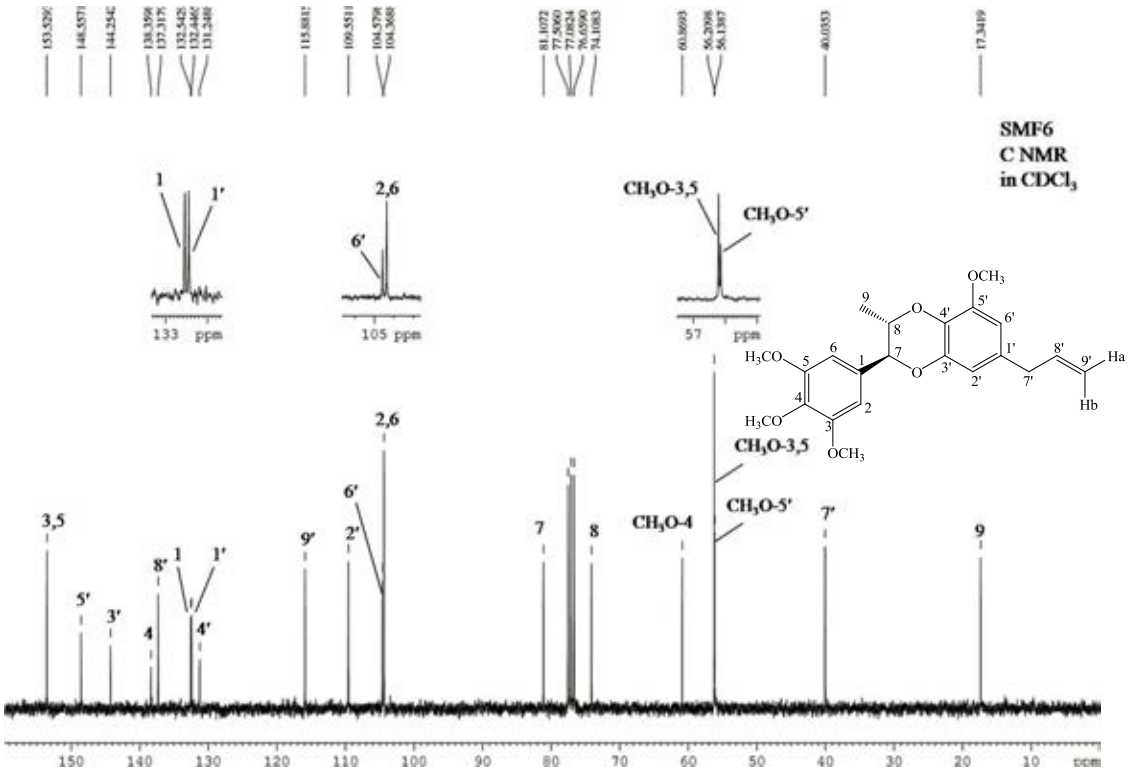

Figure 224 ^{13}C-NMR spectrum of compound SMF6 [**112**] ($CDCl_3$)

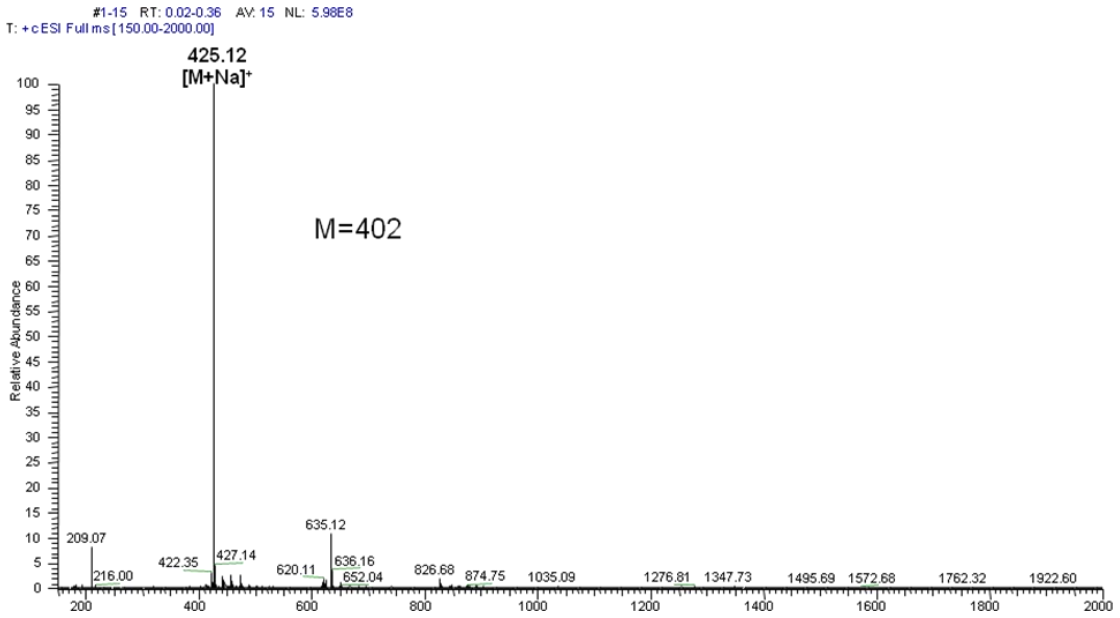

Figure 225 ESI mass spectrum of compound SMF7 [**114**]

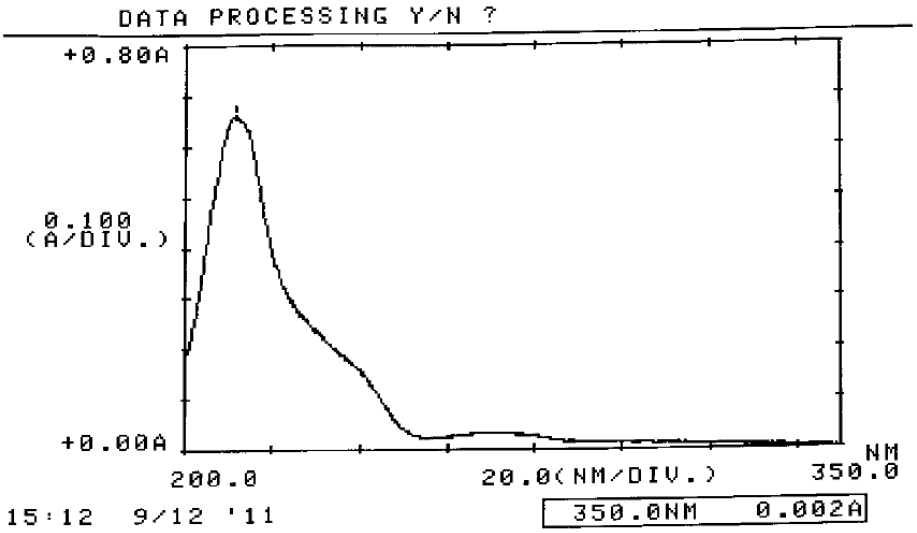

Figure 226 UV spectrum of compound SMF7 [**114**] (MeOH)

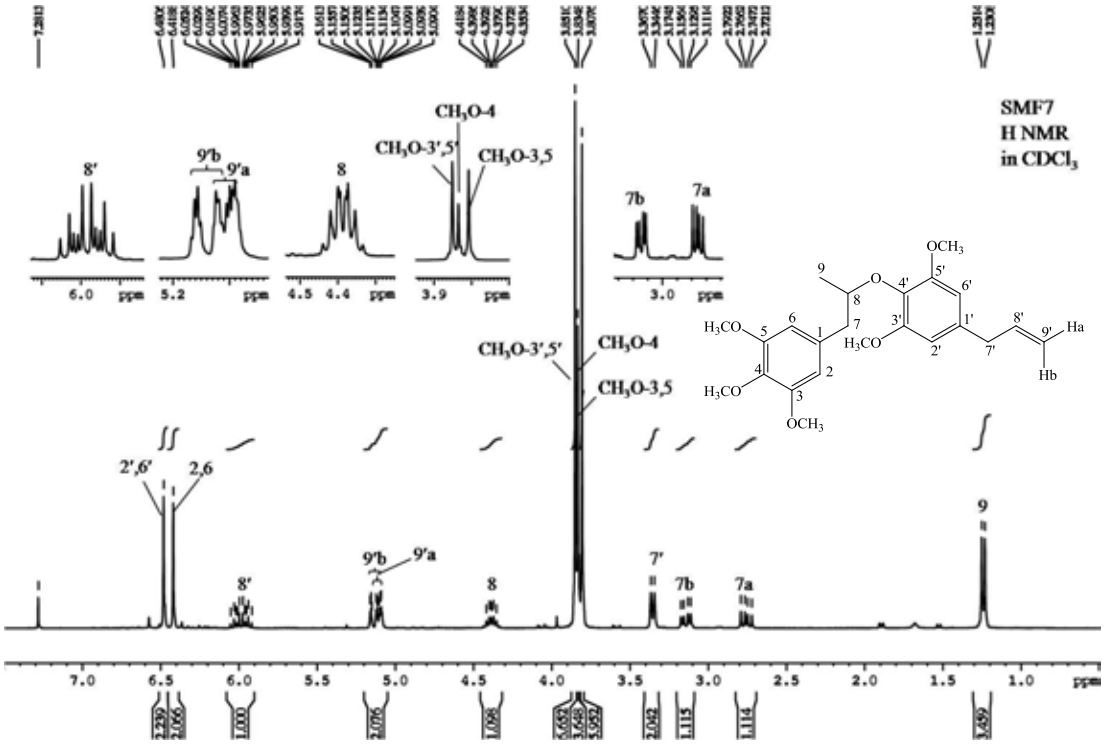

Figure 227 ^{1}H-NMR spectrum of compound SMF7 [**114**] ($CDCl_3$)

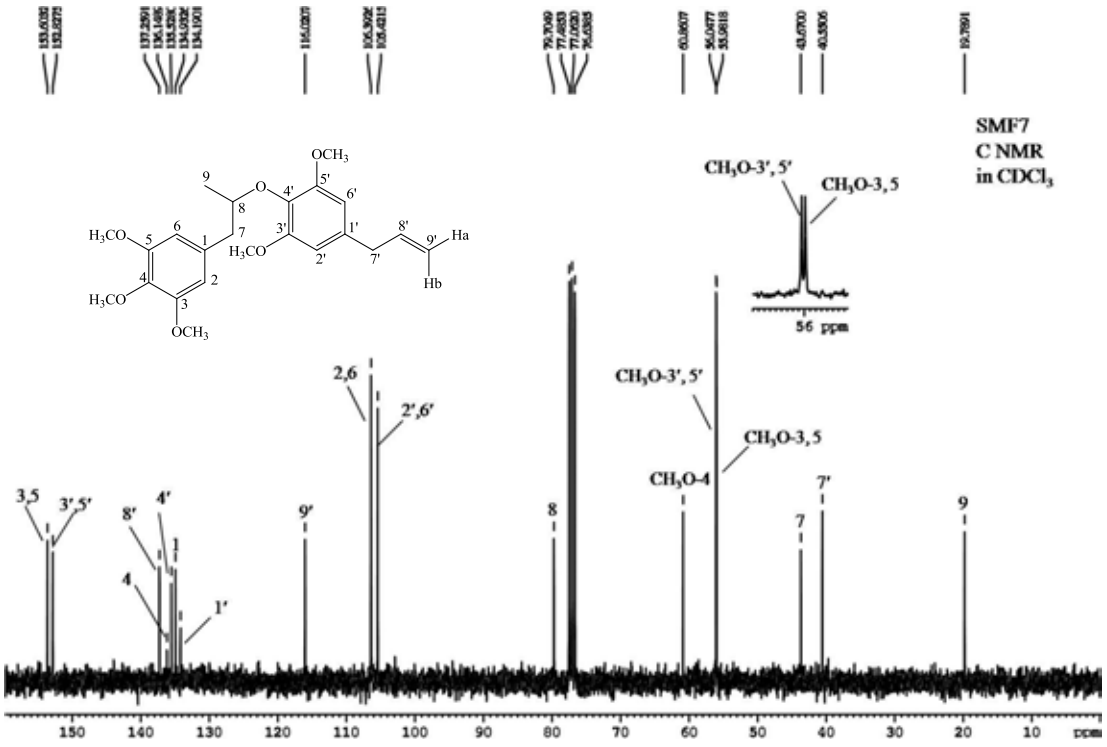

Figure 228 ^{13}C-NMR spectrum of compound SMF7 [**114**] ($CDCl_3$)

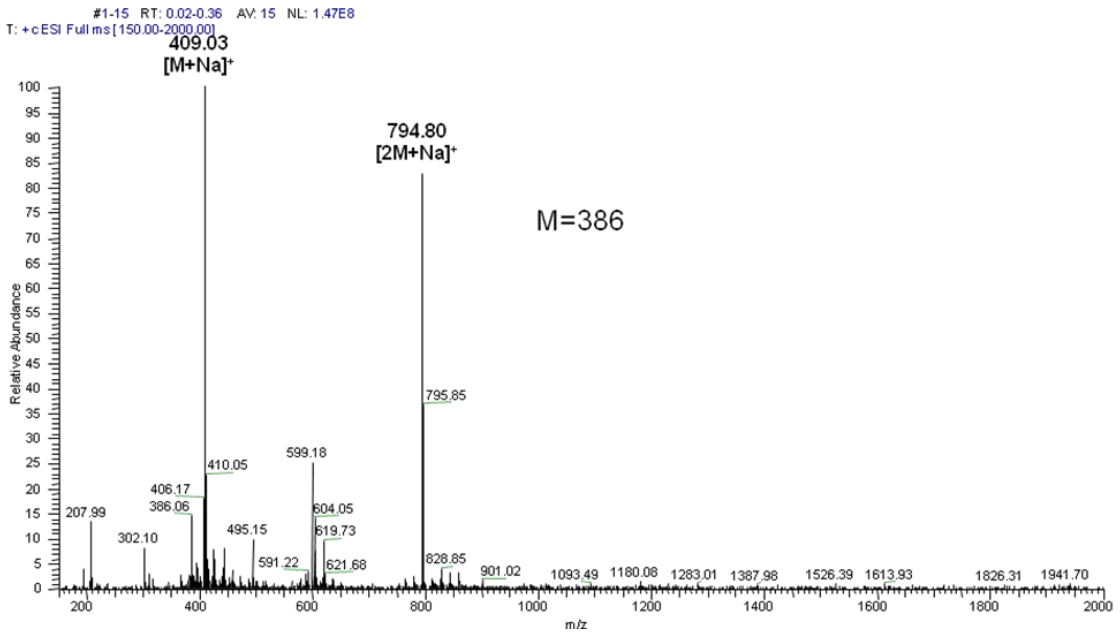

Figure 229 ESI mass spectrum of compound SMF8 [**115**]

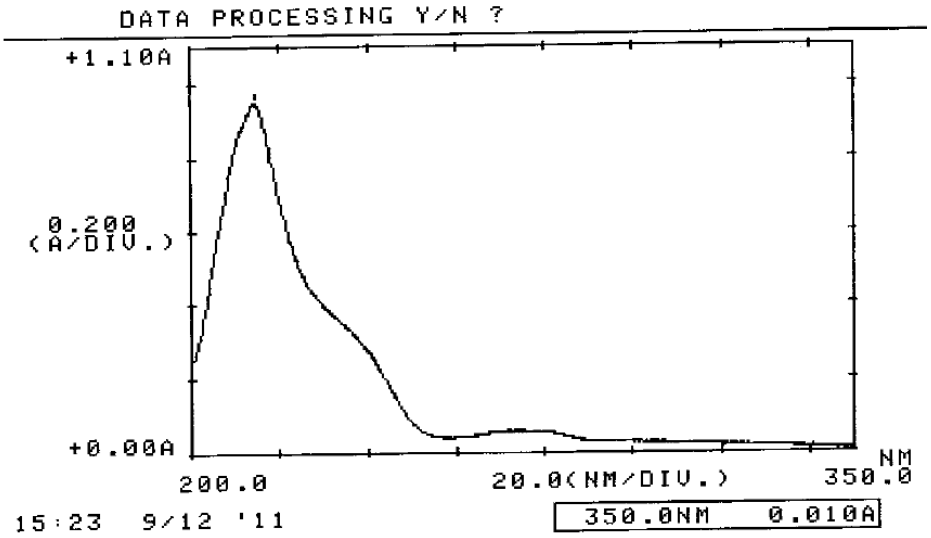

Figure 230 UV spectrum of compound SMF8 [**115**] (MeOH)

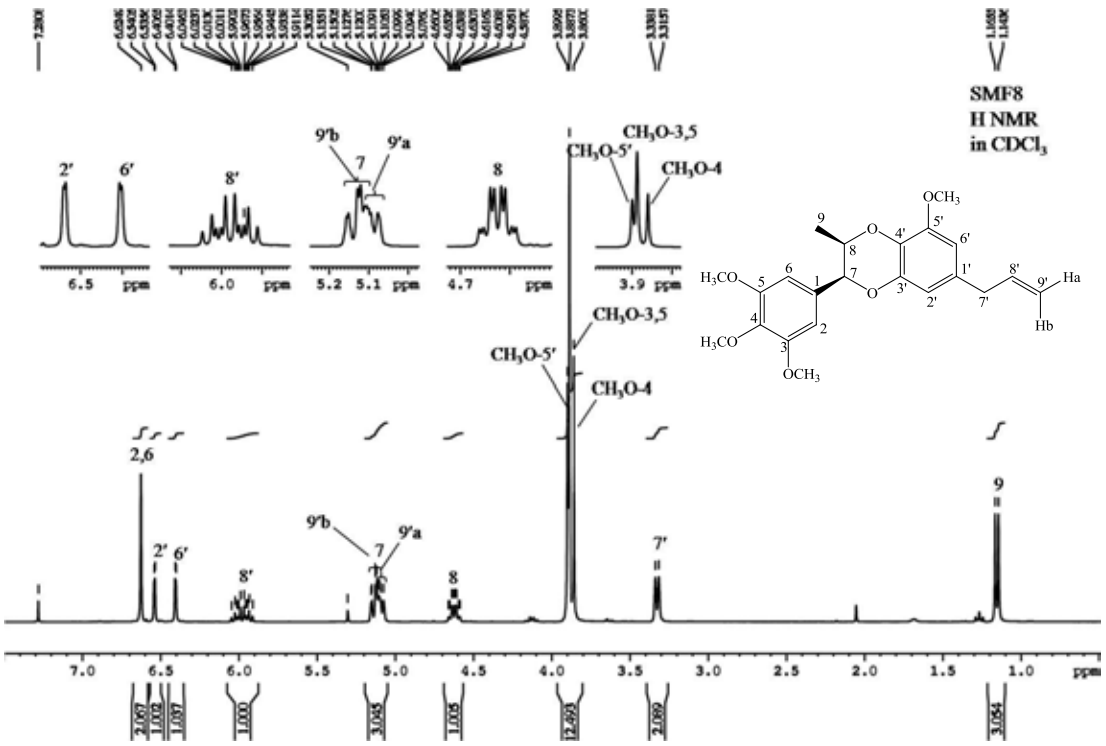

Figure 231 ^{1}H-NMR spectrum of compound SMF8 [**115**] ($CDCl_3$)

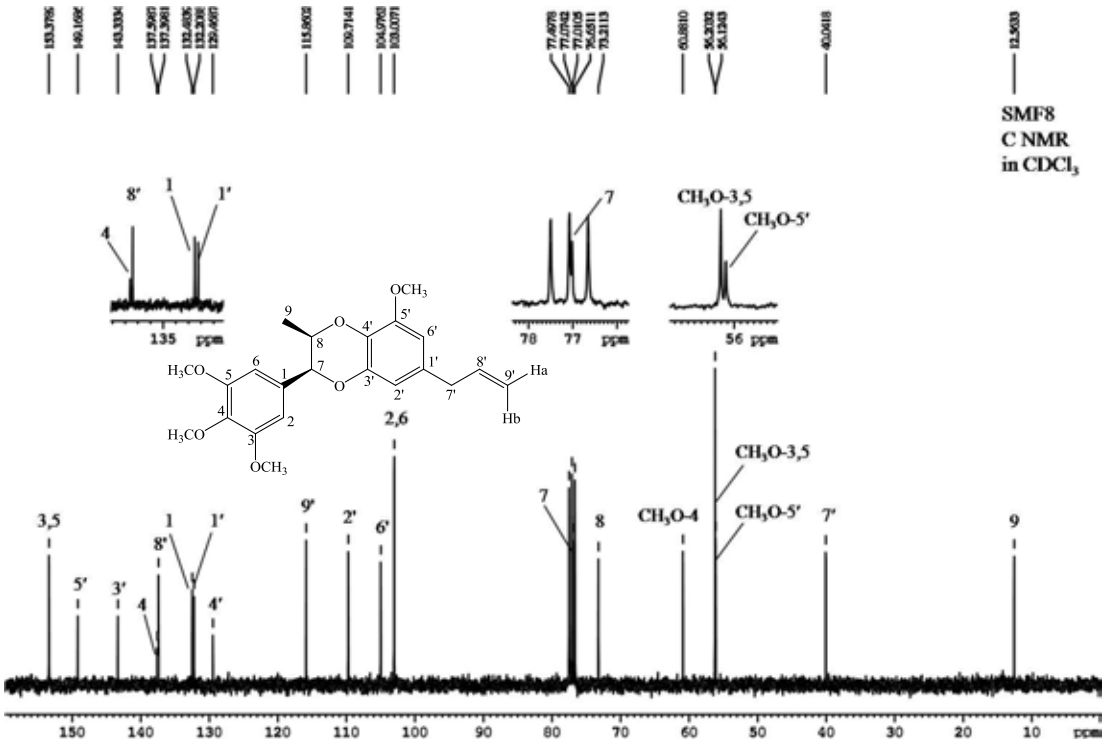

Figure 232 ^{13}C-NMR spectrum of compound SMF8 [**115**] ($CDCl_3$)

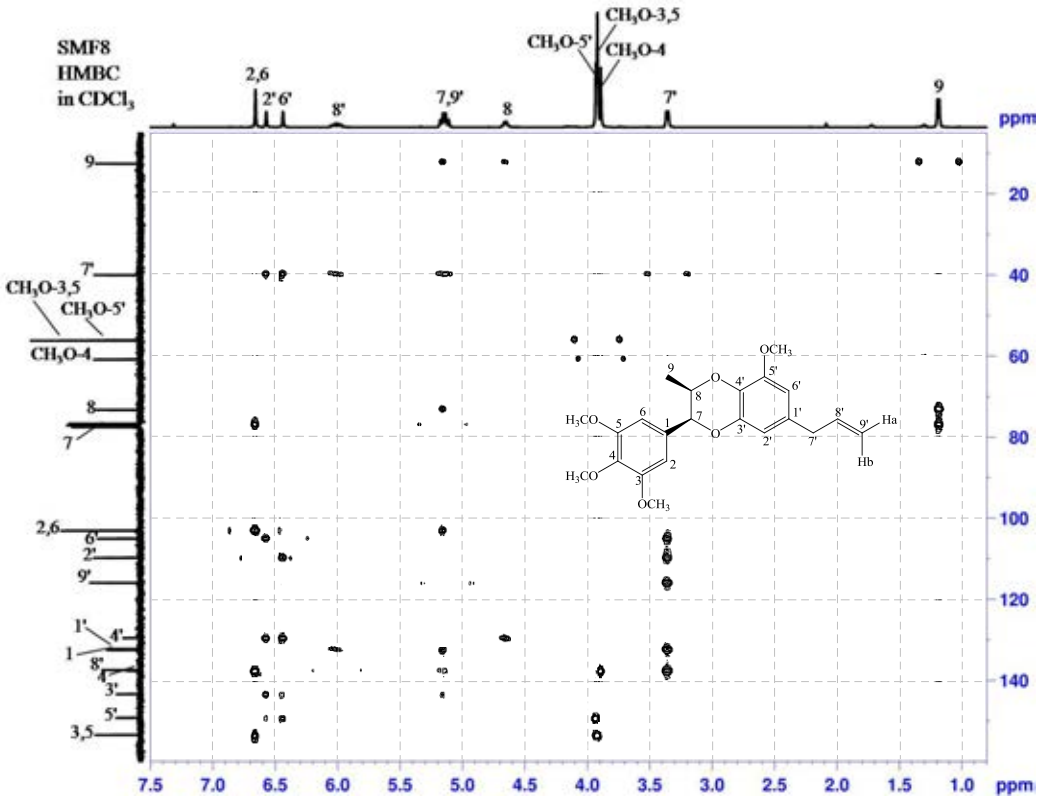

Figure 233 HMBC spectrum of compound SMF8 [**115**] ($CDCl_3$)

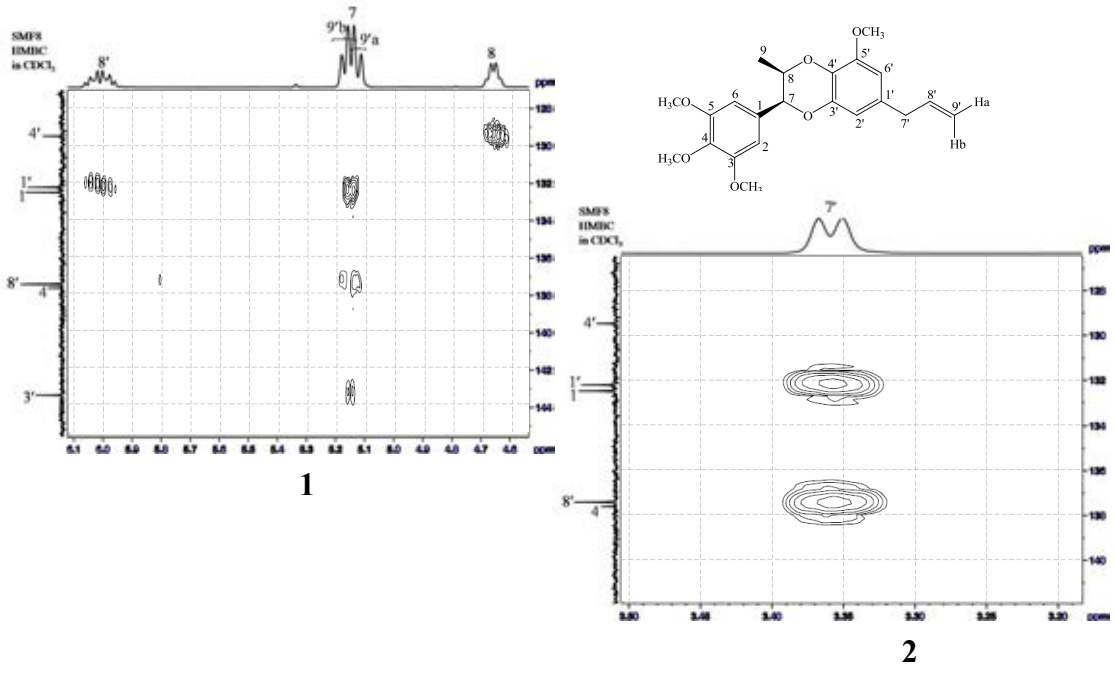

Figure 233a HMBC spectrum of compound SMF8 [**115**] ($CDCl_3$)
[δ_H 6.12-4.56 ppm, δ_C 145.5-127.0 ppm (1)] and
[δ_H 3.51-3.18 ppm, δ_C 142.0-126.5 ppm (2)]

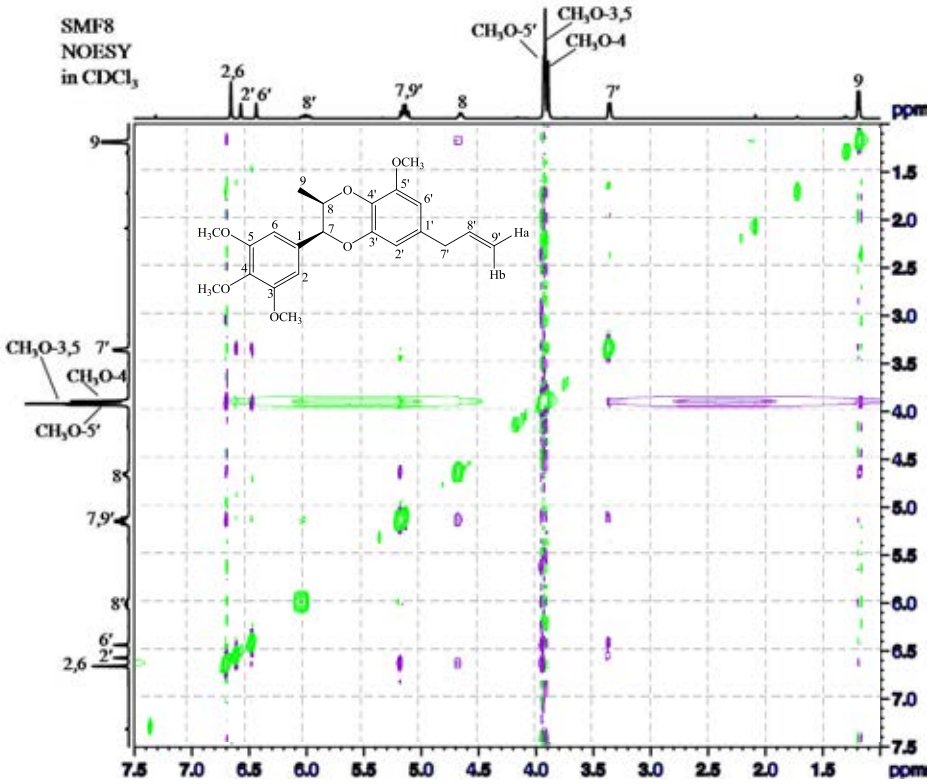

Figure 234 NOESY spectrum of compound SMF8 [**115**] ($CDCl_3$)

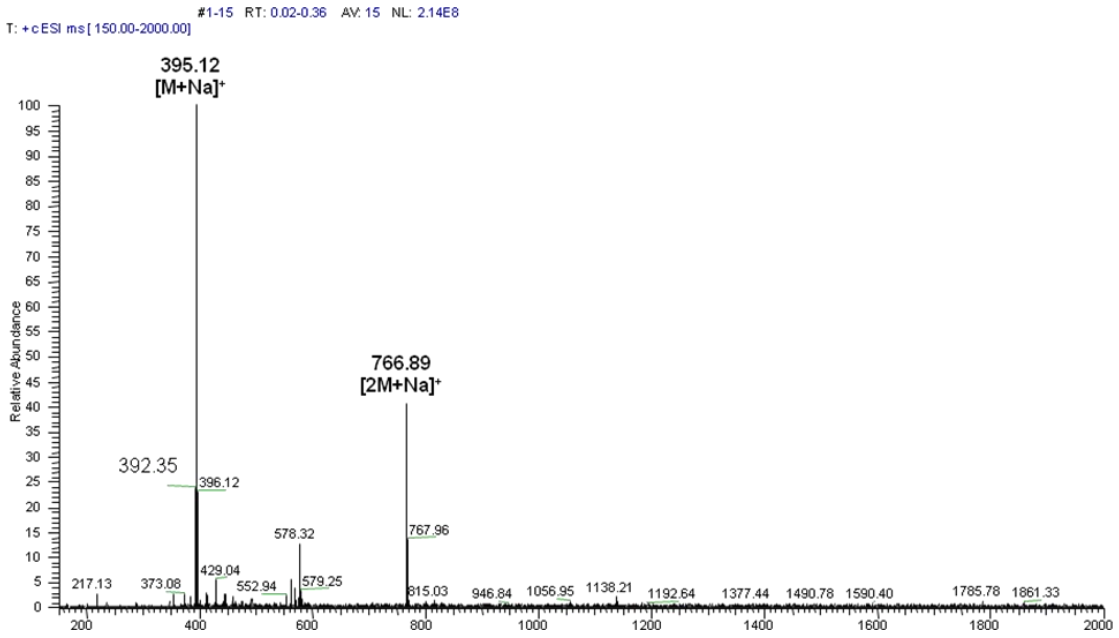

Figure 235 ESI Mass spectrum of compound SMF9 [**116**]

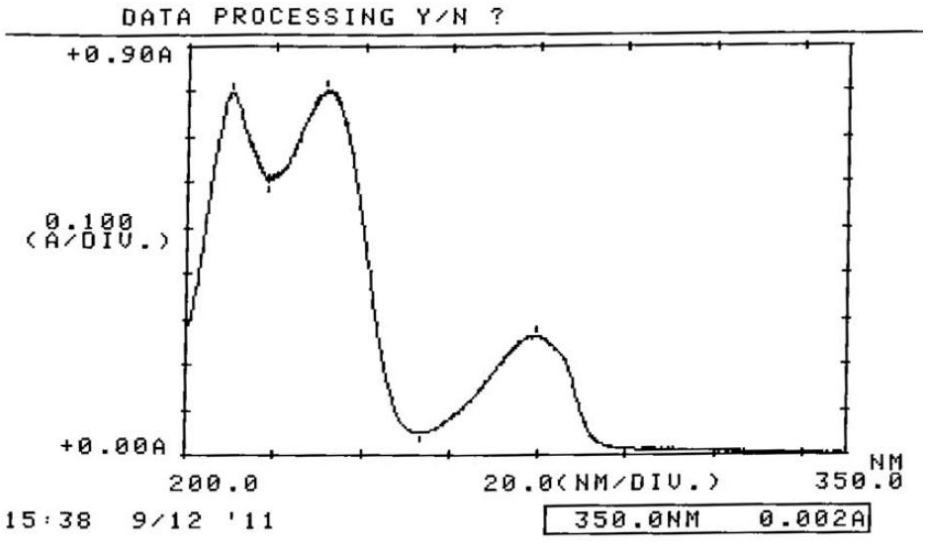

Figure 236 UV spectrum of compound SMF9 [**116**] (MeOH)

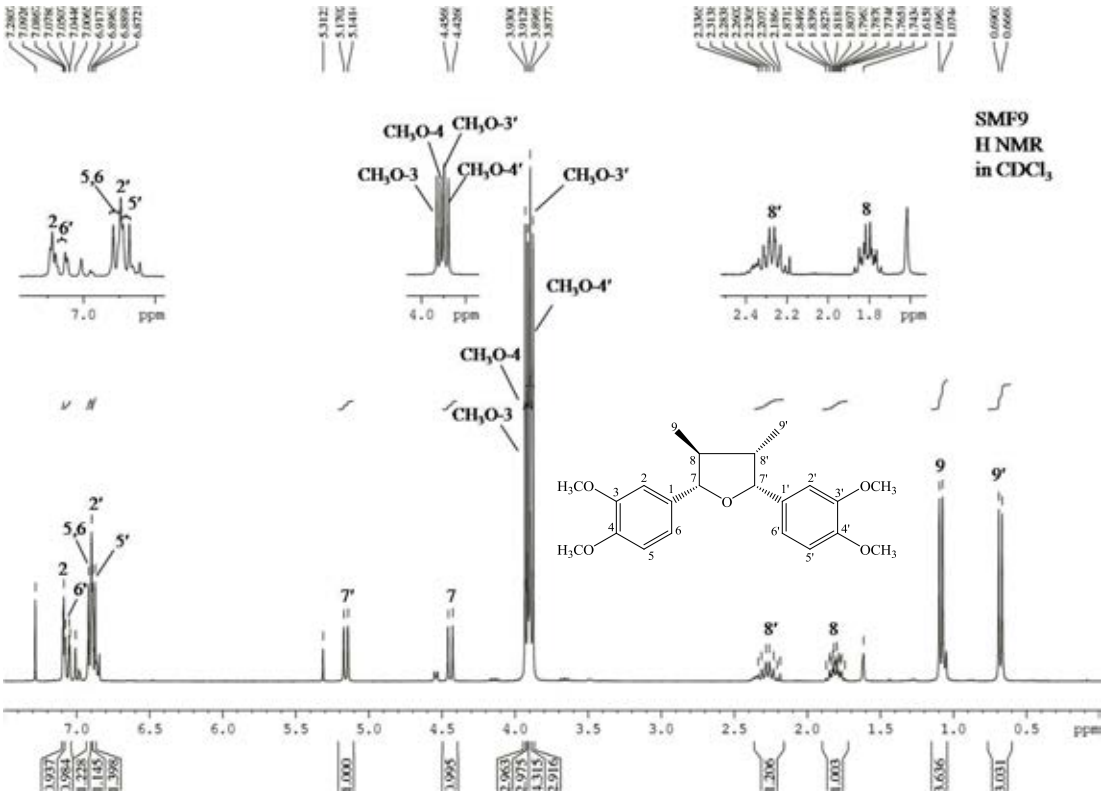

Figure 237 ^{1}H-NMR spectrum of compound SMF9 [**116**] ($CDCl_3$)

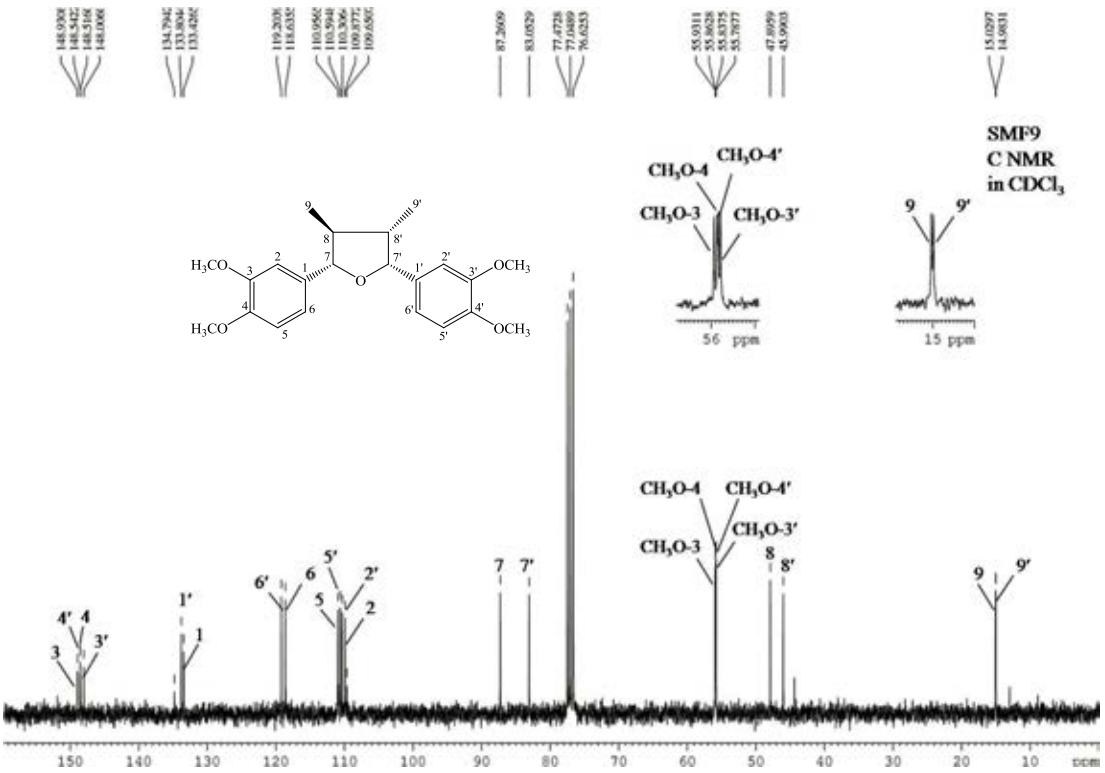

Figure 238 ^{13}C-NMR spectrum of compound SMF9 [**116**] ($CDCl_3$)

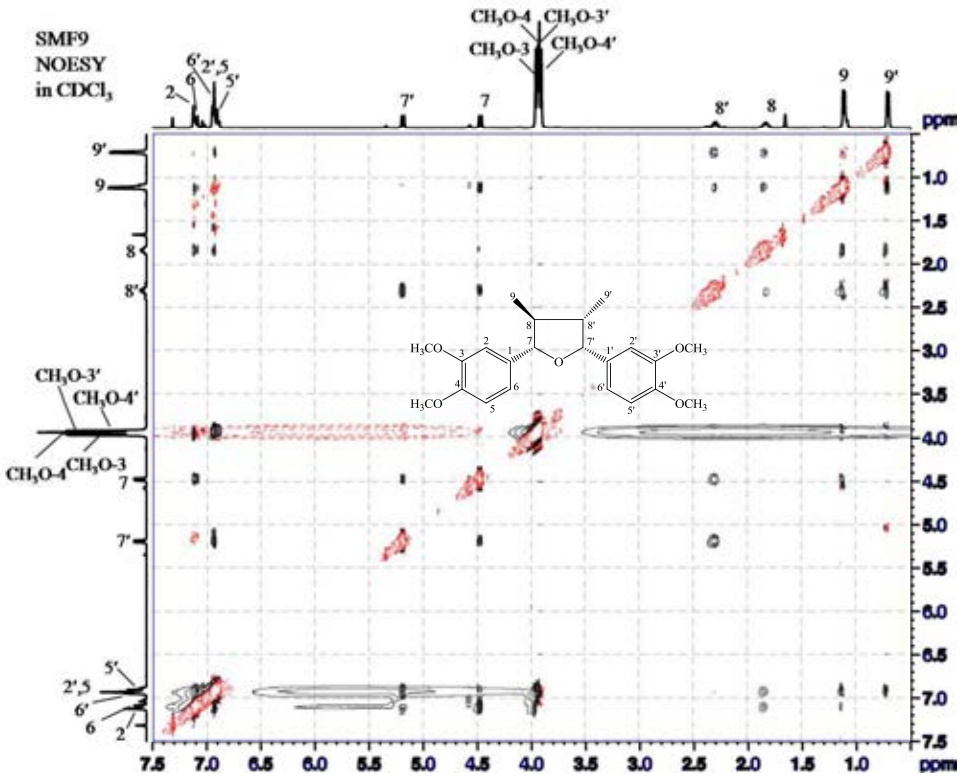

Figure 239 NOESY spectrum of compound SMF9 [**116**] ($CDCl_3$)

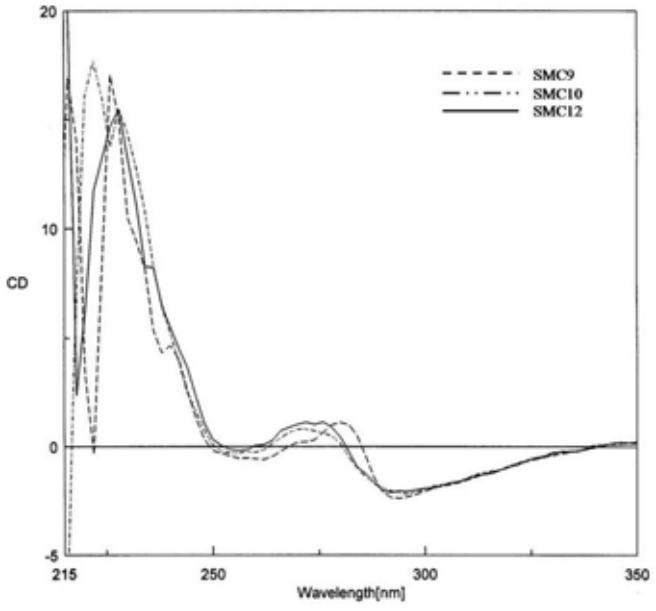

Figure 240 CD spectra (MeOH)of compounds SMF9 [**116**], SMF10 [**117**] and SMF12 [**118**]

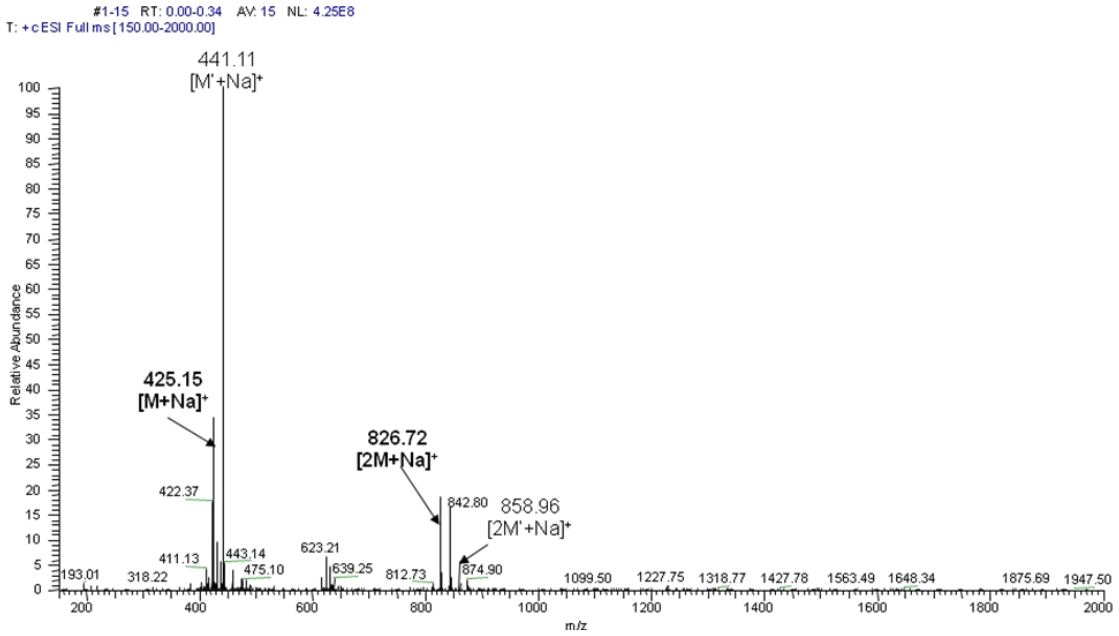

Figure 241 ESI mass spectrum of compound SMF10 [**117**]

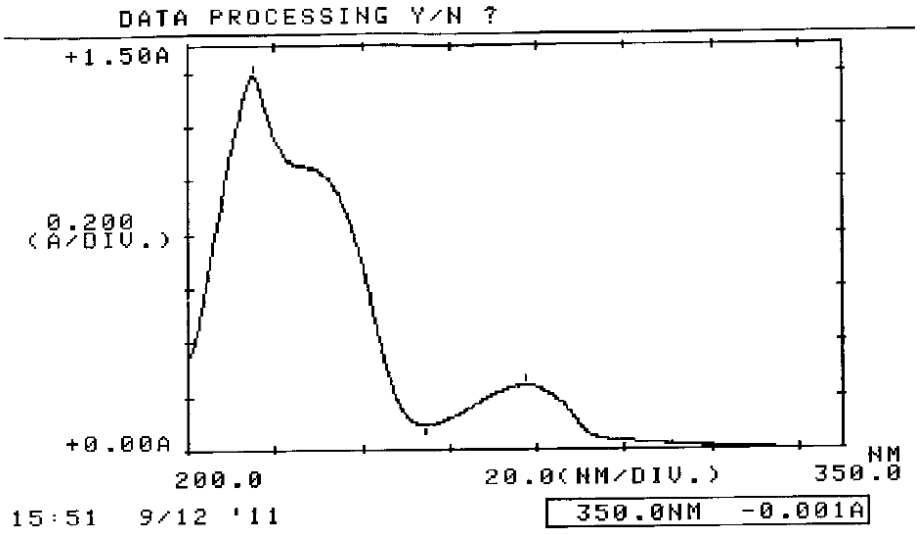

Figure 242 UV spectrum of compound SMF10 [**117**] (MeOH)

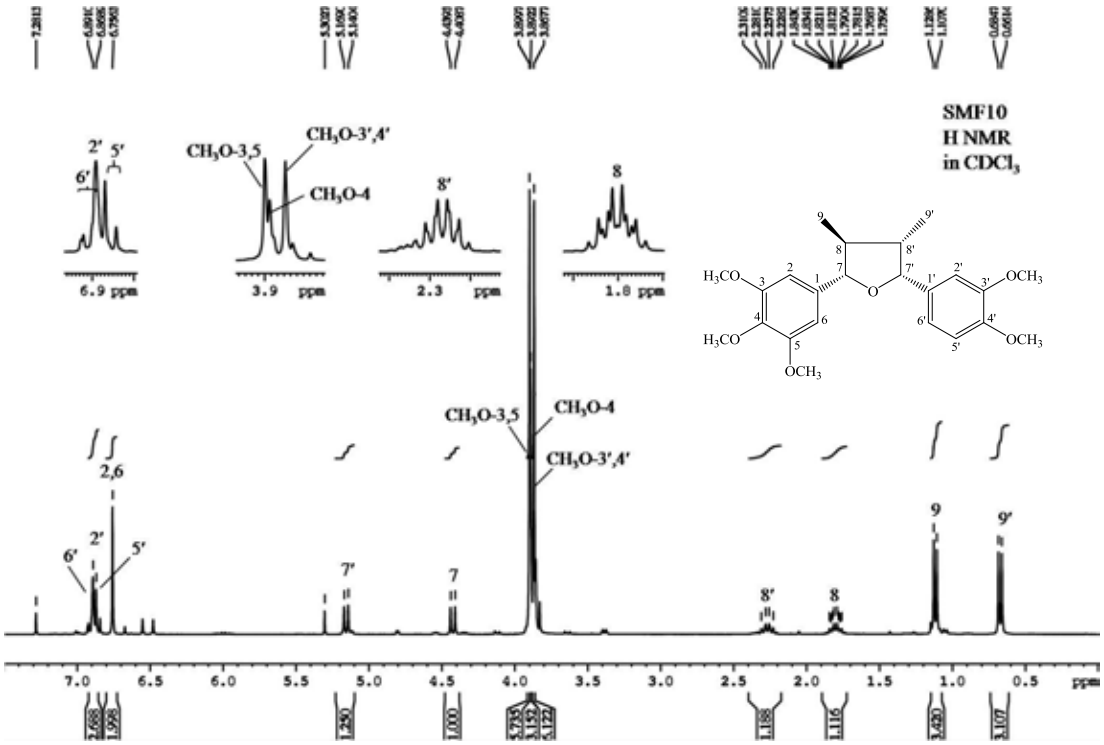

Figure 243 ^{1}H-NMR spectrum of compound SMF10 [**117**] ($CDCl_3$)

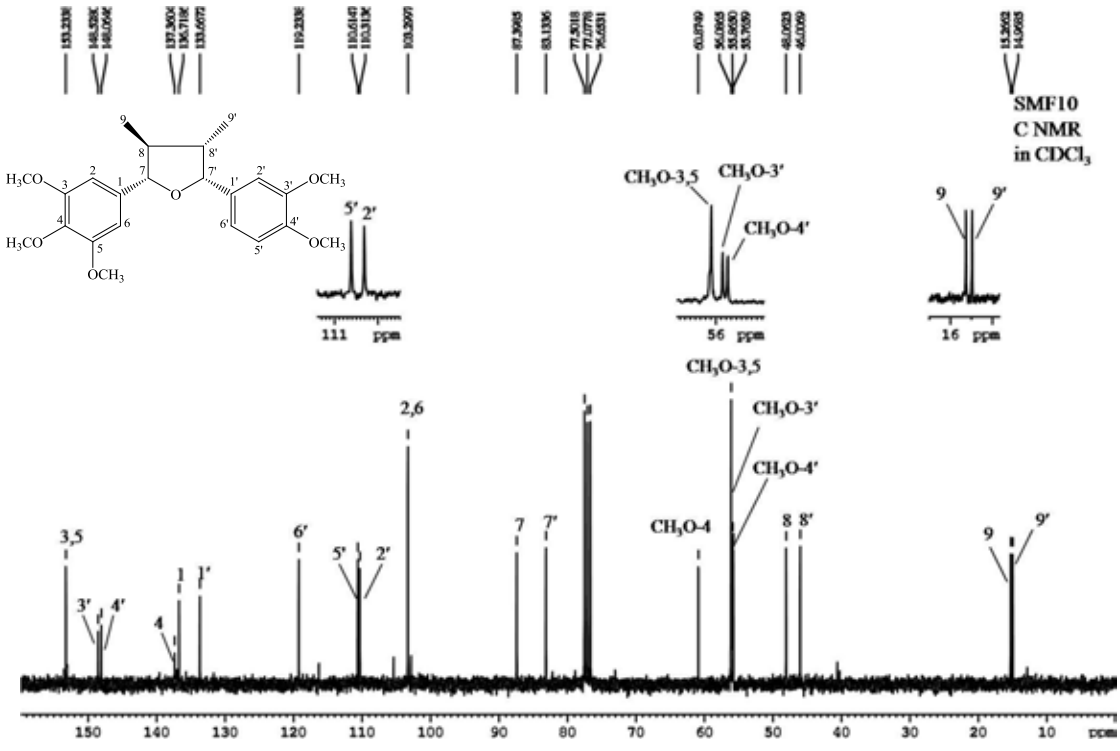

Figure 244 ^{13}C-NMR spectrum of compound SMF10 [**117**] ($CDCl_3$)

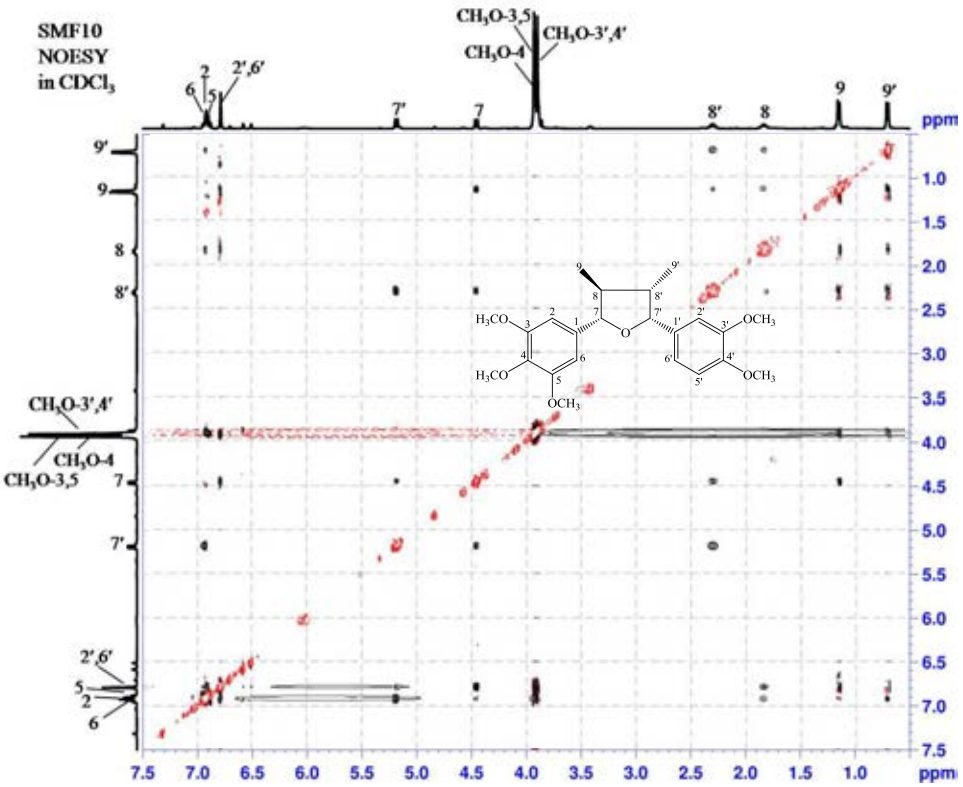

Figure 245 NOESY spectrum of compound SMF10 [**117**] ($CDCl_3$)

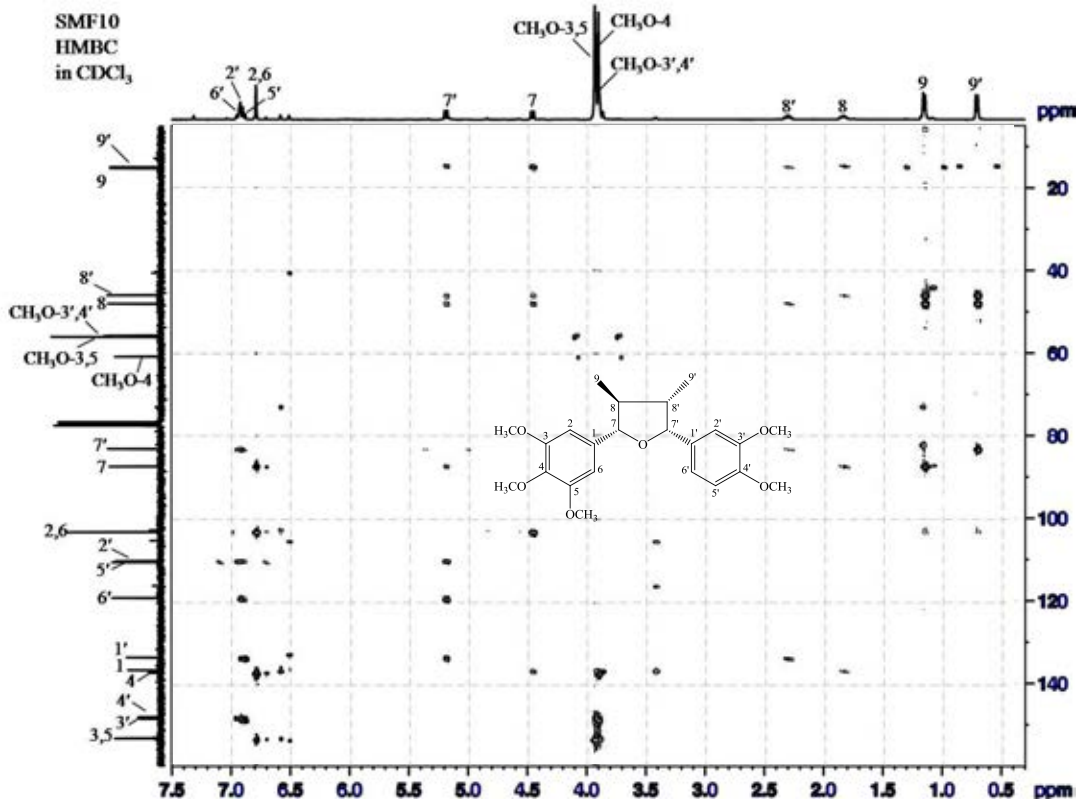

Figure 246 HMBC spectrum of compound SMF10 [**117**] ($CDCl_3$)

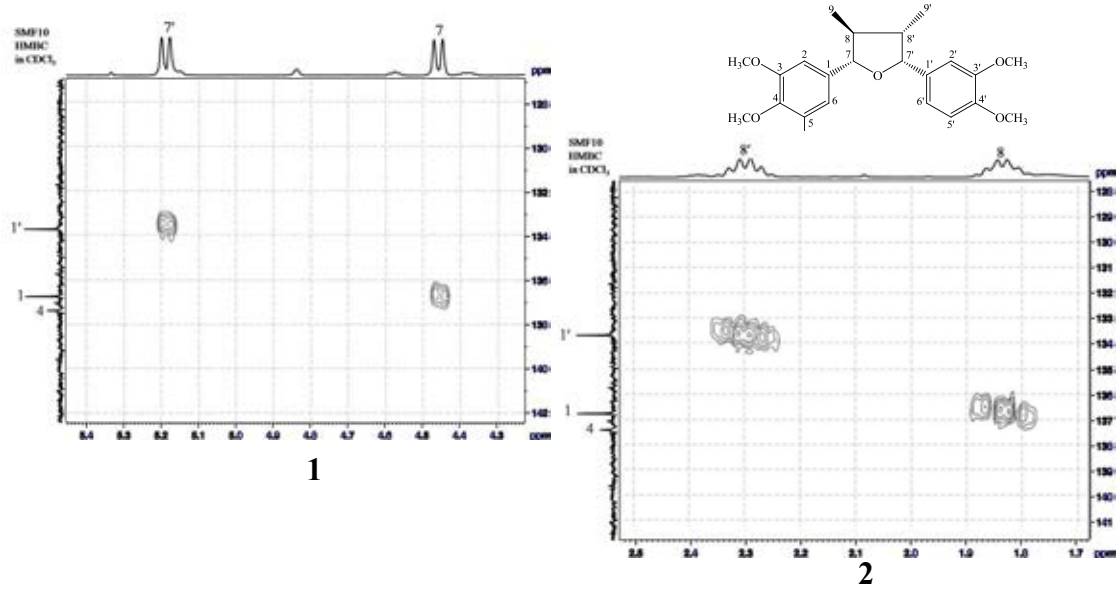

1 **2**

Figure 246a HMBC spectrum of compound SMF10 [**117**] ($CDCl_3$)
[δ_H 5.45-4.23 ppm, δ_C 142.5-127.7 ppm (1)] and
[δ_H 2.53-1.68 ppm, δ_C 141.6-127.6 ppm (2)]

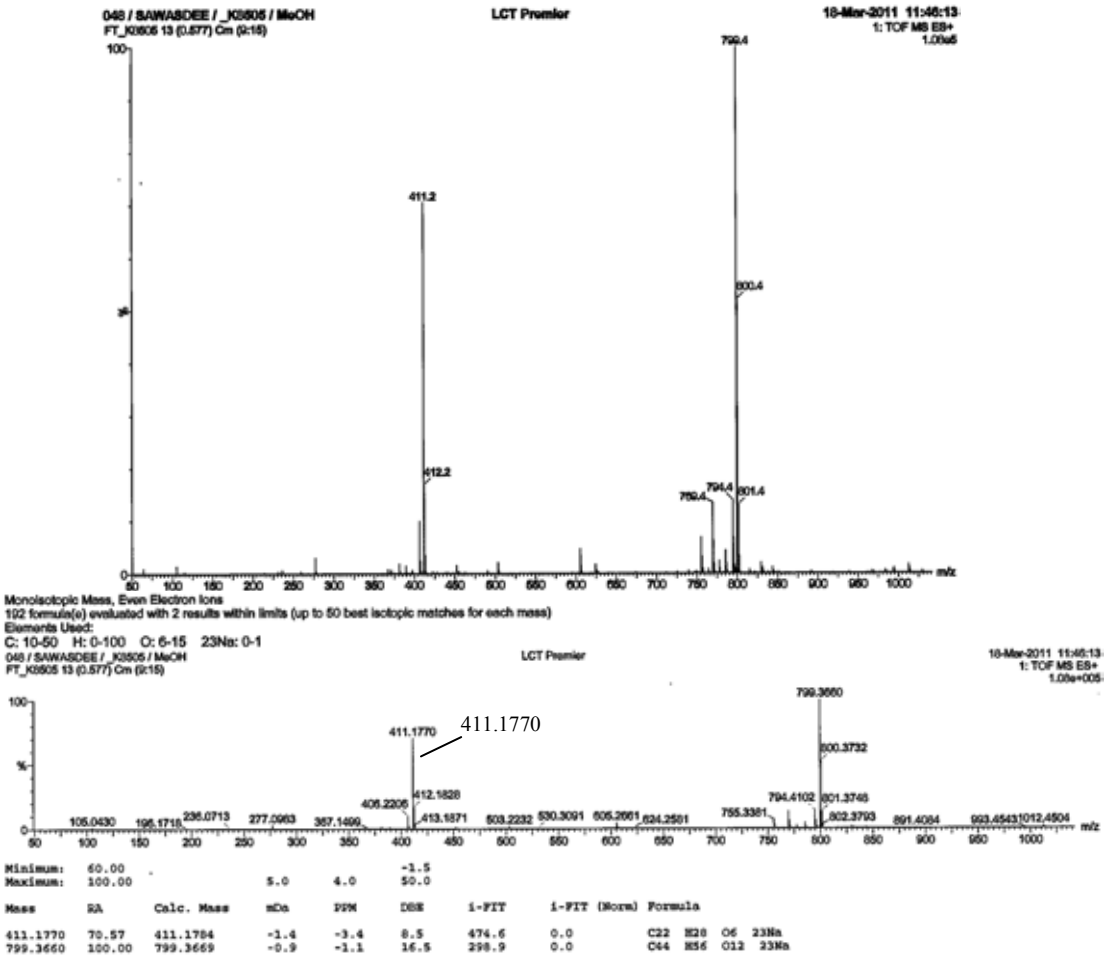

Figure 247 HRESI mass spectrum of compound SMF12 [**118**]

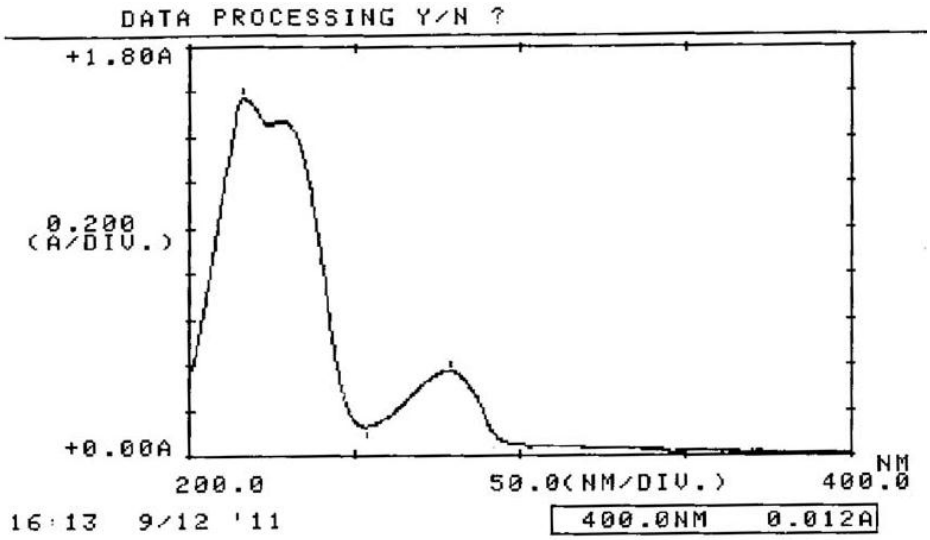

Figure 248 UV spectrum of compound SMF12 [**118**] (MeOH)

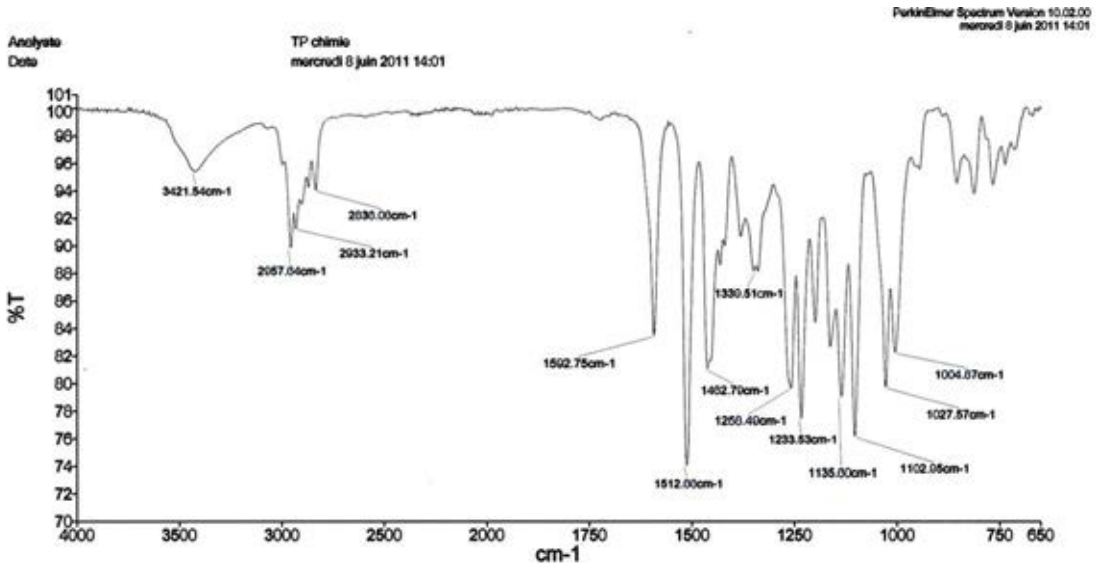

Figure 249 IR spectrum of compound SMF12 [**118**] (film)

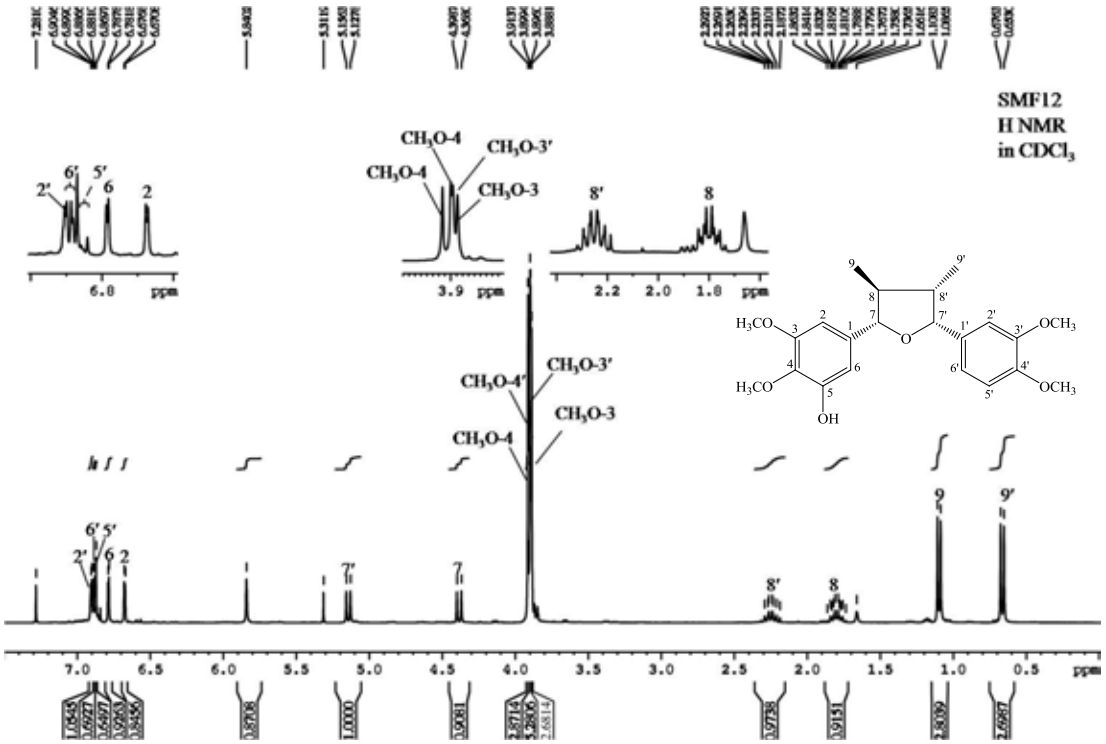

Figure 250 ^{1}H-NMR spectrum of compound SMF12 [**118**] ($CDCl_3$)

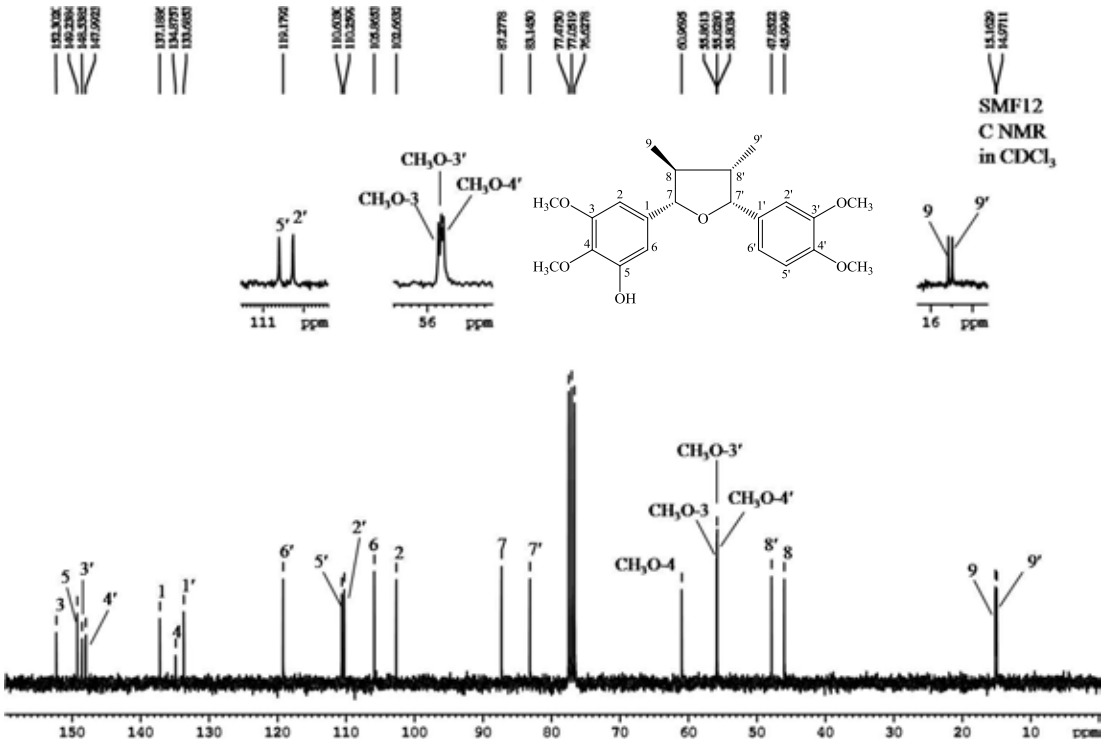

Figure 251 ^{13}C-NMR spectrum of compound SMF12 [**118**] ($CDCl_3$)

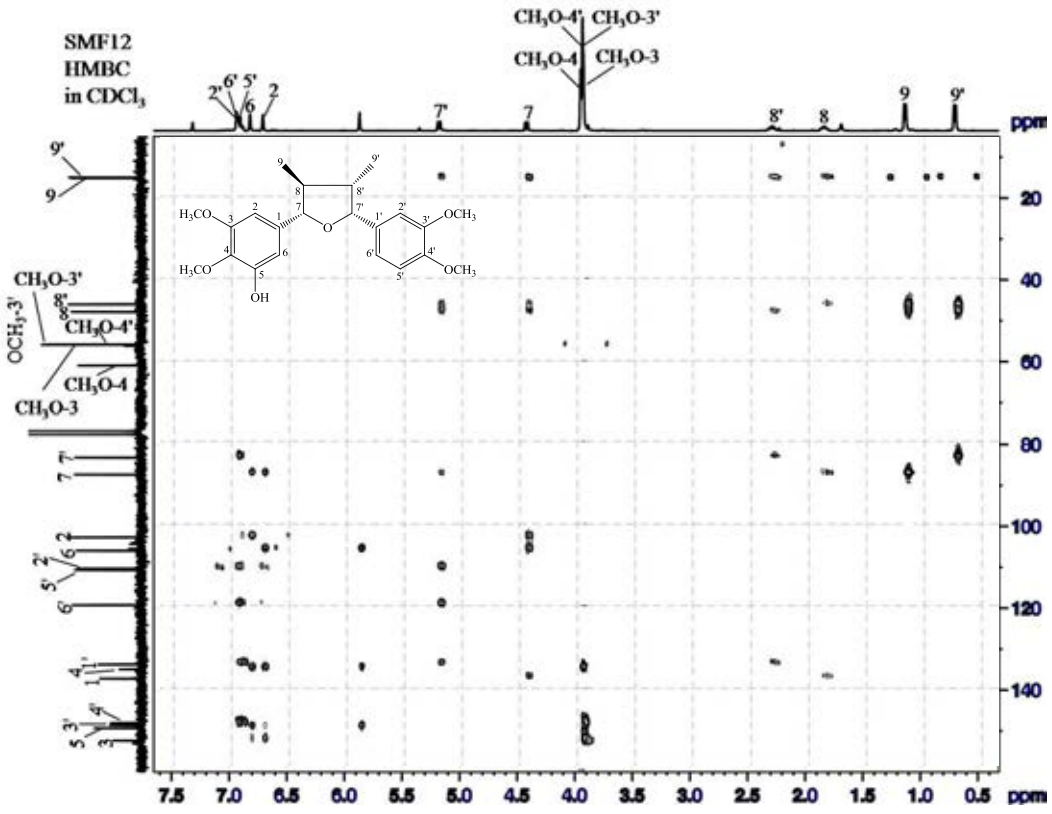

Figure 252 HMBC spectrum of compound SMF12 [**118**] ($CDCl_3$)

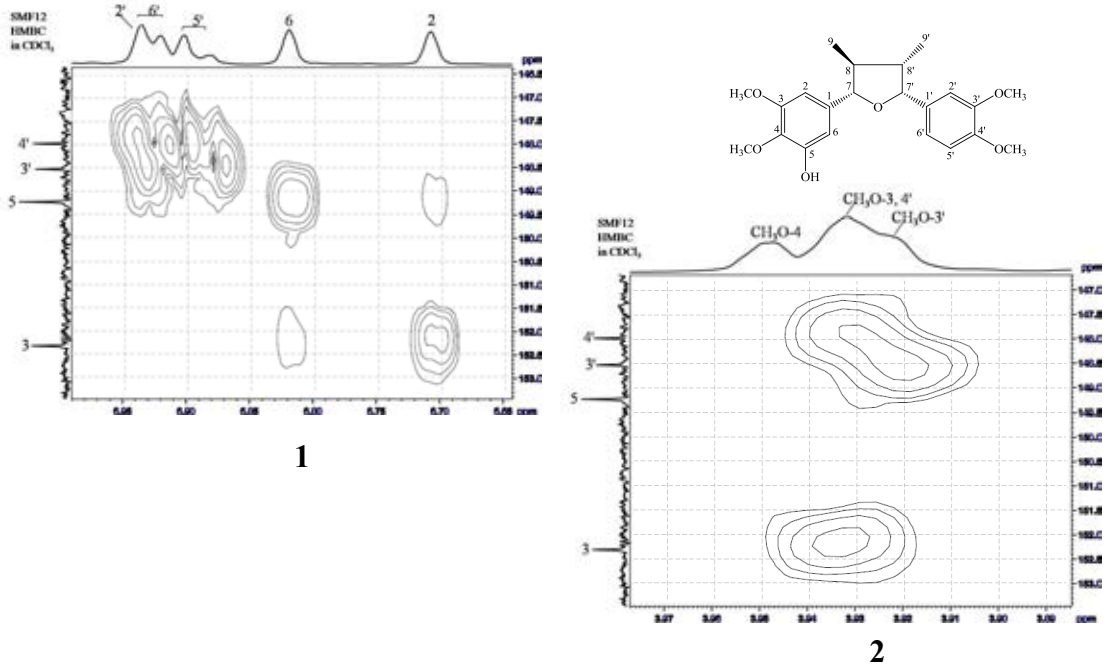

1 **2**

Figure 252a HMBC spectrum of compound SMF12 [**118**] ($CDCl_3$)
[δ_H 6.99-6.64 ppm, δ_C 153.5-146.4 ppm (1)] and
[δ_H 3.98-3.89 ppm, δ_C 153.5-146.7 ppm (2)]

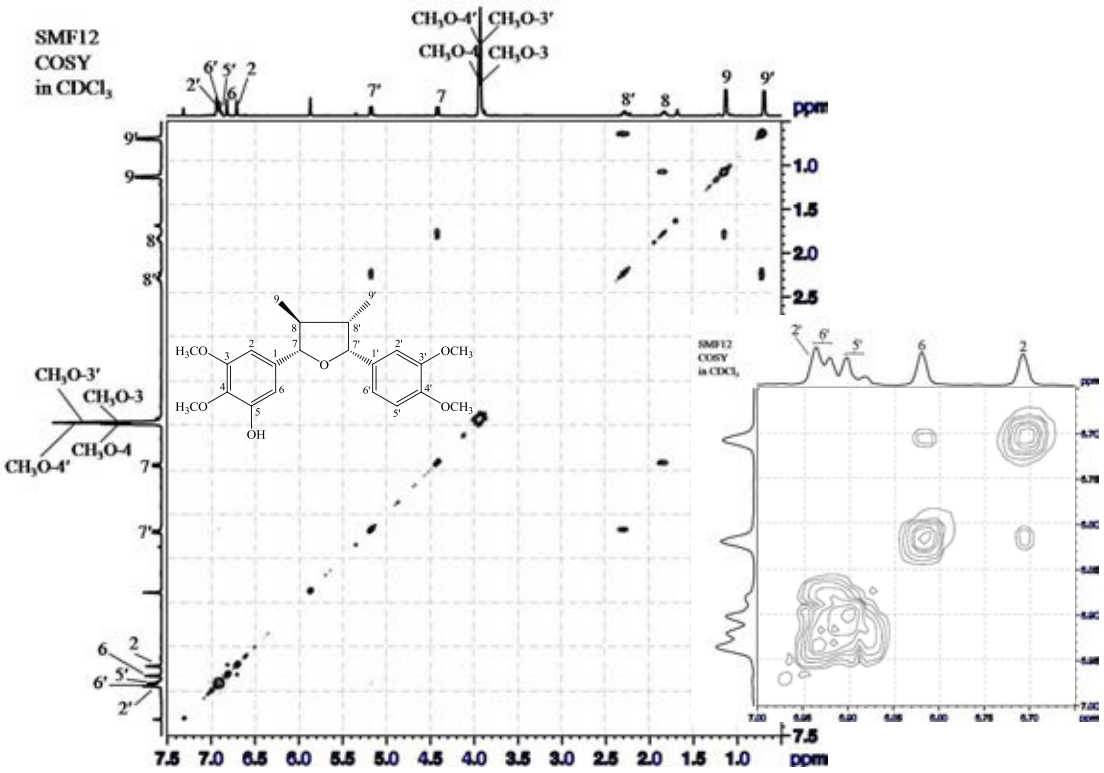

Figure 253 ^{1}H-^{1}H COSY spectrum of compound SMF12 [**118**] ($CDCl_3$)

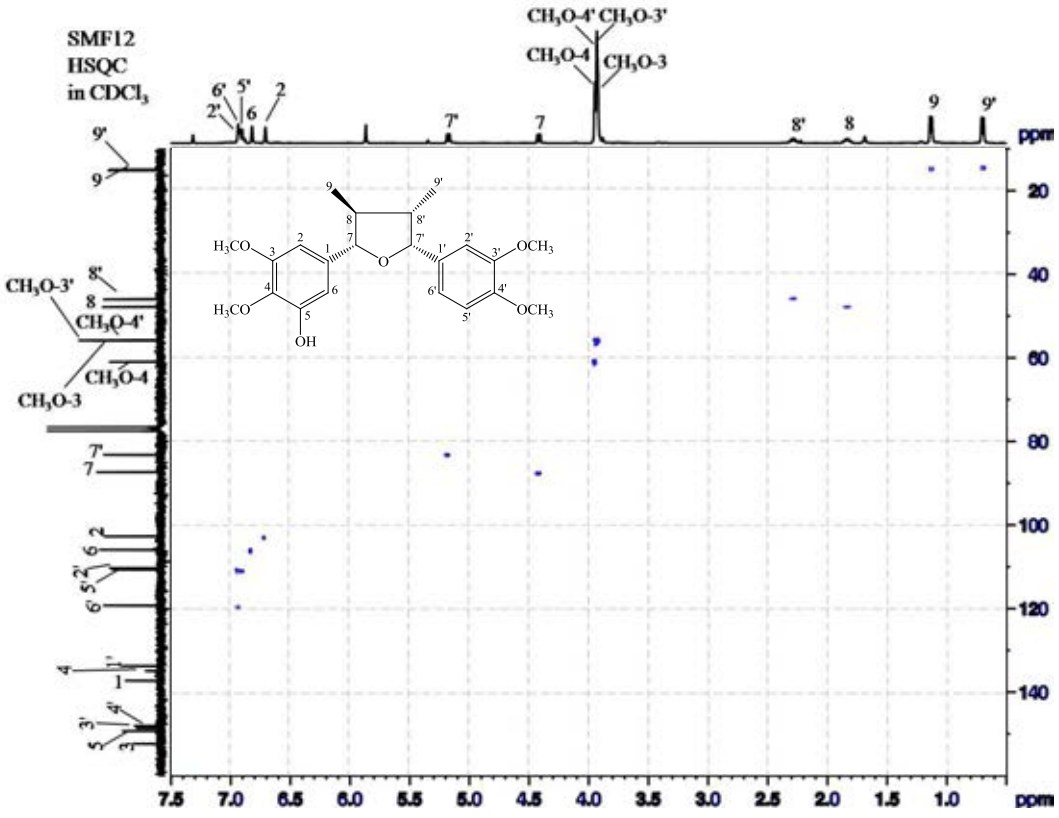

Figure 254 HSQC spectrum of compound SMF12 [**118**] ($CDCl_3$)

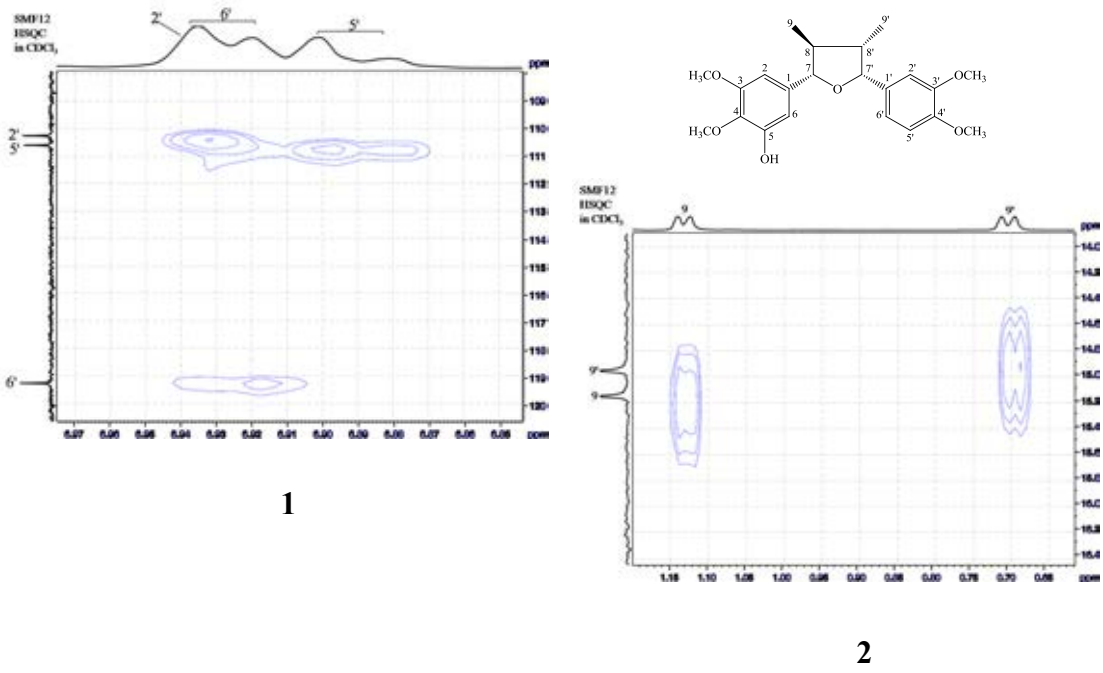

Figure 254a HSQC spectrum of compound SMF12 [**118**] ($CDCl_3$)
[δ_H 6.70-6.84 ppm, δ_C 120.5-108.0 ppm (1)] and
[δ_H 1.16-0.61 ppm, δ_C 16.5-13.9 ppm (2)]

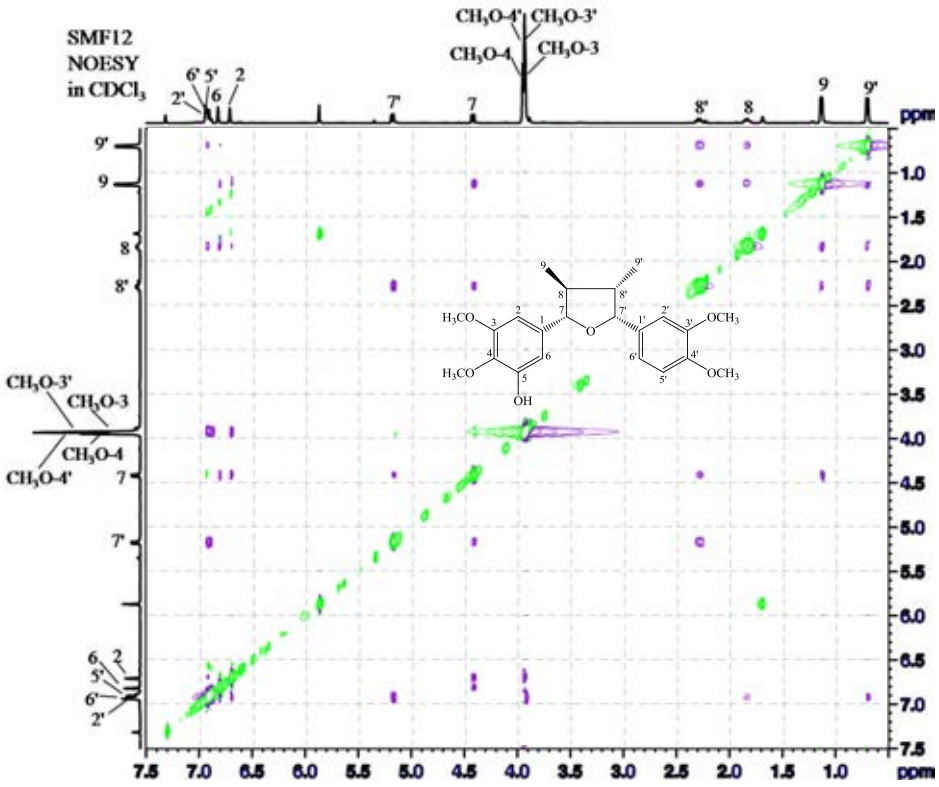

Figure 255 NOESY spectrum of compound SMF12 [**118**] ($CDCl_3$)

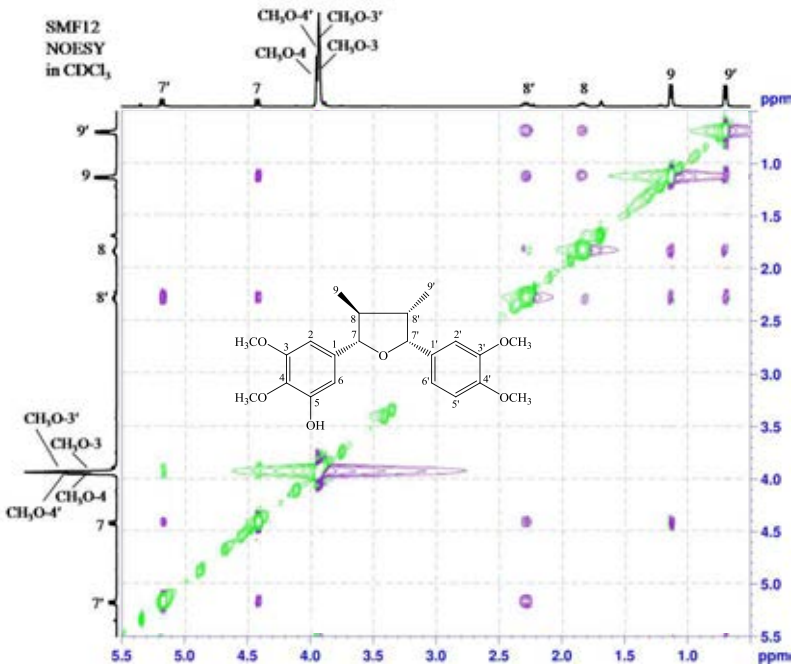

Figure 255a NOESY spectrum of compound SMF12 [**118**] ($CDCl_3$) [δ_H 5.50-0.50 ppm]

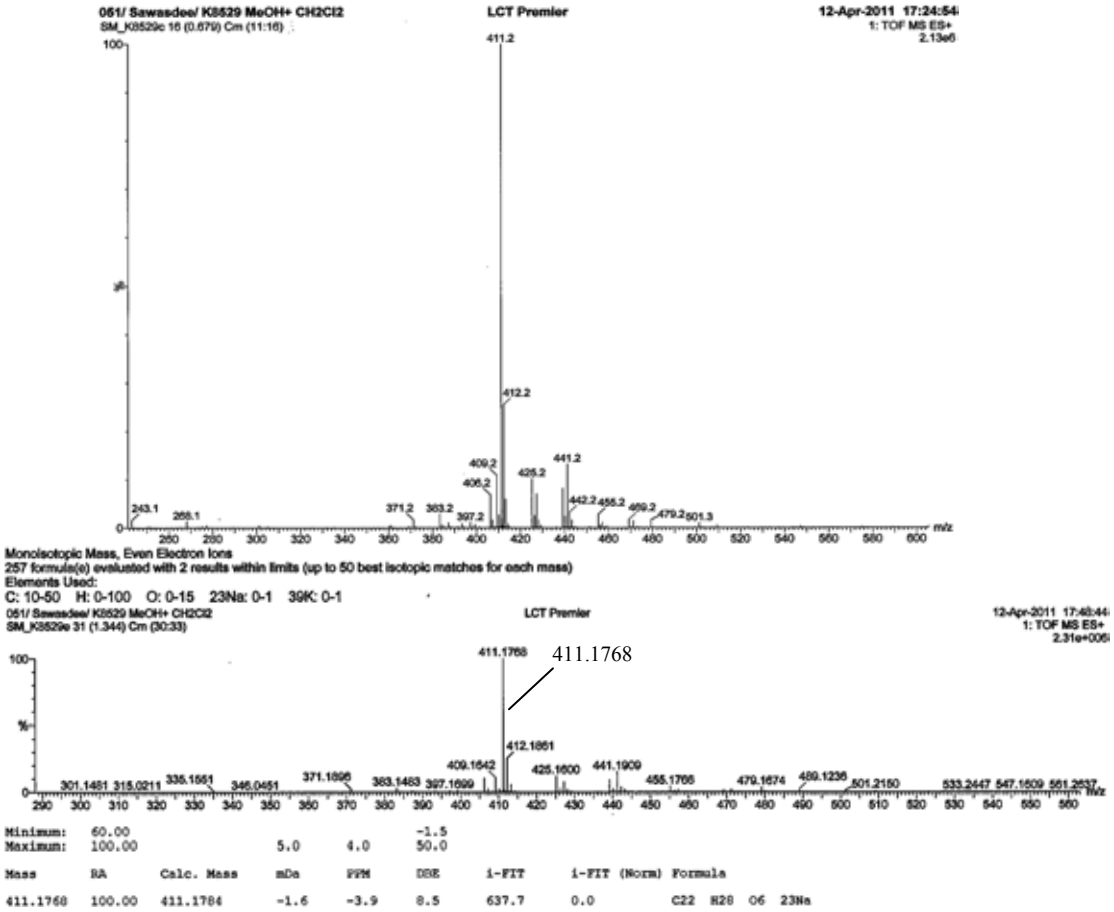

Figure 256 HRESI mass spectrum of compound SMF13 [**119**]

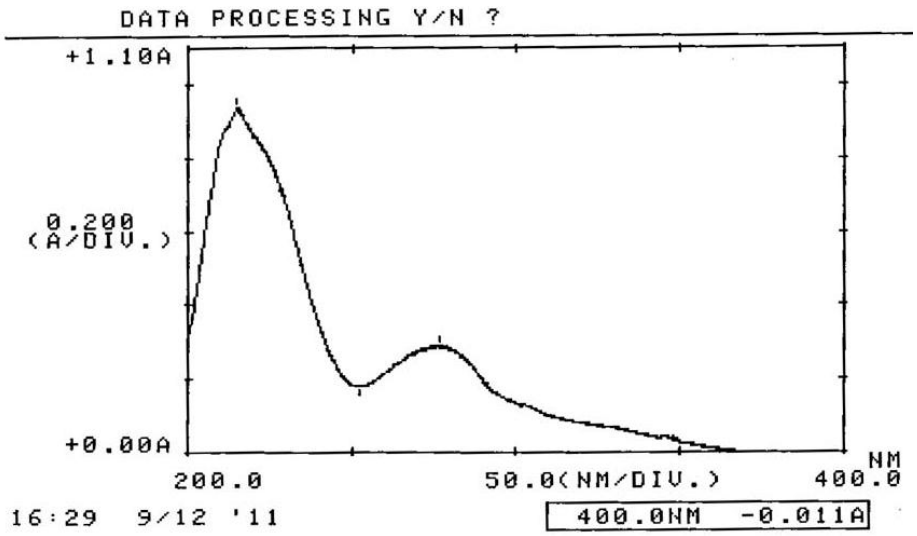

Figure 257 UV spectrum of compound SMF13 [**119**] (MeOH)

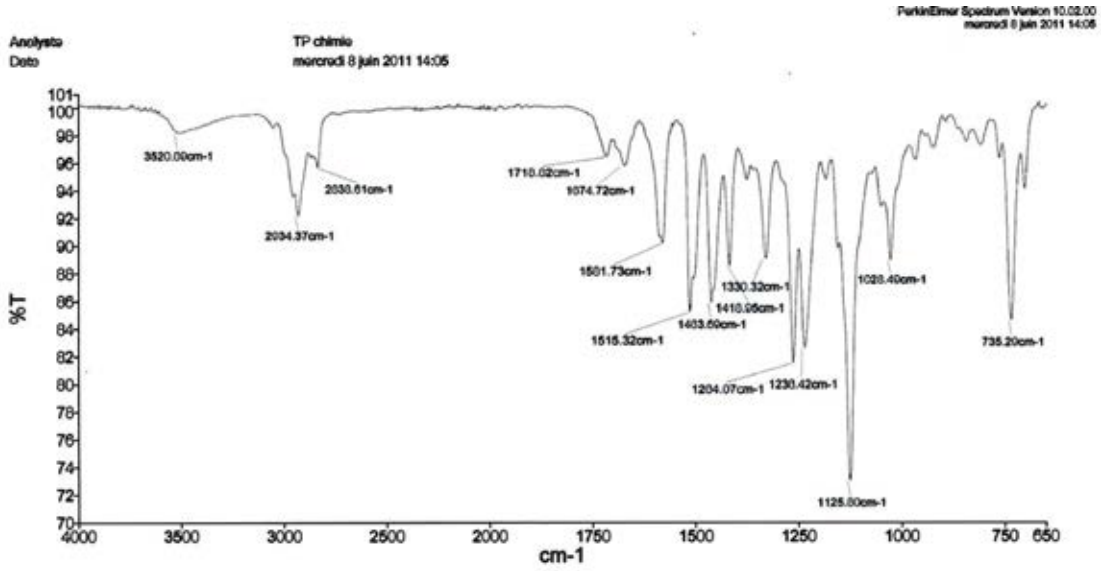

Figure 258 IR spectrum of compound SMF13 [**119**] (film)

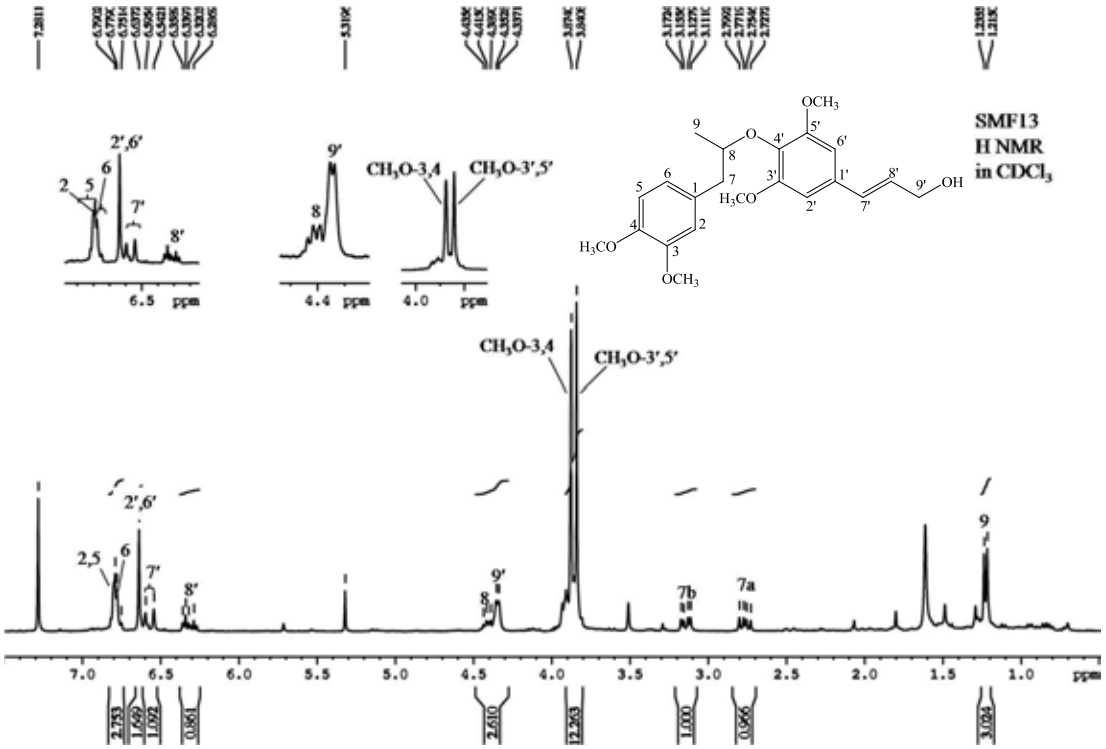

Figure 259 ^{1}H-NMR spectrum of compound SMF13 [**119**] ($CDCl_3$)

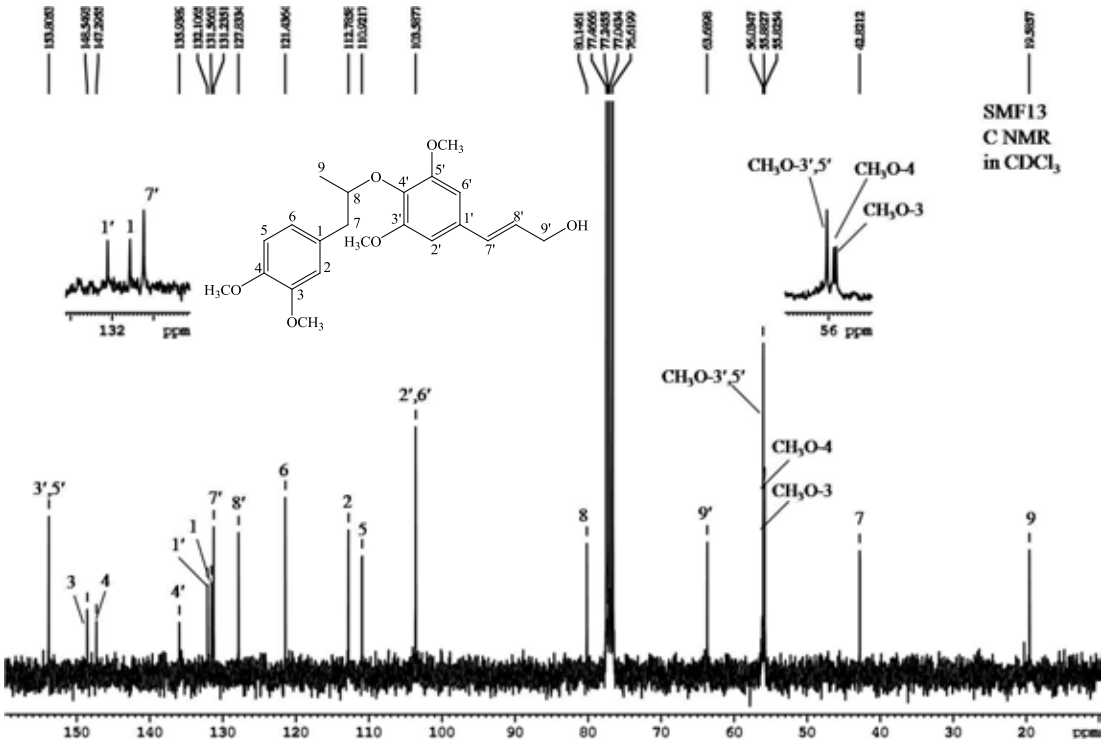

Figure 260 ^{13}C-NMR spectrum of compound SMF13 [**119**] ($CDCl_3$)

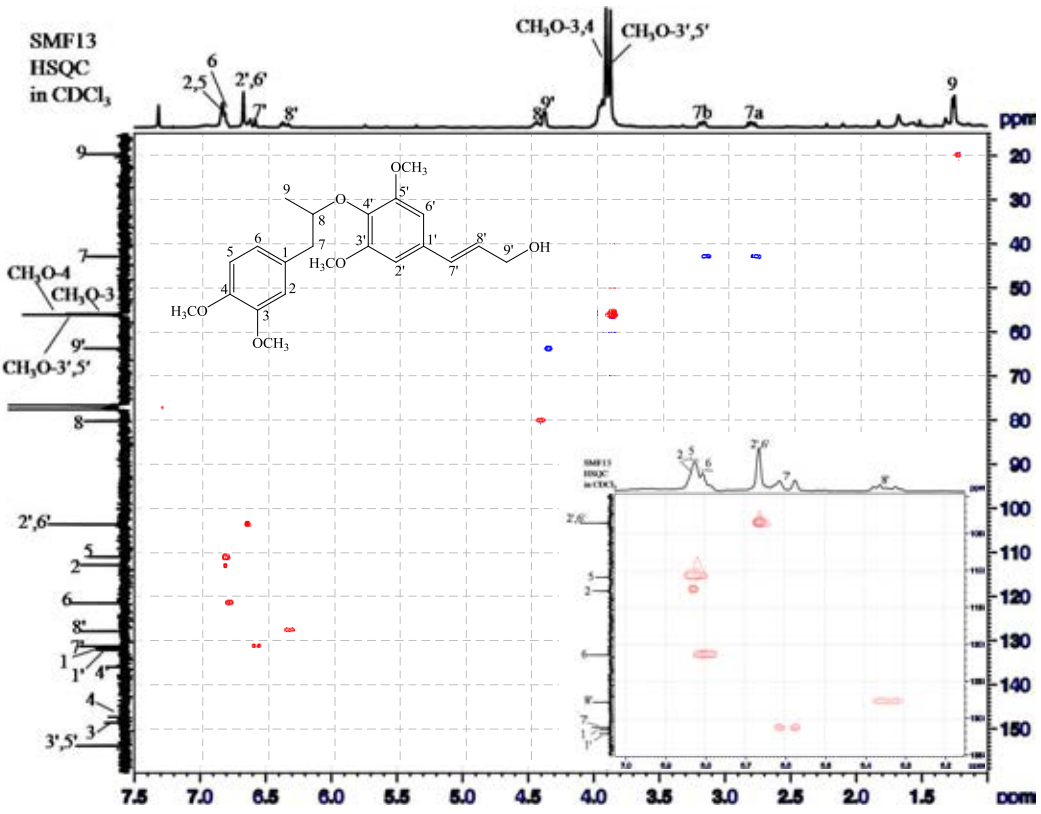

Figure 261 HSQC spectrum of compound SMF13 [**119**] ($CDCl_3$)

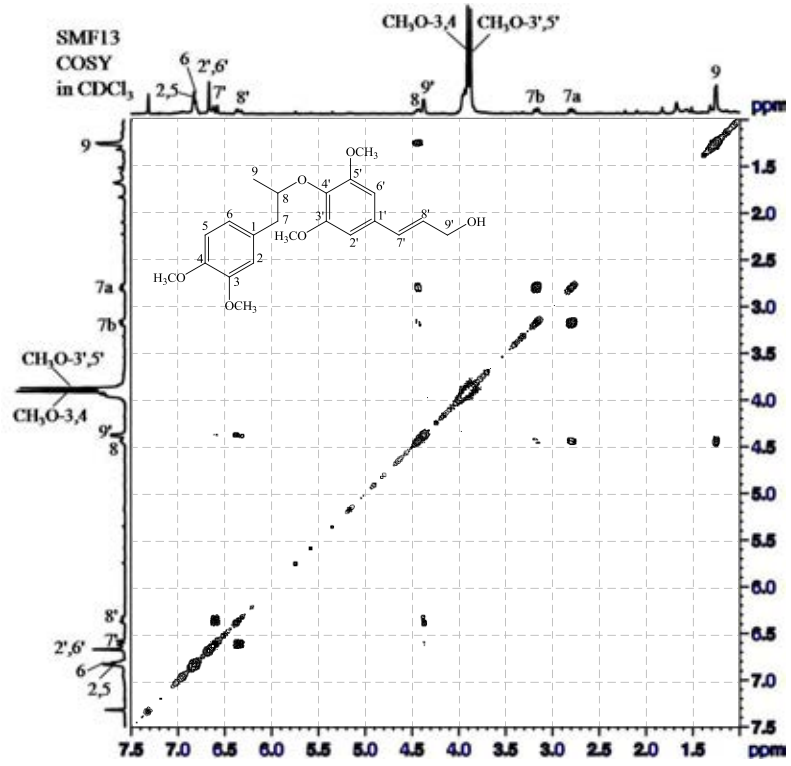

Figure 262 ^{1}H-^{1}H COSY spectrum of compound SMF13 [**119**] ($CDCl_3$)

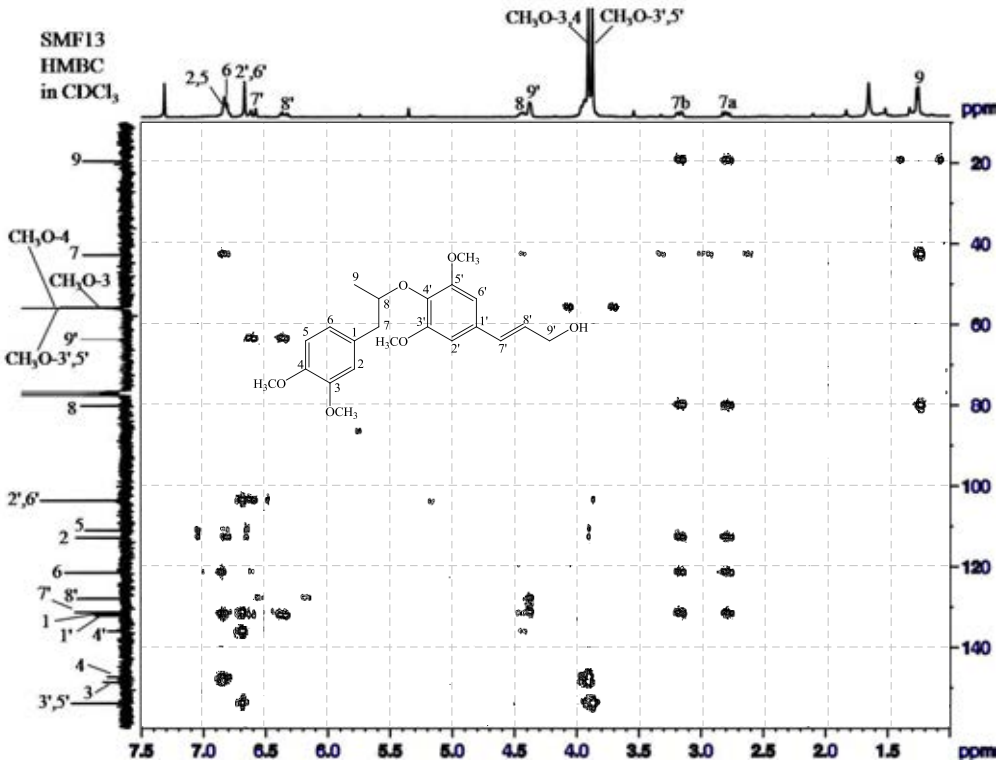

Figure 263 HMBC spectrum of compound SMF13 [**119**] ($CDCl_3$)

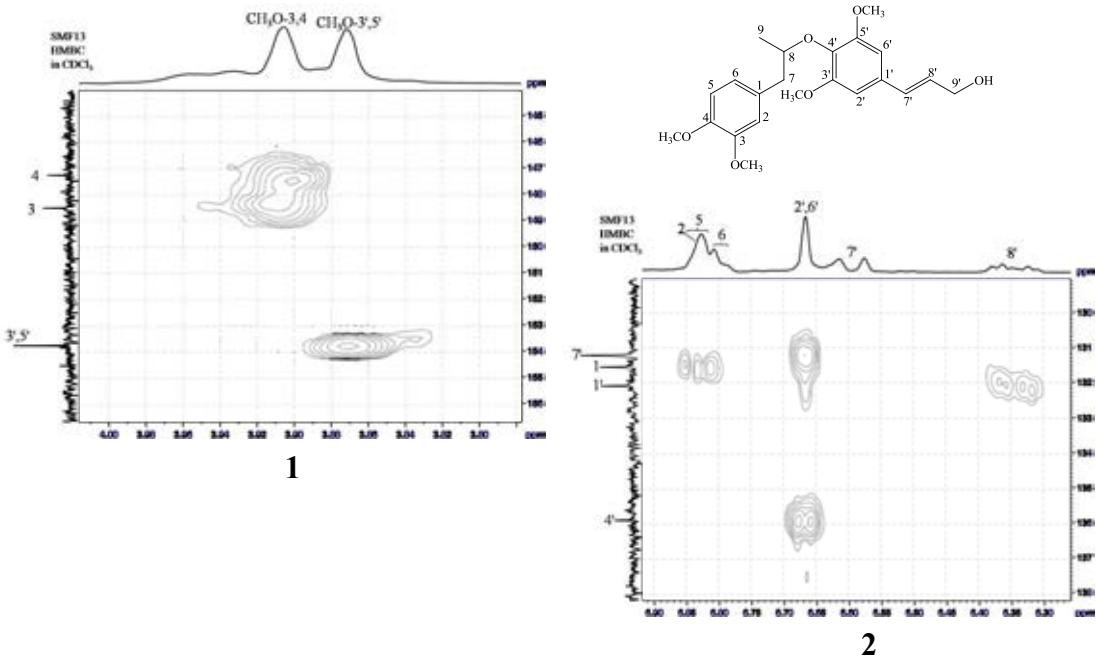

Figure 263a HMBC spectrum of compound SMF13 [**119**] ($CDCl_3$)
[δ_H 4.02-3.78 ppm, δ_C 156.7-144.0 ppm (1)] and
[δ_H 6.92-6.26 ppm, δ_C 138.2-129.0 ppm (2)]

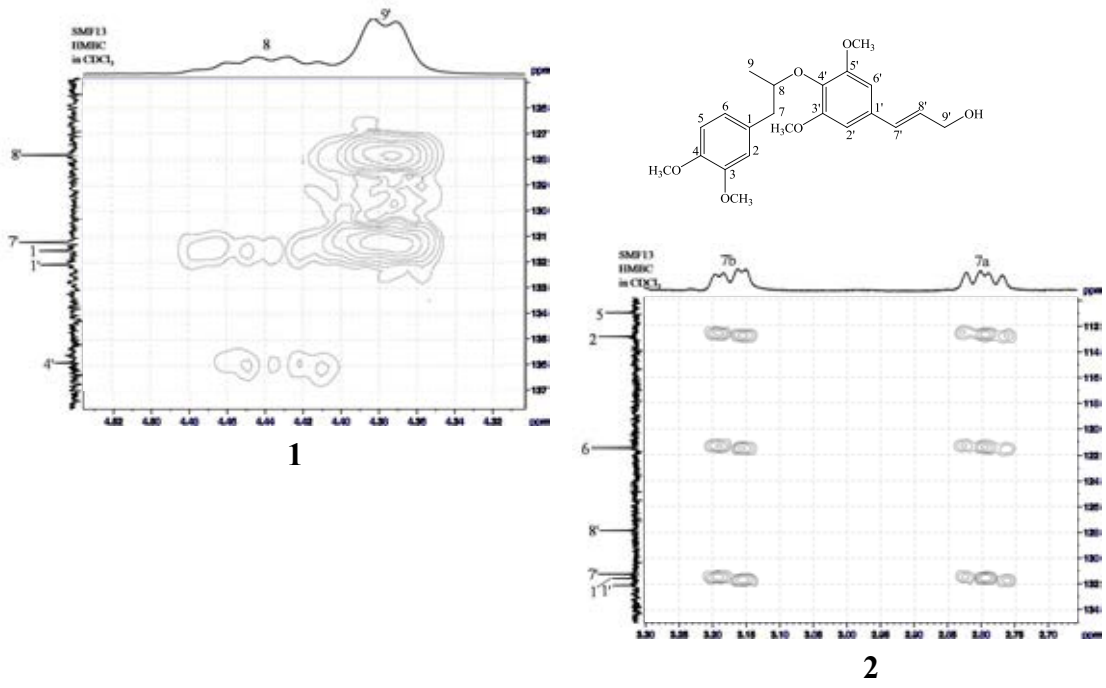

Figure 263b HMBC spectrum of compound SMF13 [**119**] ($CDCl_3$)
[δ_H 4.54-4.30 ppm, δ_C 137.7-124.9 ppm (1)] and
[δ_H 3.30-2.66 ppm, δ_C 135.0-110.0 ppm (2)]

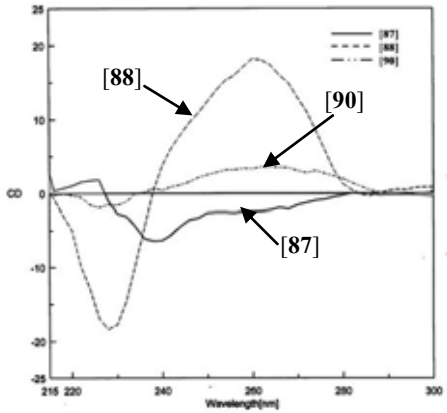

[**87**] $[\alpha]_D^{20} = -13.22$

[**88**] $[\alpha]_D^{20} = +18.39$

[**90**] $[\alpha]_D^{20} = +65.28$

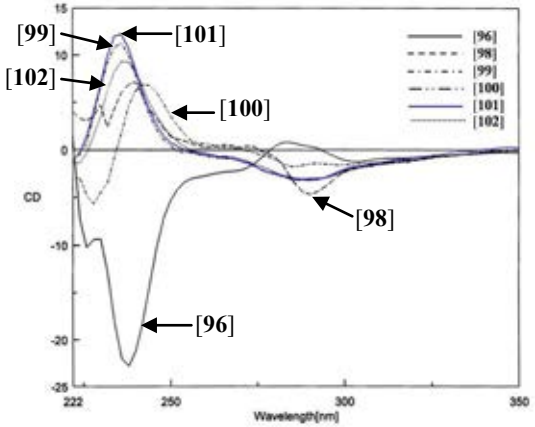

[**96**] $[\alpha]_D^{20} = -25.00$

[**98**] $[\alpha]_D^{20} = +8.57$

[**99**] $[\alpha]_D^{20} = +32.35$

[**100**] $[\alpha]_D^{20} = +15.71$

[**101**] $[\alpha]_D^{20} = +77.00$

[**102**] $[\alpha]_D^{20} = +22.96$

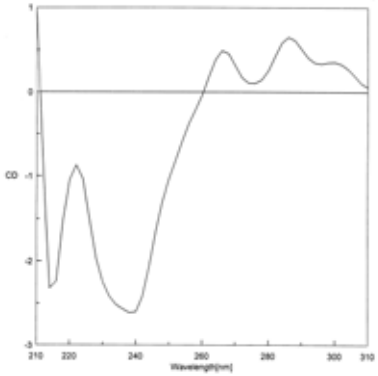

[**106**] $[\alpha]_D^{20} = +22.20$

Figure 264 CD spectra of *trans*-2-aryl-3-methyl-2,3-dihydrobenzofuran neolignans

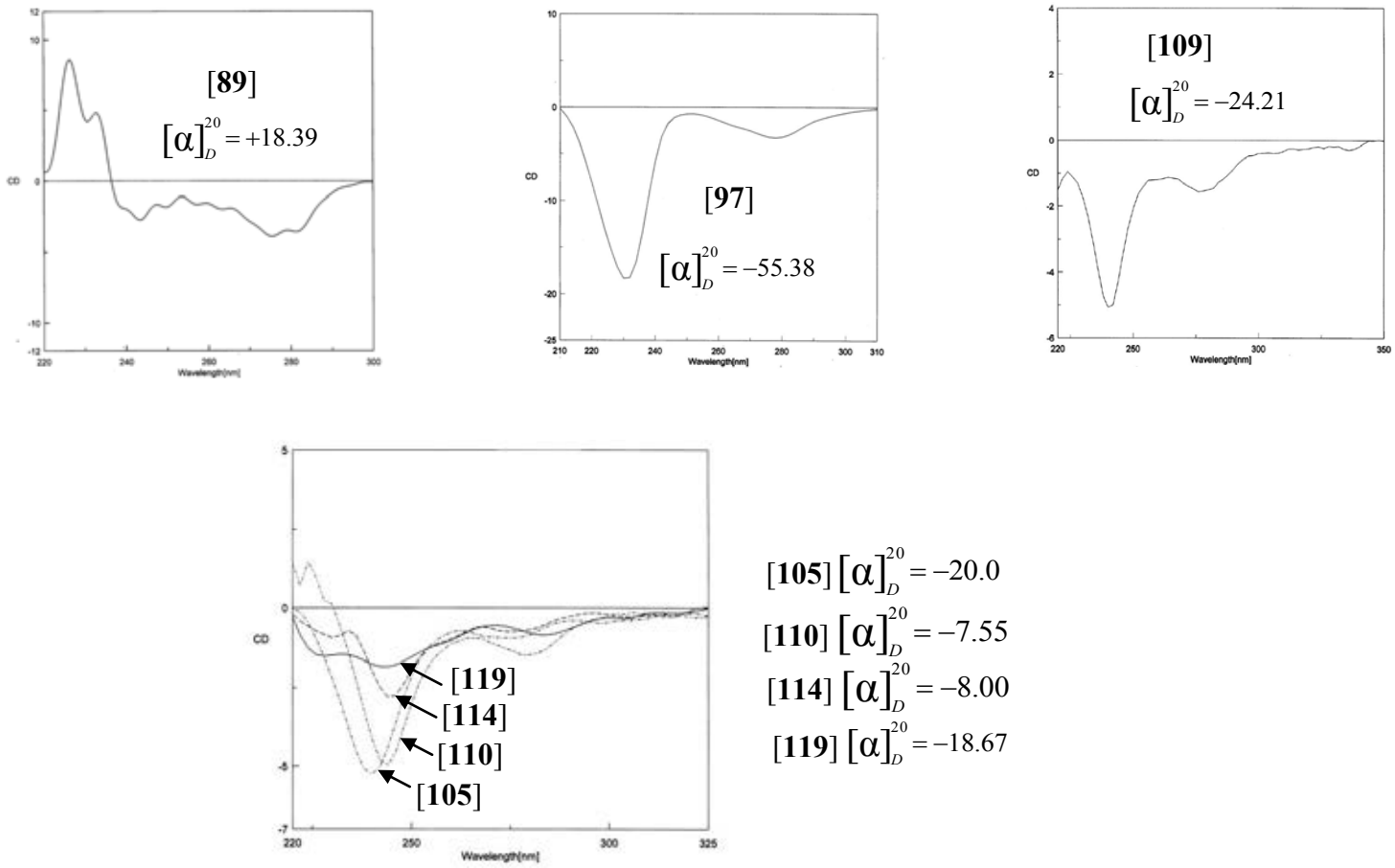

[**105**] $[\alpha]_D^{20} = -20.0$

[**110**] $[\alpha]_D^{20} = -7.55$

[**114**] $[\alpha]_D^{20} = -8.00$

[**119**] $[\alpha]_D^{20} = -18.67$

Figure 265 CD spectra of 8.O.4′ neolignans

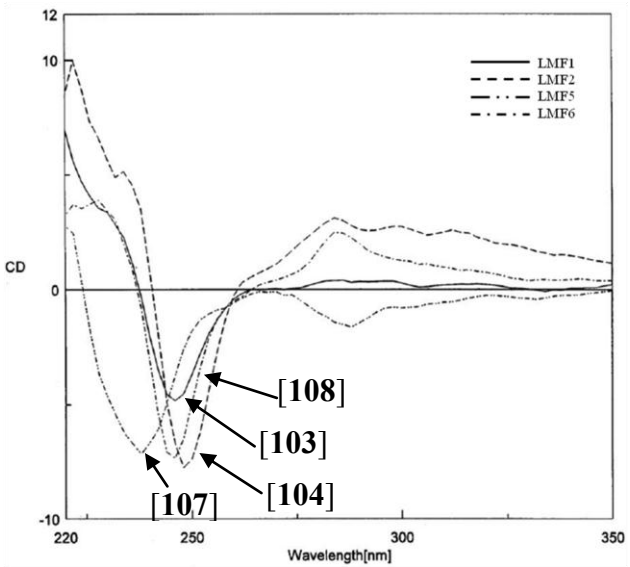

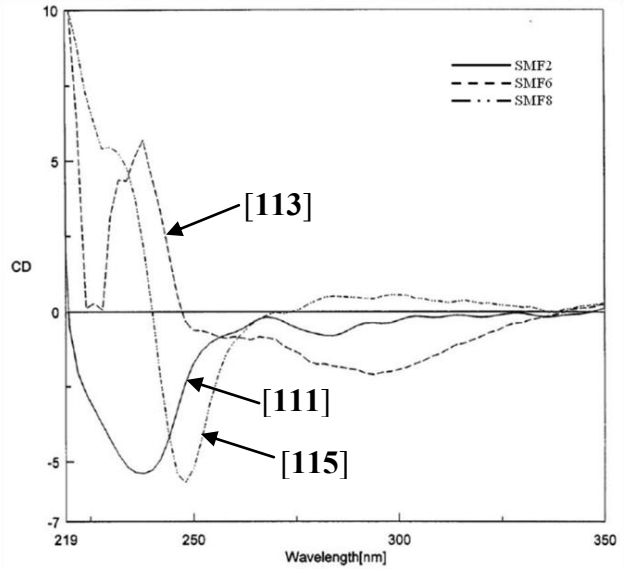

[**103**] $[\alpha]_D^{20} = +65.54$

[**104**] $[\alpha]_D^{20} = +96.88$

[**107**] $[\alpha]_D^{20} = -23.64$

[**108**] $[\alpha]_D^{20} = +80.00$

[**111**] $[\alpha]_D^{20} = -15.27$

[**113**] $[\alpha]_D^{20} = +13.64$

[**115**] $[\alpha]_D^{20} = +52.86$

Figure 266 CD spectra of 7.O.3′,8.O.4′ neolignans

VITA

Miss Kanokporn Sawasdee was born on June 7, 1976 in Bangkok, Thailand. She received her Bachelor's degree of Pharmacy in 1999 from the Faculty of Pharmacy, Huachiew Chalermprakiet University, Thailand and Master's degree of Science in Pharmacy in 2002 from the Faculty of Pharmaceutical Sciences, Chulalongkorn University, Thailand. She was awarded a 2006 Royal Golden Jubilee Scholarship from the Thailand Research Fund, a research grant from the French Embassy and a Chulalongkorn University Graduate Scholarship in Commemoration of HM King Bhumibol Adulyadej's 72nd Anniversary.

Publications

1. Likhitwitayawuid, K., Sawasdee, K., and Kirtikara, K. 2002. Flavonoids and stilbenoids with COX-1 and COX-2 inhibitory activity from *Dracaena loureiri*. Planta Med. 68: 841-843.
2. Sawasdee, K., Chaowasku, T., and Likhitwitayawuid, K. 2010. New neolignans and a Phenylpropanoid glycoside from twigs of *Miliusa mollis*. Molecules 15: 639-648.
3. Sawasdee, K., Chaowasku, T., Lipipun, V., Dufat, T. H., Michel, S., and Likhitwitayawuid, K. New neolignans from *Miliusa mollis* leaves. (in preparation).
4. Sawasdee, K., Chaowasku, T., Lipipun, V., Dufat, T. H., Michel, S., and Likhitwitayawuid, K. New neolignans and lignan from *Miliusa fragrans*. (in preparation).

Oral presentations

1. Sawasdee, K., Chaowasku, T., Lipipun, V., Dufat, T. H., Michel, S., and Likhitwitayawuid, K. 2012. New neolignans from leaves of *Miliusa fragrans*. RGJ-Ph.D. Congress XIII, April, 6-8, 2012, Pattaya, Chonburi, Thailand.